LEGIBILITY NOTICE

A major purpose of the Technical Information Center is to provide the broadest dissemination possible of information contained in DOE's Research and Development Reports to business, industry, the academic community, and federal, state and local governments.

Although a small portion of this report is not reproducible, it is being made available to expedite the availability of information on the research discussed herein.

ORNL--6508

DE89 008978

PHYSICS DIVISION

PROGRESS REPORT

for Period Ending September 30, 1988

J. B. Ball Director

F. E. Bertrand	Section Head
S. Datz	Section Head
C. M. Jones	Section Head
J. B. McGrory	Section Head
F. Plasil	Section Head
R. L. Robinson	Section Head

Edited by: A. B. Livingston

Date Published: March 1989

OAK RIDGE NATIONAL LABORATORY
Oak Ridge, Tennesee 37831
operated by
MARTIN MARIETTA ENERGY SYSTEMS, INC.
for the
U.S. DEPARTMENT OF ENERGY
under Contract No. DE-AC05-84OR21400

Reports previously issued in this series are as follows:

ORNL 2718	Period Ending March 10, 1959
ORNL-2910	Period Ending February 10, 1960
ORNL-3085	Period Ending February 10, 1961
ORNL-3268	Period Ending January 31, 1962
ORNL-3425	Period Ending May 21, 1963
ORNL-3582	Period Ending January 31, 1964
ORNL-3778	Period Ending December 13, 1964
ORNL-3924	Period Ending December 31, 1965
ORNL-4082	Period Ending December 31, 1966
ORNL-4230	Period Ending December 31, 1967
ORNL-4395	Period Ending December 31, 1968
ORNL-4513	Period Ending December 31, 1969
ORNL-4659	Period Ending December 31, 1970
ORNL-4743	Period Ending December 31, 1971
ORNL-4844	Period Ending December 31, 1972
ORNL-4937	Period Ending December 31, 1973
ORNL-5025	Period Ending December 31, 1974
ORNL-5137	Period Ending December 31, 1975
ORNL-5306	Period Ending June 30, 1977
ORNL-5498	Period Ending December 31, 1978
ORNL-5787	Period Ending June 30, 1981
ORNL-6004	Period Ending September 30, 1983
ORNL-6120	Period Ending September 30, 1984
ORNL-6233	Period Ending September 30, 1985
ORNL-6326	Period Ending September 30, 1986
ORNL-6420	Period Ending September 30, 1987

SPECIAL DEDICATION

This issue of the Physics Division Progress Report is dedicated to the memory of our colleague George Leander, who died during this past year.

Throughout his career, George worked at the forefront of theoretical nuclear structure physics. Despite the shortness of that career, he published over 100 papers. Included in his work were important contributions in the geometrical aspects of nuclei, the shape evolution preceding nuclear fission, exotic shapes in light nuclei, high-spin phenomena in nuclei, the process of fast collective rotation, and the understanding of electromagnetic nuclear decay in regions of high level density.

That George was strongly influenced by the Copenhagen school of philosophy and interpretation of nuclear phenomena is most evident in his last major paper. A detailed treatise on the ideas of spontaneous symmetry breaking in the nuclear intrinsic frame in the context of mirror-asymmetry and its profound consequences in numerous nucleon-nucleus interaction effects, the paper will remain a standard in the field for years to come.

George's enthusiasm in helping guide our programs, his obvious love of science, and his dedication to physics were an inspiration to all of us who were privileged to know him.

CONTENTS

2. EXPERIMENTAL NUCLEAR PHYSICS

NUCLEAR STRUCTURE STUDIES VIA ELASTIC AND INELASTIC SCATTERING

NUCLEAR STRUCTURE STUDIES VIA CHARGE-EXCHANGE REACTIONS

NUCLEAR STRUCTURE STUDIES VIA TRANSFER AND CAPTURE REACTIONS

NUCLEAR STRUCTURE STUDIES VIA COMPOUND NUCLEUS REACTIONS

NUCLEAR STRUCTURE STUDIES VIA RADIOACTIVE DECAY

HEAVY-ION REACTION MECHANISM STUDIES, FUSION AND FISSION

EMISSION OF LIGHT IONS, NEUTRONS, PIONS, AND PHOTONS IN HEAVY-ION REACTIONS

NUCLEAR PHYSICS WITH ULTRARELATIVISTIC PROJECTILES

MISCELLANEOUS TOPICS

INSTRUMENTATION

3. THE UNISOR PROGRAM

4. EXPERIMENTAL ATOMIC PHYSICS

ACCELERATOR-BASED ATOMIC PHYSICS

ULTRARELATIVISTIC HEAVY-ION PHYSICS COLLISIONS

INTERMEDIATE ENERGY PHYSICS

HEAVY-ION REACTIONS

NUCLEAR STRUCTURE

PHYSICS OF (e^+,e^-) SYSTEMS

COMPUTATIONAL PHYSICS

MATHEMATICAL PHYSICS

QUARKS IN NUCLEI

ATOMIC AND MOLECULAR PHYSICS

6. LASER AND ELECTRO-OPTICS LAB

7. HIGH ENERGY PHYSICS

INTRODUCTION

This report covers the research and development activities of the Physics Division for the 1988 fiscal year, beginning October 1, 1987, and ending September 30, 1988. The activities of this Division are concentrated in the areas of experimental nuclear physics, experimental atomic physics, and theoretical nuclear and atomic physics.

Operation of the Holifield Heavy Ion Research Facility as a national user facility continues to represent the single largest activity within the Division. This year saw the completion of the acceleration tube upgrade of the 25-MV tandem electrostatic accelerator and the achievement of record terminal potentials, operation for an experiment with 25 million volts on terminal, and successful tests with beam at 25.5 MV. These and other highlights, including commissioning of the new experimental devices, are summarized in Chapter 1.

The experimental nuclear physics program continues to be dominated by research utilizing heavy ions. These activities, while continuing to center largely on the Holifield Facility, have seen significant growth in the use of facilities that provide intermediate energies (GANIL) and especially ultrarelativistic beams (CERN). Results of this work are presented in Chapter 2.

The UNISOR program, since its inception, has been intimately associated with the Division and, most particularly, with the Holifield Facility. The experimental nuclear structure research of this consortium is included in Chapter 3, along with first reports from the initial operation of the Nuclear-Orientation Facility.

In addition to the Holifield Facility, the Division operates two smaller facilities, the EN Tandem and the ECR Ion Source Facility, as "User Resources." Chapter 4 reports on the operation of these two facilities and the experimental programs in accelerator-based atomic physics, based at the EN Tandem and the Holifield Facility, and the fusion-related atomic physics program based at the ECR Facility.

The efforts in theoretical physics, covering both nuclear and atomic physics, are presented in Chapter 5. Continued efforts on computational aspects of theoretical physics are highlighted and serve as the impetus for a new Division initiative to establish a Center for Computational Physics.

In addition to research with multicharged heavy ions from the ECR source, the effort on atomic physics in support of the controlled fusion program includes a plasma diagnostics development program. The concentration of this program on optical and laser technology is marked by the change in designation to the Laser and Electro-Optics Lab. This work is discussed in Chapter 6.

A small, continuing effort in elementary particle physics, carried out in collaboration with the University of Tennessee, is reported in Chapter 7.

The Division operates two efforts in data compilation and evaluation. The work of the Atomic Physics Data Center and our effort as part of the National Nuclear Data Center are summarized in Chapter 8.

Our proposal for a heavy-ion storage ring for atomic physics (HISTRAP) remains a major new initiative of the accelerator-based atomic physics program and the Division. Continuing efforts on optimizing the ring design and on component prototyping are presented in Chapter 9.

The report concludes with general information on publications, Division activities, and personnel changes.

J. B. Ball
February 1989

1. HOLIFIELD HEAVY ION RESEARCH FACILITY

OVERVIEW

J. A. Martin C. M. Jones
R. L. Robinson

Operation and development of the Holifield facility in this period was characterized by a continuation of the high quality operation achieved in FY 1987, and by exciting developments in both accelerator technology and instrumentation for the experimental program.

Fifty experimental runs were completed in FY 1988 involving 167 participants. Of this group, 44 were graduate students. The institutions represented are summarized in Table 1.1.

The third and final phase of the compressed geometry acceleration tube program was successfully completed; the tandem accelerator has now been completely equipped with acceleration tubes of the improved design. In addition to allowing us to set new voltage records, this improvement

Table 1.1. Distribution of users who participated in research programs at the HOLIFIELD during the twelve-month period between October 1, 1987, and September 30, 1988

Institutions	Number of Researchers
U.S. UNIVERSITIES	
East Carolina University	1
Eastern Kentucky University	1
Edinboro University	1
Furman University	1
Georgia State University	2
Georgia Institute of Technology	4
Hendrix College	1
JIHIR	1
Louisiana State University	1
Mississippi College	2
Mississippi State University	1
Notre Dame	1
ORAU	4
Oregon State University	2
Southern Methodist University	1
Tennessee Technological University	1
Texas A&M University	1
University of Florida	3
University of Iowa	1
University of Kentucky	1
University of Maryland	9
University of Michigan	1
University of North Carolina	1
University of Pennsylvania	4
University of Pittsburgh	4
University of Rochester	3
University of Tennessee	11
University of Tennessee/Chattanooga	1
Vanderbilt University	17
Washington University	6
Washington & Lee University	2
Western Kentucky University	4
Yale University	2
	96
NATIONAL LABORATORIES	
Idaho National Engineering Laboratory	1
Lawrence Berkeley Laboratory	1
Lawrence Livermore National Laboratory	3
Oak Ridge National Laboratory	35
	40
NON-U.S. INSTITUTES	
CEN/Saclay (France)	1
Hindi University (India)	1
Inst. Kernphysik, Frankfurt (Germany)	2
Inst. Kernphysik, Julich (Germany)	1
McMaster University (Canada)	1
Nacional de Energia Atomics (Argentina)	1
Nazionale de Fisica Nucleare (Italy)	1
Research Institute of Physics (Sweden)	1
Niels Bohr Inst. (Denmark)	2
Nuclear Research Center-Negev (Israel)	1
Ruder Boskovic Inst. (Yugoslavia)	2
Bielefeld University (Germany)	1
Univ. of Giessen (Germany)	3
Univ. of Gottingen (Germany)	1
Univ. of Heidelberg (Germany)	3
Univ. of Jyvaskyla (Finland)	2
Univ. of Montreal (Canada)	4
Sao Paulo University (Brazil)	1
	29
OTHER	
Wadsworth Laboratory	1
Webb High School, Knoxville	1
	2
Total	167

has had an immediate impact on operation for the experimental program, allowing us to provide beams which have previously not been available.

Two developments in negative ion source technology are especially notable. The first is development of a high-intensity, plasma-sputter, heavy-negative-ion source suitable for synchrotron injection. The second is development of a new technique which allows the Cs sputter source, used for normal operation of the accelerator, to be used for production of Group IA (Li, Na, K, Rb, Cs) element beams.

Utilization of the facility has been improved in this reporting period by addition of a number of diagnostic elements in ORIC beam lines. These include slits, viewers, and beam profile monitors. With the addition of these elements, it is now possible to adjust and monitor the beam transport system in a systematic way.

The close-packed Ge ball and the Nuclear Orientation Facility were commissioned and used successfully in the experimental program. The HILI, a third new experimental device which became operational late last year, was used for three major experiments during this fiscal year. These three devices considerably increase the capability of the Holifield Facility for the investigation of low-lying-level properties, high-spin states, and reaction mechanisms. The use of these devices for 30% of the research hours during FY 1988 exemplifies their importance.

Two new beam lines, to be used primarily for atomic physics programs, were completed. The merged electron beam system, which was previously used at the ORNL EN tandem accelerator, has been installed on one of these lines.

During the year, difficult and long-lead-time hardware components were developed for HISTRAP, a proposed synchrotron/cooler/storage ring. HISTRAP has a maximum bending power of 2.67 Tm, $ME/Q^2 = 355$, and would serve as an energy booster for the HHIRF tandem in addition to operation in stand-alone mode. A vacuum of 4×10^{-12} Torr has been achieved in a high-vacuum test stand which models 1/16 of the proposed ring-circumference. A prototype dipole magnet has been fabricated and will be evaluated during the coming year. A prototype rf cavity has been fabricated and is being tested. Funding for the HISTRAP is being requested for FY 1991.

ACCELERATOR OPERATIONS AND DEVELOPMENT

OPERATIONS

G. D. Alton, J. A. Biggerstaff, M. R. Dinehart, D. T. Dowling, H. D. Hackler, C. L. Haley, D. L. Haynes, C. A. Irizarry, C. M. Jones, R. C. Juras[1], S. N. Lane, C. T. LeCroy, C. A. Ludemann, C. A. Maples, J. A. Martin, R. L. McPherson, M. J. Meigs[1], G. D. Mills, S. W. Mosko, S. N. Murray, D. K. Olsen, B. K. Sizemore, B. A. Tatum, S. D. Taylor, N. F. Ziegler

Facility operating statistics for the current reporting period, FY 1988, are shown in Tables 1.2 and 1.3. As was expected, hours of beam available for research was reduced, in comparison to FY 1987, due to the installation of compressed geometry acceleration tubes in the tandem accelerator. Unscheduled maintenance continued at the low levels achieved in FY 1987.

A list of beams provided for research in FY 1988 is given in Table 1.4. During this

Table 1.2. Tandem accelerator utilization for the period October 1, 1987, through September 30, 1988

	Hours	Percent
Beam available for research (tandem-alone and coupled operation)	3362	38
Beam available during ORIC tuning (coupled operation)	303	3
Accelerator tuning (includes scheduled startup-shutdown)	494	6
Machine studies (includes conditioning not required for specific experiments)	1307	15
Total operating time	5466	62
Unscheduled maintenance	263	3
Scheduled maintenance	2695	31
Scheduled shutdown	360	4

Table 1.3. Cyclotron utilization for the period October 1, 1987, through September 30, 1988

	Hours	Percent
Beam available for research (coupled operation)	1037	12
Accelerator tuning (includes scheduled startup-shutdown and operation during tandem tuning)	272	3
Machine studies	13	0
Unscheduled maintenance	89	1
Scheduled shutdown and maintenance	7373	85

Table 1.4. Beams provided for research for the period October 1, 1987, through September 30, 1988

Ion Species	Maximum Energy (MeV)	Mode*
^{1}H	25	T
^{12}C	110	T
^{16}O	225	T
^{17}O	377	T,C
^{18}O	90	T
^{19}F	180	T
^{28}Si	701	T,C
^{32}S	230	T
^{34}S	170	T
^{36}S	165	T
^{35}Cl	529	T,C
^{37}Cl	180	T
^{40}Ca	328	T
^{44}Ca	185	T
^{58}Ni	918	T,C
^{64}Ni	170	T

*T = Tandem alone; C = Coupled mode.

period, 16 ion species, ranging in mass from ^{1}H to ^{64}Ni, were provided for research.

Two beams provided for use in the atomic physics research program are especially good examples of the enhanced capabilities which result from the tandem accelerator's improved terminal potential performance. The first, provided at a terminal potential of 23.4 MV, was 327.5 MeV $^{40}Ca^{19+}$. The second, provided at 25.0 MV, was 225.3 MeV $^{16}O^{8+}$. These beams could not have been provided prior to the compressed geometry tube installation.

1. Instrumentation and Controls Division, ORNL.

TANDEM ACCELERATOR

G. D. Alton, R. C. Juras[1]
J. A. Biggerstaff, R. L. McPherson
D. L. Haynes, M. J. Meigs[1]
C. M. Jones, G. D. Mills
N. F. Ziegler

Voltage Performance

The third and final phase of the FY 1986 Accelerator Improvement and Modification (AIM) project which provided for installation of compressed geometry acceleration tubes was completed in November 1987. Following conditioning and tests, the tandem accelerator was returned to service for the experimental program in early January 1988. After two further conditioning periods in May 1988 and September 1988, record terminal potentials were achieved for operation with beam (25.5 MV) and operation for the experimental program (25.0 MV). Further details on this effort are provided in another contribution to this report.

A distribution function of terminal potential versus number of runs is shown in Fig. 1.1. Our

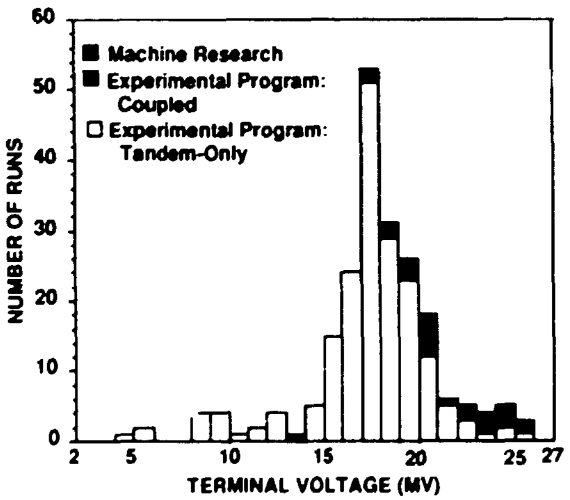

Fig. 1.1. The number of runs in 1-MV-wide intervals is shown as a function of tandem accelerator terminal potential for the period October 1, 1987, through September 30, 1988.

policy of conservative operation continued with only 23 full-column sparks during the period.

Operation

Reliability of the tandem accelerator continued to be excellent. During one period from December 1987 to April 1988, the accelerator was operated for over four months without a tank opening, providing 1741 hours of beam for research with only 30 hours of unscheduled maintenance. In FY 1988, operation for the experimental program was interrupted only once by an unscheduled tank opening.

In addition to operation for the experimental program, the accelerator was used for several "machine research" tasks. These included charge state distribution measurements and foil lifetime measurements in preparation for coupled operation with rare-earth beams and confirmation of the identity of newly developed Group IA element beams. Details of this work are described in other contributions to this report.

Operation of the SF_6 storage and recirculation system continued to be without incident. SF_6 inventory losses for the year were about 1.5%.

Improvements and Modifications

During the extended maintenance period required for installation of the compressed geometry acceleration tubes, a number of other tasks were accomplished. These included careful inspection and testing of the column structure, inspection and cleaning of the charging chains, installation of new corona points (with improved brackets), installation of new shorting rod contacts, installation of new large-diameter einzel lenses in the injector, careful realignment of ion optic components in the injector and injection beam line, and extensive modification of injector deck wiring and controls (to improve access and maintainability). Also during this maintenance period, a new corona point alignment technique was implemented. In this technique, a current-regulated high-voltage power supply is used to adjust the gaps. For a fixed current (typically 20 μA), the gaps can be aligned to a voltage tolerance of ±10%; a lower value than was achievable with the previously used mechanical adjustment technique.

Control system improvements in this period included integration of beam line 41 controls and a revision of the operating system software.

Ion Source Development

In collaboration with staff members from the National Laboratory for High Energy Physics of Japan (KEK), a new high-intensity, pulsed-mode, plasma-sputter heavy-negative-ion source has been developed. Providing multi-mA peak intensity heavy negative ion beams, this source appears to be especially well suited for synchrotron injection applications.

A new technique for the generation of useful atomic negative ion beam intensities of the Group IA elements (Li, Na, K, Rb, Cs) using a standard Cs sputter source has been developed.

Descriptions of the high-intensity pulsed negative ion source and the technique for generating atomic negative ion beams from the Group IA elements are given in other contributions to this report.

Failures of Interest

After nine years of faithful service (40,600 hours of operation), chain number three of chain set number 2 failed. After review, it was decided to continue operation; only 30 minutes of beam time were lost. During the next scheduled tank opening, it was determined that the failure occurred due to a rivet that had worked loose; there was no significant damage to the column. The broken chain was replaced with a used chain from chain set number 1 which had been removed in 1984.

As a result of a broken hose, water collected in one of the coils of the energy analyzing magnet. Due to current leakage through the wet insulation, the field of the magnet became too erratic to be usable. Our solution to this problem was to heat the coil to a temperature of about 205°F with circulating hot water (provided by a pump and modified home water heater) for two periods totaling approximately 24 days.[2] At the end of the second period, the magnet was vastly improved. The erratic behavior was gone, but the magnet exhibited a small drift in field for a short period whenever the magnet current was changed. After a month of operation, the drift in field following a current change was almost non-existent.

---

1. Instrumentation and Controls Division, ORNL.
2. With appropriate scheduling, virtually no time was lost from the experimental program.

ORIC ACCELERATOR

D. T. Dowling J. A. Martin
S. N. Lane S. W. Mosko
C. A. Ludemann D. K. Olsen
B. A. Tatum

During the period of this report, there were 12 separate beam tunings for 11 experiments with coupled operation of the cyclotron and tandem accelerators. There was no stand-alone operation of the cyclotron using the internal ion source. The internal ion source was decommissioned in mid-year. The ion source console controls will be removed to provide space for the new beam line vacuum monitoring and control system.

Coupled operation beam time available for research was 1037 hours. Operating efficiency expressed as the ratio of beam time for research to total scheduled hours was 73.5% (71.6% in FY 1987). Expressed as percent of total scheduled hours, beam tuning was 19.2% (21.0% in FY 1987), and unscheduled maintenance totaled 6.3% (5.9% in FY 1987). In FY 1988, tuning time included 48 hours of operator training.

An ORIC performance summary is given in Table 1.5. Beam extraction efficiency averaged 68% with the beam buncher in use. Beam energies were typically provided within an accuracy of ±0.5%.

Cyclotron Setup and Tuning

Most ORIC tuning parameters were either fixed, or tuned close to the predicted values from the setup calculations. This success allowed the many beams listed in Table 1.5 to be quickly tuned through the ORIC. This year, ORIC setup was further simplified by full implementation of the software for strength and balance controls to tune the inside and outside coil currents of the lower extraction channel. The balance control tunes these currents so that the first harmonic balance of ORIC is varied while the lower channel strength is fixed. The strength control tunes the lower channel currents so that the lower channel strength is varied while the first harmonic balance is fixed. These controls provide more predictable

Table 1.5. Coupled operation for research for the period October 1, 1987 - September 30, 1988

Date	Ion	Desired Energy (MeV)	Measured Energy (MeV)	Error (%)	Extraction Efficiency (%)	Injected Ion	Injection Energy (MeV)	Tandem Voltage (MV)
1/05/88	$^{58}Ni^{+22}$	638	635.6	- 0.38	76	$^{58}Ni^{+8}$	168.9	18.7
1/14/88	$^{35}Cl^{+14}$	525	528.8	+ 0.72	47(1)	$^{35}Cl^{+6}$	125.2	17.8
1/21/88	$^{58}Ni^{+23}$	900	895.2	- 0.53	77	$^{58}Ni^{+9}$	180.0	17.9
2/03/88	$^{17}O^{+8}$	375	376.2	+ 0.32	80	$^{17}O^{+3}$	77.2	19.2
3/16/88	$^{28}Si^{+14}$	700	701.2	+ 0.17	69	$^{28}Si^{+5}$	116.4	19.3
3/26/88	$^{17}O^{+8}$	375	374.6	- 0.11	40(1)	$^{17}O^{+3}$	74.9	18.6
6/08/88	$^{58}Ni^{+23}$	852	850.3	- 0.20	69	$^{58}Ni^{+9}$	200.3	20.0
6/15/88	$^{58}Ni^{+20}$	540	540.7	+ 0.13	62	$^{58}Ni^{+6}$	138.4	19.7
7/06/88	$^{17}O^{+8}$	375	376.9	+ 0.51	68	$^{17}O^{+3}$	80.5	20.1
7/14/88	$^{58}Ni^{+23}$	912	918.5	+ 0.71	51	$^{58}Ni^{+9}$	200.3	20.0
7/22/88	$^{17}O^{+8}$	375	376.2	+ 0.32	76	$^{17}O^{+3}$	80.6	20.1
9/30/88	$^{58}Ni^{+22}$	638	637.8	+ 0.03	55	$^{58}Ni^{+8}$	189.9	21.1

NOTE: (1) Buncher off.

and staightforward ORIC setup and beam extraction.

In addition, the ORIC tuning procedure was updated and expanded. The new procedure is a straightforward guide for tuning the injection beam line from the tandem accelerator, injection into ORIC, acceleration within the cyclotron, beam extraction, and transport of the beam to and through the analyzing magnet for beam energy measurements. This procedure has formed the basis for operator training classes on ORIC operation.

Control Systems

Control Computer. Software was completed for the strength and balance controls of the extraction system, and the new deflector power supply. These controls were brought into routine operation. The 153° BAM entrance and exit slits were calibrated and a new high resolution reference for this magnet's power supply was installed. These controls were placed on the computer as well. The capability for down loading ORIC setup parameters from the tandem control and supervisory computer was developed and automatic periodic logging of operating parameters was accomplished.

Beam Line Vacuum Control System. Design of a new beam line vacuum control system was completed and installation was begun. The primary components of the system are an industrial programmable logic controller (PLC) and numerous digital vacuum gauge controllers (DGCs)[1]

Beam lines are divided into "sectors" which typically consist of one pumping station (pump and pump valve), two Convectron[1] gauges (one on either side of the pump valve), a nude ionization gauge, and a beam line valve at each end of the sector. Each DGC interfaces with the three gauges in a sector. Pressure and gauge status information is transmitted to the PLC via a RS-232 link. Valves are interfaced to the PLC which uses DGC information to provide setpoint protection for ORIC and pumping stations in the event of a leak. Additionally, the PLC interlocks the valves to prevent opening a sector to air pressure.

Operator interaction with the system is provided by a color CRT and membrane control panel attached to a personal computer, all located in the ORIC control room. Graphics pages may be selected from the keyboard to display pressures and valve status for each sector, and to display alarms. Operators may open and close beam line and pump valves, and turn on, off, or degas ionization gauges from the same keyboard. Operator interface is provided at remote stations by DGCs, and toggle switches and LEDs interfaced to the PLC.

Several DGCs, gauges, and some additional cables were installed, graphics pages completed, and control software begun. Plans were made to upgrade the ORIC control console to provide room for the new system.

Cyclotron Development

Cyclotron Ion Source. The internal ion source for the cyclotron was decommissioned. All future cyclotron operation will require beam injection from the tandem accelerator. The most recent operation of the internal ion source was in 1984. Elimination of the source is a key factor in permitting the integration of the cyclotron radiation safety system with the HHIRF system. Removal of ion source controls from the cyclotron control console will provide space for the new beam line vacuum controls and instrumentation which will be installed during FY 1989.

Beam Extraction System. The coaxial magnetic channel which developed a water leak during the summer of 1987 was repaired. The leak was found to be in a solder joint on one of the power leads. The coaxial channel was leak checked after the repair and no other leaks were found. The ORIC once again has a spare coaxial channel ready for use.

Fabrication of the new lower channel continued periodically during the year. Work progressed to the point of being able to pressure check the channel's coils and water headers. Some of the expected problems with nylon insulator O-ring seals were encountered. These problems were solved by fabricating new insulators with tighter tolerances on the O-ring grooves and exercising great care during assembly so as not to cut the O-rings.

Power Supplies. The power supply upgrade program for replacement or improvement of obsolete or unreliable power supplies continues. The electrostatic deflector power supply was replaced with a new compact unit which was installed near the deflector terminal. Consequently, a 35-meter run of coaxial cable, which connected the former power supply to the deflector, has been eliminated. The new supply features current limiting, low energy storage, and remote voltage programming. Since the stored energy available for dissipation in deflector sparking has been substantially reduced, the power supply high-voltage output has been directly connected to the deflector without current-limiting resistors. Deflector performance is much improved through improved voltage regulation, reliable voltage information, reduced sparking, and reduced current drain.

A replacement power supply for the compensated magnetic channel of the beam extraction system was specified and ordered during FY 1987. Contrary to the vendor's delivery schedule, we are still waiting for the power supply. The latest information from the vendor, combined with observations made on inspection visits, suggests that delivery is likely during the early part of FY 1989.

Filter capacitors containing PCB were replaced in several power supplies. Some difficulties in matching circuit configuration occurred in the rf system anode power supply. The troublesome units were replaced by the vendor, and the anode power supply is on line and operating. It is believed that all significant PCB-containing components have been removed from the cyclotron and its peripheral equipment.

Trimming Coil Status. During the past year, the cyclotron encountered another trimming coil loss. A small, but inaccessible, water leak occurred in one sector of trim coil #8. After completion of a coil assembly drying operation, a coolant and electrical bypass connection was arranged on the faulty coil sector on the "West Trim Coil Assembly." A similar bypass was implemented on the "East Trim Coil Assembly" to retain symmetry. The remaining 2/3 of trim coil #8 is sufficient to maintain beam isochronism in the cyclotron. Recalling that trim coil #10 was totally lost in a previous incident, we are making contingency plans for possible future problems with the trim coil assembly.

Trimming coil sets were retrieved from the NRL cyclotron when it was decommissioned a few years ago. It is believed that all but one coil in these sets are operable. These coil sets are identical to those in the ORIC cyclotron, and they may be used as a direct substitution. Further evaluation and preparation is under way.

Cyclotron Vacuum System. A surplus forepump system containing a 150-cfm rotary-piston pump and a Roots blower was obtained from one of the experimental groups. This pump has been reconditioned and installed in place of the last of the World War II vintage 300-cfm rotary pumps which had been in service on the cyclotron for over 25 years. The blower will improve pumping performance in the pressure region just above that where diffusion pumps can go on line.

Environmental Compliance. Environmental compliance problems continue to impact cyclotron operation resources. Solutions have been implemented which will assure compliance with minimal future cost. Most recently, the oil reclamation system for mechanical vacuum pumps was decommissioned. Now that the oldest of our mechanical pumps is retired, our oil consumption is greatly reduced. The newer pumps are able to eliminate volatile contaminants from their oil without separate reclaiming equipment. It will be necessary to replace oil occasionally, but storage of large quantities of oil on site is no longer necessary.

Beam Line Improvements

Diagnostics Systems. The addition of new diagnostics for ORIC beam lines continued during the past year. A new beam viewer was installed at the exit of beam switching magnet BSM-4 for focusing of beams going to the 1.6-meter scattering chamber. The viewer is located just

25 cm downstream of the exit pole face of the magnet. Due to space limitations on the exit side of the magnet, the viewer is mounted inside the magnet vacuum chamber. The viewer actuator is mounted between the magnet pole faces and extends from the back to the front of the chamber and couples to a feedthrough on the magnet chamber face plate. Viewer performance and spot visibility was checked during a recent spin spectrometer experiment.

A set of motorized, remote controlled slits were installed downstream of the 153° beam analyzing magnet. These slits can be controlled either from the ORIC control room or from a control station located close to the slits. The actual slit opening is displayed on the ORIC control console. This allows more precise and varied slit settings according to the experimenter's needs without having to go into the ORIC vault.

Other beam diagnostics installed in the past year consist of a number of beam profile monitors (BPMs). The new BPMs were installed on the ORIC injection line, in front of the spin spectrometer, between the 1.6-meter scattering chamber and UNISOR, on beam line 31 just before viewer 31-4, and on beam line 3 just before the exit slits of the 153° beam analyzing magnet. These BPMs have helped the ORIC operators in tuning beams and monitoring stability.

Vacuum Systems. The upgrade of ORIC beam lines continued in the past year. Limited funds necessitated careful selection of activities to pursue. It was decided to replace one of the original diffusion pump stations which required increased maintenance and provided only marginal performance. The new pump station is a 330 ℓ/s turbomolecular pump unit. This unit is located between beam switching magnet BSM-1 and the 153° beam analyzing magnet. This beam line now has an operating pressure of approximately 3×10^{-7} Torr.

---

1. Manufactured by Granville-Phillips Co., Boulder, Colorado.

IMPROVED VOLTAGE PERFORMANCE OF THE OAK RIDGE 25URC TANDEM ACCELERATOR[1]

D. L. Haynes M. J. Meigs[2]
C. M. Jones J. E. Raatz[3]
R. C. Juras[2] R. D. Rathmell[3]
N. F. Ziegler

Installation of compressed geometry acceleration tubes and associated changes in the corona voltage grading system have resulted in significant improvement in voltage performance of the tandem accelerator. Details of the final phase of this work and initial tests on the modified accelerator are summarized in this section.

Compressed Geometry Acceleration Tubes

One of the principal changes in the present voltage improvement program was replacement of the original acceleration tubes with tubes of a compressed geometry design. In this design, which utilizes a modified NEC high-gradient 17-cm-long tube section, the 3-cm-thick heatable aperture assembly, provided as part of the original installation, is replaced with an aperture assembly of essentially zero length. With this change, seven tube sections can be installed in the space previously occupied by six, thus increasing the effective insulator length per unit column length by a factor of 7/6 = 1.17. Tests on a compressed geometry configuration, similar to that described in this report, were first reported by Assman et al.[4] A subsequent test, using a column structure more closely resembling the 25URC column, was reported by Raatz et al.[5]

The installation and tests described in this report represent the last of three phases of the tube replacement program for the 25URC accelerator. In the first phase, two tube units,[6] 26 and 27, were replaced with compressed geometry tubes in June 1986 and tested in the interval July 1986 to October 1986.[7] In the second phase, units 19-25 were replaced with compressed geometry tubes in November 1986 and tested in the interval November 1986 to March 1987.[8] In the present phase, the remaining 18 units were replaced. Detailed discussions of the results of the first and second phases, as well as details of the compressed geometry acceleration tube design and installation, have been provided in Refs. 7 and 8. In the final installation, the 30° vee-shaped aperture discussed in Ref. 8 was used in all but units 19-22. In these units, conventional, straight, 1-mm-thick apertures were used.

Voltage Grading

In order to compensate for the increased number of insulating gaps in the acceleration tube, it was necessary to decrease the point-to-plane spacing of the tube corona points from 4.4 mm to 3.3 mm. This was accomplished by fabrication and installation of new corona point assemblies with points of increased length. Corona point assemblies for both the acceleration tubes and column were mounted using holders of a new design.[9] As expected, these holders have proved more reliable than the original holders.

As noted by Weisser,[10] mechanical adjustment of corona points is not adequate to achieve good voltage homogenity. To alleviate this problem, the corona points used for the present tests were adjusted electrically in air using a current-regulated power supply to measure the voltage required to produce a constant test current, typically 20 μA, for each gap. Using this technique, it was possible to adjust the corona point spacings so that the gap voltages varied by less than ±10%.

Column Preparation and Acceleration Tube Installation

Previous measurements,[8,11] on the longitudinal voltage gradient and radial voltage capabilities of the column strongly suggest that the column is not a limiting factor in voltage performance. However, to help insure that this would continue to be the case, we carefully inspected and cleaned the column prior to installation of the compressed geometry acceleration tubes. The first step in this process was removal of the acceleration tubes, the Pelletron chains, and column corona points. Each column post insulating gap was then cleaned by blowing with compressed, dry N_2 and visually inspected. As a result of this visual inspection, approximately 15 of 8,262 gaps were subsequently cleaned with ethanol and Q-tips. The resistance and spark gap breakdown voltage of each column plane (16 column post gaps + 1 corona point support post gap) were then measured. No significant problems were noted as a result of these inspections and tests. We specifically found no indications of the column post structural problems noted by Brinkley et al.[12] As the final step in this work, the column was carefully cleaned and the tightness of column rings and transverse interconnecting elements was checked.

As noted in Ref. 8, the upper one-third of the accelerator, units 19-27, had previously been equipped with compressed geometry acceleration tubes. The tubes in units 19-25 had been in service since November 1986 and in the present phase were only removed, stored on site, and replaced. The tubes in units 26+27 were installed in June 1987 as part of an auxiliary (unsuccessful) test of surface finish technique. These tubes were replaced along with those from units 1-18.

As indicated in Ref. 8, the compressed geometry tubes were, with noted exceptions, to be assembled from previously used tube sections. Thus the tube sections removed from units 1-18 and 26+27 were returned to the NEC plant where they were visually inspected, modified, and fitted with new insert electrodes. In contrast to the tube sections previously used to assemble compressed geometry tubes, these tube sections were not sandblasted. After installation, the tubes were baked at an average temperature of about 100°C for approximately 24 hours while pumping with the major dead section and terminal sputter ion pumps. In the previous installations of compressed geometry tubes,[7,8] the tubes were not baked.

Conditioning and Testing

Conditioning of the accelerator following completion of the installation of the compressed geometry tubes in November 1987 was performed in three major phases. The first phase, which had as its primary goal return of the accelerator to service for the experimental program, ended in early January 1988. Several observations during this first period are of interest. First, the tubes in units 19-25 conditioned more easily and more rapidly than those in units 1-18 and 26+27. Thus, the removal, disassembly, storage, and installation of the used tubes did not cause them to completely revert to the behavior of tubes with new insert electrodes and apertures. The tubes in units 19-25 also exhibited "classic" pulsed X-ray conditioning while the newly assembled tubes in units 1-18 and 27+27 exhibited virtually no pulsed X-ray conditioning. When compared on the basis of achieved stable voltage as a function of time or number of sparks, the conditioning behavior of the tubes in units 1-18 and 26+27 was comparable to the initial conditioning of the tubes previously installed in units 19-27.[8] It thus appears that there are no significant differences in conditioning behavior which may be associated with baking at ~100°C for 24 hours or with sandblasting of the ceramic.

Following a period of operation for the experimental program at terminal potentials up to 20 MV, the accelerator was conditioned for a second period of 18 days in April/May 1988. At the end of this period, the tubes in units 19-25 had been (easily) conditioned to a stable gradient of 1.0 MV/unit, while the tubes in units 1-18 and 26+27 had been conditioned to an average stable gradient of 0.95 MV/unit. At the end of the period, stable operation of the accelerator, with beam, was demonstrated at 24.0 MV (for one hour, without sparks or tics).

Following a second period of operation for the experimental program at terminal potentials up to 23.4 MV, the accelerator was conditioned for a third period of 18 days in August/September 1988. At the end of this period, pairs of units and individual units had been conditioned to an average stable gradient of approximately 1.04 MV/unit, and stable operation of the accelerator with beam was demonstrated at 25.5 MV (for one hour without sparks or tics). A few days after completion of these tests, the accelerator was operated for use in the experimental program at a terminal potential of 25.0 MV.

Discussion

From an operational viewpoint, installation of compressed geometry acceleration tubes and the associated changes in the column and the tube voltage grading systems has been a success. The maximum demonstrated stable voltage with beam has increased from 23.5 MV to 25.5 MV and the maximum terminal potential used in an experiment has increased from 22.0 MV to 25.0 MV. In a more general sense, the improved terminal potential performance of the accelerator has had an immediate positive effect on our experimental program, allowing us to provide beams of higher energy and intensity.

We wish to emphasize that we believe that the results reported here are preliminary in the sense that the ultimate terminal potential capability of the accelerator has not been reached. Specifically, our experience with conventional tubes has been that voltage performance continues to improve over a period of several years with use and conditioning. It also appears that adequate tube grading currents may not be provided with the present corona points. We hope to rectify this problem in the near future. Finally, we do not believe that we have a complete understanding of how tank gas pressure should be adjusted for operation above 22 MV. We expect our understanding of this question to improve as we routinely operate the accelerator at higher potentials.

In summary, installation of compressed geometry acceleration tubes and associated changes in the corona voltage grading system have resulted in significant improvement in voltage performance of the 25URC accelerator. Further improvements, resulting from detailed changes in the corona voltage grading system and increased operating experience, are expected in the future.

---

1. Summary of a paper submitted for publication in Nuclear Instruments and Methods in Physics Research.
2. Instrumentation and Controls Division, ORNL.

3. National Electrostatics Corporation, Middleton, Wisconsin.
4. W. Assmann, G. Korschinek, and H. Münzer, Nucl. Instr. and Meth. 220 (1984) 86.
5. J. E. Raatz, R. D. Rathmell, P. H. Stelson, and N. F. Ziegler, Nucl. Instr. and Meth. **A224** (1986) 104.
6. The configuration of the 25URC accelerator is based on 27 61-cm-long live modules or "units" separated by two major and three minor dead sections. Proceeding from bottom to top, the units are grouped in the following way: 1-4, 5-9, 10-13, 14-18, 19-22, 23-27.
7. C. M. Jones, K. A. Erb, D. L. Haynes, J. T. Mitchell, N. F. Ziegler, J. E. Raatz, and R. D. Rathmell, Proc. 1986 Symp. Northeastern Accelerator Personnel, Notre Dame, Indiana (November 1986) p. 65.
8. C. M. Jones, K. A. Erb, D. L. Haynes, J. T. Mitchell, N. F. Ziegler, J. E. Raatz, and R. D. Rathmell, Nucl. Instr. and Meth. **A268** (1988) 361.
9. N. F. Ziegler, G. D. Mills, M. J. Meigs, R. L. McPherson, R. C. Juras, C. M. Jones, D. L. Haynes, and G. D. Alton, Proc. 1987 Symp. Northeastern Accelerator Personnel, Tallahassee, Florida (September 1987) p. 5.
10. D. C. Weisser, Nucl. Instr. and Meth. **A268** (1988) 419.
11. C. M. Jones, Proc. Third Int. Conf. on Electrostatic Accelerator Technology, Oak Ridge, Tennessee (April 1981) p. 23.
12. T. A. Brinkely, G. P. Clarkson, M. D. Malev, T. R. Ophel, R. B. Turkentine, and D. C. Weisser, Nucl. Instr. and Meth. **A244** (1986) 89.

A HIGH-INTENSITY PLASMA-SPUTTER HEAVY-NEGATIVE-ION SOURCE[1]

G. D. Alton Y. Mori[2]
A. Takagi[2] A. Ueno[2]
S. Fukumoto[2]

In recent years, the synchrotron has been used or considered for use for acceleration and storage of heavy ion beams for use in high-energy atomic and nuclear physics research. Facilities predicated on this principle have been constructed, or are being constructed, around the world. Other facilities, such as the Heavy Ion Storage Ring for Atomic Physics (HISTRAP) at the Oak Ridge National Laboratory (ORNL) have been proposed. If funded, the Holifield Heavy Ion Research Facility (HHIRF) tandem accelerator would serve as one of the injectors. For this type of heavy ion accelerator, high-intensity pulsed beams of widths 50-300 μs, at repetition rates of 1-50 Hz, of a wide spectrum of elements are required. The low-duty-factor injection requirements of the synchrotron (typically 10^{-3}) place a premium on ion sources with high-intensity capabilities. The specific needs of the proposed tandem accelerator injection of HISTRAP for a high-brightness negative ion source with a wide range of species capabilities was the primary motivating factor which led to the present developments.

Negative ion beam intensities of ≈200 μA (peak intensity) represent a practical requirement of the ion source when the tandem accelerator is used as an injector for the synchrotron. Intensity levels of this magnitude are achievable for a limited number of relatively high electron affinity atomic and molecular species in negative ion sources based on the cesium ion sputter generation principle (see e.g., Refs. 3-5). Such intensity levels are marginally adequate at the point of injection into the synchrotron due to charge-state fractionation during the stripping process, and beam transmission losses in the tandem accelerator and beam transport system. Increased beam intensities of a wide spectrum of negative ion species, at least to the level that the tandem accelerator becomes the limiting factor, are therefore desirable.

The multi-cusp magnetic field plasma surface source, routinely employed for the production of high-intensity pulsed H^- beams at the Los Alamos National Laboratory (LANL)[6] and at the National Laboratory for High Energy Physics,[7] has recently been modified for use as a high-intensity pulsed pulsed-mode heavy-negative-ion source.[1] The design details, operational parameters, and performance characteristics for H^- generation have been reported previously (see e.g., Refs. 6 and 7), while those for heavy ion generation have been described in Ref. 1. The source, modified for heavy negative ion generation, and the experimental set-up used during evaluation of the source, are shown schematically in Fig. 1.2.

For heavy-negative-ion generation, a high-density plasma discharge, seeded with cesium vapor, is produced by pulsing the discharge voltage of two series-connected LaB_6 cathodes maintained at ~1450°C. For this application, the negatively biased spherical geometry probe

ORNL-DWG 88-7161R

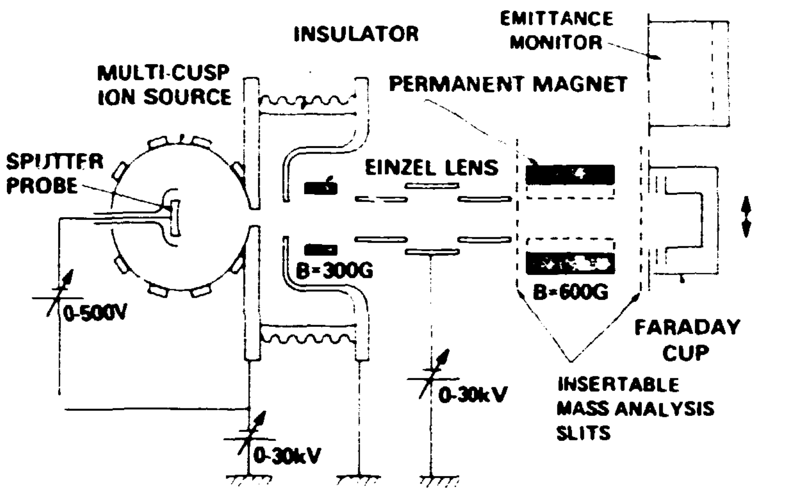

Fig. 1.2. Schematic drawing of the plasma sputter negative ion source, experimental apparatus and emittance measurement device used to evaluate the source for heavy negative ion beam generation. The dotted lines show the positions of the slit apertures and alterations to the permanent magnet used to determine the mass distribution within a particular ion beam.

(converter) is made of the material of interest and, as such, is the consumable item. That is, negative ions are formed by plasma discharge sputtering of the probe itself. In order to produce higher heavy-negative-ion beam intensities by sputter ejection at a given probe voltage, a chemically inert, heavy discharge support gas such as Ar, Kr, or Xe, is utilized. Xe was used throughout the present measurements. Cesium is introduced into the discharge from an external cesium oven operated typically at a temperature of ~214°C. The sheath surrounding the negatively biased sputter probe (spherical radius ρ = 140 mm and diameter ϕ ~ 30 mm) which is maintained at a negative voltage relative to housing (typically ≤ 1000 V) serves as the first acceleration gap and lens for focusing the ion beam through the exit aperture (diameter ϕ = 18 mm). Under pulsed-mode operation at the low duty factors utilized, (typically 2×10^{-3}), the LaB_6 cathodes exhibit very little erosion after many hours of operation. With the combined long lifetimes of the sputter probe, LaB_6 cathodes, and low cesium consumption rate (~<1 mg/h), the source can operate stably for a few thousand hours at constant peak beam intensity levels without maintenance or cleaning.

An example of an intensity versus time distribution of an ion beam extracted from a Pt probe is shown in Fig. 1.3; the measurements were made at optimum or near optimum cesium flow rate, Xe discharge pressure, and at fixed sputter probe voltage. Table 1.6 provides a partial list of total negative ion beam intensities, species, and probe materials utilized during operation of the source. Also given are the approximate mass distributions of the principal negative ion species present in the total negative ion beam.

ORNL PHOTO-7429-88

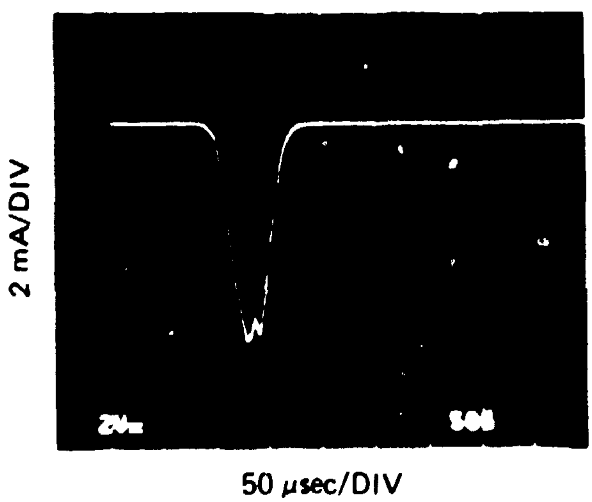

Fig. 1.3. Intensity versus time distribution of the total ion current extracted from a Pt sputter probe at a voltage of -1000 V and optimum cesium flow rate. Vertical axis: 2 mA/division. Horizontal axis: 50 μs/division.

Table 1.6. A partial list of total heavy negative ion beam intensities (peak) from the high-brightness plasma sputter negative ion source.

Sputter Probe Material	Sputter Probe Voltage (V)	Geometry	Total Peak Beam Intensity (mA)	Species (%)
Ag	937	Spherical	6.2	Ag^-(91)
Au	437	Spherical	10.3	Au^-(73)
Bi	937	Spherical	2.7	Bi^-(6); O^-(42)
C	937	Spherical	6.0	C^-(36); C_2^-(58)
Co	937	Spherical	6.0	Co^-(85)
Cu	438	Spherical	8.2	Cu^-(77)
CuO	438	Flat	4.5	Cu^-(40); O^-(60)
GaAs	937	Flat	3.7	As^-(20); As_2(52)
GaP	937	Flat	1.8	P^-(44)
Mo	438	Spherical	30.0	O^-(67)
Ni	438	Spherical	6.0	Ni^-(87)
Pd	937	Spherical	7.6	Pd^-(69)
Pt	937	Spherical	8.1	Pt^-(71)
Si	937	Spherical	6.0	Si^-(75)
Sn	937	Spherical	3.6	Sn^-(67)

Emittance measurements were made of negative ion beams extracted from Au and Ni sputter probes for intensity levels of 1 and 4 mA (Au), and 2.5 and 6 mA (Ni), by use of the stepping motor-driven emittance detector unit shown schematically in Fig. 1.2. The emittances from each of the probes were found to increase with beam intensity as expected, based on the presence of space charge. The normalized emittances were found to have typical values at the 80% contour level of $\epsilon_n \leq \approx \sim 25\pi$ mm.mrad (MeV)$^{1/2}$. This value is only ~1.5 times those of cesium sputter negative ion sources when operat in pulsed mode.[8] Yet, the beam intensities from this source are often 30 to 100 times, or more, greater than the cesium sputter negative ion sources described in Refs. 3-5.

The measured emittance values compare favorably with the calculated acceptance of the ORNL 25URC tandem accelerator[9] and, in principle, ion beams from this source should be transportable through such devices. However, consideration must be given in designing the ion extraction, postacceleration, and low-energy transport systems of the source and tandem injector in order to reduce space charge distortion of the emittances of the ion beams. The source is well suited for use in conjunction with the tandem electrostatic accelerator as a synchrotron injector. The source holds the interesting prospect for use in producing dc, mA intensities of a wide range of species, including the commonly used semiconducting material dopants (e.g., B^-, P^-, As^-, and Sb^-), as well as O^-, for high-energy isolation barrier formation.

1. G. D. Alton, Y. Mori, A. Takagi, A. Ueno, and S. Fukumoto, Nucl. Instr. and Meth. **A270** (1988) 194.
2. National Laboratory for High Energy Physics, 1-1 Oho-machi, Tsukuba-gun, Ibaraki-ken, 305 Japan.
3. R. Middleton, Nucl. Instr. and Meth. **214** (1983) 139.
4. G. D. Alton, Nucl. Instr. and Meth. **A244** (1986) 133.
5. G. D. Alton and G. D. Mills, IEEE Trans. Nucl. Sci. **NS-32** (5) (1985) 1822.
6. R. L. York and R. R. Stevens, Proc. of 3rd Int. Conf. on Production of Negative Ions and Beams, edited by Krystof Prelec (Am. Inst. of Phys. Conf. Proc. No. 111, New York, 1984) 410.
7. Y. Mori, A. Takagi, K. Ikegami, and S. Fukumoto, Proc. of 4th Int. Conf. on Production and Neutralization of Negative Ions and Beams, edited by James G. Alessi (Am. Inst. of Phys. Conf. Proc. No. 158, New York, 1987) 378.
8. G. D. Alton, Phys. Div. Prog. Rep., Sept. 30, 1987, ORNL-6420, p. 222.
9. J. D. Larson and C. M. Jones, Nucl. Instr. and Meth. 140 (1977) 489.

A TECHNIQUE FOR GENERATING ATOMIC NEGATIVE ION BEAMS OF THE GROUP IA ELEMENTS

G. D. Alton G. D. Mills

The Group IA elements constitute ~8% of the elements which are considered viable candidates for use in tandem electrostatic accelerator research programs, and the ability to form them by the sputter technique would allow a common source to be used for the generation of useful beam intensities of almost every chemically active element in the periodic chart. The development of a method based on the use of standard sputter-type negative ion sources is therefore highly desirable. Such sources are versatile, have long lifetimes, and are easy to operate.

In the past, efforts to produce useful negative ion beams by sputtering Group IA elements, e.g., Li metal, have been unsuccessful. In the course of such experiments, it was discovered that Li^- ion beams can be produced by bleeding O_2 over Li metal samples during the sputtering process. Even though some successes have been achieved by use of this method, this technique has generally proved to be erratic and undependable. In addition, the physio-chemical properties of Li metal make sample preparation and handling difficult. The properties of the other members of the group, with the possible exception of Na, preclude their use as sputter probes in elemental form.

The present developments were prompted by sputter source experiments with Li/Cu alloys in 50%/50% atomic proportions. The results of these experiments proved to be disappointing, yielding Li^- beam intensities of only a few nA. However, after exposing the Li/Cu samples to dry air for extended periods of time (several months) and thus conversion from Li/Cu to Li_2O/Cu, Li^- negative ion beams [illegible]om t[illegible] same sputter probes grew to more than 2 μA at a sputter probe voltage $\leq$3 kV. The results obtained from the Li_2O/Cu samples suggested the formation of sputter probes from mixtures of Li_2O and Cu or Ag powder. (In fact, Brand, in independent developments, has used this technique to form Li_2O + Ag powder sputter probes for use in a standard sputter negative ion source which are reported to yield a few μA of Li^-.)[1] However, the oxides of the more chemically active members of the group (Kb, Rb, and Cs) are highly deliquescent, a property which presents problems during probe formation and storage. In the belief that the Group IA carbonates would be somewhat less hygroscopic (Li_2CO_3 and Na_2CO_3) and deliquescent (K_2CO_3, Rb_2CO_3 and Cs_2CO_3) and thus easier to form into sputter samples and store, mixtures of the Group IA element carbonates and ~10% (atomic) Cu powder were pressed at 3.4×10^3 bars into pellets of diameter ϕ = 6 mm and thickness t = 4 mm for use in the ORNL cylindrical ionizer geometry source.[2,3]

The sputter probes were evaluated using the Ion Source Preparation Facility, which is equipped with provisions for mass analysis.[4] Figure 1.4 provides examples of the dependence of mass analyzed negative ion yield on sputter probe voltage. A list of mass analyzed beam intensities realized from each of the Group IA elements is displayed in Table 1.7. These results were subsequently further confirmed by accelerating each of the beams to the terminal of the 25URC tandem accelerator and performing charge-state analysis. The lifetimes of the

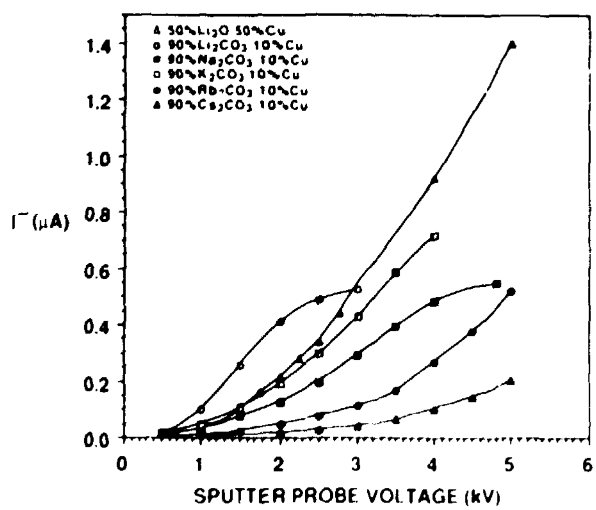

Fig. 1.4. Examples of Group IA element negative ion beam intensity versus sputter probe voltage: Source: Cylindrical geometry ionizer.

Table 1.7. Typical Group IA element atomic negative ion beam intensities produced by sputtering Group IA element carbonates

Sputter Probe	Sputter Probe Voltage (kV)	Species	Intensity (μA)
Li_2CO_3	≤ 3	Li^-	≥ 0.5
Na_2CO_3	≤ 3	Na^-	≥ 0.5
K_2CO_3	≤ 3	K^-	≥ 0.5
Rb_2CO_3	≤ 3	Rb^-	≥ 0.5
Cs_2CO_3	≤ 3	Cs^-	≥ 0.2

carbonate probes were limited by sputter erosion. Experience to date indicates that the lifetimes of the probes decrease as the mass of the Group IA element increases and range from >40 hours for Li_2O_3 probes to ~4-6 hours for Cs_2CO_3 probes.

The application of the technique described above enables the formation of atomic negative ion beams from all of the Group IA elements at intensity levels useful in tandem electrostatic accelerator research programs. This development thus adds ~8% to the inventory of species that can be produced in conventional sputter-type negative ion sources. The requirement that these materials be in compound form for production as atomic negative ion species suggests the possibility of a molecular dissociation formation mechanism rather than a surface ionization mechanism which occurs during sputtering of metal surfaces covered with minute amounts of a Group IA element. However, it should be noted that the surface work functions of the carbonates before and after ion bombardment are unknown and, in fact, may be low enough for reconsideration of the surface ionization mechanism.

1. K. Brand, private communication.
2. G. D. Alton, Nucl. Instr. and Meth. **A244** (1986) 133.
3. G. D. Alton and G. D. Mills, IEEE Trans. Nucl. Sci. **NS-32** (5) (1985) 1822.
4. G. D. Alton, J. W. McConnell, and G. D. Mills, Physics Division Progress Report, Sept. 30, 1986, ORNL-6326, p. 7.

CHARGE-STATE DISTRIBUTION OF 220 MeV ^{158}Gd IONS EMERGING FROM THIN CARBON FOILS

D. K. Olsen J. A. Martin

These measurements were made in preparation for acceleration of $^{156}Gd^{+36}$ ions to 875 MeV with coupled operation of the cyclotron and tandem accelerators. Previous measurements[1,2] with Nd and Au ions had shown significant deviations from the predictions of commonly used semiempirical charge distribution, such as the Sayer[3] formula which we routinely use at the Holifield facility.

The 90° double-focusing energy-analyzing magnet of the tandem accelerator was used for charge-state separation. Measurements were made only at 220 MeV incident energy on the foils. To assure that equilibrium distributions were determined, measurements were made with foil thicknesses of 20, 40, and 60 $\mu g/cm^2$.

The measured fractions F for charge states q were fitted by the least-squares method with skewed Gaussian distributions of the form used by Sayer; $F_q = F_m e^{-0.5t^2/(1+\epsilon t)}$, where $t = (q-q_0)/\sigma$, q_0 is the maximum intensity charge-state value, F_m is the corresponding fraction, σ is the width parameter, and ϵ is the skewness parameter. Measured and adjusted charge-state fractions are listed in Table 1.8. The adjusted values are derived by fitting the measured data with the skewed distribution and adjusting the maximum value of the fitted curve so that the sum of the fractions is unity. The measured data was adjusted by the same ratio. This procedure is necessary because the measurements were not made over a wide enough range to account for 100% of the ions. The rms error of the fits was typically 4%.

The skewed Gaussian parameters for the charge distributions are given in Table 1.9. These data suggest that the equilibrium thickness is near 40 $\mu g/cm^2$. A comparison of adjusted data and least-squares fit for the 40 $\mu g/cm^2$ foil is shown in Fig. 1.5. The previous Nd data gave $\sigma = 1.9$ and $\epsilon = -0.025$; whereas these data for Gd give $\sigma = 2.4$ and $\epsilon = -0.165$, a much larger width and more skew. The difference between the maximum intensity charge states for these data and the Sayer prediction is 1.7 units.

Table 1.8. Charge state fractions for 220 MeV $^{158}Gd^{+9}$ ions passed through thin carbon foils

Charge State q	Charge State Fractions, F_q						
	20 μg/cm²		40 μg/cm²		60 μg/cm²		
	Measured	Adjusted	Measured	Adjusted	Measured	Adjusted	Sayer
29	0.091	0.080	-	-	0.071	0.065	0.007
30	0.125	0.109	0.108	0.094	0.106	0.097	0.021
31	0.151	0.132	0.144	0.125	0.144	0.132	0.049
32	0.166	0.145	0.169	0.146	0.159	0.146	0.095
33	0.166	0.145	0.186	0.161	0.173	0.158	0.145
34	0.147	0.125	0,176	0.152	0.159	0.146	0.179
35	0.089	0.078	0.123	0.107	0.109	0.100	0.179
36	0.147	0.041	0.068	0.059	0.053	0.048	0.144
37	0.014	0.013	0.020	0.017	0.016	0.015	0.095
38	0.003	0.003	0.006	0.005	0.004	0.004	0.022

Table 1.9. Skewed Gaussian parameters for charge distributions of 220-MeV ^{158}Gd ions passed through thin carbon foils

	Skewed-Gaussian Parameters			
	20 μg/cm	40 μg/cm	60 μg/cm	Sayer
q_0	32.30	32.83	32.67	34.5
$\bar{q}$	31.78	32.27	32.01	34.5
Fq_{MAX}	0.163	0.165	0.163	0.18
σ	2.43	2.39	2.41	2.17
ε	-0.140	-0.154	-0.154	+0.01

1. J. A. Martin, R. L. Auble, K. A. Erb, C. M. Jones, and D. K. Olsen, Nucl. Instr. and Meth. **A244** (1986) 187.
2. Phys. Div. Prog. Rep. Sept. 30, 1987, ORNL-6420, p. 10.
3. R. O. Sayer, Rev. Physique Appl. 12 (1977) 1543.

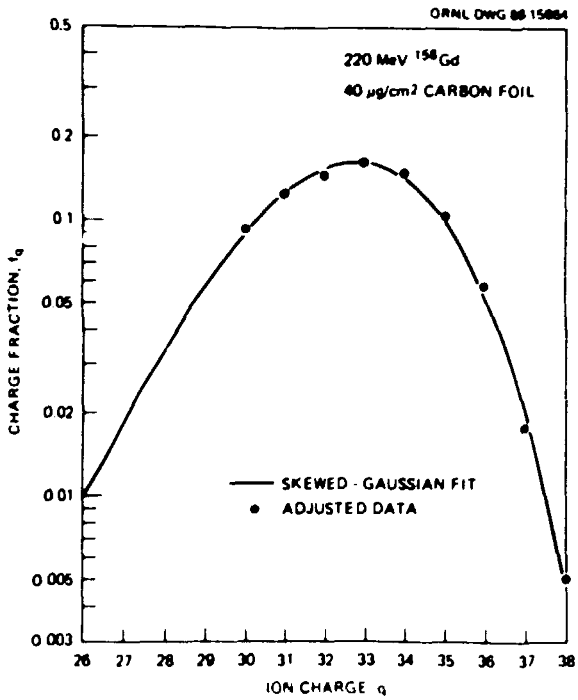

Fig. 1.5. Measured and fitted charge state fractions for 220-MeV ^{158}Gd ions through a 40 μg/cm² carbon foil.

DISPENSER-TYPE SOLID EMITTERS FOR PRODUCING GROUP IA POSITIVE ION BEAMS

G. D. Alton   P. M. Read[1]
J. Maskrey[1]

Concentrated efforts were made in collaboration with members of the Ion Beam Analysis Group, Harwell Laboratory, Oxfordshire, England, to test and evaluate solid thermal emitters for the production of Li^+ and Na^+ ion beams. The emitters consisted of mixtures of Group IA element oxides, alumina, silica, and 10% platinum metal fused together; upon heating to 1000-1100°C, a particular mixture will emit either Li or Na positive ions with a high ionization efficiency. The emitters were fabricated so that they could be easily installed and used in a porous tungsten surface ionization source such as described in Ref. 2. The porous tungsten surface ionization source, in its present form, can only be used to generate beams of K^+, Rb^+, and Cs^+. The ultimate objective of this development is to extend the species capability of this type of surface ionization source, and thus develop a universal source for the production of ion beams from all of the Group IA elements. In addition, the simplicity and low cost of the emitters (<$100) make them viable substitutes for the porous tungsten surface ionization source for the production of K^+, Rb^+, and Cs^+ ion beams of moderate intensity (<150 μA). The Li^+ ion beams are of particular interest to the Harwell Ion Beam Analysis Group in that they can be used in X-ray and Rutherford back-scattering (RBS) surface-analysis applications.

The sources were evaluated and intensity-versus-emitter temperature established for the production of Li^+ and Na^+ ion beam intensities up to ~150 μA. Figure 1.6 displays typical $^{+}Li^{6}$ intensity versus ionizer heater current extracted from two of the solid thermal emitter sources. Experiments were also performed which were designed to estimate the source lifetime for the production of Li^+ beams of a few μA (~<10 μA). The sources performed very reliably throughout the testing and evaluation period. Future efforts call for repeating these tests with K, Rb, and Cs emitters.

1. Harwell Laboratory, Oxfordshire, England.
2. G. D. Alton, Phys. Div. Prog. Rep., May 1976, ORNL-5137, p. 125.

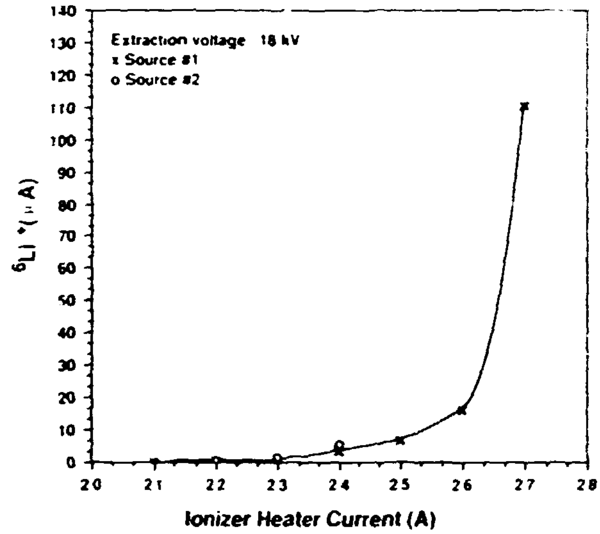

Fig. 1.6. Ion beam intensity versus ionizer heater current from a Li^+ solid thermal emitter ion source.

FACILITY OPERATIONS AND DEVELOPMENT

HHIRF EXPERIMENTS

R. L. Robinson

During FY 1988 there were 38 experiments performed at the Holifield: 28 of these were recommended by PAC for a total of 3084 research hours and 10 were approved as discretionary time, for an additional 277 research hours. These experiments are listed in Table 1.10. Experiment numbers with a prefix H denote experiments recommended by PAC and those with a prefix D, discretionary.

Some experiments were divided into several different runs throughout the year. The distributions of these runs, and of the research hours, are given by target station and by the area of physics in Tables 1.11 and 1.12, respectively. Thirty percent of the approved research hours utilized three experimental devices which were commissioned since last September: the Nuclear Orientation Facility (experiment H187), the HILI (experiments H182, H183, and H230), and the close-packed Ge ball (experiments H185, H203, D072, and H216). In the latter of the four experiments utilizing the close-packed Ge ball, the ball was used in conjunction with the broad range magnetic spectrometer to detect gamma rays emitted in coincidence with [illegible] nuclei inelastically scattered from [illegible].

Table 1.10. Experiments completed at the HHIRF during October 1, 1987-September 30, 1988

Title	Spokesman	Experiment Number	Target Station	Beam Type	Beam E(MeV)	Research Hours
TANDEM						
High Order Electric Multipoles in Convoy Electron Angular Distributions	Elston (U Tennessee)	H164	Atomic Physics	^{16}O	115	87
Lifetime Measurements of Discrete and Continuum Gamma Rays in ^{164}Yb	Lee (ORNL)	H185	γ-Ray Spectrometer	^{44}Ca	195	123
On-Line Nuclear Orientation of $^{191,193}Hg$	Girit (Vanderbilt U /ORAU)	H187	UNISOR	^{12}C	95,110,115	114
A Systematic Study of the Excitation Energy Division in Binary Reactions	Sarantites (Washington U)	H190	Spin Spectrometer	^{1}H	25	5
Search for Superdeformed Shapes in the Mass A=80 Region	Baktash (ORNL)	H192	Spin Spectrometer	^{34}S ^{1}H	120-170 9,20	183
Resonant Transfer and Excitation Investigated by Two Photon Coincidences and High Resolution X-Ray Spectroscopy	Schuch (AFI, Sweden)	H197	Atomic Physics	^{32}S	108,140,165	108
Search for Oblate Structures and Competition Between Oblate and Prolate Structures at High Spin	Ramayya (Vanderbilt U)	H203	γ-Ray Spectrometer	^{35}Cl	95	120
Sub-Barrier Inelastic and Transfer Reaction Cross Sections for ^{32}S + Ni	Hindi (Tennessee TU)	H204	Split Pole Magnet	^{58}Ni ^{64}Ni	156 170	18
Multipolarity of Electromagnetic Transitions in ^{130}Ce	Saladin (U Pittsburgh)	H210	Spin Spectrometer	^{34}S	140,164	102
Lifetimes of States through a Double Band Crossing in ^{184}Pt	Riedinger (U Tennessee)	H211	γ-Ray Spectrometer	^{36}S	165	148
High Spin States in ^{24}Mg	Zurmuhle (U Pennsylvania)	H215	Spin Spectrometer	^{16}O	51-62	120
Determination of α Widths for Uranium Nuclei Near N = 130; Search for ^{224}U, ^{225}U, and ^{226}U	Toth (ORNL)	H218	Velocity Filter	^{19}F	106	98
Electron Impact Excitation of Multiply Charged Ions in Crystal Channels	Datz (ORNL)	H219	Atomic Physics	^{32}S	120-210	98
Search for "Hyperdeformed" Shapes in Nuclei	Sarantites (Washington U)	H222	Spin Spectrometer	^{37}Cl ^{1}H	160-180 12	147
Transfer Plus Excitation from Two Electron Interactions	Datz (ORNL)	H224	Atomic Physics	^{32}S	120	68
Search for Shape Coexistence in ^{187}Au	Zganjar (Louisiana SU)	H227	UNISOR	^{19}F ^{16}O	170 125,135	105
Study of ^{70}Ge and ^{72}Ge in the Spin Spectrometer via Inelastic Scattering of ^{16}O	Hensley (ORNL)	H229	1.6-m Chamber Spin Spectrometer	^{16}O	75	28 62

Table 1.10. (Continued)

Title	Spokesman	Experiment Number	Target Station	Beam Type	Beam E(MeV)	Research Hours
Study of Intruder Structures in Odd-Neutron ^{119}Te and ^{121}Te	Walters (U Maryland)	H232	UNISOR	^{32}S	175	105
Search for Low-Spin Superdeformed States in Hg Nuclei	Henry/Akovali (LLNL/ORNL)	H236	UNISOR	^{19}F ^{12}C	180 90, 100	148
Electron Impact Excitation of Multiply Charged Ions in Crystal Channels	Datz (ORNL)	H237	Atomic Physics	^{28}Si ^{32}S ^{40}Ca	54–170 80–205 170–328	101
Radiative Electron Capture by Fully Stripped Oxygen in Gases	Vane (ORNL)	H246	Atomic Physics	^{16}O	100–225	40
Test of PSD for Study of Short-Lived α Emitters	Toth (ORNL)	D060	Velocity Filter	^{18}O	90	28
Test of Gas-Jet Target	Shapira (ORNL)	D063	Split-Pole Magnet	^{58}Ni	170	9
UNISOR Ion Source Development	Carter (ORAU)	D064	UNISOR	^{16}O ^{12}C ^{32}S ^{58}Ni	55, 157 110 175 280	38
Particle Charge Transfer Cross Sections for O^{+} in He	Datz (ORNL)	D065	Atomic Physics	^{16}O	30	5
Decay of ^{184}Au to ^{184}Pt	Carter (ORAU)	D066	UNISOR	^{16}C	160	30
Study of High T_c Superconductors through Heavy-Ion Induced X-Ray Satellite Emission	Raman (ORNL)	D067	X-Ray Spectrometer	^{32}S	96	46
Study of Pulsed Beam Characteristics	Bemis (ORNL)	D069	Beam Line 31	^{34}S	164	2
High Spin States in ^{184}Hg	Hamilton (Vanderbilt U)	D072	γ-Ray Spectrometer	^{35}Cl	175, 190	38
COUPLED						
Study of Incomplete Momentum Transfer in Multi-Fragmentation Reactions	Novotny (U Giessen)	H182	HILI	^{58}Ni	919	150
Energy and Angular Momentum Division in Deep Inelastic Collisions Studied via Light Particle Emission from the Reaction 900 MeV $^{58}Ni + ^{12}C$	Tan (JIHIR/ORNL)	H183	HILI	^{58}Ni	895	107
A Systematic Study of the Excitation Energy Division in Binary Reactions	Sarantites (Washington U)	H190	Spin Spectrometer	^{28}Si	701	157
Investigation of Target Excitations in Asymmetric Reactions	Mignerey (U of Maryland)	H196	Time of Flight	^{35}Cl	529	146
Search for Two-Octupole-Phonon States in ^{208}Pb	Bertrand (ORNL)	H216	Broad-Range Magnet	^{17}O	276	107

Table 1.10. (Continued)

Title	Spokesman	Experiment Number	Target Station	Beam		Research Hours
				Type	E(MeV)	
Study of the GQR in ^{238}U	Auble (ORNL)	H225	Broad-Range Magnet	^{17}O	375	114
Testing the Energy Dissipation Models by Means of Protons in Coincidence with Heavy Fragments from Collisions of Symmetric Nuclear Systems	Cindro (Rudjer Boskovic)	H230	HILI	^{58}Ni	540,850,919	176
Test of HILI Detector System	Shapira (ORNL)	D047	HILI	^{58}Ni	635	33
			1.6-m Chamber	^{58}Ni	638	17
Test Run for Search for Two-Octupole Phonon States in ^{208}Pb	D'Onofrio (Ns. Fisica, Italy)	D070	Broad-Range Magnet	^{17}O	377	31
						3362

Table 1.11. Use of experiment target stations for the period October 1, 1987 through September 30, 1988

Target Station	Research Hours (No. of Runs)		
	Tandem	Coupled	Total
γ-ray Spectrometer	429(4)	na	429(4)
X-ray Spectrometer	46(1)	na	46(1)
Velocity Filter	126(2)	na	126(2)
Atomic Physics	507(7)	na	507(7)
Split-Pole Magnet	27(3)	na	27(3)
Broad-Range Magnet	0	252(4)	252(4)
Time-of-Flight Facility	0	146(1)	146(1)
1.6-m Scattering Chamber	28(1)	0	28(1)
UNISOR	540(13)	0	540(13)
Spin Spectrometer	619(6)	157(1)	776(7)
HILI	na	483(6)	483(6)
Beam Line 31	2(1)	na	2(1)
Total	2,324(38)	1,038(12)	3,362(50)

na = not accessible to beam

Table 1.12. Division of research hours by research activities for the period October 1, 1987 through September 30, 1988

Activity	Research Hours (No. of Runs)		
	Tandem	Coupled	Total
Low-lying level properties	600(9)	0	600(9)
High-spin states	981(8)	0	981(8)
Quasi-elastic processes	90(2)	221(3)	311(5)
Damped reactions	5(1)	560(4)	565(5)
Reaction mechanisms	18(2)	176(2)	194(4)
Atomic physics	507(7)	0	507(7)
Applications	46(1)	0	46(1)
Tests of detectors	28(1)	50(2)	78(3)
Tests of apparatus	49(7)	31(1)	80(8)
Total	2,324(38)	1,038(12)	3,362(50)

EXPERIMENTAL APPARATUS

R. L. Auble J. W. Johnson
J. R. Beene N. R. Johnson
H. K. Carter H. J. Kim
I. Y. Lee

Following are brief updates on apparatus development projects during the past year. Major new projects are discussed in more detail elsewhere in this report.

Compton-Suppression System

A new support stand was completed which now allows the Compton-Suppression System to be used independently of the Spin Spectrometer. This device will support up to 21 detectors in a close-packed configuration with a source-detector distance of about 12 cm, as compared to about 20 cm when the detectors are mounted in the Spin Spectrometer. This enhances the double- and triple-coincidence rates by factors of about 6 and 20, respectively. The new stand also provides portability which allows the system to be moved to different experiment stations and used in conjunction with other apparatus.

The heavy usage of the Compton-Suppression System, coupled with the lack of spare Ge detectors, requires that all detectors be kept in good condition. To this end, the Ge-detector recovery system has been expanded to allow simultaneous recovery of two detectors. This has proved to be very beneficial, as detector recoveries carried out over the past year would have cost approximately $50K if done commercially.

Velocity Filter

The installation of the new scattering chamber and center support post for the velocity filter has been completed. This equipment provides a more rigid pivot point and will allow the velocity filter to be easily rotated through the full angular range of -8 to +20 degrees.

HILI Detector

The heavy-ion light-ion detector presently includes all of the original design elements with the exception of a second 96-element scintillator hodoscope. This last element is under construction. Also, work is underway to develop additional scintillator telescopes, to be located inside the scattering chamber, which will extend the angular coverage to about 28 degrees. Plans are being made for moving the HILI to the present TOF station, where it will have access to both tandem-only and coupled-accelerator beams (only coupled-accelerator beams can be accessed at present).

Nuclear Orientation Facility

The first on-line experiment using the Nuclear Orientation Facility was completed in June 1988. This is discussed elsewhere in this report. Unfortunately, the cold finger still exhibited unacceptable temperature increases when the beam line baffle was opened, despite the vendors efforts to make in situ improvements. For this reason, in July the entire dilution unit and heat shields were returned to the vendor for further modification. These are expected to be reinstalled by late November and available for further experiments by December.

Barium Fluoride Detectors

Acceptance tests of the photomultiplier tubes have been completed, and 19 of the 57 crystals on order have been received and tested. The assembly of the first 19-element array is in progress. It is planned to have 57 elements (three 19-element arrays) available by the end of 1988.

COMPUTER SYSTEMS

J. A. Biggerstaff
W. H. Atkins[1]
C. E. Bemis
D. M. Galbraith
E. E. Gross
J. W. McConnell
J. B. McGrory
W. T. Milner
C. N. Thomas[2]
R. L. Varner

Data Acquisition/Reduction Computer System

A major software item (driver for a new JORWAY-434 CAMAC interface procured earlier) was completed and implemented. This new software and hardware enable us to utilize the full 16 MB of memory available on all three CONCURRENT systems. We had been effectively limited to 4 MB by the older JORWAY-432 CAMAC interface and associated software. This implementation significantly enhances these machines which are being subjected to ever-increasing demands.

A system has been implemented that provides for the automatic transfer of histogram data (via CAMAC) from the UNISOR Tennecomp system (PDP-11 memory) to a standard disk file on one of the CONCURRENT computers. This process is controlled by special software written for the Tennecomp system which transfers data to a FIFO connected to the CONCURRENT CAMAC system. CONCURRENT software simply tests the FIFO status and copies any data sent to it.

A new very-high-density mass-storage device has been acquired and is currently being evaluated as a candidate for the next generation of data storage systems. This device (based on an Exabyte tape drive) uses video technology to record about 2 GB of data onto one standard 8-mm T-120 video cassette (cost about $8.00). Two GB of storage is equivalent to that provided by thirteen 10-inch 6250-bpi tapes recorded with 8192-byte records (cost about $180). The maximum read/write speed (248 KB/sec) is about 1/3 of that for a standard 125-ips 6250-bpi tape but is adequate for our current data acquisition and processing applications. Full implementation of such devices should significantly increase the actual processing throughput of the associated computer systems by eliminating most of the time lost while waiting for tapes to be mounted during non-prime time.

Four additional (refurbished) TELEX tape drives were acquired, bringing the total to 4 each on two of CONCURRENT CPUs and 3 on a third CPU with one spare. A color VAXstation 2000, to be used in the development of the next generation of interactive graphic software, has been procured.

Disk space management has been a perpetual problem aggravated by the fact that quotas are impractical in our environment, where resources are limited yet most users require large amounts of disk space at certain times. A fractional archiving, FARC (rhymes with lark) procedure has been implemented which works as follows: When any disk becomes more than 90% allocated, enough files are archived (copied to tape and deleted from disk) to reduce the allocation to 75%. Files to be archived are selected by considering "greed" factors (computed from the number of files and space occupied on all disks on all CPUs) associated with candidate FARCees as well as the size, age and type of file. The system has been in use for about four months (including a summer season) and has worked well. At least, most FARCees have felt too guilty of excessive greed to complain to the FARCor.

Local Area Networks

The first phase of our Ethernet Local Area Network (LAN) has been completed. At the present time about 40 terminals located in Building 6000 can connect to any of the three CONCURRENT computers, the Physics Division VAX/785 or any of five Microvax nodes. Full DECNET connectivity to the CTD[1] network is also supported. Future plans call for extending the LAN to Buildings 6003 and 6008.

VAX 11/785, FPS-164 Array Processor System

The VAX and FPS processors were utilized approximately 55% of the past year, with daytime utilization frequently above the 90% level. The reliability of both systems has been good, with the only major downtime resulting from UNIBUS problems on the VAX. In spite of the good performance of the FPS this year, we are making plans to shut it down in order to save the high maintenance cost. We are searching now for more cost-effective solutions to the Division's large-scale computing needs.

Little extra hardware has been added to these systems. We are in the process of adding an Exabyte tape drive and SCSI controller to the VAX, and we anticipate delivery soon of a DEC SA482 storage array (2.5 GB of disk storage). The Exabyte drive will provide us with the necessary extra capacity for backing up the new storage array, as well as providing the central VAX with the ability to read and translate data from the CONCURRENT computers and the WA80 collaboration at CERN.

In the past year, we connected the Physics Ethernet to the DECnet part of ESnet, a wide-area network operated by the DOE Office of Energy Research. All the VAX computers in the Physics Division are now part of this wide-area network. Our connection is currently made through a dedicated 14.4K-baud synchronous telephone line to FermiLab. ORNL is in the process of upgrading this connection to 56K baud and replacing the MicroVAX II router with a faster dedicated DECRouter 2000. This connection to ESnet has become quite important to many research activities in the Physics Division, including the WA80 collaboration, the development of the GAMMASPHERE proposal and the development of new parallel computing facilities for data reduction in the division, as based on the FermiLab ACP farm concept.

Computer System Upgrade

A committee consisting of E. E. Gross (chairman), J. R. Beene, C. E. Bemis, J. A. Biggerstaff, C. C. Havener, H. F. Krause, C. A. Ludemann, W. T. Milner, M. R. Strayer, and G. R. Young was formed to examine the computer usage and needs of the Physics Division for the next five-year period. Based on the perceived needs, the committee made the following recommendations:

(1) At least a factor of 4 increase in general computer power. Distributed computing power via workstations was considered as a means for meeting this need but the committee recommended increasing the central computing power in the Division. It was felt that a four- to six-fold increase in general computing power would better meet the needs of the Division as a whole as well as allow for an orderly buildup of distributed computing.

(2) A factor of 10 improvement in date reduction capability. The growing complexity of experiments, the large data analysis needs of the WA-80 experiment, and the phenomenal success of the Spin Spectrometer, have created a crisis in data analysis. At present, it can take up to three months to make the initial scan through a typical set of Spin Spectrometer data tapes and about one year before the data are fully reduced. The committee recommended development of parallel processing computers based on the Fermi Laboratory's "Advanced Computer Project" (ACP) concept as the means towards solving the data analysis crisis.

(3) Replacement of the Array Processor with an enhanced supercomputer. To remain competitive in large-scale calculations, the committee recommended replacement of the FPS Array Processor with a next generation parallel supercomputer.

(4) A large increase in mass storage capability. An essential ingredient in alleviating the data processing needs is mass storage capability. The committee recommended that 6 GB of disk capacity be added and that the promising new mass storage devices be evaluated.

(5) Gradual replacement of Chromatics terminals by advanced graphics workstations.

(6) A more intelligent front-end data acquisition system in the future. The committee believed that the ACP farm technology for data processing could also be adapted for a more advanced data acquisition system than the present Event Handler.

(7) A carefully thought-out communication system based on ethernet.

The committee also proposed a general implementation plan which addressed these needs within the time and budgetary constraints ($1M over a five-year period). Implementation of this plan began this year.

---

1. Computing and Telecommunications Division, ORNL.
2. Oak Ridge Associated Universities.

THE JOINT INSTITUTE FOR HEAVY ION RESEARCH

R. L. Robinson, L. L. Riedinger
J. H. Hamilton

The Joint Institute, now in its fourth year of operation, is a collaborative endeavor of the University of Tennessee, Vanderbilt University, and Oak Ridge National Laboratory. It is administrated by the University of Tennessee through the Science Alliance, which is one of the State of Tennessee's Centers of Excellence. Two-thirds of the support of the Joint Institute comes from the Science Alliance; remaining funds are provided by DOE, Vanderbilt University, and ORNL.

The primary mission of the Joint Institute is to enhance and stimulate the scientific environment of the Holifield Facility to the mutual benefit of its three sponsoring institutes. Major elements of this are its guest program and support of workshops. Table 1.13 lists scientists supported by the Joint Institute during FY 1988. The average length of appointment for these 56 guests was over 4 months.

Table 1.14 lists meetings that were held during the past fiscal year at the Joint Institute and were supported by it. The Gamma-Ray Detector Facility (GAMMASPHERE) meeting was to review, augment, and refine a preliminary draft of a proposal for a large, 4π ball of Compton suppressed Ge detectors. The strong interest in this device was demonstrated by the large attendance at this meeting and by the enthusiasm exhibited by the attendees. The preliminary draft had resulted from a similar meeting held a month before at the Lawrence Berkeley Laboratory.

The meeting on Monte Carlo Codes was in the true sense a "working" workshop and included a mix of the attendees working together, within small groups, and individually. The purpose of the meeting was to explore the application of various Monte Carlo codes to a broad range of relativistic heavy-ion experimental data. Both experimentalists and theorists were involved to insure that the experimental conditions were included properly and that the programs were used correctly. Two small meetings were held for UNISOR researchers to discuss what physics results had been obtained to date, and what are desirable future objectives.

The Joint Institute also provides short-term living accommodations, with maximum capacity of 12 per night, for Holifield users. During FY 1988 there were 286 users who stayed a total of 1848 person-days (an average of 6.5 days per guest).

Table 1.13. Guest scientists at the Joint Institute for Heavy Ion Research during the period of October 1987 - September 1988

Name	Institute	Length of Appointment
S. Ayik	Tennessee Tech. Univ.	10 weeks
K. Bhatt	Western Kentucky Univ.	1 month
N. Cindro	Ruder Boskovic Inst. (Yugoslavia)	5 months
J. Coffin	Centre Nat. Recherche Scientifique (France)	5 weeks
. D'Onofrio	National Institute of Nuclear Physics (Italy)	1 year
F. Donau	Inst. for Nuclear Research (East Germany)	2 months
H. Doubre	GANIL (France)	5 days
L. Dragon	Univ. of Muenster (West Germany)	6 weeks
J. Dudek	Centre De Recherches Nucleaires (France)	8 months
A. Faessler	Inst. fur Theoretische Physik (West Germany)	1 month
G. Garcia-Bermudez	Nacional de Energia Atomica (Argentina)	3 months
J. Garrett	Niels Bohr Inst. (Denmark)	1 week
C. Girit	Vanderbilt Univ/ORAU	4 months
W. Greiner	Univ. of Frankfurt (West Germany)	2 weeks

(Cont.)

Table 1.13. (Continued)

Name	Institute	Length of Appointment
J. Griffin	Univ. of Maryland	3 months
K. Groeneveld	Johann Wolfgang Goethe-Univ. (West Germany)	3 months
B. Herskind	Niels Bohr Inst. (Denmark)	3 days
S. Kahane	Nuclear Research Center (Israel)	1 year
P. Kienle	GSI (West Germany)	1 day
M. Korolija	Ruder Boskovic Inst. (Yugoslavia)	8 months
S. Landowne	Argonne National Lab.	2 weeks
L. Lantto	Univ. of Oulu (Finland)	5 months
R. Lemmer	Univ. of Witwatersrand (South Africa)	1 month
J. Lisantti	ORNL/JIHIR	1 year
I. Lund	GSI (West Germany)	1 month
C. Maguire	Vanderbilt Univ.	1 month
J. Maruhn	Univ. of Frankfurt (West Germany)	10 days
V. Metag	Univ. of Giessen (West Germany)	2 weeks
U. Mosel	Univ. of Giessen (West Germany)	18 days
B. Mueller	Univ. of Frankfurt (West Germany)	2 weeks 10 days
N. Neskovic	Boris Kidric Inst. (Yugoslavia)	7 weeks
V. Oberacker	Vanderbilt Univ.	7 weeks
D. Pelte	Univ. of Heidelberg (West Germany)	3 weeks
M. Pennington	Rutherford Lab. (England)	5 days
J. Rafelski	Univ. of Arizona	1 week
A. Ray	ORNL/JIHIR	1 year
P. Reinhard	Inst. fur Theoretische Physik (West Germany)	1 month
D. Rentsch	Univ. of Giessen (West Germany)	2 months
M. Riley	ORNL/JIHIR	1 year
S. Saini	ORNL/JIHIR	1 year
J. Saladin	Univ. of Pittsburgh	6 weeks
K. Schiffer	Niels Bohr Inst. (Denmark)	1 week
W. Schmidt-Ott	Univ. Gottingen (West Germany)	2 months
M. Schultz	Univ. of Heidelberg (West Germany)	1 year
M. Soyeur	CEN, Saclay (France)	1 month
K. Teh	ORNL/JIHIR	1 year
U. Thumm	Univ. of Freiburg (West Germany)	7 months
M. Tinknell	Lawrence Berkeley Laboratory	1 year
A. Virtanen	Univ. of Jyvaskyla (Finland)	1 year
T. Walkiewicz	Edinboro Univ.	1 year
R. Wang	Univ. of Science Technology (China)	1 year
J. Wells	Tennessee Technological Univ.	3 days
J. Wieleczo	CEN, Saclay (France)	1 year
C. Wu	Jilin Univ. (China)	1 year
J. Wu	ORNL/JIHIR	5 months
J. Zhang	Lanzhou Inst. (China)	1 year

Table ..14. Meetings Sponsored by JIHIR during FY 1988

Meeting	Date	Approximate Attendance	Organizer
Workshop on High Energy Nuclear Collision Monte Carlo Codes	Sept. 12-23, 1988	20	T. Awes S. Sorensen
UNISOR Information Meeting	Nov. 18, 1987	25	H. K. Carter
Workshop on the Proposal for a National Gamma-Ray Detector Facility	Nov. 19-21, 1987	94	N. Johnson, Chairman
UNISOR Workshop	June 21-22, 1988	41	H. K. Carter

USERS GROUP ACTIVITIES

R. L. Auble

Members of the Executive Committee of the HHIRF Users Group during 1987 and 1988 are listed in Table 1.15.

Table 1.15. Users Group Executive Committee

1987
Jim Beene, Oak Ridge National Laboratory
Doug Cline, University of Rochester
Mike Guidry, University of Tennessee
Joe Hamilton, Vanderbilt University
I-Yang Lee, Oak Ridge National Laboratory
Alice Mignerey[a], University of Maryland
1988
Jim Beene, Oak Ridge National Laboratory
Doug Cline[b], University of Rochester
Joe Hamilton[a], Vanderbilt University
I-Yang Lee, Oak Ridge National Laboratory
Richard Schmitt, Texas A&M University
John Wells, Tennessee Technological Univ.

[a]Chairperson
[b]Chairperson elect for 1989

The Executive Committee met with HHIRF staff on April 11 and September 8 to provide user input on the operation of the facility. These meetings gave the users an opportunity to voice their opinions regarding allocation of financial resources, make recommendations on PAC membership, and generally to take an active role in the decision making process. One change which was a direct result of committee recommendations was the appointment of a half-time liaison scientist to assist users of the Spin Spectrometer and Compton-suppression system.

In order to keep the users' membership list up to date, we require that all members indicate their wish to remain members every third year. This was done in FY 1988. The current number of reconfirming members is 360.

Each year, a nominating committee is formed to select four candidates for election to the Executive Committee of the HHIRF Users Group. The members of the nominating committee for 1988 were: K. S. Toth (ORNL)-chairman, P. E. Haustein (BNL), C. F. Maguire (Vanderbilt University), D. M. Moltz (LBL), and S. W. Yates (University of Kentucky).

The annual meeting of the HHIRF Users Group was held in Nashville on November 23, 1987 in conjunction with the meeting of the Southeastern Section of the APS. The meeting was hosted by Vanderbilt University and the JIHIR and was chaired by Alice Mignerey. Presentations included discussion of facility operations, recent accelerator and apparatus upgrades, new experimental apparatus, and long-range computer requirements.

THE PROGRAM ADVISORY COMMITTEE

R. L. Robinson

The PAC continues, as it has since 1984, to meet every six months to review proposals submitted for experiments. Recommendations of PAC are based principally on the scientific merit of the proposals. Statistics on the two PACs that met in FY 1988, and the one that will meet in November 1988, are given in Table 1.16. As a result of reliable machine operation and large backlog of data, the ratio of hours that could be recommended by PAC to those requested in the proposals has reached a new high of over 80%. This is to be compared with a typical value of 65% two years ago.

Members of one or both PACs in FY 1988 were:

J. M. Alexander	Suny, Stonybrook
H. C. Britt	LLNL
A. L. Goodman	Tulane University
T. L. Khoo	ANL
J. B. Natowitz	Texas A&M University
R. A. Phaneuf	ORNL
P. H. Stelson	ORNL
P. J. Siemens	Oregon State University

Other attendees of the meetings were L. S. Schroeder (representing DOE), J. H. Hamilton (representing the Executive Committee of the HHIRF Users Group), J. B. Ball (representing the ORNL Physics Division), and R. L. Auble (representing the users as Liaison Officer).

Table 1.16. Information on PAC-10, PAC-11, and PAC-12

	Meeting Date	Hours Requested	Hours Recommended	Rec/Req.
PAC-10	Oct. 27, 1987	2320	1888	81%
PAC-11	May 6, 1988	2088	1912	92%
PAC-12	Nov. 1, 1988	2448	est. 2000	est. 82%

2. EXPERIMENTAL NUCLEAR PHYSICS

Although the main research program in heavy-ion physics continues to be based on the beams and experimental equipment at the Holifield Heavy Ion Research Facility (HHIRF), the use of facilities elsewhere, especially at CERN and GANIL, is becoming increasingly important. The program at CERN, using ultrarelativistic heavy-ion beams, has provided a wealth of information on particle production, γ-ray production, and energy densities achievable with up to 200 GeV/nucleon light heavy-ion beams on a fixed heavy target. These are essential data required for the establishment and study of a possible quark-gluon plasma state. The results on γ decay of the giant resonances from experiments at GANIL are revealing interesting information on the microscopic composition of the resonances. In particular, these experiments have successfully located and measured the properties of an isovector giant quadrupole resonance. The program at HHIRF continues to be dominated by the Spin Spectrometer which generates a great deal of detailed information on high-spin alignment mechanisms and on the evolution of nuclear shapes with increasing spin and increasing excitation energy. The device continues to be developed as a promising tool for heavy-ion inelastic scattering. Together with measurements using the velocity filter, the Spin Spectrometer is also providing a more complete understanding of the subbarrier fusion process. Progress continues to be made in understanding the division and dissipation of excitation energy and angular momentum generated in heavy-ion collisions. The heavy-ion light-ion (HILI) detector has been successfully tested and should shortly be making contributions to this important area of research.

NUCLEAR STRUCTURE STUDIES VIA ELASTIC AND INELASTIC SCATTERING

SURFACE CONTRIBUTIONS TO THE COMPLEX NEUTRON-^{208}Pb MEAN FIELD BETWEEN -20 AND +20 MeV[1]

J.-P. Jeukenne[2] C. H. Johnson
C. Mahaux[2]

Phenomenological analyses of the experimental n-^{208}Pb differential, total, and polarization cross sections, with local optical-model potentials, indicate that the radial shape of the surface absorption depends upon energy below 10 MeV, i.e., the corresponding diffuseness decreases and the radius parameter increases with decreasing neutron energy. Because of the dispersion relation that connects the real and imaginary parts of the mean field, these features imply that the real potential contains a surface component whose radial shape also depends upon energy. This radial shape is calculated numerically for typical parametrizations of the energy dependence of the surface absorption; it turns out to be quite complicated for neutron energies between 0 and 15 MeV. In this domain, the predicted differential cross sections are sensitive to the radial shapes of both the real and imaginary surface components of the mean field even though their volume integrals are exactly the same in all the investigated models. The best agreement with the experimental data is obtained for parametrizations in which the radial shape of the surface absorption depends only weakly upon energy. It is shown that good fits to the experimental data can also be obtained in the framework of models in which the radial shape of the surface absorption is independent of energy, but in which the strength of the surface absorption depends upon the orbital angular momentum of the incoming neutron. Tentative physical interpretations of these features are proposed.

1. Summary of paper submitted to Physical Review C.
2. Consultant from Institut de Physique B5, University of Liège, B-4000 Liège 1, Belgium.

NEUTRON-^{40}Ca MEAN FIELD BETWEEN -80 AND +80 MeV FROM A DISPERSIVE OPTICAL-MODEL ANALYSIS[1]

C. H. Johnson C. Mahaux[2]

The n-^{40}Ca complex mean field is derived from a dispersive optical-model analysis of the available experimental cross sections. In this analysis the real part of the mean field contains dispersive contributions which are derived from the imaginary part by means of a dispersion relation. These dispersive contributions must be added to the Hartree-Fock potential which is assumed to have a Woods-Saxon shape, with a depth $U_{HF}(E)$ that depends exponentially upon energy. The input experimental data are fourteen differential cross sections in the energy domain [5.3, 40.0 MeV], five polarization cross sections in the domain [9.9, 16.9 MeV] and the total cross section in the domain [2.5, 80 MeV]. The resulting optical-model potential is an analytic function of energy. It can thus be extrapolated towards negative energies, where it should be identified with the shell-model potential. This extrapolation yields good agreement with the experimental single-particle energies in the two valence shells of ^{40}Ca. The model also predicts the radial shape and the occupation probabilities of the single-particle orbits and the spectroscopic factors of the single-particle excitations. In order to reproduce the experimental energies of the deeply bound 1p and 1s orbits, one must use a linear rather than an exponential energy dependence of $U_{HF}(E)$ at large negative E. It is shown that this is precisely the behavior expected from the fact that the energy dependence of $U_{HF}(E)$ actually represents the nonlocality of the original microscopic Hartree-Fock field. The model also correctly predicts the distribution of the single-particle strength of the 1d5/2 excitation in ^{39}Ca. The calculated distributions of the 1p strength in ^{39}Ca and of the 1f5/2 strength in ^{41}Ca show that the available experimental information extends over less than half the expected peak. Therefore, the positions of the peaks can not be determined from the experiment. In the energy domain [2.5, 9 MeV] the predicted total cross section deviates from the experimental data; this reflects the fact that at low energy the calculated cross section is very sensitive to small modifications of the mean field.

---

1. Summary of paper submitted to Physical Review C.
2. Consultant from University of Liège, Liège, Belgium.

RADIUS OF THE $1f_{7/2}$ ORBIT IN ^{41}Ca[1]

S. Platchkov[2], A. Amroun[2], P. Bricault[2], J. M. Cavedon[2], P. K. A. de Witt Huberts[3], P. Dreux[2], B. Frois[2], C. D. Goodman[4], D. Goutte[2], J. Martino[2], V. Meot[2], G. A. Peterson[5], X. H. Phan[2], S. Raman, I. Sick[6]

The magnetic form factor of ^{41}Ca was measured by elastic electron scattering in the momentum transfer range between 1.8 and 3.3 fm^{-1}. The two essential results deduced from this experiment are: (1) the rms radius of the $1f_{7/2}$ neutron orbit is 3.99 ± 0.06 fm and (2) the single-particle spectroscopic amplitude of this orbit is 0.83 ± 0.05, representing a depletion of the $1f_{7/2}$ orbit by (17±5%) in ^{41}Ca. The measured rms radius agrees with the mean-field value of 4.02 fm calculated by Dechargé and Gogny[7] and with the relativistic mean-field result of 4.05 fm by Kim;[8] it is slightly smaller than the 4.14 fm value of Negele.[9] The measurement of the $1f_{7/2}$ neutron radius has direct implications for the interpretation of the Coulomb energy differences for the ^{41}Ca-^{41}Se mirror pair. Knowledge of this radius rules out the explanation of the Coulomb energy anomaly[10] based on a reduction of the valence orbit radius.

---

1. Summary of published paper: Phys. Rev. Lett. 61, 1465 (1988).
2. DPhN/HE CEN Saclay, F-91191 Gif-sur-Yvette, France.
3. NIKHEF-K, 1009 AJ Amsterdam, The Netherlands.

4. Indiana University Cyclotron Facility, Bloomington, IN 47401.
5. University of Massachusetts, Amherst, MA 01003.
6. University of Basel, CH 4056 Basel, Switzerland.
7. Phys. Rev. C 21, 1568 (1980).
8. E. J. Kim, Ph.D thesis, Stanford University (1987), and private communication.
9. Nucl. Phys. A165, 305 (1971).
10. J. A. Nolen, Jr., and J. P. Schiffer, Annu. Rev. Nucl. Sci. 19, 471 (1968).

FISSION DECAY OF THE GQR IN ^{238}U

R. L. Auble, D. J. Horen, J. R. Beene, J. L. Blankenship[2], F. E. Bertrand, R. L. Varner, A. D'Onofrio[1], J. Lisantti[3]

Studies of the fission decay of the giant quadrupole resonance in ^{238}U were undertaken to examine the possibility that the quantum number K is conserved during the fission process. Such a possibility was raised in studies of the $^{238}U(\alpha,\alpha'f)$ reaction[4] where the fission fragments were limited to angles close to the recoil direction. In the present study, four position-sensitive avalanche detectors provided partial coverage at all fission angles. The GQR was excited by the $^{238}U(^{17}O,^{17}O')$ reaction using a 375-MeV beam from the HHIRF coupled accelerators. Inelastically scattered particles were analyzed in the broad-range spectrograph (BRS), and fission events were identified by coincidences between the focal plane detector and the avalanche detector array located in the BRS scattering chamber.

Inelastic spectra were gated on fragment angles (in 10° bins) between 0° and 90° with respect to the recoil direction. Relative fission probabilities were determined by dividing by the singles spectrum and normalizing in the 25-30 MeV excitation region (assumed to be isotropic). Angular distributions obtained for various excitation energies are shown in Fig. 2.1. For energies near the fission barrier, we observe the expected enhancement along the recoil direction. Above the barrier, at energies predicted for the various K-components of the GQR, the angular distribution is isotropic within the experimental uncertainties. This implies that K at the saddle point is essentially unrelated to the K component excited in the reaction.

ORNL-DWG 88-15266

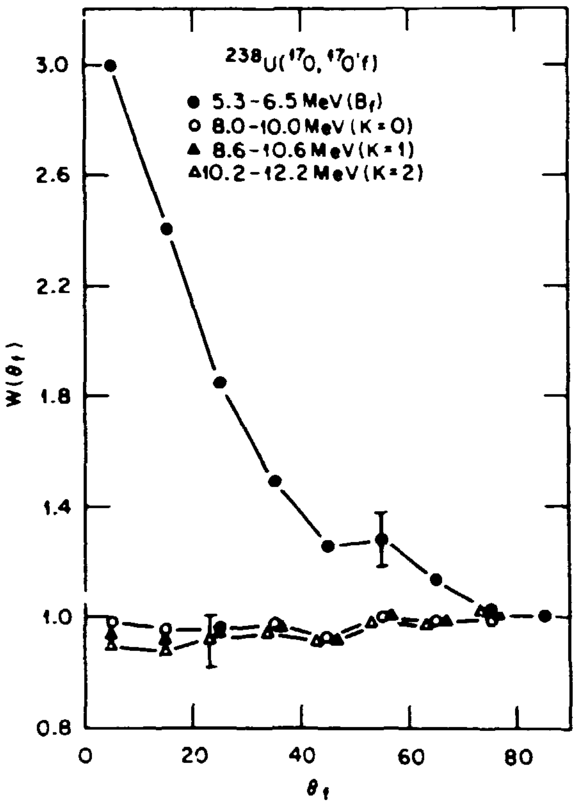

Fig. 2.1. Angular correlations, for various excitation energies, of inelastically scattered particles in coincidence with fission fragments emitted at an angle θ_f relative to the recoil direction.

---

1. Joint Institute for Heavy Ion Research and Instituto Nazionale di Fisica Nucleare, Napoli, Italy.
2. Instrumentation and Controls Division, ORNL.
3. Partial support from the Joint Institute for Heavy Ion Research, ORNL.
4. F. E. Bertrand et al., Phys. Lett. 99B, [illegible].

EXPERIMENTAL DEMONSTRATION OF COMPOUND AND PRECOMPOUND EFFECTS IN GIANT DIPOLE RESONANCE PHOTON DECAY

J. R. Beene, F. E. Bertrand, D. J. Horen, R. L. Auble, B. L. Burks[1], J. Gomez del Campo, M. L. Halbert, D. C. Hensley, R. O. Sayer[2], W. Mittig[3], Y. Schutz[3], J. Barrette[4], N. Alamanos[4], F. Auger[4], B. Fernandez[4], A. Gillibert[4], B. Haas[5], J. P. Vivien[5], A. M. Nathan[6]

The importance of the contribution of fully damped compound states to the photon decay of giant resonances excited by inelastic scattering was pointed out first in Ref. 7 and has been discussed in a number of subsequent works.[8-12] Approximate quantitative calculations based on the ideas of the theory of multistep compound emission (MSCE),[12,13] have been carried out, for the ground-state photon decay of the isoscalar giant quadrupole and isovector giant dipole resonances (IVGDR) in ^{208}Pb excited by 22-MeV/nucleon ^{17}O scattering,[11] and for the IVGDR excited by the same reaction at 84 MeV per nucleon.[14] These calculations show remarkably good agreement with the experimental photon decay data. Ground state photon decay following inelastic excitation by 84-MeV/nucleon ^{17}O is a particularly good case for further exploration of the application of the MSCE theory, since the IVGDR is very strongly excited (~2.5 b/sr at 2.5°), with a peak-to-continuum ratio of about 6 to 1, and has an average ground-state gamma branch at least two orders of magnitude larger than that of the underlying background or any nearby resonances.

According to the MSCE theory, the cross section for a particular exit channel in a nuclear reaction can be described by an incoherent sum of contributions from different stages (or levels of complexity) in the evolution of the states of the excited system.

$$\sigma_f = \sum_{i=1}^{r} \sigma_{fi} , \qquad (1)$$

The first term in this sum represents the primary doorway state excited by the reaction process (in our case the coherent giant resonance state, which can be described as a superposition of 1p1h states). The sum then runs over successively more complex states (2p2h, 3p3h ...), terminating at the fully damped compound system. In the formal expression[11-13] a depletion factor multiplies each stage, taking into account that only that fraction of systems which have not decayed in previous stages can contribute to the cross section for the ith stage. In our applications of MSCE to photon decays of giant resonances, we have simplified Eq. 1 by neglecting all stages except the first (primary doorway) and last (fully damped compound) stage. The cross section for ground-state photon emission, integrated over photon emission angle, can then be written

$$\sigma(\gamma_0, E) = \sigma(E) \left(\frac{\Gamma_{\gamma 0}}{\Gamma} + \left[\frac{\Gamma^{\downarrow}}{\Gamma}\right] R_{cn}(E)\right) \qquad (2)$$

where $\sigma(E)$ is the excitation cross section as a function of excitation energy E. The two terms in parentheses represent the primary doorway and compound contributions, respectively. $\Gamma_{\gamma 0}$ is the gamma decay width of the giant resonance, treated as a single sharp state, Γ is the total width of the resonance $\Gamma = \Gamma^{\uparrow} + \Gamma^{\downarrow}$ where $\Gamma^{\uparrow}$ and $\Gamma^{\downarrow}$ are the escape and damping widths, respectively. The width ratio in square brackets in the second term therefore represents the fraction of systems which reach the fully damped stage. $R_{cn}(E)$ is the compound ground-state gamma branching ratio obtained from a detailed statistical model calculation, including corrections for width fluctuations which have been discussed extensively by Moldauer.[15] Calculations employing the formalism have been described in more detail elsewhere.[8,11] The important qualitative feature of Eq. 2 is that the first term depends only on the gross collective properties of the giant resonance (strength and total width) while the second term is sensitive to detailed properties of the compound states. This means that a good test of the basic features of Eq. 2 should be provided by a comparison of data on nuclei which have similar strength distributions, but compound states with very different properties.

One of the best examples of such a comparison is ^{208}Pb and ^{209}Bi. The collective properties of these nuclei are remarkably similar. The average ground-state gamma branch from fully damped states is, however, expected to be much smaller in ^{209}Bi than in ^{208}Pb, due primarily to the substantially larger neutron decay widths of the ^{209}Bi compound states. These larger widths result from the larger density of final states available in ^{207}Bi, compared to ^{207}Pb. The similarity of the strength distributions is emphasized by the data in Fig. 2.2, showing the almost indistinguishable spectra for inelastic excitation of these two nuclei by 84-MeV/nucleon ^{17}O at a center-of-mass angle of 2.7°. Figure 2.3a shows the ground-state photon decay coincidence (^{17}O,$^{17}O'\gamma$) yields for ^{208}Pb divided by those for ^{209}Bi. The coincidence data was acquired under identical conditions for the two targets; a range of scattering angles spanning 2° to 4° and a combination of photon data from nine multiple detector arrays of BaF_2 (see Ref. 10 for details of experimental geometry). The gamma decay yields are clearly quite different near 11 MeV, in spite of the almost identical excitation cross sections (Fig. 2.2). Equation 2 predicts a ratio of yields in good agreement

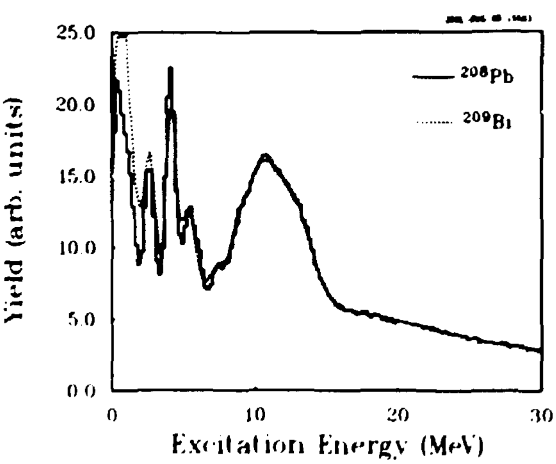

Fig 2.2. Excitation energy spectra obtained with inelastic scattering of 84-MeV/nucleon ^{17}O on ^{208}Pb (solid histogram) and ^{209}Bi (dashed line).

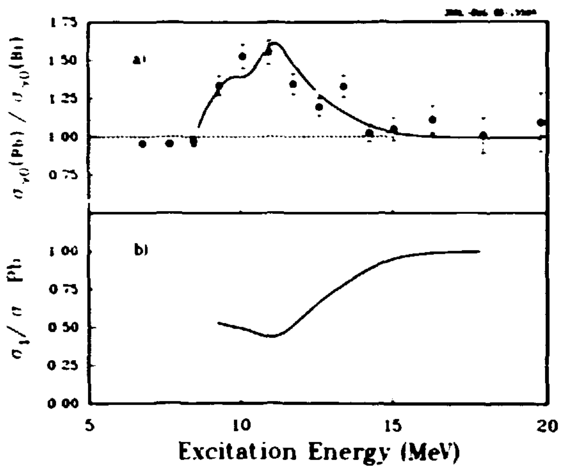

Fig 2.3. Ground-state gamma-ray coincidence data. Figure 2.3a shows the ratio of experimental yields for ^{208}Pb divided by ^{209}Bi (data points) and the result of a calculation of this ratio obtained using Eq. 2 (solid line). Figure 2.3b illustrates the contribution of the two terms of Eq. 2 to the predicted ground-state photon yield from ^{208}Pb. The quantity plotted is the ratio of the first term of Eq. 2 to the sum of the two terms.

with the data, as shown by the solid line in Fig. 2.3a. The difference between the predicted yields for the two nuclei lies almost entirely in the second term of Eq. 2, which makes about a five times larger contribution in ^{208}Pb than in ^{209}Bi in the vicinity of the GDR. The energy dependence of the two terms in Eq. 2 is illustrated in Fig. 2.3b which shows the ratio of the first term to the sum of both terms in Eq. 2 for ground-state photon decay of the IVGDR in ^{208}Pb.

We draw two conclusions from these results:
(1) The decay of fully damped states makes a significant contribution to ground-state photon decay in ^{208}Pb, as conjectured in Ref. 7
(2) The calculation using Eq. 2 gives a quantitative account of the data. This is somewhat surprising in view of our rather schematic and approximate implementation of the MSCE theory. We would have regarded even qualitative agreement between the data and the calculation as confirmation of the usefulness of the MSCE theory in this situation.

---

1. Engineering Physics and Mathematics Division, ORNL.

2. Computing and Telecommunications Division, ORNL.
3. Grand Accelerateur National d'Ions Lourds, 14021 Caen Cedex, France.
4. Centre d'Etudes Nucleaires de Saclay, 91191 Gif-sur-Yvette Cedex, France.
5. Centre de Recherches Nucleaires, 67037 Strasbourg Cedex, France.
6. University of Illinois, Champaign, IL 61820.

7. J. R. Beene et al., Phys. Lett. B164, 19 (1985).
8. J. R. Beene, F. E. Bertrand, and R. L. Varner, Nucl. Phys. A482, 407c (1988).
9. H. Dias et al., Phys. Lett. 173B, 355 (1985).
10. H. Dias, M. S. Hussein, and S. K. Adhikari, Phys. Rev. Lett. 57, 1998 (1986).
11. J. R. Beene et al., submitted to Physical Review C.
12. H. Feshbach, A. Kerman, and S. Koonin, Ann. Phys. 125, 429 (1980).
13. M. Hussein and K. McVoy, Phys. Rev. Lett. 43, 1645 (1979).
14. J. R. Beene et al., Phys. Div. Prog. Rep. for Period Ending Sept. 30, 1987, ORNL 6420, p. 41.
15. P. A. Moldauer, Phys. Rev. C 11, 426 (1975).
16. F. E. Bertrand et al., "A Photon Decay Study of the Isovector Giant Quadrupole Resonance in ^{208}Pb," this report.

STUDY OF THE BREATHING MODE OF ^{208}Pb THROUGH NEUTRON DECAY[1]

A. Bracco[2], J. R. Beene, N. Van Giai[3], P. F. Bortignon[4], F. Zardi[5], R. A. Broglia[6]

The neutron decay of the giant monopole resonance region between 13 and 15 MeV in ^{208}Pb is analyzed in terms of collective and statistical doorway states. The direct escape widths of the giant monopole resonance populating the lowest five valence hole states of ^{207}Pb are determined, and compared with the results obtained from complex collective states. This comparison discriminates sharply between different model Hamiltonians which predict similar energies and collectivities for the resonance.

---

1. Abstract of published paper: Phys. Rev. Lett. 60, 2603 (1988).
2. Universita di Milano and Istituto Nazionale di Fisica Nucleare, I-20133 Milano, Italy.
3. Institut de Physique Nucleaire, F-91406 Orsay Cedex, France.
4. Centro Studi Nucleari Enrico Fermi, Politecnico di Milano, I-20133 Milano, Italy.
5. Istituto Nazionale di Fisica Nucleare, I-35131 Padova, Italy.
6. Universita di Milano, I-20133 Milano, Italy, and the Niels Bohr Institute, Copenhagen, Denmark.

COULOMB EXCITATION OF GIANT RESONANCES IN ^{208}Pb BY E = 84 MeV/NUCLEON ^{17}O PROJECTILES[1]

J. Barrette[2], N. Alamanos[2], F. Auger[2], B. Fernandez[2], A. Gillibert[2], D. J. Horen, J. R. Beene, F. E. Bertrand, R. L. Auble, B. L. Burks, J. Gomez del Campo, M. L. Halbert, R. O. Sayer, W. Mittig[3], Y. Schutz[3], B. Haas[4], J. P. Vivien[4]

Inelastic scattering of 84 MeV/nucleon ^{17}O on ^{208}Pb has been measured between $1.5° < \theta CM < 5.0°$. The giant resonance structure near 12 MeV is excited with a differential cross section of more than 2b/sr and exhibits a peak-to-continuum ratio as large as 6 to 1. The major part of the cross section can be ascribed to Coulomb excitation of the isovector giant dipole and the giant quadrupole resonance. From the Coulomb excitation of the GQR we deduce a $B(E2)\uparrow = 0.53 \pm 0.11$ $e^2 b^2$ which is that expected for a nearly pure isoscalar resonance which exhausts ≈60% of the EWSR.

---

1. Abstract of published paper: Phys. Lett. B209, 182 (1988).
2. Centre d'Etudes Nucleaires de Saclay, 91191 Gif-sur-Yvette Cedex, France.
3. Grand Accelerateur National d'Ions Lourds, 14021 Caen Cedex, France.
4. Centre de Recherches Nucleaires, 67037 Strasbourg Cedex, France.

ELECTROMAGNETIC DECAY OF THE GIANT RESONANCE REGION IN ^{209}Bi

R. L. Varner, R. L. Auble, J. R. Beene, F. E. Bertrand, B. L. Burks[1], M. L. Halbert, D. C. Hensley, D. J. Horen, R. L. Robinson, R. O. Sayer[2]

We have made a series of measurements of the absolute cross section for the ground-state electromagnetic decay of nuclei excited into their giant resonance region by the inelastic scattering of approximately 23-MeV/nucleon ^{17}O ions. The nuclei studied so far are ^{208}Pb (Ref. 3), ^{90}Zr (Ref. 4), and ^{209}Bi; this is a report on the work with ^{209}Bi.

Our interest in the ^{209}Bi system arose because of the unusual properties of the gamma decay in ^{208}Pb, in which the cross section is much larger than can be accounted for by direct giant resonance decays alone. This discrepancy can be understood in terms of the multistep theory of nuclear reactions. We should consider photon decay not only from the initial (doorway) stage, i.e., the coherent giant resonance state, but also from subsequent stages, including the fully damped compound nuclear states into which the resonance strength is eventually mixed. In the case of ^{208}Pb, the small neutron decay widths of the compound states, resulting from the low density of final states in ^{207}Pb, lead to unusually large compound contributions to the photon decay.[5] The ^{209}Bi system provides a contrast with ^{208}Pb in that it has a much higher density of final states for neutron decay than ^{208}Pb, yet should have nearly identical direct decay properties for the giant resonances.

The ^{209}Bi measurement was performed using basically the same setup as in the earlier ^{208}Pb experiment, using a 2.3 mg/cm^2 target and a 376-MeV ^{17}O beam. We attempted to enrich the data on-line, chiefly by eliminating events in which the total gamma energy was below the excitation energy by more than the neutron separation energy and by scaling down counts in the elastic scattering peak. Better hardware in the Spin Spectrometer interface permitted much more accurate and stable application of this technique than in the earlier ^{90}Zr measurement. As a check on this experiment we measured the same decays using a 3.7 mg/cm^2 target of ^{208}Pb in an otherwise identical setup.

We measured the excitation cross section of the giant quadrupole resonance (GQR) at 10.7 MeV to be 40 mb/sr at a lab angle of 13°, consistent with 80% of the sum rule in ^{209}Bi. This is quite similar to GQR yields measured[6] in ^{208}Pb, as we would expect. There is additional excitation cross section at 13.5 MeV of about 10 mb/sr, consistent with 100% sum rule depletion of both the giant dipole and giant monopole resonances (GDR and GMR).[6]

In Fig. 2.4 we show the ground-state electromagnetic decay cross section from the giant resonance region, including calculations of that decay using the program ONESTEP.[5] The calculations shown are made in a parameter-free model of the multistep decay, assuming that all gamma decays result from either the doorway giant resonance or the fully equilibrated compound nucleus. As can be seen, the data show little evidence of any decays except dipole decays from the doorway GDR, whose gamma branching to the ground state is dramatically larger than that of the GQR. At this time we think that the normalization of the cross sections may be uncertain by 20%. Work is now in progress to improve the normalization uncertainty and refine the calculations.

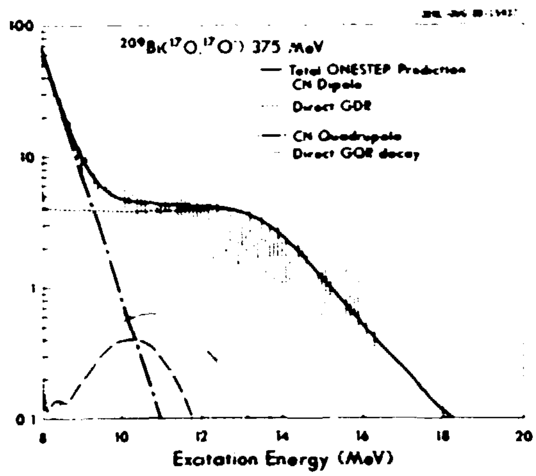

Fig. 2.4. Cross section for gamma decay of the giant resonance region in ^{209}Bi. The curves are from calculations with ONESTEP.

---

1. Engineering Physics and Mathematics Division, ORNL.
2. Computing and Telecommunications Division, ORNL.
3. J. R. Beene et al., submitted to Physical Review C.
4. R. L. Varner et al., Phys. Div. Prog. Rep. for Period Ending Sept. 30, 1986, ORNL-6326, p. 26.

5. J. R. Beene, Phys. Div. Prog. Rep. for Period Ending Sept. 30, 1987, ORNL-6420, p. 44.
6. T. P. Sjoreen et al., Phys. Rev. C 29, 1370 (1984).

ISOLATION OF THE ISOVECTOR QUADRUPOLE RESONANCE IN ^{208}Pb VIA PHOTON DECAY

F. E. Bertrand, J. R. Beene, R. L. Auble, M. L. Halbert, D. C. Hensley, D. J. Horen, Y. Schutz[1], W. Mittig[1], J. Barrette[2], B. Fernandez[2], F. Auger[2], N. Alamanos[2], A. Gillibert[2]

For the electric giant resonances there is presently a great deal of systematic data on the isoscalar modes, quadrupole (ISGQR), monopole (ISGMR), and octopole (ISGOR), and some information on the isoscalar hexadecapole (ISGHR) and isoscalar dipole resonances. There is, however, very little firm information on the electric isovector modes, other than for the long-established isovector giant dipole (IVGDR) and the isovector giant monopole resonances. This dearth of information on the isovector electric resonances arises from several factors. First, the excitation of isovector states in direct nuclear reactions is much weaker than for isoscalar resonances. Second, direct reactions, in general, are not multipole-selective and thus excite many giant resonances, leading to a very complicated resonance structure that is difficult to unfold and interpret. Third, the isovector electric resonances are expected to be located at higher excitation energies and to be broader than their isoscalar counterparts, thus making their observation above the underlying continuum more difficult. Finally, in general the continuum underlying the giant resonances is at best comparable to the size of the isoscalar quadrupole and would be much larger than the cross section for an isovector resonance at twice the isoscalar excitation energy. This would greatly increase the difficulty of observing a broad, weakly excited resonance at high excitation energy.

In a recent paper[3] by Speth et al., it was pointed out that the photon decay of the isovector giant quadrupole (IVGQR) in ^{208}Pb should proceed very strongly via a branch to the 2.618-MeV, 3- state. This is in marked contrast to the measured[4] and calculated[3,5] photon decay of the isoscalar giant quadrupole resonance (ISGQR) which shows no decay to the first 3$^-$ state in ^{208}Pb. The calculation[3] suggests a branch to the 2.618-MeV state that is ~1.8 times larger than the branch to the ground state with an overall ratio of gamma to neutron emission of ~10^{-3} for the IVGQR. For this reason, detection of the photon decay from the expected excitation energy region of the IVGQR may provide a means to isolate this state from the excitation of other resonances and the underlying continuum in the same excitation energy region.

We have carried out experiments using the 84-MeV/nucleon ^{17}O beam from the GANIL accelerators in Caen, France. At these beam energies, Coulomb excitation dominates the cross section for the IVGQR. Oxygen-17 was used because its low neutron separation energy (about 4 MeV) minimizes the contribution to the inelastic scattering spectra from such processes as projectile excitation and nucleon pickup and subsequent decay. Inelastically scattered particles were detected in the magnetic spectrograph facility SPEG with an energy resolution of about 800 keV and unit mass separation. The spectrograph was set to accept events in the angular range from 1.5 to 5.0 degrees. The vertical acceptance was 45 mrad.

Photons in coincidence with inelastically scattered ^{17}O were detected in 99 BaF_2 detectors arranged in clusters of 19 (x clusters) or 7 (y clusters) detectors. The detectors in the y clusters were right hexagons with face-to-face dimension of 8.7 cm and length 14 cm, while those in the x clusters were 5.7- by 20-cm-long. The clusters were placed at angles (θ,ϕ) of (70,172), (138,30), (138,50), (109,68), (109,187), (109,232), (109,352), and (109,111) degrees, where (0,0) was the beam direction and the inelastically scattered particles were detected in the ϕ = 180° half-plane. Pulse heights and times relative to the cyclotron rf were stored for each of the detectors along with the data from SPEG. Neutrons were identified and separated from photons by time of flight using pulse height (energy) dependent time gates. The photon time resolution at fixed pulse height was less than 800 ps for pulse heights corresponding to 2 MeV or more. Pulse shape identification was used for charged particle rejection. Each detector cluster was treated as a single detector by summing the individual pulse heights to produce a total pulse height, subject to the condition that the central detector (y clusters) or the sum of the pulses from the central seven detectors (x clusters) accounted for > 50% of the total. Energy and efficiency calibrations were made using radioactive sources (up to photon energy of 4.42 MeV) and on-line data for the 2.613-, 4.085-, and 5.512-MeV states in ^{208}Pb which decay by emission of a single photon to the ground state. The results were extrapolated to higher energy using simulations based on the computer code GEANT.

Photons were measured in coincidence with inelastic scattering for the entire excitation energy region studied, ~1-40 MeV. For the detection of the IVGQR, triple coincidences were utilized between the inelastically scattered ^{17}O ion, a photon of energy 2.61 MeV, and a photon having energy greater than 10 MeV. Use of the triple coincidence insured observation of photon decays directly from the region of the IVGQR to the 2.61-MeV state rather than via a cascade through intermediate states.

Typical gamma widths for E1 decays are orders of magnitude greater than those for other multipolarity for photons of these energies. Thus, contributions to the triple coincidence data from states other than 2^+ or 4^+ in the 20-MeV region is negligible. We do not expect to find $T = 0$, 2^+ strength in that region since such strength is fully accounted for at lower energies. In the case of 4^+ strength, we first point out that isovector 4^+ strength should be located at much higher excitation energies and will undoubtedly be very spread out. It is much more likely that isoscalar 4^+ strength may be located in the region of 20 MeV. Since L = 4 strength can be located at $0\hbar\omega$, $2\hbar\omega$, and $4\hbar\omega$, it is unlikely that more that 50% of the isoscalar 4^+ strength would be found near 20 MeV ($4\hbar\omega$). If it is assumed that 50% of the $T = 0$, 4^+ strength is found at 20 MeV of excitation energy, we calculate a maximum differential cross section for the L = 4 strength (3 deg.) to be about five times less than the expected cross section for 100% of the IVGQR cross section. Furthermore, as is shown in Ref. 3, we expect a very large suppression of the photon decay between an isoscalar giant resonance state and the low-lying isoscalar, 2.61 MeV, state in ^{208}Pb. Another possible important source of background which is very effectively suppressed by the coincidence with 2.61-MeV photons is that due to complex reaction processes producing multiparticle final states. The simultaneous detection of the ^{17}O ejectile and the ^{208}Pb 2.61-MeV photons uniquely identifies the two-body final state. For these reasons we feel that the photons detected in the triple coincidence measurements are dominated by transitions from the isovector giant quadrupole resonance to the 2.61-Mev, 3^-, level in ^{208}Pb.

The histogram in Fig. 2.5 shows the yield of photons from the triple coincidence data, where

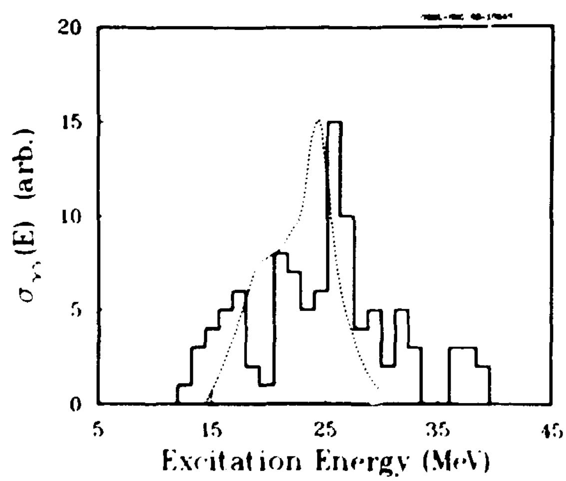

Fig. 2.5. The histogram shows the measured relative distribution of $\gamma\gamma$ coincidence yield (E_γ > 10 MeV, E_γ = 2.6 MeV) as a function of excitation energy, subject to the conditions discussed in the text. The dashed curve is the IVGQR spectrum predicted by the calculation in Ref. 9.

$E_{\gamma 1} + E_{\gamma 2} \sim E^*$ and $E_{\gamma 1} = 2.6$ MeV. There are a total of 109 events in this spectrum which were accumulated during about 128 hours of beam time. For reasons detailed in the preceding paragraph, we attribute this spectrum to the IVGQR. Although the counts are few, the results are very clean and yield the values for the centroid, width (sigma), and strength of the IVGQR as shown in Table 2.1. Also shown in Table 2.1 are results from two inelastic electron scattering measurements,[6,7] a recent observation[8] from the (γ,n) reaction, and RPA calculations.[9] We also measure the ground-state photons from the same region of excitation energy in ^{208}Pb and find a ratio of ground-state photon decay to photon decay through the 2.61-MeV, 3^- state to be approximately one. The calculations of Ref. 3 indicate a branching ratio between ground state photons and photons through the 2.61 MeV level of about 0.5. Considering the uncertainty due to the low number of counts in our data, we do not consider the difference between the calculation and the measurement to be significant. The ground state decay from this region is likely to contain a large contribution from the tail of the IVGDR. We hope to estimate the relative contributions using gamma-ray angular correlations.

The curves in Fig. 2.5 show the strength distribution for the IVGQR calculated by Bortignon et al.[9]

---

1. Grand Accelerateur National d'Ions Lourds, 14021 Caen Cedex, France.
2. Centre d'Etudes Nucleaires de Saclay, 91191 Gif-sur-Yvette Cedex, France.

3. J. Speth et al., Phys. Rev. C 31, 230 (1985).
4. J. R. Beene et al., submitted to Physical Review C.
5. P. F. Bortignon, R. A. Broglia, and G. F. Bertsch, Phys. Lett. 148B, 20 (1984).
6. M. Nagao, Y. Torizuka, Phys. Rev. 302, 1068 (1973).
7. R. Pitthan, F. R. Buskirk, E. B. Dally, J. N. Dyer, and X. K. Maruyama, Phys. Rev. Lett. 33, 849 (1974); erratum, Phys. Rev. Lett. 34, 848 (1975).
8. T. Murakami, I. Halpern, D. W. Storm, P. T. Debevec, L. J. Morford, S. A. Wender, and D. H. Dowell, Phys. Rev. C 35, 479 (1987).
9. P. F. Bortignon, private communication.

HEAVY-ION COULOMB EXCITATION AND PHOTON DECAY OF THE GIANT DIPOLE RESONANCE IN ^{208}Pb[1]

J. R. Beene, F. E. Bertrand, D. J. Horen, R. L. Auble, B. L. Burks[2], J. Gomez del Campo, M. L. Halbert, R. O. Sayer[3], W. Mittig[4], Y. Schutz[4], J. Barrette[5], N. Alamanos[5], F. Auger[5], B. Fernandez[5], A. Gillibert[5], B. Haas[6], J. P. Vivien[6]

Measurements are presented of the photon decay of the isovector giant dipole resonance in ^{208}Pb following Coulomb excitation by 84-MeV/nucleon ^{17}O. By studying the angular correlation between ^{17}O ions and single photons to the ground state we are able to isolate the

Table 2.1. Isovector giant quadrupole resonance ^{208}Pb

	Present Experiment $(^{17}O,^{17}O'\gamma\gamma)$	Bortignon[9] Calculation	(γ,n)[8] Forward/ Backward Asy.	(e,e')[6]	(e,e')[7]
Centroid (MeV)	22.6 ± 0.4	22.4	23.5 ± 1.5	~22	22.5
Width (MeV)	6 ± 2	3.6			5 ± 1
EWSR (%)	~50%	61		60 ± 25	85 ± 28

IVGDR without elaborate peak fitting or background subtraction. The angular correlations and yields are accounted for quantitatively by a pure Coulomb excitation model of the reaction process. The distribution in energy of the ground-state photon decay cross section is well described by an approximate application of the multistep theory of nuclear reactions. Use of the shape of the dipole resonance obtained in the photon decay measurements leads to the extraction of differential cross sections for the isoscalar giant quadrupole and monopole resonances with low uncertainty.

---

1. Abstract of paper submitted to Physical Review C.
2. Engineering Physics and Mathematics Division, ORNL.
3. Computing and Telecommunications Division, ORNL.
4. Grand Accelerateur National d'Ions Lourds, 14021 Caen Cedex, France.
5. Centre d'Etudes Nucleaires de Saclay, 91191 Gif-sur-Yvette Cedex, France.
6. Centre de Recherches Nucleaires, 67037 Strasbourg Cedex, France.

SEARCH FOR THE TWO OCTUPOLE PHONON STATES IN ^{208}Pb

J. R. Beene, M. L. Halbert, A. D'Onofrio[1], R. L. Varner, R. L. Auble, D. J. Horen, F. E. Bertrand, J. Lisantti[2], R. T. VanHook[3]

The description of nuclear states in terms of elementary degrees of freedom has been of great importance in the development of our understanding of nuclear structure. Quadrupole and octupole surface vibrations are examples of elementary modes which have been most successfully applied in many nuclei. It is surprising and troubling that one of the most collective vibrational states known, the 2.6-MeV, 3^- state in ^{208}Pb, has not yet provided, in spite of extensive searches, a clear indication that it produces a two-phonon excitation.[4,5]

As a by-product of our studies of giant resonance gamma decay using the ^{208}Pb(^{17}O,^{17}O'γ) reaction at 22 MeV/nucleon and the Spin Spectrometer, we uncovered less than definitive indications that the two octupole phonon multiplet might be excited with reasonable cross section by this reaction.[6] Based on this tempting but equivocal result, we recently carried out a high resolution experiment to search for these states. The experiment again employed the ^{208}Pb(^{17}O,^{17}O'γ) reaction at 22 MeV/nucleon, but scattered ^{17}O ions were detected in the HHIRF Broad Range Spectrograph (BRS) in coincidence with gamma rays detected in 18 Compton-suppressed Ge detectors in the newly available stand-alone configuration. The BRS was specially modified to make it more easily used in this and other gamma ray coincidence experiments. These modifications included removal of the quadrupole lens at the entrance to the spectrometer and the construction of a new, small scattering chamber about 50 cm upstream of the normal BRS target position. These changes allowed the Compton suppression array to be positioned around the target in its normal configuration and made room for a beam dump/Faraday cup to be constructed, and surrounded by borated paraffin and lead, at a distance from the Ge detectors such that radiation from the beam dump was not a significant problem. In spite of this unusual configuration, the BRS, with its focal plane counter based on the vertical drift chamber,[7] produced more than adequate resolution (< 300 keV at 375 MeV).

Data analysis is still in the preliminary stages, and no firm conclusions can be drawn as yet. It is already clear that (as anticipated) the experiment suffers from a low coincidence efficiency and consequently poor statistics. Nevertheless, if the excitation cross sections (1 to 5 mb/sr) inferred from the earlier Spin Spectrometer data prove to be correct, a definitive assignment of at least some states of the multiplet should be possible.

---

1. Joint Institute for Heavy Ion Research and Instituto Nazionale di Fisica Nucleare, Napoli, Italy.
2. Partial support from the Joint Institute for Heavy Ion Research, ORNL.
3. Oak Ridge Science and Engineering Research Semester Participant from Hendrix College, Conway, AR 72032.

4. P. Curutchet et al., Phys. Lett. 208B, 331 (1988).
5. P. Schuck, Z. Physik A279, 31 (1976).
6. J. R. Beene et al., p. 503 in Proceedings of Niels Bohr Centennial Conference on Nuclear Structure, eds. R. Broglia, G. Hagemann, and B. Herskind (North Holland, Amsterdam, 1985).
7. T. P. Sjoreen et al., Nucl. Instrum. Methods Phys. Res. 224, 421 (1984) and M. V. Hynes et al., Nucl. Instrum. Methods Phys. Res. 224, 89 (1984).

INELASTIC SCATTERING OF ^{16}O ON ^{58}Ni AND $^{70,72,74}Ge$

D. C. Hensley, F. E. Bertrand, E. E. Gross, J. R. Beene, M. L. Halbert, G. Vourvopoulos[1]

A study of the inelastic scattering of 75-MeV ^{16}O on various isotopes of Ge has been conducted in order to study the properties of the first 2^+ and first 4^+ states in these nuclei. It was felt that these nuclei represented an interesting challenge for the technique of measuring inelastic scattering in the Spin Spectrometer. Nickel-58 was added to the list since it was a case that had been studied previously with it as the projectile. Lead-208 was studied briefly to provide a direct means of calibrating the detectors.

Thorough measurements of the charged particle scattering of ^{16}O on the various targets were conducted in the large scattering chamber with a single position-sensitive detector (PSD). The silicon PSD was 8 mm high and 47 mm long with a fully depleted depth of 500 microns. It was fronted by a rectangular collimator with wire defining slits which separated the detector into 14 roughly equal area slices. The detector was positioned so that it spanned about 9 degrees. Measurements were taken on all targets from a central setting of 15° (most forward slit at 9°) out to a setting of 50°. The ^{208}Pb data were extended out to a 65° setting. Extensive left, right measurements were taken in order to determine precisely the zero point of the angle scale. This entire data set has been processed to provide gain-corrected energy projections from all of the slices, for all of the settings. Special corrections were made to the data because, near the end of the experiment, the position signal was found to be wandering. The energy projections are being analyzed to extract the full angular distributions.

The scattering measurements were then moved to the Spin Spectrometer where three PSDs were used for charged particle detection. Two 27-mm-long detectors were positioned with their centers at 20° and 45°, respectively, and a 47-mm-long PSD was positioned with its center at 35°. This setup provided charged particle detection from 14° to 53°; the grazing angle was near 30°. These detectors were run in coincidence with the 70 NaI detectors of the Spin Spectrometer, and the coincidence events were stored on tape. Approximately 12 hours of beam on target was run for each of the light targets. The beam current was held to under 10 nA so that the trigger rate in the most forward detector was of the order of 6000 counts per second. The two other detectors then had typical rates of 1000 and 100, respectively. The NaI gamma-ray rates ranged from 10 kHz to 20 kHz.

A preliminary scan of the data indicates that the yield for the first 4^+ state and additional excited states will be adequate for detailed analysis. There is a moderate excitation of the ^{16}O projectile to its first few excited states near 6 MeV. Analysis of all of the data is continuing both at HHIRF and at Western Kentucky University.

---

1. Western Kentucky University, Bowling Green, KY 42101.

DETERMINING THE EXPERIMENTAL GEOMETRY FOR INELASTIC SCATTERING IN THE SPIN SPECTROMETER

D. C. Hensley

In the study of inelastic scattering of heavy ions on ^{208}Pb in the Spin Spectrometer, a continuing source of uncertainty in the method pertains to the determination of the absolute normalization and angles for the various measured angular distributions. An uncertainty of 5% or less in the absolute normalization and 0.1 degrees or less in the angles is needed for this study to be uniquely useful. But the detector mounts and target holder hardware in the 17-cm-radius scattering chamber in the spectrometer make it difficult to fix precisely the location of the beam spot and the positions of the detectors. Further, since we use position sensitive detectors (PSD) without special geometry determining collimators, the relation between angle and position channel for a given detector is difficult to determine. A technique has been developed which appears to establish a very low uncertainty in both the absolute normalization and the angles.

First, the "raw elastic" spectrum is measured in the 1.6-m scattering chamber with a PSD fronted by a geometry defining collimator. The "raw elastic" refers to the yield measured within an energy gate on the scattering which includes all of the elastic and essentially all of the scattering to the first 2^+ state of the projectile. Normally the first 2^+ state is poorly, if at all, resolved in the bare silicon detectors, and smaller uncertainties in determining the yield are incurred by studying the composite peak. Vertical wires divide the detector into 14 fixed angle bins. The relative angles of these wires were determined using the precision goniometer of the 1.6-m chamber to rotate the detector while viewing the wires with a transit. Data were then measured to as small an angle as possible, about 10° in the lab, and several measurements were made, both beam left and beam right, to establish the zero angle with respect to the beam. Finally, measurements are made at angles as far beyond the grazing angle as is practical.

After the relative efficiencies of the 14 slits and the absolute angles were determined for the data sets, the overall normalization was fixed by requiring that the average ratio to Rutherford of the scattering from 10° through 29° in the lab be equal to one. This normalization procedure essentially circumvents knowing the geometry, the target thickness, and the integrator calibration. The final angular distribution thus determined has an uncertainty of less than 2% in the absolute normalization and an uncertainty of less than 0.5 degrees in the angle scale.

The same "raw elastic" yield was extracted for two PSD detectors mounted in the scattering chamber of the Spin Spectrometer. These two spectra of "raw elastic" yield were then compared with the distribution determined in the large scattering chamber. What is not known is the detailed dependence of lab angles and efficiencies on position channels for the two PSD detectors in the Spin Spectrometer.

The technique for accurately determining the geometry assumes that there is a linear relationship between position channel and distance along the detector. The precise raw-elastic angular distribution determined in the 1.6-m scattering chamber was first transformed to take into account all of the known geometry of the spectrometer PSDs and was then renormalized to best fit the differential raw elastic yield. The fitting procedure automatically determines the two coefficients required to provide the best linear relation between channel number and distance along the detector. The procedure works so well that it was immediately obvious in the Spin Spectrometer data that the two PSDs have a slightly nonlinear dependence of distance on position channel. The following formula was then tried and appeared to give very good results:

$$X = X_0 + \delta*\text{Chan} + \varepsilon*(\text{Chan}-\text{Chan}_z)^2$$

where the third term, involving ε, is zero unless $\text{Chan}>\text{Chan}_z$.

A least squares search was made for the values of X_0, δ, ε, Chan_z, and the normalization which gave the best fit to one of the spectra. Figure 2.6 shows the best fit to the spectrum for the second detect whose angle range included the grazing angle. The bump in the center of the spectrum indicates the position of the grazing angle. The dots belong to the Spin Spectrometer spectrum and the nearly solid line corresponds to the transformed raw elastic angular distribution.

The fit in Fig. 2.6 is uniquely determined because of the grazing angle bump. The fit to

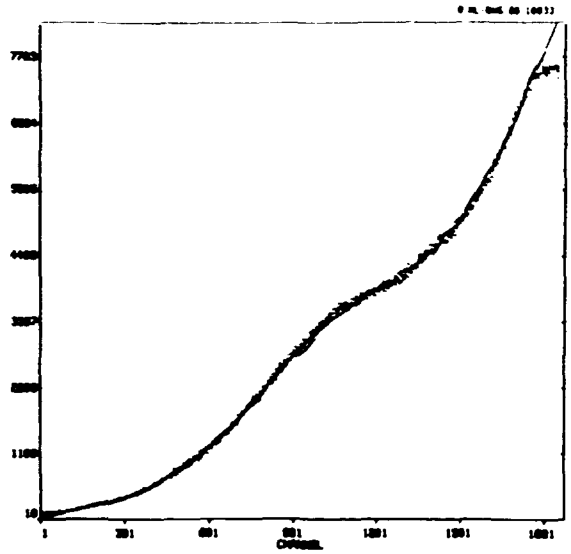

Fig. 2.6. Spectrum of "raw elastic" yield (dots) measured in the Spin Spectrometer compared to the transformed raw elastic angular distribution (solid line) determined from the 1.6-m chamber data. The bump in the center of the spectrum corresponds to the position of the grazing angle.

the spectrum for the forward detector is not uniquely determined as its spectrum has no unusual identifying features, hence some additional information was applied to the fitting procedure. There is about a 0.4 degree overlap in angle of the two detectors, and in this overlap region it is possible, by using the gamma ray detecting capability of the Spin Spectrometer, to find the ratio of the yield of the raw elastic to that of the first 2^+ state as a function of channel for both detectors. This ratio should be independent of any differences between the two detectors and should be a unique function of angle because of the fast decrease of the elastic scattering with angle. By comparing the two resulting sets of ratios, it was possible to reference a channel of the forward detector to that of a channel in the back detector for which the corresponding angle could be determined. The best values for the various parameters were then obtained for the spectrum for the forward detector while holding the value of the angle for the reference channel fixed.

It was found that both of the detectors were essentially linear over more than 75% of their range and the nonlinearity for both detectors was fairly small. (Note that any nonlinearity in the PSD used in the 1.6-m chamber could be totally ignored since the wire mask in front of the detector determined the geometry, irrespective of the response of the detector.) The absolute normalization for the two spectra turned out to agree within 1%, and were within a few percent agreement with that for the angular distribution determined in the 1.6-m scattering chamber. The latter few percent difference is easily attributable to the fact that two similar ^{208}Pb targets were used in the two different phases of the experiment, and while they had the same nominal thickness, a few percent variation between the two targets should be expected.

As a check on the consistency of this fitting procedure, the results for the forward detector were also obtained by doing a least squares fit for just the linear region of the detector, but no angles and channels were fixed. The χ^2 values were somewhat flat but did yield two solutions. One fit essentially agreed with the fixed reference channel fit, and the other fit required a mere 0.17-degree shift for the reference channel.

Consequently, it is probable that the angle determination for the forward detector is uncertain to no more than 0.1 degrees, and the overall absolute normalization is uncertain to less than 2%. Because this normalization was obtained from about half of the data set, and since there was some small detector drift noted during the run, but corrected for, the final uncertainty for both detectors in the Spin Spectrometer in the absolute normalization is 4% and in the angles is 0.1 degrees.

ELASTIC AND INELASTIC SCATTERING OF 200 MeV ^{26}Mg FROM ^{208}Pb

E. E. Gross — F. E. Bertrand
D. C. Hensley — G. Vourvopoulos[1]
M. L. Halbert — D. Humphrey[1]
J. R. Beene — T. VanCleve[1]

Although the M(E2) systematics for 2^+ states of even-even nuclei are well established, and have recently been updated by Raman et al.,[7] the same is not the case for M(E4) matrix elements. These depend on direct excitation of low-lying 4^+ states, but such information is relatively scarce because cross sections are low and because the states are hard to resolve with conventional charged particle detectors. In the previous Progress Report,[3] we presented a method to overcome these difficulties by using the Spin Spectrometer in coincidence with position-sensitive solid-state particle detectors. The advantage of this technique is that the γ-ray detectors of the Spin Spectrometer provide the resolution while the particle detectors provide the information for the differential cross sections. With this technique, we have gathered differential cross section data on states excited by ~200 MeV beams of ^{24}Mg, ^{26}Mg, ^{28}Si, and ^{30}S scattered from a ^{208}Pb target. In the same Progress Report, we presented results[4] on the coupled channels analysis of the ^{24}Mg data as well as a cursory look at the ^{26}Mg data.[5]

The ^{26}Mg levels that we observe from 200-MeV ^{26}Mg scattering from a ^{208}Pb target are the ground state (elastic scattering), and the $2_1{}^+$ (1.87 MeV), $2_2{}^+$ (2.94 MeV), $4_1{}^+$ (4.32 MeV), and $4_2{}^+$ (4.90 MeV) excited states. This level scheme has been difficult to understand from the nuclear structure point of view particularly as to the nature of the second 2^+ state, i.e., whether or not this state can be attributed to a triaxial shape configuration for ^{26}Mg. Furthermore, it is not clear which of the two 4^+ states belong to the ground state rotational band. The present data and analysis make a contribution to the resolution of both questions. The differential cross section data were analyzed in rotational model-coupled channels using the program ECIS.[6]

The optical potential is most sensitive to elastic scattering data which is shown in Fig. 2.7 as a ratio to Rutherford scattering. The sum of elastic and inelastic scattering was normalized to Rutherford scattering for $\theta < 30°$ c.m. A "shallow" real potential, about 25 MeV, and a "deep" real potential, about 200 MeV, were tried, together with their corresponding imaginary potentials. They give the same results for both the fit to all the differential cross sections and for the values of the matrix elements. The fit to elastic scattering is shown as the solid curve in Fig. 2.7.

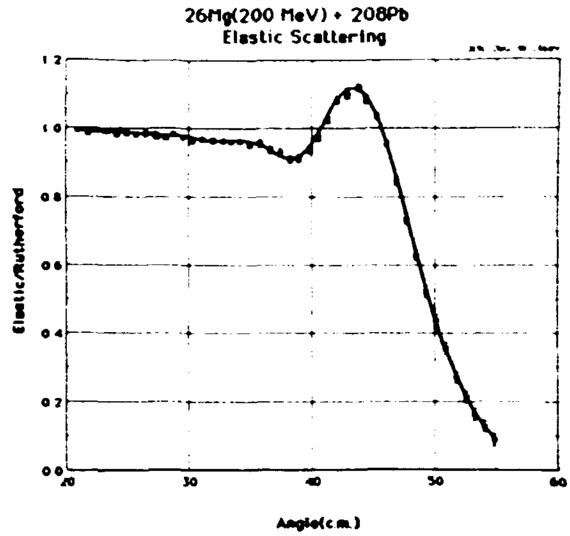

Fig. 2.7. Ratio of elastic scattering to Rutherford scattering for 200-MeV ^{26}Mg incident on a ^{208}Pb target. The solid curve results from a coupled channels fit.

The B(E2) to the first 2^+ state is most sensitive to the forward angle, Coulomb dominated, differential cross section. These data are shown in Fig. 2.8. We find that B(E2) = (253 ± 6) $e^2 fm^4$ provides the best fit, a value which is 20% smaller than the value quoted in the recent Nuclear Data Tables article.[2] The E2 reorientation matrix element, which is related to the static quadrupole moment, Q_2, is most dependent on the large angle $2_1{}^+$ cross section data which, in turn, depends on nuclear excitation as well as Coulomb excitation. In our analysis, the nuclear deformations are tied to the charge deformation by the Hendrie scaling procedure[7] and are, therefore, not treated as independent variables. From a fit to our data, the solid line in Fig. 2.8, we obtain a value Q_2 = (-11.4 ± 2) efm^2 which agrees with Coulomb reorientation measurements.[8,9]

The second 2^+ state at 2.94 MeV has often been attributed to a triaxial character for

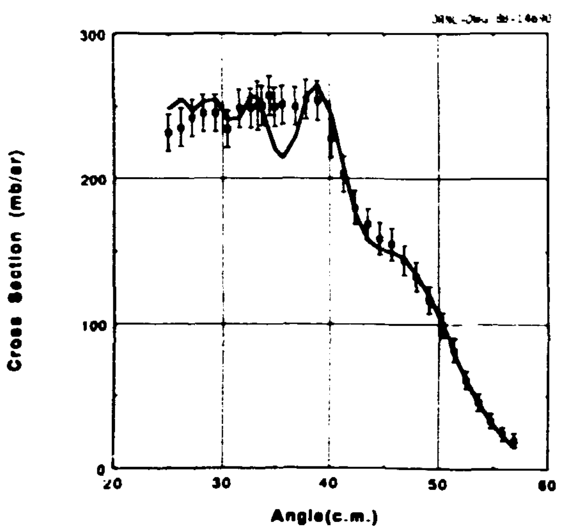

Fig. 2.8. Differential cross section for exciting the first 2^+ state (1.87 MeV) of ^{26}Mg from 200-MeV ^{26}Mg scattering from a ^{208}Pb target. The solid curve is a coupled-channels rotational-model fit.

^{26}Mg. However, a symmetric rotor model calculation, the solid curve in Fig. 2.9, gives a reasonable account of the measured differential cross section data. These data and analysis are sensitive to the sign of $p_3 = M(E2;0_1 \leftrightarrow 2_1)$

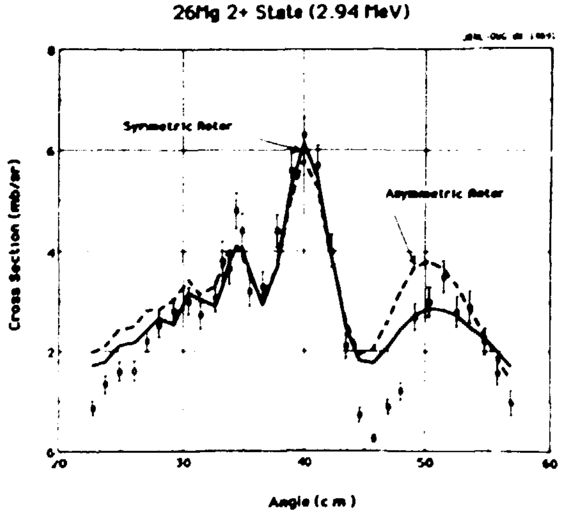

Fig. 2.9. Differential cross section for exciting the second 2^+ state (2.94 MeV) of ^{26}Mg from 200-MeV ^{26}Mg scattering from a ^{208}Pb target. The solid curve is a coupled-channels fit using rotational model form factors. The dashed curve is an asymmetric-rotor model fit.

$M(E2;0_1 \leftrightarrow 2_2)\ M(E2;2_1 \leftrightarrow 2_2)$; we find $p_3 > 0$ thus resolving a long standing ambiguity in Coulomb reorientation measurements[8,9] of Q_2. An asymmetric rotor calculation, shown as a dashed curve in Fig. 2.9, gives a fair representation of the shape of the differential cross section but with a χ^2 value a factor of four larger than the solid curve. Furthermore, the sign of the E2 matrix element between the two 2^+ states, $M(E2;2_1 \leftrightarrow 2_2)$, predicted by the asymmetric rotor model is opposite to the sign deduced from the symmetric rotor model fit and the predicted 4^+ cross section is a factor of three larger than either of the two 4^+ states observed. We conclude that the asymmetric rotor model is not a good representation of ^{26}Mg. The addition to the analysis of the third 2^+ state at 4.84 MeV had no noticeable affect on Q_2; however, the addition of a 2^+ state at 21 MeV (which would be the location of the GQR from simple systematics) with 60% of the sum rule strength, as indicated by the high resolution work of Bertrand et al.,[10] would increase Q_2 by 2-4% depending on the sign of the $2_1^+ \leftrightarrow$ GQR matrix element. This may be compared with the influence of the GDR which has been estimated[11] to decrease Q_2 by 0.5%.

The first 4^+ state (4.32 MeV) eludes description by the rotational model (shown as the solid curve in Fig. 2.10) especially as regards the data in the grazing angle region near 43°. The second 4^+ state at 4.90 MeV, however, is well described by the model as can be seen by the solid curve in Fig. 2.11. The dashed and dotted curves in Fig. 2.11 illustrate the sensitivity to the hexadecapole matrix element. These results are convincing evidence that the 4.90-MeV state is the member of the ground state rotational band and that the 4.32-MeV level is not a collective state.

---

1. Western Kentucky University, Bowling Green, KY 42101.
2. S. Raman, C. H. Malarkev, W. T. Milner, C. W. Nestor, and P.H. Stelson, Atom, and Nucl. Data Tables 36, 1 (1987).
3. Phys. Div. Prog. Rep. for Period Ending Sept. 30, 1987, ORNL-6420, p. 60.

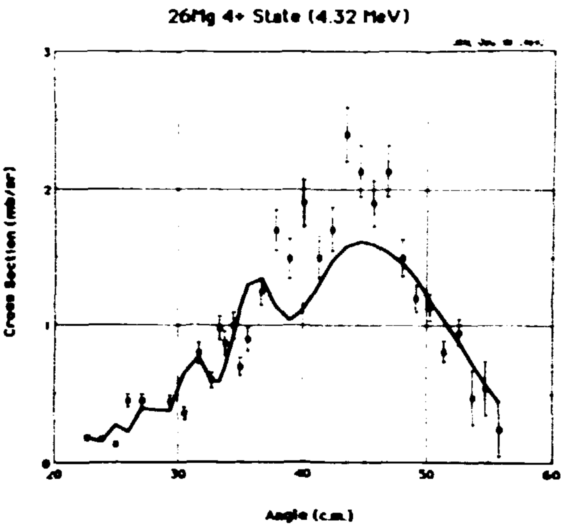

Fig. 2.10. Differential cross section for exciting the first 4^+ state (4.32 MeV) of ^{26}Mg from 200-MeV ^{26}Mg scattering from a ^{208}Pb target. The solid curve is the best fit obtainable assuming that this state belongs to the ground state rotational band.

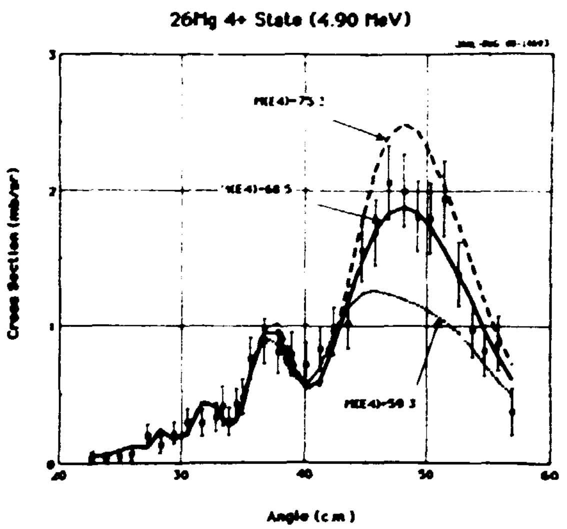

Fig. 2.11. Differential cross sect'on for exciting the second 4^+ state (4.90 MeV) of ^{26}Mg from 200-MeV ^{26}Mg scattering from a ^{208}Pb target. The solid curve is a coupled-channels fit using rotational model form factors. The dashed and dotted curves illustrate the sensitivity of the calculation to the $M(E4;0_1^+\to 4_2^+)$ matrix element.

4. Ibid., p. 65.
5. Ibid., p. 63.
6. J. Raynal, private communication.
7. D. L. Hendrie, Phys. Rev. Lett. 31, 478 (1973).

8. D. Schwalm, A. Bamberger, P. G. Bizzeti, B. Povh, G.A.P. Engelbertink, J. W. Olness, and E. K. Warburton, Nucl. Phys. **A192**, 449 (1972).
9. R. H. Speer, T. H. Zebel, M. T. Eset, A. M. Baxter, and S. Hinds, Nucl. Phys. **A378**, 559 (1982).
10. F. E. Bertrand, K. van der Borg, A. G. Drentje, M. N. Harakeh, J. van der Plicht, and A. van der Woude, Phys. Rev. Lett. **40**, 635 (1978).
11. M. P. Fewell, Ph.D. Thesis, The Australian National University, October 1978 (unpublished).

ASYMMETRIC ROTOR MODEL CALCULATIONS FOR ^{24}Mg

E. E. Gross — F. E. Bertrand
D. C. Hensley — G. Vourvopoulos[1]
M. L. Halbert — D. Humphrey[1]
J. R. Beene — T. VanCleve[1]

Symmetric rotor model calculations for 200-MeV ^{24}Mg + ^{208}Pb scattering reported in the previous Progress Report[2] provided satisfactory fits to elastic scattering and to inelastic excitation of the 2_1^+ (1.37 MeV), 4_1^+ (4.12 MeV), and 2_2^+ (4.24 MeV) states of ^{24}Mg. A few asymmetric rotor model analyses,[3,4] have been applied to previous ^{24}Mg data and several theoretical calculations,[5,6,7] have predicted triaxial shapes for this nucleus in order to account for the second 2^+ state. We therefore subjected our data to an asymmetric rotor model analysis using the generalization of the Davydov-Filippov model[8] due to Baker[9] who included hexadecapole deformation and a method for calculating the proper scaling for the nuclear β and γ parameters of the model. The best asymmetric rotor fit to the 2_2^+ state is shown as the dashed curve in Fig. 2.12 which has a χ^2 value five times larger than that for the symmetric rotor fit (the solid curve in Fig. 2.12). The asymmetric rotor fit to the first 2^+ state, shown as the dashed curve in Fig. 2.13, also has a χ^2 value five times larger than that for the symmetric rotor fit, shown as the solid curve in Fig. 2.13, primarily because it fails to provide the necessary amount of reorientation to account for the behavior of the large angle data. A further failure of the asymmetric rotor model for ^{24}Mg is the prediction that the product of the three matrix elements $M(E2;0_1^+\to 2_1^+)$

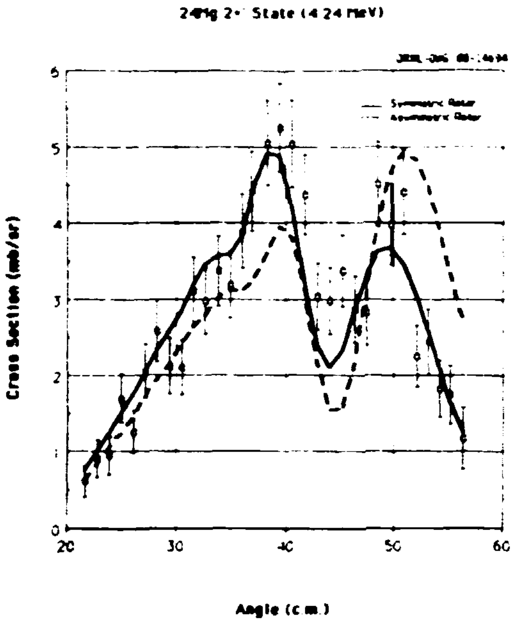

Fig. 2.12. Differential cross section for exciting the 2^+ state at 4.24 MeV in ^{24}Mg by 200-MeV ^{24}Mg scattering from a ^{208}Pb target. The solid curve is a coupled channels fit using rotational model form factors. The dashed curve is a coupled channels fit in the asymmetric-rotor model where the parameter γ of the model was adjusted to minimize χ^2.

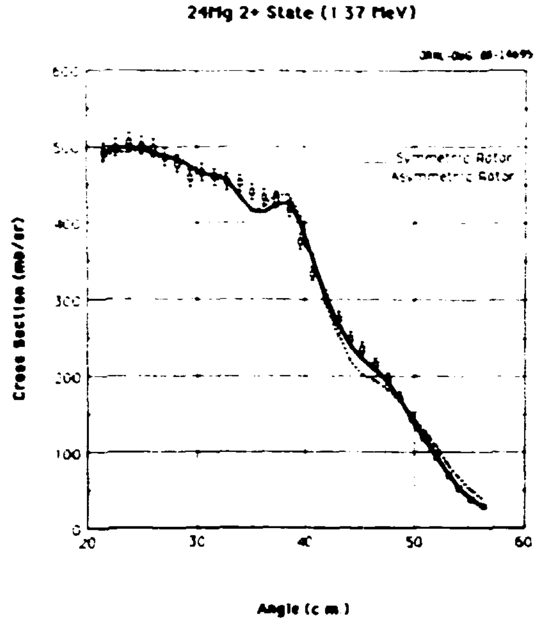

Fig. 2.13. Differential cross section for exciting the 2^+ state at 1.37 MeV in ^{24}Mg by 200-MeV ^{24}Mg scattering from a ^{208}Pb target. The solid curve is a coupled channels fit using rotational model form factors. The dotted curve is the asymmetric rotor model prediction corresponding to the fit to the second 2^+ state shown in Fig. 2.12.

$M(E2;0_1 \leftrightarrow 2_2)\ M(E2;2_1 \leftrightarrow 2_2)$ is less than zero, whereas the symmetric rotor model fit (the solid curve in Fig. 2.12) requires this product to be positive. We conclude that the asymmetric rotor model is not capable of representing the necessary matrix elements to fit this set of data.

---

1. Western Kentucky University, Bowling Green, KY 42101.
2. Phys. Div. Prog. Rep. for Period Ending Sept. 30, 1987, ORNL-6420, p. 65.
3. K. van der Borg, M. N. Harakeh, and B. S. Nilsson, Nucl. Phys. **A125**, 31 (1979).
4. J. Nurzynski, C. H. Atwood, T. R. Ophel, D.F. Hebbard, B. A. Robson, and R. Smith, Nucl. Phys. **A399**, 259 (1983).
5. D. Kurath, Phys. Rev. C **5**, 768 (1972).
6. G. Leander and S. E. Larsson, Nucl. Phys. **A239**, 93 (1975).
7. B. Grammaticos, Nucl. Phys. **A252**, 90 (1975).
8. A. S. Davydov and G. F. Filippov, Nucl. Phys. **8**, 237 (1958).
9. F. T. Baker, Nucl. Phys. **A331**, 39 (1979).

ANALYSIS OF ^{40}Ca(p,p') AT 500 MeV USING $t\rho$ OPTICAL POTENTIALS IN A COLLECTIVE FRAMEWORK[1]

K. H. Hicks[2]   J. Lisantti[3]

Inelastic scattering to the low-lying collective states in ^{40}Ca excited by 500-MeV protons is examined using both relativistic and nonrelativistic microscopic optical model potentials in the Tassie model. The nonstandard shapes produced by these microscopic models do not produce different deformation lengths than those obtained using standard Woods-Saxon shapes. For comparison, calculations using the distorted-wave impulse approximation are presented.

---

1. Abstract of published paper: Nucl. Phys. **A484**, 432 (1988).
2. TRIUMF, Vancouver, British Columbia, Canada V6T 2A3.
3. Partial support from Joint Institute for Heavy Ion Research, ORNL.

APPLICATION OF THE RELATIVISTIC COLLECTIVE MODEL TO INTERMEDIATE-ENERGY PROTON-NUCLEUS SCATTERING

J. Lisantti[1]

With the recent success of the use of the Dirac equation to describe the elastic scattering of intermediate energy protons from nuclei, it was only natural to extend this formalism to the study of inelastic scattering. As with the nonrelativistic formalism based on the use of the Schrodinger equation there are two different methods which have evolved in the use of the Dirac equation. One method is based on using the microscopic impulse approximation,[2] the other is to use the macroscopic deformed potential model.[3]

We have analyzed our 500-MeV $^{40}Ca(\vec{p},p')$ data using this latter method. The optical potentials used for the analysis come from Raynal[4] in which he observed that there is considerable ambiguity in the imaginary vector potential (W_V) in an analysis of data[5] which covered a limited angular range. Values ranging from 0 to -180 MeV gave good fits with the best results obtained for the range of -80 to -120 MeV. We have analyzed a set of data[6] which went to larger scattering angles than Ref. 5. Our results as calculated using the code ECIS87[7] are shown on Fig. 2.14 for two potentials labeled W_V = -80 MeV and W_V = -120 MeV in comparison to the elastic data of Ref. 6. Both potentials fit the data equally well. In order to investigate these potentials further, we then calculated the inelastic scattering cross sections and analyzing powers for the 3_1^- (3.736 MeV), 2_1^+ (3.904 MeV), and the 5_1^+ (4.49 MeV) states, using both of these potentials. The results of these calculations are shown in Fig. 2.15. The inelastic data shows no preference for either potential and in fact both potentials give the same deformation lengths as shown in Fig. 2.15. These deformation lengths are compared in Table 2.2. The relativistic model is higher for the 3_1^- and 5_1^- states than the nonrelativistic model, while both methods agree for the 2_1^+ state. The last column of Table 2.2 shows the average value of δ_{NR} obtained from various proton scattering experiments in the range of 25 to 800 MeV. We observe that the relativistic model gives higher values for the 3_1^- and 2_1^+ states but agrees for the 5_1^- state. Therefore, there appears to be no clear trend between the relativistic and nonrelativistic models as far as the deformation parameters are concerned for ^{40}Ca, and data for inelastic scattering show no preference for either of the relativistic potentials.

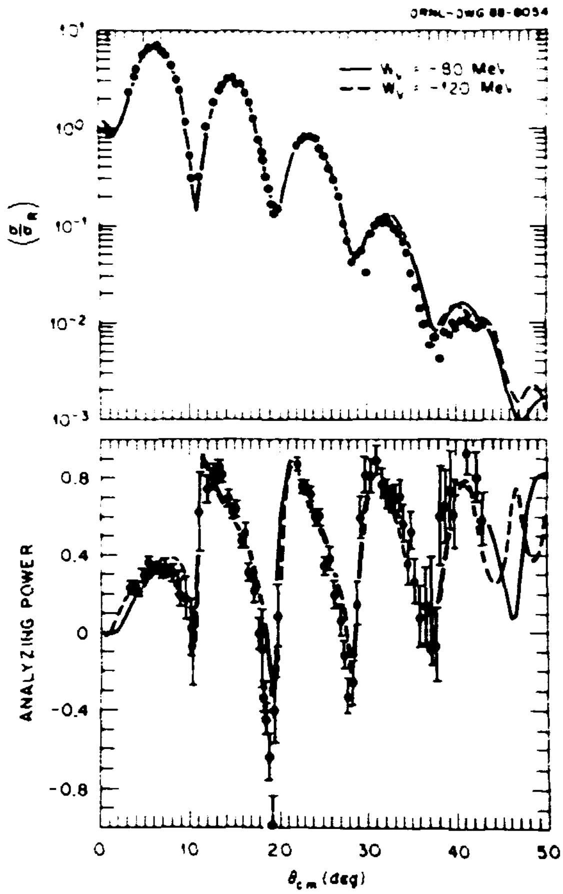

Fig. 2.14. Proton elastic scattering at 500 MeV. The data are from Ref. 6. The solid curve is the relativistic optical model fit for the imaginary vector potential having a depth of -80 MeV, while the dashed line is for -120 MeV.

A further application of the Dirac relativistic collective model has been to fit the optical potential parameters to 280- and 489-MeV proton elastic scattering data from ^{58}Ni. The

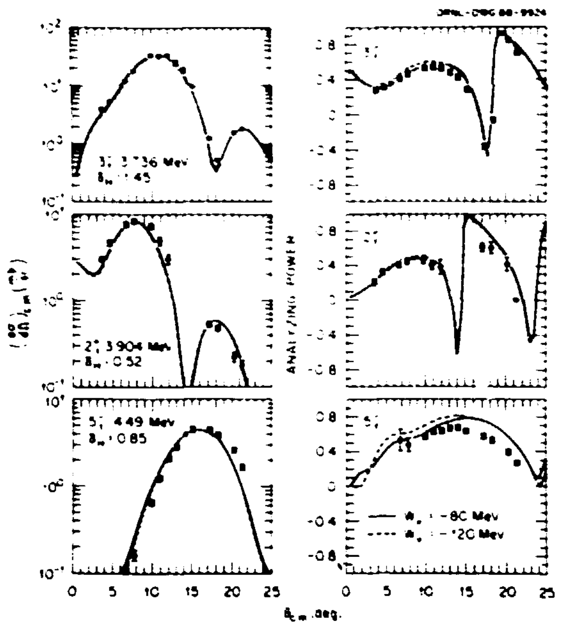

Fig. 2.15. Relativistic collective deformed potential calculations compared with 500 MeV $^{40}Ca(p,p')$ data. The solid curve is from the calculations using an imaginary potential of -80 MeV, while the dashed curve results from -120 MeV. The deformation lengths, δ_H, are also given.

Table 2.2. Hadronic deformation lengths obtained for states in ^{40}Ca using 500-MeV proton scattering. δ_R is the deformation lengths for the relativistic model, while δ_{NR} are the deformation lengths for the non-relativistic model, $\langle\delta_{NR}\rangle$ is the average value of δ_{NR} obtained from proton studies from 25 to 800 MeV.

State	δ_R	δ_{NR}	$\langle\delta_{NR}\rangle$
3_1^- 3.736 MeV	1.45±0.07	1.33±0.03	1.35±0.01
2_1^+ 3.904 MeV	0.52±0.03	0.50±0.03	0.44±0.01
5_1^- 4.49 MeV	0.85±0.04	0.69±0.03	0.83±0.01

fits obtained to the data are shown in another contribution to this report. The optical potentials obtained are given in Table 2.3. The fits again show no sensitivity to the imaginary vector part of the potential so the final values used are the same for both energies. These optical potentials were then used to calculate the inelastic scattering cross sections for a

Table 2.3. Relativistic optical model parameters obtained for 280- and 489-MeV $^{58}Ni(p,p)$ scattering. R refers to real, I to imaginary, V to vector and S to scalar; potential depths in MeV, geometries in fm.

		280 MeV	489 MeV
V_{RS}	=	-538.7263	-292.7794
r_{RS}	=	0.9467	1.0528
a_{RS}	=	0.6604	0.6604
V_{RV}	=	392.0168	201.0615
r_{RV}	=	0.9515	1.0486
a_{RV}	=	0.6279	0.6279
V_{IS}	=	58.4439	58.7449
r_{IS}	=	1.0477	1.0796
a_{IS}	=	0.5722	0.5722
V_{IV}	=	-82.195	-82.195
r_{IV}	=	1.057	1.057
a_{IV}	=	0.575	0.575

variety of states. The fit to the data for these calculations are given in another contribution to this report. The deformation lengths obtained are given in Table 2.4 for the two energies, along with the average values of the

Table 2.4. Deformation lengths δ_R obtained by using the relativistic collective model for the $^{58}Ni(p,p')$ reaction, and also the average values for the deformation lengths $\langle\delta_{NR}\rangle$ obtained using the nonrelativistic model for proton energies of $178 < E_p < 800$ MeV.

State	280 MeV δ_R	489 MeV δ_R	$\langle\delta_{NR}\rangle$
2^+ 1.45 MeV	0.76±0.04	--	0.82±0.04
2^+ 3.04 MeV	0.26±0.03	0.32±0.03	0.26±0.03
2^+ 3.26 MeV	0.32±0.03	0.39±0.03	0.35±0.02
3^- 4.47 MeV	0.64±0.04	0.77±0.06	0.68±0.05
4^+ 2.46 MeV	0.36±0.03	0.39±0.02	0.36±0.03
4^+ 3.63 MeV	0.30±0.04	0.32±0.02	0.31±0.03
4^+ 4.75 MeV	0.45±0.04	0.48±0.03	0.42±0.02

deformation lengths obtained using the nonrelativistic model. There is good agreement between the values given for each state. The only trend is that the 489 MeV results are consistently higher than the 280 MeV values. This may possibly be due to the differences in the distortions and or the form factors since the optical parameters are different.

---

1. Partial support from Joint Institute for Heavy Ion Research, ORNL.
2. J. R. Shephard, E. Rost, and J. Piekarewica, Phys. Rev. C **30**, 1604 (1984); E. Rost and J. R. Shepard, Phys. Rev. C **35**, 681 (1987).
3. J. I. Johansson, E. D. Cooper, and H. S. Sherif, Nucl. Phys. **A476**, 663 (1988).
4. Jacques Raynal, Phys. Lett. **196B**, 7 (1987).
5. K. K. Seth et al., Phys. Lett. **158B**, 23 (1985).
6. D. A. Hutcheon, private communication.

ELASTIC AND INELASTIC SCATTERING OF 280- AND 489-MeV PROTONS FROM ^{58}Ni

J. Lisantti[1] — K. H. Hicks[4]
D. K. McDaniels[2] — M. C. Vetterli[5]
Z. Tang[2] — L. W. Swenson[6]
Z. Xu[2] — X. Y. Chen[6]
D. M. Drake[3] — F. Farzanpay[6]

Our group over the last four years has been studying the application of the collective, deformed potential, model to the analysis of intermediate-energy-proton scattering for the elastic and inelastic channels. These studies have covered the nuclei of ^{208}Pb (Ref. 7), ^{40}Ca (Ref. 8), and ^{28}Si (Ref. 9). As a further extension of this work we have measured elastic and inelastic scattering of 280- and 489-MeV protons in ^{58}Ni. The experiment was performed at the TRIUMF accelerator using the MRS (Medium Resolution Spectrometer) to detect the scattered protons. Elastic and inelastic scattering to seven bound states over an angular range of 6.9 to 27.0 degrees was measured at 280 MeV, while the 489-MeV data covered 5.7 to 27.7 degrees. We have analyzed our data using two different theoretical models based on the collective, deformed potential, model. The differences between the two are that one method utilizes the Schrodinger equation (nonrelativistic model, NROMP), while the other model uses the Dirac equation (relativistic model, ROMP). The fits to the elastic scattering for the 280-MeV data is shown in Fig. 2.16 (the $A_y(\theta)$ data are 290-MeV ^{54}Fe($\vec{p}$,p), results of Hausser[10] et al., which have the scattering angles' momentum shifted to match a 280-MeV experiment). The solid line is from the nonrelativistic optical model parameter fit, while the dashed curve is for the relativistic optical model parameters. The relativistic model fits both the cross section and analyzing power data better than the nonrelativistic model. The parameters for the

ORNL-DWG 88-14790

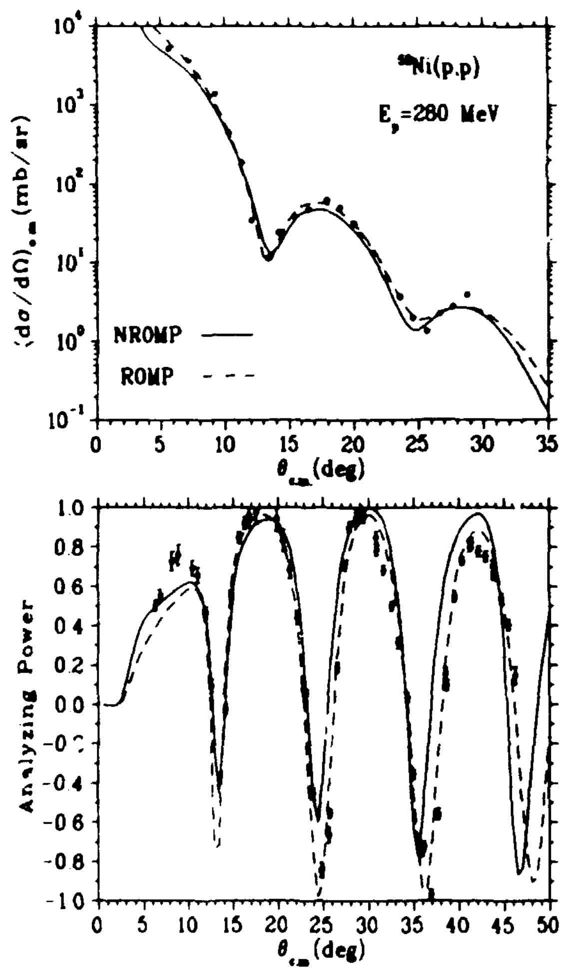

Fig. 2.16. Optical model fits to 280-MeV ^{58}Ni(p,p) elastic scattering. The solid line is for the nonrelativistic model (NROMP), as calculated in ECIS79, while the dashed curve is for the relativistic model (ROMP).

relativistic model are given in another contribution to this report. The NROMP for both energies are given in Table 2.5. After the NROMP and ROMP were obtained, the next step was to analyze our inelastic data. Results for the

Table 2.5. Nonrelativistic optical model parameters (NROMP) for 280- and 489-MeV $^{58}Ni(p,p)$ elastic scattering. Potential depths are in MeV, while the geometry units are in fermis.

		280 MeV	489 MeV
V_R	=	12.228	11.443
r_R	=	1.255	1.255
a_R	=	0.7632	0.763
V_I	=	29.774	55.004
r_I	=	1.007	1.007
a_I	=	0.5276	0.528
V_{RSO}	=	1.866	0.741
r_{RSO}	=	1.136	1.154
a_{RSO}	=	0.6415	0.642
V_{ISO}	=	-0.645	-2.228
r_{ISO}	=	0.816	1.038
a_{ISO}	=	0.7281	0.728

r_c = 1.2

analysis of three 2^+ states excited by 280-MeV protons are given in Fig. 2.17, while results for the excitation by 489-MeV protons of three 4^+ states are shown in Fig. 2.18. Both of the models fit the data fairly well and give similar shapes for the angular distributions with the exception that, at smaller scattering angles the relativistic model gives consistently larger cross sections, and this effect is more pronounced at the lower incident proton energies. Whether this effect is due to differences in distortions at the different incident energies is unclear at this time, and needs further study. However, it does point to an interesting

ORNL DWG 88 14789

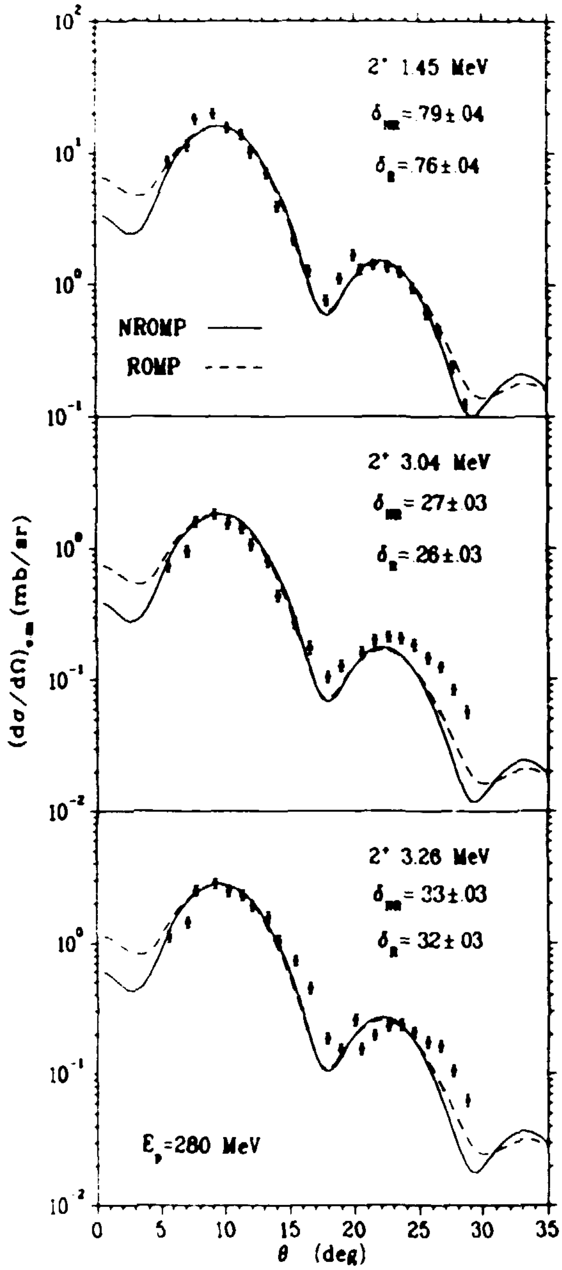

Fig. 2.17. Collective, deformed-potential-model calculations for inelastic scattering of 280-MeV protons from ^{58}Ni for three 2^+ states. The calculated angular distribution come from nonrelativistic (solid) or relativistic (dashed) models.

experiment, in that doing small-angle ^{58}Ni elastic scattering at lower energies (E_p < 300 MeV), may be a possible way to study relativistic effects.

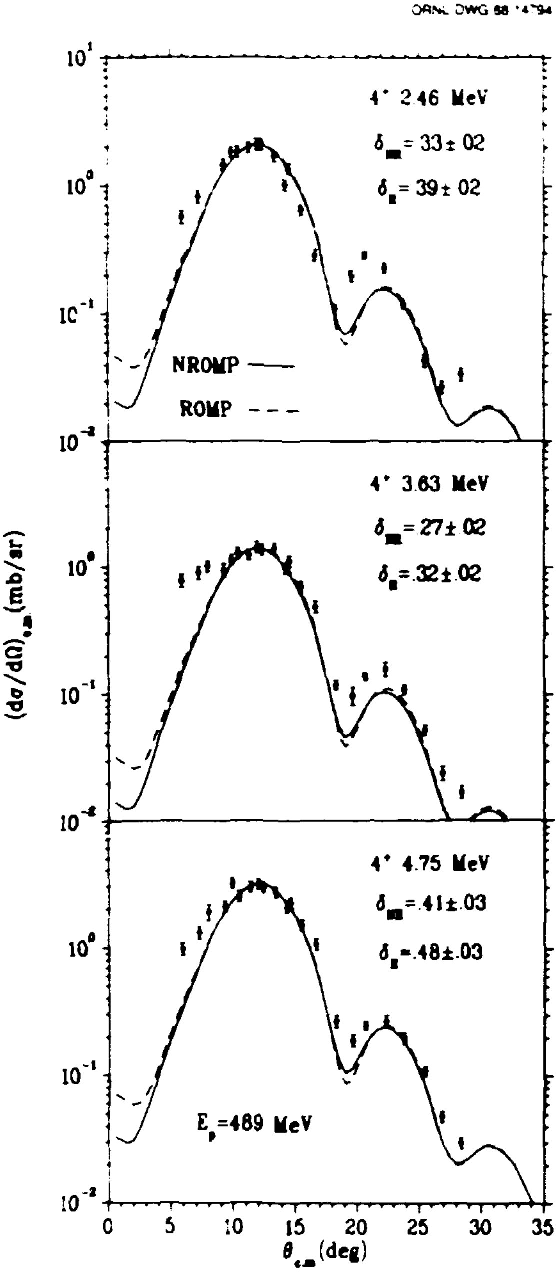

Fig. 2.18. Collective, deformed-potential-model calculations for inelastic scattering of 489-MeV protons from ^{58}Ni for three 4^+ states. The calculated angular distributions come from nonrelativistic (solid) or relativistic (dashed) models.

Table 2.6 lists the nonrelativistic deformation lengths, δ_H, obtained in the present study along with results from other studies. No dependence of δ_H on incident proton energy is observed, and this is reflected in Fig. 2.19 for three 2^+ states and one 3^- state. This reinforces our contention that, for those states which have surface-peaked Gaussian-like shape transition densities, the collective model should describe these states quite well,[8] and that there is no energy dependence of the hadronic deformation lengths.

---

1. Partial support from the Joint Institute for Heavy Ion Research, ORNL.
2. University of Oregon, Eugene, OR 97403.
3. Los Alamos National Laboratory, Los Alamos, NM 87545.
4. Ohio University, Athens, OH 45701.
5. TRIUMF, Vancouver, B.C., Canada.
6. Oregon State University, Corvallis, OR 97330.
7. D. K. McDaniels, J. Lisantti, I. Bergqvist, L. W. Swenson, X. Y. Chen, D. J. Horen, F. E. Bertrand, E. E. Gross, C. Glover, R. Sayer, B. L. Burks, O. Hausser, and K. Hicks, Nucl. Phys. **A467**, 557 (1987).
8. J. Lisantti, D. J. Horen, F. E. Bertrand, R. L. Auble, B. L. Burks, E. E. Gross, R. O. Sayer, D. K. McDaniels, K. W. Jones, J. B. McClelland, S. J. Seestrom-Morris, L. W. Swenson, submitted to Physical Review C; D. J. Horen, F. E. Bertrand, E. E. Gross, T. P. Sjoreen, D. K. McDaniels, J. R. Tinsley, J. Lisantti, L. W. Swenson, J. B. McClelland, T. A. Carey, S. J. Seestrom-Morris, and K. Jones, Phys. Rev. C **30**, 709 (1984).
9. J. Lisantti, F. E. Bertrand, D. J. Horen, B. L. Burks, C. W. Glover, D. K. McDaniels, L. W. Swenson, X. Y. Chen, O. Hausser, and K. Hicks, Phys. Rev. C **37**, 2408 (1988).
10. O. Hausser, private communication (unpublished).
11. 178 and 1047 MeV: A. Ingemarsson, T. Johansson, and G. Tibell, Nucl. Phys. **A322**, 285 (1979); 280 and 489 MeV: present work; 333, 497, and 800 MeV: Norton M. Hintz, D. Cook, M. Gazzaly, M. A. Franey, M. L. Barlett, G. W. Hoffmann, R. Fergerson, J. McGill, G. Pauletta, R. L. Boudries, J. B. McClelland, and K. W. Jones, Phys. Rev. C **37**, 692 (1988).

COMPARISON OF COLLECTIVE TRANSITION POTENTIALS TO TRANSITION CHARGE DENSITIES

J. Lisantti[1] D. J. Horen

The collective model has been used quite successfully for many years to describe direct nuclear reactions for a variety of probes at a variety of energies.[2] The basic model for direct reactions assumes that the nuclear potential is modeled by an optical potential which

Table 2.6. Deformation lengths obtained for various states in ^{58}Ni using inelastic proton scattering at different incident energies. Units are in fermis.

State (MeV)	178[1]	280	333[1]	489	498	800[1]	1047[1]
2^+ 1.45	0.805±0.08	0.79±0.04	0.82±0.08	--	0.81±0.08	0.89±0.09	0.805±0.08
2^+ 3.04	--	0.27±0.03	0.21±0.02	0.29±0.03	0.26±0.03	0.27±0.03	--
2^+ 3.26	--	0.33±0.03	0.35±0.03	0.35±0.03	0.35±0.03	0.37±0.04	--
3^- 4.47	0.674±0.07	0.66±0.04	0.59±0.06	0.68±0.06	0.72±0.07	0.75±0.07	0.674±0.07
4^+ 2.46	--	0.36±0.03	0.37±0.04	0.33±0.02	0.36±0.04	0.40±0.04	--
4^+ 3.63	--	0.31±0.04	0.31±0.03	0.27±0.02	0.29±0.03	0.36±0.04	--
4^+ 4.75	--	0.45±0.04	0.40±0.04	0.41±0.03	0.40±0.04	0.43±0.04	--

[1]No uncertainties were given in the references listed in Ref. 11, so a reasonable value of 10% uncertainty was applied.

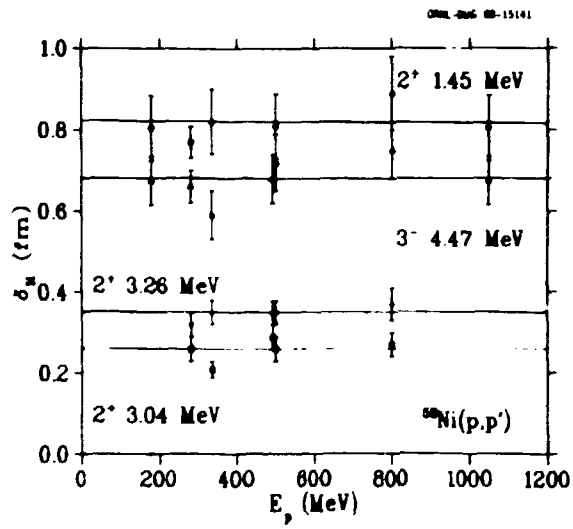

Fig. 2.19. Deformation lengths extracted for four states in ^{58}Ni using the nonrelativistic model plotted against incident proton energy. The references for the various energies is Ref. 11 of this paper.

has a radial form of Woods-Saxon shape. This potential has the form

$$U(r) = V_C - V_R f(r, r_R, a_R) - iV_I f(r, r_I, a_I) +$$

$$\left(\frac{\hbar}{2m_\pi c}\right)^2 \frac{1}{r}\frac{d}{dr} [V_{RSO} f(r, r_{RSO}, a_{RSO}) +$$

$$iV_{ISO} f(r, r_{ISO}, a_{ISO})] \vec{\sigma}\cdot\vec{\ell} \ , \qquad (1)$$

where V_C is the Coulomb, V_R the real, V_I the imaginary, V_{RSO} the real spin-orbit, and V_{ISO} the imaginary spin-orbit potentials, and the f's are Woods-Saxon forms. Hence, there are 12 adjustable parameters (depth, radii, and diffusenesses) in this model which are obtained from fitting elastic scattering data. In the collective, deformed potential model one assumes that the excitation of collective states (shape oscillations) can be described by a transition potential that has the same form as the transition density. To first order this is given by the radial derivative of the optical potential.[2] Therefore, the shape of the transition potential ΔU (form factor) is that obtained from the derivative of a Woods-Saxon shape, namely, a Gaussian-like shape centered on the nuclear surface.

In a microscopic description of nucleon-nucleus scattering, the impulse approximation can be used to describe the scattering event. Here one assumes that the incident nucleon interacts with one nucleon in the nucleus to cause the scattering. The potential to describe this event can be either the free or medium modified nucleon-nucleon interaction. This interaction is then folded with a transition density $\rho_{tr}(r)$ to obtain the form factor to describe the inelastic scattering. The transition density can be obtained either from shell model calculations or charge transition densities measured by inelastic-elastic scattering.

Since the effective nucleon-nucleon interaction is short range, one would expect the form factor for the microscopic description to have the same shape as the transition density. Therefore, one would expect the two model calculations to be similar when the transition densities have shapes which approximate a derivative of the OMP. This condition is satisfied for collective shape oscillations.

Since the availability of measured transition densities is rather sparse, one usually analyzes inelastic data using deformed potential model calculations. Hence, we have examined some cases for which both (p,p') and (e,e') data are available. As we discuss below, calculations using derivative Woods-Saxon form factors provide good fits to the data for those states which have charge transition densities which are well described by Woods-Saxon form factors.

These conclusions are based on an analysis of our 500-MeV $^{40}Ca(p,p')$(Ref. 3) and 280- and 489-MeV $^{58}Ni(p,p')$ data. Examples are given in Fig. 2.20 for three 3^- states in ^{40}Ca. The measured angular distributions are shown on the left. The data for the well-known collective 3_1^- state at 3.736 MeV is shown in the upper left hand side and compared with collective, deformed potential model calculations using two different sets of optical parameters. As can be seen both sets fit the data very well. The figure immediately to the right shows the shape of the imaginary transition potential (solid line), which accounts for most of the inelastic cross section at 500 MeV and the shape of the charge transition density (dashed line) obtained from (e,e') studies.[4] As is seen, both shapes are very similar, hence the agreement of the collective model to the data. The middle and bottom angular distributions of Fig. 2.20 show the data and collective model calculations for the 3_2^- (6.29 MeV), and 3_3^- (6.58 MeV) states. The data are not nearly as well fit as that for the 3_1^- state, particularly the data have a much higher cross section at the second maximum than the calculations. This disagreement

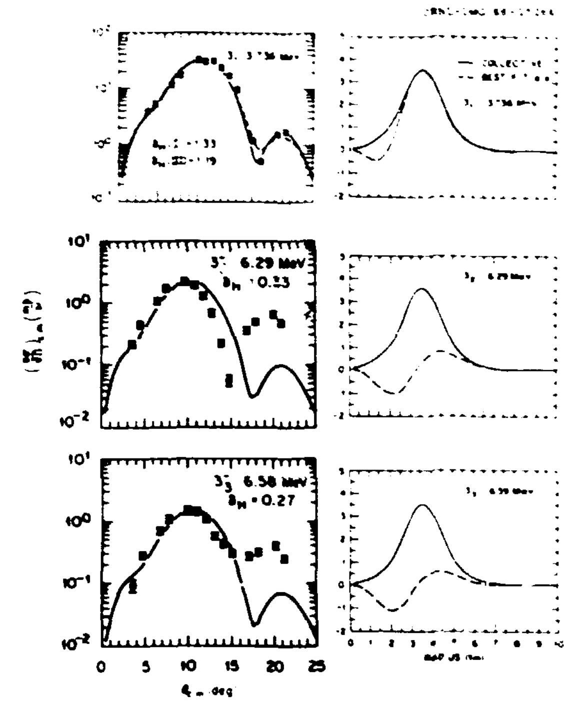

Fig. 2.20. The left hand column shows angular distributions for three 3^- states in ^{40}Ca excited in the 500-MeV $^{40}Ca(p,p')$ reaction. The solid and dashed lines are collective, deformed-potential model calculations using two different sets of optical model parameters. The right hand side shows imaginary transition potentials (solid line) in comparison to transition charge densities from (e,e')[3] (dashed line).

between the data and the collective model calculations is reflected in the shape of the charge transition densities (dashed lines) in comparison to the imaginary transition potentials (solid lines). Large differences are seen between these two shapes. In fact, if one replaces the transition potential shape with the charge transition density shapes the 3_2^- and 3_3^- data can be fit fairly well as shown in Fig. 2.21 for the 3_2^- state, indicating that intermediate energy protons can be used to extract proton and possibly neutron transition densities.

Similar results are obtained for our analysis of states in ^{58}Ni.

---

1. Partial support provided by the Joint Institute for Heavy Ion Research, ORNL.
2. Direct Nuclear Reactions, G. R. Satchler (Oxford University Press, 1983).

3. J. Lisantti, D. J. Horen, F. E. Bertrand, R. L. Auble, B. L. Burks, E. E. Gross, R. O. Sayer, D. K. McDaniels, K. W. Jones, J. B. McClelland, S. J. Seestrom-Morris, L. W. Swenson, submitted to Physical Review C.
4. K. Itoh, M. Oyamada, and Y. Torizuka, Phys. Rev. C 2, 2181 (1970).

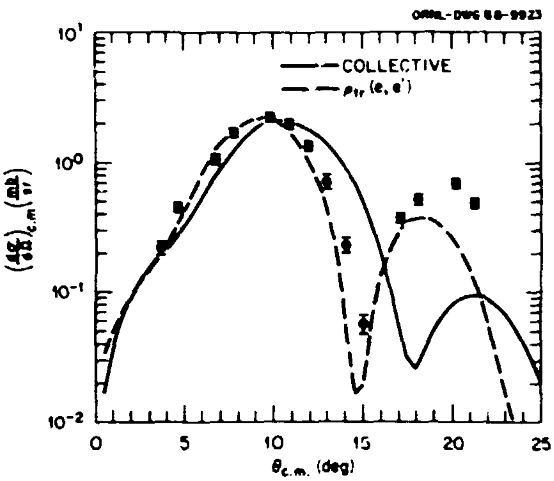

Fig. 2.21. Cross section data for the 3_2^- (6.29 MeV) state in comparison to a collective model calculation (solid line), and a distorted wave calculation using the charge transition density from inelastic electron scattering and a zero range fore (dashed line). The dashed curve was normalized to match the magntiude of the data at the first maximum.

GIANT RESONANCE STRENGTH DISTRIBUTION IN ^{40}Ca FROM INELASTIC SCATTERING OF 500 MeV PROTONS[1]

J. Lisantti[2] R. O. Sayer[4]
D. J. Horen D. K. McDaniels[5]
F. E. Bertrand K. W. Jones[6]
R. L. Auble J. B. McClelland[6]
B. L. Burks[3] S. J. Seestrom-Morris[6]
E. E. Gross L. W. Swenson[7]

Differential cross section measurements have been made for the giant resonance region (13.2 to 40 MeV) in ^{40}Ca using 500 MeV protons with an experimental energy resolution of 70 keV. Fine structure was observed in this energy region. After fixing the energy weighted sum rule (EWSR) depletion for the isovector giant dipole resonance at 70%, EWSR's of 70 ± 14% for the isoscalar giant quadrupole resonance and 15 ± 3% for the isoscalar giant hexadecapole resonance were deduced. The $3\hbar\omega$ giant octupole resonance observed at 31 MeV with a width of 10 MeV exhausted 30 ± 6% of the EWSR. All of these EWSR depletions agree well with theoretical predictions.

---

1. Abstract of paper submitted to Physical Review C.
2. Partial support from Joint Institute for Heavy Ion Research, ORNL.
3. Engineering Physics and Mathematics Division, ORNL.
4. Computing and Telecommunications Division, ORNL.
5. University of Oregon, Eugene, OR 97403.
6. Los Alamos National Laboratory, Los Alamos, NM 87545.
7. Oregon State University, Corvallis, OR 97331.

EXCITATION OF GIANT RESONANCES IN ^{28}Si WITH 250 MeV PROTONS[1]

J. Lisantti[2] D. K. McDaniels[4]
F. E. Bertrand L. W. Swenson[5]
D. J. Horen X. Y. Chen[5]
B. L. Burks[3] O. Hausser[6]
C. W. Glover[3] K. Hicks[7]

Differential cross section measurements have been made for 250-MeV proton inelastic scattering from ^{28}Si. Hadronic deformation lengths for the states at 1.78 MeV (2^+), 4.62 MeV (4^+), 6.8 MeV (3^- and 4^+), 9.70 MeV (5^-) and 10.2 MeV (3^-) have been extracted using a first order vibration model DWBA description. Deformation lengths for the 2^+ and 4^+ states are found to be independent of proton energy from 40 to 500 MeV. Cross sections for the excitation of the giant resonance region are found to be highly fragmented between 16 and 25 MeV. This region of excitation is found to contain an energy weighted sum rule depletion of 70% for the isovector giant dipole resonance, 26% for the isoscalar giant quadrupole resonance and 5% for the isoscalar hexadecapole resonance. No structure was observed in the inelastic continuum region of 25 to 45 MeV of excitation energy.

---

1. Abstract of published paper: Phys. Rev. C 37, 2408 (1988).
2. Partial support from Joint Institute for Heavy Ion Research, ORNL.
3. Engineering Physics and Mathematics Division, ORNL.
4. University of Oregon, Eugene, OR 97403.
5. Oregon State University, Corvallis, OR 97331.

6. Simon Fraser University, Burnaby, British Columbia, Canada V5A 1S6.
7. TRIUMF, Vancouver, British Columbia, Canada V6T 2A3.

COLLECTIVE MODEL DWBA ANALYSIS OF 500-MeV PROTON SCATTERING FROM ^{40}Ca[1]

J. Lisantti[2]	R. O. Sayer[4]
D. J. Horen	D. K. McDaniels[5]
F. E. Bertrand	K. W. Jones[6]
R. L. Auble	J. B. McClelland[6]
B. L. Burks[3]	S. J. Seestrom-Morris[6]
E. E. Gross	L. W. Swenson[7]

A vibrational collective model has been used to analyze 15 bound states in ^{40}Ca excited by inelastic scattering of 500-MeV polarized protons. It is shown that for those states which have surface-peaked charge transition densities the collective model describes the shape and magnitude of the angular distributions quite well. The hadronic deformation lengths extracted are shown to be constant over the incident proton energy range of 25 to 800 MeV with the exception of data at 185 MeV. The average values for the hadronic deformation lengths are used to calculate the ratio of the neutron-to-proton multipole matrix elements for 5 states. Elastic scattering and the 3_1^-, 2_1^+, and 5_1^- transitions have also been studied, using the relativistic collective model.

---

1. Abstract of paper submitted to Physical Review C.
2. Partial support from Joint Institute for Heavy Ion Research, ORNL.
3. Engineering Physics and Mathematics Division, ORNL.
4. Computing and Telecommunications Division, ORNL.
5. University of Oregon, Eugene, OR 97403.
6. Los Alamos National Laboratory, Los Alamos, NM 87545.
7. Oregon State University, Corvallis, OR 97331.

MICROSCOPIC $t\rho$ OPTICAL POTENTIALS USED TO DESCRIBE INTERMEDIATE-ENERGY PROTON ELASTIC SCATTERING

J. Lisantti[1]

Traditionally, elastic scattering of nucleons from nuclei has been treated phenomenologically using the optical potential model. This model describes the cross section and analyzing powers fairly well for the large body of data that exists. However, one problem with this model is that it does not describe the scattering using a more fundamental microscopic nucleon-nucleon interaction, along with not using ground-state properties of the nucleus. Also the optical model suffers from the ambiguity of fitting 12 parameters to the data.

One way to study the elastic scattering of nucleons from nuclei in a parameter-free microscopic model is to use the impulse approximation. The optical potential in this method is found from folding a nucleon-nucleon interaction, t_{NN}, with the ground-state charge distribution, $\rho_{ch}(r)$, obtained from elastic electron scattering. This method generates what is known as "$t\rho$" optical potentials. The nucleon-nucleon interaction used depends on how the scattering is treated. If one assumes that the single-step nucleon-nucleon interaction occurs in the nucleus in the same manner as in free space, one can use the Love-Franey force[2] as determined by fitting the SP84 phase shift results of the program SAID[3] (this will be referred to as the L-F Interaction). However, if one assumes density-dependent (Pauli blocking, Fermi motion) effects for the interaction in the nucleus, there are effective interactions to use. One is the G-matrix approach of von Geramb,[4] using the Paris potential which includes one π, two π, and ω exchange. A more recent effective interaction, similar to von Geramb's, is HM86 of Nakayama and Love[5] using the Bonn potential.

Therefore, with the experimentally determined model independent $\rho_{ch}(r)$ folded with each of the interactions, one obtains optical potentials which can then be used to calculate elastic scattering observables.

We have analyzed our 280- and 489-MeV ^{58}Ni elastic and inelastic proton data in such a manner. Figure 2.22 shows the results of the use of three different interactions folded with the same ground-state charge distribution of a three-parameter Fermi distribution from de Jager, de Vries, and de Vries.[6] Before

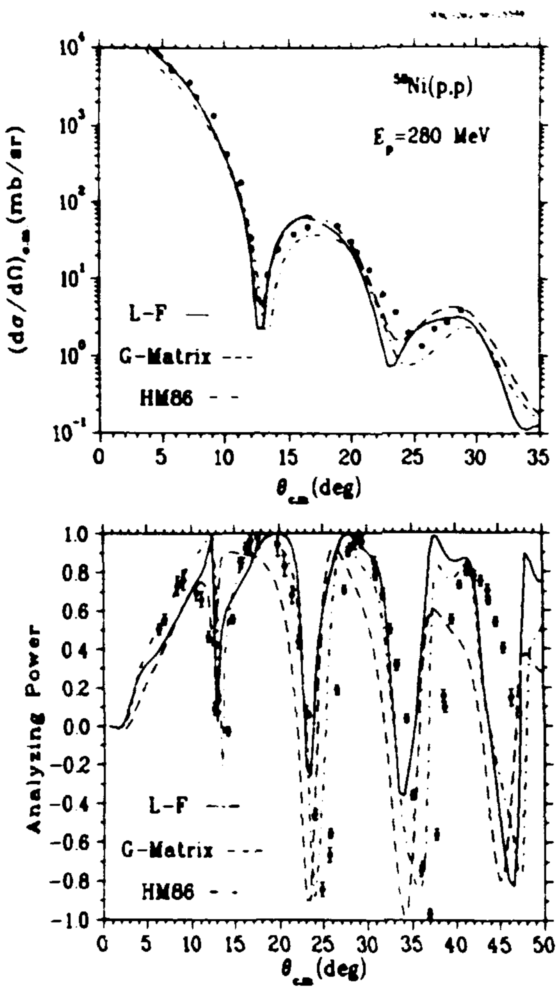

Fig. 2.22. Elastic scattering data at 280 MeV for the ^{58}Ni(p,p) reaction. The three calculations are from microscopic optical potentials generated in the program ALLWRLD, and then used to calculate the observables in the program ECIS79. The solid curve is for the Love-Franey interaction, the dashed curve is the G-matrix approach of von Geramb based on the Paris potential, and the dot-dashed curve is the HM86 interaction of Nakayama-Love, based on the Bonn potential. The analyzing power data are q-shifted results of Hausser et al.[7] at 290 MeV for ^{54}Fe(p,p) elastic scattering.

discussing the results, remember that the calculations shown are not fits, there are no free parameters in these calculations! The solid curve uses the Love-Franey interaction, and gives the poorest match to the data, especially at the largest angles, but still it matches the data fairly well. The dashed curve is the G-matrix result using the Paris potential at 400 MeV; as is observed, it gives a similar description of the data as the Love-Franey interaction. The last interaction used is the dot-dashed calculation using the HM86 interaction. It fits the data the best of the three, but, as with the other two interactions, it does not fit the data as well as the phenomenological optical potentials as shown in another contribution to this report.

At the higher ($E_p \gtrsim 400$ MeV) incident proton energies it is known that density dependence is not important, therefore we calculated optical potentials using only the Love-Franey interaction. The data for elastic ^{58}Ni(p,p) scattering is shown in Fig. 2.23 along with two calculations. The solid line is a nonrelativistic

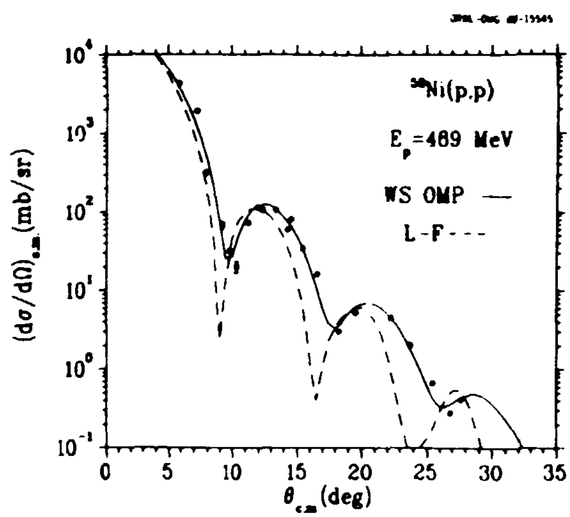

Fig. 2.23. Elastic scattering data at 489 MeV for the ^{58}Ni(p,p) reaction. The solid curve is from a nonrelativistic phenomenological optical model fit to the data using ECIS79. The dashed curve is from the Love-Franey interaction.

optical model fit, using parameters given in another contribution to this report. It does a much better job of describing the data than the dashed curve of the Love-Franey interaction. An interesting characteristic observed in both Figs. 2.22 and 2.23 is that, for both the cross sections and analyzing powers, the microscopic calculations begin to get out of phase with the data at the larger scattering angles. It is unclear if this is attributable to the effective interaction or to the ground-state charge distribution having large uncertainties in the interior of the nucleus which would be observed in the larger angle (p,p) scattering.

---

1. Partial support from the Joint Institute for Heavy Ion Research, ORNL.
2. M. A. Franey, W. G. Love, Phys. Rev. C 31, 488 (1985); W. G. Love and M. A. Franey, Phys. Rev. C 24, 1073 (1981); Phys. Rev. C 27, 438(E) (1983).
3. "Scattering Analysis Interactive Dial In," Phase shift code of Roper and Arndt.
4. H. V. von Geramb, The Interaction Between Medium Energy Nucleons in Nuclei – 1982, AIP Conference Proceedings, No. 97, p. 44.
5. K. Nakayama, W. G. Love, Phys. Rev. C 38, 51 (1988).
6. C. W. de Jager, H. de Vries, and C. de Vries, At. Data Nucl. Data Tables 14, 479 (1974).
7. O. Hausser, private communication (unpublished).

NUCLEAR STRUCTURE STUDIES VIA CHARGE-EXCHANGE REACTIONS

TRANSFER REACTIONS AT HIGH ENERGY AND AMBIGUITIES IN HEAVY-ION POTENTIALS[1]

D. J. Horen, M. A. G. Fernandes[2], G. R. Satchler, B. L. Burks[3], R. L. Auble, F. E. Bertrand, E. E. Gross, D. C. Hensley, R. O. Sayer[4], D. Shapira

The smaller impact parameters that contribute to transfer reactions between heavy ions at high energies make them more sensitive to different types of optical potentials than is the case at lower energies. This may allow one to distinguish between potentials that otherwise generate similar elastic scattering cross sections within the limited angular region over which typical elastic data are available. We cite as evidence results for nucleon transfers induced by $^{18}O + ^{28}Si$ at 352 MeV which rule out surface transparent potentials.

---

1. Abstract of published paper: Z. Phys. A-Atomic Nuclei 328, 189 (1987).
2. Present address: Instituto de Fisica, Universidade de Sao Paulo, Sao Paulo, Brazil.
3. Engineering Physics and Mathematics Division, ORNL.
4. Computing and Telecommunications Division, ORNL.

THE $^{52,54}Cr(p,n)^{52,54}Mn$ AND $^{57,58}Fe(p,n)^{57,58}Co$ REACTIONS AT E_p = 120 MeV[1]

D. Wang[2], J. Rapaport[2], D. J. Horen, B. A. Brown[3], C. Gaarde[4], C. D. Goodman[5], E. Sugarbaker[6], T. N. Taddeucci[7]

Differential cross sections for the (p,n) reaction on $^{52,54}Cr$ and $^{57,58}Fe$ have been measured for angles up to θ_{lab} = 10.5° and 14.6°, respectively, using 120 MeV protons. The observed anglular distributions are used to evaluate the location and strength of Gamow-Teller resonances. A shell-model calculation of this strength distribution is presented and compared with the experimental results. The M1 strength for ^{52}Cr is also calculated and compared with available results from (e,e') and (p,p') experiments. A comparison is made with other $1f_{7/2}$ nuclei.

---

1. Abstract of published paper: Nucl. Phys. A480, 285 (1988).
2. Ohio University, Athens, OH 45701.
3. Michigan State University, East Lansing, MI 48824.
4. Niels Bohr Institute, Copenhagen, Denmark.
5. Indiana University, Bloomington, IN 47405.
6. Ohio State University, Columbus, OH 43215.
7. Los Alamos National Laboratory, Los Alamos, NM 87545.

ℓ = 1, SPIN-DIPOLE STRENGTH IN ^{40}Ca[1]

D. J. Horen, J. Lisantti, R. L. Auble, F. E. Bertrand, B. L. Burks[2], E. E. Gross, R. O. Sayer[3], D. K. McDaniels[4], K. W. Jones[5], J. B. McClelland[5], S. J. Seestrom-Morris[5], L. W. Swenson[6]

Spin-dipole strength in ^{40}Ca has been studied by inelastic scattering of 500-MeV protons and the dipole response in ^{40}Ca is compared with the spin-dipole data from the $^{40}Ca(p,n)$ reaction and nonspin-dipole data from photonuclear studies.

---

1. Abstract of paper submitted to Zeitschrift fur Physik A - Atomic Nuclei.

2. Engineering Physics and Mathematics Division, ORNL.
3. Computing and Telecommunications Division, ORNL.
4. University of Oregon, Eugene, OR 97403.
5. Los Alamos National Laboratory, Los Alamos, NM 87545.
6. Oregon State University, Corvallis, OR 97331.

NUCLEAR STRUCTURE STUDIES VIA TRANSFER AND CAPTURE REACTIONS

TWO-NEUTRON PAIRING ENHANCEMENT FACTORS[1]

X. T. Liu[2] X. L. Han[5]
C. Y. Wu[2] M. W. Guidry[3]
S. P. Sorensen[3] D. Cline[4]
R. W. Kincaid[2] W. J. Kernan[4]
E. Vogt[4] T. Czosnyka[4]
A. E. Kavka[4]

The enhancement of two-nucleon transfer cross sections by factors of approximately 50 over that expected from uncorrelated transfer of two particles is well documented in (t,p) or (p,t) reactions on superfluid nuclei.[6] In the collision of two superfluid heavy ions it is expected that the enhancement could be considerably larger, due to the strong pairing correlation in both interacting nuclei.[7] Various experiments have attempted to study two-particle transfer in the collision of two heavy nuclei,[8] and typically have concluded that the enhancement factors for these collisions are compa-able to those for (t,p) or (p,t) reactions. These experiments had low energy resolution and thus there was little information as to which states were being populated in the reaction.

In this paper we report on the first measurement of enhancement factors with sufficient resolution to distinguish transfer to the ground-state band from transfer to other bands. We find two components in this population, with very different enhancement factors. The bulk of the reaction, > 80%, populates 2-quasiparticle (2-QP) bands with enhancements of ≈ 7-20, but the transfer to the ground band is found to have enhancement factors ≈ 30-500. Examples, are shown in Fig. 2.24. Thus the average enhancement for all bands populated is small (< 50), but the enhancement for the pairing rotational

ORNL-DWG 88-16645

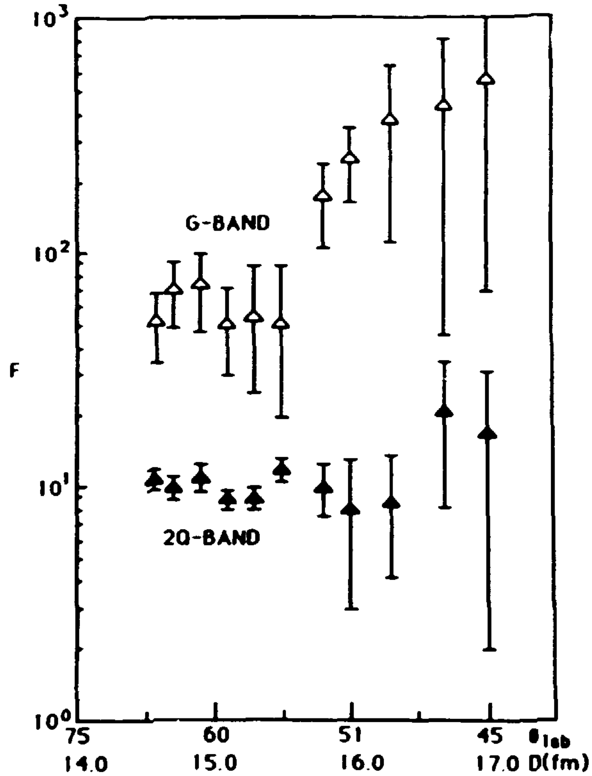

Fig. 2.24 Two-neutron enhancement factors $F \equiv P_{2n}/P_{1n}^2$, constructed from transfer probabilities.

transition to the ground-state band is large, indicating that collisions between two heavy ions may approximate the scattering of two macroscopic superfluid objects.

---

1. Summary of paper submitted to Physics Letters B.
2. University of Tennessee, Knoxville, Tennessee.
3. Adjunct staff member, University of Tennessee, Knoxville, Tennessee.
4. University of Rochester, Rochester, New York.
5. Joint Institute for Heavy Ion Research, ORNL, Permanent address: Jilin University, Changchun, People's Republic of China.
6. R. Broglia, O. Hansen, and C. Riedel. Adv. Nucl. Phys. 6, 287 (1973).
7. R. A. Broglia, C. H. Dasso, S. Landowne, B. S. Nilsson, and A. Winther, Phys. Lett. 73B, 401 (1978).
8. For example, W. von. Oertzen, H. G. Bohlen, B. Gebauer, R. Künkel, F. Pühihlnofer, D. Schüll, Z. Phys. A326, 463 (1987).

OSCILLATING TWO-NEUTRON TRANSFER PROBABILITIES AT LARGE RADIAL SEPARATION IN HEAVY-ION REACTIONS[1]

X. T. Liu[2] C. Y. Wu[2]
M. W. Guidry[3] W. J. Kernan[4]
S. P. Sorensen[3] D. Cline[4]
R. W. Kincaid[2] E. Vogt[4]
T. Czosnyka[4] B. Kotlinski[4]
A. E. Kavka[4]

In this paper we show that the large-distance probabilities for two-neutron transfer in the reactions $^{162}Dy(^{58}Ni,^{60}Ni)^{160}Dy$ and $^{162}Dy(^{116}Sn,^{118}Sn)^{160}Dy$ exhibit the expected exponential dependence for transfer to the 2-quasiparticle bands, but oscillations, interpreted as an interference between scattering from different spatial orientations of deformed nuclei, are observed for transfer to the ground band. Fig. 2.25 illustrates this behavior. We suggest that the superposition of these two disparate behaviors is a plausible explanation for all previously reported anomalies in 2-neutron transfer reactions with heavy ions on deformed nuclei: the slope anomaly results from a superposition of two independent components of the transfer population. The first component dominates the transfer cross section near the grazing angle and is associated with population of 2-quasiparticle bands; it decays exponentially. The second component is associated with transfer to the ground-state rotational band. It is a small fraction of the transfer cross section at the grazing angle, but accounts for about half the total 2-neutron transfer at large distances. This component exhibits a slowly decaying oscillation.

---

1. Summary of paper submitted to Physical Review C, Rapid Communication.
2. University of Tennessee, Knoxville, Tennessee.
3. Adjunct staff member, University of Tennessee, Knoxville, Tennessee.
4. University of Rochester, Rochester, New York.
5. S. Landowne, C. Price, and H. Esbensen, Nucl. Phys. A484, 98 (1988).

INTERPLAY OF DIRECT AND COMPOUND-NUCLEUS MECHANISMS IN NEUTRON CAPTURE BY LIGHT NUCLIDES[1]

S. Raman S. Kahane[2]
J. E. Lynn[3]

We discuss the direct-capture theory pertaining to primary electric-dipole (E1) transitions following slow-neutron capture. For approximately 20 light nuclides that we have

ORNL-DWG 88-16646

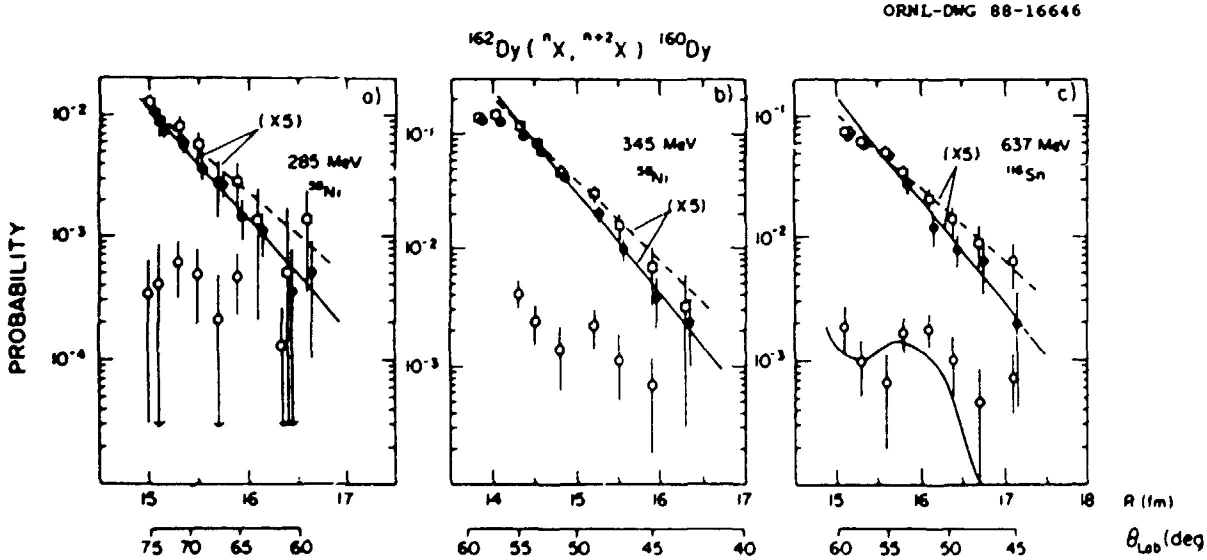

Fig. 2.25. Radial behavior for two-neutron transfer reactions. Shown for each case are the probability for two-neutron transfer to the ground-state band (open circles), the 2-qp bands (closed circles), and the sum of these two (open squares). The dashed and solid lines are the best fits of straight lines through the data for total and 2qp respectively. The undulating solid curve in (c) is the summed probability of 4+, 6+, and 8+ states from the calculation of Ref. 5. All probabilities are plotted on an absolute scale, but displaced by the factors shown for clarity.

studied, estimates of direct-capture cross sections using optical-model potentials with physically realistic parameters are in reasonable agreement with the data. Minor disagreements that exist are consistent with extrapolations to light nuclides of generally accepted formulations of compound-nucleus capture. In dealing with nuclei "soft" to vibrations, we have considered the possible effects of coupling of the collective motion with the optical potential in the framework of R-matrix theory. In such cases, we find that the inclusion of "inelastic" channels results in systematic changes in the calculated cross sections.

---

1. Abstract of an invited paper presented at the International Conference on Nuclear Data for Science and Technology, Mito, Japan (May 30-June 3, 1988).
2. Nuclear Research Centre-Negev, Beer Sheva, Israel.
3. Atomic Energy Research Establishment, Harwell OX11 ORA, England.

GROUND-STATE PHOTONEUTRON REACTIONS IN ^{18}O[1]

J. W. Jury[2]
P. C.-K. Kuo[2,3]
K. G. McNeill[3]
C. K. Ross[4]
H. R. Weller[5]
S. Raman

Differential cross sections have been measured for the reaction $^{18}O(\gamma,n_0)^{17}O$ over the region of excitation energy from 14 to 26 MeV. The angle-integrated cross section for the ground-state transition reveals that this channel accounts for less than 20% of the total photoneutron cross section in the structured pygmy resonance region (near 14 MeV) and is a small fraction (10-15%) of the cross section in the region of the giant resonance (near 25 MeV). The values of angular distribution coefficients fitted to the data are consistent with a description of this reaction in which electric dipole excitations dominate the cross section in the pygmy resonance. Narrow regions exist near 15.0, 16.0, and 20.0 MeV where nonzero a_1 coefficients are observed, indicating the absorption of non-E1 radiation. The measured cross section and a_2 coefficients are compared with a direct-semidirect calculation, which gives reasonable agreement and suggests that f-wave neutron emission dominates the ground-state channel and that there is little justification for the introduction of E2 amplitudes other than a pure direct E2 term.

---

1. Abstract of published paper: Phys. Rev. C 36, 1243 (1987).
2. Trent University, Peterborough, Ontario, Canada K9J 7B8.
3. University of Toronto, Toronto, Ontario, Canada M5S 1A7.
4. National Research Council of Canada, Ottawa, Ontario, Canada K1A 0R6.
5. Triangle Universities Nuclear Laboratory, Duke University, Durham, North Carolina 27706.

NUCLEAR STRUCTURE STUDIES VIA COMPOUND NUCLEUS REACTIONS

IRREGULARITIES AT HIGH SPIN IN THE ODD-ODD NUCLEUS ^{158}Tm[1]

M. A. Riley[2]
Y. A. Akovali
C. Baktash
M. L. Halbert
D. C. Hensley
N. R. Johnson
I. Y. Lee
F. K. McGowan
A. Virtanen[3]
L. H. Courtney[4]
V. P. Janzen[4]
L. L. Riedinger[4]
L. Chaturvedi[5]
J. Simpson[6]

Many high-spin ($I > 30\ \hbar$) studies have been performed in the N = 88-90 transitional rare-earth region. However, these studies using the large anti-Compton arrays have focused on the even-even and odd-even nuclei. Some work has been performed on the odd-odd nuclei, but only at lower spins. In the present work we observe states in ^{158}Tm up to spin $I^{\pi} = 36^{(+)}$ (tentatively 38^{+}), the highest spin currently observed in an odd-odd nucleus. More importantly, however, we find the high-spin structure to be very different from that previously proposed for this nucleus.[7]

High-spin states in ^{158}Tm were populated by using the reaction ^{110}Pd (^{51}V,3n) at a beam energy of 220 MeV. De-excitation γ rays were detected with the Oak Ridge Compton Suppression System, an array of 19 Compton-suppressed spectrometers, each of which is comprised of a high resolution germanium detector surrounded by a bismuth germanate (BGO) or sodium iodide (NaI) anti-Compton shield. In the present experiment, 12 BGO and 7 NaI anti-Compton shields were used. A total of 165 x 10^6 events were recorded when two or more germanium detectors were in coincidence. While the 4n, ^{157}Tm channel was the dominant channel populated (see following article) at this beam energy (~ 35%), events corresponding to the 3n, ^{158}Tm channel accounted for ~ 20% of the reaction cross section.

On the basis of the γ-γ coincidence data, together with angular correlation measurements, we have established the high-spin-level scheme of ^{158}Tm to spin 23$^-$ (tentatively 25$^-$) in the negative parity sequence. These data agree with the level scheme of Holzmann et al.,[8] and also with that of Foin et al.,[7] up to spin 22$^-$. In addition, we observe another strongly coupled sequence, most likely of positive parity, up to spin 36$^{(+)}$(38$^+$). It is with this band, which we place in parallel rather than on top of the yrast sequence, that we find disagreement with Ref. 7. On the other hand, many of the main γ-ray transitions and their coincident relationships are, indeed, retained in the present work. However, the differences are significant enough to totally change the high-spin interpretation of this nucleus.

In Fig. 2.26, experimental alignments (i) and routhians (e') are plotted for the N = 89 isotones ^{157}Er (Refs. 9 and 10), ^{158}Tm and ^{159}Yb (Refs. 11 and 12). The subtracted reference had as parameters $\mathscr{I}_0$ = 20 MeV$^{-1}\hbar^2$ and $\mathscr{I}_1$ = 60

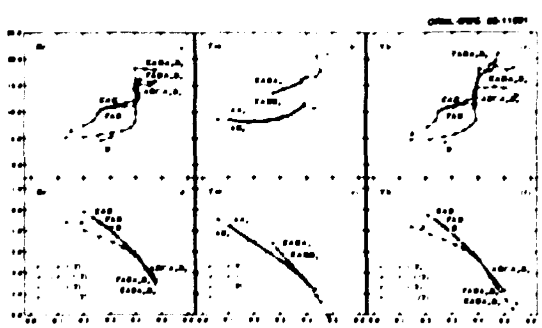

Fig. 2.26. Experimental alignments (i) and routhians (e') plotted versus rotational frequency ħω for bands in the N = 89 isotones. The bands are labeled both by parity and signature (π,α) and also by their quasiparticle composition.

MeV$^{-3}\hbar^4$. This reference choice gives nearly constant alignments for bands in ^{157}Er and ^{159}Yb below and above the $\pi h_{11/2}$ band crossing. Experimental band sequences are labeled by their parity and signature (π,α) and also by their quasiparticle composition. In the region of the neutron $i_{13/2}$ and proton $h_{11/2}$ intruder shells, the following conventions are used: A = $(\pi,\alpha)_n$ = $(+,1/2)_1$, B = $(+,-1/2)_1$, C = $(+,1/2)_2$, D = $(+,-1/2)_2$, E = $(-,1/2)_1$ and F = $(-,-1/2)_1$, where n denotes the nth such aligned quasineutron. For quasiprotons, A_p = $(-,-1/2)_1$, B_p = $(-,+1/2)_1$ and C_p = $(-,-1/2)_2$. The similarity between the three isotones in Fig. 2.26 is very striking indeed. In the odd-odd ^{158}Tm case, however, one may expect a doubling of bands, as the two signatures (A_p and B_p) of the high-K, $\pi h_{11/2}$ level observed as yrast in the odd-Z even-N nuclei, couple to the odd quasineutron bands. Bands involving the F quasineutron are not observed, however, in the present study of ^{158}Tm.

Figure 2.26 shows that in all three isotones the sequences containing the configuration EAB become yrast above ħω = 0.40 MeV, explaining the high intensity observed in these sideband sequences. At ħω = 0.30 MeV the energy difference between the bands containing the configurations A and EAB is 0.50 MeV in ^{157}Er, 0.41 MeV in ^{158}Tm, and 0.44 MeV in ^{159}Yb. Also, the observed alignments for the various bands in ^{158}Tm of 8.9ħ, 8.6ħ, 14.1ħ and 13.9ħ at ħω = 0.30 MeV for the AA_p, AB_p, $EABA_p$, and $EABB_p$ assigned configurations are in good agreement with the estimated values of 8.6ħ, 8.2ħ, 13.9ħ and 13.5ħ, respectively, obtained from the neighboring ^{157}Er, ^{159}Yb and ^{157,159}Tm nuclei. Such good agreement in these isotones is strong evidence in support of the presently proposed high-spin interpretation and quasiparticle assignments for ^{158}Tm.

In ^{158}Tm the sideband shows a sharp gain in alignment at ħω ~ 0.45 MeV in the (+,1) sequence (see Fig. 2.26), which behavior may be interpreted as the B_pC_p crossing. Alternatively, in these soft transitional (N ~ 88,89) nuclei it is expected and observed at high spin (I = 30-40) that the yrast line will be crossed by less collective structures which terminate in aligned single-particle states. In ^{158}Tm, calculations predict such crossings just above spin 30 for positive parity, with favored terminations at spins 33^+, 38^+ and 39^+. Such crossings could also explain the observed anomaly at $\hbar\omega$ = 0.45 MeV. More detailed studies are required to decide this issue or to determine if, in fact, both suggestions play a part in the very high spin spectrum of ^{158}Tm.

---

1. Summary of paper submitted to Physical Review C, Rapid Communications.
2. ORNL and JIHIR. Present address: University of Liverpool, Liverpool, U.K.
3. ORNL and JIHIR. Present address: University of Jyväskyla, Jyväskyla, Finland.
4. University of Tennessee, Knoxville, TN 37996.
5. Vanderbilt University, Nashville, TN 37235. Present address: Banaras Hindu University, Varanadi 221005, India.
6. Daresbury Laboratory, Warrington WA44AD, U.K.

7. C. Foin et al., Phys. Lett. 159B, 5 (1985).
8. R. Holzmann et al., Phys. Rev. C 31, 421 (1985).
9. M. A. Riley et al., Phys. Lett. 135B, 275 (1984).
10. J. Simpson et al., submitted to J. Physics G.
11. T. Bryski et al., Nucl. Phys. A474, 193 (1987).
12. L. Courtney, University of Tennessee Ph.D. Thesis (1987) and Progress Report, University of Tennessee, June 1985 - May 1986, p. 46.

ALIGNMENTS, SHAPE CHANGES, TRANSITION RATES AND BAND TERMINATIONS IN ^{157}Tm

M. A. Riley[1]	I. Y. Lee
Y. A. Akovali	F. K. McGowan
C. Baktash	A. Virtanen[2]
M. L. Halbert	V. P. Janzen[3]
D. C. Hensley	L. L. Riedinger[3]
N. R. Johnson	L. Chaturvedi[4]

The even-even N = 88 nuclei ^{158}Yb (Ref. 5), ^{156}Er (Ref. 6) and ^{154}Dy (Refs. 7 and 8) have been well studied at high spin and there is evidence for a shape transition from prolate to oblate (band termination) between spins I ≈ 30-42. It is important to study this shape transition in an odd-Z isotone since a particular systematic trend is expected and also because odd-Z nuclei possess special characteristics not found in the even-even cases. Some of these special features were discussed in detail in last year's progress report.[9]

High spin states in ^{157}Tm were populated via the ^{110}Pd(^{51}V,4n) reaction at a beam energy of 220 MeV. Gamma rays were detected in coincidence by using our 19-detector Compton Suppression System. Approximately 165 million events were recorded, with events corresponding to the 4n, ^{157}Tm channel accounting for ~ 35% of the reaction cross section. For further experimental details, see the ^{158}Tm contribution to this report. The level scheme analysis of these data is now complete. We have identified nine rotational cascade sequences in the level scheme of ^{157}Tm. Over 80 γ-ray transitions are observed, whereas previously only 6 γ rays had been assigned[10] to this nucleus. High-spin states are observed up to I = 83/2 for negative parity and I = 55/2 for positive parity. Spin and parity assignments are based on angular correlation information and strong systematics that exist in this region.

At low spins the yrast band, based on the π[523]7/2 $h_{11/2}$ Nilsson level, shows large signature splitting which disappears (and even inverts slightly) after the $i_{13/2}$ neutron alignment at spin I = 31/2. Similar behavior is observed in the N = 90, odd-Z nuclei and has been interpreted as a change in shape from negative to zero or slightly positive values of the asymmetry shape parameter γ (see Ref. 11). The interaction strength at the $i_{13/2}$ crossing is very weak with the main intensity flow actually bypassing the $31/2^-$ yrast level via a 934-keV transition. Such a weak interaction, and also a slightly higher than normal crossing frequency, is expected for nuclei where the Fermi surface λ lies below the Ω = 1/2 intruder level.[12]

A special feature of the odd-proton nuclei is that it is possible to obtain electromagnetic B(M1)/B(E2) transition rates by measuring the ΔI = 1 to ΔI = 2 branching ratios in the two strongly coupled $h_{11/2}$ yrast sequences. These results show similar characteristics to other odd-proton nuclei in this region, displaying a sharp rise at the $i_{13/2}$ neutron alignment. Above spin I = 25, the ratio rises sharply again which is also true for the N = 90, odd-Z nuclei. It is not clear whether the underlying explanation for this increase is the same for all these nuclei. In the case of ^{157}Tm we would suggest that the effect is caused by the influence on the yrast sequence by band termination structures which cross the yrast line just below spin I = 30, leading to a reduction in the B(E2) values.

Plotted in Fig. 2.27a is the excitation energy minus a rigid rotor reference for the

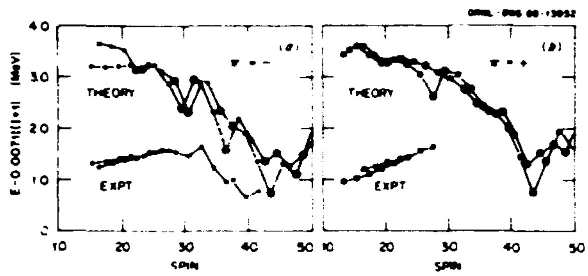

Fig. 2.27. Excitation energy minus a rigid rotor reference for (a) negative parity levels and (b) positive parity levels in ^{157}Tm. The calculated[12] levels have been shifted up by 2 MeV.

yrast (negative parity) band of ^{157}Tm. Also plotted (shifted 2 MeV up in energy) are some very recent band-termination predictions by Ragnarsson and Bengtsson.[13] These calculations omit pairing and, therefore, some care should be taken when interpreting the theory values for low spins, I < 30. The similarity between experiment and theory is striking! The strong down sloping, ending in a particular favored oblate state (encircled), is a characteristic feature of terminating bands. The predicted low states at spins I = 61/2 and 73/2 indeed coincide with low experimental states. The observation of an intense, very high energy γ ray (1080 keV) above I = 30 and the observation of a dipole transition (557 keV) at spin I = 75/2 are also phenomena which may be explained in these band termination calculations. The high spin experimental spectrum, I ≳ 57/2, however, is not readily understood within a standard cranked shell model framework.

We show in Fig. 2.27b the two strongly coupled signatures of the high-spin positive-parity sequence. The latter is not observed to high enough spin to expect any strong direct correspondence with theory (again shifted up 2 MeV in energy). It is interesting to note, however, that a drop in the γ-ray energy spacing does occur at spin I = 55/2, and this coincides with the favored theoretical state in this figure.

These observations are consistent with similar effects seen in the lighter N = 88 nuclei and support the interpretation[5,13] for band terminating behavior in the heavier ^{158}Yb nucleus, which had been questioned in Ref. 14.

---

1. ORNL and JIHIR. Present address: University of Liverpool, Liverpool, U.K.
2. ORNL and JIHIR. Present address: University of Jyväskyla, Jyväskyla, Finland.
3. University of Tennessee, Knoxville, TN 37996.
4. Vanderbilt University, Nashville, TN 37235. Present address: Banaras Hindu University, Varanadi 221005, India.

5. C. Baktash et al., Phys. Rev. Lett. **54**, 978 (1985).
6. F. Stephens et al., Phys. Rev. Lett. **54**, 2584 (1985).
7. H. W. Cranmer-Gordon et al., Nucl. Phys. **A465**, 506 (1987).
8. W. C. Ma et al., Phys. Rev. Lett.
9. M. A. Riley et al., Phys. Div. Prog. Rep. for Period Ending Sept. 30, 1987, ORNL-6420, p. 89.
10. R. Kossakowski et al., Phys. Rev. C **32**, 1612 (1985).
11. S. Frauendorf and F. May, Phys. Lett. **125B**, 245 (1983).
12. R. Bengtsson, I. Hamamoto and B. Mottelson, Phys. Lett. **73B**, 259 (1978).
13. I. Ragnarsson and T. Bengtsson, private communication.
14. I. Ragnarsson et al., Phys. Rev. Lett. **54**, 982 (1985).
15. S. B. Patel et al., Phys. Rev. Lett. **57**, 62 (1986).

HIGH-SPIN STUDIES OF ^{172}Os: COMPLEX ALIGNMENT MECHANISM

J. C. Wells[1] A. Virtanen[4]
N. R. Johnson F. K. McGowan
M. A. Riley[2] C. Baktash
J. Dudek[3] I. Y. Lee

The nuclei in the light-mass tungsten-osmium region exhibit both shape coexistence effects and shape evolution tendencies and, thus, present good cases for comprehensive experimental investigations and theoretical calculations to understand their behavior at a microscopic level.

One interesting case in this region is ^{172}Os. Previous studies[5,6] of this nucleus have defined the yrast sequence up to $I = 24^+$, but have provided only limited information on side bands. Both Durell et al.[5] and Wells et al.[6] reported two anomalies (discontinues from a rotational-like trend) in the yrast sequence moment of inertia below a rotational frequency $\hbar\omega = 0.27$ MeV. Since this earlier work had left many interesting and unanswered questions about ^{172}Os, we have made a reinvestigation of its high-spin properties and, in the course of the work, have obtained some information on the previously unstudied nucleus, ^{173}Os.

For the current γ-γ coincidence measurements, a 1-mg/cm² target of enriched ^{144}Nd and a 162-MeV beam of ^{32}S ions from the HHIRF tandem accelerator was used, with the 4n-reaction channel producing ^{172}Os. The measurements were made with the Oak Ridge Compton Suppression System, using 19 Compton-suppressed large-volume Ge detectors. This system was incorporated into the Spin Spectrometer, a 4π array of NaI detectors, by replacing 19 of the NaI units with Compton-suppressed Ge units. In this way, γ-γ coincidence data was collected while recording the associated total energy and γ-ray multiplicity. The γ-ray spectra from the 19 Ge detectors were gain-matched and a 4k- by 4k-channel coincidence matrix was generated using coincidences between all possible pairs of detectors.

The level scheme for ^{172}Os deduced from the coincidence data is shown in Fig. 2.28, where the ^{172}Os γ rays have been grouped into five bands. Ordering of the γ rays in the level scheme is based on the observed coincidence relationships and on intensity arguments and energy systematics. Spin assignments are based on our γ-γ-angular-correlation data.

We have also identified γ rays belonging to other reaction channels besides the 4n channel which leads to ^{172}Os. In addition to ^{169}W and ^{170}W, we observe five other distinct bands belonging to unidentified nuclides, which, based on x-ray spectra, are probably odd-mass Os and Re isotopes. We have made a tentative identification of one of these bands as being that of ^{173}Os. The energies and intensities are given in Table 2.7.

The experimental aligned angular momenta for the five bands in ^{172}Cs are shown in Fig. 2.29

ORNL-DWG 88-14568R

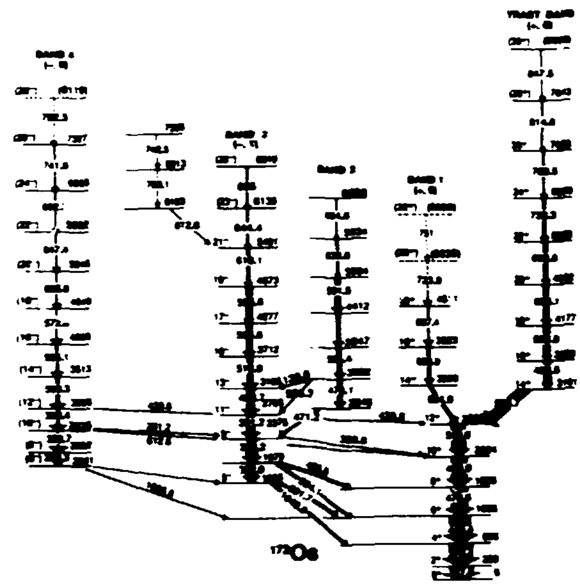

Fig. 2.28. Level scheme of ^{172}Os.

Table 2.7 Gamma-ray energies and intensities of a band assigned to ^{173}Os

E_γ(keV)[a]	Intensity[b]	E_γ(keV)[a]	Intensity[b]
232.4			
389.5	100±8	645.7	45±5
484.1	88±8	687.7	32±5
535.5	79±8	735.5	22±5
572.2	59±6	781.0	19±4
608.6	50±6	819.4	11±4

[a]Uncertainty in transition energies is 0.1 keV.

[b]Relative γ-ray intensities are normalized to the intensity of the 389.5-keV transition (=100). The transitions are assumed to be ordered in the band according to increasing energy.

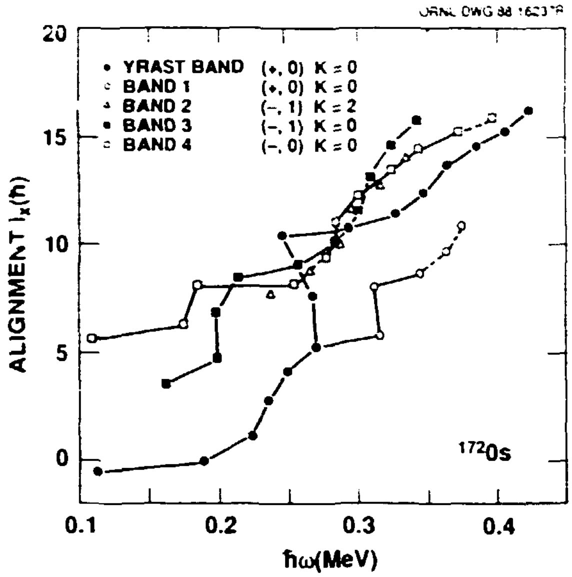

Fig. 2.29. Aligned angular momentum (i_x) for bands in ^{172}Os deduced from experiment.

These are labeled by their parity and signature quantum numbers (π,α). The rotational references, subtracted in determining these curves, used Harris parameters $J_0 = 15\ \hbar^2\ MeV^{-1}$ and $J_1 = 90\ \hbar^4\ MeV^{-3}$.

To understand the high-spin behavior of ^{172}Os illustrated in Fig. 2.29, we have carried out theoretical analyses where the first step involved calculations of the total-energy surfaces for the four assigned parity-signature combinations as a function of spin. These were performed with the generalized Strutinsky approach and the deformed Woods-Saxon potential (without pairing). These surfaces reveal a large number of varied-deformation configurations for ^{172}Os. For the even-parity states, only moderate deformations are involved in the spin range of our measurements, with (β_2,γ) remaining essentially constant (0.21,-16°) up to about spin 18^+ and there evolving to (0.18,-6°).

A microscopic analysis was next carried out with Hartree-Fock-Bogoliubov cranking (HFBC) calculations which included pairing correlation effects and particle-number projection. Some of the interesting conclusions we have reached based on these calculations and our experimental data follow: (1) The proton orbital most active in the alignment process has the quantum labels $h_{9/2}$, K = 1/2 (i.e., $1/2^-$ [541]) and crosses the Fermi level for Z = 76 at $\hbar\omega \approx 0.4$ MeV. Thus, it plays no significant role in the lower-frequency phenomena of our present investigation, contrary to the previous suggestions of this possibility. (2) The low-Ω orbitals of the $i_{13/2}$ quasineutrons interact strongly over the frequency range of $\hbar\omega$ = 0.22-0.27 MeV, corresponding to at least AB, BC, and AD crossings in the common nomenclature and, therefore, can account for the low-frequency anomalies in the moment of inertia. (3) The continuation of the s-band beyond the "forking" in the yrast sequence probably takes on the AB quasineutron character while the continuation of the ground-state band has primarily a BC description (or perhaps BCAD in analogy to the description applied in ^{158}Er by Simpson et al.[7] (4) The first anomaly in the ^{172}Os moment of inertia at I ≈ 6^+ probably results from the strong interaction with the ground band by the extension of the BC (BCAD) configuration, whereas the anomaly at I ≈ 14^+ is due to the AB crossing. (5) Finally, the negative parity bands denoted by (π,α) = (-,1) and (-,0) in Fig. 2.28 can be attributed to the AE and AF configurations, respectively, at low frequencies and to AEBC and AFBC configurations after the band crossings.

---

1. Adjunct staff member from Tennessee Technological University, Cookeville, TN.
2. ORNL and JIHIR. Present address: University of Liverpool, Liverpool, U.K.
3. JIHIR, Oak Ridge. Present address: Universite Louis Pasteur, F-67037, Strasbourg CEDEX, France.
4. ORNL and JIHIR. Present address: University of Jyväskyla, Jyväskyla, Finland.
5. J. L. Durell et al., Phys. Lett. 155B, 367 (1982).
6. J. C. Wel et al., Phys. Rev. C 36, 431 (1987).
7. J. Simpson et al., J. Phys. G 13, 847 (1987).

INVESTIGATION OF THE EVOLUTION OF COLLECTIVITY IN ^{172}Os VIA LIFETIME MEASUREMENTS

A. Virtnen[1] I. Y. Lee
N. R. Johnson C. Baktash
F. K. McGowan J. Dudek[3]
M. A. Riley[2] J. C. Wells[4]

In earlier[5,6] γ-γ coincidence measurements on ^{172}Os, it was established that there are two "anomalies" (discontinuities from a rotational-like trend) in its yrast-sequence moment of inertia below a rotational frequency of $\hbar\omega \approx$ 0.27 MeV. These studies[5,6] led to several suggestions for this behavior, but were unable to single out the cause.

In an effort to better understand the behavior of ^{172}Os — and to address some of the questions about other nuclei in this region — we recently launched new experimental investigations involving lifetime measurements with the recoil-distance apparatus and detailed γ-ray spectroscopy measurements with our Compton Suppression System. The spectroscopy studies are discussed in the previous article.

Excited states in the nucleus ^{172}Os were produced by the reaction ^{144}Nd(^{32}S,4n)^{172}Os at a beam energy of 162 MeV. The thickness of the enriched, self-supporting ^{144}Nd target was 1.35 mg/cm^2. The stopping medium for the recoiling nuclei consisted of 34 mg/cm^2 lead evaporated onto a 0.2-mm nickel foil. Target-stopper separations were determined by a digital micrometer and by capacitance measurements.

The ^{172}Os γ rays were detected in seven high-resolution Ge detectors. The shifted and unshifted γ-ray lines were measured in a BGO Compton-suppressed Ge detector placed at 0° and 9.7 cm from the target. The other six Ge detectors were in a ring perpendicular to the beam axis and at 5.9 cm from the target. Coincidence counts between any of the 90° detectors and the 0° detector were recorded on magnetic tape for 21 different target-stopper distances ranging from 0 to 20,128 μm. A lead-backed target was used for the zero-distance measurement.

Three sets of coincidence spectra from these experiments were analyzed. One of these we refer to as "Total Projected Data" (TPD) since they result from a coincidence count in the 0° detector gated by any event in the 90° detectors. From these spectra, the velocity of the recoiling ^{172}Os ions was found to be 4.767 ± 0.060 μm/ps, which corresponds to 1.59% of the velocity of light. We also analyzed the spectra generated by gating on γ rays below the transitions of interest — the "Gated Below Data" (GBD).

We can eliminate difficulties caused by long-lived side-feeding by gating on the band members higher than the transition of interest; we refer to coincidence spectra generated in this manner as "Gated Above Data" (GAD). All three types of data were analyzed with the computer program LIFETIME.[7] Decay curves from the data yielding the best fits for the 4$^+$ through 20$^+$ states of the yrast sequence are shown in Fig. 2.30.

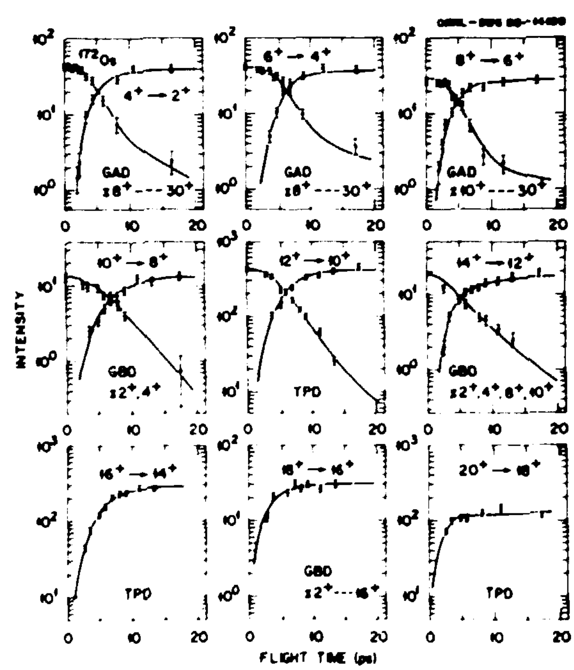

Fig. 2.30. Decay curves for the 4$^+$ through 20$^+$ states in ^{172}Os. The solid lines are the fits to the experimental points as extracted with the program LIFETIME. The notations GAD, GBD and TPD designate the type of coincidence data used as explained in the text.

A summary of the lifetimes (τ) and transition quadrupole moments (Q_t) determined in preliminary analyses of the three types of data is presented in Table 2.8. These Q_t values, plotted as a function of spin in Fig. 2.31, show an enhancement in the collectivity in the vicinity of the 6^+ state where the first anomaly in $\mathcal{J}$ occurs, while beyond the backbend there is a decrease in collectivity. Theoretical estimates of the transition quadrupole moments involve, in principle, the microscopic initial- and final-state wave functions and are rather complicated. They can often be replaced by an approximate expression[8] of the form

$$Q_t = \left(\frac{12}{5\pi}\right)^{1/2} (Ze)\, r_0^2\, A^{2/3}\, \beta_2 \cos(30° + \gamma) \ , \quad (1)$$

where $r_0 = 1.2$ fm. As pointed out [see preceding article] our potential energy surface calculations for ^{172}Os yield values of the deformation parameters (β_2, γ) of (0.212, -16°) up to I = 18 ħ, where a transition to (β_2, γ) = (0.185, -5°) takes place. In Fig. 2.31 the solid lines, corresponding to Q_t values computed from these deformations, mark the respective trends of the shape evolution.

A significant deviation between experimental and theoretical Q_t values is observed at I = 6^+ - 8^+. The fact that we find an enhanced collectivity for these states goes counter to earlier suggestions[6,9] that the $h_{9/2}$ protons in the 1/2$^-$ [541] orbital may be responsible for the behavior of the moment of inertia at these spins. The influence of this orbital is to drive the shape toward positive γ deformation (noncollective triaxiality) which should produce a drop in Q_t values. This conclusion is reinforced by our microscopic analysis carried out with Hartree-Fock-Bogoliubov cranking

Table 2.8 Summary of lifetimes and transition quadrupole moments of ^{172}Os yrast states obtained from the preliminary analyses of the total projected data (TPD), gated below data (GBD) and gated above data (GAD).

J_i^π	Eγ,keV	Weighted Average τ(ps)[a,b]	Q_t(eb)[b]
2^+	227.8	165±11	5.7±0.2
4^+	378.4	$10.1^{+1.1}_{-0.7}$	$5.7^{+0.3}_{-0.2}$
6^+	448.4	2.3±0.2	$7.6^{+0.4}_{-0.3}$
8^+	470.5	$1.7^{+0.7}_{-0.2}$	$7.7^{+1.7}_{-0.5}$
10^+	498.9	$1.6^{+0.3}_{-0.2}$	$6.8^{+0.7}_{-0.5}$
12^+	540.6	$1.1^{+0.4}_{-0.1}$	$6.7^{+1.1}_{-0.4}$
14^+	536.7	$1.2^{+0.7}_{-0.6}$	$6.3^{+2.0}_{-1.7}$
16^+	488.5	$3.2^{+0.8}_{-0.5}$	$4.9^{+0.6}_{-0.4}$
18^+	586.8	$1.5^{+0.6}_{-0.5}$	$4.6^{+1.0}_{-0.8}$
20^+	655.1	0.3±0.2	6.9±2.4

[a]Standard modeling was used in the fitting procedure. It involved two-state cascade side feeding to each level and a four-state rotational band built on the highest member of the cascade.

[b]These values are weighted averages of TPD, GBD and GAD. Error analyses were carried out statistically including the fact that the three sets of data are not fully independent.

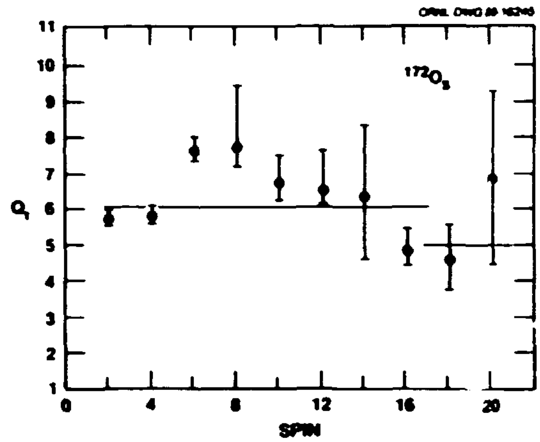

Fig. 2.31. Transition quadrupole moments, Q_t, as a function of spin for the yrast sequence of ^{172}Os. The solid lines show the trends predicted by theory.

calculations which treated pairing self-consistently and included particle-number projection. These calculations indicated the $h_{9/2}$ protons play no role below a frequency of $\hbar\omega$ = 0.4 MeV.

Although these calculations seem to rule out an appreciable $h_{9/2}$ proton contribution to the observed behavior of ^{172}Os, they do indicate that there are at least three two-quasineutron band crossings (AB, BC, and AD in the standard terminology) in the narrow frequency range of 0.22 to 0.27 MeV. Our spectroscopy results have shown that there is a strong interaction between these bands and the ground band in this region, and thus may give rise to the deviations of the Q_t values from a smooth trend, as seen in Fig. 2.31. We also note that the quantum effects in the Q_t moment, not present in Eq. (1), can contribute changes of the order of those indicated in the experimental Q_t evolution. The analysis of these contributions from quantum effects is in progress.

---

1. ORNL and JIHIR. Present address: University of Jyväskyla, Jyväskyla, Finland.
2. ORNL and JIHIR. Present address: University of Liverpool, Liverpool, U.K.
3. JIHIR, Oak Ridge. Present address: Universite Louis Pasteur, F-67037, Strasbourg CEDEX, France.
4. Adjunct staff member from Tennessee Technological University, Cookeville, TN.
5. J. L. Durell et al., Phys. Lett. 115B, 367 (1982).
6. J. C. Wells et al., Phys. Rev. C 36, 431 (1987).
7. J. C. Wells, M. P. Fewell and N. R. Johnson, LIFETIME: A Computer Program for Analyzing Doppler Shift Recoil Distance Nuclear Lifetime Data, ORNL/TM-9105 (1985).
8. P. Ring et al., Phys. Lett. 110B, 423 (1982).
9. H. T. Hsieh, M. M. King Yen and I. T. S. Kuo, J. Phys. G. 14, L31 (1988).

TRANSITION QUADRUPOLE MOMENTS OF HIGH-SPIN STATES IN ^{172}W

F. K. McGowan I. Y. Lee
N. R. Johnson C. Baktash

Recently, Raman et al.[1] questioned the large B(E2, 0 → 2) value of 5.78 ± 0.37 e^2b^2 for ^{172}W extracted from lifetime measurements carried out by us and our collaborators[2] by the recoil-distance technique. This disagreement was based on empirical and theoretical systematics[3] of B(E2, 0 → 2) values for even-even nuclei. To investigate factors which could have caused a decrease in the extracted lifetimes, we have reanalyzed the total-projected data with a focus on the normalization of the γ-ray spectra at different target-stopper distances. In our previous analysis[2] the γ-ray spectra were normalized to have the same number of events for the sum of the 4^+ to 1[illegible] transitions.

In the new analysis, we have normalized the spectra to only the sum of the (corrected) intensities of the shifted and unshifted components of the well-resolved $2^+ \to 0^+$ and $4^+ \to 2^+$ transitions in ^{172}W. These normalization factors reflect the integrated beam current on the target. The shifted component corrections are the positional solid angle and recoil velocity-dependent solid angle. For the unshifted component the only significant correction is the positional solid angle. The line-shape correction can be neglected because the stopping time in the stopper is calculated to be 1.16 ps, whereas the lifetimes of the 4^+ and 2^+ states are 51 and 1040 ps, respectively. Deorientation effects in the directional correlations of γ rays in the yrast band of ^{172}W are insignificant (≤ 2%) for our arrangement of the detectors in the γ-γ coincidence mode due to the small directional correlation (see Ref. 4).

With the new normalization factors, there are significant changes in the normalized intensities for the decay of the 2^+ and 4^+ states at the the larger recoil distances. The revised value of the transition quadrupole moment, Q_t, is 7.05 ± 0.30 eb for the $2^+ \to 0^+$ transition which is 8% smaller than our previously published value.[2] This corresponds to B(E2, 0 → 2) = 4.94 ± 0.42 e^2b^2 which is still 20% larger than the proposed systematics.[3]

So far, only the total-projected data have been reanalyzed for the yrast band in ^{172}W. In Fig. 2.32 the transition quadrupole moments deduced from the lifetime results are presented

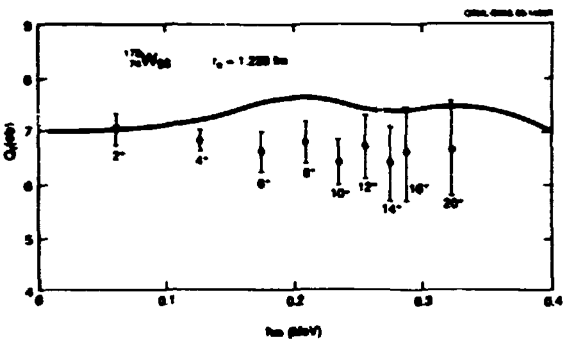

Fig. 2.32. Transition quadrupole moments, Q_t, for the yrast sequence of ^{172}W as a function of rotational frequency ($\hbar\omega = E_\gamma/2$). The solid curve shows the results of a cranked Woods-Saxon-Bogolyubov calculation.

as a function of the rotational frequency. The solid curve shows the results of a cranked Woods-Saxon-Bogolyubov calculation by Bengtsson and Xing.[2] The deformations (β_2, γ) from these calculations were converted to Q_t using

$$Q_t = \frac{6eZA^{2/3}}{(15\pi)^{1/2}} r_0^2 \beta_2 (1 + .360\beta_2)\cos(30° + \gamma) .$$

The solid curve corresponds to r_o = 1.228 fm (adjusted to reproduce the Q_t of the 2^+ state). The data for I < 8 do not show the increase in collectivity from centrifugal stretching at low spins. For states with I > 10 the Q_t values are all near a constant value of 6.5 eb. This is, of course, the trend predicted by the cranked-shell-model calculations for a nucleus with the Fermi surface near the middle of the $i_{13/2}$ neutron shell.

We are continuing the reanalysis of the other types of data (gated-above and sum-gated-below) for ^{172}W. When this is finished, we will take an average of all the reanalyzed data to see if the trend of the Q_t values in Fig. 2.32 is sustained. At that point we will address the role played by the $h_{9/2}$ protons in the interpretation of the results and present the information in a forthcoming paper.

---

1. S. Raman, C. W. Nestor, Jr., S. Kahane, and K. H. Bhatt, At. Data Nucl. Data Tables, to be published; S. Raman et al., Comment submitted to Phys. Rev. Lett.

2. M. N. Rao, N. R. Johnson, F. K. McGowan, I. Y. Lee, C. Baktash, M. Oshima, J. W. McConnell, J. C. Wells, A. Larabee, L. L. Riedinger, R. Bengtsson, Z. Xing, Y. S. Chen, P. B. Semmes, and G. A. Leander, Phys. Rev. Lett. 57, 667 (1986).

3. S. Raman, C. W. Nestor, Jr., and K. H. Bhatt, Phys. Rev. C 37, 805 (1988).

4. James E. Draper, Nucl. Instr. and Meth. A247, 481 (1986).

LIFETIME MEASUREMENT OF THE CORRELATED CONTINUUM GAMMA RAYS IN ^{170}Hf

I. Y. Lee, N. R. Johnson, C. Baktash, F. K. McGowan, J. R. Beene, M. A. Riley[2], W. B. Gao[1], A. Virtanen[3], Y. R. Jiang[1], L. Zhou[4], S. Zhu[1]

Continuum gamma rays are generally emitted at the early stages of the gamma decay of a compound nucleus. These gamma rays are from states with higher angular momentum and excitation energy than the discrete gamma rays. Therefore, from the study of continuum gamma rays it is possible to obtain information on nuclear properties in regions unreachable through studies of discrete gamma rays.

It is known experimentally that in most nuclei the continuum gamma rays are stretched E2 in nature and that they follow rotational-like sequences (i.e., energy increases with spin). The "singles" continuum spectra show a high energy edge which moves to higher energy as more angular momentum is brought into the nucleus. In a two-dimensional gamma-gamma coincidence matrix, the rotational-like behavior shows up as a valley along the $E_1 = E_2$ diagonal and as ridges parallel to the valley. The separation of the ridges is directly proportional to the nuclear moment of inertia.

Recent studies have shown that only a small fraction of the expected continuum intensity is observed in the ridge structure which has a width of about 20 keV. Level-mixing calculations for the region above the yrast line indicate that the effect of the damping of the collective strength is to spread the correlation through a region as wide as 200 keV. Such a large width will lead to a reduction of the intensity of the ridge structure that rises above the valley. In addition, this rotational damping will also change the lifetime of the E2 decay. Hence, a measurement of the lifetime of the gamma-ray continuum can provide information on the degree of rotational damping.

Lifetime measurements of the continuum gamma rays were first[5] carried out on singles spectra using the Doppler-Shift Attenuation Method (DSAM). Spectra from experiments with a thin target and a gold-backed target were compared, and, from the difference in the Doppler-shift of the edge of the E2 continuum, the lifetime of the gamma rays near the edge was derived. The results indicated that the collectivity of the continuum gamma rays is as high as, and possibly higher than, the low-spin rotational states. However, these experiments have limited value because they were done with NaI detectors which have low energy resolution and because the singles method can measure only the lifetimes of gamma rays near the edge. In the current measurements we have applied the DSAM to the full gamma-gamma correlation matrix, enabling us to determine the lifetime of the ridge in ^{170}Hf over a large range of energy. With our Compton Suppression Spectrometer System, it was possible to carry out these measurements with good energy resolution and a high peak-to-Compton ratio.

The experiments were carried out with a 195-MeV ^{44}Ca beam from the HHIRF tandem accelerator. Two ^{130}Te targets were used in separate runs. A 1 mg/cm^2 target on a 16 mg/cm^2 gold backing was used for the DSAM measurement and a thin target of thickness 1 mg/cm^2 was used for comparison. The gamma rays were detected in 20 anti-Compton shielded Ge detectors placed in a compact support structure with a target to Ge detector distance of about 12 cm. Triple-coincidence data were taken at a rate of 1000 events per second. We collected 150 x 10^6 events with the backed target and 50 x 10^6 events with the thin target.

Two-dimensional E_γ vs E_γ matrices were generated from these data. For the thin target, data were corrected for both the gain and the angular dependence of the Doppler shift. From the data with the backed target, a matrix was generated with coincidence events between the four 45° detectors and the four 135° detectors. Only the gain was corrected for this matrix. Thus, depending on the lifetime, the gamma ray will show a different amount of Doppler-shift. To measure the shifts, the 2-D matrices were cut perpendicular to the diagonal, and 1-D spectra were obtained by projection. Cuts were made in 50-keV steps from 700 to 1100 keV on both matrices. Figure 2.33 shows the comparison of several of these projected spectra.

It can be seen from these data that from 700 keV to 1000 keV the shift increases from 15% to

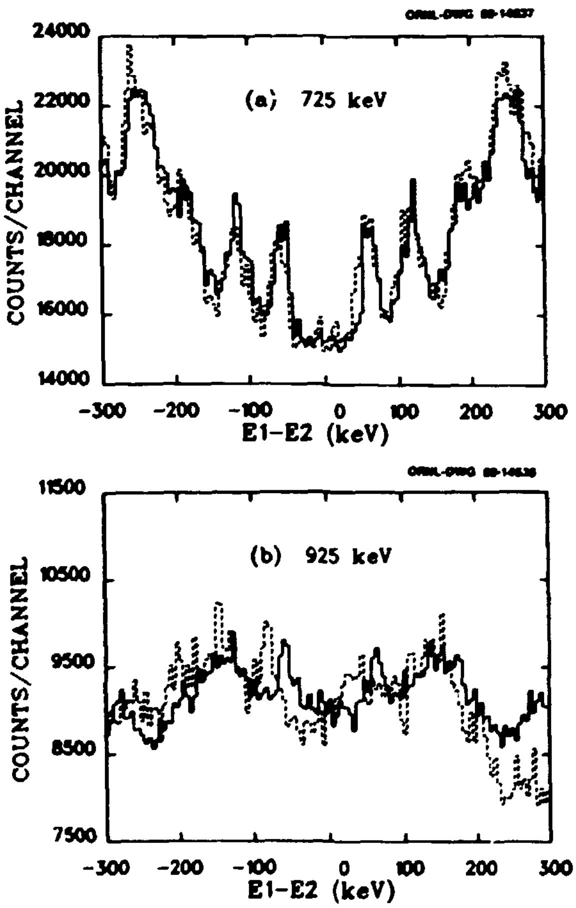

Fig. 2.33. Gamma-ray spectra from backed- and thin-target experiments. Spectra are obtained by cutting and projecting the 2-D matrice perpendicular to the $E_1 = E_2$ diagonal in 50-keV steps centered at (a) E_γ = 725 and (b) 925 keV, respectively.

90% of the fully shifted value, indicating a movement toward shorter lifetimes. Since the apparent lifetime reflects the total time from the formation of the compound nucleus to the emission of the gamma ray, to obtain the collectivity of a given transition, we have to understand the lifetimes of all the preceding gamma rays. The total decay time is dependent on the spin I_i of the starting point of the cascade, the energy of the gamma rays in the cascade, and the B(E2) values of the transitions. In a simple model, if a constant value for the moment of inertia is assumed, the gamma-ray energy can be calculated by $E_\gamma = (4I-2)/2\mathcal{J}/\hbar^2$; and if a constant value for Q_t is assumed, the B(E2) can be obtained by the expression

$$B(E2) = (16\pi/5)\, Q_t^2 \langle I\ 0\ 2\ 0 | I{-}2\ 0\rangle^2 .$$

The value of I_i can be determined from the average multiplicity of the gamma ray. Using this information, together with the recoil velocity calculated as a function of time from the stopping power, we can calculate the expected Doppler shift as a function of the gamma-ray energy. Figure 2.34 compares the calculated results with the experimental values. In these calculations, we used I_i = 50 which is determined from our measured average gamma-ray multiplicity, $2\mathcal{J}/\hbar^2$ = 114 MeV^{-1} which reproduces the separation of the ridges. The three curves correspond to Q_t values of 6, 7, and 8 eb, where 7 eb is the value for 2+ → 0+ transition of ^{170}Hf.

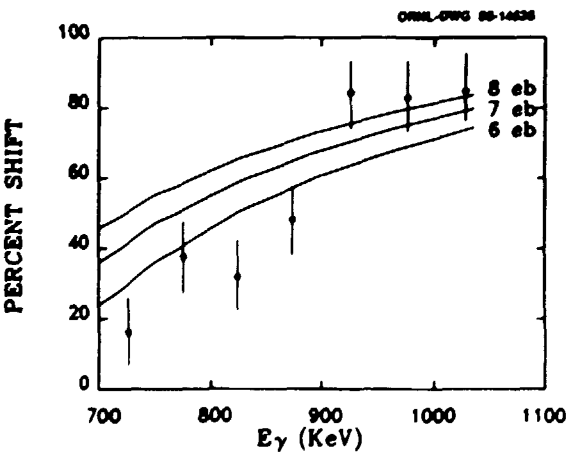

Fig. 2.34. Measured and calculated Doppler shift as a function of gamma-ray energy. The calculations were carried out using I_i = 50, $2\mathcal{J}/\hbar^2$ = 114 MeV^{-1} and Q_t = 6, 7, and 8 eb.

The experimental results in Fig. 2.34 indicate that the collectivity of gamma rays with energy less than 900 keV is smaller than that of the 2+ → 0+ transition, and above 900 keV the collectivity is higher. The reduction of the collectivity at E_γ < 900 keV has been observed[6] in many nuclei. It is interpreted as the change of the nuclear shape to smaller β deformation or to more triaxial or oblate deformation (γ > 0), due to the rotational alignment of high-j particles. The increasing of the collectivity at higher energies can also be due to a shape change. However, it is possible that this increase could be due to rotational damping. According to the calculation, the spreading width of the E2 strength for A = 160 nuclei is about 100-200 keV at an excitation energy of 2-4 MeV. Due to the E_γ^5 factor in the E2 transition rate, such a spread will increase the transition rate and reduce the lifetime by a factor of 10-30% which is comparable to our experimental values.

---

1. Vanderbilt University, Nashville, TN.
2. ORNL and JIHIR. Present address: University of Liverpool, Liverpool, U.K.
3. ORNL and JIHIR. Present address: University of Jyväskyla, Jyväskyla, Finland.
4. University of Tennessee. Knoxville, TN.
5. H. Hübel, V. Smilansky, R. M. Diamond, F. S. Stephens, and B. Herskind, Phys. Rev. Lett. 41, 791 (1978).
6. M. P. Fewell et al., Phys. Rev. C 37, 101 (1988).

HIGH-SPIN DATA BASE

J. D. Garrett, N. R. Johnson, M. A. Riley, F. McGowan, C. Baktash, L. Courtney[1], I. Y. Lee, L. L. Riedinger[2]

In recent years nearly all laboratories involved in the study of nuclei at high spins have established some kind of computerized data base for the nuclei that they are studying and the neighboring isotopes and isotones. The most comprehensive such data base probably is that established jointly by the Niels Bohr Institute, Oak Ridge National Laboratory, and their various collaborators. Although this data base is rather complete for the deformed even-even and odd-A rare earth and A = 120-140 isotopes, with time, the data base at the various institutes diverge as different data is added.

Therefore, we are preparing the guidelines for a central high-spin data base to be established at ORNL. The results of this data base will be accessible via a computer network to all high-spin groups participating. Some control will be exercised for data to be included. Likewise, a computer bulletin board will contain what data is included in the data base. The quick access to this data should also be helpful to nuclear structure theorists.

---

1. University of Tennessee, Knoxville, TN.
2. Adjunct staff member from the University of Tennessee, Knoxville, TN.

DESCRIPTION OF ONE-QUASIPARTICLE PROTON STATES IN RARE-EARTH NUCLEI

W. Nazarewicz[1,2] J. D. Garrett[3]
M. A. Riley[3,4] J. Dudek[5]

The valence single-proton configurations of rare earth nuclei represent a variety of orbital shapes. Thus the occupation of such configurations can have a significant influence on the nuclear shape. To study these effects, systematic calculations of noncollective single-proton states in odd-Z rare-earth nuclei have been performed, using the shell correction method with an average Woods-Saxon potential[6] and a monopole pairing interaction. Approximate particle number projection was carried out by using the method proposed by Lipkin and Nogami.[7] Deformation space was defined by means of quadrupole and hexadecapole deformation parameters (β_2,β_4).

The present calculations for neutron deficient isotopes with Z = 63-75 is a considerable extension of the number of nuclei considered in a previous paper[8] where the Nilsson-Strutinski approach was utilized. Equilibrium deformations of the even-even rare earth nuclei also are computed and compared with experimental values. Strong polarization effects due to the odd proton explain systematic trends of known band heads. A sample of results from these calculations for the Lu isotopes is shown in Fig. 2.35.

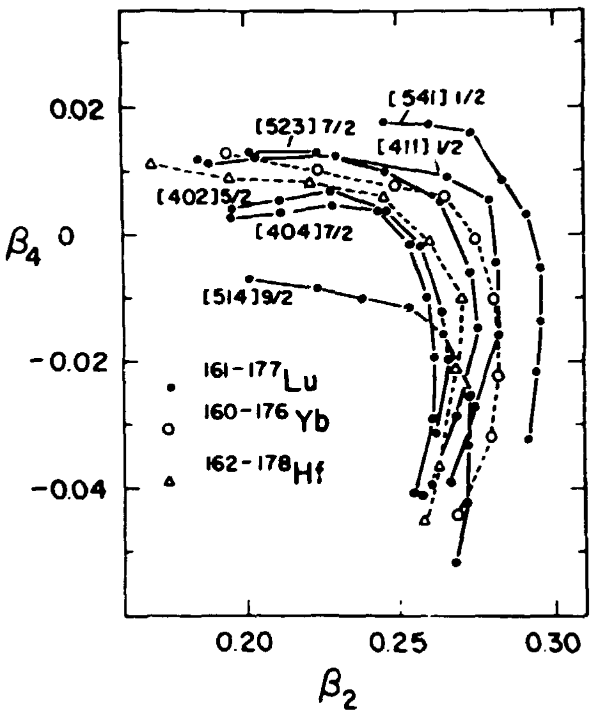

Fig. 2.35. Configuration dependence of the band-head quadrupole β_2 and hexadecapole β_4 deformations for the lutetium isotopes, $^{161-177}Lu_{90-106}$. For comparison, the ground-state deformations of ytterbium and hafnium isotopes also are shown.

Equilibrium deformations of lowest single-proton states in $^{161-177}Lu$ isotopes are compared to that of the corresponding even-even Yb and Hf cores. A pronounced configuration-dependent spread in the equilibrium shapes is seen.

---

1. The Niels Bohr Institute, Copenhagen, Denmark.
2. Institute of Physics, Warsaw Institute of Technology, Poland.

3. ORNL and The Niels Bohr Institute, Copenhagen, Denmark.
4. JIHIR. Present address: University of Liverpool, Liverpool, U.K.
5. JIHIR, Oak Ridge. Present address: Centre de Recherches Nucleaires et Universite Louis Pasteur, Strasbourg, France.
6. S. Cwiok, J. Dudek, W. Nazarewicz, J. Skalski and T. Werner, Computer Physics Communications, in press.
7. H. C. Pradhan, Y. Nogami and J. Law, Nucl. Phys. A201, 357 (1973).
8. B. S. Nilsson and M. E. Bunker, Nucl. Phys. A245, 376 (1975).

MOMENTS OF INERTIA AND SHAPE EVOLUTION AT HIGH SPINS IN ^{170}Hf

C. Baktash, J. W. McConnell, M. L. Halbert, F. K. McGowan, D. C. Hensley, C. M. Steele[1], N. R. Johnson, M. Carpenter[2], I. Y. Lee, V. P. Janzen[2], L. L. Riedinger[2]

This study was motivated by several reports in the literature on the observation of rigid-rotor behavior in ^{168}Hf (Ref. 3) and ^{168}Yb (Ref. 4), as well as a few other nuclei in this and the mass A = 80 regions.[5-7] The authors of these papers have attributed such a behavior to the collapse of neutron pairing in these nuclei. Experimentally, assessment of the strength of pairing forces has proven to be a difficult task. Therefore, it is important that the above interpretation be tested. If verified, it would provide a rather simple test of the pairing collapse. One way of testing the above interpretation is to examine the moments of inertia of similar bands in neighboring nuclei. Since the pairing strength is expected to be similar for the same configurations at the same rotational frequencies in the neighboring nuclei, the moments of inertia of these bands should behave very similarly. Therefore, if the above hypothesis is valid, one would expect to observe a rigid-rotor behavior in ^{170}Hf, which is two protons and two neutrons away from ^{168}Yb and ^{168}Hf, respectively.

The experimental setup consisted of the ORNL Compton Suppression Spectrometer System (18 Ge), and the Spin Spectrometer. The fusion-evaporation reaction ^{130}Te(^{44}Ca,4n) at a beam energy of 195.5 MeV was used to populate the high-spin states in ^{170}Hf. To select the high spin states, and to reduce the contamination due to other exit channels, only events with a fold of K > 17 were accepted in the off-line analysis of the data. These events amounted to slightly more than half of the total data (nearly 400 million events), and resulted in spectra which were dominated by the γ rays from ^{170}Hf.

The above γ-γ coincidence data were used to establish a partial decay scheme for ^{170}Hf, shown in Fig. 2.36. In addition to extending the three previously known[8] bands in this nucleus by more than 10ħ, we have established five new bands. We have also observed transitions that originate from three other bands, including one built on a high-K isomeric state. However, we have not yet firmly established the interband transitions that connect these cascades to the known level scheme.

The spin values shown in Fig. 2.36 were assigned on the basis of DCO measurements using detectors at 24 and 87 degrees. The parity assignments for bands 2 and 3 were adopted from Ref. 8. Two pieces of information suggest that bands 3 and 4 are signature partners: (1) the Routhians of the two bands are very similar; and (2) several interband transitions connect the two bands. Therefore, we have suggested a negative parity for band 4. We have also assumed positive parities for bands 7 and 8. (A negative parity assignment makes these bands yrast, which is unlikely in view of their weak population.)

The general features of the yrast sequence, and the negative-parity bands 2- are in qualitative agreement with the results of cranked-shell-model calculations. They show the first $i_{13/2}$ neutron band crossing at a frequency of $\hbar\omega$ = 0.25-0.30 MeV, and the onset of the first proton band crossing around $\hbar\omega$ = 0.5 MeV. The two side bands, however, show some unusual features which will be discussed in the following.

Figure 2.37 shows the kinematic and dynamical moments of inertia ($\mathcal{J}^{(1)}$ and $\mathcal{J}^{(2)}$, respectively) for the positive-parity yrast sequence, and the side bands 6 and 8. In contrast to its

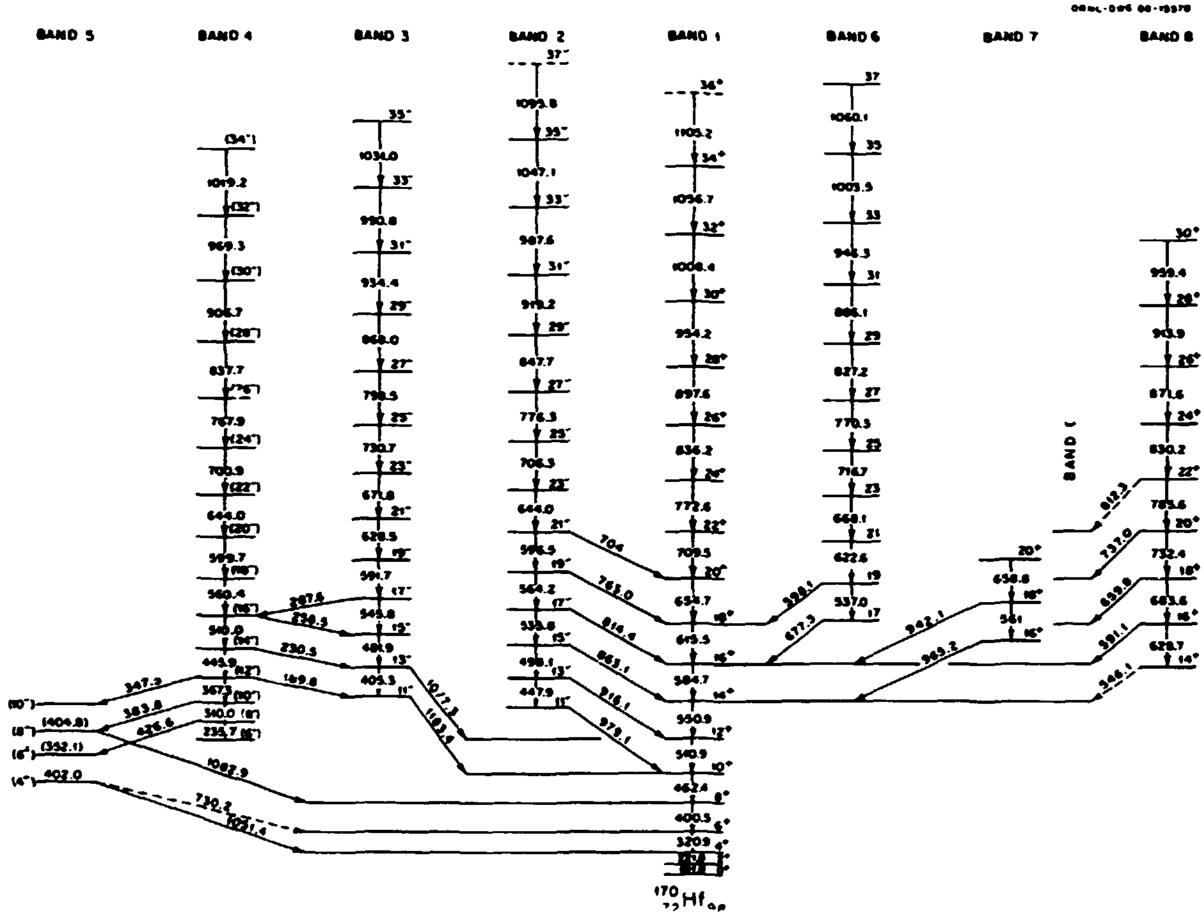

Fig. 2.36. Partial level scheme of ^{170}Hf.

isotope ^{168}Hf and isotone ^{168}Yb, the ^{170}Hf nucleus does not show a rigid-rotor behavior (i.e., $\mathscr{I}^{(1)} = \mathscr{I}^{(2)}$) for the positive-parity yrast sequence (see Fig. 2.37a). This result clearly indicates that moments of inertia are influenced by more factors than just the pairing strength; a not-too-surprising conclusion. Being microscopic quantities, in addition to the neutron and proton pairing force, the moments of inertia reflect the shape parameters that describe the mean field (β_2,β_4,γ), as well as the integral and local aligned angular momentum. It is, therefore, far too simplistic to ascribe its constancy (or variations) to a single influencing factor, namely the pairing strength. The fact that moments of inertia offer little quantitative information regarding the pairing force is further demonstrated by self-consistent CHFB calculations. These calculations show that the neutron pairing force is dramatically reduced following the first neutron band crossing around $\hbar\omega = 0.25$ MeV in this nucleus and its immediate neighbors. However, despite this similarity of the neutron pairing strength, the moments of inertia for the three nuclei under consideration are different.

In contrast to the positive-parity yrast sequence, band 6 shows a rigid-rotor behavior (Fig. 2.37b), and becomes energetically yrast at high spins. Nevertheless, this band receives little side-feeding intensity. This unusual side-feeding pattern for an yrast sequence suggests that it may be structurally different from the other bands in the level scheme. Calculations of the potential-energy surfaces, using microscopic-macroscopic methods and a

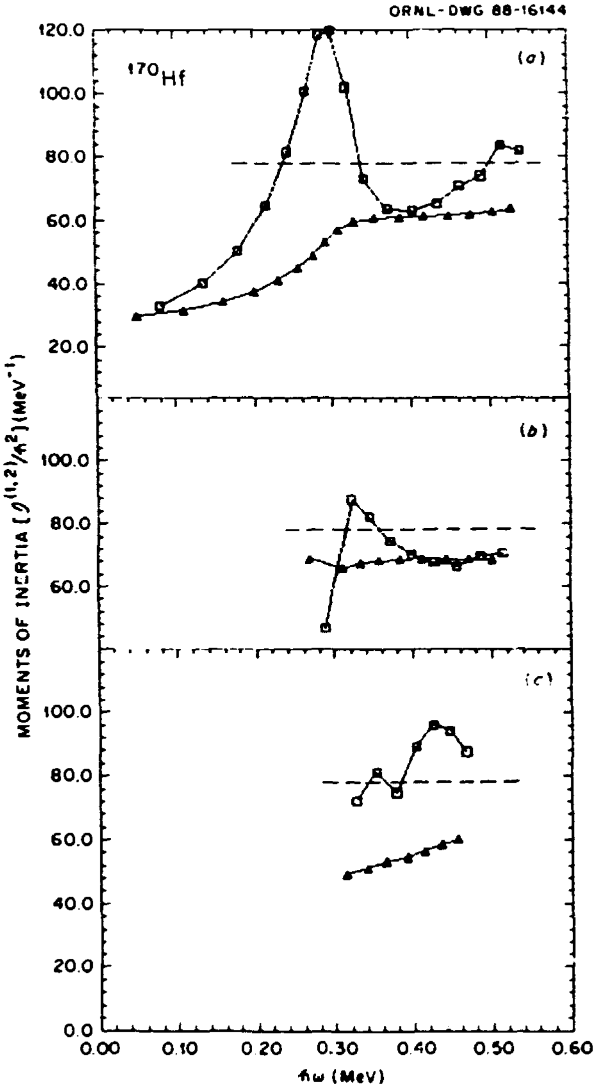

Fig. 2.37. Dynamical (squares) and kinematic (triangles) moments of inertia for (a) the positive-parity yrast sequence, (b) band 6, and (c) band 8 in ^{170}Hf.

deformed Woods-Saxon potential, indicate an excursion toward negative values of γ ($\gamma \approx -30°$), and more collective structures at spins of $I > 40\hbar$. This band may be associated with such collective oblate structures. Recent lifetime measurements of the continuum γ rays also indicate enhanced collectivity at high rotational frequencies in this nucleus (see contribution by I. Y. Lee et al., in this publication).

Figure 2.37c shows the moments of inertia for band 8. There are several unusual features associated with this band: (1) it has the least amount of aligned angular momentum and, thus, is highly nonyrast; (2) its kinematic moment of inertia is smoothly rising and barely reaches the average values of the other bands at the highest spin; and (3) its dynamical moment of inertia is bell-shaped and exceeds the rigid-rotor value by nearly 25%. Naturally, the behavior of $\mathcal{J}^{(2)}$ may be trivially explained by a band crossing at $\hbar\omega = 0.4$ MeV. However, no other band in this nucleus shows a band crossing at this frequency, which falls between the critical frequencies of the first neutron and proton band crossings. To reproduce such a crossing, one needs to invoke a very different quadrupole deformation for this band. A value of $\beta = 0.40$ will indeed give rise to an $i_{13/2}$ proton crossing at this frequency.

To substantiate the presence of a large-deformation minimum in this frequency range and in this region, we have examined the potential-energy surfaces that have been calculated by the computer code of Dudek and Nazarewicz. Interestingly, when the pairing strength is reduced to zero, one obtains a secondary minimum at $\beta \approx 0.35$. This minimum, however, disappears if a strength of $\Delta_n \approx \Delta_p \approx 0.5$ MeV is assumed. Naively, this may be taken as indirect evidence for a significantly reduced pairing strength at $\hbar\omega > 0.5$ MeV in this nucleus. However, before reaching such a conclusion, one needs to carefully examine and rule out other explanations for the observed behavior of the moments of inertia of this band.

---

1. Oak Ridge Science Semester Student. Present address: Department of Nuclear Engineering, Massachusetts Institute of Technology, Cambridge, Massachusetts.
2. University of Tennessee, Knoxville, Tn 37996-1200.
3. R. Chapman et al., Phys. Rev. Lett. 51, 2265 (1983).
4. J. C. Bacelar et al., Nucl. Phys. A442, 509 (1985).
5. C. Schuck et al., Phys. Lett. 142B, 253 (1984).

6. H. G. Price et al., Phys. Rev. Lett. 51, 1842 (1983).
7. L. K. Peker and J. H. Hamilton, BAPS 31, 1765 (1986).
8. J. C. Lisle et al., Nucl. Phys. A366, 281 (1981).

SEARCH FOR SUPERDEFORMED BANDS IN ^{82}Sr

C. Baktash	M. A. Riley[2]
G. Garcia-Bermudez[1]	A. Virtanen[3]
M. L. Halbert	V. Abenante[4]
D. C. Hensley	D. G. Sarantites[4]
N. R. Johnson	T. M. Semkow[4]
I. Y. Lee	H. C. Griffin[5]
F. K. McGowan	X. T. Liu[6]

Since the discovery of the fission isomers, it has been realized that, as a result of the interplay between the macroscopic and microscopic forces in nuclei, superdeformed nuclei (i.e., long-to-short axis ratio of 2:1) can appear in certain nuclear mass regions. Specifically, cranked-shell-model calculations point to the mass A = 150 and A = 80 regions as the most favorable candidates for the study of superdeformed (SD) shapes. In the past few years, a sequence of discrete transitions emanating from the high-spin SD states in ^{152}Dy, (Ref. 7) and several of its neighboring Gd, Tb, and Dy nuclei have been found. However, no SD band has been reported outside the actinide and A ≈ 150 regions. Therefore, it remains an exciting challenge to search for SD shapes in other mass regions. The importance of the observation of superdeformation in the lighter nuclei (A ≈ 80) lies in the fact that it not only provides a further test of the current theories, but also valuable insight into the competition between the microscopic and macroscopic forces that act to stabilize large deformations in nuclei.

In an extensive set of calculations, Nazarewicz et al.[8] have concluded that the single-particle energy spectra show large gaps at large deformations for N, Z = 38, 42 and 44. In particular, the N = 44 gap is expected to survive at large angular frequencies, and gives rise to SD structures at high spins in ^{82}Sr and ^{84}Zr nuclei.

In our current studies, we have concentrated on the investigation of ^{82}Sr and its odd neighboring isotopes. The fusion-evaporation reaction $^{52}Cr(^{34}S,2p2n)$ at a beam energy of 130 MeV was used to populate the high-spin states in ^{82}Sr. The experimental setup consisted of the ORNL Compton Suppression Spectrometer System (18 Ge), Spin Spectrometer, and the 4π CsI Dwarf Ball of Washington University. This system provided for both high-resolution γ-ray spectroscopy and complete exit-channel selection. In addition to light charged-particle identification, the 72 elements of the Dwarf Ball also provide angular-distribution and particle-energy information for the emitted particles. This information will be used to obtain the anisotropy of the charged particles in the center-of-mass frame and, thereby, to deduce the deformation of the parent compound nucleus.[9]

In the off-line analysis of these data, we generated a 3000 x 3000-channel γ-γ coincidence matrix subject to the requirements that: (1) the Dwarf Ball detects at least one proton; and (2) the total coincidence fold from the Spin Spectrometer should exceed a minimum value of K = 7. These conditions resulted in spectra that were dominated by γ-rays from ^{82}Sr. Figure 2.38 shows a partial level scheme for ^{82}Sr, which was constructed using the above data. In addition to establishing two new bands, we have extended four of the previously known[10] bands to spins that range from 20 to 27ħ. Together, they represent the most extensive high-spin band structure obtained in a medium-heavy nucleus.

The spin-parity assignments for states below ≈ 5 MeV of excitation energy were adopted from Ref. 10. The spin assignments for the higher-lying members of the bands were made using DCO measurements. The positive-parity, even-spin yrast sequence in this nucleus feeds both the ground-state band, and the γ-vibrational band. The kinematic and dynamic moments of inertia ($\mathcal{J}^{(1)}$ and $\mathcal{J}^{(2)}$, respectively) for this band is shown in Fig. 2.39a. In contrast to the yrast sequence in ^{84}Zr (Ref. 11), this band does not show a rigid-rotor behavior (i.e., $\mathcal{J}^{(1)}$ ≈

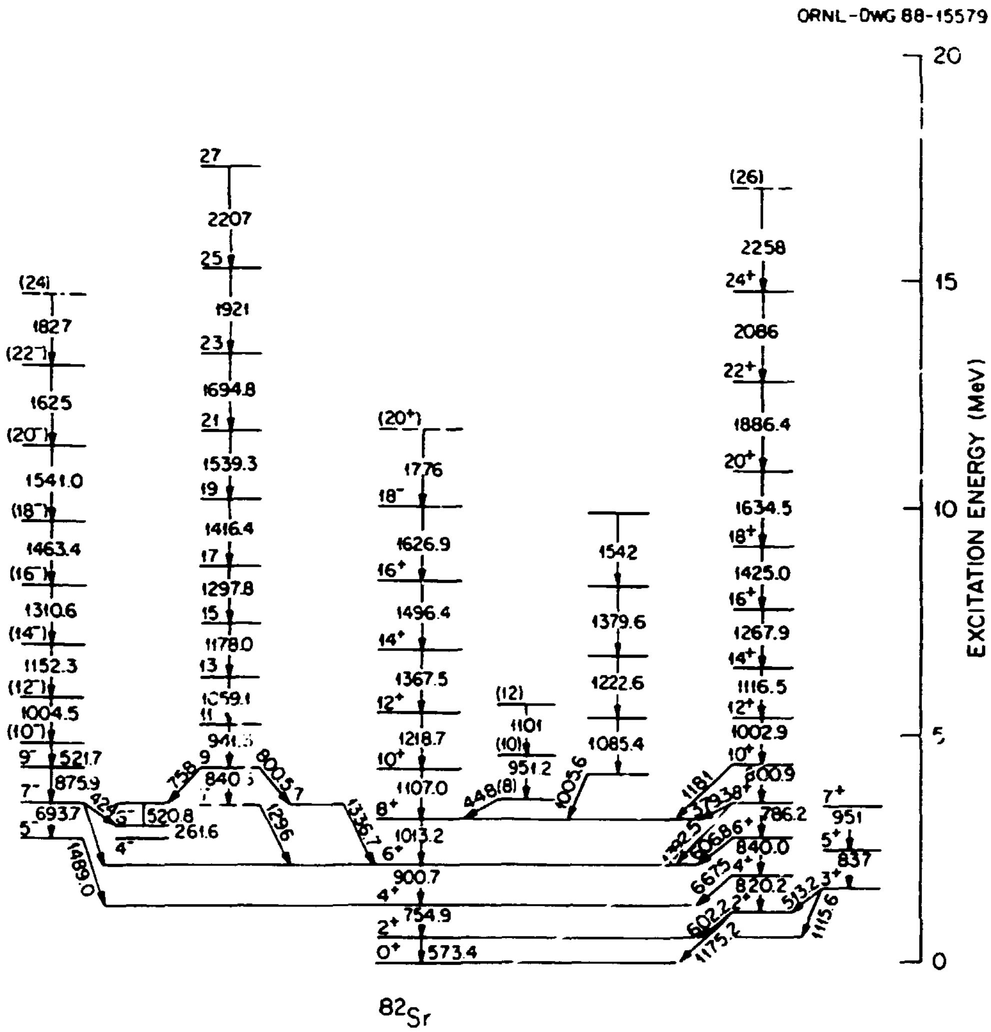

Fig. 2.38. Partial level scheme for ^{82}Sr.

$\mathcal{J}^{(2)} \approx \mathcal{J}_{rigid}$.) A rigid-rotor behavior in ^{84}Zr was interpreted[11] as evidence for the collapse of pairing correlations at high spins. Again, as discussed in our contribution on ^{170}Hf in this publication, our results for ^{82}Sr indicate that a rigid-rotor behavior conveys little information regarding the strength of pairing correlations.

The odd-spin band, extending to spin 27, becomes energetically yrast at high-rotational frequencies. The moments of inertia of this band, and of the negative-parity band are shown in Figs. 2.39b and 2.39c, respectively. Above an angular frequency of $\hbar\omega \approx 0.8$ MeV, they both show an alignment of $i \approx 15\hbar$. In collaboration with W. Nazarewicz, we are currently performing cranked-shell-model calculations (with a deformed Woods-Saxon potential) to interpret the structure of the high-spin bands in this nucleus.

Searching for superdeformed states, we have closely examined the above two-dimensional γ-γ coincidence matrix. Figure 2.40 shows this matrix following subtraction of the uncorrelated background of coincidence γ rays. A weak ridge-valley structure is evident in this figure. The first ridges are separated by approximately 300 keV, which implies a dynamic moment of inertia of $2\mathcal{J}^{(2)}/\hbar^2 \approx 50$ MeV^{-1}. This corresponds to a deformation of $\beta \approx 0.5$-0.6. Lack of sufficient

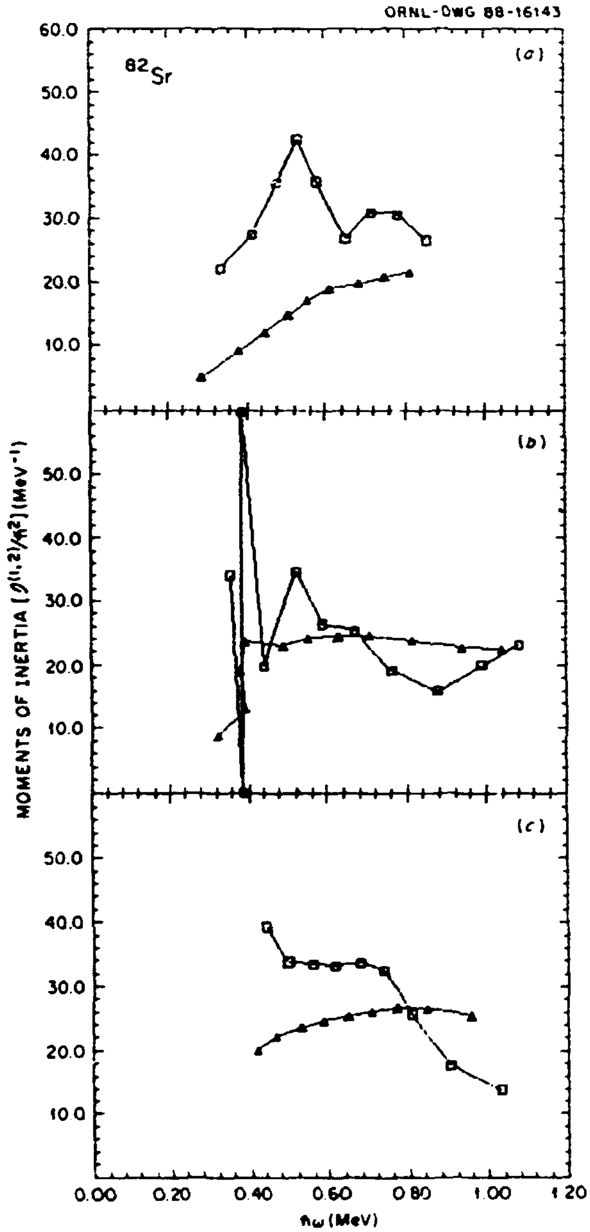

Fig. 2.39. Dynamical (squares) and kinematic (triangles) moments of inertia in ^{82}Sr as a function of $\hbar\omega$ for (a) the positive-parity yrast sequence, (b) the odd-spin band, and (c) the negative-parity band.

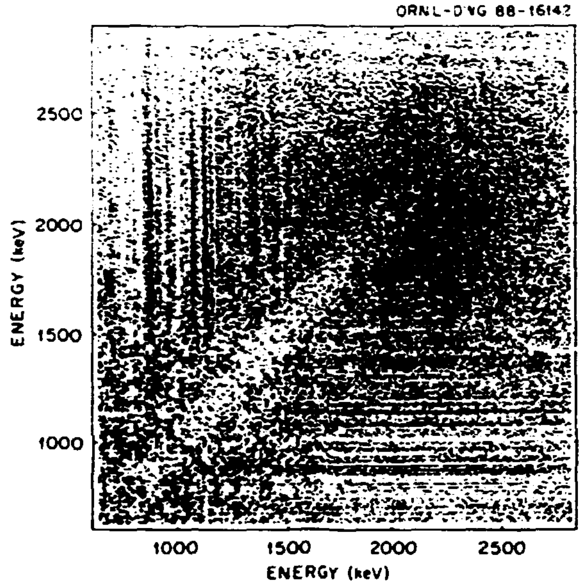

Fig. 2.40. Eγ-Eγ two-dimensional map for ^{82}Sr from the proton-gated data. The energy dispersion is 8 keV/channel.

statistics has so far prevented us from establishing a SD discrete band that is associated with the ridge-valley structure. We will perform a high-statistics experiment on one of the neighboring $^{81,83}Sr$ isotopes in the near future.

---

1. JIHIR. Permanent address: Comision Nacional de Energia Atomica, 1429 Buenos Aires, Argentina.

2. ORNL and JIHIR. Present address: University of Liverpool, Liverpool, U.K.

3. ORNL and JIHIR. Present address: University of Jyväskyla, Jyväskyla, Finland.

4. Washington University, St. Louis, MO 63130.

5. University of Michigan, Ann Arbor, MI 48108.

6. University of Tennessee, Knoxville, TN 37996-1200.

7. P. J. Twin et al., Phys. Rev. Lett. 57, 811 (1986).

8. W Nazarewicz et al., Nucl. Phys. A435, 397 (1985); and private communication.

9. Z. Majka et al., Phys. Rev. Lett. 58, 322 (1987).

10. P. S. Haskins et al., Phys. Rev. C32, 1897 (1985).

11. H. G. Price et al., Phys. Rev. Lett. 51, 1942 (1983).

TRANSITION QUADRUPOLE MOMENTS OF HIGH SPIN STATES IN $^{162,163}Yb$

F. K. McGowan C. Baktash
N. R. Johnson A. J. Larabee[2]
Y. Schutz[1] J. C. Wells[3]
I. Y. Lee

Transition quadrupole moments of states with spins up to ≈20 in collective bands near the yrast line have proved to be a valuable tool for tracing changes in nuclear shape. A reduction of collectivity at high spins has been observed in several N = 90 nuclei.[4-6] This effect in

^{156}Dy, ^{158}Er, and ^{160}Yb is understood qualitatively in terms of the cranked-shell-model theory[7] as a result of rotational alignment of two $i_{13/2}$ neutrons. The driving forces of the aligned neutrons with low-Ω orbitals changes the deformation of the nucleus from a prolate shape at low spin to a triaxial shape at high spin with positive γ-values which reduces the collectivity of the rotation. The calculated systematics[8] of triaxial shape-driving orbitals suggest that, unlike the N = 90 nuclei, the collectivity should not decrease at higher neutron number around N = 96 and 98. This arises from the fact that the aligned $i_{13/2}$ orbitals are different for the Fermi level near the middle of the $i_{13/2}$ shell. Our measurements for ^{170}W (N = 96) showed no reduction of the transition quadrupole moments after the backbend and up to spin I = 22^+. This confirms the cranked-shell-model theory prediction. The present study of ^{162}Yb is of particular interest because the N = 92 nuclei are closer to the region of N = 90 nuclei where nuclear shape changes have been observed to occur.

A comparison of the structure of the isotone ^{158}Dy with ^{162}Yb is of interest because it should contain information pertaining to modifications of the neutron degree of freedom resulting from proton-dependent changes to the nuclear field. For ^{158}Dy there is an upbend at the crossing frequency ħω = 0.29 MeV and the transition quadrupole moments[4] in the upbend connect smoothly, features indicative of a strong interaction between the ground and s-bands. Somewhat above the crossing frequency, the transition quadrupole moments Q_t show an appreciable reduction of 17%. In contrast, ^{162}Yb (N = 92) has a sharp backbend at ħω = 0.27 MeV. This small isotonic dependence of the crossing frequency can be explained by the expected[3] decrease in quadrupole deformation with increasing proton number. The interband transition $14^+ \to 12^+$ of 492.4 keV in the yrast sequence was not observed[10] (see Fig. 2.41) in previous work. Based on an intensity limit for this transition, the B(E2, 14 → 12) is less than

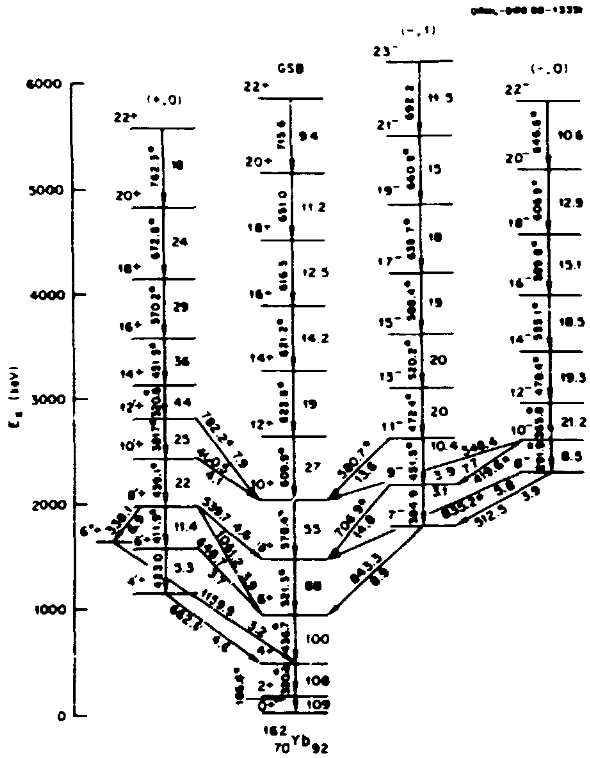

Fig. 2.41. A portion of the level scheme for ^{162}Yb taken from Ref. 9. Decay curves were obtained for those transitions with an asterisk. Transition energies and intensities also are given for each transition.

0.23 $B(E2)_{sp}$. The interaction matrix element between the ground and s-bands is exceedingly small in ^{162}Yb. Therefore, the yrast line above the sharp backbend describes the s-band very well. This interesting situation presents a good case to trace nuclear shape changes in an unperturbed two-quasineutron band over an appreciable range of spin I. The level scheme[10] for ^{162}Yb from the ^{122}Sn(^{44}Ca, 4n) reaction contains several other interesting features. The s-band feeds mainly into a vibrational-like band. There is relatively strong population of the side bands, e.g., the negative parity bands. The relative transition intensities are also given in Fig. 2.41.

Lifetimes of states in ^{162}Yb have been measured by the Doppler-shift recoil-distance method operated in the "singles" mode, using the reaction ^{116}Cd(^{50}Ti, 4n) at 215 MeV. Decay curves were extracted for those transitions with an asterisk in Fig. 2.41. A serious problem in the analysis was the number of multiplets (γ-rays of equal energy): 320.6 keV $4^+ \to 2^+$ and $14^+ \to 12'^+$; 451.5 keV $16^+ \to 14^+$ and $11^- \to 9^-$; 521 keV $8^+ \to 6^+$ and $15^- \to 13^-$. With the use of the very extensive results[10] from γ-ray spectroscopy, we have analyzed the decay curves from these multiplets. In Fig. 2.42 the transition

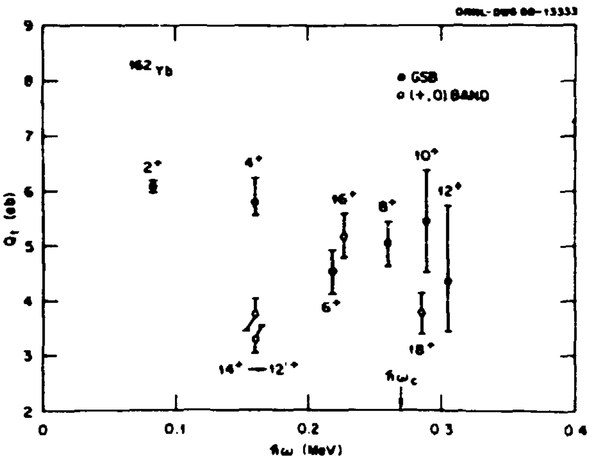

Fig. 2.42. Transition quadrupole moments Q_t for the yrast sequence of ^{162}Yb as a function of the rotational frequency ($\hbar\omega = E_\gamma/2$).

quadrupole moments Q_t deduced from the lifetime results are presented as a function of the rotational frequency. At low spins the data do not show the increase in collectivity from centrifugal stretching as predicted by cranked-shell-model calculations. This is the trend which we have also observed in ^{160}Yb, ^{170}W, and ^{172}W. For both ^{160}Yb and ^{162}Yb, the Q_t values for the states in the ground-state band and the (+,0) band tend to decrease with increasing rotational frequency. The Q_t values for the $i_{13/2}$ band in ^{163}Yb also show a decrease with increasing ħω.

A number of Q_t values extracted for states in the negative parity bands, (-,1) and (-,0), and the vibrational-like band are given in Table 2.9. The Q_t values of the (-,1) band are larger than those of the (-,0) band. The relatively large Q_t values for states in the vibrational-like band would account for the feature that the

Table 2.9 Transition quadrupole moments for states in the (-,1), (-,0), and vibrational-like bands in ^{162}Yb

Transition	Eγ(keV)	Q_t(eb)
$9^- \to 7^-$	384.9	7.8±1.2
$11^- \to 9^-$	451.5	7.5±1.0
$19^- \to 17^-$	635.7	$6.3^{+2.6}_{-1.2}$
$10^- \to 8^-$	291.8	5.7±0.4
$12^- \to 10^-$	365.8	5.4±0.6
$14^- \to 12^-$	478.4	$5.9^{+1.9}_{-0.6}$
$16^- \to 14^-$	555.1	6.1±1.0
$8' \to 6''$	338.1	8.0±1.2
$8' \to 6'$	411.9	6.3±0.4
$10' \to 8'$	439.1	$8.0^{+0.4}_{-0.8}$
$12' \to 10'$	381.7	5.8±0.4

(+,0) band feeds mainly into this vibrational-like band.

Finally, a number of interband Eλ transition probabilities, extracted from the data, are given in Table 2.10. Since the interband reduced E2 transition probabilities are very small, we are able to extract reduced M1 transition probabilities. For the transitions $10'^+ \to 10^+$ and $8'^+ \to 8^+$, the B(M1) values are $(9.6\pm1.6) \times 10^{-2}\mu_N^2$ and $(2.8\pm0.4) \times 10^{-2}\mu_N^2$, respectively. These B(M1) values are relatively large for transitions between low spin states. The B(E1) values between the natural parity states are also large.

---

1. ORNL. Present address: Grand Accelerateur National d'Ions Lourd, Caen, France.
2. University of Tennessee. Present address: TRIUMF, Vancouver, Canada.
3. Adjunct staff member from Tennessee Technological University, Cookeville, TN.
4. H. Emling et al., Nucl. Phys. A419, 187 (1984).
5. M. Oshima et al., Phys. Rev. C 33, 1988 (1986).
6. M. P. Fewell et al., Phys. Rev. C 37, 101 (1988).

7. R. Bengtsson et al., Nucl. Phys. A405, 221 (1983).
8. S. Frauendorf and F. R. May, Phys. Lett. 125B, 245 (1983).
9. R. Bengtsson et al., At. Data Nucl. Data Tables 35, 15 (1986).
10. J. N. Mu et al., Nucl. Phys. A472, 295 (1987).

Table 2.10 Interband reduced transition probabilities in single-particle units

Transition	Eλ	B(Eλ)/B(Eλ)sp
$14^+ \to 12^+$	E2	<0.23
$12'^+ \to 10^+$	E2	2.0±0.8
$10'^+ \to 8^+$	E2	<0.5
$8'^+ \to 6^+$	E2	0.78±0.12
$11^- \to 10^+$	E1	$(1.1\pm0.1)\times10^{-3}$
$9^- \to 8^+$	E1	$(1.0\pm0.1)\times10^{-3}$
$10^- \to 10^+$	E1	$(2.7\pm0.4)\times10^{-5}$
$8^- \to 8^+$	E1	$(1.0\pm0.2)\times10^{-4}$

HIGH-SPIN STUDIES IN LIGHT Ir NUCLEI

H. Q. Jin[1] C. Baktash
C. R. Bingham[2] M. L. Halbert
M. P. Carpenter[1,3] N. R. Johnson
V. P. Janzen[1] I. Y. Lee
L. L. Riedinger[2] F. K. McGowan
L. Zhou[1] M. A. Riley[4]

The first backbend throughout the deformed rare-earth nuclei results from the alignment of the $\nu i_{13/2}$ orbital. However, the proton orbitals $\pi h_{9/2}$ and $\pi i_{13/2}$ play an increasingly important role for the nuclei at the upper end of this region of deformation. Prolate rotational bands have been identified previously,[5] built on these high-j band heads in $^{181-187}$Au; and they show the $\pi i_{13/2}$ excitation energy relative to that of the $\pi h_{9/2}$ decreasing steadily, a sign that the nuclear deformation in the $\pi i_{13/2}$ band is increasing for lighter isotopes.[6]

Experiments have recently been performed on the high-spin states in ^{179,181}Ir at the Oak Ridge Holifield Tandem accelerator. The purpose of this program has been to investigate the deformation driving tendency of the high-j quasiproton orbitals, and to understand alignment processes in the bands built on these states. A key question is whether or not there occurs in ^{179,181}Ir (N = 102,104) a band crossing due to the alignment of the $\pi h_{9/2}$ pair, as found at N = 106 (^{183}Ir) and 107 (^{185}Pt).[7] The $\pi h_{11/2}$ band in ^{181}Ir seems to show two crossings, which could again be evidence of a very low-frequency $\pi h_{9/2}$ crossing and therefore the double-crossing scenario[7,8] (i.e., $\nu i_{13/2}$ and $\pi h_{9/2}$ alignments).

The Holifield experiments were performed using ^{156,158}Gd(^{27}Al,4n)^{179,181}Ir reactions at a beam energy of 134 MeV. The Compton Suppression System (with 19 suppressed Ge counters) was loaded into the Spin Spectrometer and used for these measurements. Lead-backed targets were used to avoid Doppler shifting in the γ-ray energies at different detector angles. Due to the absence of any previously assigned states in ^{179}Ir, excitation function measurements were performed at three energies (134, 139, and 144 MeV). The (^{27}Al,4n) reaction at 134 MeV was chosen to populate the strong 4n channel and reduce the secondary p4n channel, which gives the known nucleus ^{178}Os. Three bands have been established, based on the systematic analysis of Ir isotopes in this region: $1/2^-[541]$, $\pi h_{9/2}$; $1/2^+[660]$, $\pi i_{13/2}$; and $5/2^+[402]$, $\pi d_{5/2}$. The $\pi h_{9/2}$ band has been identified as the ground configuration of light Au and Ir isotopes, and it has a large signature splitting (K = 1/2). So far, we have not identified the unfavored signature of this band in ^{179}Ir.

The resulting ^{179}Ir alignment plots in Fig. 2.43 show that the $\pi h_{9/2}$ band has a crossing around $\hbar\omega$ = 0.35 MeV, due to the alignment of a pair of $i_{13/2}$ neutrons. The I = 17/2 and 21/2 members of the $\pi i_{13/2}$ band lie close in energy to those in the $\pi d_{5/2}$ structure, and it is at this point where the former band feeds into the latter. This interaction between the two structures produces the slight perturbation in two points around $\hbar\omega$ = 0.2 MeV for the $\pi d_{5/2}$ band

ORNL-DWG 88-14473

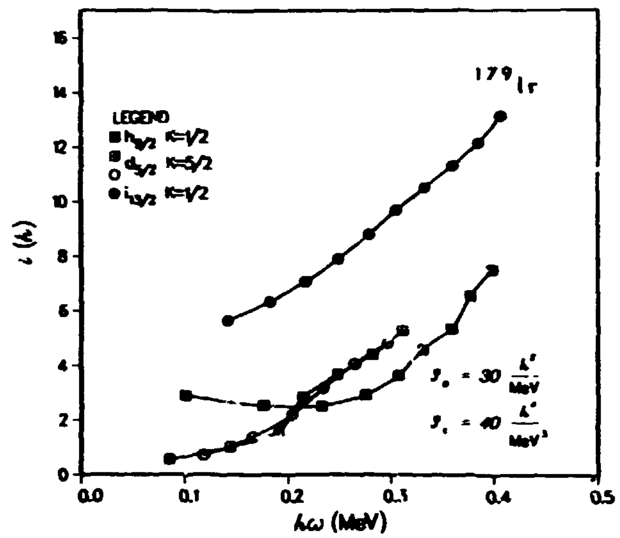

Fig. 2.43. Plot of aligned angular momentum (i) versus rotational frequency for the 1/2[541], the 1/2[660] and the 5/2[402] bands in ^{179}Ir. The rotational reference was subtracted according to J_0 = 30 ħ²/MeV and J_1 = 40 ħ⁴/MeV³.

ORNL-DWG 88-14474

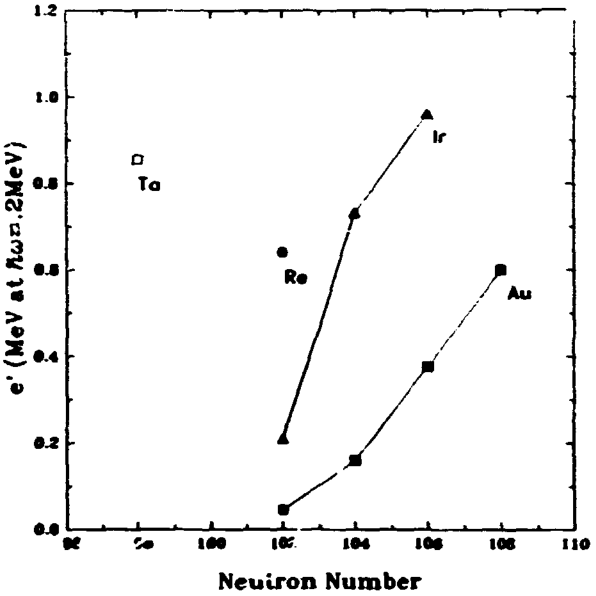

Fig. 2.44. Plot of the excited energies of $\pi i_{13/2}$ band relative to that of the $\pi h_{9/2}$ band for some rare earth nuclei.

(see Fig. 2.44). A large gain in alignment for the $\pi i_{13/2}$ band is apparent over an unusually long range in frequency. The moment of inertia is significantly larger for that band as well, indicating a possible change in deformation. The $\pi i_{13/2}$ band appears at a surprisingly low excitation energy with a rotational pattern that is very intriguing. In fact, while the $\pi h_{9/2}$ band is the yrast band at low rotational frequency, the $\pi i_{13/2}$ band becomes yrast at higher frequency. Figure 2.44 illustrates the observed energy of the $\pi i_{13/2}$ band relative to the $\pi h_{9/2}$ band for nuclei where the 1/2$^+$[660] band has been identified. There is a clear drop in relative energy for the lighter Ir isotopes as well as the Au isotopes. It is well known that the $\pi h_{9/2}$ band-head energy for Au isotopes decreases as the neutron number decreases and the deformation of this band increases. The rapid fall in energy of the $\pi i_{13/2}$ band for Au in Fig. 2.44 is an indication that the $\pi i_{13/2}$ band might possess a deformation larger than that of the $\pi h_{9/2}$ excitation. The energies of $\pi i_{13/2}$ bands for the Ir isotopes also show the same pattern, which could suggest larger deformations for the $\pi i_{13/2}$ bands in the Ir isotopes as well. The alignment of the $\pi i_{13/2}$ band increases smoothly, perhaps because of a $\nu i_{13/2}$ crossing of very large interaction strength, in contrast to the more normal interaction expected in the less-deformed orbitals. A Total Routhian Surface (TRS) contour diagram for the lowest positive-parity configuration in ^{179}Ir shows that there is a significant difference in the predicated deformation due to occupation of the $\pi d_{5/2}$ vs. $\pi i_{13/2}$ orbitals (β_2 = 0.2 vs. 0.3).[9] The large gain in experimental alignment could be due to a very substantial change in reference parameters, pointing to a corresponding change in deformation even larger than that suggested by the TRS calculations.

The level scheme of ^{179}Ir has not been completed. The analysis of the data is still in progress and we have seen another unidentified, strongly-coupled band. B(M1)/B(E2) values are to be extracted and should be very sensitive to the quasiparticle nature of band crossings. We hope that such a branching-ratio analysis will be able to help determine whether there is indeed one or two low-frequency alignment processes in this region of nuclei.

---

1. University of Tennessee, Knoxville, TN.
2. Adjunct staff member from the University of Tennessee, Knoxville, TN.
3. Present address: The Niels Bohr Institute, University of Copenhagen, Denmark.
4. Present address: University of Liverpool, Oliver Lodge Lab., Liverpool L69 BX, England.
5. L. Zhou, et al., Nuclear Phys. Prog. Rept., Univ. of Tenn., 21 (1988) and H.-Q. Jin, et al., ibid. p. 26.
6. V. P. Janzen, et al., Phys. Div. Prog. Rept. September 1987, ORNL-6420, p. 90.
7. V. F. Janzen, et al., Phys. Rev. Lett. 59, 2073 (1988).
8. A. J. Larabee, et al., Physics Lett. 169B, 21 (1986).
9. V. P. Janzen, et al., in Proc. of the Conf. on High-Spin Nucl. Structure and Novel Shapes, Argonne National Laboratory, April, 1988, ANL-PHY-88-2, p. 211.

LIFETIME MEASUREMENTS OF HIGH-SPIN STATES IN ^{185}Pt AND ^{186}Pt

L. Zhou[1] M. Riley[2]
V. Janzen[1] A. Virtanen
H. Jin[1] U. Garg[3]
L. Riedinger[1] G. Kajrys[4]
N. Johnson S. Monara[4]
I. Y. Lee N. Nadon[4]
F. McGowan S. Pilotte[4]

A measurement of the lifetimes of high-spin states in ^{185}Pt and ^{186}Pt has been performed at the Holifield facility. The purpose of the measurement was primarily to deduce which quasiparticle alignment is responsible for the yrast band crossing in ^{185}Pt, by measuring the B(E2) values before and after the band crossing, comparing it to our previously measured B(M1)/B(E2) values,[5] and concluding how the M1 matrix elements behave in the 9/2[624] band after the crossing. This should be a clear signature whether it is the $h_{9/2}$ protons or the $i_{13/2}$ neutrons responsible for this band crossing.

The lifetime experiment was performed with the recoil-distance device located in the center of an array of seven Ge detectors. One Compton-suppressed detector was located at 0°, and six unsuppressed detectors were positioned at 90°. The reaction used was ^{36}S + ^{154}Sm at a beam energy of 165 MeV, which produces ^{185}Pt by the 5n channel and ^{186}Pt by 4n. Gamma-gamma coincidence data were acquired at 23 plunger distances. Analysis has, so far, been performed on the projected spectra, i.e., the total-coincidence data. Shifted and unshifted peaks are seen in these projected spectra for transitions up to I = 18 in the yrast band of ^{185}Pt and up to 43/2 in the yrast 9/2[624] band of ^{185}Pt. Only preliminary results are available at this time. It is clear that the B(E2) value for the first 2^+ of ^{186}Pt is smaller than that for the previously measured ^{184}Pt.[6] This is logical in view of the prediction that the Pt nuclei become more deformed for smaller N.

The importance of performing this measurement is exemplified in Fig. 2.45. This figure shows the measured B(M1)/B(E2) values from our earlier spectroscopy work on ^{185}Pt and ^{183}Ir.[5] There is

ORNL-DWG 88-14475

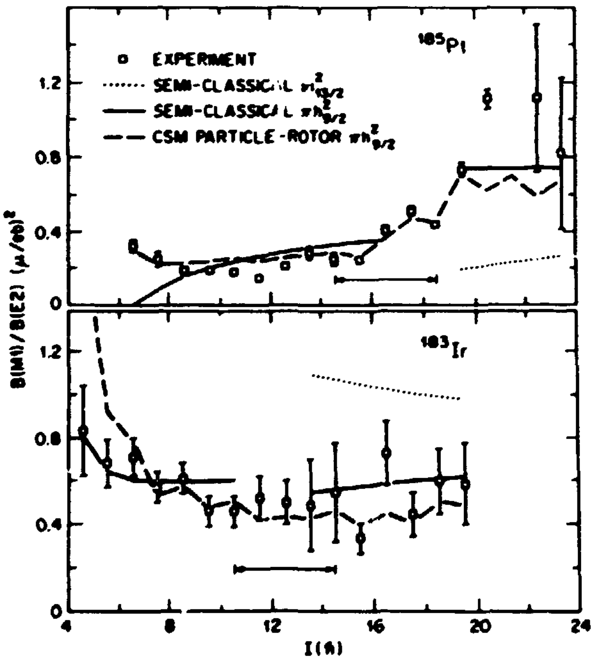

Fig. 2.45. Experimental and calculated B(M1;I → I-1)/B(E2;I → I-2) ratios in ^{185}Pt and ^{183}Ir. The semi-classical geometrical predictions assuming a $\pi h_{9/2}$ crossing are shown as a solid line; the dotted line assumes a $\nu i_{13/2}$ alignment. The dashed line shows the results of the cranked shell model particle-rotor calculation. The spin ranges for proposed $\pi h_{9/2}$ crossings are marked.

a crossing in the 9/2[624] ($\nu i_{13/2}$) band of ^{185}Pt in the I = 14 to 18 range, resulting in an increase in the M1/E2 ratio. Self-consistent calculations of the shape of this nucleus in various one- and three-quasiparticle configurations are used to estimate the effect of either a $\pi h_{9/2}$ or $\nu i_{13/2}$ alignment on the B(E2) values. From this, it was concluded that the E2 matrix elements should not vary much between the one- and three-quasiparticle components of this 9/2[624] band of ^{185}Pt. It seems then that the rise in the M1/E2 ratio can be attributed to the increase in the M1 matrix element, which requires this to be the $\pi h_{9/2}$ crossing.[5] This scenario is supported by the corresponding data on the 5/2[402] ($\pi d_{5/2}$) band of ^{183}Ir, also shown in Fig. 2.45. There is no rise in the M1/E2 ratio through the crossing in this band, which supports the proposed $\pi h_{9/2}$ crossing here also. The existence of such a low-frequency ($\hbar\omega$ = 0.24 MeV) band crossing due to the alignment of a pair of $h_{9/2}$ protons is very surprising and unexpected from theory. The lifetime experiment on ^{185}Pt is intended, then, to settle this issue by measuring directly the B(E2) values in the $\nu i_{13/2}$ band and allowing the extraction of the M1 matrix elements from the earlier branching ratios.[5]

---

1. University of Tennessee, Knoxville, TN.
2. Partial support provided by JIHIR and the University of Tennessee.
3. University of Notre Dame, Notre Dame, Indiana.
4. University of Montreal, Canada.
5. V. P. Janzen, et al., Phys. Rev. Lett. 59, 2073 (1988).
6. U. Garg, et al., Phys. Lett. B180, 319 (1986).

NUCLEAR STRUCTURE STUDIES VIA RADIOACTIVE DECAY

BETA DECAY PROPERTIES OF ^{148}Er AND ^{148}Ho[1]

K. S. Toth J. M. Nitschke[3]
D. C. Sousa[2] P. A. Wilmarth[3]

The decay properties of ^{148}Er and ^{148}Ho, produced in ^{58}Ni bombardments of ^{94}Mo, were investigated following on-line mass separation. New γ rays were observed for both nuclides. Transitions assigned to ^{148}Ho decay are predominantly from the decay of the high-spin isomer; based on its decay characteristics (see Fig. 2.46), we propose that this state in ^{148}Ho has a

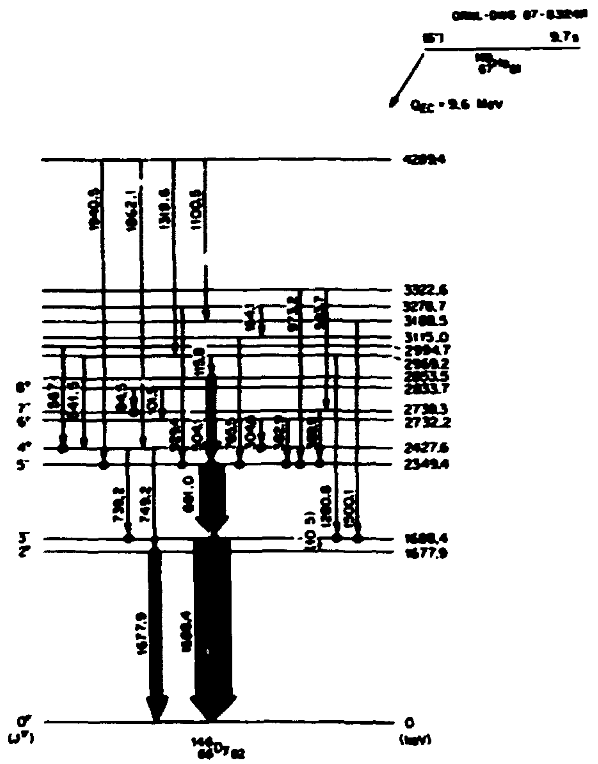

Fig. 2.46. Proposed decay scheme for the ^{148}Ho high-spin isomer. Observed coincidence relationships are indicated by dots placed at the top and bottom of transition lines. The 6^- assignment for this isomer is suggested because: (1) γ rays deexciting the lowest 10^+ level at 2920 keV (seen in an in-beam study of ^{148}Dy states) are not observed, (2) deexcitations from the 8^+ and 7^- levels at 2833.7 and 2739.3 keV on the other hand are observed, and, (3) the log ft value for the β transition feeding the 5^- 2349.4-keV level is ~ 5.3.

spin assignment of 6^-. The decay pattern of ^{148}Er shows that the J^π of the ^{148}Ho low-spin isomer is 1^+. Coincidences between protons and x and γ rays establish ^{148}Er and ^{148}Ho to be β-delayed-proton precursors. In the β decay of ^{148}Dy, three weak γ rays were observed in addition to the one intense 620.2-keV transition that has been known to follow the nuclide's decay.

1. Summary of published paper: Phys. Rev. C 37, 1196 (1988)
2. Summer visitor from Eastern Kentucky University, Richmond, KY 40475.
3. Lawrence Berkeley Laboratory, Berkeley, CA 94720.

DELAYED PROTON EMISSION OF N = 81 ODD-ODD PRECURSORS: ^{148}Ho, ^{150}Tm, AND ^{152}Lu[1]

J. M. Nitschke[2] J. Gilat[2]
P. A. Wilmarth[2] K. S. Toth
F. T. Avignone III[3]

Beta-delayed proton decay was observed in ^{148}Ho, ^{150}Tm, and ^{152}Lu for the first time. Contrary to neighboring even-Z, N = 81 isotones, the proton spectra appear structureless and statistical in nature. Proton branching ratios for the high-spin isomers in these isotopes, based on the intensity of γ-ray transitions in the intermediate nuclei, are $(8\,^{+1}_{-2}) \times 10^{-4}$, $(1.2\,^{+0.2}_{-0.4}) \times 10^{-2}$, and $(1.5 \pm 0.7) \times 10^{-1}$, respectively. The onset of proton emission in all three cases occurs at a proton-to-gamma width ratio of about 10^{-4}. Protons were found to be in coincidence with X rays, γ rays, and positrons. Coincident K X rays served to identify the Z of the precursor, while the γ rays gave quantitative information about proton decay to excited states in the daughter nuclei. By comparing the final state branching ratios with statistical model calculations, it was concluded that both ^{148}Ho and ^{150}Tm have isomers with probable spin values of 1^+ and 6^-. Statistical model calculations with "standard" prescriptions for level densities and γ widths, and with a reduced level density parameter, were compared to experiment. To reproduce the shape of the proton spectrum, it was necessary to assume Gaussian-shaped Gamow-Teller β strength functions centered near 8-MeV excitation energy. Figure 2.47 shows the calculated fit and the experimental spectrum measured for ^{150}Tm.

1. Summary of a published paper: Phys. Rev. C 37, 2694 (1988).
2. Lawrence Berkeley Laboratory, Berkeley, CA 94720.
3. University of South Carolina, Columbia, SC 29208.

ORNL-DWG 88-15161

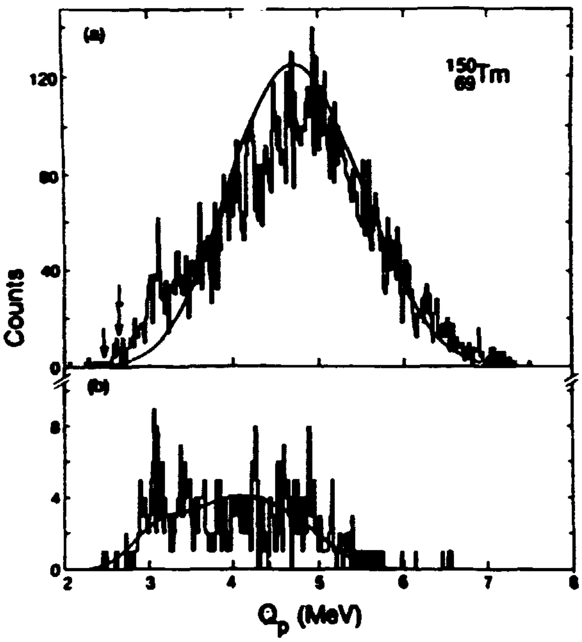

Fig. 2.47. (a) Proton spectrum observed at mass 150. The smooth curve is the result of a statistical model calculation normalized to the total number of observed protons. Based on experimentally measured final state feedings in the proton-decay daughter, ^{149}Ho, the contributions of the 6^- and 1^+ states of ^{150}Tm were assumed to be 80% and 20%, respectively. (b) Protons observed in coincidence with positrons. The curve overlaying the data was obtained by smoothing the proton spectrum in part (1) and multiplying it by the ratio of the Fermi functions $f^+/(f^+ + f^{EC})$.

BETA-DELAYED PROTON DECAY OF THE N = 83 PRECURSOR ^{153}Yb[1]

P. A. Wilmarth[2] K. Vierinen[2]
J. M. Nitschke[2] K. S. Toth
M. Kortelahti[3]

Beta-delayed proton emission was observed for the N = 83 precursor ^{153}Yb. This extends the region of delayed proton emission in the lanthanides across the N = 82 shell for the first time. The 4.0 ± 0.5 s delayed proton activity was assigned to ^{153}Yb on the basis of mass separation, coincident Tm K x rays, and coincident γ-ray transitions in the daughter nucleus ^{152}Er. Proton final state branching ratios are consistent with a $7/2^-$ precursor spin. The proton branching ratio is $(8 \pm 2)\times10^{-5}$. Fig. 2.48 summarizes schematically the ^{153}Yb β-delayed-proton decay scheme.

---

1. Summary of a published paper: Z. Phys. A323, 503 (1988).
2. Lawrence Berkeley Laboratory, Berkeley, CA 94720.
3. Louisiana State University, Baton Rouge, LA 70803; Permanent address: University of Jyväskylä, SF-40100 Jyväskylä 10, Finland.

ORNL-DWG 88-15163

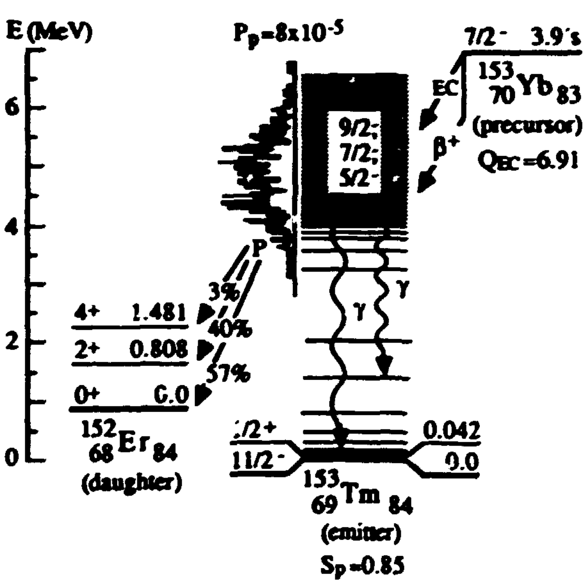

Fig. 2.48. Energetics and branching ratios for ^{153}Yb delayed proton decay.

FINE STRUCTURE IN ^{153}Tm α DECAY[1]

K. S. Toth, R. B. Firestone[2], P. A. Wilmarth[2], K. Vierinen[2], J. M. Nitschke[2], M. O. Kortelahti[3], F. T. Avignone, III[4]

In an investigation of A = 153 isotopes, fine structure was observed in ^{153}Tm α decay. Besides the previously known α transitions that feed the ^{149}Ho $h_{11/2}$ (0.0 keV) and $d_{5/2}$ (49.9 keV) isomers, two very much weaker α groups were found to populate the $d_{3/2}$ (220.4 keV) and $d_{5/2}$ (564.4 keV) states in ^{149}Ho. Based on the ^{149}Ho level scheme and on the Q_α values for the two main ^{153}Tm α transitions, we determine that the $h_{11/2}$ level in ^{153}Tm is the ground state and that the $s_{1/2}$ state lies 43 ± 7 keV above it (see Fig. 2.49). Energy systematics for the $s_{1/2}$ and $h_{11/2}$ proton states in even-N odd-Z nuclei near N = 82 are discussed.

---

1. Summary of a published paper: Phys. Rev. C38, 1932 (1988).
2. Lawrence Berkeley Laboratory, Berkeley, CA 94720.
3. Louisiana State University, Baton Rouge, LA 70803; permanent address: University of Jyväskylä, SF-40100, Jyväskylä 72, Finland.
4. University of South Carolina, Columbia, SC 29208.

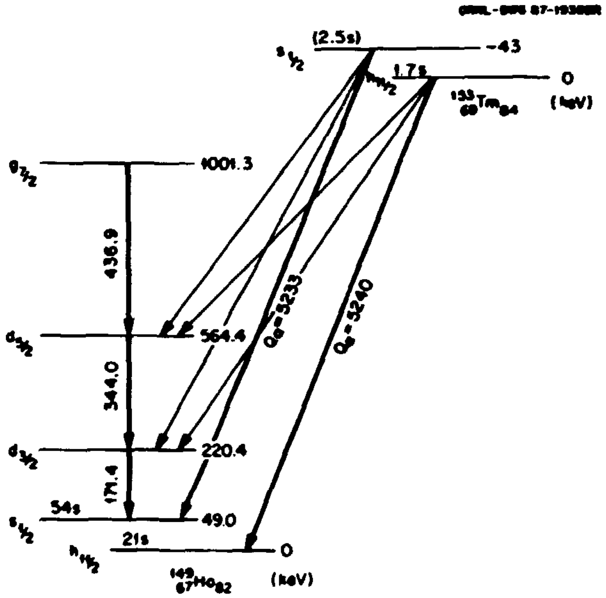

Fig. 2.49 Alpha-decay scheme of ^{153}Tm. Because of the 60-keV (FWHM) resolution of our particle telescope we could not determine from which of the two isomers the fine structure ^{153}Tm α groups originate. Thus, transitions from both isomers to the 220.4- and 564.4-keV ^{149}Ho levels are indicated.

BETA-DECAY OF ^{154}Lu AND ^{154}Yb[1]

K. S. Vierinen[2], P. A. Wilmarth[2], A. A. Shihab-Eldin[2], R. M. Chasteler[2], J. M. Nitschke[2], R. B. Firestone[2], K. S. Toth

By using mass-separated sources the β-decay properties of ^{154}Lu and ^{154}Yb were investigated. Limits of ^{154}Lu decay to the first 8^+ and 6^+

levels in ^{154}Yb suggest a 7^+ spin for the odd-odd parent; also, delayed proton emission and an indication of delayed α-particle emission were observed to follow ^{154}Lu β decay. The β-decay branch of the α-emitting nucleus ^{154}Yb was identified for the first time by the observation of one intense 133.2-keV γ ray. This transition deexcites a 1^+, 133.2-keV level in ^{154}Tm, which is fed by an allowed $0^+ \rightarrow 1^+$ β transition with a log*ft* value of 3.6 ± 0.3. The decay schemes of ^{154}Lu and ^{154}Yb are shown in Fig. 2.50.

---

1. Summary of a published paper: Phys. Rev. C 38, 1509 (1988).
2. Lawrence Berkeley Laboratory, Berkeley, CA 94720.

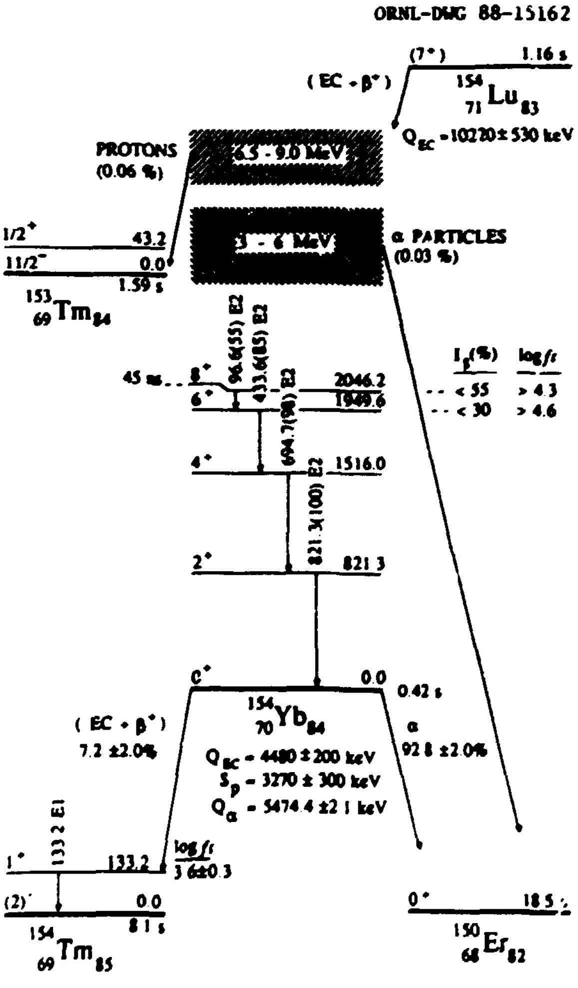

Fig. 2.50. Decay schemes of ^{154}Lu and ^{154}Yb.

NUCLEAR STRUCTURE EFFECTS ON α REDUCED WIDTHS[1]

K. S. Toth	J. W. McConnell
Y. A. Ellis-Akovali	H. K. Carter[2]
H. J. Kim	D. M. Moltz[3]

Figure 2.51 shows reduced widths for s-wave (ground-state-to-ground-state) α transitions of even-even nuclei with Z from 78 to 100. The widths exhibit a generally smooth behavior. Deviations from this smoothness can be interpreted as being due to nuclear structure effects; for example, the discontinuity at N = 126 results from the shell closure.

Above the N = 126 shell, around N = 130, the reduced widths are rather large; in particular, the ^{218}Ra value (labeled as "Previous Measurement") exhausts 75% of the Wigner-sum-rule limit. Suggestions have been made that these large widths are an indication of α clustering on the nuclear surface. We re-measured[4] the ^{218}Ra α half-life with the use of the HHIRF velocity filter and a novel experimental technique,[5] and found it to be 25.6 μs instead of the adopted value of 14 μs. This larger half-life yields an α width which, in the figure, is indistinguishable from those of ^{216}Rn and ^{220}Th. The result is a smooth trend of α widths from the N = 130 region to the well-deformed, prolate, Cm, Cf, and Fm nuclei, which thus weakens the argument for the existence of α clusters in the heavy elements.

However, contrary to an expected shell effect at Z = 82, the α-decay rates of ^{186}Pb, ^{188}Pb, ^{190}Pb, and ^{192}Pb (open points with N from 104 to 110) are less hindered than those of neighboring Hg isotopes; this may imply that midway between N = 82 and N = 126 the 82-proton shell is not magic.[6] We recently[7] used the UNISOR facility to identify the α decay of ^{194}Pb for the first time and to determine the isotope's α branch. The resultant width (N = 112) together with the estimate for ^{184}Pb (N = 102) indicate that the influence of the Z = 82 shell may reassert itself for both N > 112 and N < 102.

---

1. Summary of published invited talk: Proc. 5th Int. Conf. on Nuclei Far From Stability,

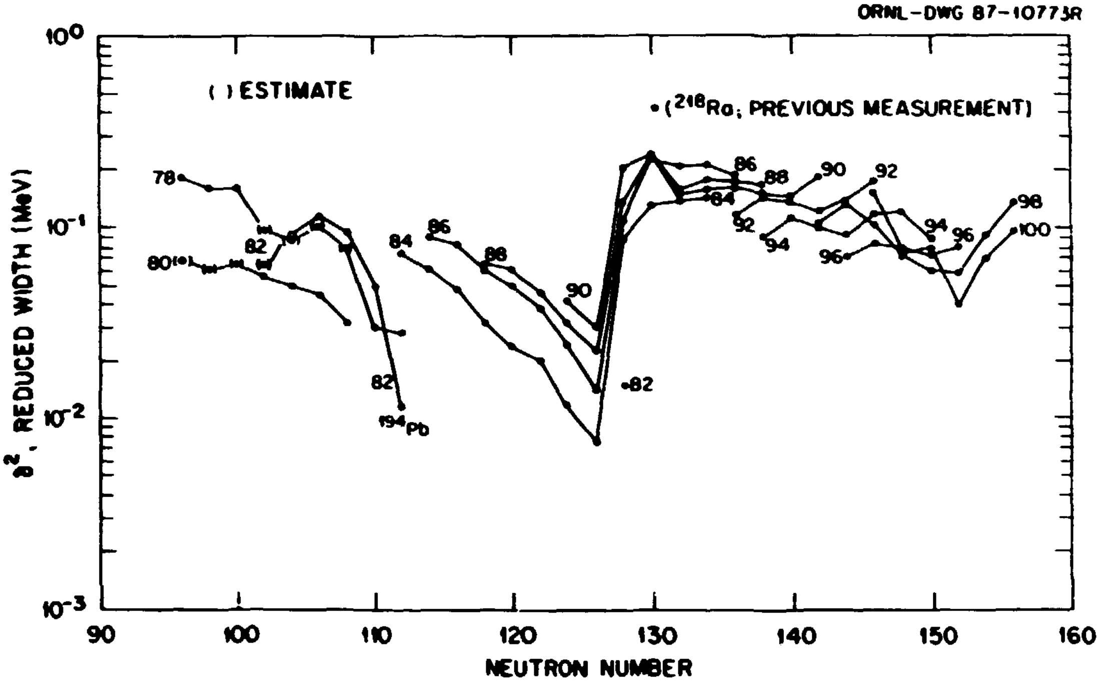

Fig. 2.51. Reduced widths for s-wave α transitions plotted as a function of N for even-even isotopes with Z from 78 to 100. Widths for Pb nuclei are indicated by open points.

Rosseau Lake, Ontario, Canada. Sept. 14-19, 1987, I. S. Towner ed., American Institute of Physics Publication No. 164, p. 665.

2. UNISOR, Oak Ridge, TN 37831.

3. Lawrence Berkeley Laboratory, Berkeley, CA 94720.

4. K. S. Toth, H. J. Kim, M. N. Rao, and R. L. Mlekodaj, Phys. Rev. Lett. 56, 2360 (1986).

5. H. J. Kim, K. S. Toth, M. N. Rao, and J. W. McConnell, Nucl. Instrum. Methods A249, 386 (1986).

6. K. S. Toth, Y. A. Ellis-Akovali, C. R. Bingham, D. M. Moltz, D. C. Sousa, H. K. Carter, R. L. Mlekodaj, and E. H. Spejewski, Phys. Rev. Lett. 53, 1623 (1984).

7. Y. A. Ellis-Akovali, K. S. Toth, H. K. Carter, C. R. Bingham, I. C. Girit, and M. O. Kortelahti, Phys. Rev. 36, 1529 (1987).

RADIOACTIVITIES WITH 145<A<155 INVESTIGATED AT THE OASIS FACILITY

K. S. Toth, J. Gilat[1], J. M. Nitschke[1], D. M. Moltz[1], P. A. Wilmarth[1], M. N. Rao[2], Y. A. Akovali, D. C. Sousa[3], K. Vierinen[1]

Over the past four years a collaborative program between LBL and ORNL has been in progress at the OASIS separator[4] to investigate properties of short-lived nuclides near N = 82 (see Fig. 2.52). Table 2.11 lists the isotopes investigated and summarizes some of the data obtained. Our purpose has been primarily two-fold: (1) to study levels in nuclei whose structures should be describable in single-particle terms, and (2) to understand the nature of the sharp peaks observed in delayed-proton spectra of N = 81, even-Z precursors. In the course of this collaboration: (1) systematics of neutron states in N = 81 and N = 83 nuclei, and of proton states in N = 82 nuclei have now been extended to $^{149}_{68}Er_{81}$, $^{151}_{70}Yb_{81}$, $^{149}_{66}Dy_{83}$, $^{151}_{68}Er_{83}$, $^{149}_{67}Ho_{82}$, and $^{151}_{69}Tm_{82}$; (2) five isotopes, three isomers, and ten delayed-proton emitters have been discovered; and (3) the pronounced structure in the delayed-proton spectra of ^{147}Dy, ^{149}Er, and ^{151}Yb has been shown[5] to be associated with the $s_{1/2}$ ground states of these even-Z, N = 81 precursors.

---

1. Lawrence Berkeley Laboratory, Berkeley, CA 94720.

2. Present address: University of São Paulo, São Paulo, Brazil 01498.

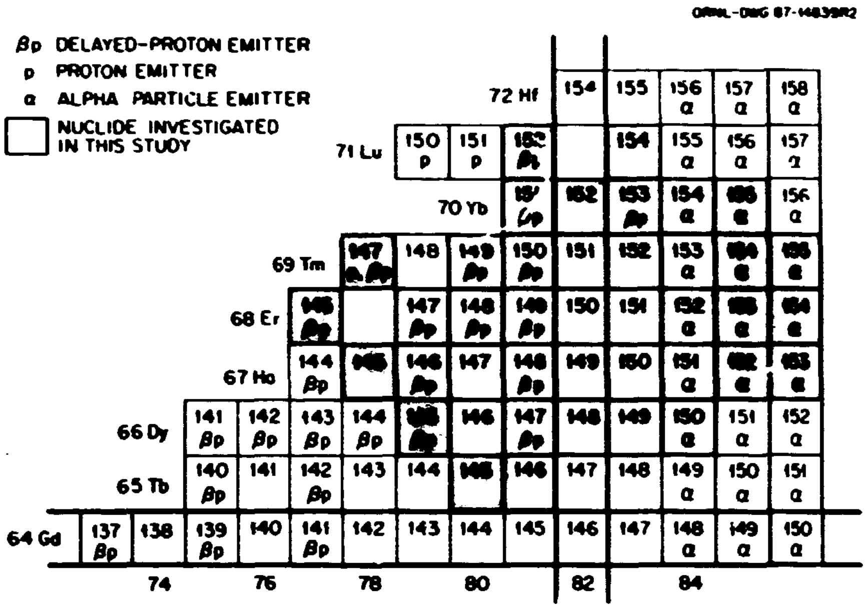

Fig. 2.52. Portion of nuclidic chart; isotopes investigated in this study are indicated by shaded squares.

Table 2.11 Isotopes investigated in this study.

Isotope	J^{π}	$T_{1/2}(s)$	Delayed protons
$^{145}Er^{a}$		0.5(2)	Yes[b]
$^{145}Ho^{a}$	$11/2^-$	2.4(1)	
^{145}Dy	$11/2^-$	15(2)	Yes
$^{145}Dy^{a}$	$1/2^+$	8(2)	Yes[b]
^{146}Ho		3.6(3)	Yes[b]
^{146}Dy	0^+	29(3)	
^{146}Tb	1^+	~8	
$^{147}Tm^{c}$	$(11/2^-)$	0.65(7)	
^{147}Er	$(11/2^-)$	2.5(2)	Yes
^{147}Er	$(1/2^+)$		Yes
^{147}Ho	$(11/2^-)$	5.8(2)	
^{148}Er	0^+	4.4(2)	Yes[b]
^{148}Ho	(6^-)	9.7(3)	Yes[b]
^{148}Ho	(1^+)		Yes[b]
$^{149}Tm^{a}$	$(11/2^-)$	0.9(2)	Yes[b]
^{149}Er	$11/2^-$	9(1)	Yes
^{149}Er	$1/2^+$		Yes
^{149}Ho	$11/2^-$	21(1)	
^{149}Ho	$1/2^+$	54(5)[d]	
^{150}Tm	(6^-)	2.2(2)[d]	Yes[b]
^{150}Tm	(1^+)		Yes[b]
^{150}Er	0^+	20(1)	
$^{151}Yb^{a}$	$11/2^-$	1.6(1)	Yes[b]
$^{151}Yb^{a}$	$1/2^+$		Yes[b]
^{151}Tm	$11/2^-$	4.3(2)	
$^{151}Tm^{a}$	$1/2^+$	~11	
$^{152}Lu^{a}$	(6^-)	0.7(1)	Yes[b]
^{152}Yb	0^+	3.1(2)	
^{152}Tm	(2^-)		
^{153}Yb	$7/2^-$	3.9(1)	Yes[b]
^{153}Tm	$11/2^-$	1.7(2)	
^{153}Tm	$1/2^+$	(2.5)	
^{154}Lu	(7^+)	1.2(1)	Yes[b]
$^{154}Yb^{c}$	0^+	~0.4	
$^{155}Yb^{c}$	$(7/2^-)$	1.7(2)	

[a] New isotope or new isomer.
[b] Delayed-proton emission observed for the first time.
[c] Beta-decay branch of nuclide identified.
[d] New half-life.

3. Summer visitor from Eastern Kentucky University, Richmond, KY 40475.
4. J. M. Nitschke, Nucl. Instrum. Methods 206, 341 (1983).
5. K. S. Toth, Y. A. Ellis-Akovali, J. M. Nitschke, P. A. Wilmarth, D. M. Moltz, and F. T. Avignone III, Phys. Lett. B178, 150 (1986).

DECAYS OF ^{118}In, ^{120}In, and ^{122}In ISOMERS TO LEVELS IN ^{118}Sn, ^{120}Sn, AND ^{122}Sn[1]

S. Raman K. G. Tirsell[3]
T. A. Walkiewicz[2] G. Bonsignori[4]
L. G. Multhauf[3] K. Allaart[5]

The nuclear excited states of ^{118}Sn, ^{120}Sn, and ^{122}Sn were studied by means of the decays of 4.45-min ^{118}In isomer, 46.2-s and 47.3-s ^{120}In isomers, and 10.3-s and 10.8-s ^{122}In isomers, respectively. The In activities were produced by the (n,p) reaction with 14-MeV neutrons on enriched samples of ^{118}Sn, ^{120}Sn, and ^{122}Sn. The γ rays, measured with a Ge(Li) detector, were incorporated into separate level schemes, each resulting from the decay of an individual In isomer. The experimental level schemes of ^{118}Sn, ^{120}Sn, and ^{122}Sn were compared with level schemes calculated on the basis of a broken-pair model that includes up to two broken pairs in the $50 < N < 82$ shell. This model is reasonably successful in explaining the experimental data for these nuclides.

---

1. Abstract of published paper: Phys. Rev. C 37, 1203 (1988).
2. Edinboro University, Edinboro, Pennsylvania 16444.
3. Lawrence Livermore National Laboratory, Livermore, California 94550.
4. Università Bologna, Bologna, Italy.
5. Vrije Universiteit, Amsterdam, The Netherlands.

SINGLE-PARTICLE STATES IN ^{151}Tm AND ^{151}Er; SYSTEMATICS OF NEUTRON STATES IN N = 83 NUCLEI[1]

Y. A. Akovali P. A. Wilmarth[3]
K. S. Toth D. M. Moltz[3]
A. L. Goodman[2] M. N. Rao[4]
J. M. Nitschke[3] D. C. Sousa[5]

With the use of mass-separated sources, the β-decay properties of ^{151}Yb and ^{151}Tm were investigated. Based on these radioactivity measurements, the $h_{11/2}$, $s_{1/2}$, $d_{3/2}$, $d_{5/2}$, and $g_{7/2}$ single-proton states in ^{151}Tm and the $f_{7/2}$, $h_{9/2}$, $p_{3/2}$, $i_{13/2}$, and probably the $p_{1/2}$ single-neutron states in ^{151}Er, were identified. Systematics of neutron states in even-Z, N = 83 isotones (see Fig. 2.53) are compared with predictions of spherical Hartree-Fock-Bogoliubov

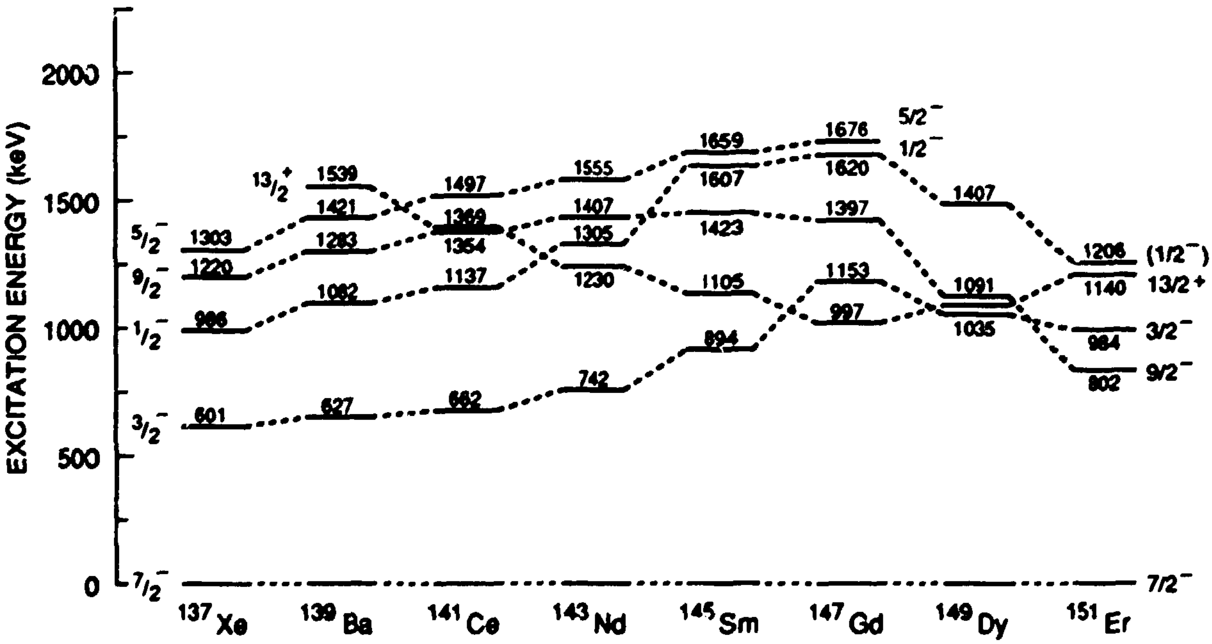

Fig. 2.53. Experimental energy systematics of single-neutron states in even-Z, N = 83 isotones.

cal ulations (see Fig. 2.54). It is found that if a proper effective interaction is used, the calculated energy levels agree with experimental excitation energies.

---

1. Submitted for publication in Physical Review C.
2. Tulane University.
3. Lawrence Berkeley Laboratory.
4. Universidade de São Paulo.
5. Eastern Kentucky University.

SEARCH FOR LOW-SPIN SUPERDEFORMED STATES IN ^{186}Hg

Y. A. Akovali, E. A. Henry[1], J. A. Becker[1], J. Kormicki[4], C. R. Bingham[2], R. Meyer[1], H. K. Carter[3], W. Schmidt-Ott[5], I. C. Girit[2,4], Y-s. Xu[6], H. Carmichael[7]

Spontaneously fissioning isomers discovered[8] in the heavy actinide nuclei were explained[9] by a second minimum in the nuclear potential. These highly deformed fissioning isomers have since been studied extensively and are very well established (for a review, see for example, Ref. 10).

Investigations of high-spin nuclear states in a wide range of nuclides have played an important role in providing crucial information on nuclear structure. About two years ago, coexistence of prolate and oblate deformations at high spins in ^{152}Dy was found[11] which led to the discovery of the superdeformed rotational band in that nucleus.[12] This breakthrough has been followed by other investigations of superdeformation at high spins in ^{132}Ce (Ref. 13), $^{134-136}$Nd (Ref. 14), and ^{149}Gd (Ref. 15). These high-spin superdeformed states which originate from a second prolate minimum in the nuclear potential had been predicted by many calculations[16] long before they were found experimentally.

ORNL-DWG 86-15110

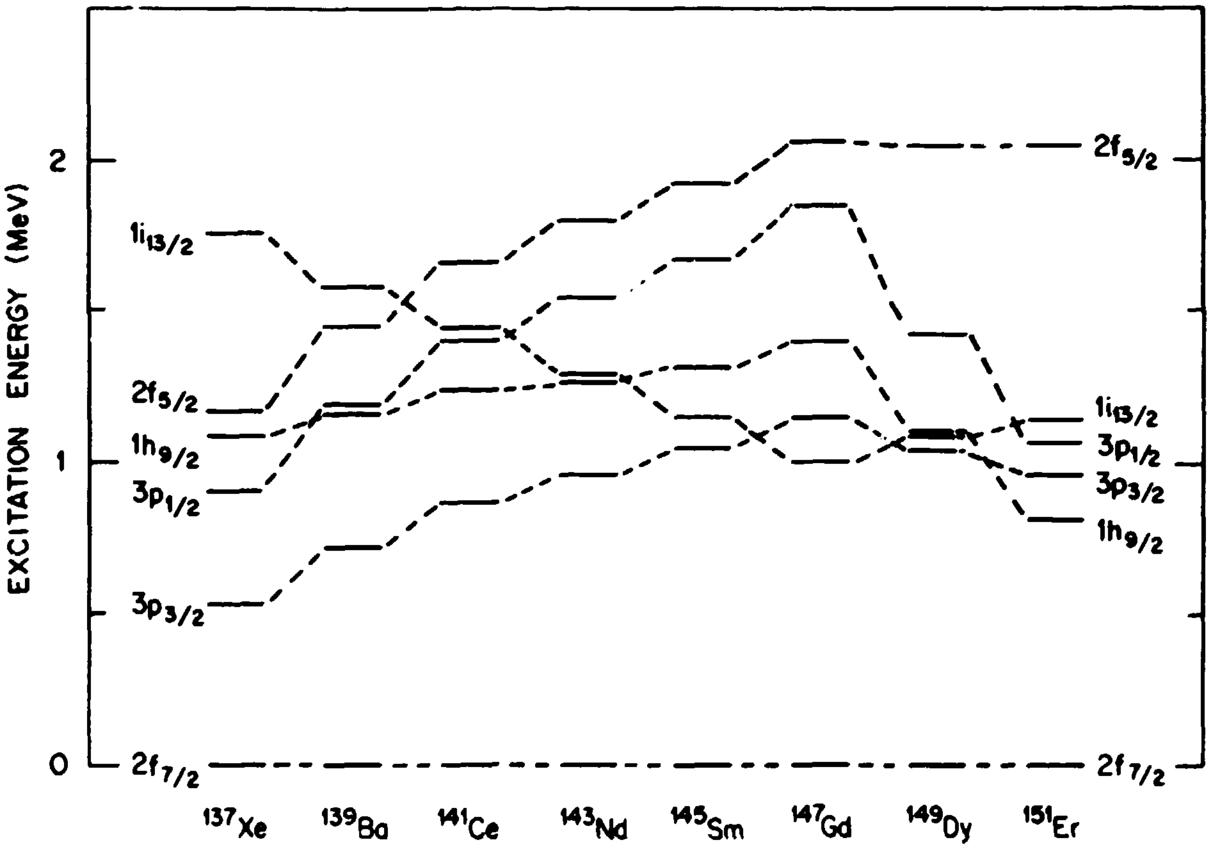

Fig. 2.54. Energy systematics of HFB single-neutron states in N = 83 even-Z nuclei.

Superdeformation in the neutron-deficient Pt, Hg, and Pb nuclei is predicted[17] at low spins. Prolate and oblate shapes in $^{184-188}$Hg isotopes have been found to coexist. No investigation has been reported for levels above 3 MeV in these nuclei where superdeformed states should appear. We estimate that alpha emission from these states would compete with deexcitation by gamma transitions.

The Q values for (positron + electron capture) decays of $^{184-188}$Tl isotopes to Hg nuclei are favorably high: 9190 keV for ^{184}Tl, 8530 keV for ^{186}Tl, and 7730 keV for ^{188}Tl. We expect their 2- isomeric states to populate the expected superdeformed bands in Hg daughters.

An experiment on the ^{186}Tl → ^{186}Hg decay was performed in September 1988. The isotope was produced by bombarding a ^{172}Hf target with 180-MeV ^{19}F ions from the Holifield Heavy Ion Research Facility tandem accelerator. Following production, the A = 186 nuclei were mass-separated with the UNISOR on-line facility, collected onto an automated tape system, and transported to two counting stations. Two large-volume Ge(Li) γ-ray detectors and a Si α-particle detector were placed at the first station in calibrated geometries in order to measure absolute counting rates. Singles γ, singles α, and αγ, γγ coincidence data were accumulated. At the second station three Ge(Li) detectors were utilized for γγ-angular correlation measurements.

The experiment was done with three different collection and counting cycles so that the decays of known ^{186}Tl 7^+, 10^- isomers with 27.5-s, 2.9-s half-lives, and the expected 2^- ground state could be identified from relative transition intensities. At the conclusion of each collection and counting cycle, the computer-controlled tape was moved such that collected isotopes were brought to the first station and the ones at the first station were taken to the second station. Production and counting cycles were chosen as 60 s, 25 s and 9 s in duration. The assay times for the α and γ singles were divided into three 20-s, five 5-s and six 1.5-s intervals, respectively, for half-life information.

Examples of the γ and α spectra taken are shown in Fig. 2.55 and Fig. 2.56, respectively. Besides γ rays in ^{186}Hg following ^{186}Tl β^+ decay, transitions from ^{186}Hg, ^{186}Au, ^{186}Pt, ^{186}Ir decays are also present in the spectra. We also identified gamma rays in ^{182}Au following ^{186}Tl α decay in the αγ coincidence spectrum which had not been observed before.

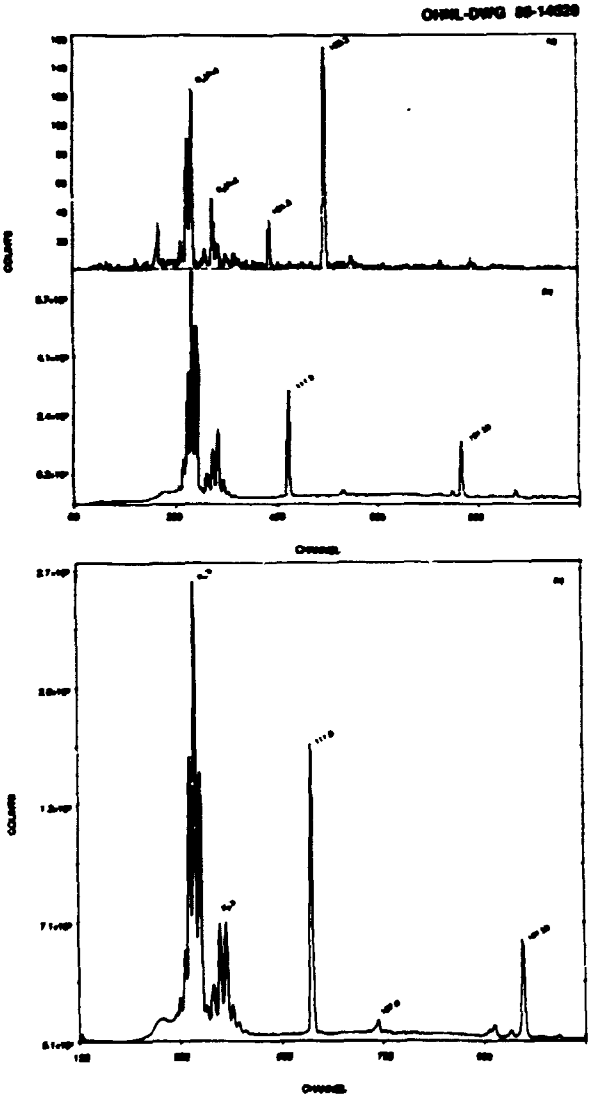

Fig. 2.55. Low-energy portions of the γ-ray spectra: (a) Singles γ spectrum; (b) γ projection in coincidence with γ rays; (c) γ rays in coincidence with α particles.

ORNL-DWG 88-14819

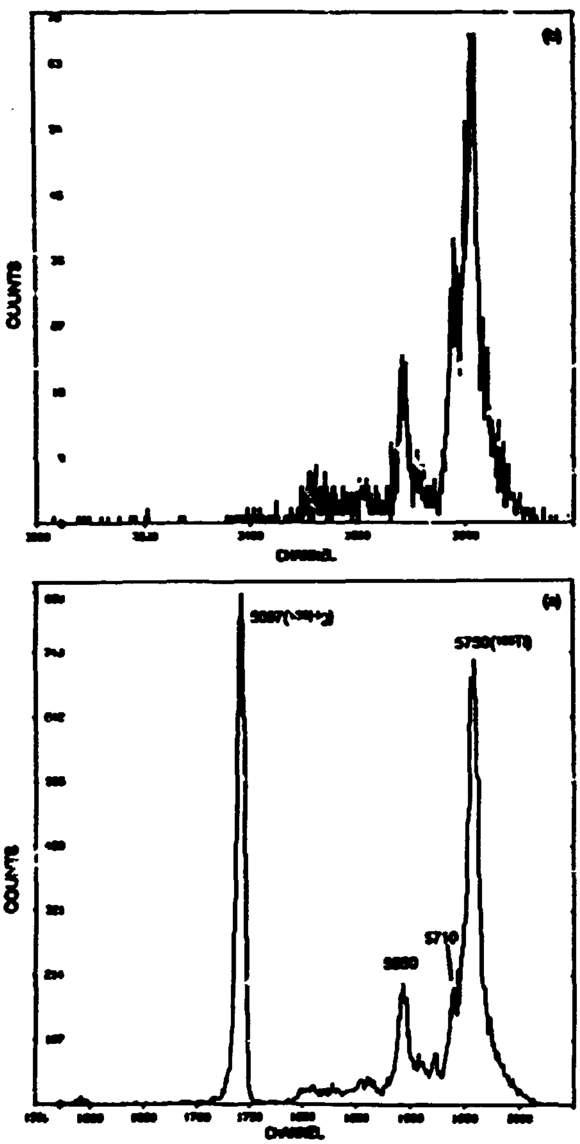

Fig. 2.56. Alpha-particle spectra: (a) singles α spectrum, (b) α's in coincidence with γ rays.

Multiscale spectra indicate that the α peaks observed are complex. Although α groups from ^{186}Hg ground state and ^{186}Tl isomers are identified, definite assignments of all peaks require additional analyses which are in progress.

---

1. Lawrence Livermore National Laboratory.
2. University of Tennessee, Knoxville, TN.
3. UNISOR, Oak Ridge Associated Universities, Oak Ridge, TN.
4. Vanderbilt University, Nashville, TN.
5. University of Göttingen, Göttingen, West Germany.
6. Oregon State University, Corvallis, Oregon.
7. University of Tennessee, Knoxville, TN.
8. S. M. Polikanov et al., Sov. Phys. JETP 15, 1016 (1962).
9. V. M. Strutinsky, Nucl. Phys. A95, 420 (1967).
10. S. Bjørnholm and J. E. Lynn, Rev. Mod. Phys. 52, 725 (1980).
11. B. M. Nyako et al., Phys. Rev. Lett. 56, 2680 (1986).
12. P. J. Twin et al., Phys. Rev. Lett. 57, 811 (1986).
13. A. J. Kirwan et al., Phys. Rev. Lett. 58, 467 (1987).
14. E. M. Beck et al., Phys. Rev. Lett. 58, 2182 (1987); E. M. Beck et al., Phys. Lett. 195B, 531 (1987).
15. B. Haas et al., Phys. Rev. Lett. 60, 503 (1988).
16. I. Ragnarsson et al., Nucl. Phys. A347, 287 (1980); T. Bengtsson et al., Phys. Scr. 24, 200 (1981); J. Dudek and W. Nazarewicz, Phys. Rev. C 31, 298 (1985).
17. J. Dudek et al., Phys. Rev. Lett. 59, 1405 (1987); J. Dudek, private communication (1988).

HEAVY-ION REACTION MECHANISM STUDIES, FUSION AND FISSION

PIONS IN SPONTANEOUS FISSION? THE SAGA CONTINUES

J. R. Beene   C. E. Bemis, Jr.
M. L. Halbert

The results of our experimental search for the spontaneous fission of ^{252}Cf accompanied by the emission of neutral pions have been reported previously[1] and have been the topic of a recent publication.[2] Briefly, we have used the HHIRF Spin Spectrometer as a neutral pion detector in conjunction with a fast fission ionization detector which served as a fission event trigger. Coincident high energy photon pairs, which could arise from the decay of neutral pions, and, in prompt (<2 ns) coincidence with a fission event from the decay of ^{252}Cf, were completely absent in our experiment. We have quoted an upper limit of one such decay of the above type in 10^9 fissions at the 90% confidence level.

The original suggestions of exotic decay modes that might accompany spontaneous fission were proffered by Ion, Ion-Mihai, and Ivascu[3] and were based on the favorable energetics for such processes and on phase-space arguments. Because the dynamics of the postulated decay modes are unknown, an exact branching ratio, relative to "normal" fission, cannot be estimated with any high degree of confidence. The unknown dynamics have not deterred these authors however, and numerous papers have subsequently appeared which relate to these exotic decay modes.[4-7] In addition to the light mesons, i.e., pions, the speculations have been extended to include the heavy leptons, i.e., muons, and the strangeness -1 baryons, e.g., the lambda-0. Together with additional co-workers, Ion, Ion-Mihai, and Ivascu have presented some experimental upper limits for pion-accompanied fission processes[8-10] but none are as sensitive as the experimental limit that we have presented for neutral pions, namely, less than one event in 10^9 fissions at the 90% confidence level.[1-2] An experimental upper limit of less than one event in 2×10^8 fissions has also recently been published by Cerruti and coworkers[11] and we are aware of other experiments that have been completed, or are in progress, that will set comparable limits.

Ion et al., Refs. 5 and 7, have attempted to provide some rate estimates for the pion processes above, but the estimates they provide are naive. They define a modified fissility parameter for pion-accompanied fission by the subtraction of the pion rest mass from the usual Coulomb or electrostatic energy of a spherical liquid drop, a procedure with little validity. This modified fissility parameter is subsequently used by them as a substitute in semi-empirical expressions that relate the usual fissility parameter to fission barriers and to spontaneous fission lifetimes. This is, then, the basis for the "dynamical" prediction of the rates of pion-accompanied fission: for ^{252}Cf, the prediction for the branching decay ratio, pion-accompanied fission/normal spontaneous fission, is approximately 1×10^{-14}. For ^{258}Fm, the prediction is for more than half of the spontaneous fissions to be pion-accompanied events!!

Despite the short-comings of the rate estimates above, and our lack of understanding of the dynamics of the pion-accompanied fission process, the topic continues to be of interest. We are contemplating an improved experiment designed to address branching ratios for the neutral pion-accompanied fission process in the range of 1×10^{-12}. An improved experiment would take advantage of the improved timing and energy resolution characteristics of BaF_2 detectors using the detector arrays described in Ref. 12. The experimental methodology would be similar to that described in Refs. 1 and 2 and we would expect interference from cosmic rays to be negligible.

---

1. J. R. Beene, C. E. Bemis, Jr., and M. L. Halbert, Phys. Div. Ann. Prog. Rep. for Period Ending Sept. 30, 1987, ORNL-6420, p. 96.
2. J. R. Beene, C. E. Bemis, Jr., and M. L. Halbert, Phys. Rev. C 38, 569 (1988).
3. D. B. Ion, R. Ion-Mihai, and M. Ivascu, Ann. Phys. (NY) 171, 237 (1986).
4. D. B. Ion, R. Ion-Mihai, and M. Ivascu, Rev. Roum. Phys. 31, 205 (1986); 31, 209 (1986); 31, 551 (1986); 32, 299 (1986); 32, 1037 (1987); 33, 109 (1988).
5. D.B. Ion, R. Ion-Mihai, and M. Ivascu, "Spontaneous Pion Emission as a New Natural Radioactivity-Dynamical Prediction," Central Institute of Physics, Bucharest, preprint No. FT-324-1988, Jan. 1988, (unpublished).
6. D. B. Ion, M. Ivascu, and R. Ion-Mihai, "Hyperfission-A New Mode of Nuclear Fission," GSI, Darmstadt, preprint No. GSI-88-05, Feb. 1988, (unpublished).
7. D. B. Ion, R. Ion-Mihai, and M. Ivascu, "Predictions for Pionic Radioactivity from Fission Data of Even-Even Nuclei," Central Institute of Physics, Bucharest, preprint No. FT-332-1988, May 1988, (unpublished).
8. D. Bucurescu et al., Rev. Roum. Phys. 32, 849 (1987).
9. M. Ivascu et al., Rev. Roum. Phys. 32, 937 (1987).
10. M. Ivascu et al., Rev. Roum. Phys. 33, 105 (1988).
11. C. Cerruti et al., Z. Phys. A239, 383 (1988).
12. J. R. Beene, F. E. Bertrand, and J. Blankenship, "BaF_2 Array Project," this report.

ANGULAR MOMENTUM EFFECTS IN SUBBARRIER FUSION

M. L. Halbert T. M. Semkow[1]
J. R. Beene V. Abenante[1]
D. C. Hensley D. G. Sarantites[1]
K. Honkanen[1] Z. Li[1]

Experimental data[2,3] on fusion of ^{64}Ni and ^{100}Mo taken with the Spin Spectrometer at and below the Coulomb barrier have been analyzed in several ways.[4,5] Coupled-channels calculations[6] can reproduce the low-energy portion of the excitation function only if additional couplings are incorporated beyond those known for inelastic scattering. Either the inelastic β_λ need to be increased by 50% over the values in the literature[4] or unusually large couplings to fictitious transfer states need to be included.[5] But even if such measures are taken to match the experimental excitation function, the predicted L distributions at low energies are not well reproduced, as shown in Fig. 2.57. This suggests that the couplings required to reproduce the data lie outside the degrees of freedom explicitly included in the calculations.

Several optical-model approaches have been tried which exhibit varying degrees of success. In our investigations we used a nucleus-nucleus potential given by a folding potential based on the M3Y interaction;[7] actually, a Woods-Saxon representation[8] was used. We found[4] that varying the real-well depth V_0 to match the fusion cross section σ_{fus} at each bombarding energy gives L distributions that do not extend to high enough L values (open circles in Fig. 2.57). Allowing the shape of the real well to vary in addition leads to somewhat better success.[5] As an example, Fig. 2.58 shows, as a function of the diffuseness a_V, the moments of L predicted for a family of Woods-Saxon wells, with V_0 adjusted to fit σ_{fus} at 132.8 $MeV_{c.m.}$. All of these fits for reasonable values of a_V (0.4 to 0.7 fm), give <L> and <L²> that are smaller than the experimental values (dashed lines), although the moment of L for the limiting case (a_V = 0, infinite square well) comes fairly close to the data.

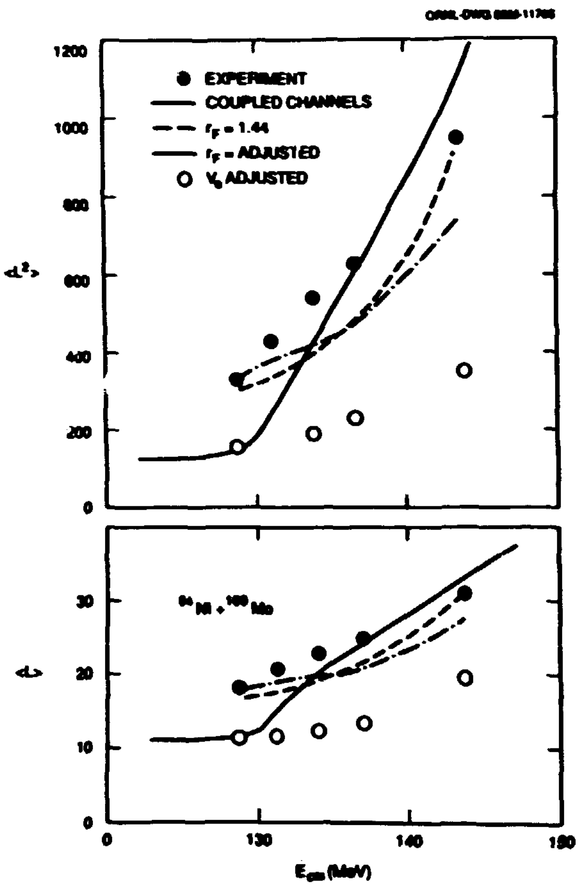

Fig. 2.57. Bombarding energy dependence of the moments of L. Full points are from experiment. The open circles show the results for potentials with V_0 adjusted to fit the measured excitation function. The full curves are for coupled channels calculations (Ref. 6). The dashed curves show one-dimensional barrier penetration results similar to those of Ref. 8.

Calculations have been made recently[9] for other systems in which the radius parameter r_F of the absorptive well for fusion was empirically adjusted to fit σ_{fus}. Typically a value of r_F ~ 1.4 fm is deduced;[9] for our data, r_F comes out between 1.40 and 1.455 fm. The moments of L for this parameterization, shown by the dash-dot curve in Fig. 2.57, represent the experimental data well at the lowest and highest energies. In traditional barrier-penetration models, the colliding nuclei must approach to distances similar to the nuclear half-density radius (r_0 ~ 1.0 fm) for fusion to occur; such distances are well inside the Coulomb-barrier

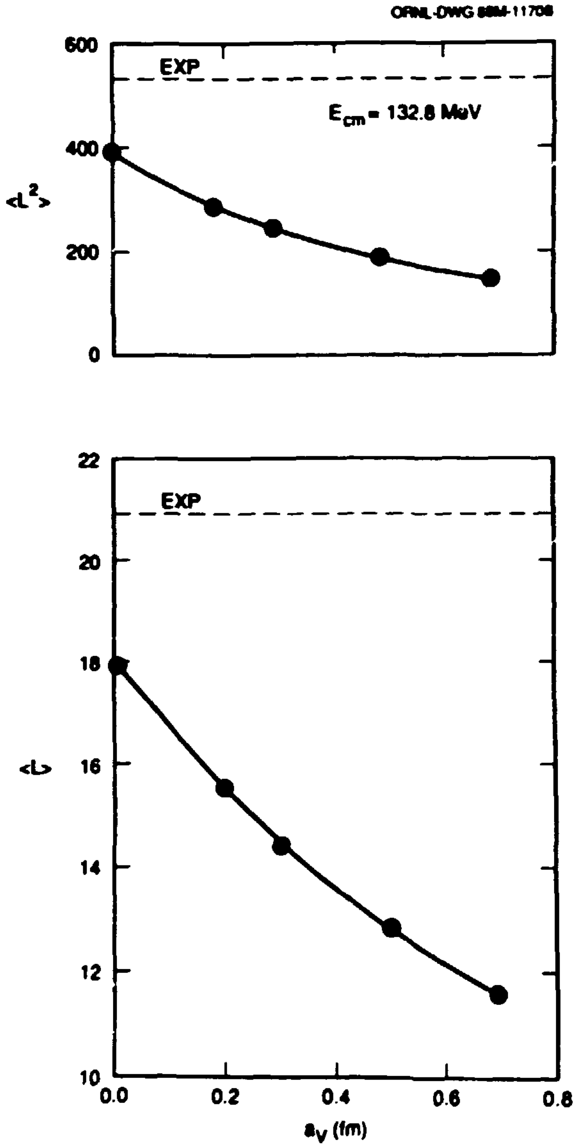

Fig. 2.58. Moments of L for ^{64}Ni + ^{100}Mo fusion at E_{cm} = 132.8 MeV. The experimental values are shown by the dashed lines. The points are results of barrier-penetration calculations in which the diffuseness a_V was varied. The well depth V_0 was adjusted in each case to match σ_{fus}.

radius. The empirical approach taken in Ref. 9 does not discuss the physical phenomena that might be responsible for fusion at large distances, similar to (or even outside of) the Coulomb-barrier radius.

Stelson has made empirical fits to σ_{fus} for ^{64}Ni + ^{100}Mo with a slightly rounded rectangular distribution of barriers at each energy.[10] At the lowest energies the predicted L distributions do not match the experimental ones unless the barrier radii are assumed to be very much larger than at the highest energies.

In summary, neither the coupled-channels calculations nor the single-barrier-penetration models appear able to reproduce the excitation function and the σ_L distribution simultaneously. Models in which the fusion radius is permitted to be substantially larger than the nuclear-matter radius are more successful. Some recent macroscopic calculations indicate that neck formation leading to fusion can occur well outside the unperturbed barrier.[11] We should also mention that Stelson has shown[12] that the parameters for his empirical barrier distributions can be related, via arguments employing the summed single-neutron potentials, to sudden opening of a window for neutron flow between the reactants. The nuclear separation at which such flow would commence is similar to that found from the empirical adjustments used here and in Ref. 9.

Despite these suggestive results, we feel it is premature to claim that our data demonstrate that fusion occurs at large distances. As Vandenbosch has pointed out,[13] it may be inaccurate to assume that during the course of a fusion event the reduced mass and the barrier are (a) invariant and (b) independent of L. These questions have not been specifically addressed in any models of fusion as far as we know.

---

1. Washington University, St. Louis, MO 63130.
2. M. L. Halbert et al., Phys. Div. Prog. Rep. for Period Ending Sept. 30, 1985, ORNL-6233, p. 130.
3. M. L. Halbert et al., Symposium on the Many Facets of Heavy-Ion Fusion Reactions, ANL-PHY-86-1, 311 (1986).
4. M. L. Halbert et al., p. 323 in Frontiers of Heavy-Ion Physics, eds. N. Cindro, W. Greiner, and R. Caplar (World Scientific, 1987).
5. M. L. Halbert et al., Symposium on Heavy-Ion Reaction Dynamics in Tandem Energy Region, Hitachi, Japan, August 1-3, 1988 (Universal Academic Press, Tokyo, in press).
6. C. H. Dasso and S. Landowne, Phys. Lett. B183, 141 (1987); Computer Phys. Comm. 46, 187 (1987).

7. G. R. Satchler and W. G. Love, Phys. Reports 55, 183 (1979).
8. G. R. Satchler (private communication).
9. T. Udagawa et al., Phys. Rev. C 32, 1922 (1985); B. T. Kim et al., Phys. C 33, 370 (1986).
10. P. H. Stelson, private communication.
11. A. Iwamoto and K. Harada, Z. Phys. A326, 201 (1987).
12. P. H. Stelson, Phys. Lett. 205B, 190 (1988).
13. R. Vandenbosch et al., Phys. Rev. Lett. 57, 1499 (1986).

THE GIANT DIPOLE RESONANCE IN VERY HOT A = 170 SYSTEMS

H. P. Morschl[1] M. L. Halbert
W. Spang[1] D. C. Hensley
J. R. Beene I. Y. Lee
F. E. Bertrand R. L. Varner
R. L. Auble D. G. Sarantites[2]
D. W. Stracener[2]

We have measured coincidences between gamma rays and heavy recoils in the $^{17}O + ^{159}Tb$ reaction at 300 and 400 MeV. Details of the experimental setup have been given elsewhere.[3] Events were characterized by linear momentum transfer to the heavy fragment determined from its time of flight to a recoil detector 37 cm downstream of the target. Excitation energies produced in the composite systems were estimated from the linear momentum transfer using relations given in Ref. 4. Gamma ray spectra were generated for four momentum transfer bins at each bombarding energy centered at values ranging from about 60% to 90% of full momentum transfer and corresponding to nuclear temperatures ranging from 2.5 to 3.9 MeV.

A preliminary analysis, in which we extract some properties of the giant dipole resonance (GDR) built on the excited states through which the de-excitation of the hot nuclei proceeds from the gamma ray continuum spectra has been completed and the results submitted for publication in Physical Review Letters. Two main conclusions were drawn from this analysis. The widths of the components of the deformation split GDR, which we observe at T = 2.5 MeV, are much smaller than those observed for similar nuclei at lower temperature[5,6] (lower panel of Fig 2.59). It has been observed that the resonance widths approximately double as the temperature is raised from T = 0 to about T = 2 MeV.[5,6] We observe widths at T = 2.5 MeV close to the T = 0 values. The GDR widths remain almost constant with increasing excitation energy up to just above 3 MeV, then increase rapidly to about 75% of the T = 2 MeV value by T = 3.9 MeV. A narrowing of the GDR at high temperature has been predicted,[7] but the effect observed here is much more dramatic than anticipated. The other main result concerns the ratio, S1/S2, of intensities of the two components of the deformation split GDR (see the upper panel of Fig. 2.59). At T = 2.5 MeV we find S1/S2 = 0.5, which is the value expected for a prolate nucleus (the 1 refers here to the lower energy component), and is consistent with

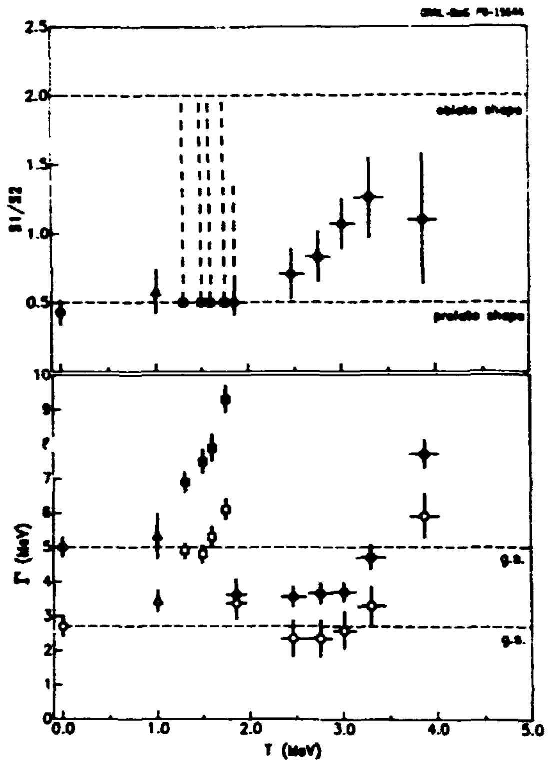

Fig. 2.59. Strength ratios S1/S2 (upper part) and GDR widths (lower part) as a function of T. The open and closed symbols correspond to the low and high energy component of the GDR. The circles for large T indicate our results. The circles at T = 0 are the average g.s. values (Ref. 8), the triangles are from Ref. 5, the squares from Ref. 6 and the trapezoids from Ref. 9.

results obtained below T = 2 MeV. With increasing T, S1/S2 increases smoothly, reaching about 1.2 at T = 3.9, indicating an evolution via triaxial shapes toward an oblate deformation.

This initial analysis has a number of shortcomings, among which is the fact that it provides no information on the absolute collective strength of the GDR. A much more detailed and complete analysis is now underway. Very preliminary results obtained from early phases of this analysis indicate what appears to be a rapid reduction in collective E1 strength near the position of the T = 0 GDR for the highest temperatures observed in our study. The apparent GDR strength in this region falls from about 80% of the classical energy weighted sum rule (EWSR) at T = 2.5 MeV to only about 10% at T = 3.9 MeV. This abrupt decline could reflect either a real loss of collectivity in the GDR for these hot systems, or a failure of the statistical model, which is used to extract the strength, to correctly describe the decay cascade at high T. Preliminary indications favoring the former of these hypotheses has been obtained in the form of evidence that a substantial fraction of missing E1 strength is redistributed from the vicinity of GDR peak (~15 MeV) to lower energies, concentrating near the location of the unperturbed $1\hbar\omega$ states at about 8 MeV.

---

1. Institut fur Kernphysik, Kernforschungsanlage Julich, West Germany.
2. Washington University, St. Louis, MO 63130.
3. J. R. Beene et al., Phys. Div. Prog. Rep. for Period Ending Sept. 30, 1987, ORNL 6420, p. 97.
4. J. B. Natowitz et al., Z. Physik A325, 467 (1986).
5. D. R. Charkrabarty et. al., Phys. Rev. C 37, 1437 (1988).
6. C. A. Gosset et al., Phys. Rev. Lett. 54, 1486 (1986).
7. R. A. Broglia, Nucl Phys A482, (Legnaro proceedings).
8. B. L. Berman and S. C. Fultz, Rev. Mod. Phys. 47, 713 (1975).
9. H. P. Morsch, Nucl Phys A482, 45c (1988).

EXCITATION ENERGY DIVISION IN THE QUASIELASTIC REGION FROM REACTIONS OF 12 MeV/NUCLEON ^{48}Ti WITH ^{150}Nd[1]

T. M. Semkow[2] M. Ross[2]
D. G. Sarantites[2] J. R. Beene
K. Honkanen[2,3] M. L. Halbert
Z. Li[2] D. C. Hensley

Internal excitation of projectilelike fragments and targetlike fragments was investigated for the system 12 MeV/nucleon ^{48}Ti + ^{150}Nd, by measuring the discrete γ rays emitted by both fragments in coincidence with the charge-separated projectilelike fragments. Two quasielastic exit channels of the projectilelike fragments were studied: Z = 20 and Z = 22. Characteristic γ rays were used to determine the average masses of products, after separation and neutron evaporation, as a function of kinetic energy loss. Our results show that the mass-to-charge equilibration occurs quickly for the Z = 20 exit channel, but is slower for the Z = 22 channel. Comparison between the average masses of products and the masses calculated using the statistical model show that the excitation energy is divided approximately equally between the projectilelike and the targetlike fragments for the Z = 20 exit channel. The excitation energy appears to be divided equally up to ~105 MeV of the kinetic energy loss corresponding to ~36% of kinetic energy damping. This result is consistent with predictions made by the stochastic nucleon-exchange models for a small kinetic energy loss.

---

1. Abstract of published paper: Phys. Rev. C 37, 169 (1988).
2. Washington University, St. Louis, MO 63130.
3. Deceased.

EXCITATION ENERGY DIVISION IN $^{35}Cl + ^{209}Bi$ AT 15 MeV/NUCLEON

A. A. Marchetti[1] B. Libby[1]
A. C. Mignerey[1] H. Madani[1]
W. L. Kehoe[1] K. B. Morley[1]
F. E. Obenshain

It is presently accepted that the excitation energy division (EED) in deep-inelastic reactions is a degree of freedom that is slow relative to the time scale of a nuclear reaction. The EED seems to evolve gradually from equal partition between projectilelike and targetlike fragments towards division proportional to mass (equal temperature) as energy loss increases. However, its behavior in the quasi-elastic region has not yet been clarified. A systematic study of this degree of freedom in this particular energy region will help the understanding of the early stages of the dinuclear reaction mechanism. It will also serve as a test for models addressing the transition from direct to deep-inelastic reactions. Unfortunately, the EED is not susceptible to direct measurement and has to be inferred from other observables. Coincident detection of the projectilelike and targetlike fragments has been used for this purpose.[2] The basic assumption of this method is that the average primary angles are preserved during the evaporation process. This assumption becomes less reliable when small energy (masses) losses are involved. A complementary method that our group has employed is based on fitting the centroids of the evaporation component of the secondary kinetic energy spectra.[3] These centroids are a function of the mean EED, the EED variance, and the assumed primary energy distribution; but they are most sensitive to the mean EED.

According to calculations based on the PACE evaporation code,[4] excited projectilelike fragments (PLFs) should decay mainly by emitting light-charged particles, while targetlike fragments (TLFs) should deexcite primarily via neutron evaporation. A light-charged-particle gate should, therefore, enhance channels in which the projectile receives a large fraction of the excitation energy.

An experiment was performed by our group in January 1988 at HHIRF with the time-of-flight system. The reaction studied was $^{35}Cl + ^{209}Bi$ at 15 MeV/nucleon. The time-of-flight system allows the determination of mass and atomic number of PLFs. The detection angle chosen was 18°, which is close to the grazing angle. Two ΔE-E plastic phoswich detectors were used to determine the light-charged particles in coincidence with PLFs. These were located downstream on each side of the beam. The plastic detectors were designed and built by the group at Maryland. Each one consisted of four ΔE-E plastic phoswich paddles. The ΔE element of each paddle was BC400 plastic with dimensions 0.05 x 10 x 12 cm^3. The E element was BC444 plastic with dimensions 3 x 10 x 12 cm^3. Each ΔE-E pair was coupled to a Hamamatsu R1166 photomultiplier tube (PMT). All eight PMT signals were processed separately. The charge-integrating ADCs were triggered by an ~20 nsec time gate for the ΔE signal and ~400 nsec for the E signal.

Some preliminary results are presented in Fig. 2.60, where the effect of requiring light-charged particles in coincidence with the projectilelike fragment on the inclusive $Z = 18$ spectrum is shown. There is an important enhancement in the separation of the primary peak and the evaporation component. We are now trying to obtain the mass information. Experimental problems decreased the energy and time resolution, thereby causing the mass determination to be more difficult. The EED determination will follow as soon as reliable mass results are obtained.

---

1. University of Maryland, College Park, Maryland 20742.
2. D. R. Benton et al., Phys. Rev. C 38, 1207 (1988).
3. A. P. Weston-Dawkes, Ph.D. thesis ORO-5172-0027, University of Maryland (1986).
4. A. Gavron, Phys. Rev. C 21, 230 (1980).

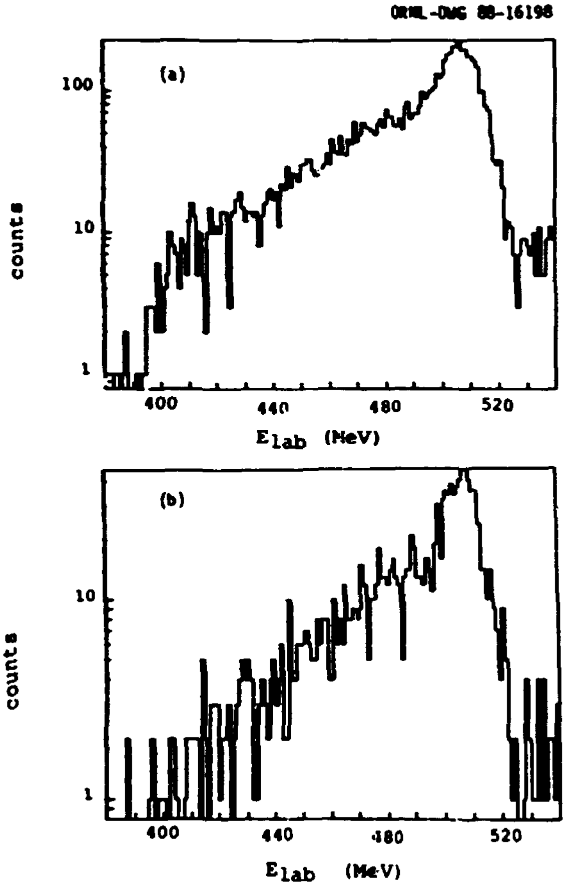

Fig. 2.60. Laboratory kinetic energy spectra for Z = 18 products produced in $^{35}Cl + ^{209}Bi$ collisions at 15.0 MeV/nucleon: (a) inclusive spectrum and (b) spectrum with a light-charged particle coincidence requirement.

ANGULAR MOMENTUM DEPENDENCE OF COMPLEX FRAGMENT EMISSION[1]

L. G. Sobotka[2] J. C. Lisle
D. G. Sarantites[2] R. P. Schmitt[3]
Ze Li[2] Z. Majka[3]
E. L. Dines[2] G. Nebbia[3]
M. L. Halbert H. C. Griffin[4]
D. C. Hensley A. J. Sierk[5]

The angular momentum dependence of large fragment production in long lived reactions is studied by measurements of fragment cross sections from reactions with substantially different angular momentum distributions and the coincident γ-ray multiplicity distributions. The results indicate that the primary ℓ-wave distributions move to larger mean values and decrease in width and skewness with increasing mass symmetry in the decay channel. The results also confirm that the partition of angular momentum in kinetic energy relaxed heavy-ion reactions is that expected for a rigidly rotating intermediate.

---

1. Abstract of published paper: Phys. Rev. C 36, 2713 (1987).
2. Washington University, St. Louis, MO 63130.
3. Texas A and M University, College Station, TX 77843.
4. University of Michigan, Ann Arbor, MI 48109.
5. Los Alamos National Laboratory, Los Alamos, NM 87545.

STUDIES OF EMISSIONS OF COMPLEX FRAGMENTS AND EFFECTIVE TEMPERATURES FOR COLLISIONS OF $^{58}Ni + ^{58}Ni$ AT 11 MeV/NUCLEON[1]

J. Gomez del Campo R. L. Auble
J. L. Charvet[2,3] J. R. Beene
A. D'Onofrio[3,4] M. L. Halbert
H. J. Kim

Complex fragments of nuclear charge (Z) from 4 to 13 were measured at five laboratory angles using surface barrier detector telescopes. Coincident γ-rays were measured in a 4π geometry using 64 NaI detectors. Kinematical analysis of the fragments revealed that those of Z between 4 and 9 are consistent with the decay of a compound nucleus formed in a complete fusion reaction. Gamma rays of excited states of ^{12}C, ^{15}N, and ^{16}O were measured, and effective temperatures of about 2 MeV were extracted. Hauser-Feshbach calculations reproduce the measured cross sections and the effective temperatures very well.

---

1. Abstract of paper: Phys. Rev. Letts. 61, 290 (1988).
2. Centre d'Etudes de Bruyeres-le-chatel, France and Joint Institute for Heavy Ion Research, Oak Ridge, TN 37831.
3. Joint Institute for Heavy Ion Research, Oak Ridge, TN 37831.
4. Istituto Nazionale di Fisica Nucleare, Napoli, Italy.

PROGRESS ON THE HILI DETECTOR

K. Teh[1] H. J. Kim
D. Shapira R. Novotny[2]
M. Korolija[3]

Efforts are now underway for the completion of the final phase of the HILI detector system.[4] Among them is the assembly and installation of the second phoswich array. This hodoscope is identical in all respects to the present one except that the light guides that couple the phoswich elements to the photomultiplier tube have been redesigned to improve the light collection efficiency by 50%.

In addition, a scheme for measuring flight times for ions detected in the hodoscope arrays has been implemented. These measurements may be used to separate protons from deuterons and beam velocity neutrons from prompt gamma rays. The light ion TOF is obtained by timing the scintillator pulse with respect to the rf signal from ORIC. A plot of the energy versus TOF for hodoscope element showing the p-d separation is given in Figure 2.61. The implementation of a time-of-flight capability on the HILI light-ion hodoscopes was made possible by the availability of the Phillips 10C6 FASTBUS TDC. Its high channel density, fast conversion time, picosecond time resolution, and sparse data-handling ability were necessary in implementing TOF for the 192 detector elements. In order to integrate the Phillips TDCs into the present FASTBUS component of the HILI system,[5] specialized microcode for the LeCroy Segment Manager was developed to handle the different word formats used by the LeCroy and Phillips modules. The addition of this capability to the detector required a few revisions to the front-end signal-processing scheme. The revised block diagram is included in Figure 2.62.

Another feature that was added to the HILI system is the auto-ranging A/D conversion of the hodoscope energy-loss signals. The LeCroy 1885 ADCs are capable of switching conversion ranges automatically when the integrated charge exceeds a nominal value of 160 pC. The high range which extends to 1400 pC gives the ADC an additional

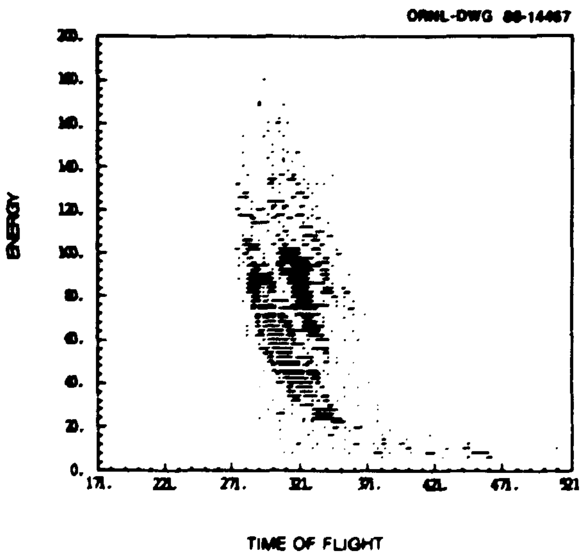

Fig. 2.61. A plot of the total energy deposited versus the time-of-flight shows the separations of the $Z = 1$ group into protons and deuterons.

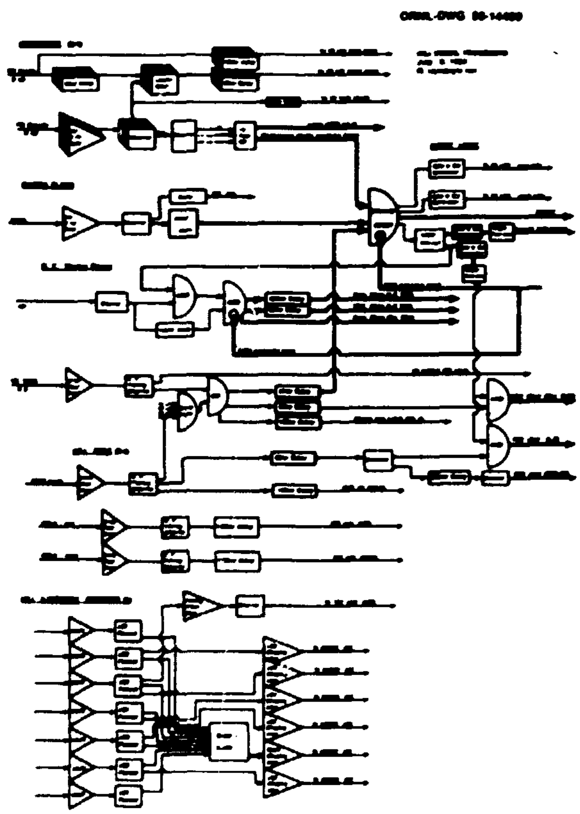

Fig. 2.62. The block diagram showing the electronics setup for the HILI detector.

order of magnitude in dynamic range. With this feature we were able to detect light heavy ions up to Z = 8 without sacrificing ΔE resolution for the protons and alphas. An example of this is given in Figure 2.63.

1. Joint Institute for Heavy Ion Research, Vanderbilt University, Nashville, Tennessee, and Physics Division, ORNL.
2. Physikalisches Institut, University of Giessen, Heinrich-Buff-Ring 16, D-6300 Giessen, West Germany.
3. Laboratory for Nuclear Spectroscopy, Ruder Boskovic Institute, 41001 Zagreb, Yugoslavia.
4. D. Shapira et al., Phys. Div. Prog. Rep. Sept. 30, 1984, ORNL-6120, p. 114.
5. K. Teh et al., IEEE Trans. Nucl. Sci., NS-35, 272 (1988).

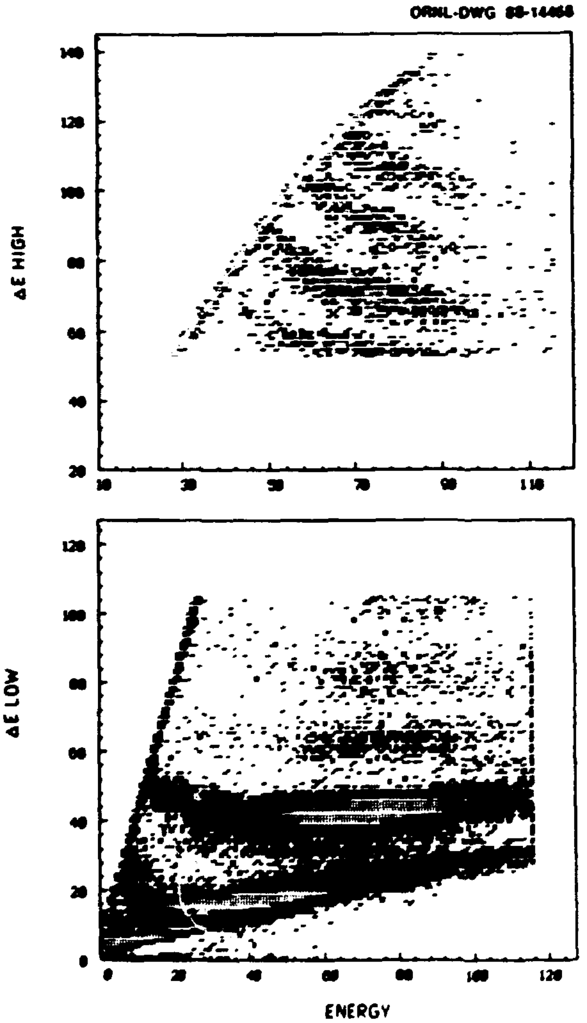

Fig. 2.63. The upper figure is a plot of the high-range ΔE versus E while the lower figure is a plot of the low-range ΔE versus E. Ions up to Z = 8 can be detected without sacrificing ΔE resolution.

ALIGNMENT MEASUREMENT IN $^{28}Si + ^{12}C$ REACTION

A. Ray, D. Shapira, J. Gomez del Campo, H. J. Kim, J. Sullivan[1], B. Shivakumar[2], M. Jeff[2], M. L. Halbert

We are continuing our investigation of the reaction dynamics of damped orbiting reactions. Recent measurements of yields[3-5] and alignment[6,7] of orbiting nuclei have shown the non-compound signature of these reactions. On the other hand, the observation of (1/sinθ) angular distributions at back-angles has indicated that the timescale of these reactions is long compared with that of the direct reaction process. Previous alignment measurements[6] performed on $^{28}Si + ^{12}C$ system at E = 34.5 MeV and 43.5 MeV have shown that both ^{12}C and ^{28}Si nuclei emitted at θ_{cm} = 180° are predominantly (95%) in m = 0 magnetic substate with respect to the beam axis. This result agrees with a simple dinuclear orbiting picture. If we consider a simple-minded dinuclear orbiting picture where the orbiting complex suddenly breaks apart tangentially, then both orbiting nuclei should have their spins perpendicular to the reaction plane when they are detected away from the beam axis. Should the reaction go via the compound nucleus process, then one also expects, from phase-space consideration, about 65-70% alignment of the spins of the emitted nuclei perpendicular to the reaction plane.

We recently performed an experiment to measure the alignment of the damped reaction products emitted at back-angles. We studied the $^{28}Si + ^{12}C$ system at E_{cm} = 43.5 MeV and 48 MeV. Natural carbon foils (150 μg/cm² thick) were bombarded by a ^{28}Si beam from the HHIRF tandem accelerator at E_{lab} = 145 MeV and 160 MeV. Six ΔE-E solid-state particle telescopes were placed at θ_{lab} = 10°, 15°, 19.5°, 23°, 25.3°, 25.6°, and 30°. The experiment was performed in the Spin Spectrometer. Coincidence between the E-detectors and the Spin Spectrometer was required. Gamma spectra, in coincidence with carbon particles emitted at back angles, were obtained in each NaI detector. A 0.25-in.-thick lead plate was placed in front of each NaI detector to stop charged particles and attenuate low-energy gamma rays. The relative efficiencies of the NaI detectors for 4.44-MeV gamma rays were obtained by measuring the 4.44-MeV gamma-ray yield in the detectors with a plutonium-berillyum source placed at the target position. The reaction $^{12}C(1H,1H)^{12}C$ at E(1H) = 17 MeV was used to determine the absolute efficiencies of NaI detectors for 4.44-MeV gamma rays. The efficiency for 1.78-MeV gamma rays was obtained by measuring 1.84-MeV gamma yield in each NaI detector with a ^{88}Y source placed at the position of the target.

Figure 2.64 shows the gamma spectra obtained in coincidence with carbon particles emitted at θ_{lab} = 10°. We see the 1.37-MeV line from ^{24}Mg, the 1.78-MeV line from ^{28}Si and the Doppler-shifted 4.44-MeV line from ^{12}C. The polar angles (θ,ϕ) subtended by the NaI detectors are measured in a coordinate system where the z-axis is along the normal to the scattering plane, and the x-axis is along the direction of motion of emitted carbon nuclei. We find the corresponding Doppler shift of the gamma-ray lines. We average the gamma yield over all the NaI detectors subtending a fixed angle with the normal to the scattering plane. We get rid of the interference of different magnetic substates in this way. We finally obtain the angular

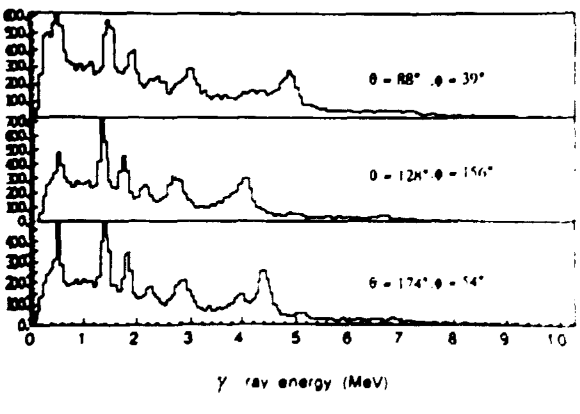

Fig. 2.64. Coincidence gamma-ray spectrum obtained at (θ = 88°, ϕ = 39°), (θ = 128°, ϕ = 156°) and (θ = 174°, ϕ = 54°) for the reaction ^{28}Si + ^{12}C at E(Si) = 145 MeV. The polar angles are measured in a coordinate frame with the z-axis along the normal to the scattering plane and the x-axis along the direction of motion of the detected particle.

correlation at different angles by taking into account the relative efficiencies. We find very poor alignment (20%) for both ^{28}Si and ^{12}C. This result is in disagreement with both the compound nucleus and with the simple-minded orbiting pictures. This result may indicate that the twisting mode of the orbiting nuclei is important when they break apart. We are still investigating other possible sources of this apparent misalignment.

---

1. Cyclotron Institute, Texas A and M University, College Station, TX 77843.
2. Physics Department, Yale University, New Haven, CT 06511.

3. D. Shapira et al., Phys. Lett. B114, 111 (1982).
4. D. Shapira, J. L. C. Ford, Jr. and J. Gomez del Campo, Phys. Rev. C 26, 2470 (1982).
5. A. Ray et al., Phys. Rev. C 31, 1573 (1985).
6. A. Ray et al., Phys. Rev. Lett. 57, 815 (1986).
7. W. Dunnweber, presented at the XXV International Winter Meeting, Bormio, Italy, 1987.

TRANSFER REACTIONS FOR THE ^{50}Ti + ^{90}Zr SYSTEM BELOW THE COULOMB BARRIER[1]

H. J. Kim M. M. Hindi[2]
J. Gomez del Campo D. Shapira
P. H. Stelson

The analysis of quasi-elastic cross section data for the ^{90}Zr projectile plus ^{50}Ti target system shows that the probability for $^{50}Ti(^{90}Zr,^{49}Ti)^{91}Zr$, 1n-transfer reaction near the barrier is much larger than estimates based on semiclassical theory. The probability for $^{50}Ti(^{90}Zr,^{51}V)^{89}Y$, 1p-transfer reaction, on the other hand, agrees with the same theory. The internuclear distance where the 1n-transfer probability first deviates from tunneling predictions coincides with the threshold of the fusion barrier distribution deduced from the experimental fusion cross sections of the ^{50}Ti + ^{90}Zr system, suggesting a common mechanism for the large enhancement of 1n-transfer and fusion cross sections.

---

1. Abstract of paper to be published in Physical Review C.
2. Tennessee Technological University, Cookeville, Tennessee.

NEUTRON FLOW BETWEEN NUCLEI AS THE PRINCIPAL ENHANCEMENT MECHANISM IN HEAVY-ION SUBBARRIER FUSION[1]

P. H. Stelson

Most theories developed to account for the observed enhanced cross sections for heavy-ion fusion in the barrier region have barrier transmission and coupling to low-lying collective states as cornerstone concepts. We present a different picture based on neutron transfer which relegates enhancement caused by collective states to the region far below the barrier (<10 mb). The overlap of the projectile and target shell-model potentials indicate that the valence neutrons of the colliding nuclei can begin to flow between the nuclei at distances which are typically 1.5 fm outside of the mean barrier distance. This neutron flow may precipitate a neck between the nuclei which provides the driving force for fusion. The cross sections in the near-barrier region (10 to 200 mb) are well represented by a parabolic energy dependence which follows from the integration of the simple expression (1-B/E) from a threshold energy to the bombarding energy. The threshold energies for fusion correlate well with the binding energies of the valence neutrons of the colliding nuclei. The heaviest isotopes of each element, which have the smallest neutron binding energies, have the largest cross sections in the near-barrier region. The collective properties of the colliding nuclei (mainly the low-lying quadrupole states) are then considered to modulate the thresholds for neck formation. This modulation produces cross sections in the region far below the barrier (.01 to 10 mb), which are in agreement with experiment and which correlate well with the collective properties of the colliding nuclei. We will use these concepts to interpret the fusion cross sections of the following systems: (^{58}Ni + ^{58,64}Ni); (^{64}Ni + ^{64}Ni); (^{40}Ca + ^{40,44,48}Ca); (^{44}Ca + ^{44}Ca); (^{24}Mg + ^{90,92,94,96}Zr); (^{40}Ar + ^{144,148,154}Sm); and (^{74}Ge + ^{74}Ge). The broad spin distributions for the system (^{64}Ni + ^{100}Mo) observed by Halbert et al.[2] have been difficult to understand using theories based only on coupling to collective states. The model presented here provides broad bell-shaped spin distributions, in good agreement with the experimental measurements.

---

1. Abstract of paper to be published in Proceedings of the International Symposium on Heavy-Ion Reaction Dynamics in Tandem Energy Region, Hitachi, Japan, Aug. 1-3, 1988

2. M. L. Halbert et al., Phys. Div. Prog. Rep., Sept. 30, 1986, ORNL-6326 (March 1987), p. 100 and Phys. Div. Prog. Rep., Sept. 30, 1987, ORNL-6420 (March 1988), p. 105.

EMISSION OF LIGHT IONS, NEUTRONS, PIONS, AND PHOTONS IN HEAVY-ION REACTIONS

PREEQUILIBRIUM EMISSION AND TARGET-PROJECTILE-LIKE CORRELATIONS FOR ^{20}Ne + ^{60}Ni AT E(^{20}Ne) = 740 MeV[1]

A. D'Onofrio[2,3] F. Andreozzi[5]
J. Gomez del Campo A. Brondi[5]
B. Delaunay[4] R. Moro[5]
J. Delaunay[4] M. Romano[5]
H. Dumont[4] F. Terrasi[5]

Inclusive γ rays at 90° and 125° and particle spectra (for Z = 1-6) at 14° and (Z = 1-4) at 120° and 150° were measured. Particle γ-ray coincidences were obtained. Cross sections for heavy residuals were extracted from in-beam γ-ray and radioactivity measurements. Target-projectile-like correlations were well reproduced using a geometrical abrasion model plus preequilibrium and equilibrium decay.

---

1. Abstract of paper to be published in Physical Review C.

2. Guest Assignee from Istituto Nazionale di Fisica Nucleare, 80125 Napoli, Italy.

3. Joint Institute for Heavy Ion Research Oak Ridge, TN 37831.

4. Service de Physique Nucleaire-Basse Energie, Centre d'Etudes Nucleaires de Saclay, 91191 Gif-sur-Yvette Cedex, France.

5. Istituto Nazionale di Fisica Nucleare, 80125 Napoli, Italy.

EXTENDED EMISSION SOURCES OBSERVED VIA TWO-PROTON CORRELATIONS[1]

T. C. Awes, R. L. Ferguson, F. E. Obenshain, F. Plasil, G. R. Young, S. Pratt[2], Z. Chen[3], C. K. Gelbke[3], W. G. Lynch[3], J. Pochodzalla[3], H. M. Xu[3]

Two-proton correlations were measured as a function of the total energy and relative momentum of the protons. The correlation is analyzed for different orientations of the relative momentum, which allows information on the size and lifetime of the emission source to be extracted. The most energetic particles are emitted from a short-lived source of compound nucleus dimensions while the lower energy protons appear to be emitted from a source considerably larger than the compound nucleus.

---

1. Abstract of paper to be published in Physical Review Letters
2. Department of Physics, University of Tennessee, Knoxville, Tennessee 37996.
3. National Superconducting Cyclotron Laboratory, Michigan State University, East Lansing, Michigan 48824.

NEUTRON EMISSION FROM PRODUCTS OF STRONGLY DAMPED REACTIONS OF ^{58}Ni + ^{165}Ho AT 930 MeV

G. A. Petitt[1], C. Butler[1], V. Penumetcha[1], T. C. Awes, J. R. Beene, R. L. Ferguson, F. E. Obenshain, F. Plasil, S. P. Sorensen[2], G. R.Young

At energies above 10 MeV/nucleon, nonequilibrium nucleon emission is observed to become a significant aspect of heavy-ion-induced reactions. At present, the mechanism of nonequilibrium emission is not firmly established. In particular, models with drastically different assumptions are found to reproduce many of the features observed in inclusive measurements of nonequilibrium light-particle emission. One characteristic of the emission process which may be used to distinguish between the various models is the apparent velocity of the rest frame in which the nonequilibrium emission appears isotropic. For nucleon-nucleon collision models[3] and hot spot models,[4] the emission is expected to appear to occur from a frame moving at about half of the beam velocity, essentially independent of impact parameter. On the other hand, for other models such as those which interpret the nonequilibrium emission as a result of field-induced emission[5] or, for example, Fermi jets,[6] the emission is expected to appear to occur from a frame which has a velocity greater than the outgoing projectile-like fragment (or less than the targetlike fragment for nonequilibrium target emission).

Neutrons emitted in and out of the reaction plane have been measured in coincidence with projectilelike fragments (PLFs) resulting from damped reactions of ^{58}Ni + ^{165}Ho at 930-MeV incident energy. The charge, energy, and angle of the PLFs were measured in a gas ΔE position-sensitive silicon E detector which permitted the total kinetic energy loss (TKEL) to be determined for each event. Neutrons were measured in coincidence with projectilelike fragments using an array of 12 liquid scintillator detectors which provided pulse-height, pulse-shape, and time-of-flight information. The neutron coincidence spectra were analyzed in 25-MeV-wide TKEL bins over the TKEL loss range from 0 to 450 MeV. The neutron spectra were fitted with a moving source parameterization to determine the temperatures, multiplicities, velocities, and angles of the projectilelike, targetlike, and nonequilibrium emission sources.

The source velocities obtained from the moving source fits are shown by the open points in Fig. 2.65 for the PLF (triangles), the TLF (squares), and the nonequilibrium (circles) sources. The extracted PLF and TLF velocities are in good agreement with the velocities determined directly from the measured PLF and calculated for the corresponding TLF assuming two-body kinematics, as shown by the solid points. The nonequilibrium source velocities are extracted reliably over the total kinetic energy loss range from 275 < TKEL < 450 MeV. The velocities are found to be approximately half of the beam velocity and to be independent of TKEL. This result is in qualitative agreement with expectations for nonequilibrium

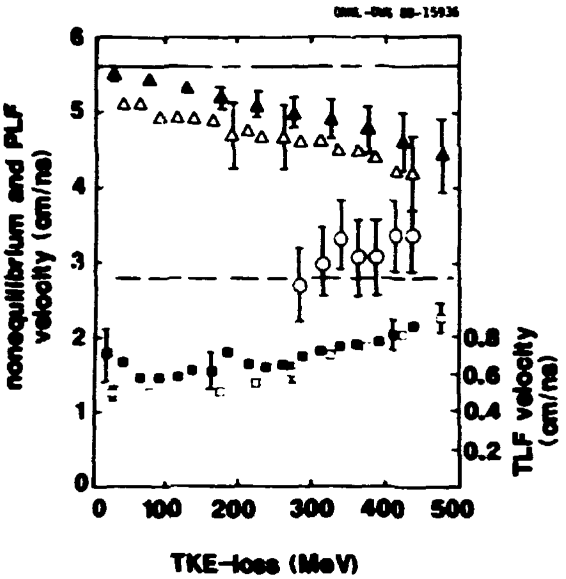

Fig. 2.65. Velocities of neutron emission sources as a function of TKE loss. Triangles are for the PLF source, with open points for the velocities extracted from the moving source fits and solid points corresponding to the mean velocities of the measured PLF. Squares are for the TLF source, with solid points for velocities extracted from the fits and open points extracted from measured PLF assuming two-body kinematics. The open circles are the fitted source velocities of the nonequilibrium neutron component.

emission due to nucleon-nucleon collisions or due to emission from a hot spot consisting of nearly equal target and projectile participants. It is not in accordance with expectations for field-induced emission.

1. Georgia State University, Atlanta, Georgia.
2. Adjunct research participant from the University of Tennessee, Knoxville, Tennessee.
3. William A. Friedman, Phys. Rev. C 29, 13 (1986).
4. T. C. Awes et al., Phys. Rev. C 25, 2361 (1982).
5. A. S. Umar et al., Phys. Rev. C 30, 1934 (1984).
6. J. P. Bondorf et al., Phys. Lett. 84B, 162 (1979).

FRAGMENTATION OF ^{16}O PROJECTILES AT 100 MeV PER NUCLEON[1]

J. D. Silk[2] | P. H. Stelson
H. D. Holmgren[2] | S. Raman
D. L. Hendrie[3] | R. L. Auble
T. J. M. Symons[3] | J. R. Wu
G. D. Westfall[3] | K. Van Bibber[4]

Energy and angular distributions of heavy ($Z \geq 4$) projectilelike residues of ^{16}O have been measured at 100 MeV/nucleon with better than unit A and Z resolution. Global fits to the isotopic distributions show close correspondence to the relativistic results. Closer examination reveals angle-dependent damping of the fragmentation peak. The dependence of this damping upon the target mass gives evidence that the scattering outside the grazing angle is to positive angles.

1. Abstract of published paper: Phys. Rev. C 37, 158 (1988).
2. University of Maryland, College Park, Maryland 20742.
3. Lawrence Berkeley Laboratory, Berkeley, California 94720.
4. Stanford University, Stanford, California 94305.

NUCLEAR PHYSICS WITH ULTRARELATIVISTIC PROJECTILES

OVERVIEW OF ORNL ULTRARELATIVISTIC HEAVY-ION PROGRAM

T. C. Awes | A. Ray
C. Baktash | S. Saini
R. L. Ferguson | D. Shapira
A. Franz[1] | S. P. Sorensen[2]
I. Y. Lee | M. L. Tincknell
F. E. Obenshain | K. M. Teh
F. Plasil | G. R. Young

The ORNL involvement in studies of nucleus-nucleus collisions at ultrarelativistic (>10 GeV/nucleon) energies has grown significantly over the last few years. At the present time, we are engaged in three activities: the CERN WA80 experiment, RHIC-related research and development, and the AGS experiment dedicated to the study of low-energy photon production.

The first two activities are centered in the High-Energy Reactions Group, while the AGS experiment is a project of the Nuclear Collision Dynamics Group. We summarize here the status of these activities, together with future plans.

During this reporting period our most intensive effort has continued to be associated with the WA80 collaboration. The second WA80 run took place at CERN during the first half of October 1987 with 3.2-TeV ^{32}S projectiles. The sulfur beam never attained the high degree of stability that was achieved with oxygen during the first run in the fall of 1986. However, satisfactory event statistics were obtained with four targets: Au, Ag, Cu, and Al. Preliminary results have been presented at a number of conferences, and calorimetric results are described in a separate contribution to this report.[3] The most significant preliminary findings from the sulfur run are that the observed transverse energy continues to scale with the number of participating nucleons, as was deduced from the oxygen data, and that the volume-averaged energy density does not increase significantly with projectile size at a given bombarding energy. In other WA80 activities, data reduction and analysis have continued. New results from the 1986 oxygen run have become available, including preliminary results on the prime WA80 quark-gluon plasma probe — the observation of direct photons.[4]

Future plans at CERN call for the availability of sulfur beams in 1990, for which extension requests have been solicited by CERN management. WA80 has submitted such a request in the spring of 1988 for the purpose of obtaining greatly increased γ/π^0 statistics in order to: (i) study the variation of γ/π^0 with event centrality; (ii) study γ/π^0 for $p_T > 3$ GeV/c (region of perturbative QCD); and (iii) study γ/π^0 for very light systems where quark-gluon plasma formation is not expected. In the original extension request, WA80 had planned to upgrade the multiplicity detectors to handle higher beam intensities, double the solid angle for photon detection by building a second lead-glass electromagnetic calorimeter (SAPHIR), and increase the maximum data-taking rate by converting from CAMAC to FASTBUS ADCs. The appropriate CERN program advisory committee approved WA80 for sulfur beam in 1990 on the condition that the second SAPHIR not be built and that, instead, a more highly-segmented high-resolution (probably sampling) calorimeter be designed and implemented. This new device currently constitutes the highest-priority project of WA80.

Longer-term plans at CERN anticipate approval of the construction of a new injector leading to the availability of lead beams in the early 1990s. Should these plans become a reality, ORNL intends to remain associated with WA80 or with its successor. The primary interest of our group is the measurement of intrinsic photons with very large coverage. This would require a large-scale deployment of the highly-segmented high-resolution calorimeters currently under development. In addition, there is significant interest within the collaboration in the design and construction of a time-projection chamber (TPC). Since similar interests exist in the NA35 (streamer chamber) collaboration and since consolidation of future heavy-ion experiments is deemed desirable by various laboratory managements, discussions are underway between WA80 and NA35, exploring the possibility of a merger.

Turning from CERN to BNL facilities, our efforts to obtain approval for an experiment to study electron-pair emission at the AGS have been terminated, and the fledgling collaboration has been dissolved. This development followed action by the AGS Program Advisory Committee, which considered the proposal in October 1987 and, having found it too costly, decided not to approve it. Subsequently, the collaboration considered a number of alternatives, including the submission of a revised, scaled-down proposal. The ORNL group decided to leave the collaboration in April 1988, partly because we did not feel that a less expensive version of the dielectron experiment could address the physics issues adequately and partly to enable us to concentrate on research and development associated with the proposed Relativistic Heavy-Ion Collider (RHIC) to be built at BNL. Specifically, it is the intent of the Oak Ridge group to play a major role in developing a proposal for an experiment designed to measure muon pairs at RHIC. In September 1988, ORNL responded to a DOE call by submitting an R&D proposal with colleagues from BNL, LLNL, MIT, University of California at Riverside, and the University of Tennessee. The proposal is described in a separate contribution to this report.[5]

In another new initiative on a somewhat smaller scale, ORNL is involved in studies of the production of relatively low-energy photons at the AGS and at CERN. Earlier experiments at CERN have indicated that an anomalous excess yield of soft photons is produced. A letter of intent of a BNL-CERN-ORNL collaboration was submitted to the AGS Program Advisory Committee late in 1987. The BaF_2 detector system to be used in this experiment is described in a separate contribution to this progress report.[6] A test of the new detector was carried out with a negative pion beam at the AGS in late spring of 1988. It was followed by a test measurement using a 450-GeV proton beam at CERN in August 1988. An AGS proposal, based on the letter of intent, for p-nucleus and nucleus-nucleus studies at 15 GeV/nucleon is in preparation.

1. University of Tennessee, Knoxville, Tennessee 37996.

2. Adjunct research participant from the University of Tennessee, Knoxville, Tennessee 37996.

3. R. Albrecht et al., "Energy Measurements from Sulfur-Induced Reactions at 200 GeV/Nucleon," this report.

4. R. Albrecht et al., "Intrinsic Photon Spectra from ^{16}O-Induced Reactions at 200 GeV/Nucleon," this report.

5. S. Aronson et al., "Calorimeter and Absorber Optimization Proposal for the RHIC Dimuon Experiment," this report.

6. D. Shapira et al., "An Array of BaF Detectors for the Study of Soft Photons Emitted in Ultrarelativistic Proton-Nucleus and Nucleus-Nucleus Collisions," this report.

FORWARD AND TRANSVERSE ENERGY DISTRIBUTIONS IN OXYGEN-INDUCED REACTIONS AT 60 A GeV AND 200 A GeV[1]

R. Albrecht[2]
T. C. Awes
C. Baktash
P. Beckmann[3]
F. Berger[3]
R. Bock[2]
G. Claesson[4]
L. Dragon[3]
R. L. Ferguson
A. Franz[4]
S. Garpman[5]
R. Glasow[3]
H. A. Gustafsson[5]
H. H. Gutbrod[2]
J. W. Johnson
K. H. Kampert[3]
B. W. Kolb[2]
P. Kristiansson[4]
I. Y. Lee
H. Loehner[3]
I. Lund[2]
F. E. Obenshain
A. Oskarsson[5]
I. Otterlund[5]
T. Peitzmann[3]
S. Persson[5]
F. Plasil
A. M. Poskanzer[4]
M. Purschke[3]
H. G. Ritter[4]
R. Santo[3]
H. R. Schmidt[2]
T. Siemiarczuk[2,6]
S. P. Sorensen[7]
E. Stenlund[5]
G. R. Young

Results are presented from reactions of 60 A GeV and 200 A GeV ^{16}O projectiles with C, Cu, Ag, and Au nuclei. Energy spectra measured at zero degrees and transverse energy distributions in the pseudorapidity range from 2.4 to 5.5 are shown. The average transverse energy per participant is found to be nearly independent of target mass. Estimates of nuclear stopping and of attained energy densities are made.

1. Abstract of published paper: Phys. Lett. B 199, 297 (Dec. 1987)

2. Gesellschaft fuer Schwerionenforschung (GSI), D-6100 Darmstadt, West Germany.

3. University of Muenster, D-4400 Muenster, West Germany.

4. Lawrence Berkeley Laboratory, Berkeley, California 94720.

5. University of Lund, S-22362 Lund, Sweden.

6. On leave of absence from the Institute of Nuclear Studies, Warsaw, Poland.

7. Adjunct research participant from the University of Tennessee, Knoxville, Tennessee 37996.

PHOTON AND NEUTRAL PION DISTRIBUTIONS IN 60 AND 200 A GeV ^{16}O + NUCLEUS AND PROTON + NUCLEUS REACTIONS[1]

R. Albrecht[2], T. C. Awes, C. Baktash, P. Beckmann[3], F. Berger[3], R. Bock[2], G. Claesson[2], L. Dragon[3], R. L. Ferguson, A. Franz[4], S. Garpman[5], R. Glasow[3], H. A. Gustafsson[5], H. H. Gutbrod[2], K. H. Kampert[3], B. W. Kolb[2], P. Kristiansson[4], I. Y. Lee, H. Loehner[3], I. Lund[2], F. E. Obenshain, A. Oskarsson[5], I. Otterlund[5], T. Peitzmann[3], S. Persson[5], F. Plasil, A. M. Poskanzer[4], M. Purschke[3], H. G. Ritter[4], R. Santo[3], H. R. Schmidt[2], T. Siemiarczuk[2,6], S. P. Sorensen[7], E. Stenlund[5], G. R. Young

Transverse momentum (p_T) distributions of inclusive photons and neutral pions at mid-rapidity are measured with a lead glass calorimeter in 60 and 200 A GeV ^{16}O + nucleus and proton + nucleus reactions. The variation of the average transverse momentum is investigated as a function of centrality, determined by measurements of the remaining energy of the projectile and the charged-particle multiplicity. For small values of the entropy, deduced from the multiplicity density, an increase in average p_T is observed levelling off for larger values of entropy. The target-mass and energy dependence of π^0 p_T distributions are presented.

---

1. Abstract of published paper: Phys. Lett. B 201, 390 (Feb. 1988).
2. Gesellschaft fuer Schwerionenforschung (GSI), D-6100 Darmstadt, West Germany.
3. University of Muenster, D-4400 Muenster, West Germany.
4. Lawrence Berkeley Laboratory, Berkeley, California 94720.
5. University of Lund, S-22362 Lund, Sweden.
6. On leave of absence from the Institute of Nuclear Studies, Warsaw, Poland.
7. Adjunct research participant from the University of Tennessee, Knoxville, Tennessee 37996.

CHARGED-PARTICLE DISTRIBUTIONS IN ^{16}O-INDUCED NUCLEAR REACTIONS AT 60 AND 200 A GeV[1]

R. Albrecht[2], T. C. Awes, C. Baktash, P. Beckmann[3], F. Berger[3], R. Bock[2], G. Claesson[2], L. Dragon[3], R. L. Ferguson, A. Franz[4], S. Garpman[5], R. Glasow[3], H. A. Gustafsson[5], H. H. Gutbrod[2], J. W. Johnson, K. H. Kampert[3], B. W. Kolb[2], P. Kristiansson[4], I. Y. Lee, H. Loehner[3], I. Lund[2], F. E. Obenshain, A. Oskarsson[5], I. Otterlund[5], T. Peitzmann[3], S. Persson[5], F. Plasil, A. M. Poskanzer[4], M. Purschke[3], H. G. Ritter[4], R. Santo[3], H. R. Schmidt[2], T. Siemiarczuk[2,6], S. P. Sorensen[7], E. Stenlund[5], G. R. Young

Results from ^{16}O-induced nuclear interactions with C, Cu, Ag, and Au targets at 60 and 200 A GeV are presented. Multiplicity and pseudorapidity-density distributions of charged particles and their dependence on the target mass number are reported. The increase in the particle density with increasing centrality, characterized by the energy flux at zero degrees, is investigated. Comparisons with the FRITIOF model reveal systematic differences.

---

1. Abstract of published paper: Phys. Lett. B 202, 596 (Mar. 1988).
2. Gesellschaft fuer Schwerionenforschung (GSI), D-6100 Darmstadt, West Germany.
3. University of Muenster, D-4400 Muenster, West Germany.
4. Lawrence Berkeley Laboratory, Berkeley, California 94720.
5. University of Lund, S-22362 Lund, Sweden.
6. On leave of absence from the Institute of Nuclear Studies, Warsaw, Poland.
7. Adjunct research participant from the University of Tennessee, Knoxville, Tennessee 37996.

TARGET FRAGMENTATION IN PROTON-NUCLEUS AND ^{16}O-NUCLEUS REACTIONS AT 60 AND 200 GeV/NUCLEON[1]

H. R. Schmidt[2]	P. Kristiansson[4]
R. Albrecht[2]	I. Y. Lee
T. C. Awes	H. Loehner[3]
C. Baktash	I. Lund[2]
P. Beckmann[3]	F. E. Obenshain
F. Berger[3]	A. Oskarsson[5]
R. Bock[2]	I. Otterlund[5]
G. Claesson[2]	T. Peitzmann[3]
L. Dragon[3]	S. Persson[5]
R. L. Ferguson	F. Plasil
A. Franz[4]	A. M. Poskanzer[4]
S. Garpman[5]	M. Purschke[3]
R. Glasow[3]	H. G. Ritter[4]
H. A. Gustafsson[5]	R. Santo[3]
H. H. Gutbrod[2]	T. Siemiarczuk[2,6]
K. H. Kampert[3]	S. P. Sorensen[7]
B. W. Kolb[2]	E. Stenlund[5]

G. R. Young

Target remnants with $Z < 3$ from proton-nucleus and ^{16}O-nucleus reactions at 60 and 200 GeV/nucleon were measured in the angular range from 30° to 160° ($-1.7 < \eta < 1.3$) employing the Plastic Ball detector. The excitation energy of the target spectator matter in central oxygen-induced collisions is found to be high enough to allow for complete disintegration of the target nucleus into fragments with $Z < 3$. The average longitudinal momentum transfer per proton to the target in central collisions is considerably higher in the case of ^{16}O-induced reactions (~300 MeV/c) than in proton-induced reactions (~130 MeV/c). The baryon rapidity distributions are roughly in agreement with one-fluid hydrodynamical calculations at 60-GeV/nucleon ^{16}O + Au but are in disagreement at 200 GeV/nucleon, indicating the higher degree of transparency at the higher bombarding energy. Both the transverse momenta of target spectators and the entropy produced in the target fragmentation region are compared to those attained in head-on collisions of two heavy nuclei at Bevalac energies. They are found to be comparable or to even exceed the values for the participant matter at beam energies of about 1-2 GeV/nucleon.

---

1. Abstract of published paper: Z. Phys. C **38**, 109 (April 1988).

2. Gesellschaft fuer Schwerionenforschung (GSI), D-6100 Darmstadt, West Germany.
3. University of Muenster, D-4400 Muenster, West Germany.
4. Lawrence Berkeley Laboratory, Berkeley, California 94720.
5. University of Lund, S-22362 Lund, Sweden.
6. On leave of absence from the Institute of Nuclear Studies, Warsaw, Poland.
7. Adjunct research participant from the University of Tennessee, Knoxville, Tennessee 37996.

A NEURAL NETWORK APPROACH TO THE PROBLEM OF PHOTON PAIR COMBINATORICS

Terry C. Awes

Photon measurements provide a means to investigate a broad range of phenomena in relativistic hadron-hadron, hadron-nucleus, and nucleus-nucleus collisions. Directly radiated high transverse momentum (P_T) photons are expected to be produced in hadronic collisions predominantly through the process of gluon Compton scattering, and when valence antiquarks are available, through quark-antiquark annihilations, and, to a lesser extent, by bremsstrahlung from the decelerated quarks. Recently, there has been a great deal of experimental activity to measure high P_T direct photons in pp, πp, and $p\bar{p}$ collisions since such measurements should provide a sensitive probe of the gluon structure functions. In nucleus-nucleus collisions enhanced thermal photon radiation at low P_T might provide a possible signature for quark-gluon plasma formation should sufficiently high energy densities be attained.

Although directly radiated photons are highly interesting, by far the dominant source of photons is from the decay of neutral pions, η's, and higher resonances. Therefore, in order to extract the direct photon component, the contribution from decays must be determined. With increasing photon multiplicities in the final state, it becomes increasingly problematic to make the correct association of photon pairs resulting from π^0 and η decay. This is due to the fact that it becomes more probable, simply due to combinatorics, that random photon pairs may have an apparent invariant mass which falls into the π^0 or η region. A technique has been developed which uses the full information carried in the multiphoton final state to select the most probable set of photon pairs, suppressing the selection of unwanted combinatorial background pairs. The selection is accomplished using a neural network type algorithm.

The basis of the technique is to assign a number to each photon pair combination representing a relative probability that the pair might be correct. The relative probability indicates the likelihood that the pair is a true pair, based primarily on the invariant mass of the photon pair. The optimum set of photon pairs is to be chosen such that each photon is used in only one photon pair combination and such that the set of selected pairs has the largest probability for being correct. This result is obtained within a neural network scheme by using the initial relative probabilities as input to a set of neurons with one neuron for each possible photon pair combination. For a given photon pair, the output of the corresponding neuron is used to stimulate itself while simultaneously inhibiting the neurons of all other photon pair combinations involving either of the two photons which provide the primary input to the neuron. The final set of neurons which remain turned on corresponds to the set of photon pairs which maximizes the overall probability and minimizes the selection of incompatible photon pairs in which a given photon is used more than once.

It is a straightforward matter to encode the neural network described above as an iterative algorithm to be used on a digital computer. The probability that the photon pair consisting of photon i and photon j is correct is given by P^n_{ij}, which corresponds to the output of the neurons after the n'th iteration. The initial probabilities P^0_{ij}, corresponding to the input, are determined from any initial information which may be used to estimate the likelihood that a given pair is correct. The probability that pair ij is correct at iteration n + 1 is given by the expression

$$P^{n+1}_{ij} = P^n_{ij} + g\cdot\left[f\cdot P^n_{ij} - \frac{1}{N_{con}} \sum_{k\neq i,j} (P^n_{ik} + P^n_{kj})\right] \quad (1)$$

where the parameter f is the relative feedback gain. It gives the strength of the positive self-feedback relative to the negative input from the other neurons. The factor $1/N_{con}$ normalizes the negative feedback terms by the number of neurons connected to neuron ij so that the relative feedback is essentially independent of photon multiplicity. The parameter g corresponds to the overall gain of the neurons and determines how quickly the probabilities saturate. The property of saturation is introduced by setting

$$P^{n+1} = \begin{array}{l} 0 \text{ if } P^{n+1}_{ij} < 0 \\ 1 \text{ if } P^{n+1}_{ij} > 1 \end{array} \quad (2)$$

The procedure is then to iterate Eq. 1 until all probabilities have saturated either on or off.

We consider an example of photon measurements using a detector with an energy resolution typical of lead glass and with an energy threshold of 250 MeV. We consider the detector to have complete geometrical acceptance for the photons produced in the 12-GeV p + Au reaction as predicted by the FRITIOF[1] Monte Carlo code. Some photons will fall below the detection threshold and hence will not be available for determination of the other photon to which they are paired. A similar loss of pair information will result from an incomplete geometrical acceptance or from an imperfect photon identification. The invariant mass distribution of the photon pairs is shown in Fig. 2.66. In Fig. 2.66a it is seen that the π^0 and η peaks are observed to lie on a large combinatorial background when using all possible photon pairs within an event. The invariant mass distribution of the photon pairs selected by using the neural network algorithm is shown in Fig. 2.66b. The algorithm is observed to suppress strongly the combinatorial background, with the result that the peak-to-total ratio for the π^0 and η are improved. The invariant mass distribution of the actual photon pairs, that is the desired result, is shown in Fig. 2.66c.

---

1. B. Nilsson-Almqvist and E. Stenlund, Comput. Phys. Commun. 43, 387 (1987).

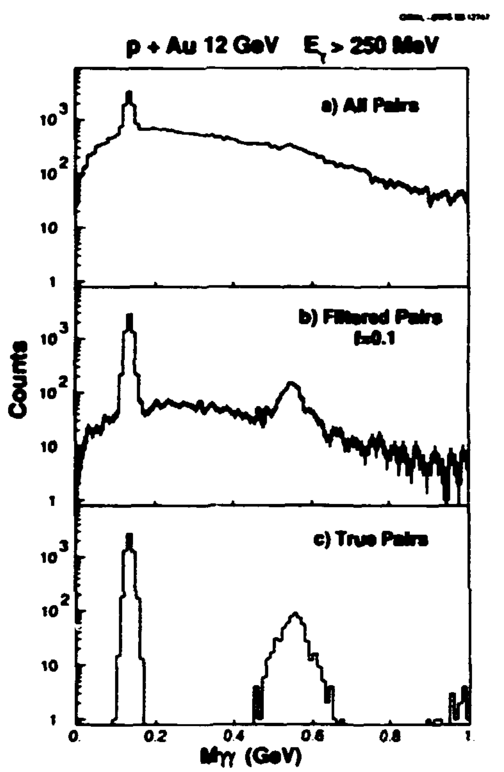

Fig. 2.66. The gamma-gamma invariant mass distribution for reactions of protons on Au at 12 GeV with a gamma energy threshold of 250 MeV. The invariant mass is calculated (a) for all possible gamma-gamma combinations and (b) for those selected after filtering with the neural-net algorithm with parameters g = 0.3 and f = 0.1. The mass distribution of the true pairs of (a) and (b) are shown in (c).

ENERGY MEASUREMENTS FROM SULFUR-INDUCED REACTIONS AT 200 GeV/NUCLEON

WA80 Collaboration

R. Albrecht[1], T. C. Awes, C. Baktash, P. Beckmann[2], F. Berger[2], R. Bock[1], G. Claesson[1], L. Dragon[2], R. L. Ferguson, A. Franz[3], S. Garpman[4], R. Glasow[2], H. A. Gustafsson[4], H. H. Gutbrod[1], K. H. Kampert[2], B. W. Kolb[1], P. Kristiansson[3], I. Y. Lee, H. Loehner[2], I. Lund[1], F. E. Obenshain, A. Oskarsson[4], I. Otterlund[4], T. Peitzmann[2], S. Persson[4], F. Plasil, A. M. Poskanzer[3], M. Purschke[2], H. G. Ritter[3], S. Saini, R. Santo[2], H. R. Schmidt[1], T. Siemiarczuk[1], S. P. Sorensen[5], E. Stenlund[4], M. L. Tincknell, G. R. Young

The goal of relativistic heavy-ion experiments is to study hadronic matter at high energy density, in an interacting volume that is large compared to the size of an individual hadron. These conditions are obtained experimentally by colliding projectile ions at relativistic energies with target nuclei of similar or greater mass. It is predicted that a sufficiently hot and dense system of hadrons will dissolve briefly into a state of deconfined quarks and gluons, the quark-gluon plasma (QGP). Since the interesting properties of the QGP, and of any othe collective effects that are not mere superpositions of nucleon-nucleon collisions, are believed to manifest themselves more clearly with larger volumes and higher energy densities, it is important to compare the results obtained with projectiles of increasing mass. In the fall of 1987, experiment WA80 completed its second run with heavy-ion beams from the SPS accelerator at CERN. The major difference from the first run was that the beam, ^{32}S at 200 GeV/nucleon, had double the mass and total energy of the ion beam in 1986, ^{16}O. Many of the ^{16}O results obtained from the 1986 run have been presented earlier.[6]

The WA80 experiment contains several components designed to measure different features of high-energy nuclear collisions. This report discusses results from two of these detectors, the MIRAC (MId-RApidity Calorimeter) and the ZDC (Zero-Degree Calorimeter). These measure the total energy of emitted particles in the (approximately) forward hemisphere of the nuclear collision and the residual energy of the projectile spectator nucleons, respectively. Both of these detectors, as well as the other detector systems in WA80, have been described in detail elsewhere.[7] Either device can be used as an on-line or off-line trigger to classify collision violence: both increasing scattered energy in the MIRAC and decreasing residual projectile energy in the ZDC correspond to shrinking impact parameters in the reactions. Thus, calorimeters can identify what fraction of the projectile energy is contributing to the reactions, and can trace where that energy is deposited by the participating particles.

The energy spectra from the ZDC for the 1987 ^{32}S run with four targets of increasing mass are shown in Fig. 2.67. The trend of increasing cross section at low ZDC energy with increasing target mass can be understood simply by the geometry of colliding nuclear spheres. Since the lightest target, ^{27}Al, is actually smaller than ^{32}S, there is virtually no cross section for losing more than 75% of the beam energy (i.e., 1.6 TeV remaining out of 6.4 TeV). For the heaviest target, ^{197}Au, there is actually a small peak at 1 TeV (15% of beam energy) corresponding to the complete "dive-in" of the smaller ^{32}S projectile into the target. For comparison, 1986 data with a ^{16}O beam on four similar targets are shown. The spectral shapes obtained with the two different projectiles are qualitatively very similar for each target. The main difference to be noted is that the ^{32}S projectile always has a smaller cross section for losing a large fraction of the beam energy than does the ^{16}O projectile. This is because at any impact parameter the larger ^{32}S nucleus has more nucleons that will either miss the target completely or may pass through the periphery of the target and lose little energy.

The energy of the interacting particles, as detected by the MIRAC, is conventionally reported as transverse energy:

$$E_T = \sum_{i=1}^{N} E_i \sin\theta_i \ .$$

For particles in the forward hemisphere with energies large compared to their rest masses, e.g., pions, this quantity is approximately the same as transverse momentum and, thus, is nearly Lorentz invariant. The transverse energy spectra from ^{32}S incident on the four targets are shown in Fig. 2.68. The angular range of the

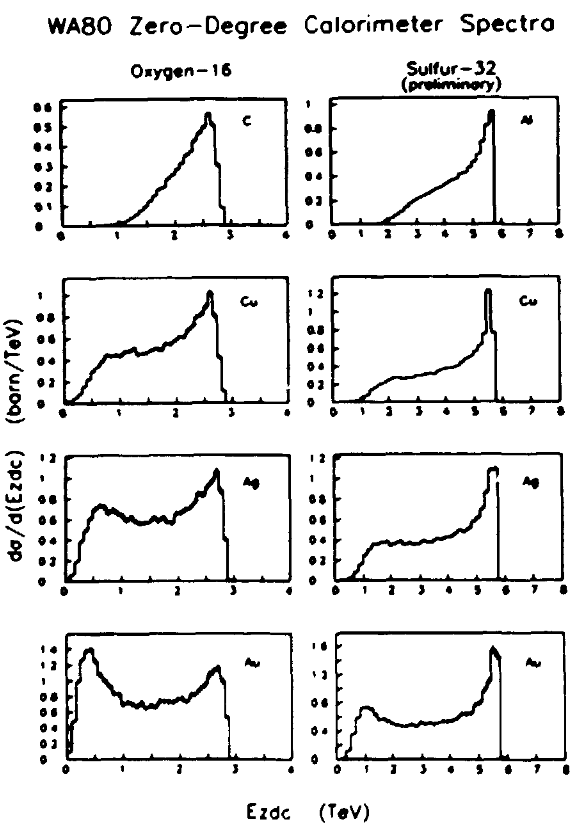

Fig. 2.67. Zero-Degree Calorimeter energy spectra from the interactions of ^{32}S (right side) and ^{16}O (left side) with various targets at E/A = 200 GeV.

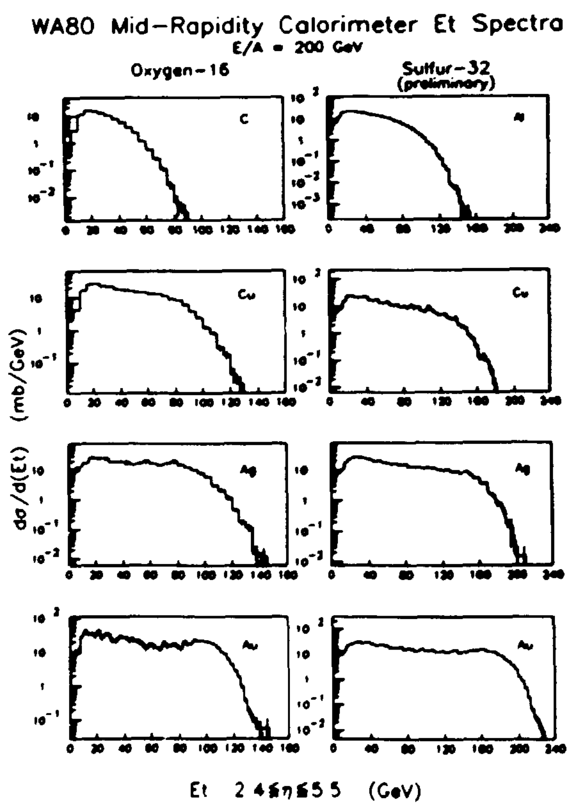

Fig. 2.68. Transverse energy spectra from ^{32}S (right side) and ^{16}O (left side) interactions with various targets at E/A = 200 GeV, obtained with the Mid-Rapidity Calorimeter, in the pseudorapidity interval $2.4 < \eta < 5.5$.

MIRAC used in these figures is from 10.5 to 0.5 degrees, or from 2.4 to 5.5 in pseudorapidity. The shapes of these spectra are again determined primarily by nuclear geometry. The peak at low E_T is caused by the large differential cross sections for large impact parameters and by the threshold of the experimental trigger. The broad plateau is a region where the increasing number of participating particles with decreasing impact parameter produces E_T at a rate that compensates for the decreasing cross section. At very high E_T there is a nearly-Gaussian tail that derives from fluctuations in the violence of collisions at nearly-zero impact parameter. Shown for comparison, the ^{16}O data exhibit quite similar features. In these data, for the heavy targets, a second peak at high E_T is visible; however, there is no prominent bump at high E_T for the ^{32}S data. This is because a larger fraction of the total cross section results from the smaller ^{16}O nucleus, completely "diving into" the large target nucleus and generating roughly the same large E_T signal.

Because E_T is a direct measure of the reacting energy in the collision, it is interesting to study how E_T scales with increasing projectile mass. Until new accelerators become available, e.g., RHIC, increasing projectile mass is the only available means to try to increase the reacting energy. Shown in Fig. 2.69 are E_T spectra for ^{16}O + Au and ^{32}S + Au at 200 GeV/nucleon. The ^{16}O E_T scale has been multiplied by a factor of 1.60 to approximately align the high-E_T tails of the two spectra. This demonstrates that doubling the projectile's mass and energy produces significantly less than a factor of 2.0 greater E_T, contrary to naive expectations. The reason for this is that (at least at SPS energies and for emitted particles in the forward hemisphere), E_T per participant nucleon is almost constant. This is demonstrated in Fig. 2.70, where E_T per participant is shown to be roughly constant as a function of residual ZDC energy for eight separate beam-target combinations at 200 GeV/nucleon. The constant value, about 2 GeV/participant, is nearly the same in each case. The number of

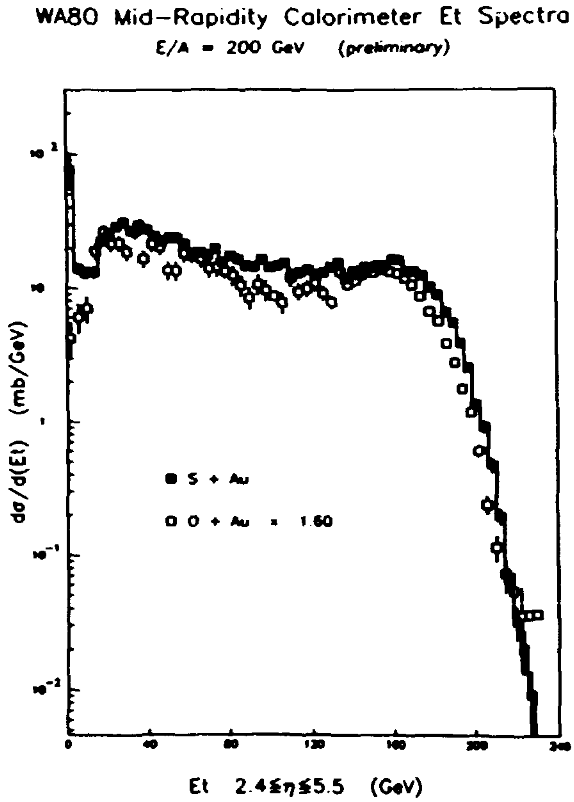

Fig. 2.69. A comparison of transverse energy distributions from ^{16}O and ^{32}S reactions with Au. The transverse energy scale of the ^{16}O data has been multiplied by 1.60 to approximately align the right-hand tails of the distributions.

participants was calculated from the event ZDC energy, using the correlation of the average number as a function of ZDC energy in the FRITIOF Monte Carlo event simulation code. Returning to the E_T scaling law, the number of projectile participants obviously scales as A_p in a central collision. However, the number of target participants is determined by the cylindrical volume the projectile cuts out of the center of the target sphere, which scales only as $A_p^{2/3} * A_T^{1/3}$, and, thus, the total sum scales as less than A_p^1. Since E_T/participant is constant, E_T also scales as A_p^x, where $x \sim 2/3$ when comparing ^{16}O and ^{32}S results.

Although the energy density threshold for the transition to a QGP is not accurately predicted by current theories, many sources concur that the critical value is in the range 1-3 GeV/fm^3.

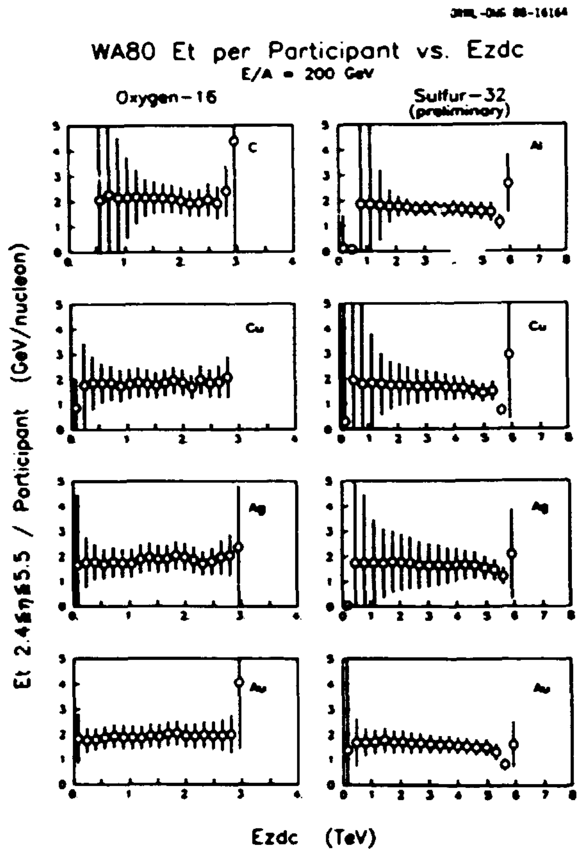

Fig. 2.70. Average transverse energy per participating nucleon as a function of the energy observed in the Zero-Degree Calorimeter. Sulfur-32 data at E/A = 200 GeV are shown on the right side; ^{16}O data at the same energy are depicted on the left side. Vertical bars indicate the degree of uncertainty in the average transverse energy values.

At present, a reliable and well-established way to measure the energy density experimentally is not available. The oft-quoted Bjorken formula is:

$$\epsilon_{BJ} = (dE_T/dy)/(F\tau) ,$$

where dE_T/dy is the transverse energy per unit rapidity, F is the face area of the participating sections of the nuclei, and τ is the proper formation length, canonically taken to be 1 fm. This expression was derived under the assumption that there is a flat plateau in dE_T/dy as a function of rapidity y, which is a poor approximation for energies as low as those of the SPS experiments.

The questionable applicability of Bjorken's formula has launched a search for alternative formulations. One such alternative is a fireball model, in which the energy density is merely the fireball energy divided by the fireball volume:

$$\epsilon_{FB} = E_{FB}/V_{FB} .$$

For an isotropic fireball, the total energy is simply proportional to the total transverse energy:

$$E_{FB} = \frac{4}{\pi} \cdot E_T(\text{total}) .$$

The volume may be estimated from the cylinder taken at a time in the c.m. frame just after the rear edges of the nuclei have finished passing through each other. The volume of the cylinder is the product of the face area of the participants, and a length equal to the sum of the Lorentz-contracted diameters of the participating sections plus a 1-fm formation length for the produced particles to satisfy the energy-time uncertainty relation after the collisions of the rear-most nucleons. This formula:

$$V_{FB} = F\left(\frac{\langle D_p\rangle}{\gamma_p} + \frac{\langle D_t\rangle}{\gamma_t} + \tau\right)$$

lessens the dependence of ϵ_{FB} on the unknown parameter τ.

As defined above, both ϵ_{BJ} and ϵ_{FB} can be calculated for each event from the observed $dE_T/d(\eta) \approx dE_T/dy$ distribution, and from the impact parameter of the collision which is deduced from the ZDC energy with the help of the FRITIOF model. Shown in Fig. 2.71 are scatter plots of ϵ_{BJ} vs E_{zdc} and ϵ_{BJ} vs E_T for three colliding systems: ^{16}O + Au at 60 GeV/nucleon, ^{16}O + Au at 200 GeV/nucleon, and ^{32}S + Au at 200 GeV/nucleon. These plots show that the Bjorken energy density is indeed in the range of 1-3 GeV/fm^3. Note that the most probable energy densities increase significantly going from 60 GeV to 200 GeV, and that the increase in going from ^{16}O to ^{32}S at 200 GeV is small. There is also a strong anticorrelation of ϵ_{BJ} with E_{zdc}, and a strong positive correlation of ϵ_{BJ} with

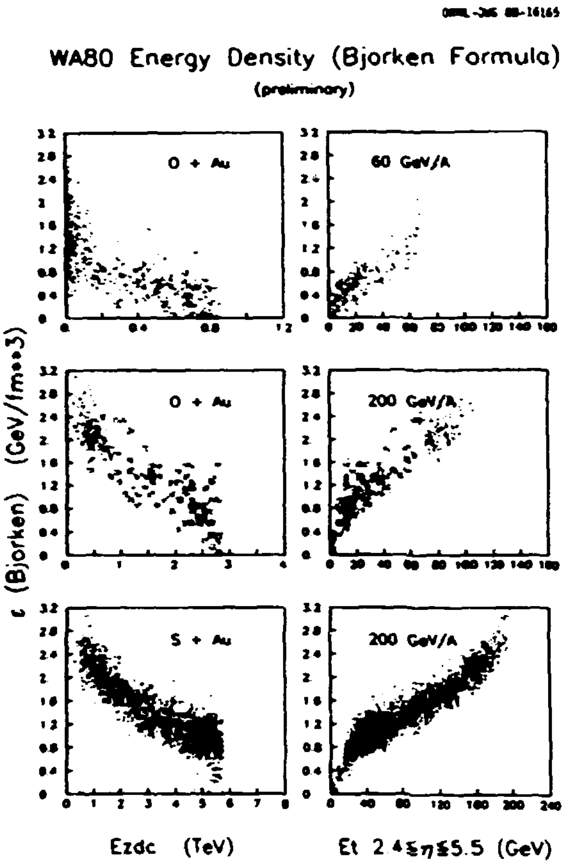

Fig. 2.71. Energy densities associated with individual events determined from the Bjorken model (see text). In the left column are energy densities plotted against E_{zdc}; on the right are energy densities plotted against transverse energy. The top two figures are ^{16}O + Au at 60 GeV/nucleon; the middle two are ^{16}O + Au at 200 GeV/nucleon; and the bottom two are ^{32}S + Au at 200 GeV/nucleon.

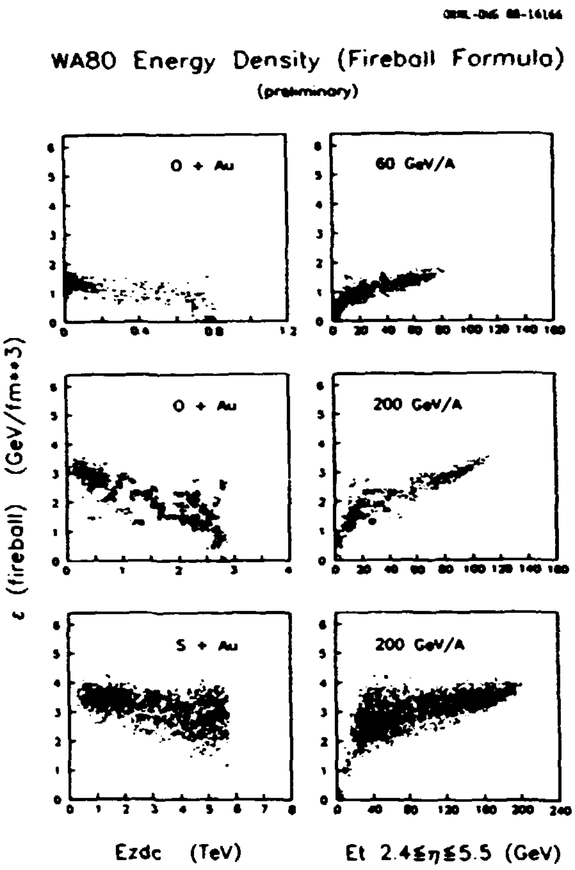

Fig. 2.72. Same as Fig. 2.71 but for energy densities determined from the fireball model (see text).

E_T; thus, the Bjorken energy density is a function of impact parameter.

In Fig. 2.72 are displayed scatter plots for ϵ_{FB} vs E_{zdc} and ϵ_{FB} vs E_T for the same three cases. The fireball model estimates of energy density are in the range 1 to 4 GeV/fm^3, even higher than Bjorken's estimates. The increase in going from 60 GeV to 200 GeV is still a factor of 2, corresponding directly to the difference in c.m. energy. It is interesting to note that ϵ_{FB} is much less anticorrelated with E_{zdc} and less correlated with E_T than ϵ_{BJ} is. This behavior may, in fact, be reasonable since these (anti)correlations imply that energy density does not depend strongly on the number of participants, but merely on the colliding energy. Increasing the participants does, however, increase the volume and time over which the fireball may equilibrate, and it may, thus, enhance the possibility for observing the QGP.

In conclusion, the 1987 ^{32}S data taken with the WA80 MIRAC and ZDC have been presented. Both the ZDC energy spectra and the MIRAC E_T spectra are qualitatively similar in shape to their counterparts from the 1986 ^{16}O data. The features of the spectra can be simply understood by a clean-cut model of nuclear spheres colliding at various impact parameters. The transverse energy increases by less than a factor of two when the projectile mass and total energy double. This is a consequence of the fact that E_T per participant nucleon is constant at a given bombarding energy regardless of the projectile, target, or impact parameter. The energy density can be estimated on an event-by-event basis by either Bjorken's model or by a fireball model. Both estimates result in energy densities in the range of 1 to 3 GeV/fm^3, which is encouraging for the possible formation of the quark-gluon plasma at SPS energies.

---

1. Gesellschaft fuer Schwerionenforschung (GSI), D-6100 Darmstadt, Fed. Rep. Germany.
2. University of Muenster, D-4400 Muenster, Fed. Rep. Germany.
3. Lawrence Berkeley Laboratory, Berkeley, California 94720.
4. University of Lund, S-22362 Lund, Sweden.
5. Adjunct research participant from the University of Tennessee, Knoxville, Tennessee 37996.
6. Phys. Div. Prog. Rep., Sept. 30, 1987, ORNL-6420 (Mar. 1987), pp. 110-13.
7. Ibid., pp. 115-20.

STUDY OF FLUCTUATIONS IN CHARGED-MULTIPARTICLE PRODUCTION IN 200-GeV/NUCLEON NUCLEUS-NUCLEUS COLLISIONS

WA80 Collaboration

R. Albrecht[1], T. C. Awes, C. Baktash, P. Beckmann[2], F. Berger[2], R. Bock[1], G. Claesson[1], L. Dragon[2], R. L. Ferguson, A. Franz[3], S. Garpman[4], R. Glasow[2], H. A. Gustafsson[4], H. H. Gutbrod[1], K. H. Kampert[2], B. W. Kolb[1], P. Kristiansson[3], I. Y. Lee, H. Loehner[2], I. Lund[1], F. E. Obenshain, A. Oskarsson[4], I. Otterlund[4], T. Peitzmann[2], S. Persson[4], F. Plasil, A. M. Poskanzer[3], M. Purschke[2], H. G. Ritter[3], R. Santo[2], H. R. Schmidt[1], T. Siemiarczuk[1], S. P. Sorensen[5], E. Stenlund[4], G. R. Young

One of the goals of the WA80 experiment is a search for fluctuations in the number of particles produced per unit rapidity. Such fluctuations had been suggested by van Hove[6] and others as possible signals of the rather violent reversion of a quark-gluon plasma back into a hadronic state. Recent theoretical work by Hwa[7] and by Bialas and Pescnanski[8] has suggested that moments of the multiplicity distribution taken as a function of the rapidity interval would yield information on whether dynamical correlations and one (or a few) characteristic scales exist or whether, instead, a "continuum" of scales characterizes the observed distributions.

The WA80 setup includes large arrays of streamer tubes which are read out by pads of a few square centimeters in size. A reasonably accurate measurement of the multiplicity of charged particles emitted as a function of pseudorapidity (η) and azimuth is obtained. (Information on neutral particles and on particle momenta is not available, so the above analyses can only be made for charged particles as a function of pseudorapidity.) The pseudorapidity resolution of the counters has been studied and has been shown to have an rms deviation of 0.067 units (averaged over the range $2.4 < \eta < 4.0$), meaning that structures larger than that could be identified, should they exist.

Hwa considered the case where a phase transition (e.g., from a quark-gluon plasma state back to a hadron gas) exhibits a large correlation length, similar to the dynamical effects seen in critical phenomena, such as critical opalescence. In this case, the ratio of the dispersion to the mean of the multiplicity distribution is expected to become large. However, in order to examine this effect, the geometrical part of the observed fluctuations, which arise from impact parameter variation, must first be removed. One can restrict the impact parameter range by restricting the mean multiplicity studied. In order to avoid problems which would arise as a result of this restriction, Hwa suggested varying the mean multiplicity by changing the η-window studied, while keeping its center fixed. The dispersion/mean can then be studied as a function of this η-window size. The fluctuations arising from geometry should be nearly independent of the window size, while those arising from dynamical effects should be enhanced for a small window size. This latter result arises from an enhanced two-particle correlation in phase space (if there are dynamical correlations), which itself arises from a large correlation length at a phase transition.

The following definitions refer to the method proposed by Hwa:

$P(n)$ = probability for measuring n charged particles,

$\langle n \rangle$ = mean of $P(n)$ distribution,

D = $\sqrt{(\langle n^2 \rangle - \langle n \rangle^2)}$ is the dispersion,

$C2$ = $\langle n^2 \rangle / \langle n \rangle^2$ is the second central moment.

Hwa has shown that the quantity $S2 = C2 - 1/\langle n \rangle$ can be expressed as the sum of two terms, where the first reflects geometrical effects and must be larger than 1.0, and the second contains any effects due to dynamical correlations. Any enhancements due to the latter are expected to appear for small values of the η window studied.

The results of the WA80 1986 runs with 200-GeV/nucleon ^{16}O have been analyzed according to the above suggestions. A similar analysis has also been carried out for events generated by the VENUS (version 1.06) event generator.[9] Results are presented in Table 2.12 for both minimum bias events and for "central" events selected by requiring that the energy in the Zero-Degree Calorimeter (ZDC) be less than 20% of the projectile energy.

Given the similarity of the results from the data and the VENUS model events, and also given the nearness of the values of S2 to 1.0, particularly for the central events, there does not appear to be strong evidence present for the existence of dynamical correlations in the present data. We have also checked that the use of pseudorapidity instead of rapidity (the phase-space variable) in the analysis does not alter the results: calculations using VENUS events and an analysis in terms of rapidity yield the same result.

The analysis method proposed by Bialas and Peschanski is, in some sense, a more general version of the above analysis. They propose that the "scaled factorial moments," F_i, of the multiplicity distribution be extracted and examined for the presence of large, nonstatistical fluctuations. They pointed out that the variation of these moments with the "window" selected in rapidity would give an indication of the existence of a particular scale in rapidity for the creation of the final particles; such a scale might reflect the conditions at hadronization of a quark-gluon plasma. These authors also suggested that one might, instead, observe a pattern in these moments that is characteristic of what is known as "intermittency" in hydrodynamics. This is a pattern known from studies of turbulent fluid flow in which fluctuations appear on a range of different scales but are limited to small parts of phase space.

These moments can be defined as:

$$F_i = \frac{1}{M} \sum_{i=1}^{M} (M^i) \times \frac{K_m * (K_m - 1) * \ldots * (K_m - i + 1)}{\langle N \rangle^i}$$

Table 2.12. Results of analysis of WA80 $^{16}O + ^{197}Au$ data at E/A = 200 GeV and of corresponding VENUS simulation events using the method of Ref. 7 (see text). The bin center was taken at $\eta = 3.0$.

	Minimum Bias				Central			
	WA80		VENUS		WA80		VENUS	
η-window	Mean	S2	Mean	S2	Mean	S2	Mean	S2
0.30	15.1	1.36	14.8	1.40	26.5	1.03	27.6	1.04
0.60	29.6	1.39	28.3	1.45	53.6	1.02	54.8	1.03
0.90	44.1	1.39	42.0	1.46	80.0	1.02	81.4	1.03
1.20	57.6	1.39	55.3	1.45	104.6	1.02	107.2	1.02
1.50	70.2	1.38	68.2	1.45	127.3	1.02	132.1	1.03
1.80	82.2	1.38	80.4	1.45	148.8	1.02	155.4	1.02
2.10	94.1	1.38	91.9	1.44	170.2	1.02	177.1	1.02
2.40	106.1	1.38	102.6	1.44	191.7	1.02	197.3	1.02

where M is the total number of equally sized "bins" into which a given rapidity interval is subdivided, N is the total multiplicity in the rapidity interval, and K_m is the number of particles in the m'th bin. These moments are straightforward to compute from the data. Bialas and Peschanski showed that if the F_i are averaged over many events, the resulting moments are equal to the moments of the true probability distribution of particles in phase space. This then avoids the problem of having only integral numbers of particles in a given rapidity interval in a real event and the problem of having counting statistics fluctuations present in the rapidity distribution for a specific event.

The presence of nonstatistical fluctuations will influence the absolute values of F_i and will also influence the variation of F_i with the size of the rapidity bins, ΔY, into which the overall rapidity interval is subdivided. For example, if there exists a set of fluctuations on a rapidity scale S, then F_i will increase with decreasing ΔY until the scale S is reached, after which point F_i will become constant. If, on the other hand, an intermittent pattern exists, where F_i depend on ΔY via a power law relation, then F_i will be observed to increase with decreasing ΔY down to the resolution limits of the data.

A plot of the logs of the 2nd, 3rd, 4th, and 5th moments, $\ln(F_i)$, vs the negative log of the width of the pseudorapidity bin, $-\ln(\Delta\eta)$, is shown in Fig. 2.73. Results are presented for "peripheral" and "central" collisions of E/A = 200-GeV ^{16}O with ^{197}Au. The "peripheral" events are given as filled triangles and correspond to observed energies in the ZDC of 1.0-1.8 TeV (31-56% of the projectile energy). The "central" events correspond to observed energies of less than 0.4 TeV in the ZDC (12% of the projectile energy). For both classes of events the log of the observed moments rises linearly with the negative log of the pseudorapidity bin. The observed rise is not unlike that expected for an intermittent pattern. Also included on this figure are the results of the same analysis done by using events created by the string-model program FRITIOF. These are shown as open squares and are observed to show little, if any, dependence of the log of the factorial moments on the pseudorapidity window. Note that the smallest pseudorapidity bin used throughout this analysis was $\Delta\eta = 0.1$.

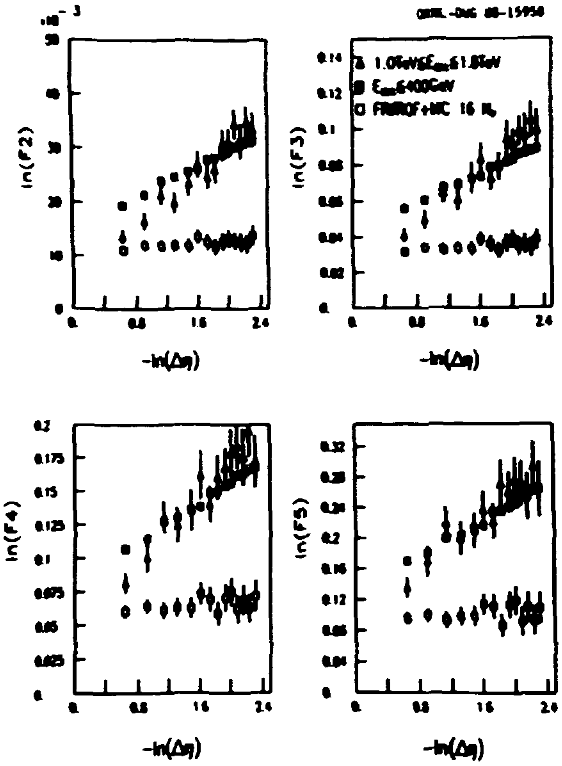

Fig. 2.73. Plot of the log of the 2nd thru 5th factorial moments for the E/A = 200-GeV ^{16}O + ^{197}Au multiplicity data of WA80 vs the log of the pseudorapidity interval for which the moments were calculated. The moments used are the scaled factorial moments proposed by Bialas and Peschanski, as defined in Ref. 8. The pseudorapidity interval covered is 2.4 to 4.0 units.

These results thus do not show any evidence for dynamical correlations (using the analysis method of Hwa), nor for a "fixed" scale of the observed fluctuations (using the analysis method of Bialas and Peschanski). The observed pattern is not unlike that expected for an intermittent source, at least down to the scale in pseudorapidity (0.1) observable with the WA80 apparatus.

---

1. Gesellschaft fuer Schwerionenforschung (GSI), D-6100 Darmstadt, Fed. Rep. Germany.

2. University of Muenster, D-4400 Muenster, Fed. Rep. Germany.
3. Lawrence Berkeley Laboratory, Berkeley, California 94720.
4. University of Lund, S-22362 Lund, Sweden.
5. Adjunct research participant from the University of Tennessee, Knoxville, Tennessee 37996.
6. L. van Hove, Nucl. Phys. A447, 443c (1985).
7. R. Hwa, Z. Phys. C 38, 277 (1988); R. Hwa, University of Oregon preprints OITS-385 and OITS-393.
8. A. Bialas and R. Peschanski, Nucl. Phys. B273, 703 (1986); A. Bialas and R. Peschanski, Jagellonian University preprint TPJU/4/88.
9. K. Werner and M. Kutschera, Phys. Lett. 183B, 385 (1987); K. Werner, Brookhaven National Laboratory preprint 39726.

INTRINSIC PHOTON SPECTRA FROM ^{16}O-INDUCED REACTIONS AT 200 GeV/NUCLEON

WA80 Collaboration

R. Albrecht[1], T. C. Awes, C. Baktash, P. Beckmann[2], F. Berger[2], R. Bock[1], G. Claesson[1], L. Dragon[2], R. L. Ferguson, A. Franz[3], S. Garpman[4], R. Glasow[2], H. A. Gustafsson[4], H. H. Gutbrod[1], K. H. Kampert[2], B. W. Kolb[1], P. Kristiansson[3], I. Y. Lee, H. Loehner[2], I. Lund[1], F. E. Obenshain, A. Oskarsson[4], I. Otterlund[4], T. Peitzmann[2], S. Persson[4], F. Plasil, A. M. Poskanzer[3], M. Purschke[2], H. G. Ritter[3], R. Santo[2], H. R. Schmidt[1], T. Siemiarczuk[1], S. P. Sorensen[5], E. Stenlund[4], G. R. Young

The WA80 experiment at the CERN SPS is designed to measure the distribution of charged particles over a large fraction of phase space, to analyze the forward and transverse energy distributions, and to investigate the target fragmentation region. In addition, photons and neutral pions are identified near midrapidity in a high-resolution lead-glass electromagnetic calorimeter (SAPHIR). This allows a detailed analysis of the photon and π^0 transverse momentum (p_T) distributions based on centrality selections made using the energy measurements or the charged-particle multiplicity measurements. The experimental setup has been described in detail elsewhere.[6] The SAPHIR detector consists of 1278 individually readout lead-glass modules with a total pseudorapidity coverage of $1.5 < \eta > 2.1$ and a solid angle of 0.13 steradian. Charged particles are identified in SAPHIR by a double layer of streamer tubes with pad readout located in front of SAPHIR. The streamer tube material contributes 4% to the photon conversion probability. The target vacuum chamber contributes an additional 0.4%. Details of the construction and performance of SAPHIR are given elsewhere.[7]

Besides the investigation of pion momentum distributions[8] and correlation studies, the ultimate objective of photon detection in relativistic heavy-ion collisions has been the detection of direct photons which promise to provide a clean signal of thermal radiation from the expected quark-gluon plasma.[9] However, this analysis is severely hampered by the presence of decay photons from the various meson decays. Among those, the π^0 and the η are clearly the dominant source of single-photon background which must be subtracted from the inclusive photon yield to determine the yield of direct photons. Other possible sources of photon background from beam halo and misidentified hadrons have been shown to be negligible for the WA80 detector setup. A Monte Carlo code, which uses the measured π^0 and η cross sections and known branching ratios and kinematics for photon decay of these mesons, is used to calculate the photon yield from π^0 and η decays within the SAPHIR detector acceptance. It is, therefore, essential to determine the π^0 and η cross sections in order that the contribution of decay photons can be calculated accurately. The extraction of the π^0 cross section has been described elsewhere.[8] Unfortunately, the determination of the η cross section is more difficult because the η acceptance of SAPHIR is much lower than for the π^0, due to the larger opening angle for the η-decay photons. Nevertheless, we obtain the mass spectrum shown in Fig. 2.74, where a clear η signal is observed in a limited p_T region with a peak width compatible with the measured detector resolution. From the observed peak, the ratio $\eta/\pi^0 = 0.74 \pm 0.23$ is derived, which is in accordance with results from p + p reactions. The η spectrum in other p_T regions

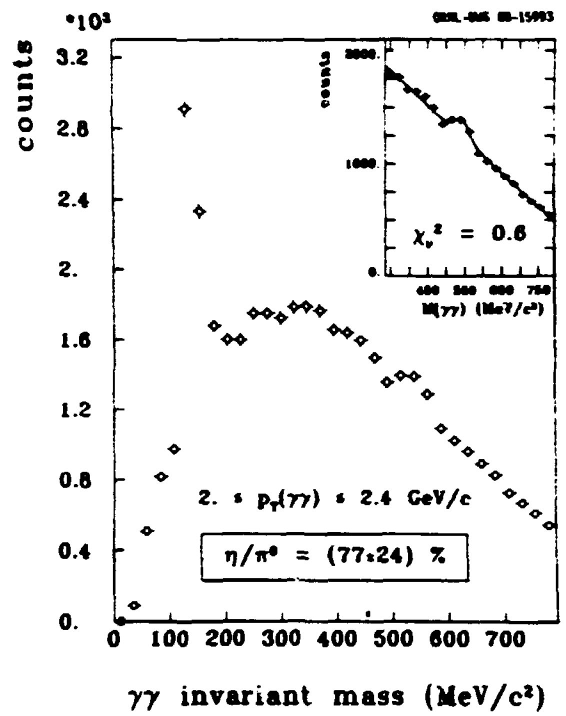

Fig. 2.74. Invariant mass spectrum of $\gamma\gamma$ pairs from minimum bias data, showing the π^0 and η peaks for ^{16}O + Au at 200 A GeV. Only photons with E_γ > 500 MeV and 2 GeV/c < $p_T(\gamma\gamma)$ < 2.4 GeV/c are considered. The small inset shows the mass region around the η peak.

is obtained with the assumption that, as observed in p + p reactions, the η yield is simply proportional to the π^0 yield, when scaled by the respective transverse masses. Finally, heavier mesons, which also photon decay, are expected to produce only an additional small fraction of the η contribution and have been neglected thus far in the preliminary analyses. By comparing the photon measurements in different event classes, uncertainties due to detector response, such as nonlinearities, acceptance, and geometry, automatically cancel. Also, uncertainties due to the photon contributions from η- and heavier-meson decays will cancel if their production scales with the π^0 production, independent of the event type. Thus, comparisons of the direct photon production in central versus peripheral reactions allows a comparison of results for high density nuclear matter to those for low density matter (cf. as in hadron-hadron collisions), with approximately the same systematic errors for each. However, an important difference in the analysis of the photon results for the different event types is that the photon reconstruction efficiency is found to be multiplicity-dependent. This situation will be improved in the future by more sophisticated analysis techniques currently under development.

The measured inclusive γ/π^0 ratio for peripheral reactions of ^{16}O + Au at 200 A GeV is shown by the solid crosses in Fig. 2.75. Also shown are the calculated contributions of decay photons from π^0 decay (solid histogram) and from both π^0 and η decays together (dashed histogram). The errors indicate the statistical errors plus the error due to the uncertainty in the η/π^0 ratio. The preliminary estimate of the direct γ/π^0 ratio is then obtained by subtracting the dashed histogram from the inclusive photon measurement. Thus, the peripheral direct γ/π^0 ratio is seen to be consistent with a value of zero. This is in agreement with results observed in hadron-hadron collisions[10] in which γ/π^0 is observed to differ significantly from zero only in the p_T region above about 3 GeV/c. On the other hand, the preliminary result for central collisions shown in Fig. 2.76 indicates that there is an excess of direct photons which is not observed in peripheral collisions. This trend is in qualitative agreement with predictions for the formation of a quark-gluon plasma.[9] It remains to be determined whether this preliminary result will be verified in further, more complete analyses, and, if so, whether it might also have other more conventional explanations in terms of dense hadronic matter.

---

1. Gesellschaft fuer Schwerionenforschung (GSI), D-6100 Darmstadt, Fed. Rep. Germany.
2. University of Muenster, D-4400 Muenster, Fed. Rep. Germany.
3. Lawrence Berkeley Laboratory, Berkeley, California 94720.
4. University of Lund, S-22362 Lund, Sweden.
5. Adjunct research participant from the University of Tennessee, Knoxville, Tennessee 37996.

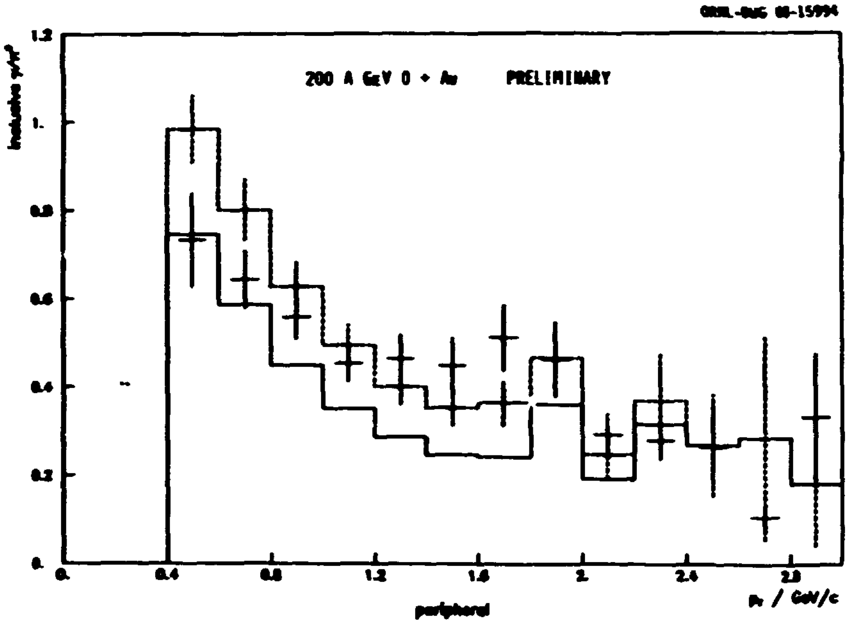

Fig. 2.75. γ/π^0 ratio for peripheral reactions of ^{16}O + Au. The solid crosses indicate the inclusive ratio and it's statistical error. The full-line histogram shows the contribution to this ratio due to photons from π^0 decays. The dashed-line histogram shows the sum of decay photons from the π^0 and η mesons, together with the statistical uncertainty from the Monte Carlo simulations and from the measured η/π^0 ratio. The preliminary direct γ/π^0 ratio is extracted from the difference between the crosses and dashed-line histogram.

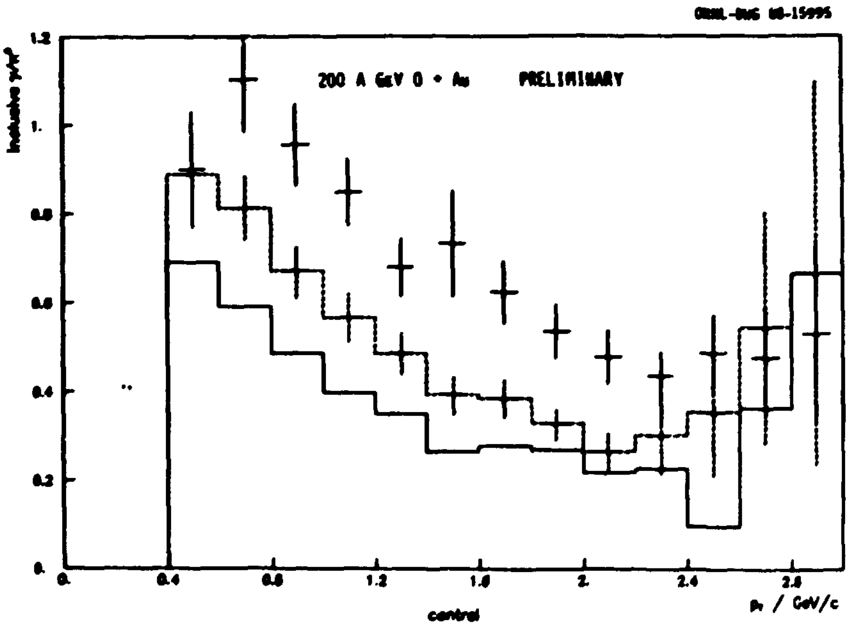

Fig. 2.76. Same as Fig. 2.75 for central reactions.

6. "Study of Nucleus-Nucleus Collisions at Relativistic Energies: CERN-SPS WA80 Experiment," Phys. Div. Prog. Rep., Sept. 30, 1985, ORNL-6233 (April 1986), p. 149.

7. H. Löhner et al., WA80 Collaboration, Z. Phys. C 38, 97 (1988).

8. "π^0 Momentum Distributions from Central and Peripheral ^{16}O + Au Collisions at 200 GeV/Nucleon," Phys. Div. Prog. Rep., Sept. 30, 1988, ORNL-6508.

9. R. C. Hwa and K. Kajantie, Phys. Rev. D 32, 1109 (1985).

10. T. Ferbel and W. R. Molzen, Rev. Mod. Phys. 56, 181 (1984).

π^0 MOMENTUM DISTRIBUTIONS FROM CENTRAL AND PERIPHERAL ^{16}O + Au COLLISIONS AT 200 A GeV

WA80 Collaboration

R. Albrecht[1]	I. Y. Lee
T. C. Awes	H. Loehner[2]
C. Baktash	I. Lund[1]
P. Beckmann[2]	F. E. Obenshain
F. Berger[2]	A. Oskarsson[4]
R. Bock[1]	I. Otterlund[4]
G. Claesson[1]	T. Peitzmann[2]
L. Dragon[2]	S. Persson[4]
R. L. Ferguson	F. Plasil
A. Franz[3]	A. M. Poskanzer[3]
S. Garpman[4]	M. Purschke[2]
R. Glasow[2]	H. G. Ritter[3]
H. A Gustafsson[4]	R. Santo[2]
H. H. Gutbrod[1]	H. R. Schmidt[1]
K. H. Kampert[2]	T. Siemiarczuk[1]
B. W. Kolb[1]	S. P. Sorensen[5]
P. Kristiansson[3]	E. Stenlund[4]

G. R. Young

First results from ultrarelativistic heavy-ion experiments at the CERN SPS have shown that with 200-A-GeV ^{16}O projectiles high energy densities are created, which approach the critical values for a quark-gluon phase transition predicted by QCD lattice calculations. One means of studying the properties of the compressed and highly excited reaction zone is the investigation of the transverse momentum (p_T) spectra of produced pions and their dependence on the centrality of the reaction. To distinguish different contributing processes and to provide a reliable basis for comparisons with p + p scattering, a large p_T coverage is required. In particular, data at high p_T values are desirable, where hard processes become important and may be calculated by perturbative QCD. The present investigation of π^0 spectra has, therefore, concentrated on a detailed measurement of p_T spectra up to 2.8 GeV/c and on the selection of data according to the centrality of the reaction.

The experiment has been performed at the CERN SPS. The WA80 experimental arrangement has been described earlier.[6] A schematic drawing of it is shown in another contribution to this progress report.[7] The pion data were obtained with the lead-glass electromagnetic calorimeter (SAPHIR), and the degree of collision centrality was deduced from data obtained with the Zero-Degree Calorimeter (ZDC). In the data presented here, the minimum bias trigger is defined by the requirement that less than 88% of the total oxygen projectile energy is measured in the ZDC and that at least one charged particle is recorded by the multiplicity detectors in the pseudorapidity range $4.4 > \eta > 1.2$. Neutral pions are identified by their decay photons ($\pi^0 \rightarrow 2\gamma$), and π^0 *dN/dp_T distributions are obtained from invariant mass spectra by a procedure described elsewhere.[8]

Figure 2.77 shows the minimum bias π^0 data for p + Au and ^{16}O + Au together with an exponential fit [$1/p_T dN/dp_T \sim \exp(-p_T/T)$] to the data in the range $0.8 < p_T < 2$ GeV/c. The difference between the ^{16}O + Au and p + Au spectra of Fig. 2.77 is clearly displayed by plotting the ratios of the spectra (Fig. 2.78). A similar representation has been used previously by Cronin et al.[9] to discuss the nuclear enhancement of p + A compared to p + p data. In their work, a scaling of the minimum-bias cross-section ratios with A^{α}_{target} and a rise of α with p_T has been observed for charged pions in the range $0.8 < p_T < 5$ GeV/c. A similar enhancement due to the different projectile masses involved is obviously seen here in going from p + Au to ^{16}O + Au reactions.

More insight into the mechanism of heavy-ion reactions at high energies can be gained by selecting central and peripheral collisions. Collective efforts or the formation of new states of nuclear matter are expected predominantly in very central collisions. Data from peripheral collisions may, on the other hand,

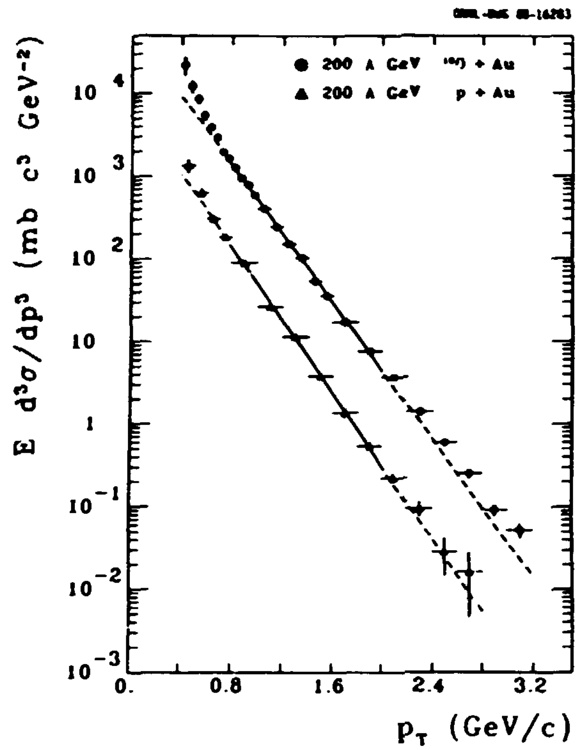

Fig. 2.77. Invariant π^0 cross sections from collisions of p and ^{16}O projectiles with an Au target at 200 A GeV measured in the pseudorapidity range $1.5 < \eta < 2.1$. An exponential is fitted to the data in the p_T region from 0.8 to 2 GeV/c (solid line) and is continued over the full p_T range (dashed line). The slope parameters are $T = 210 \pm 3$ MeV/c for ^{16}O + Au and $T = 196 \pm 4$ MeV/c for p + Au, respectively.

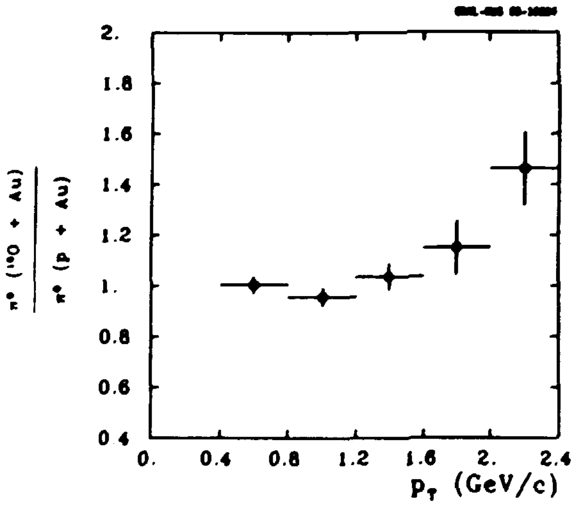

Fig. 2.78. Ratio $(^{16}O + Au)/(p + Au)$ of minimum-bias π^0 *p_T spectra normalized to unity.

provide a link between p + A and p + p reactions. The centrality selection has been achieved by cuts in the ZDC energy. Central events are defined by $0 < E_{ZDC}/E_{beam} < 30\%$, corresponding to 37% of the minimum-bias cross section, while peripheral events are defined by $40 < E_{ZDC}/E_{beam} < 88\%$, corresponding to 54% of the minimum-bias cross section. In Fig. 2.79 spectra of central and peripheral events are displayed. Exponential fits are again shown for $0.8 < p_T < 2$ GeV. The following differences between central and peripheral collisions are apparent in the data of Fig. 2.79: (i) the steeper slope observed in the minimum-bias data at lowest-p_T values ($p_T < 0.8$ GeV/c; see also Fig. 2.77) is

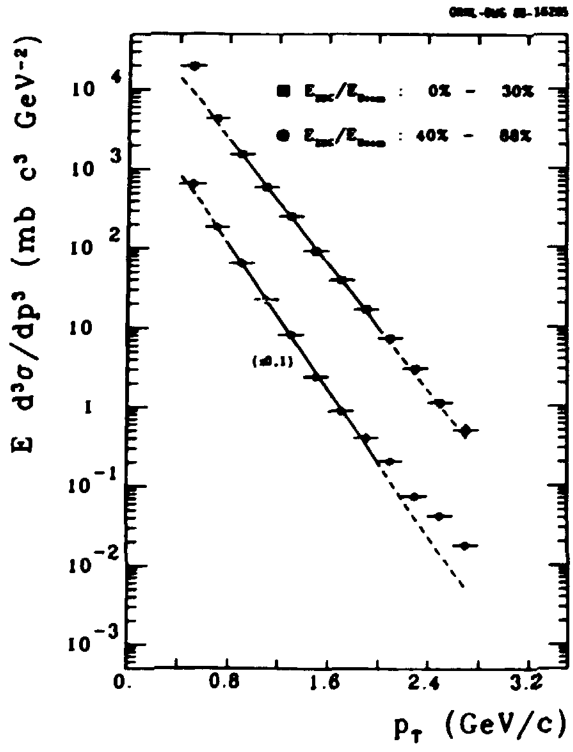

Fig. 2.79. Invariant π^0 cross sections from collisions of ^{16}O projectiles with an Au target at 200 A GeV measured in the pseudorapidity range $1.5 < \eta < 2.1$ for different E_{ZDC} windows. The squares correspond to central collisions, the dots to peripheral collisions. An exponential is fitted to the spectra for $0.8 < p_T < 2$ GeV/c (solid line) and is continued over the full p_T range as a dashed line. The slope parameters are $T = 189 \pm 5$ MeV/c for the peripheral-collision data and $T = 220 + 5$ MeV/c for the central-collision data, respectively.

also seen in the central-collision data, but not in the peripheral-collision data; (ii) in the intermediate region, $0.8 < p_T < 1.8$ GeV/c, the spectra show a well-developed exponential shape with a significantly flatter slope for central collisions compared to peripheral collisions; (iii) for $p_T > 1.8$ GeV/c, central-collision spectra maintain the slope of the lower-p_T range while the peripheral-collision spectra show a clear deviation from the low-p_T behavior with a much flatter slope in the higher-p_T region.

Figure 2.80 shows the comparison of peripheral π^0 spectra from ^{16}O + Au at 200 A GeV (19.4-GeV nucleon-nucleon c.m. energy) with charged-pion spectra from p + p collisions at a similar c.m. energy.[10] There is a remarkable agreement in the spectral slope of the data up to the highest p_T of the present experiment. The flattening of the slope in the p + p data beyond ~2 GeV/c has been interpreted as the onset of hard QCD scattering, which is expected to become important

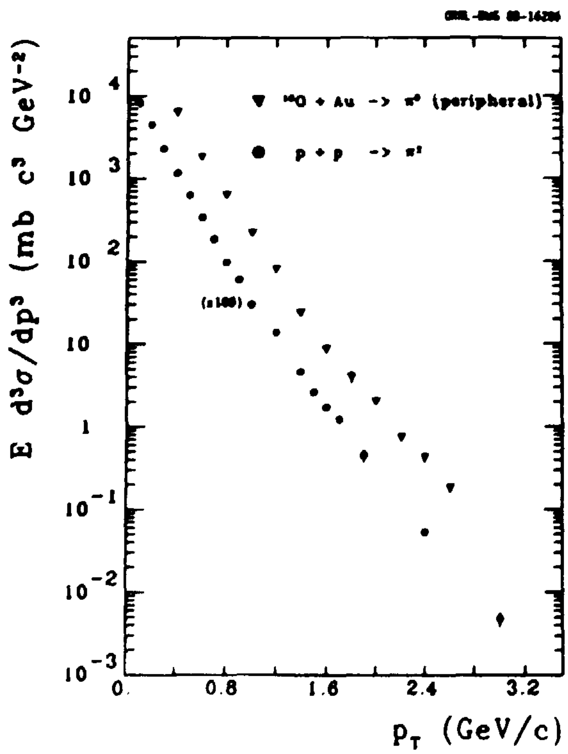

Fig. 2.80. Comparison of peripheral π^0 spectra from the present ^{16}O + Au experiment at nucleon-nucleon c.m. energy of 19.4 GeV with charged pion spectra from minimum-bias p + p data at 23 GeV.[10] (π^- and π^+ data are averaged and plotted as one common set of data points.)

for p_T values of several GeV/c. It, therefore, appears that the hard scattering component of the elementary p + p interaction survives in peripheral heavy-ion collisions, but — in the present p_T range — is strongly obscured in central collisions by nuclear effects. Forthcoming experiments in an extended p_T range may reveal whether the hard component emerges in central collisions at higher-p_T values.

---

1. Gesellschaft fuer Schwerionenforschung (GSI), D-6100 Darmstadt, Fed. Rep. Germany.
2. University of Muenster, D-4400 Muenster, Fed. Rep. Germany.
3. Lawrence Berkeley Laboratory, Berkeley, California 94720.
4. University of Lund, S-22362 Lund, Sweden.
5. Adjunct research participant from the University of Tennessee, Knoxville, Tennessee 37996.

6. H. H. Gutbrod et al., Proc. Int. Workshop on Gross Properties of Nuclei and Nuclear Excitations XV, Hirschegg, Austria, Jan. 12-17, 1987, GSI and Institut fuer Kernphysik, Darmstadt, 1987, p. 42.
7. R. Albrecht et al., "Nuclear Stopping in Oxygen-Induced Reactions at 200 A GeV," this report.
8. P. Beckmann et al., to be submitted to Nuclear Instruments and Methods in Physics Research.
9. J. Cronin et al., Phys. Rev. D 11, 3105 (1975); D. Antreasyan et al., Phys. Rev. D 19, 764 (1979).
10. B. Alper et al., Nucl. Phys. B100, 237 (1975).

NUCLEAR STOPPING IN OXYGEN-INDUCED REACTIONS AT 200 A GeV[1]

WA80 Collaboration

R. Albrecht[2], T. C. Awes, C. Baktash, P. Beckmann[3], F. Berger[3], R. Bock[2], G. Claesson[2], L. Dragon[3], R. L. Ferguson, A. Franz[4], S. Garpman[5], R. Glasow[3], H. A. Gustafsson[5], H. H. Gutbrod[2], K. H. Kampert[3], B. W. Kolb[2], P. Kristiansson[4], I. Y. Lee, H. Loehner[3], I. Lund[2], F. E. Obenshain, A. Oskarsson[5], I. Otterlund[5], T. Peitzmann[3], S. Persson[5], F. Plasil, A. M. Poskanzer[4], M. Purschke[3], H. G. Ritter[4], R. Santo[3], H. R. Schmidt[2], T. Siemiarczuk[2], S. P. Sorensen[6], E. Stenlund[5]

G. R. Young

A primary goal of relativistic heavy-ion studies is to verify the existence of the postulated quark-gluon plasma (QGP). Since most of the possible plasma signatures are indistinguishable from background created by nonplasma events, thorough understanding of reaction mechanisms is an important prerequisite in any QGP search. To isolate collective features of nucleus-nucleus collisions from those that may be expected on the basis of a linear superposition of nucleon-nucleus collisions, we compare measured quantities with results of calculations that reproduce data from nucleon-induced reactions and that make predictions for nucleus-nucleus reactions. Here we discuss the data obtained from our Zero-Degree Calorimeter (ZDC) and the transverse energy obtained from the Mid-Rapidity Calorimeter (MIRAC).[7] The experimental arrangement for WA80 is shown in Fig. 2.81.

The geometry of nucleus-nucleus collisions is important in order to describe the general features of the reaction mechanism. To a large extent qualitative features of the reaction may be described by such simple parameters as the relative size of the nuclei, the overlap volume, and the impact parameter. Simple geometrical considerations can be used for a qualitative understanding of the ZDC energy spectra, Fig. 2.82. At 200 A GeV, the $^{16}O + {}^{12}C$ reaction has essentially no cross section for events

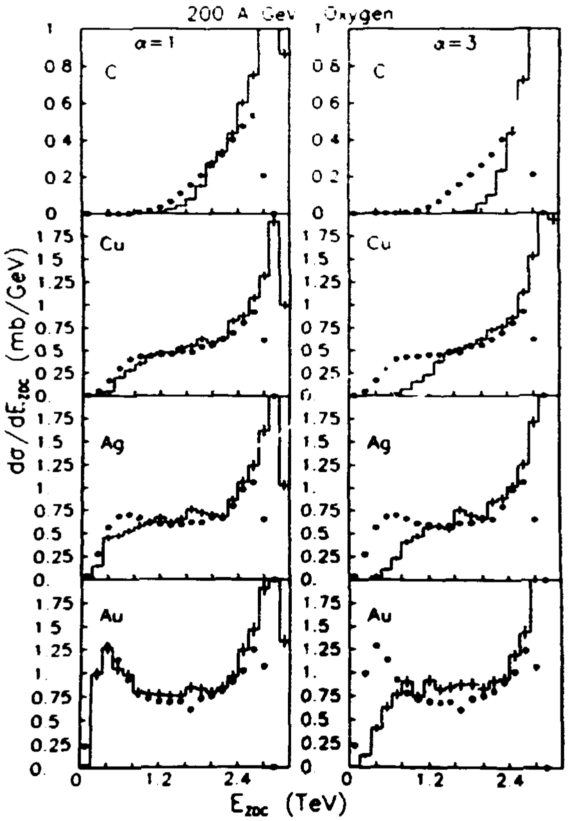

Fig. 2.82. The data points shown as a function of energy are cross sections which were obtained from the WA80 Zero-Degree Calorimeter, and the histograms are calculated (see text) with no trigger conditions. The parameter α = 1 indicates maximal stopping.

ORNL-DWG 88-14841

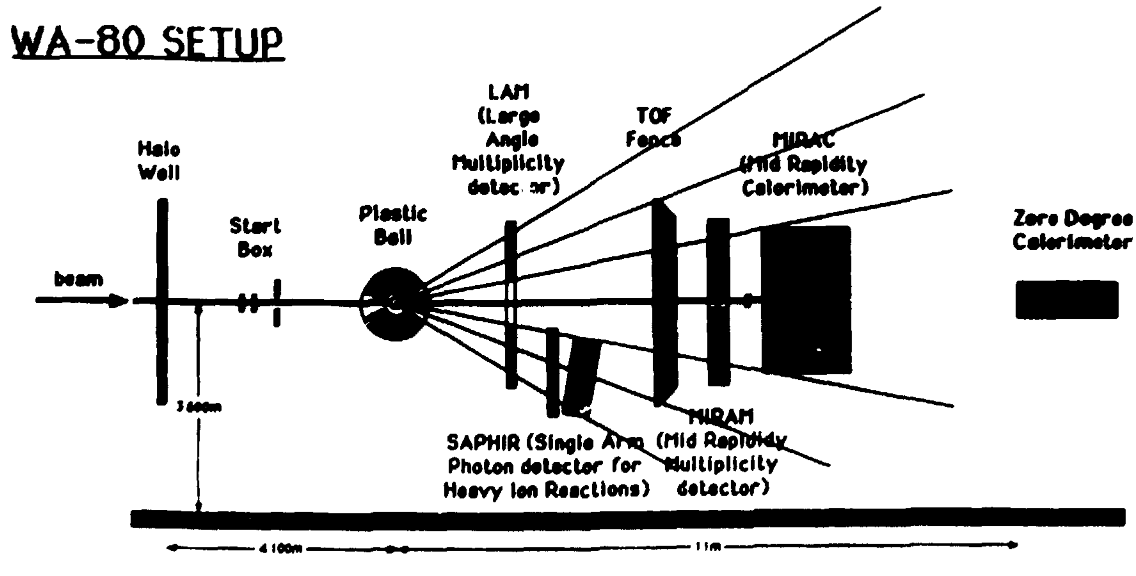

Fig. 2.81. Experimental arrangement for WA80, side view. The energy resolution of the Zero-Degree Calorimeter is 2.5% at 3.2 TeV.

depositing a small amount of energy in the ZDC because, even in the most central collisions, several projectile spectator nucleons, each with an energy of 200 GeV, continue in the beam direction. The particles measured with the ZDC are within 0.3 deg of the beam. In contrast, a peak is seen at small ZDC energies for the ^{16}O + ^{197}Au reaction. In this case, events with low ZDC energies arise from central collisions (impact parameter near zero) and result in the emission of only a few leading particles at angles less than 0.3 deg. And, in fact, collisions with a wide range of impact parameters around zero lead to interaction of the entire projectile with a nearly constant number of nucleons and contribute to the low-energy peak.

Figure 2.83a shows the relative sizes of Lorentz-contracted oxygen and gold nuclei with an impact parameter near zero. The dashed lines shown in the figure represent a tube drawn through the two nuclei, in this case at central density. The number of nucleons within the tube will depend on the relative sizes of the nuclei involved. If a uniform distribution of nucleons in the nucleus is assumed, then the number within the tube will be given by the volume of the tube divided by the total volume times the number of nucleons in the nucleus.

The Glauber-type multiple collision model[8] which we have used is based on this geometry. The sequential nature of the collisions and subsequent energy loss is illustrated in Fig. 2.83b. The model assumes a specific law for nuclear stopping, which will be discussed below. The formation of the QGP will depend on the degree of nuclear stopping. It has been shown for proton-proton scattering at energies above a few tens of GeV that the cross section is nearly independent of energy and of the light cone variable, x; i.e., $d\sigma/dx$ = constant:

$$x = (E_0^b + p_z^b)/(E_0^a + p_z^a) .$$

The denominator and numerator are four momenta of the parent particle, a, and daughter particle, b. For nucleus-nucleus collisions we assume, in a series of many collisions, that the individual baryons interact continuously with all the colliding baryons. By a baryon-baryon collision we mean a nondiffractive inelastic collision with a cross section σ_{in} = 29.4 mb. The particle production is parametrized by simple functions in the Glauber theory. In

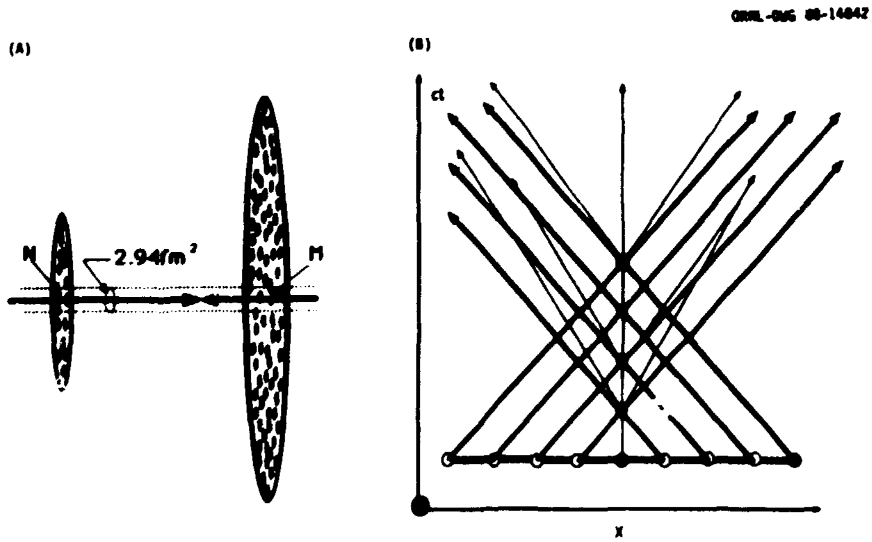

Fig. 2.83. The collision geometry is shown. The dashed lines represent a tube through the nuclei. The area of the tube is 29.4 mb. (b) Shows a space-time diagram with nuclear stopping indicated by the lighter lines.

order to simplify the calculations further, we choose the placement of baryons within the target and projectile by random selection, and divide each nucleus into tubes of cross section 2.94 fm^2 extending through the nuclei as described above. The impact-parameter dependence is taken into account by random sampling of the distribution. It is assumed that the energy is so high that the baryons and produced particles remain within a given tube.

The stopping law should depend on the number of collisions and has been investigated in some cases with the functional form $\alpha = 1 + \beta(n-1)$, where β is a constant of order 0.5 and n is the collision number. However, theoretical results indicate that α can be taken as a constant. It is assumed that the baryon-baryon collisions lead to particle clusters and that the momentum state of the leading clusters is given by $P(x) = \alpha x^{\alpha-1}$, where α is a constant for a given calculation. Nuclear stopping is large for $\alpha = 1$ and decreases for larger values of α. The histograms shown on the left and on the right in Fig. 2.82 are calculated with $\alpha = 1$ and $\alpha = 3$, respectively. We see that $\alpha = 1$, large stopping, yields the best fit to our ZDC data. By "nuclear stopping," we refer to the fraction of the incident kinetic energy that is converted to "heat" (particle production, etc.). The energy loss for proton-nucleus collisions will be the order of 45% for the first interaction, and after, say, three subsequent interactions within the nucleus, 87% of the incident energy will have been lost.

Since the model is quite general, we may compare transverse energy calculations of this model with those measured with the Mid-Rapidity Calorimeter. Figure 2.81 shows the location of this calorimeter. The calculations, corrected for acceptance, and the experimental data for the transverse energy, E_T, are shown in Fig. 2.84, and again we see that $\alpha = 1$ yields the best fit. There may be additional contributions to E_T from secondary collisions or other sources. These results show that for this model, the maximal degree of nuclear stopping is required to fit our data. In a multiple scattering theory, it would be reasonable to expect that the cross section would change after each collision because of baryon excitations. However, it appears that this assumption is not necessary in order to fit our data with this model.

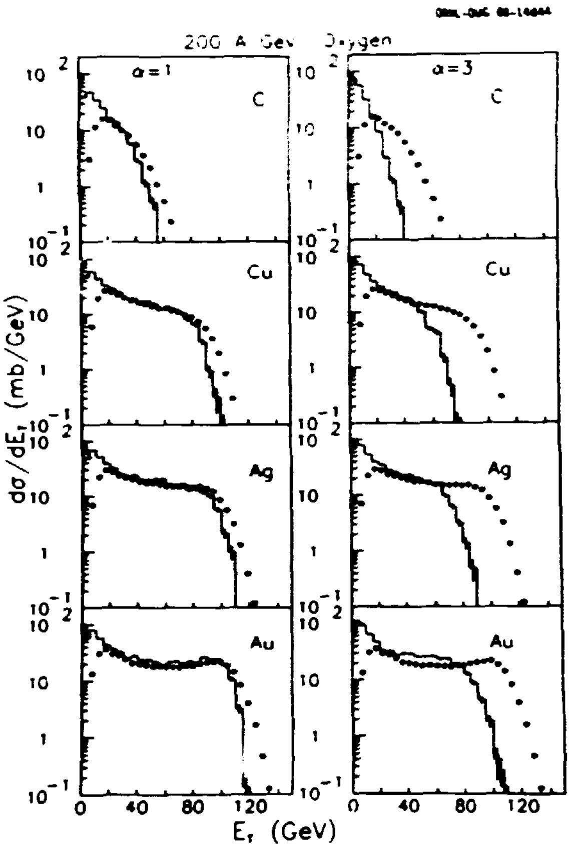

Fig. 2.84. The transverse energy measured in MIRAC at 200 A GeV (points) is shown. The calculated spectra, shown as histograms, have been corrected for geometrical acceptance.

It is of interest to extract, under the same conditions and with the same parameters as for the cross section calculation, the energy density produced within the tubes (at the moment when the produced particles have not streamed out from the tube).[9] The energy densities are shown in Fig. 2.85. It should be stressed that the tube volumes are based on the nucleon-nucleon cross section and that the longitudal region over which the collisions take place is determined from the Monte Carlo calculations.

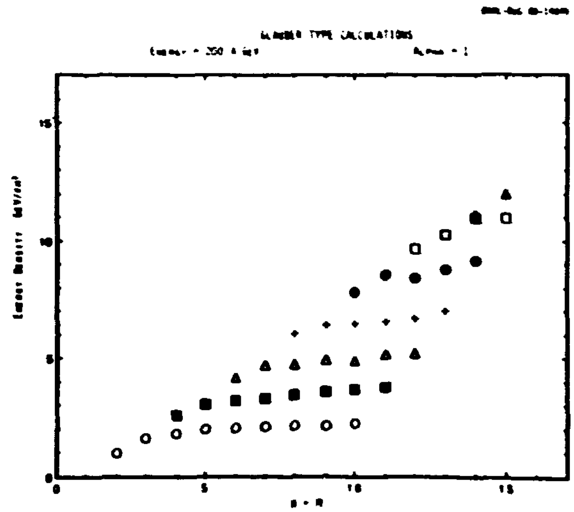

Fig. 2.85. Energy densities calculated for colliding tubes of nucleons. The abscissa is the sum of the nucleons in each of the tubes. The symbols are o, 1+M; ■, 2+M; ▲, 3+M; +, 4+M; ●, 5+M; □, 6+M; ▲, 7+M.

The densities shown in the figure are based on the calculated longitudal values and a transverse dimension comensurate with the classical nucleon radius (~1.2 fm). These parameters have been the subject of much discussion,[7] with no definite conclusions as to the values one should use.[10] Therefore, the absolute values shown in Fig. 2.85 should be viewed with caution. However, the relative values should be independent of these assumptions.

As in the calculations of the cross section, the number of nucleons in a tube drawn through the projectile and target nuclei will vary according to $A^{1/3}$, and the calculations are for combinations of N incident nucleons on M target nucleons where N and M vary from 1 to 7. For example, 5 + 5 would represent a central collision for Pb + Pb at 200 A GeV. The abscissa in Fig. 2.85 displays the sum (N + M) of nucleons in the tubes, and the ordinate displays the energy density produced within the interaction volume.

CONCLUSION

Comparision of our data with this theoretical model indicates that large nuclear stopping is required. The stopping parameter $\alpha = 1$ gives the best fit to our data. Calculations of the energy density with this model show that for a fixed incident energy per nucleon, one may expect that the energy density will increase with increasing mass of the projectile and target combination.

---

1. Summary of paper presented at XIXth International Symposium on Multiparticle Dynamics — New Data and Theoretical Trends, Arles, France, June 13-17, 1988
2. Gesellschaft fuer Schwerionenforschung (GSI), D-6100 Darmstadt, Fed. Rep. Germany.
3. University of Muenster, D-4400 Muenster, Fed. Rep. Germany.
4. Lawrence Berkeley Laboratory, Berkeley, California 94720.
5. University of Lund, S-22362 Lund, Sweden.
6. Adjunct research participant from the University of Tennessee, Knoxville, Tennessee 37996.
7. R. Albrecht et al., Phys. Lett. B 199, 297 (1987)
8. C. Y. Wong and Z. Lu, to be published
9. C. Y. Wong, Phys. Rev. C 33, 1340 (1986)
10. T. C. Awes et al., Proc. Int. Workshop XVI on Gross Properties of Nuclei and Nuclear Excitations, Hirschegg, Austria, Jan. 18-22, 1988, to be published; S. P. Sorensen, Proc. Sixth Int. Conf. on Ultrarelativistic Nucleus-Nucleus Collisions, Nordkirchen, Fed. Rep. Germany, Aug. 24-28, 1987, Z. Phys. C 38, 3 (1988).

CALORIMETER AND ABSORBER OPTIMIZATION PROPOSAL FOR THE RHIC DIMUON EXPERIMENT

S. Aronson[1]	F. E. Obenshain
T. C. Awes	F. Plasil
C. Baktash	S. Saini
M. Fatyga[1]	S. P. Sorensen[6]
R. L. Ferguson	S. G. Steadman[5]
A. Franz[2]	G.S.F. Stephans[5]
S. Y. Fung[3]	J. H. Thomas[7]
T. A. Gabriel[4]	M. L. Tincknell
R. J. Ledoux[5]	M. Vient[3]
T. Ludlam[1]	G. R. Young

A proposal has been made to the Department of Energy to address directly the question of feasibility of dimuon measurements at RHIC. The principal uncertainty at present for muon pair measurements at RHIC is the design of the hadron absorber, which must do double duty as a calorimeter. The two major questions addressed are the level of background behind the hadron calorimeter/absorber in the muon experiment and the calorimeter design for the muon experiment. The results obtained will be of use for designing muon absorbers for the various experiments in which they have been proposed for RHIC, for the general problem of designing calorimeters for low-energy hadrons at RHIC, and for the general problem of designing fine-grained EM calorimeters for photon detection at RHIC.

Dimuons have the nice property that they can penetrate a quark-gluon plasma, while hadrons do not. Dimuons can also penetrate thick detectors, while hadrons cannot. This makes it possible to design detectors of large acceptance concentrating on this promising diagnostic of the quark-gluon plasma with little interference from the numerous hadrons produced during the transition back to a hadron gas. This large acceptance makes a dimuon experiment particularly attractive for studying the postulated suppression of the J/ψ and higher mass vector mesons.

Considerable interest is centered in the high-mass region ($M = 1$-4 GeV/c^2), and a good dynamic range in p_T acceptance (up to $p_T = 5$ GeV/c) is essential. Events at the high-end of the mass range can be studied easily at low rapidities, since the relatively energetic muons can penetrate an absorber thick enough to suppress the "punch-through" background. For small values of mass or p_T (soft muons or small opening angles), dimuons can be measured only at large rapidities where muons with boosted laboratory momenta are capable of traversing the absorber. In this case, however, angular resolution is very important. Thus, in this region, an absorber with a small ratio of interaction length to radiation length must be used in order to minimize the effects of multiple scattering on resolution.

Problems associated with resolution are most severe in the forward region, due to the above considerations and due to the large background of relatively energetic particles. In the central region, problems associated with dynamic range are most severe, since the muons receive only a small boost (low rapidity). In this region, one wishes to use a relatively thin absorber shell to help the dynamic range. The general softness of the spectrum of secondaries produced at midrapidity at RHIC makes it feasible to consider such a thin absorber, although detailed information on the spectrum of punch-through products is lacking, particularly for the low-incident hadron energies that will be encountered in the central region at RHIC.

Muons are detected after traversing material that is sufficiently thick so as to absorb electrons, photons, and hadrons. Hadrons can "fake" direct muons by two main processes: (a) hadrons may decay into muons before interacting; (b) hadrons or the products of a shower caused by them may "punch-through" the absorber. Together, these requirements cause serious difficulties in the case of relativistic heavy-ion collisions, for the following reasons. A thick absorber is needed to obtain a very low probability per incident hadron that any charged particle exits its back face. This probability must be multiplied by the very large multiplicity of charged hadrons produced in a relativistic heavy-ion collision to obtain the resulting number of "fake muons" per interaction. However, using an extremely thick and high-Z absorber will also stop low-energy muons before they reach the detector.

The measurement of muons behind a massive hadron calorimeter/absorber requires answers to several background-related questions:

(1) What are the punch-through probabilities for pions, kaons, and protons in the range of 0.3-10 GeV/c incident on a specific absorber?
(2) How do these vary as a function of the absorber composition, e.g., solid carbon, aluminum, steel, copper, tungsten, lead, or the same materials interleaved with a second material which would be a suitable active material for a sampling calorimeter?
(3) How do the results vary with absorber thickness?
(4) What is the momentum and particle ID spectrum of the punch-through particles?
(5) What fraction of them can penetrate a second shield and cause a "muon" trigger?

(6) How many of the punch-through particles will be rejected by position, angle, and momentum cuts appropriate to a muon-finding analysis program?

A layout for the proposed experiments to investigate these matters is shown in its various stages in Fig. 2.86.

It has been suggested that direct photons may provide a possible probe for quark-gluon plasma formation. Also, measurement of high-p_T photons provides a means to determine the gluon structure functions necessary to obtain a thorough understanding of the vector meson, e.g., J/ψ, production rates for nuclear collisions. Since dimuon measurements and photon measurements have similar rate requirements due to the relatively weak electromagnetic coupling of the probes, it is desirable to attempt to make both measurements simultaneously in the same experiment. Furthermore, any electromagnetic calorimetry for photon measurements will provide an instrumented absorber layer for subsequent dimuon measurements. The electromagnetic calorimetry may also be used to provide necessary event characterization.

It is clear that in the high particle multiplicity environment of RHIC, single photon identification and measurement are feasible only in the central rapidity region. Even in this region, it will be necessary to have good segmentation and large distances from the interaction region in order to avoid overlapping showers. To extract the single photon information it is necessary to determine the contribution of photons which arise from meson decays. In order to extract this contribution accurately, it is necessary to have good invariant mass resolution for the photon pairs. This also serves to minimize the contribution from combinatorial pairs. This requires good energy and position measurements for the photons. For reasons of cost, sampling calorimetry is an interesting detector technology for such measurements. However, the use of sampling calorimeters to provide the necessary position and energy resolution and photon identification has not been demonstrated, particularly for the relatively low energies ($\lesssim$0.5 GeV) expected in the central rapidity region. Therefore, one purpose of the proposed research is to investigate thoroughly the feasibility of using sampling electromagnetic calorimetry for photon measurements at RHIC.

The response of calorimeters to low-energy hadrons is not well studied and is an important issue for the central rapidity region at RHIC.

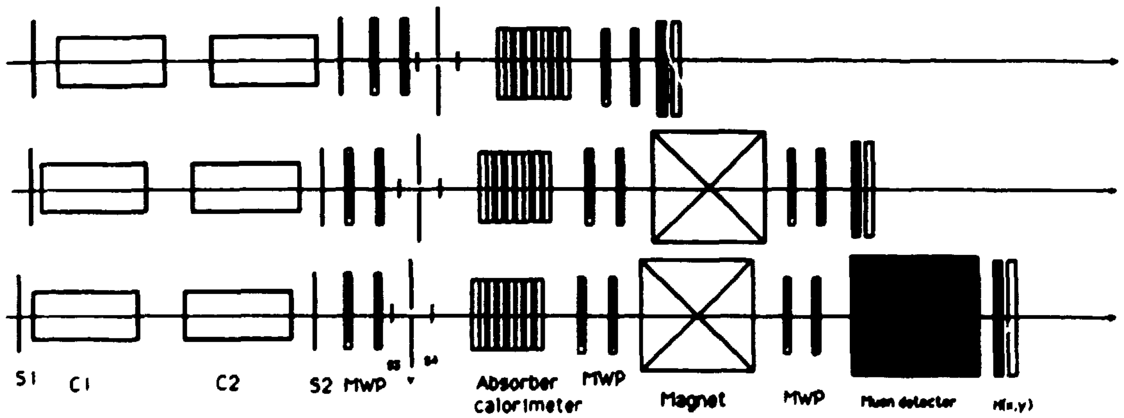

Fig. 2.86. Schematic layout of an experiment to measure punch-through and decay backgrounds for a muon experiment. Three increasing levels of complexity are shown. The various components are (a) plastic, position and beam identification detectors (S1, S2, S3, S4, and V); (b) Cerenkov detectors (C1, C2); (c) multiwire proportional counters (MWP); and (d) highly-segmented position-sensitive detector.

One to two thousand such particles will fill the region for $|y| < 1$. It is important to know how calorimeters respond to this flux. For example, is it possible to detect an energetic jet (>10-20 GeV) in the midst of the soft background, where the soft background may sum to over 1 GeV per tower? Our ability to sum energies in jets at RHIC depends on the answer to this question.

The background level for the muon measurement is closely tied to the details of the calorimeter construction. The calorimeter design is thus driven by these background considerations, the desire to measure direct photons also, and the need to obtain an accurate measurement of the energies of the soft hadrons. This leads us to propose an investigation of the properties of three different types of calorimeters. These will be studied both in parallel with the muon background measurements and in conjunction with it. The three devices are:

(1) A modular sampling calorimeter of the plate + scintillator type that may be easily reassembled with absorber plates of various types and thicknesses. This calorimeter is composed of a number of identical modules which may be stacked in a variety of configurations. Each module is separated transversely into 11 "trays" which are 4 cm x 4 cm in cross section and 70 cm deep, where each tray forms a "tower" (see Fig. 2.87).

(2) A compact EM calorimeter made of alternating thin sheets of Pb (800 μ) and scintillating optical fiber that has been formed into 200-μ-thick ribbons (lasagna calorimeter). We anticipate constructing a medium-scale, say 30 cm x 30 cm x 15 cm, EM "lasagna" calorimeter with full readout and investigating its properties for detecting energetic electrons and photons. This device has a very short radiation length (7 mm), making it useful for localizing EM showers in the transverse plane. However, this requires a highly segmented transverse readout to take full advantage of the short radiation length (see Fig. 2.88).

ORNL-DWG 88-15960

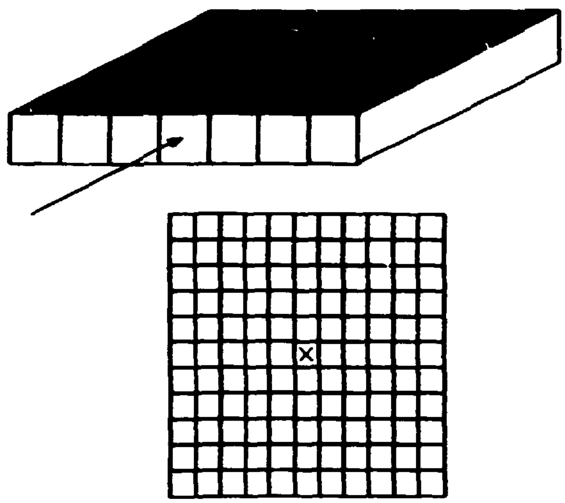

Fig. 2.87. Upper part of the figure: schematic view of seven 4 cm x 4 cm towers of the "tray" calorimeter. The scintillator and absorber material in each tower can be exchanged to test different configurations. The trays will be stacked to form an array of towers shown in the lower part of the figure. The arrow and the "x" indicate the incident test particles.

(3) A variant of the EM lasagna calorimeter scaled up in size for hadron shower containment. This device will need to be roughly 1 m x 1 m x 1 m to contain hadronic showers. Its readout and granularity can be coarser than the EM device. Present ideas suggest that 5- to 10-mm Cu interleaved with 1-mm fiber and readout in 5 cm x 5 cm or 10 cm x 10 cm cells would be an interesting geometry.

The first calorimeter is designed for easy variability in order to study the above questions of muon-detection background and to study the closely related question of hadronic shower development. The second and third devices are test versions of calorimeters that might actually be used in a dimuon experiment. They offer the advantage of a very compact overall structure. It is anticipated that these lasagna EM and hadronic calorimeters will be installed in the

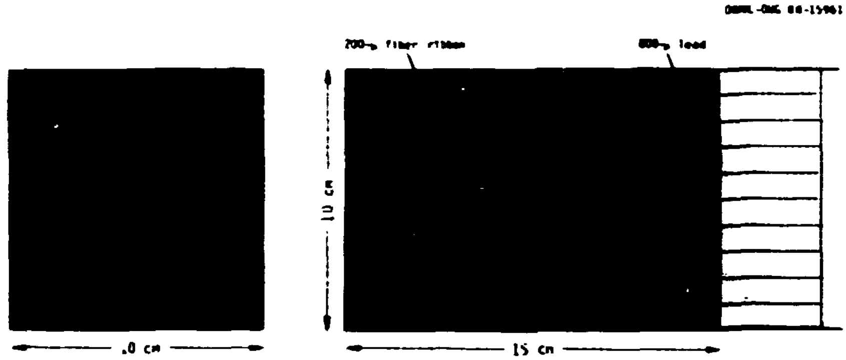

Fig. 2.88. A "lasagna" type EM calorimeter with interleaved sheets of 800-micron-thick lead and 200-micron-thick scintillating optical fiber. The fiber is square in cross section and has been glued into sheets for ease in construction. The shaded section represents the detector array, photomultipliers, or photodiodes.

dimuon test setup. The absorber leakage studies made with this arrangement will provide a good base of information for a RHIC dimuon experiment design.

---

1. Brookhaven National Laboratory, Upton, New York 11973.
2. University of Tennessee, Knoxville, Tennessee 37996.
3. University of California, Riverside, California 92521.
4. Engineering Physics and Mathematics Division, ORNL.
5. Massachusetts Institute of Technology, Cambridge, Massachusetts 02139.
6. Adjunct research participant from the University of Tennessee, Knoxville, Tennessee 37996.
7. California Institute of Technology, Pasadena, California 91125, and Lawrence Livermore National Laboratory, Livermore, California 94550.

WORKSHOP ON MONTE CARLO CODES FOR HIGH-ENERGY NUCLEAR COLLISIONS

T. C. Awes S. P. Sorensen[1]
S. Saini M. L. Tincknell
C. Y. Wong

The primary goal in the field of high-energy heavy-ion collisions is to identify and study the Quark-Gluon Plasma (QGP). It is, however, also recognized that this goal cannot be achieved without a thorough understanding of the underlying nonplasma physics. One way of summing up our knowledge about the reaction mechanisms is to create large computer codes, often in the form of Monte Carlo programs, which are able to fit most of the important experimental data.

Within the High-Energy Reactions Group at ORNL, it was felt that the time was ripe for a structured confrontation between, on one hand, the available experimental data and, on the other hand, a set of the most well-known models for high-energy nuclear collisions. In order to provide a productive environment for this interface between experiment and theory, a workshop was arranged on High-Energy Nuclear Collision Monte Carlo Codes at the Joint Institute for Heavy-Ion Research, September 12-23. The idea behind the workshop was to invite representatives from most major experimental groups and representatives for several nuclear collision models and let them interact through the two-week period. The theorists brought and incorporated their codes within a new software package, MC, which was created before the workshop. By writing a few small interface subroutines, which convert the output from each code into a standardized event format, all of the codes could be compared on equal footing, either to each other or to all of the experimental data. The experimentalists brought selected important parts of their data in a form to be fitted directly by the MC codes, and they created an "experiment filter" to be added to the MC codes to incorporate the effects of the acceptance of their experiment.

At the workshop the following models were represented: FRITIOF and ATTILA (based on the LUND string picture); VENUS, IRIS, and MCFM (all different versions of the Dual Parton Model); MARCO (Cheuk-Yin Wong's code emphasizing the nuclear stopping problem); HIJET (an extension of ISAJET with secondary interactions implemented); RQMD (a relativistic extension of the Quantum Molecular Dynamics Model); and HICOL (based on the Coherent Tube Model). Experimental data from the following groups were included: WA80, NA5, NA34/2, NA35, E597, E802, EMU01, and KLM. The many hours of CPU time consumed during the workshop were distributed among a whole array of VAXes (in ORNL's Physics Division, at the University of Tennesse, and at CERN) and the Livermore CRAYs, where we had obtained 40 hours of CPU time from DOE.

It is still too early to make a final comparison between the models, since it was realized during the workshop that several of the models still need more development. Both FRITIOF and VENUS were, in general, close to the major part of the experimental data. At the lowest beam energy of 15 A GeV, however, the string picture with infinite formation time becomes questionable and other models, like RQMD, which are extensions of nuclear physics codes, might be more relevant.

First attempts to move away from the simplified spectator-participant picture were seen. Both HIJET, MCFM, and RQMD include secondary interactions between the produced particles and the spectators. These secondary interactions were shown to be important at 15 A GeV and in the target-rapidity region at higher beam energies. The careful implementation of secondary interactions might eventually lead to a determination of the formation time parameter, which is crucial for an understanding of the attained energy densities in the heavy-ion collisions.

A full description of the Monte Carlo models involved and of the results obtained during the workshop will be published in Physics Reports.

1. Adjunct research participant from the University of Tennessee, Knoxville, Tennessee 37996.

MISCELLANEOUS TOPICS

ELECTRON-IMPACT IONIZATION OF U-88+ - U-91+: A NOVEL APPLICATION OF HIGH ENERGY HEAVY-ION CHANNELING

C. E. Bemis, Jr. C. R. Vane
J. Gomez del Campo N. Claytor[1]
C. A. Ludemann B. Feinberg[1]
H. Gould[1]

The high energy heavy-ion channeling experiments using 405-MeV uranium ions described in a previous report,[2] have been analyzed to yield electron-impact ionization cross sections for uranium ions with charge states +88 to +91. Well-channeled ions in single crystals make only large-impact parameter collisions with the distant nuclei that compose the crystal and collide only with the electrons in the axial crystal channel, which may be viewed as a dense "electron gas." In the rest frame of the uranium ions traversing the axial channel, the electrons in the channel have an energy of 222 keV which is more than sufficient to ionize U-91+ (BE ≈ 133 keV). The electron density integrated along the path of the channeled ions is determined in our experiments by measuring the radiative electron capture process for U-92+, a cross section that has been measured in previous experiments and which has been shown to scale with electron density and is in agreement with theory. Our measured cross sections for electron impact ionization by 222-keV electrons are given in Table 2.13 for the ions U-88+ to U-91+. We estimate the uncertainty in the cross sections to be a factor of two (50% smaller to 100% larger), due primarily to the

Table 2.13. Electron impact ionization cross sections (barns) for uranium ions by 222 keV electrons.

Ion	State	Cross Section
U-91+	1s	3.9
U-90+	$1s^2$	11.0
U-89+	$1s^2,2s$	27.0
U-88+	$1s^2,2s^2$	42.0

large statistical uncertainties in our experiments. A brief letter describing this experiment has been submitted for publication.

---

1. Lawrence Berkeley Laboratory, Berkeley CA 94720.
2. C. E. Bemis, Jr. et al., Phys. Div. Prog. Rep. for Period Ending Sept. 30, 1987, ORNL-6420, p. 120.

INSTRUMENTATION

THE BaF_2 ARRAY PROJECT

J. R. Beene F. E. Bertrand
J. L. Blankenship[1]

Large solid angle gamma-ray detectors with a high degree of segmentation and moderate energy resolution have played a central role in experimental heavy-ion physics in the 1980's. The Spin Spectrometer has long been the most heavily used single piece of experimental equipment at the HHIRF. The relatively large central cavity (~18 cm radius) in the Spin Spectrometer, which allows complex charged particle detector systems to be mounted inside the NaI shell, has proved to be one of the most important characteristics of the device. Recently the need for even more space for complex detector systems, particularly in the forward direction, has become more and more obvious. In parallel to this need for more complex charged particle detector systems in the Spin Spectrometer, an interest in experiments devoted to the study of high-energy gamma rays has developed at HHIRF. The gamma energies of interest range from the 10- to 30-MeV gammas encountered in the study of high-lying collective strength in nuclei to the 20- to over 100-MeV gammas found in the study of nuclear bremsstrahlung. High-energy gamma experiments of all sorts are bedeviled by the copious background of high energy protons and, especially, neutrons which are produced in heavy-ion reactions.

These needs of experimental programs at HHIRF became acute just as large BaF_2 crystals were becoming available at a reasonable cost. BaF_2 has a number of properties which make it especially attractive as a gamma detector for heavy-ion physics. It offers roughly five times better time resolution than NaI, while delivering essentially the same energy resolution for gamma energies above ~2 MeV (and only slightly worse below). In addition, BaF_2 is non-hygroscopic, has a density ~30% larger than NaI, is substantially less sensitive to neutrons than NaI, and offers the possibility of identification and separation of charged particles through pulse shape analysis.

We are constructing an array of BaF_2 detectors to help serve these needs at HHIRF and to provide a portable high-energy gamma detector system for use by ORNL staff in outside experiments. Our goal is a flexible, easily reconfigurable array, with reasonable performance up to ~200-MeV photons, and a self-contained electronics package including setup, control, and monitoring capabilities. To achieve the required stacking flexibility, the array is based upon identical BaF_2 crystals in the form of right hexagonal prisms 20-cm long and 6.5-cm edge to edge on the hexagonal faces (volume = 731 cm^3). These dimensions are illustrated in Fig. 2.89, which also shows what is expected to

ORNL-DWG 88-15992

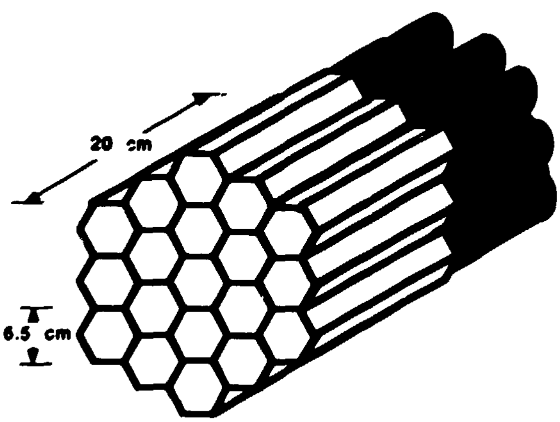

Fig. 2.89. A close-packed 19-detector bundle of BaF_2 detectors, showing the dimensions of the individual crystals. The shaded cylinders represent phototube and base assemblies.

be the most common stacking geometry, consisting of 19 close-packed crystals. Housings and mounting rigs will be provided for this 19-pack stacking.

The R2059 quartz window phototube and an integral tube base and magnetic shield, manufactured by Hamamatsu, have been selected for the project.[2] This tube provides excellent timing and pulse-height stability characteristics,[2] along with the UV sensitivity required with BaF_2 (which scintillates primarily at 210 and 310 nm).

The BaF_2 array will be used primarily to investigate extremely small cross section processes. Because of this, and because of the simple modular geometry of the array design, the size of the completed array is open-ended, essentially determined by financial considerations. The initial detector and phototube purchase includes 57 BaF_2 crystals and 63 phototubes and bases (three 19 packs). As of October 1988, 21 crystals and all 63 phototubes have been delivered, with the remainder of the crystals due by February 1988. We expect to purchase 20 additional phototubes and crystals in 1989, giving a total of 77 detector systems plus spare phototubes; enough for four 19 detector packs. This is the number of detectors required to provide the enhancement to the Spin Spectrometer alluded to earlier. For this purpose four 19 packs will be configured as a segmented wall in the forward ($\theta \lesssim 35°$ direction. The forward-most ring of 5 NaI detectors surrounding the normal beam exit pipe will be removed and replaced by an existing funnel-shaped addition to the standard target chamber, making much more space available for charged particle detection in the forward direction. BaF_2 detectors will fill ~85% of the solid angle lost by removal of the forward NaI elements if the wall is placed at a distance of 45 cm. For some applications, the wall will be moved to greater distances, with consequent loss of solid-angle coverage. The wall configuration will also provide a much finer segmentation for gamma and neutron detection. At 45 cm we will have $\Delta\theta$ ~8°, compared to $\Delta\theta$ ~24° now.

The performance of the 21 accepted crystals and 63 phototubes has been carefully studied and characterized. Results most directly relevant to use as high-energy gamma detectors are energy and time resolution. The energy resolution ($FWHM/E_\gamma$) ranges from 9.5% to ~11.7% at 660 keV and 3.9% to 4.9% at 4.4 MeV, scaling very accurately as $(E_\gamma)^{-1/2}$ over this range for all detectors. Time resolution of 350 ps FWHM has been obtained for the BaF_2 crystals in coincidence with a small plastic scintillator, using a ^{60}Co source. Since the principal advantage of BaF_2 lies in the ability to separate neutrons and protons from high energy gamma rays by time of flight, this excellent timing is especially important. We expect to be able to easily achieve our goal of ~600 ps timing for ~1-MeV gamma rays and $\lesssim$ 500 ps for $E_\gamma \gtrsim$ 10-MeV gammas.

These characteristics, along with the self-contained electronics, setup and control systems which we expect to be available in 1989, will make this array an extremely powerful tool for high energy gamma ray studies.

---

1. Instrumentation and Controls Division, ORNL.
2. J. L. Blankenship, Phys. Div. Prog. Rep. for Period Ending Sept. 30, 1987, ORNL-6420, p. 123.

GAMMASPHERE RESEARCH AND DEVELOPMENT

I. Y. Lee J. R. Beene
A. D'Onofrio[1] J. W. Jonhson
R. T. VanHook[2]

GAMMASPHERE is a proposal for the construction of a national gamma ray facility. As shown in Fig. 2.90, the current design consists of 110 large-volume high-purity n-type Ge detectors surrounded by 360 anti-Compton BGO shields which also serve as total energy and multiplicity detectors. Behind each Ge detector an additional BGO plug is placed to detect the forward scattered gamma rays. These detectors are arranged to cover 4π solid angle with the symmetry of an icosahedron.

In order to have the highest possible photo efficiency, the largest available Ge detector with size 7-cm-diam x 7-cm-long will be used.

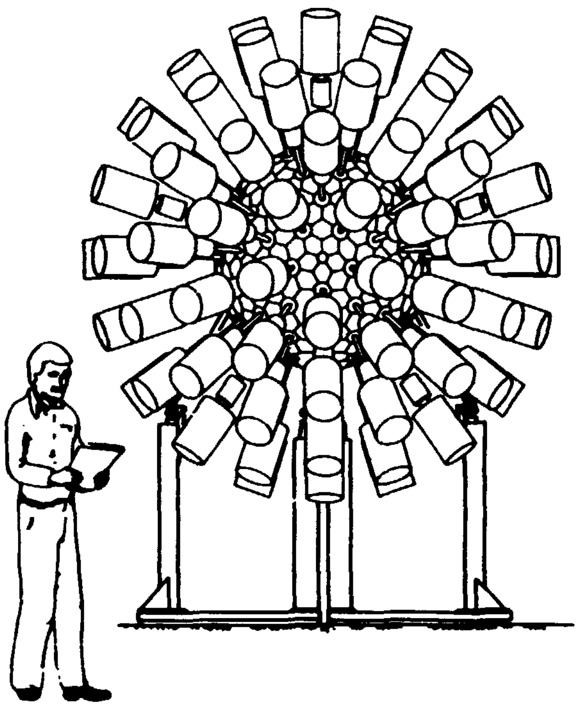

Fig. 2.90. A sketch of the GAMMASPHERE detector system.

There is sufficient flexibility in the size and shape of the BGO shield to permit its suppression properties to be optimized. We have carried out design studies of the shield based on the efficiency calculations done with the Monte Carlo simulation program GEANT. The design of the shield, as shown in Fig. 2.91, was obtained by maximizing the performance-to-cost ratio. The important dimensions are the following: (1) total length of shield = 16 cm; (2) length of the lip = 4 cm; (3) the thickness of the shield at the thinnest point = 1.4 cm; (4) the collimation covers the front face of the Ge detector; and (5) the length of the plug behind the Ge = 4 cm. With this shield, the peak-to-total ratio of the Ge detector is improved from an unsuppressed value of 0.25 to 0.85.

For high-energy gamma-ray detection, 55 BaF_2 detectors will be used to replace the Ge detectors in the forward hemisphere and operated with the BGO shield in the "energy add-back mode."

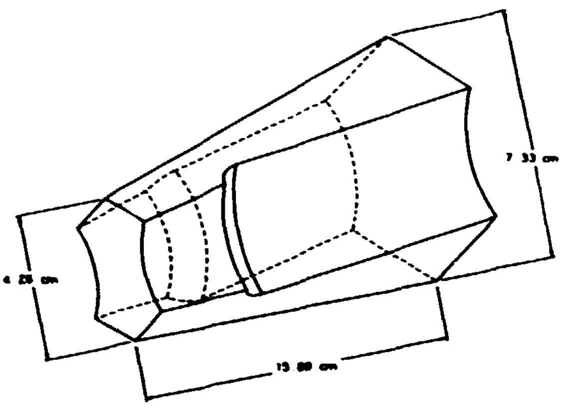

Fig. 2.91. The design of the BGO element of the GAMMASPHERE.

This arrangement provides higher efficiency and much better neutron rejection than is provided by the Ge detector. The design of the BaF_2 insert is shown in Fig. 2.92. It has a total length of 20 cm with a total volume of 740 ml. The performance, as determined by the simulations is shown in Table 2.14 for two representative gamma-ray energies, 15 and 100 MeV. The quantities tabulated are the mean and standard deviation of the add-back energy spectrum, both

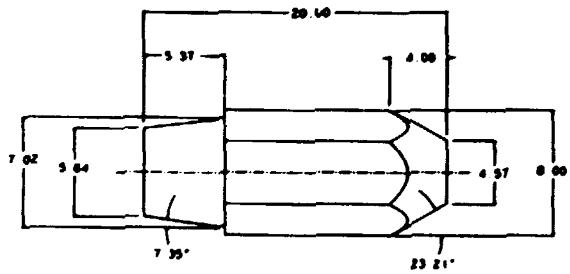

Fig. 2.92. The design of the BaF_2 insert of the GAMMASPHERE.

Table 2.14. Calculated performance of BaF_2 detectors for GAMMASPHERE.

E_γ (MeV)	$\langle E \rangle / E_\gamma$	σ / E_γ	Efficiency
15	0.93	0.12	0.370 %
100	0.89	0.11	0.358 %

expressed as a fraction of the incident energy, and the total trigger efficiency per detector. The simulated spectra from which these parameters were extracted were generated subject to the condition that >50% of the total energy (energy deposited in the BaF_2 plus its surrounding BGO) was deposited in the BaF_2.

The concept of the mechanical structure for the support of the detectors has been developed. The design is to construct a spherical shell split into hemispheres that is a heavy-wall (~3 cm) shell of nominally 1.4-m diameter. Each hemisphere will be supported by a low carriage which allows each hemisphere to be moved to give access to the target chamber. Each Ge detector and BGO shield will be inserted through a hole machined at the proper location in the support shells and mounted at attachment points machined around each hole. The dewars for the Ge detectors will be outside the structure. The BGO shield will be cantilever-supported by a hollow (deep cup-shaped) strut attached to the structure. This arrangement provides for: (1) easy access to target chamber, (2) convenient removal and replacement of Ge detectors and BGO shields, (3) good alignment of all components, and (4) economic construction.

---

1. JIHIR and Instituto Nazionale di Fisica Nucleare, Napoli, Italy.
2. Oak Ridge Science and Engineering Research Semester Participant from Hendrix College, Conway, Arkansas 72032.

AN ARRAY OF BaF_2 DETECTORS FOR THE STUDY OF SOFT PHOTONS EMITTED IN ULTRARELATIVISTIC PROTON-NUCLEUS AND NUCLEUS-NUCLEUS COLLISIONS

D. Shapira, C. Woody[2], A. Ray, D. Lissauer[2], K. Teh[1], J. Schuckraft[3], W. Willis[3]

Single-photon measurements to study the excess in soft-photon production (5 to 100 MeV P_T) in hadron-hadron collisions depend critically on one's understanding of the underlying "normal" photon spectrum. This requires implementing an extremely high dynamic range for the proposed detector. The response of this detector to photons must be well known over an energy range extending from 10 MeV to above 1 GeV. In addition, high efficiency in collection and localization of high-energy electromagetic showers and good neutron- and charged-particle rejection are desirable.

An array of 38 BaF_2 hexagons 15-cm-deep and 5-cm-wide (surface to surface) were stacked in a close-packed array as shown in Fig. 2.93. High viscosity Si oil (GE Viscasil 600 M) was used to couple every two 15-cm crystals to form a 30-cm-deep detector. Hamamatsu R2059 α (2") PM tubes with quartz windows were used because of their good timing characteristics (less then 2-ns risetime) and good response to ultraviolet light. Beam tests have shown that the detector is capable of better then 500 ps time resolution for all 19 double elements. This timing resolution is sufficient to separate 1-GeV neutrons from prompt photons when the detector is placed about one meter away from the target. Charged-particle rejection is provided by a 0.5-cm-thick plastic scintillation counter placed in front of the array (Paddle). Figure 2.94 is a block diagram showing the signal- and data-handling used during a test run at the AGS (π^- test beam) and a proton run at the SPS at CERN.

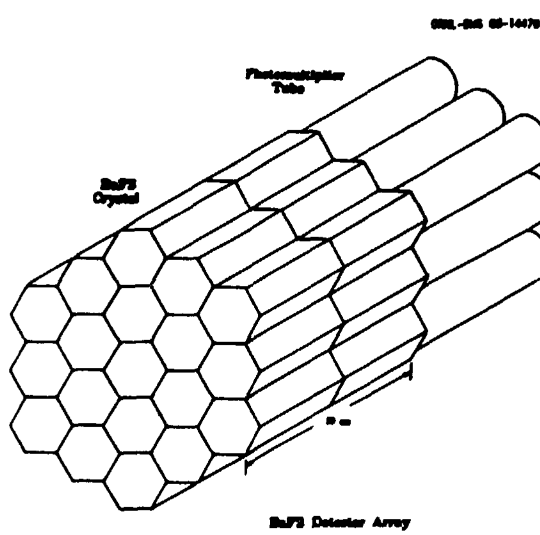

Fig. 2.93. The stack of closely-packed 19 pairs of BaF_2 scintillation detectors.

ORNL-DWG 88-14471

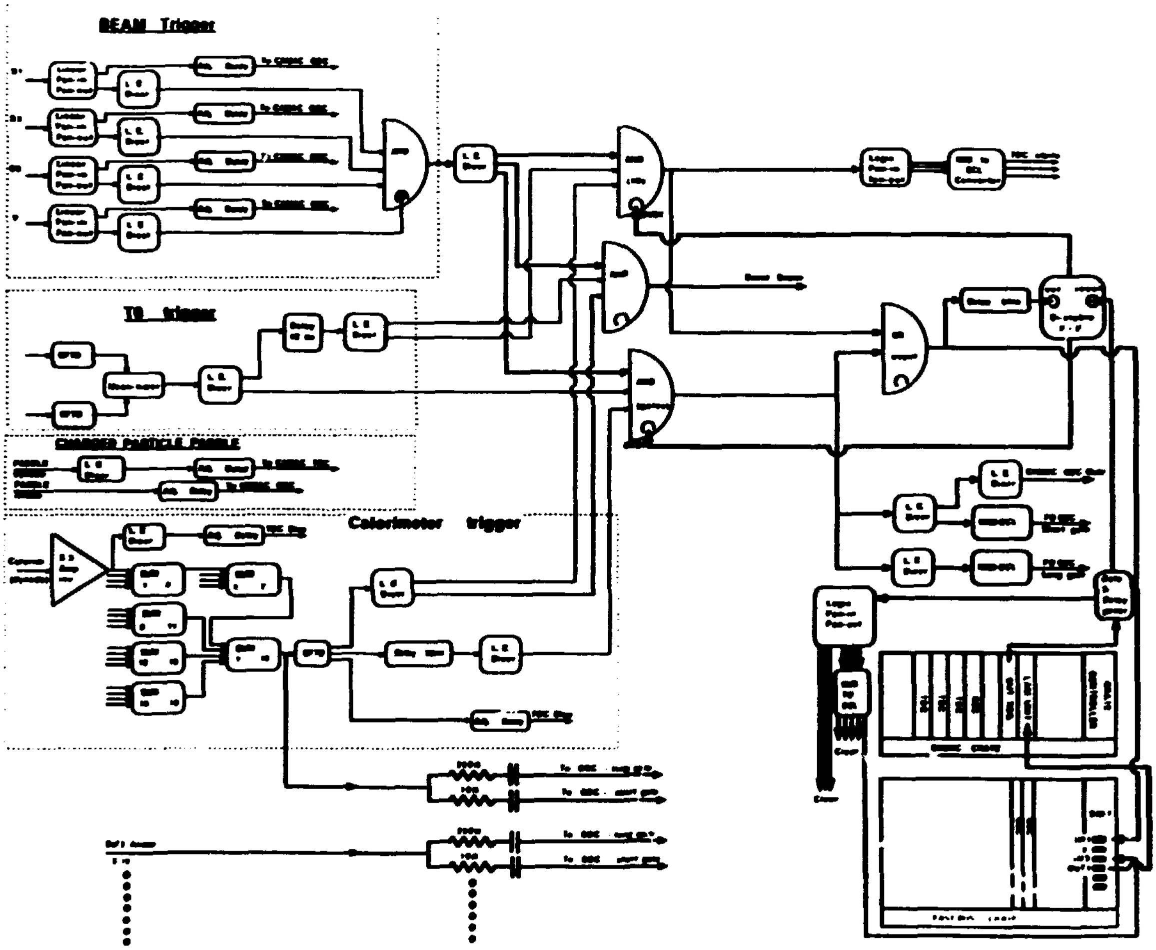

Fig. 2.94. Signal processing scheme used with the photon detector during π^- + Be test runs at the AGS.

Preliminary gain matching was done with a Co gamma-ray source and run-time gain adjustments as well as gain-drift monitoring were done with the 200-MeV energy loss suffered by minimum ionizing charged particles. Extensive calibrations with high-energy tagged photons and with electron beams are now in progress.

SAMPLING CALORIMETERS FOR THE RELATIVISTIC HEAVY-ION EXPERIMENT WA80 AT CERN[1]

T. C. Awes, C. Baktash, R. P. Cumby, R. L. Ferguson, A. Franz[2], T. A. Gabriel[3], H. A. Gustafsson[4], H. H. Gutbrod[5], J. W. Johnson, B. W. Kolb[5], I. Y. Lee, F. E. Obenshain, A. Oskarsson[6], I. Otterlund[6], S. Persson[6], F. Plasil, A. M. Poskanzer[3], H. G. Ritter[3], H. R. Schmidt[5], S. P. Sorensen[7], G. R. Young

Sampling calorimeters designed for use in the relativistic heavy-ion experiment WA80 at CERN are described. Calibration and performance results are presented for a calorimeter used at

1. Joint Institute for Heavy Ion Research, Vanderbilt University, Nashville, Tennessee, and Physics Division, ORNL.
2. Brookhaven National Laboratory, Upton, NY 11973.
3. CERN, Geneva, Switzerland.

midrapidity and for a calorimeter used at zero degrees. Over the energy range of 2 to 50 GeV, the response of the Midrapidity Calorimeter (MIRAC) was linear, and its energy resolution σ/E was found to be given by $0.014 + 0.11/\sqrt{E}$ and $0.034 + 0.34/\sqrt{E}$ for electromagnetic and hadronic showers, respectively. Signal ratios of 1.20 and 1.4 were obtained for the e/h ratio of the lead-scintillator electromagnetic section and the iron-scintillator hadronic section, respectively. The MIRAC provided an accurate transverse energy trigger with a response and resolution for high-energy heavy ions which was somewhat better than anticipated on the basis of the low-energy calibrations. The uranium-scintillator Zero-Degree Calorimeter (ZDC) was found to have a linear response to heavy ions and an in-beam hadronic resolution ranging from $\sigma/E = 0.013 + 0.33/\sqrt{E}$ at low intensities to $\sigma/E = 0.02 + 0.67/\sqrt{E}$ at higher intensities. The e/h ratio of the electromagnetic section was measured to be 1.12 at 135 GeV. The ZDC operated reliably with incident beams of 3.2-TeV oxygen and 6.4-TeV sulfur at intensities of over 10^6 nuclei per spill. It provided a trigger both for minimum bias events and for violent central collisions.

---

1. Abstract of paper submitted to Nuclear Instruments and Methods in Physics Research.
2. Engineering Physics and Mathematics Division, ORNL.
3. Lawrence Berkeley Laboratory, Berkeley, California 94720.
4. University of Lund, S-223 62 Lund, Sweden and European Laboratory for Particle Physics, CH-1211 Geneva 23, Switzerland.
5. Gesellschaft fuer Schwerionenforschung, D-6100 Darmstadt, West Germany.
6. University of Lund, S-223 62 Lund, Sweden.
7. Adjunct research participant from the University of Tennessee, Knoxville, Tennessee 37996.

3. THE UNISOR PROGRAM

The University Isotope Separator - Oak Ridge is a cooperative venture of universities, Oak Ridge Associated Universities, Oak Ridge National Laboratory, the U.S. Department of Energy, and the State of Tennessee. The primary purpose of the UNISOR consortium is to investigate the structures and decay mechanisms of rare, short-lived atomic nuclei which are prepared by means of a magnetic isotope separator coupled to the accelerators in the Holifield Heavy Ion Research Facility. The accounts which follow describe work at the UNISOR facility or work associated with UNISOR research performed principally by investigators outside the Physics Division. Research and development activities at UNISOR by Physics Division staff members are included in the Nuclear Physics Section.

LASER ION SOURCE DEVELOPMENT

G. A. Barrera[1] W. M. Fairbank, Jr.[1]
H. K. Carter[2]

A prototype laser ion source has been constructed at Colorado State University and tests are now beginning to determine the efficiency obtainable with this concept for refractory elements. The new experimental setup (Fig. 3.1) consists of a vacuum chamber with ports for: (1) a He-jet which will be used to deposit radioactive isotopes on the sample substrate; (2) windows for two laser beams, one which vaporizes a small area of the deposited sample and a second which resonantly ionizes isotopes of the desired element in the vapor cloud; (3) extraction and focusing ion optics, which is a scaled replica of the UNISOR separator optics; and (4) a time-of-flight mass spectrometer for analysis of the generated species.

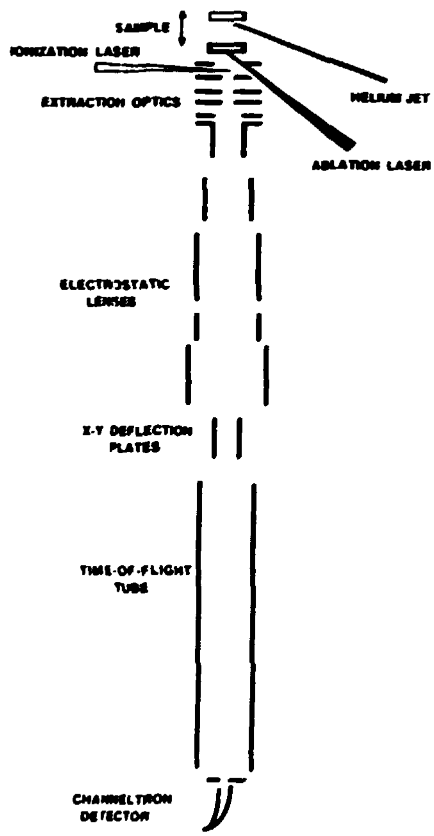

Fig. 3.1. Experimental apparatus constructed.

The major part of our effort in laser ion source development in the last year has gone into constructing this apparatus and into testing existing lasers at Colorado State University for suitability for this project. We are currently exploring two promising new ideas with this system. The first is the use of copper vapor lasers. While providing distinct advantages in terms of high pulse repetition rate (6000 Hz vs 30 Hz for a Nd:YAG laser) and therefore sample throughput, the reduced pulse energy of a copper laser can be a concern in applications such as this which require high efficiency. The second new idea is the use of fiber optics to transport the laser beams. This, we believe, will solve the pulse energy problem by making tight focusing and accurate laser alignment possible, and will also eliminate the need for two lasers. The latter factor represents an important cost-saving feature which should reduce the initial cost of setting up a laser ion source at UNISOR.

In tests to date, we have demonstrated separately laser ablation of ions from several different samples (LiCl, CsCl, Fe, etc.) with a copper laser and resonant ionization of Li and Fe atoms with a Nd:YAG-pumped dye laser. In the latter case the Li and Fe atoms were vaporized by a pulsed argon ion beam. The ions were detected and analyzed with good mass resolution in the time-of-flight mass spectrometer.

We have now seen with several elements (In, Fe, and Li) an interesting resonance enhancement by a factor of ten in the ablated ion signal when the tunable dye laser is used for ablation. We do not know yet if this effect will offer an alternative for operating a laser ion source with a single laser.

We have not yet been able to measure an efficiency for laser ablation and resonance ionization (i.e., the original laser ion source concept) with this apparatus because we have had difficulty getting a second borrowed copper laser working reliably. With more repair work on this laser or the implementation of the fiber optic system, the long-awaited laser ion source efficiency tests should begin. We plan to conduct our tests with hafnium, a refractory element of interest for future nuclear physics experiments at UNISOR.

---

1. Colorado State University, Fort Collins, Colorado.
2. UNISOR, Oak Ridge Associated Universities, Oak Ridge, Tennessee.

THE ON-LINE ORIENTATION OF ^{191}Hg AND ^{193}Hg

I. C. Girit[1] E. F. Zganjar[8]
C. R. Bingham[2] H. K. Carter[7]
J. D. Cole[3] W. L. Croft[9]
J. H. Hamilton[4] P. M. Gore[4]
E. F. Jones[4] B. D. Kern[10]
H. Xie[4] M. O. Kortelahti[11]
J. Kormicki[4] P. M. Mantica[12]
K. S. Krane[5] W. B. Newbolt[13]
W. G. Nettles[6] Y. S. Xu[5]
M. L. Simpson[7] B. E. Zimmerman[12]

The nuclei ^{191,193}Au were chosen for the first UNISOR/NOF on-line experiment to determine whether their low-lying spectrum can be described by the dynamical supersymmetry classification scheme criteria proposed by Iachello.[14] Among others, one test of supersymmetry in these nuclei is to determine whether the E2 transitions satisfy the selection rules appropriate to the scheme. This test requires precise measurements of δ(E2/M1) since for the heavier Au isotopes, the measured B(E2) of the τ-forbidden transitions are often only about 10 percent of the B(E2)s of the allowed transitions. Also, the allowed transition itself may have only a 5-10 percent E2 component, and the selection rules apply to E2 transitions only.

The excited states of ^{191}Au and ^{193}Au, studied by radioactive decay of the ^{191}Hg high-spin isomer ($T_{1/2}$ = 51 min.) and ^{193}Hg high-spin isomer ($T_{1/2}$ = 11 h), respectively, were produced by using a 110-MeV ^{12}C beam from the HHIRF tandem accelerator on natural W target. Throughout the experiment, the beam intensity on target was 2 x 10^5 ions/sec for ^{191}Hg and 4 x 10^4 for ^{193}Hg. The data were collected in eight cycles, each of which consisted of 12 to 14 ten-minute runs. Data were acquired from six detectors placed at 0°, 45°, 90°, 180°, 225°, and 270°. At the end of each cycle, the sample foil was replaced by a new iron foil in order to avoid the buildup of daughter activity. The activity was collected on the target while warm data were being taken. At the end of this period, the target was isolated by a 4-K baffle and the target allowed to cool for about 30-40 minutes.

Values of $A_k = B_k U_k A_k$ for k = 0, 2, and 4 have been obtained for 102 transition in ^{191}Au. Analysis of these data and that from the ^{193}Hg decay are in progress. A particular interest is the 331-keV transition in ^{191}Au. If the level at 331 keV belongs to the j = 3/2 orbit, then this transition is a τ-forbidden transition in the U(6/4) supersymmetry scheme, because it links the (τ_1 = 5/2, τ_2 = 1/2) state with the (τ_1 = 1/2) state, where τ changes more than one unit. The measured A_2 and A_4 directional distribution coefficients produce, without ambiguity, a very small E2 content (δ(E2/M1 = 0.007 ± 0.026) for this transition, as the model predicts.

The UNISOR/NOF system has now successfully demonstrated a new design for on-line nuclear orientation refrigerators, whereby the beam enters the system from the bottom. The option of placing detectors at 45° angles around the target, a unique feature of this system, has a number of advantages. The 45° angle enables a unique determination of the multipole mixing ratio, while the cylindrical geometry about the target enables a reduction of systematic errors, such as count rate fluctuations due to beam movement and changes in distance between the sample holder and the bottom 90° detector due to thermal contractions. This results in unambiguous determination of multipole mixing ratios, which will enhance our understanding of nuclear structure.

---

1. Vanderbilt University, Nashville, Tennessee and UNISOR, Oak Ridge Associated Universities, Oak Ridge, Tennessee.
2. University of Tennessee, Knoxville, Tennessee.
3. Idaho National Engineering Laboratory, Idaho Falls, Idaho.
4. Vanderbilt University, Nashville, Tennessee.
5. Oregon State University, Corvallis, Oregon.
6. Mississippi College, Clinton, Mississippi.
7. UNISOR, Oak Ridge Associated Universities, Oak Ridge, Tennessee.
8. Louisiana State University, Baton Rouge, Louisiana.
9. Mississippi State University, Mississippi State, Mississippi.
10. University of Kentucky, Lexington, Kentucky.
11. Louisiana State University, Baton Rouge, Louisiana. Present address: University of Jyvaskyla, Finland.
12. University of Maryland, College Park, Maryland.
13. Washington & Lee University, Lexington, Virginia.
14. F. Iachello, Phys. Rev. Lett. 44, 772 (1980).

HIGHLY CONVERTED TRANSITIONS IN ^{189}Au

M. O. Kortelahti[1] J. L. Wood[2]
E. F. Zganjar[3]

The extensive data obtained earlier for the ^{189m,g}Hg → ^{189}Au decay schemes are essentially completely analyzed. Some major details have been reported.[4,5] We observe at least one highly converted transition of 913 keV feeding the $J^\pi = 13/2^-$ member of the $h_{9/2}$ intruder band. This is shown in Fig. 3.2. The level at 1559 keV can be interpreted as due to the coupling $\pi h_{9/2}^{+1}$ X ^{188}Pt (deformed). The parallel couplings in ^{187}Au and ^{185}Au (Ref. 6) are shown in Fig. 3.3. The implication is that a blocking effect is present which makes the $\pi h_{9/2}^{+1}$ X Pt (deformed) coupling higher in energy than in the core: this supports the idea[7] that the Pt (deformed) structure involves a proton pair in the $h_{9/2}$ orbital. Other highly converted transitions are being sought.

---

1. Louisiana State University, Baton Rouge, Louisiana. Present address: University of Jyvaskyla, Finland.
2. School of Physics, Georgia Institute of Technology, Atlanta, Georgia.
3. Louisiana State University, Baton Rouge, Louisiana.
4. M. O. Kortelahti et al., Phys. Div. Prog. Rep., Sept. 30, 1987, ORNL-6420, p. 144.
5. M. O. Kortelahti et al., J. Phys. G (in press).
6. C. D. Papanicolopulos et al., Z. Phys. A330, 371 (1988).
7. K. Heyde et al., Nucl. Phys. A466, 189 (1987).

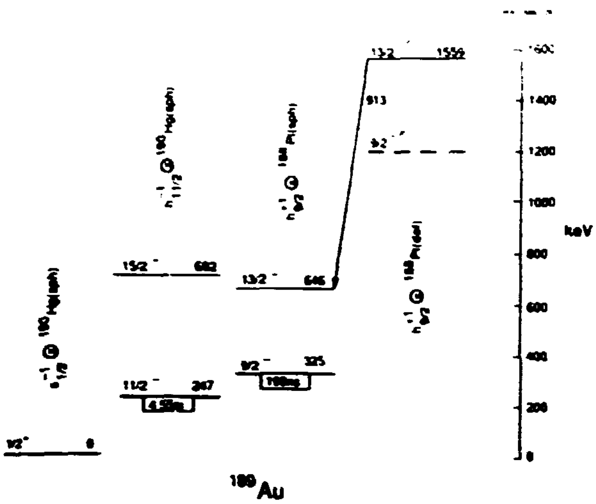

Fig. 3.2. The band heads for $s_{1/2}$, $h_{11/2}$, and $h_{9/2}$ coupling in ^{189}Au. Shown also are the $15/2^-$ and $13/2^-$ members of the bands involving $h_{11/2}$ holes and $h_{9/2}$ particles, respectively. The terms sph and def stand for more spherical and more deformed respectively. The 913-keV transition is highly converted (see text).

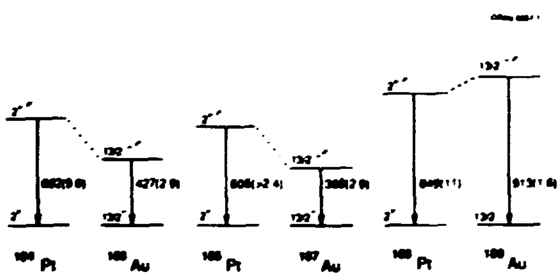

Fig. 3.3. A comparison of the $h_{9/2}^{+1}$ x ^{188}Pt(def) couplings in ^{185,187,189}Au and the corresponding $13/2^{-'} \rightarrow 13/2^{-'}$ highly converted transitions. The numbers in parentheses are the ratio α_K(expt)/α_K(M1, theory).

STUDY OF HIGHLY CONVERTED TRANSITIONS IN ^{185}Pt

J. Schwarzenberg[1] J. L. Wood[2]
R. W. Fink[1] E. F. Zganjar[3]

The extensive data obtained last year for the ^{185}Au → ^{185}Pt decay scheme are in the process of being analyzed. Besides the previously observed,[4] highly converted transitions at 340 and 542 keV, we have identified at least nine other highly converted [i.e., α_K(expt) > α_K(M1)] transitions. Prompt coincidences rule out high-multipolarity (retarded) transitions. There is considerable controversy[5] regarding the nature of these transitions. Our previous studies of such transitions in ^{185,187}Au (Ref. 6) support an electric monopole origin. In ^{185}Pb the claim is made[4,5] that the origin, at least of the 542-keV transition, is magnetic dipole with highly anamolous penetration effects. This is unprecedented. We are unable to agree with the earlier work[4,5] regarding the location of the 542-keV transition. We find it is to be at least a doublet, possibly a triplet. Our data differ from that of the previous study[4,5] in that we have e-γ coincidence data and about 30 times higher statistics for the γ-γ coincidence data. The goal of this work is to unambiguously resolve the nature of these highly converted transitions and to better understand their relationship to shape coexistence.

---

1. School of Chemistry, Georgia Institute of Technology, Atlanta, Georgia.
2. School of Physics, Georgia Institute of Technology, Atlanta, Georgia.
3. Louisiana State University, Baton Rouge, Louisiana.
4. B. Roussière et al., Nucl. Phys. A438, 93 (1985).
5. B. Roussière et al., Nucl. Phys. A485, 111 (1988).
6. C. D. Papanicolopulos et al., Z. Phys. A330, 371 (1988).

SEARCH FOR STRONGLY COUPLED BANDS IN ^{187}Au

E. F. Zganjar[1] J. L. Wood[2]

In our study of ^{185}Au, evidence for strongly coupled bands was obtained.[3] These bands are interpreted as resulting from the couplings $\pi h_{11/2}^{-1}$ x ^{186}Hg (deformed) and $\pi d_{3/2}^{-1}$ x ^{186}Hg (deformed). Such structures are unprecedented in odd-Z nuclei. Similar structures can be expected in ^{187}Au. A study of the ^{187m,g}Hg → ^{187}Au decay schemes has been undertaken to observe these structures.

The tandem accelerator at the Holifield Heavy Ion Research Facility provided beams that were used to produce radioactive nuclei through the ^{176}Hf(^{19}F,8n)^{187}Tl and ^{176}Hf(^{16}O,5n)^{187}Hg reactions for projectile energies of 160 and 125 MeV, respectively. The ^{187m}Hg ($T_{1/2}$ = 8.7 min.) was produced directly and the ^{187g}Hg ($T_{1/2}$ = 7.7 min.) was produced indirectly following the radioactive decay of ^{187}Tl. The radioactive nuclei were ionized by a FEBIAD-B2 ion source and passed through the UNISOR mass separator. Gamma rays and conversion-electron spectrum multiscaling and γ-γ-γ, γ-x-t, γ-ce-t, and ce-x-t coincidence measurements were conducted on-line. The data are in the process of being analyzed.

1. Louisiana State University, Baton Rouge, Louisiana.
2. School of Physics, Georgia Institute of Technology, Atlanta, Georgia.
3. C. D. Papanicolopulos et al., Phys. Div. Prog. Rep., Sept. 30, 1987, ORNL-6420, p. 146.

LOW-ENERGY LEVEL STRUCTURE IN ^{193}Pb, ^{193}Tl, and ^{193}Hg

C. R. Bingham[1] L. L. Riedinger[1]
H. V. Carmichael[1] E. F. Zganjar[2]
G. Zhang[1] M. O. Kortelahti[3]
H. K. Carter[4]

The coexistence of deformed and nearly spherical 0^+ states in the light Hg isotopes[5] and Pb isotopes[6] lead to an expected rich structure in the adjacent odd-A nuclei. The deformed band has not been observed in ^{192}Hg, but judging from systematics, it would probably be at an energy of about 2 MeV, and thus would not have a strong influence on the low-energy level structure of adjacent mass 193 nuclei. However, the deformed 0^+ state in Pb has dropped to about 800 keV in this mass region and possibly has a significant effect on the structure of ^{193}Pb and ^{193}Tl. Some evidence of coexisting deformed states was evident in our latest study[7] of the decay of ^{195}Bi; the deformed states should have a greater effect on the levels of ^{193}Pb and ^{193}Tl since the deformed states are at lower energies in the cores of these nuclei. Thus, the present study was initiated to establish the low-level structure of these nuclides.

Data were taken via the movable tape collector at the exit of the UNISOR separator. Three datasets were accumulated from sources produced by bombardment of: (1) an 18-mg/cm^2 solid Re target with 155-MeV ^{16}O; (2) a stacked-foil target of Re/Mo alloy with 165-MeV ^{16}O; and (3) a W-carbide target with 155-MeV ^{16}O. The experiment was designed to populate both low-spin and high-spin isomers in ^{193}Pb. Each dataset contains γ-ray and conversion electron multiscaled-singles spectra and γ-γ-t and e-γ-t coincidence data. During this particular run, the direct production of ^{193}Tl was much larger than observed in similar earlier runs, a result which was probably a consequence of the FEBIAD-B2 ion source used in this run.

Because of the dominance of the Tl activity, the presence of lines orginating from Bi decay was difficult to establish. Nevertheless, careful analysis of the multiscale data revealed six gamma-ray transitions which decay with the ^{193}Bi half-life. Preliminary analysis of the γ-γ coincidence data shows a number of other transitions in coincidence with these six transitions. Analysis of spectra, gated by the other transitions, is in progress and should result in the establishment of a decay scheme with ten to twenty levels in ^{193}Pb.

The data taken, using a Re target (Bi compound nuclei), appear to contain ^{193}Pb decay with the amount of low-spin isomer enhanced relative to data taken earlier. Also, the dataset taken with the WC target contains essentially only the high-spin isomer of ^{193}Pb. Thus, we hope to combine these datasets to obtain separate decay schemes for the high-spin and low-spin isomers of ^{193}Pb.

Conversion-electron data were not accumulated in earlier UNISOR experiments[8] on the decay of ^{193m}Tl. Since ^{193m}Tl seemed to dominate the sources produced in the present experiment, it is clear that this piece of information, which is very important in the search for coexisting deformed states in ^{193}Tl, is now available. Also, the γ-γ data from the present experiment appear to have about 20 times as many counts as the previous results for the decay of ^{193m}Tl. The present data will be used to check the previous decay scheme of ^{193m}Tl, to add a number of new levels to the scheme, and to obtain conversion coefficients, thus enabling assignment of spins to several levels where this was not possible with the earlier data.

---

1. University of Tennessee, Knoxville, Tennessee.
2. Louisiana State University, Baton Rouge, Louisiana.
3. Louisiana State University, Baton Rouge, Louisiana. Present address: University of Jyvaskyla, Finland.
4. UNISOR, Oak Ridge Associated Universities, Oak Ridge, Tennessee.
5. J. H. Hamilton et al., Phys. Rev. Lett. 35, 562 (1975); Phys. Div. Prog. Rep., Sept. 30, 1987, ORNL-6420, p. 143.
6. P. Van Duppen et al., Phys. Rev. C35, 1861 (1984).
7. Phys. Div. Prog. Rep., Sept. 30, 1987, ORNL-6420, p. 137.
8. J. L. Wood, private communication.

THE INTERPRETATION OF SELECTED STATES IN ^{195}Tl IN TERMS OF PARTICLES COUPLED TO A TRIAXIAL ROTOR

H. V. Carmichael[1] C. R. Bingham[1]
P. B. Semmes[2]

Preliminary results from calculations of energy levels in ^{195}Tl resulting from coupling $h_{9/2}$ protons to a triaxial rotor core were given in the previous progress reports.[3,4] The results were compared with the corresponding levels and relative intensities observed in the decay scheme of ^{195}Pb. While the calculations could predict the energy levels rather well, there were considerable discrepancies in the calculated and measured relative intensities. For the mixed transitions, a natural question arises as to whether either the electric or magnetic transition rates are predicted more accurately. This year we have determined the errors on the measured conversion coefficients and thus, it is now possible to separate the measured intensity into M1 and E2 parts. Consequently, new comparisons with the results of the particle-core coupling model provide additional insight into the success or failure of the model to predict the properties of the intruder states in ^{195}Tl.

In the particle core coupling model, one must provide several parameters. A triaxial rotor core has been utilized in the current calculations that require two parameters, the deformation, β, and the asymmetry, γ. The single particle is assumed to be in an $h_{9/2}$ orbital described by a Fermi level parameter, λ, and pairing gap, Δ. Δ was taken as 0.7 MeV in accordance with proton calculations in this mass region.[5] β is related to the intrinsic quadrupole moment, which has been measured for some of the odd Tl isotopes[6] and is taken to be 0.15 in agreement with these measurements. The energy of the first $5/2^-$ state was found to be sensitive to γ. Fitting this energy resulted in a γ of 37 degrees. The energy of the first $7/2^-$ state is sensitive to the Fermi level and was fit to give a value of λ = -1.39 MeV.

The predicted level scheme is compared with the corresponding experimental levels in Fig. 3.4 and the overall agreement is rather good. We note that the $(9/2)_3$ and $(11/2)_2$ states deviate considerably from the calculations. The relative intensities and mixing ratios for many transitions are given in Table 3.1 along with comparisons with the theory. Using the mixing ratios, we have deduced relative intensities of the E2 and M1 parts of the mixed transitions. Thus, we are able to compare calculations for electric and magnetic transitions with the data. These comparisons are

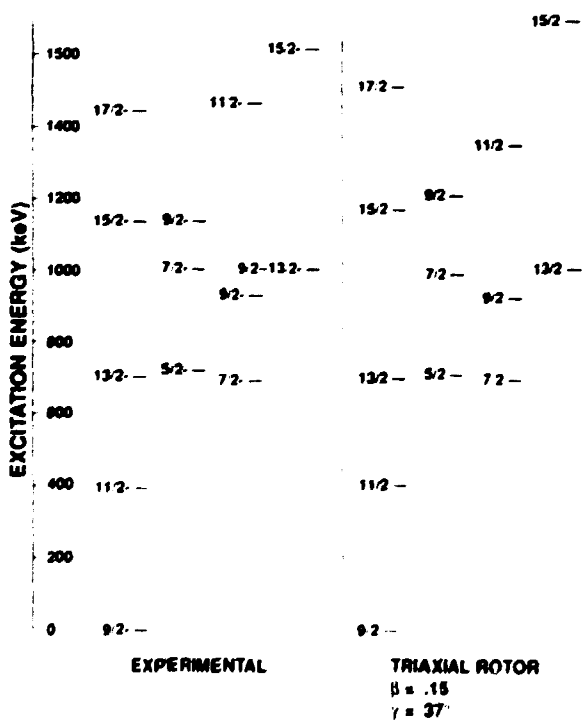

Fig. 3.4. Comparison of observed energy levels of ^{195}Tl with predictions of a rigid triaxial rotor model.

Table 3.1. Comparison of relative intensities and mixing ratios from triaxial rotor calculations with experimental data.

		Experimental				Theoretical[a]			
K	$I_i^\pi \rightarrow I_f^\pi$	Rel.Int.	I(E2)	I(M1)	$\|\delta\|$	Rel.Int.	I(E2)	I(M1)	$\|\delta\|$
9/2	$11/2^- \rightarrow 9/2^-$	100	$10.6^{+0.43}_{-0.52}$	$89.4^{+0.32}_{-0.43}$	$.403^{+.131}_{-.100}$	100	56.1	43.9	1.13
	$13/2^- \rightarrow 9/2^-$	100	—	—	—	100	100	0	∞
	$\rightarrow 11/2^-$	49	$2.52^{+4.30}_{-2.52}$	$46.5^{+2.30}_{-4.52}$	$.233^{+.176}_{-.233}$	6	1.23	4.77	.507
	$15/2^- \rightarrow 11/2^-$	100	>99.7	<.326	>17.473	100	100	0	∞
	$\rightarrow 13/2^-$	77	$8.92^{+6.97}_{-6.97}$	$68.1^{+6.96}_{-6.90}$	$.362^{+.160}_{-.201}$	16	8.18	7.84	1.02
	$\rightarrow (13/2^-)_2$	—	—	—	—	0	—	—	1.11
	$17/2^- \rightarrow 13/$	100	—	—	—	100	100	0	∞
	$\rightarrow (13/2^-)_2$	—	—	—	—	2	2	0	∞
	$\rightarrow 15/2^-$	27	1^{+4}_{-1}	26^{+1}_{-4}	$.234^{+.318}_{-.234}$	4	.010	3.00	.546
7/2	$7/2^- \rightarrow 9/2^-$	100	$31.6^{+6.70}_{-6.70}$	$68.3^{+0.06}_{-0.06}$	$.680^{+.143}_{-.136}$	100	42.3	57.7	.856
	$\rightarrow 11/2^-$	—	—	—	—	0.1	0.1	0	∞
	$(9/2^-)_2 \rightarrow 9/2^-$	100	100	0	b	100	87.0	13.0	2.50
	$\rightarrow 11/2^-$	13[c]	—	—	—	29	.542	28.5	.136
	$\rightarrow 13/2^-$	—	—	—	—	0.1	0.1	0	∞
	$\rightarrow 7/2^-$	15	$8.65^{+1.37}_{-1.37}$	$8.35^{+1.37}_{-1.37}$	$.892^{+.180}_{-.156}$	3	.683	2.32	.543
	$\rightarrow 5/2^-$	4	—	—	—	0	—	—	∞
5/2	$5/2^- \rightarrow 9/2^-$	100	>96.9	<3.12	>5.572	100	100	0	∞
	$\rightarrow 7/2^-$	—	—	—	—	0	—	—	.0158
	$(7/2^-)_2 \rightarrow 9/2^-$	100	—	—	d	100	99.5	.473	14.5
	$\rightarrow 11/2^-$	e	—	—	—	6[e]	65	0	∞
	$\rightarrow 7/2^-$	—	—	—	—	0.3	.117	.183	.801
	$\rightarrow 5/2^-$	69	$14.7^{+7.01}_{-7.74}$	$54.4^{+7.64}_{-7.70}$	$.519^{+.172}_{-.184}$	15	4.25	10.7	.629
	$\rightarrow (9/2^-)_2$	—	—	—	—	0	—	—	.424
13/2	$(13/2^-)_2 \rightarrow 9/2^-$	14	—	—	d	0	0	0	∞
	$\rightarrow 11/2^-$	100[e]	$49.4^{+6.00}_{-6.00}$	$50.6^{+6.00}_{-6.00}$	$.990^{+.141}_{-.134}$	100	78.5	21.5	1.01
	$\rightarrow 13/2^-$	—	—	—	—	2	1.00	0.0070	4.43
	$\rightarrow (9/2^-)_2$	—	—	—	—	0	—	—	∞

[a]Calculated with particle-core coupling model of Dönau & Frauendorf for an $h_{9/2}$ particle coupled to a rigid triaxial rotor with: $\beta = .15, \gamma = 37°, \lambda = -1.30, E(1^{st}2^+) = 0.327$ MeV.
[b]$\alpha_K \approx \alpha_K(E2)$, doublet with line in Tl-decay.
[c]Doublet.
[d]unresolved line.
[e]Doublet, energy closest to the $(13/2)_2 \rightarrow 11/2$.

also displayed in Table 3.1. For the K = 9/2 band, the E2 intensities agree well, whereas the calculated M1 intensities are less than the measured ones by about a factor of eight.

This discrepancy in the intraband transition intensities persists in other bands, but the interband transitions are described much better by the calculations. We are pursuing the calculations in order to better understand these difficulties.

---

1. University of Tennessee, Knoxville, Tennessee.
2. Tennessee Technological University, Cookeville, Tennessee.
3. C. R. Bingham et al., Phys. Div. Prog. Rep., Sept. 30, 1987, ORNL-6420, p. 135.
4. P. B. Semmes, Ibid., p. 148.
5. J. Meyer-ter-Vehn, Nucl. Phys. A249, 111 (1975).
6. J. A. Bounds et al., Phys. Rev. C36, 2560 (1987).

SYSTEMATICS OF LIGHT EVEN-EVEN RARE-EARTH NUCLEI WITH N < 82

B. D. Kern[1] R. A. Braga[3]
M. O. Kortelahti[2] R. W. Fink[3]

An investigation of the deformation of light rare-earth nuclei with A = 129-140 and Z = 38-63 is being continued. Through the use of beta decay, low-lying levels not populated in the yrast cascades have been observed, especially those which form the gamma bands. Techniques in use have been described elsewhere.[4]

Figure 3.5 illustrates the progression toward increased deformation of the Sm, Nd, and Ce even-N nuclei as the neutron number decreases. The obvious indication of deformation is the decrease in energy of the 2^+ and other levels of the ground-state yrast bands. This behavior has been known for many years, with contributions from many workers. Our contribution to this region has been the measurement, through the use of beta decay, of the energies of the levels and of some of the parameters of the gamma bands of $^{130,132}Ce$, $^{132,134,136}Nd$, and $^{136,140}Sm$.[4,5] It will be noted that the gamma bands behave differently from the ground-state bands. The $2\gamma^+$ level energy decreases more slowly than the $2g^+$ and at N = 72 (74 in Sm) crosses above the $4g^+$.

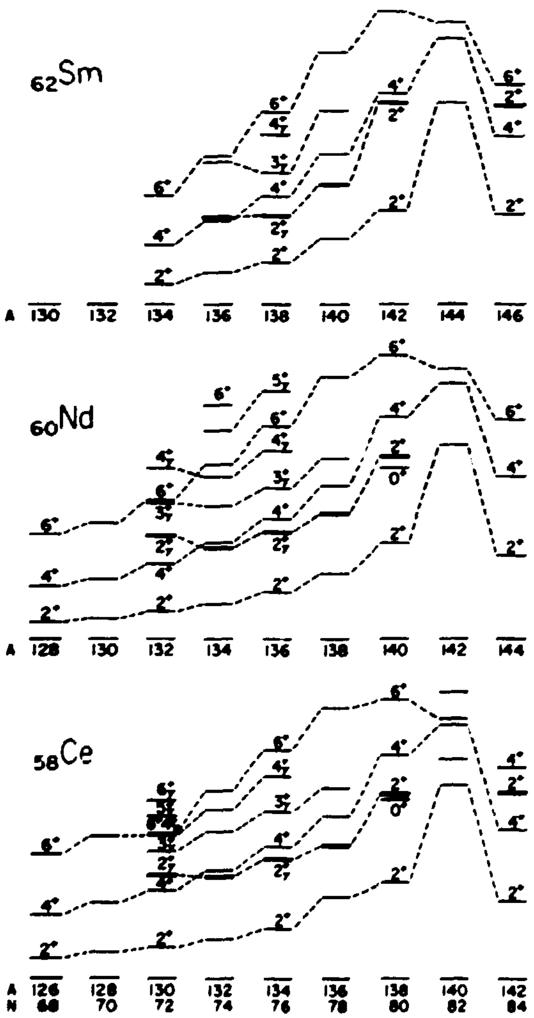

Fig. 3.5. Systematic behavior of the low lying ground-state band and gamma-band levels of Ce, Nd, and Sm for N < 82.

This effect has been predicted by Puddu et al.[6] in an IBA-2 calculation for Ce, with the crossing expected to occur at N = 68. However, they did not attempt to fit any particular nuclei and say that a slight variation of their parameters should give a more accurate description of a particular nucleus. Our experimental energy levels and relative B(E2)'s for these nuclei closely follow the predictions. Effects of the varying of the IBA-2 parameters are being investigated.

The systematic behavior of the energy levels may be interpreted as a progression from an SO(6)-like structure going towards an SU(3)-like structure as N decreases.

---

1. University of Kentucky, Lexington, Kentucky.
2. Louisiana State University, Baton Rouge, Louisiana. Present address: University of Jyvaskyla, Finland.
3. School of Chemistry, Georgia Institute of Technology, Atlanta, Georgia.

4. B. D. Kern et al., Z. Phys. A-Atomic Nuclei 330, 37 (1988).
5. B. D. Kern et al., Phys. Rev. C 36, 1514 (1987).
6. G. Puddu et al., Nucl. Phys. A348, 109 (1980).

NON-YRAST LEVEL STRUCTURE OF ^{135}Nd VIA BETA DECAY OF ^{135}Pm

M. O. Kortelahti[1] R. A. Braga[3]
H. K. Carter[2] R. W. Fink[3]
B. D. Kern[4]

The isotope ^{135}Nd has been studied through the β-decay of mass-separated ^{135}Pm. From earlier work on the β-decay of ^{135}Pm by Gizon and Alkhanov,[5] the half-life of 49 ± 7 s for the $11/2^-$ level of ^{135}Pm which decays to the $9/2^{(-)}$ ground state of ^{135}Nd was known, and four excited states in ^{135}Nd at 198.8 keV $(11/2^-)$, 463.5 keV, 561.2 keV $(13/2^-)$, and 1177.0 keV had been identified. The reported level scheme[5] is inconsistent with present data, which enables a corrected decay scheme.

In this work, the ^{135}Pm isotopes were produced at the Holifield Heavy Ion Research Facility. The reaction of 240-MeV ^{46}Ti projectiles on an enriched ^{92}Mo target was used. The mass identification was done using the on-line magnetic mass separator, UNISOR. This same reaction at 250 MeV and that with 190-MeV ^{28}Si projectiles on an enriched ^{112}Sn target were used, with the aid of a He-jet transport system.

The 198.8-keV γ ray, shown in Fig. 3.6, was the most intense one seen when using the ^{112}Sn + ^{28}Si reaction. It is due to the $11/2^-$ parent in ^{135}Pm, whose half-life was measured as 40 ± 3 s in reasonable agreement with the earlier measurements. With the ^{92}Mo + ^{46}Ti reaction, the most intense γ ray was the one with energy of 128.7 keV, indicating that a low-spin isomer in ^{135}Pm was decaying. On the left side of the diagram, the more intense 98.1-, 128.7-, 208.0-, and 270.1-keV γ rays decay with a 49 ± 3 s half-life. The possible 65.1 keV $(1/2^+) \to 9/2^-$ internal-conversion transition was not seen with the electron spectrometer and mass-separated samples. This level may be the 5.5-m half-life isomer which has been proposed.[6]

The level at 713.2 keV is the only one which decays to the 198.8-keV $11/2^-$ level and the $9/2^-$ ground state of the yrast g.s. band and also to the low-spin $(1/2^+)$ to $(7/2^+)$ levels of the left side of the diagram. This has made it possible to identify the levels on the left side of Fig. 3.6 as levels which decay to the 65.1-keV isomeric level which is not reached by yrast cascades.

---

1. Louisiana State University, Baton Rouge, Louisiana. Present address: University of Jyvaskyla, Finland.
2. UNISOR, Oak Ridge Associated Universities, Oak Ridge, Tennessee.
3. School of Chemistry, Georgia Institute of Technology, Atlanta, Georgia.
4. University of Kentucky, Lexington, Kentucky.
5. Yu. V. Sergeenkov, Nucl. Data Sheets 52, 205 (1987).
6. A. A. Abdurazakov et al., Bull. Acad. Sci., USSR (Phys. Ser.) 34, 706 (1971).

DECAY OF MASS SEPARATED ^{137}Sm

R. A. Braga[1] R. W. Fink[1]
M. O. Kortelahti[2] B. D. Kern[3]
R. L. Mlekodaj[4]

Large nuclear deformations are expected in neutron-deficient nuclei with N < 82 and Z > 50. Leander and Möller[5] have predicted that this

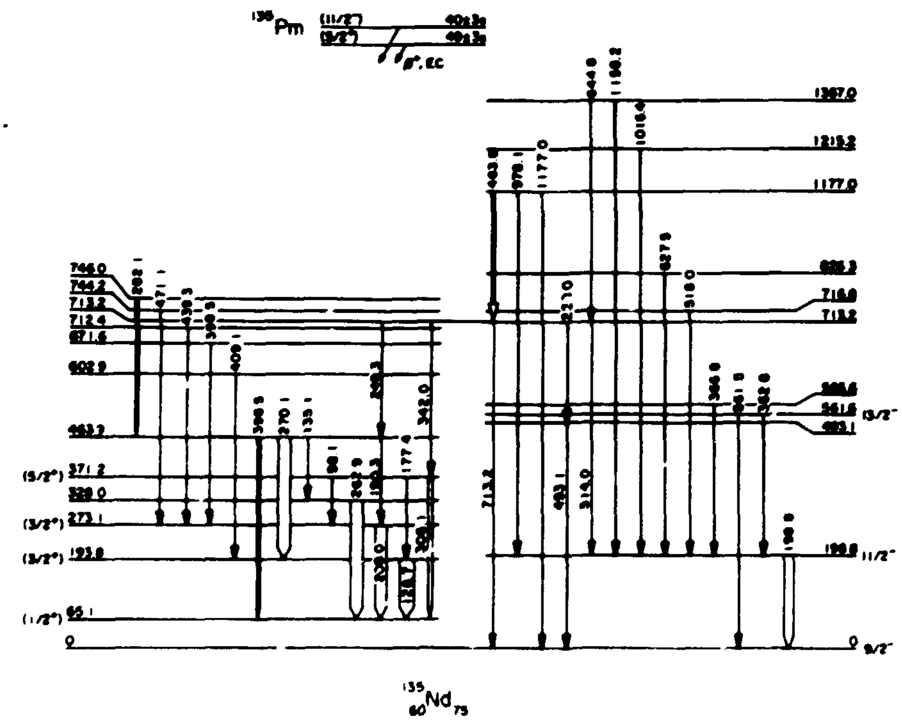

Fig. 3.6. Level diagram of ^{135}Nd, including levels due to β-decay of low-spin and high-spin isomers of ^{135}Pm. Note that the middle of the diagram is drawn to emphasize that the 713.2-keV level and several γ-ray transitions connect the non-yrast levels to the yrast g.s. band.

region of deformation is close enough to the line of stability in the neutron-deficient Sm and Pm isotopes that the possibility of producing and studying their structures exists. Macroscopic calculations by Ragnarsson et al.[6] around the neutron-deficient Sm, Gd nuclei have predicted stable prolate shapes except for the N = 76 isotones where the γ-degree of freedom is expected to come into play. Recently, the nucleus ^{138}Sm was found to have not only a small prolate-oblate energy difference, but also a triaxial equilibrium shape.[7]

Our current activity in this region of deformation is the study of the decay of 45 ^{137}Sm to levels in ^{137}Pm (an N = 76 isotone). The activities of ^{137}Sm were produced by bombarding stacked foils of natural molybdenum targets with ^{48}Ti beams from the 25-MV folded tandem accelerator at HHIRF with on-line separation at UNISOR. The experiments consisted of γ-γ-t and ce-γ-t coincidence, as well as γ-ray singles and ce-singles, spectrometry. The decay scheme for ^{137}Sm is shown in Fig. 3.7.

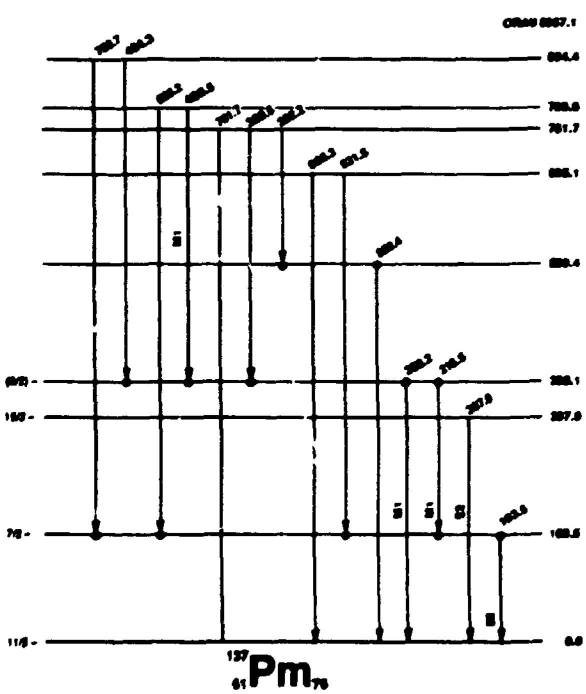

Fig. 3.7. Level scheme of ^{137}Pm from the decay of 45 sec. ^{137}Sm.

This level scheme is in essential agreement with that of Redon et al.,[8] with the exception of the spin-parity assignments, which in their case were based solely on systematics. Whereas in the heavier odd-mass Pm isotopes, the $11/2^-$ state is observed to be an excited state; in ^{137}Pm this odd-proton state drops in energy to become the ground state. In-beam spectroscopy[9] confirms this assignment of $11/2^-$ as the ground state. The $7/2^+$ assignment of Redon et al. for the 163.5-keV level is not consistent with our measurement of the conversion coefficient for the 163.5-keV transition. The α_K value of 0.264, along with L/K and L/M conversion electron ratios of 2.0 and 2.9, respectively, result in the establishment of E2 multipolarity for the 163.5-keV transition and, therefore, a spin assignment of $7/2^-$ for the 163.5-keV level. Our measured conversion coefficients also indicate that the 216.7- and 380.5-keV transitions de-exciting the 380.5-keV level are both M1 in nature. This leads to a tentative assignment of $9/2^-$ to the 380.5-keV level. The 408.5-keV transition in ^{137}Pm populating the 380.5-keV level is also M1 in character. However, due to the tentative assignment of $9/2^-$ to the 380.5-keV level, no spin assignment is made for the 789.0-keV level. The $11/2^-$ assignment for the ground state of ^{137}Pm is of particular interest in relation to the heavier odd-mass Pm isotopes. In the heavier odd-A Pm isotopes, E3 transitions are observed between the $11/2^-$ excited state and the $5/2^+$ ground state. In ^{137}Pm, however, no transition with E3 multipolarity is established. The lack of this observation reinforces our conclusion that, as with other N = 76 isotones, a decoupled band structure exists with both the $11/2^-$ and $7/2^-$ members coming low enough in energy to be below the $5/2^+$ state.

---

1. School of Chemistry, Georgia Institute of Technology, Atlanta, Georgia.
2. Louisiana State University, Baton Rouge, Louisiana. Present address: University of Jyvaskyla, Finland.
3. University of Kentucky, Lexington, Kentucky.

4. Environmental Compliance and Health Protection Division, Oak Ridge National Laboratory, Oak Ridge, Tennessee.
5. G. Leander and P. Möller, Phys. Lett. 110B, 17 (1982).
6. I. Ragnarsson et al., Nucl. Phys. A233, 329 (1974).
7. B. D. Kern et al., Phys. Rev. C36, 1514 (1987).
8. N. Redon et al., Z. Physik, A325, 127 (1986).
9. C. W. Beausang et al., Phys. Rev. C36, 602 (1987).

ENERGY LEVELS OF ^{136}Pm AND ^{136}Nd VIA BETA DECAY OF ^{136}Sm AND ^{136}Pm

B. D. Kern[1] M. O. Kortelahti[3]
R. L. Mlekodaj[2] R. A. Braga[4]
R. W. Fink[4]

^{136}Pm and ^{136}Nd were studied using the β decay of ^{136}Sm and ^{136}Pm. The radioactive nuclei were produced by the ^{92}Mo (^{48}Ti,xpyn) reactions. The UNISOR isotope separator enabled mass identification. Typically, many more low-lying, low-spin levels were populated via β-decay than in the in-beam experiments. The previously unknown level scheme of ^{136}Pm was constructed and the half-life of ^{136}Sm was determined to be 47 ± 2 s. Six new levels and thirteen new γ-ray transitions have been added to the level scheme of ^{136}Nd. The gamma band, from 2_γ^+ to 5_γ^+, was identified in ^{136}Nd. Where γ-ray branching from gamma-band levels occurred in ^{136}Nd, the relative B(E2)'s were deduced from the data and compared to predictions of the IBA SO(6) gamma-soft model and of the gamma = 30° rigid rotator model. The results indicate preference for the SO(6) model.

Additional details are given in the published paper (Ref. 5).

---

1. University of Kentucky, Lexington, Kentucky.
2. Environmental Compliance and Health Protection Division, Oak Ridge National Laboratory, Oak Ridge, Tennessee.
3. Louisiana State University, Baton Rouge, Louisiana. Present address: University of Jyvaskyla, Finland.
4. School of Chemistry, Georgia Institute of Technology, Atlanta, Georgia.
5. B. D. Kern et al., Z. Phys. A 330, [illegible]7 (1988).

SEARCH FOR LOW-SPIN SUPERDEFORMED STATES IN ^{194}Hg

E. A. Henry[1] C. R. Bingham[4]
Y. A. Akovali W. D. Schmidt-Ott[5]
J. A. Becker[1] R. A. Meyer[1]
H. K. Carter[2] Y. S. Xu[6]
J. Kormicki[3] H. V. Carmichael[4]

Recent theoretical calculations have suggested that low-spin isomeric states with large deformation will occur in the mercury nuclei.[7,8] These states would be the analogues of the fission isomers in the actinide nuclei, with J^π values of 0^+ and β_2 values of about 0.6, that is a 2:1 axis ratio. However, because the fusion barrier is much higher for the mercury nuclei, the main decay mode will be gamma-ray emission or alpha emission. These states are distinct from the high-spin superdeformed states recently found in the rare earth nuclei, where larger angular momentum stabilizes the deformation.

We have chosen two experiments that utilize beta decay of thallium nuclei to try to identify low-spin superdeformed states in mercury isotopes: alpha spectroscopy following ^{186}Tl decay and gamma-ray spectroscopy following ^{194}Tl decay. These thallium isotopes are both produced in useful quantities by the UNISOR facility. Both have a high-spin and a low-spin isomer, and both have favorable Q values. Details of the ^{186}Tl experiment are given in Section 2 of this report by Y. A. Akovali et al.

In ^{194}Hg, the superdeformed state is calculated to be at about 4 MeV of excitation and could be populated by decay of the 2^- ground state (Q_{EC} = 5.15 MeV) or the $(7)^+$ isomer (Q_{EC} = 5.45 MeV). The most easily observed signature for decay of a superdeformed isomer in ^{194}Hg would be an ~ 3.6-MeV E2 gamma ray to the first excited state in ^{194}Hg at 428 keV. Gamma-ray and alpha-singles data, and $\gamma\gamma$ and $\alpha\gamma$ coincidence data were accumulated. The data were of high quality, and many previously unobserved features are apparent. Gamma rays are observed that indicate direct population of levels at about 4 MeV of excitation in ^{194}Hg. However, only an upper limit can be placed on the intensity of a 3.6-MeV gamma ray in coincidence with the 428-keV transition from the first excited state. Further analysis of these data are necessary to quantify the population implied by these results and examine other potential decay routes.

---

1. Lawrence Livermore National Laboratory, Livermore, California.
2. UNISOR, Oak Ridge Associated Universities, Oak Ridge, Tennessee.
3. Vanderbilt University, Nashville, Tennessee.
4. University of Tennessee, Knoxville, Tennessee.
5. Joint Institute for Heavy Ion Research, Oak Ridge, Tennessee. Present address: University of Göttingen, Göttingen, West Germany.
6. Oregon State University, Corvallis, Oregon.
7. M. S. Weiss, Lawrence Livermore National Report, UCRL-96773, (Dec. 1987).
8. J. Dudek et al., Phys. Rev. Lett. 59, 1405 (1987).

LEVEL STRUCTURE OF ^{119}Te

P. F. Mantica[1] M. O. Kortelahti[3]
B. E. Zimmerman[1] W. D. Schmidt-Ott[4]
W. B. Walters[1] H. K. Carter[5]
E. F. Zganjar[2] W. L. Croft[6]
W. B. Newbolt[7]

In August, we performed our first experiment at the Holifield Heavy Ion Research Facility (HHIRF) at Oak Ridge National Laboratory. The experiment consisted of the collection of gamma-ray and conversion-electron singles spectra and gamma-electron and gamma-gamma coincidence data from the decay of ^{119}Te and ^{121}Te. Through the analysis of these data, we would calculate the amount of E0 admixture for the $1/2^+$ to $1/2^+$ and $3/2^+$ to $3/2^+$ transitions in these odd-neutron Te nuclides to determine how much of a role intruder states play in the structure of the odd-mass, odd-neutron nuclides near the Z = 50 proton shell closure.

By use of the isotope separator at the UNISOR target station, ^{119}Cs and ^{121}Cs, produced in the heavy ion reaction between a 175-MeV ^{32}S tandem beam at 1- and an 8-mg/cm^2 ^{92}Mo target, were separated from the other masses produced in the reaction and deposited on a moving tape. The transitions between levels in ^{119}Te populated through the beta/electron capture-decay of ^{119}I were then studied after allowing ample time for the removal by decay of the Cs grandparent and Xe parent from the deposited sample.

The experimental setup involved the use of parent- and daughter-decay stations. The study of the ^{119}Te and ^{121}Te nuclides was performed at the daughter station, where gamma-ray singles data up to energies of 2.0 MeV were collected, using a Ge detector with 1.9-keV full-width at half-maximum (FWHM) resolution for the 1332-keV transition in ^{60}Co. A Si(Li) detector with 2.4-keV FWHM resolution for the 975-keV K-electron-conversion transition in ^{207}Bi was used to collect conversion electron data up to energies of 3.0 MeV. Coincidences were collected between the Ge gamma-ray and Si(Li) conversion-electron detectors and between the Ge gamma-ray detector and a Ge(Li) gamma-ray detector which had a FWHM of 2.6 MeV for the 1332-keV transition in ^{60}Co and an energy range set to 3.0 MeV. At the parent station, a Si(Li) electron detector (FWHM = 3.2 keV for 975 keV) equipped with a miniorange spectrometer, and a Ge gamma-ray detector (FWHM = 2.1 MeV for 1332 keV) were used to collect conversion-electron and gamma-ray singles data for the transitions in the parent ^{119}I and ^{121}I nuclides.

Although analysis of all the data is not yet complete, some of the initial results of the analysis are interesting. Figures 3.8-3.11 show the proposed level scheme for ^{119}Te, obtained from the analysis of the gamma-gamma and electron-gamma coincidence spectra and the gamma-ray singles spectra. The proposed level scheme includes 62 gamma-ray transitions between 23 levels, and spin-parity assignments for 13 of those levels. The level scheme is much more extensive than any previously reported level scheme[8] evaluated through the beta/electron-capture population of excited states in ^{119}Te, as 14 of the levels identified in our study were not identified in any of the earlier beta/electron capture-decay studies of ^{119}I. Spin-parity assignments for the levels identified here were made with the aid of a recent in-beam study of ^{119}Te.[9]

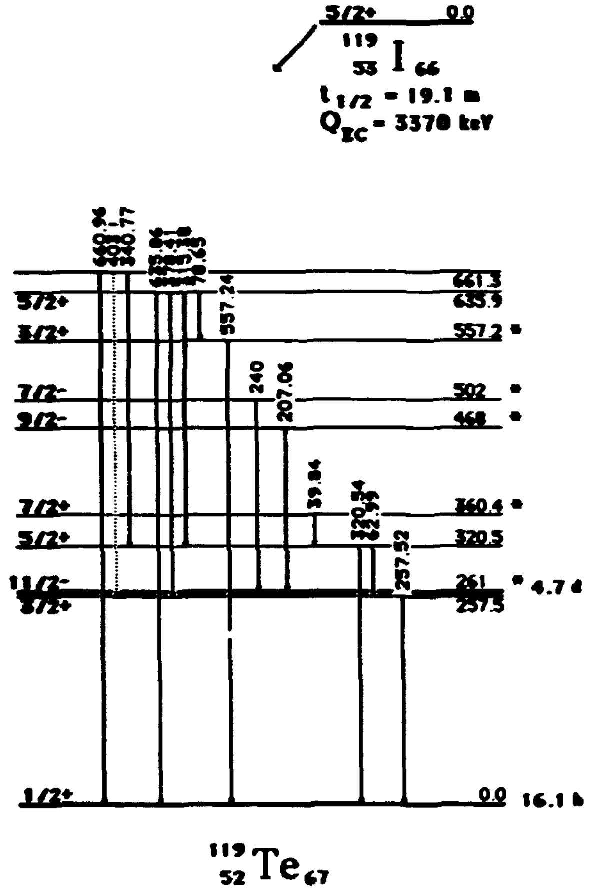

Fig. 3.8. Level scheme for ^{119}Te up to 661 keV. Levels marked with an asterisk have not been previously identified in beta-decay studies.

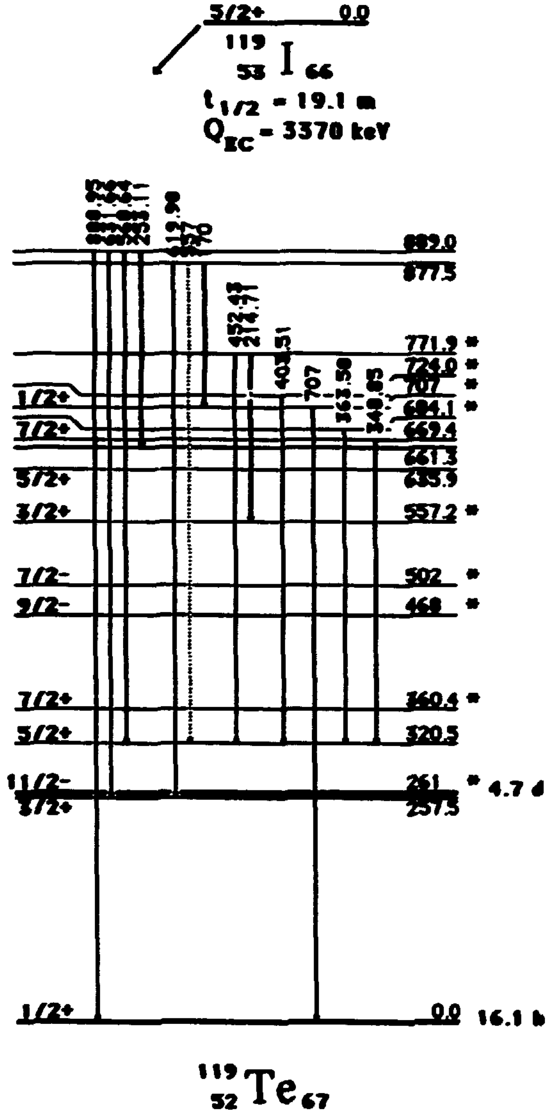

Fig. 3.9. Level scheme for ^{119}Te from 669 keV to 889 keV. Levels marked with an asterisk have not been previously identified in beta-decay studies.

Detailed analysis of the conversion-electron singles data will begin shortly for the $1/2^+$ to $1/2^+$ and $3/2^+$ to $3/2^+$ transitions in ^{119}Te. From the conver·ion-electron and gamma-ray singles data, conversion coefficients will be calculated for the $1/2^+$ to $1/2^+$ and $3/2^+$ to $3/2^+$ transitions to determine the amount of E0 admixture in these transitions. Analysis of the ^{121}Te data and the singles data collected for the *odd-mass I nuclides* will commence with the conclusion of the ^{119}Te analysis.

---

1. University of Maryland, College Park, Maryland.
2. Louisiana State University, Baton Rouge, Louisiana.
3. Louisiana State University, Baton Rouge, Louisiana. Present address: University of Jyvaskyla, Finland.
4. Joint Institute for Heavy Ion Research, Oak Ridge, Tennessee. Present address: University of Göttingen, Göttingen, West Germany.
5. UNISOR, Oak Ridge Associated Universities, Oak Ridge, Tennessee.
6. Mississippi State University, Mississippi State, Mississippi.
7. Washington and Lee University, Lexington, Virginia.
8. E. H. Spejewski et al., Nucl. Phys. A146, 192 (1970).
9. T. Rodland et al., Nucl. Phys. A469, 407 (1987).

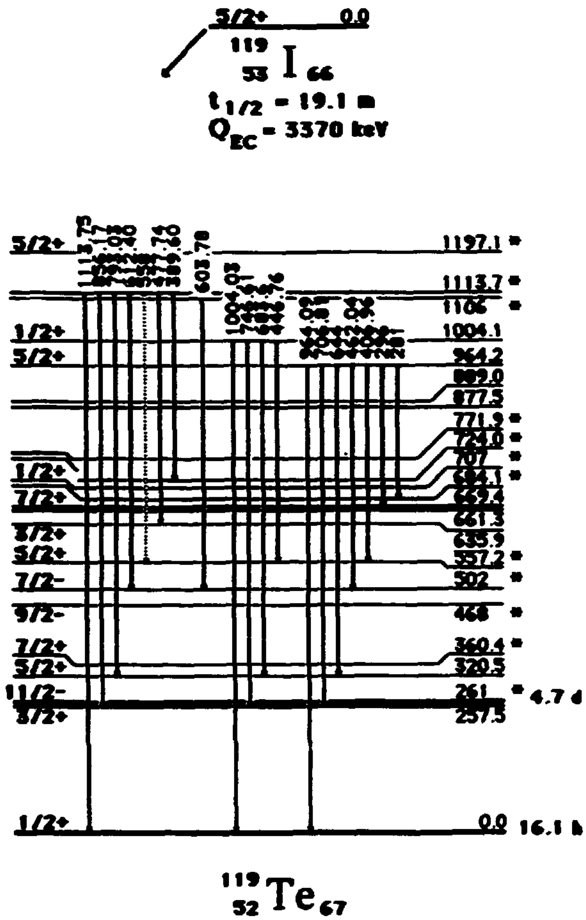

Fig. 3.10. Level scheme for ^{119}Te from 964 keV to 1113.7 keV. Levels marked with an asterisk have not been previously identified in beta-decay studies.

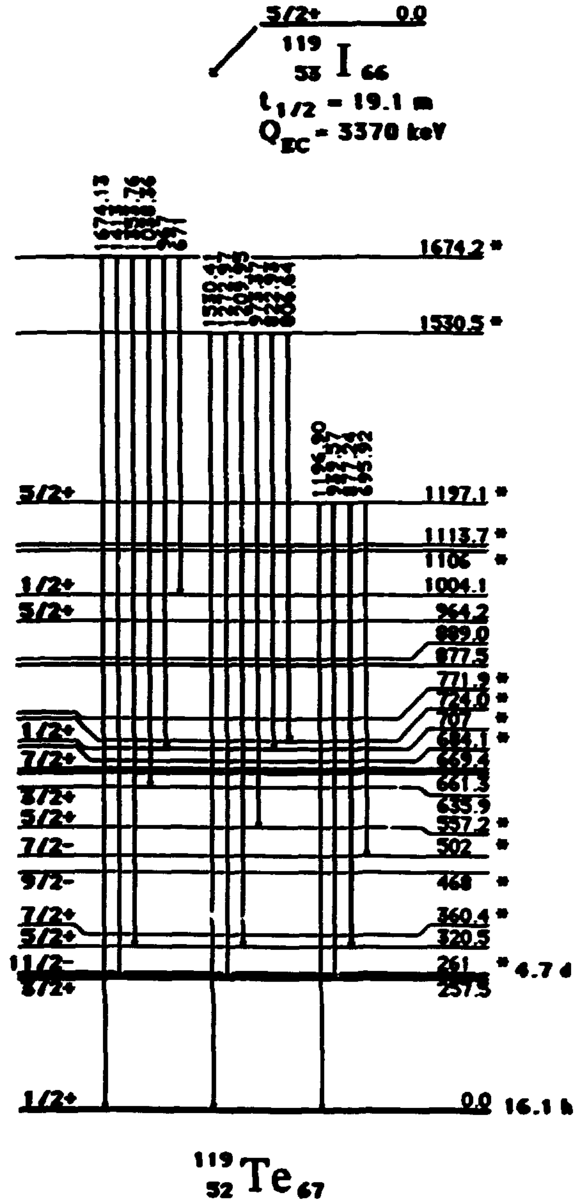

Fig. 3.11. Level scheme for ^{119}Te from 1197 keV to 1674 keV. Levels marked with an asterisk have not been previously identified in beta-decay studies.

4. EXPERIMENTAL ATOMIC PHYSICS

The experimental atomic physics program within the Physics Division is carried out by two groups, whose reports are given in this section. Work of the accelerator atomic physics group is centered around the 6.5-MV EN Tandem accelerator and the Holifield 25-MeV tandem accelerator; consequently, most of its research is concerned with atomic processes occurring to, or initiated by, few MeV/nucleon heavy ions. The second group is concerned with lower energy atomic collision physics in support of the Fusion Energy Program. These studies utilize the multiply charged ion beams obtained from an electron cyclotron resonance source. In addition to these two activities in experimental atomic physics, other chapters of this report describe the progress in related activities of these groups in theoretical atomic physics, experimental plasma diagnostic development, and atomic data center compilations.

ACCELERATOR-BASED ATOMIC PHYSICS

CHARGE AND ANGULAR CORRELATED INELASTICITIES IN MeV/amu ION-ATOM COLLISIONS

H. Schöne[1] J. P. Giese[3]
R. Schuch[2] H. F. Krause
S. Datz M. Schulz[4]
P. F. Dittner Q. C. Kessel[5]

We report on simultaneous measurements of scattering angle, recoil charge state and inelasticity in MeV/amu collisions using an Elbek high-resolution magnetic spectrograph. In general, for inelastic collisions of this type, much of the energy is carried off by either direct ionization or by ionization following inner-shell ionization or excitation. In the case of capture, a balance between energy gain (or loss) due to an increase in binding energy on the projectile and energy loss due to an increase in translational energy of the captured electron determine the inelasticity. We find that a large fraction of the total transferred energy is carried off by the continuum electrons. For this experiment, a 10-MeV carbon beam was poststripped after passing through a 90° magnet. The C^{6+} beam was energy- and charge-state selected with a second 90° magnet in combination with two sets of slits. The angular divergence was limited by a third slit in front of the gas cell. The degree of multiple target ionization by a given projectile was determined by a time-of-flight technique. A more detailed description of the setup used is given elsewhere.[6] A two-dimensional (2D) position-sensitive multichannel plate placed in the focal plane of the Elbek magnetic spectrograph[7] was used to detect the recoiling projectiles. Since the spectrograph is double focusing in the plane of dispersion (X) and nonfocusing in the perpendicular plane (Y), a displacement in Y is a measure of the angular differential cross section $d\sigma/d\theta$. With the given properties of detector and spectrograph, the angular resolution is limited to 0.005°.

With direct ionization, larger impact parameters are favored more than in the transfer reaction and the differential cross sections are more sharply peaked at small angles. Subtracting the sum of the ionization potentials (SIP) necessary to create a given ionization state in Ne from the relative inelasticity (RI), we obtain (assuming that the recoil energy and excitation energy is low) the total kinetic energy of the continuum electrons.

In Fig. 4.1a, we plot total energy given to continuum electrons for direct ionizing collisions of 10 MeV C^{6+} with He, Ne, and Ar. In Fig. 4.1b, we show the data for charge capture collisions of 10 MeV C^{6+} with He, Ne, Ar, and Kr targets. We use Q = 1 as an arbitrary zero of inelasticity because the absolute energy loss of recoil charge state 1^+ could not be determined

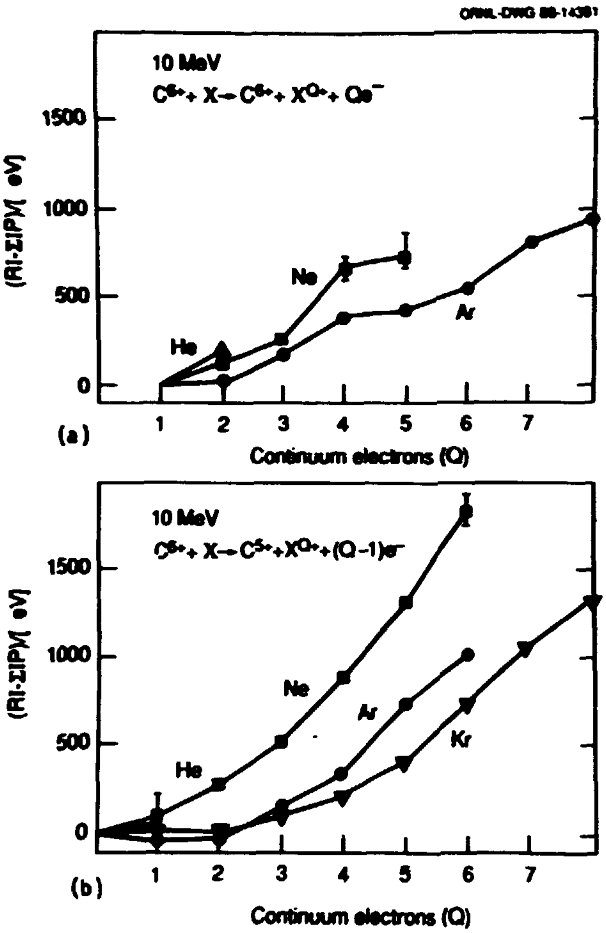

Fig. 4.1. Total energy deposited into continuum electrons (= measured projectile energy loss relative to recoil-ion charge state 1+ (R1) minus the sum of the ionization potentials (ΣIP)) necessary to form that charge state number of continuum electrons for (a) direct ionization and (b) charge capture into C^{5+} plus multiple ionization of 10 MeV C^{6+}.

with sufficient accuracy. Statistical errors are, in most cases, smaller than the data point symbols. Systematic errors are indicated only for Ne. In either channel, the kinetic energy is quite high, with 100 – 200 eV per emitted electron. Furthermore, for both reaction channels, the kinetic energy per continuum electron decreases with higher target Z. A qualitative understanding of these processes can be made using the heuristic assumption that the electrons are ejected by a binary encounter mechanism. The impact parameter for ionizing a given target electron extends to larger impact parameters for higher target Z. Hence, for high Z targets, we expect relatively less energy transfer to the removed electrons due to larger impact parameters. This trend is reflected in the ionization measurements (Fig. 4.1a). At 20 MeV, we expect the total cross section to decline, but the impact parameter dependence of the cross section should peak at and extend to larger distances. The experimental finding of decreased inelasticity with increasing energy is in agreement with the energy deposition model which predicts less energy transfer for distant collisions. ΔE may be treated likewise as direct ionization only with a smaller and closer impact parameter range defined by the requirement of simultaneous capture. As a result, the continuum electron energies are lower for increasing target Z, while, for a given target Z, the kinetic energy of an ejected electron is larger in coincidence with electron capture than for direct ionization. Since one electron in the capture channel is not released to the continuum, recoil charge state Q-1 corresponds to charge state Q for direct ionization. The direct comparison of both channels shows qualitatively good agreement with this simple model.

1. Graduate student on assignment from the University of Heidelberg, Heidelberg, FRG.
2. MSI, Frescativägen 24, S-104 05 Stockholm 50, Sweden.
3. ORAU Postdoctoral Research Associate.
4. Partial support provided by the Joint Institute for Heavy Ion Research.
5. Department of Physics, University of Connecticut, Storrs, CT 06268.
6. R. Schuch et al., Phys. Rev. Lett. 60, 10 (1988).
7. J. Borggreen et al., Nucl. Instrum. Meth. 24, 1 (1963).

ELECTRON ENERGY DISTRIBUTIONS ACCOMPANYING MULTIPLY IONIZING COLLISIONS

S. Datz, J. P. Giese[2]
H. Schöne[1], R. Hippler[3]
C. R. Vane, H. F. Krause
P. F. Dittner, M. Schulz[4]
J. K. Swenson[5]

In experiments that have measured the inelastic losses of energetic ions which accompany multiple ionization of the target, it has been observed that these losses far exceed the minimum necessary for the release of a given number of electrons. For the reaction

C^{6+} (10 MeV) + Ne → C^{6+} + Ne^{q+} + qe^- ,

the measured energy loss of C^{6+} implied that an average kinetic energy of ~200 eV has been imparted to the emitted electrons.[6]

To investigate this further, two approaches were followed: (1) We measured the forward (zero degree) electron spectra in coincidence with capture or direct ionization. This approach accents that part of the spectrum which is associated with electrons moving at low velocity in the projectile rest frame. (2) We measured the energy distribution of electrons resulting mainly from emission in the target rest frame by extraction and retardation analysis.

For the first part, we used a zero degree electron spectrometer and measured the spectrum in coincidence with charge capture for collisions of C^{6+} + Ne → C^{5+} + Ne^{q+} + $(q-1)e^-$ and with projectile charge loss in C^{5+} + Ne → C^{6+} + Ne^{q+} + $(q+1)e^-$. Higher electron energies are observed for both channels as compared with simple target ionization, C^{6+} + Ne → C^{6+} + Ne^{q+} + qe^-, indicative of the smaller impact parameters associated with these processes. A more prominent binary encounter peak in the charge-capture coincidence spectrum is observed, which gives additional evidence for the nature of the close encounters required for this process.

To measure the energy distribution of electrons released predominantly in the target frame, we applied a drawout potential of 150 volts to the scattering cell perpendicular to the direction of the ion beam. The recoil ions were thus extracted on one side while the electrons were ejected in the opposite direction. The arrival of the electrons at a channeltron initiated a pulse which was then used to measure the time-of-flight and hence the charge state of the recoil ions. We then introduced a retarding grid on the electron side and measured the recoil-ion spectrum as a function of this retarding voltage. For collisions of 20 MeV C^{6+} + Ne, Fig. 4.2 shows some representative spectra and Fig. 4.3 shows the charge fractions as a function of repeller voltage. The principal features are the initial decline of the Ne^{1+} fraction within the first 50 volts of retarding potential and the relative constancy in the ratios thereafter.

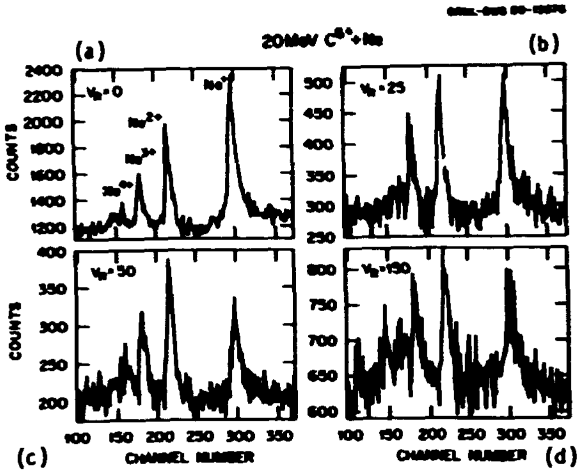

Fig. 4.2. Time-of-flight charge state spectra for Ne recoil ions from C^{6+} (20 MeV) + Ne collisions. The peaks from right to left are due to Ne^{+}, Ne^{3+}, and Ne^{4+}. Electron retarding voltages are (a) 0 V, (b) 25 V, (c) 50 V, and (d) 150 V.

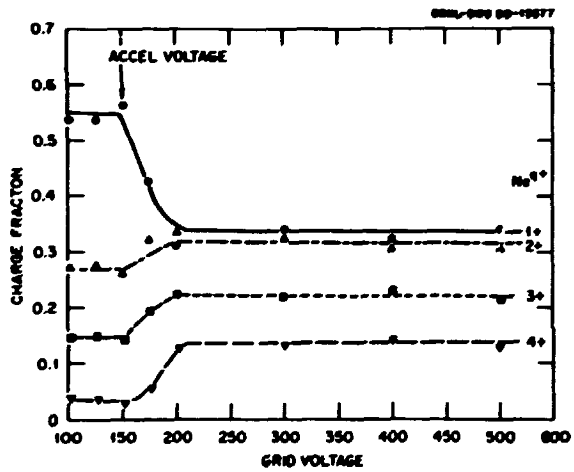

Fig. 4.3. Charge fractions as a function of electron retarding voltage.

A long-range Coulomb impulse can result in the liberation of a single electron from the target. Within the impulse approximation, such long-range interactions lead to small energy transfer and account for the low-energy dominance of the single ionization events. More significant is the relative constancy of the charge state ratios with increasing repeller voltage, i.e., the ejected electron-energy distribution is independent of the number of electrons released. This implies the validity of an energy deposition model in which a fixed amount of energy is deposited into the system and is then statistically distributed to the emerging electrons. In this case, the energy distribution among the electrons is independent of the number of electrons ejected.

---

1. Graduate student on assignment from the University of Heidelberg, Heidelberg, FRG.
2. ORAU Postdoctoral Research Associate.
3. Universität Bielefeld, Fakultät für Physik, Postfach 8640, 4800 Bielefeld 1, FRG.
4. Partial support provided by the Joint Institute for Heavy Ion Research.
5. University of Tennessee Postdoctoral Research Associate.
6. R. H. Schuch et al., Phys. Rev. Lett. 60, 925 (1988).

ELECTRON-ELECTRON INTERACTIONS IN TRANSFER AND EXCITATION IN F^{8+} + H_2 COLLISIONS

M. Schulz[1] H. F. Krause
J. P. Giese[2] H. Schöne[4]
J. K. Swenson[3] C. R. Vane
S. Datz M. Benhenni[5]
P. F. Dittner S. M. Shafroth[5]

Transfer and excitation processes have been studied intensively the last couple of years.[6-8] The interest was focussed on resonant transfer and excitation (RTE). In this process, a weakly bound target electron excites a projectile electron and is captured to a bound state of the projectile.

In last year's progress report (ORNL-6420), we presented evidence for RTE in F^{6+} + H_2 collisions. In that work, a dominance of high n state KLn RTE resonances over the KLL resonances was found. Furthermore, a maximum in the cross section was found at projectile energies higher than the RTE resonance energies. The causes for this maximum could not be conclusively clarified in that experiment. However, as one possible explanation, a process proposed by Y. Hahn[9] was discussed. In this process, which is termed "Two Electron Transfer and Excitation" (2eTE), a projectile electron is excited by one target electron and simultaneously a second target electron is captured by the projectile. In the present work, we present evidence for 2eTE in F^{8+} + H_2 collisions by measuring F Auger electrons. Furthermore, we show that the n-state dependence of the RTE resonances is entirely different in the Auger decay channel than the X-ray decay channel studied in the previous experiment.

At the EN Tandem, we obtained F^{8+} beams at energies between 17 and 33 MeV. The beam was passed through a differentially pumped H_2 gas target. The electrons produced here were decelerated by a high voltage, energy analyzed by a high-resolution electron spectrometer,[10] and detected by a position-sensitive micro-channel-plate detector. The beam was collected in a Faraday cup and used for normalization.

In Fig. 4.4, the F Auger electron emission cross sections for KLL, KLM, KLN, and KLO transitions are plotted vs the projectile

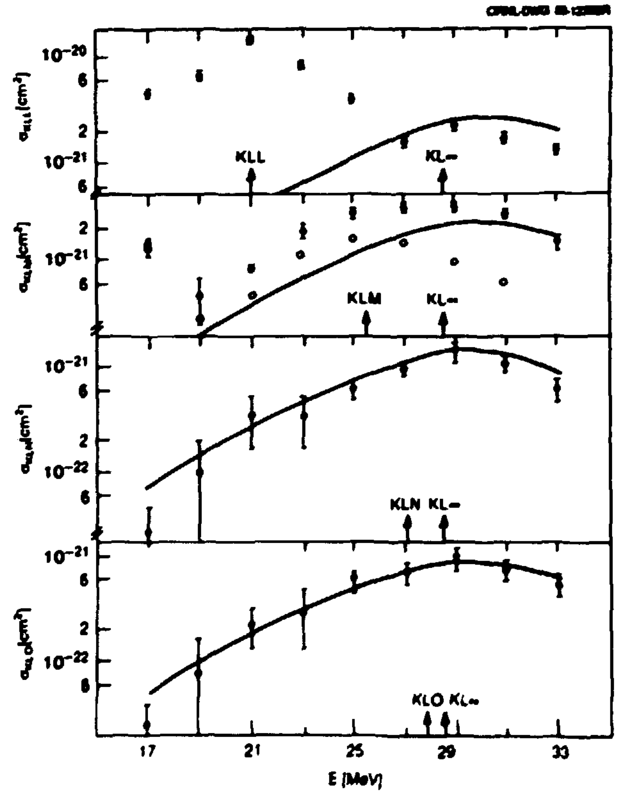

Fig. 4.4. F Auger electron emission cross sections vs projectile energy for KLL, KLM, KLN, and KLO transitions. The full curves are estimated 2eTE cross sections. The open circles in σKLM are the difference between the measured cross sections and the curve.

energy. In σ_{KLL}, two maxima can be seen at 21 and 29 MeV. For all the other transitions, the cross sections have a maximum at 29 MeV. For initially H-like ions, an Auger electron can be produced only by a transfer and excitation process (except for higher order processes). The arrows in Fig. 4.4 show the RTE resonance energies for the corresponding Auger transition and the RTE KLn series limit (KL∞). Only the first maximum in σ_{KLL} agrees with the corresponding resonance energy. The second maximum, as well as the maxima for the other transitions, are slightly above the KLn series limit. Thus it is clear that these contributions cannot be due mainly to RTE and must be explained by a different transfer and excitation process.

One obvious candidate is 2eTE. The curves in Fig. 4.4 show estimated 2eTE cross sections. Since at these projectile energies a K electron can be excited to the L shell only by free electron impact, the n distribution of the states populated by 2eTE is determined by the capture probabilities which we calculated within the OBK approximation. The energy dependence in our estimate is a combination of the OBK energy dependence and the momentum distribution (Compton profile) of the exciting target electron. The absolute magnitude was obtained by fitting the estimated 2eTE cross sections with the excitation cross section by a free electron as the only free parameter to the data point in σ_{KLN} at 29 MeV. The agreement of our estimate with σ_{KLN} and σ_{KLO} is very good. In σKLM, the curve approaches the data only at high energies. In σ_{KLL}, the agreement is reasonable in the region of the second maximum where the contributions from RTE are small. If in σ_{KLM}, the curve is subtracted from the data, then the resulting cross sections (open circles) have an energy dependence which is consistent with a KLM RTE resonance. However, these cross sections are about one order of magnitude lower than the KLL resonance. In σ_{KLN} and σ_{KLO}, no indication for RTE resonances can be seen.

We conclude that in the Auger decay channel RTE is clearly dominated by KLL states and falls off rapidly with increasing n. Taking contributions from RTE into account, the n-dependence and the projectile energy-dependence of the present data are consistent with what is expected for 2eTE cross sections. We take this as strong evidence for the occurrence of the 2eTE process.

---

1. Partial support provided by the Joint Institute for Heavy Ion Research.
2. ORAU Postdoctoral Research Associate.
3. University of Tennessee Postdoctoral Research Associate.
4. Graduate student on assignment from the University of Heidelberg, Heidelberg, FRG.
5. University of North Carolina, Chapel Hill, NC 27514.
6. J. A. Janis et al., Phys. Rev. Lett. 53, 2551 (1984).
7. M. Schulz et al., Phys. Rev. Lett. 58, 1734 (1987).
8. S. Reusch et al., Nucl. Instr. Meth. in Phys. Res. B23, 137 (1987).
9. Y. Hahn, private communication.
10. J. K. Swenson, Nucl. Instrum. Meth. in Phys. Res. B10/11, 899 (1985).

DOUBLE EXCITATION OF He BY FAST BARE IONS

J. P. Giese[1] S. M. Shafroth[4]
M. Schulz[2] H. Schöne[5]
J. K. Swenson[3] P. F. Dittner
M. Benhenni[4] C. R. Vane
S. Datz

The double excitation of He by fast bare projectiles has been investigated in order to probe the role that electron-electron correlation plays in this process. The importance of electron correlation has been clearly demonstrated in transfer ionization[6,7] and is suggested in double ionization.[8,9] The double excitation of He by bare projectiles is conceptually and computationally simpler than these ionization processes where one or two electrons end up in the continuum.[10] A qualitative examination of the probable excitation mechanisms suggests there should be a difference in the dependence of the excitation cross section on the projectile charge. The first mechanism involves a close collision between the projectile and one of the He electrons. This electron in turn collides with the second electron and both are excited. This mechanism can also be pictured as a "shake-up" transition. The initial single excitation of the first electron is known to vary as Z^2, where Z is the charge of the projectile. Thus, this mechanism might be expected to vary as Z^2. The second mechanism involves a close collision of the projectile with both electrons and would most likely vary as Z^4.

We have measured the double excitation of He by F^{q+} (q = 7 – 9) and C^{q+} (q = 4 – 6) projectiles at 1.5 MeV/amu at the ORNL EN Tandem. The doubly excited He atoms decay primarily via autoionzation producing electrons with line energies between 30 and 45 eV. These electrons have been detected using a high-resolution electron spectrometer[11] at laboratory observation angles between 9.6° and 60° relative to the beam axis. The preliminary results indicate that the dominant excitations are to the $2p2p(^1D)$ and $2p3p(^1D)$ states of He. As would be expected, there is no sign of population of triplet states when using bare projecile (F^{9+} and C^{6+}). A strong Fano profile is seen for all the states, indicating interference between the double excitation and ionization processes. A detailed analysis of these Fano profiles will be necessary in order to determine the Z-dependence of the excitation process. Our plans are to continue this series with protons at 1.5 MeV/amu and to measure the energy dependence using protons between 1.0 and 10 MeV/amu. It is also possible that a complete analysis of the Fano profiles will require measurements at larger observation angles.

---

1. ORAU Postdoctoral Research Associate.
2. Partial support provided by the Joint Institute for Heavy Ion Research.
3. University of Tennessee Postdoctoral Research Associate.
4. University of North Carolina, Chapel Hill, NC 27514.
5. Graduate student on assignment from the University of Heidelberg, Heidelberg, FRG.
6. E. Horsdal Pedersen and L. Larsen, J. Phys. B 12, 4085 (1977).
7. L. H. Andersen et al., Phys. Rev. Lett. 57, 2147 (1987).
8. J. P. Giese and E. Horsdal, submitted for publication in Nuclear Instruments and Methods in Physics Research.
9. J. H. McGuire, private communication.
10. J. H. McGuire, Nucl. Instrum. and Meth. in Phys. Res. A262, 48 (1987).
11. J. K. Swensen, Nucl. Instrum. and Meth. in Phys. Res. B10/11, 899 (1985).

RESONANT DIELECTRONIC EXCITATION IN CRYSTAL CHANNELS

S. Datz, C. R. Vane, P. F. Dittner, J. P. Giese[1], J. Gomez del Campo, N. L. Jones, H. F. Krause, P. D. Miller, M. Schulz[2], H. Schöne[3], T. M. Rosseel[4]

Energetic ions traveling through crystals under channeling conditions interact directly only with loosely bound electrons. In this approximation, the electrons in a channel may be treated as a dense electron gas characterized by a Fermi distribution of momenta. Ions traveling through this medium at velocities v_i equivalent to electron velocities required for, e.g., excitation or ionization of an electron bound to the moving ion, should experience events similar to those in a dense plasma but with a relatively narrow electron energy distribution.

To test this hypothesis, we have sought, and observed, effects due to resonant dielectronic excitation (RDE) in one-electron ions of Si, S, and Ca by electron collisions while passing through a <110> axial channel in a silicon crystal.

An electron colliding with the ion moving in the channel excites a previously bound electron and, in so doing, loses energy and is captured to a bound state, e.g.,

$$A^{(Z-1)+}\,(1s) + e \rightarrow \left[A^{(Z-2)+}\,(2p^2)\right]^{**} .$$

In the spirit of Auger notation, we refer to this as a KLL excitation. This process is resonant at a collision energy equal to the KLL energy. Since the electrons in the channel have a Fermi distribution in energy, the resonance will be spread by the Compton profile of the momentum distribution.

In vacuum under single collision conditions, the doubly excited state would decay either by an Auger process (resonant elastic scattering) back to $A^{q+} + e^-$ or by radiative stabilization (dielectronic recombination = DR) via two photons; first to $\left[A^{(Z-2)+}\,(1s2p)\right]^* + h\nu_1$ and then to $A^{(Z-2)+}\,(1s)^2 + h\nu_2$. However, if the state is created in a dense electron medium (i.e., a dense plasma or a crystal channel), collisional processes leading to further excitation and ionization come into play and may even dominate.

The experiments were carried out using the HHIRF tandem to obtain beams of H-like S^{15+} at energies ranging from 80 to 210 MeV and Ca^{19+} at energies from 150 to 3?0 MeV. The ion beams passed through the <110> axis of a silicon crystal 1.4 μm thick. Measurements were made of (a) the emerging charge-state distributions using electrostatic deflection and a solid-state position-sensitive detector, and (b) the X-ray spectra using a Si(Li) detector (130 eV resolution at 5.6 keV).

If we assume 6 electrons per atom, the electron density in the channel is $3.6 \times 10^{23}/cm^3$. If we take, as an example, KLL excitation of S^{15+}, the requisite electron-collision energy is 1.87 keV or a S^{15+} ion energy of 110 MeV on a stationary electron (note that this is well below the energy required for direct 1s → 2p excitation or for ionization). This gives an electron flux of 9.4×10^{32} cm^{-2} sec^{-1}. Coupling this with the appropriate cross sections for excitation and ionization, we obtain the rates for these processes and compare them with autoionizing and radiative rates in Fig. 4.5 for the configuration $[S^{14+}(2p^2)]^{**}$. (Note that the most rapid rate is for 2s-2p mixing.)

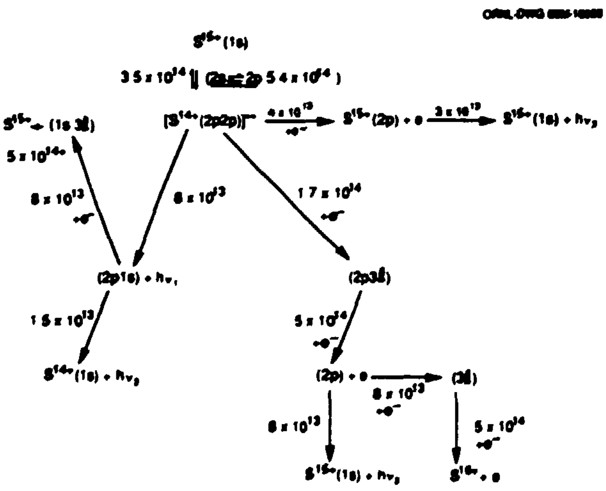

Fig. 4.5. Collisional and radiative rates (in sec^{-1}) for the various possible paths into and out of the $S^{14+}(2p^2)$ configuration at the velocity corresponding to a KLL resonance.

The observables are: stabilized charge capture to S^{14+}; collisional excitation and ionization of two electrons to form S^{16+}; X-radiation of the doubly excited state $S^{14+}(2p^2 \rightarrow 2s2p) + h\nu_1$; X-radiation of the He-like $S^{14+}(1s2p \rightarrow 1s^2) + h\nu_2$; and X-radiation from the one-electron excited system $S^{15+}(2p \rightarrow 1s) + h\nu_3$. From these rates, the predicted relative yields are:

$$Y(16+) = 0.?5$$
$$Y(14+) = 0.06$$
$$Y(h\nu_1) = 0.31$$
$$Y(h\nu_2) = 0.06$$
$$Y(h\nu_3) = 0.23.$$

However, the $h\nu_1$ and $h\nu_3$ are indistinguishable with our Si(Li) detector resolution and the yields should be added.

The results shown in Fig. 4.6 for the charge-state fractions as a function of energy and Fig. 4.7 for the X-ray yields as a function of energy are in qualitative accord with these expectations. Fig. 4.6a shows no discernable deviation in the charge 14+ fraction from a monotonic trend; and Fig. 4.7a, showing the $S^{14+}(1s2p) \rightarrow 1s^2$ X-ray yield, likewise shows a monotonic decline with increasing energy. Marked oscillations are seen in Fig. 4.6b for the S^{16+} charge fraction and Fig. 4.7b for the X rays ($h\nu_1 + h\nu_3$). Subtracting a monotonic background reveals the following features: (1) a peak at 110 MeV, the predicted position of the KLL resonance; (2) a peak at ~145 MeV, corresponding to the peak previously observed[5] for the complex of higher KLn resonances; (3) an apparent peak at 185 MeV, which is due to direct collisional excitation 1s → 2p (see below); and (4) a rise in the S^{16+} near 200 MeV, due to direct ionization.

In the case of $Ca^{19+}(1s) + e \rightarrow Ca^{18+}(2p^2)$, the radiative rates are faster, and the collisional ionization and excitation cross sections are lower than for the S^{15+} case. Here the radiative rates dominate and lead to the following set of anticipated yields:

$$Y(20+) = 0.09$$
$$Y(18+) = 0.38$$
$$Y(h\nu_1) + Y(h\nu_3) = 0.91$$
$$Y(h\nu_2) = 0.38.$$

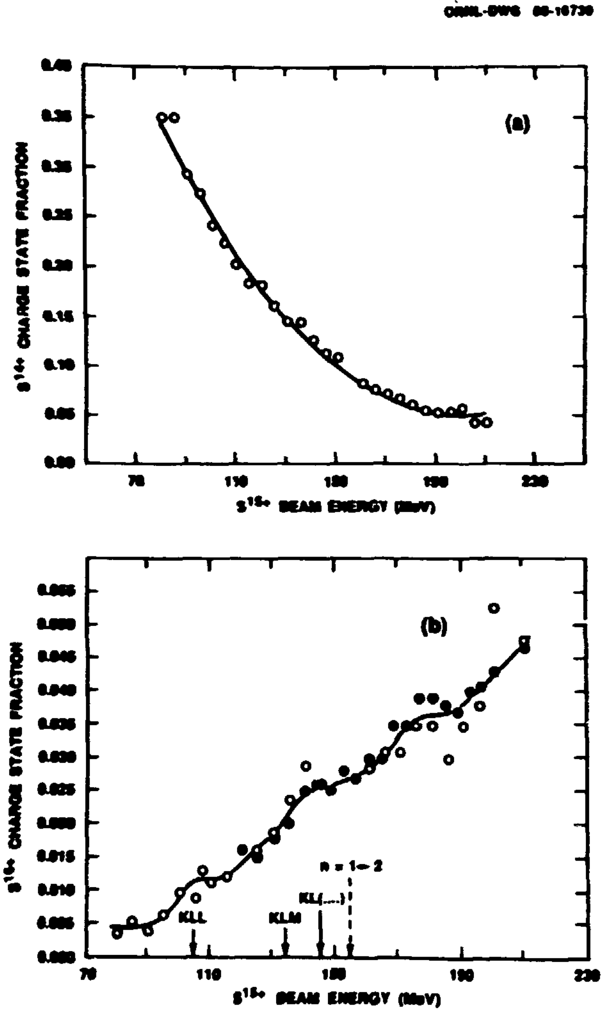

Fig. 4.6. Charge state fractions of (a) S^{14+} and (b) S^{16+}, emerging from a 1.4-μm Si <110> channel as a function of entering S^{15+} ion energy.

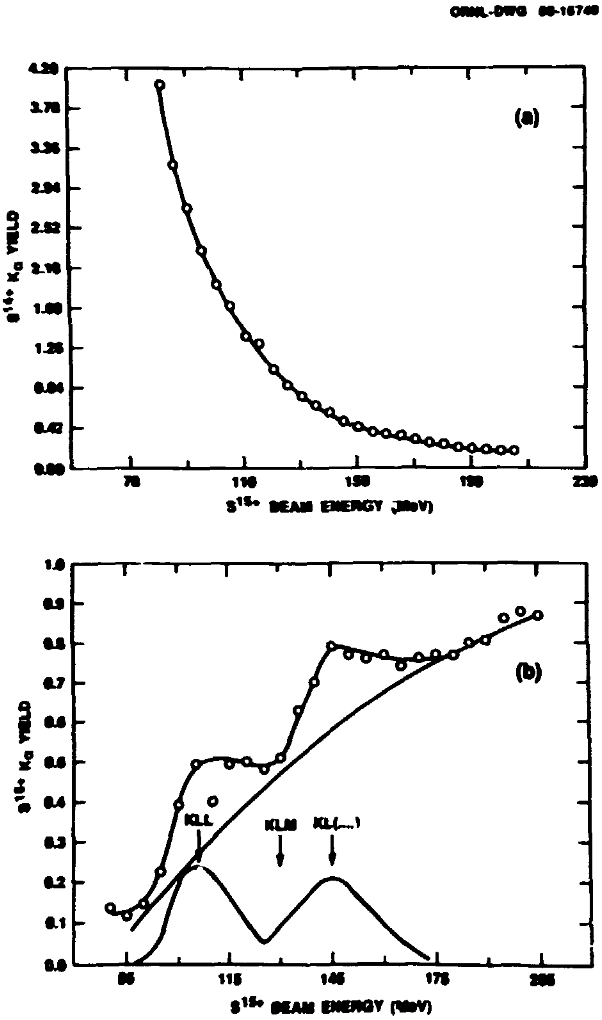

Fig. 4.7. Relative yields of X rays from (a) S^{14+} (1s2p) → $1s^2$ + $h\nu_2$ and (b) the sum of S^{14+} ($2p^2$) → (1s2p) + $h\nu_1$ and S^{15+} (2p) → 1s + $h\nu_3$.

The data for Ca^{19+} are shown in Figs. 4.8 and 4.9. Fig. 4.8a shows the formation of He-like Ca^{18+} on a large, but smooth, monotonic background. The effect, though perhaps more evident in Fig. 4.8b for Ca^{20+}, is actually smaller than the Ca^{18+} effect by a factor of ~4, as anticipated. Fig. 4.8b also shows the effect of direct 1s-2p excitation which has a threshold E_{th} = 300 MeV. Since the excitation cross section is a step function followed by a very gradual decline, we expect that, with a Compton fold, the yield will reach half its maximum at E_{th}.

The X-ray yields are shown in Fig. 4.9 The $Y(h\nu_1)$ + $Y(h\nu_3)$ in Fig. 4.9b show the expected KLL and KLn features, as well as an indication of the 1s → 2p direct excitation; but no hint of a peak due to $Y(h\nu_2)$ is seen in Fig. 4.9a, even though we expect a peak with a height of ~1/2 that is seen for KLL in Fig. 4.9a. This lack may be due to the large background attributable to direct excitation of non-channeled Ca^{18+} or capture to form excited states of Ca^{18+} at the exit surface. To alleviate the background problems in these experiments, it will be necessary to measure coincidences between the He-like K_α X rays and charge capture.

---

1. ORAU Postdoctoral Research Associate.
2. Partial support provided by the Joint Institute for Heavy Ion Research.
3. Graduate student on assignment from the University of Heidelberg, Heidelberg, West Germany.
4. Analytical Chemistry Division, ORNL.
5. M. Schulz et al., Phys. Rev. Lett 58, 1734 (1987).

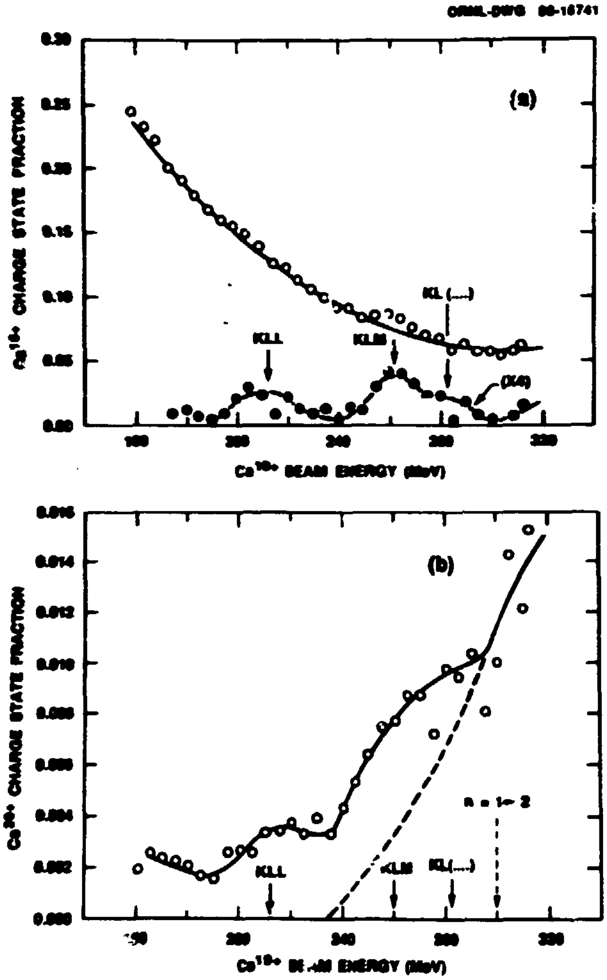

Fig. 4.8. Charge state fractions of (a) Ca^{18+} and (b) Ca^{20+}, emerging from a 1.4-µm Si <110> channel as a function of entering Ca^{19+} ion energy.

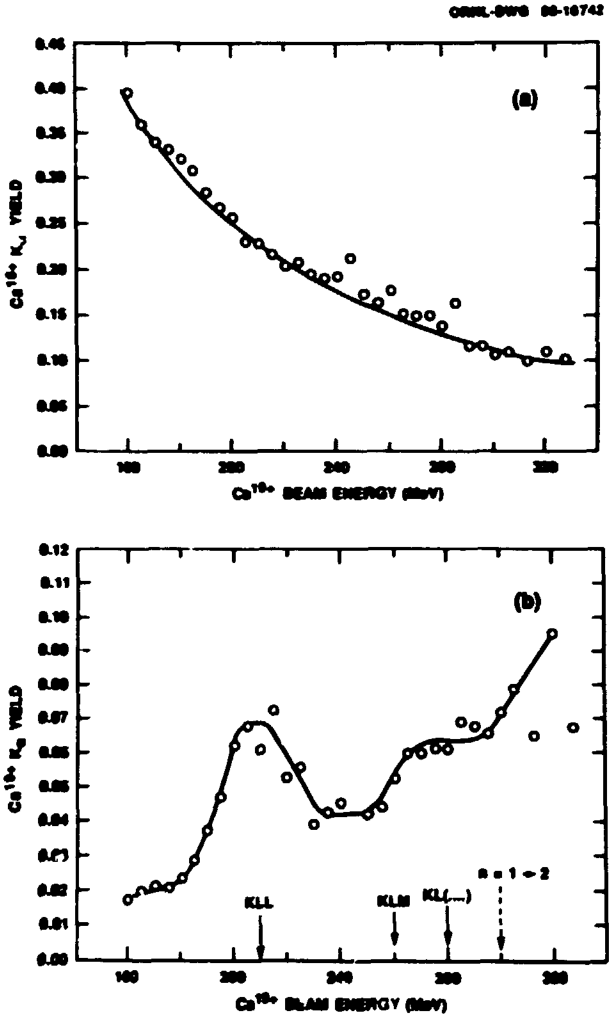

Fig. 4.9. Relative yields of X rays from (a) Ca^{18+} $(1s2p) \rightarrow 1s^2 + h\nu_2$ and (b) the sum of Ca^{18+} $(2p^2) \rightarrow (1s2p) + h\nu_1$ and Ca^{19+} $(2p) \rightarrow 1s + h\nu_3$.

RADIATIVE ELECTRON CAPTURE BY BARE- AND ONE-ELECTRON IONS

C. R. Vane, P. D. Miller, S. Datz, H. Schöne[2], P. F. Dittner, M. Schulz[3], J. P. Giese[1], T. M. Rosseel[4], H. F. Krause, R. S. Peterson[5]

The phenomenon of radiative electron capture (REC), wherein a weakly bound target electron is directly captured by a moving ion and an energy- and momentum-stabilizing photon is emitted, has been studied for bare- and/or one-electron O, Si, S, and Ca ions at energies ranging from 50 to 329 MeV on gas and solid targets. Intensities and energies of X rays emitted were precisely measured under controlled conditions in order to determine the absolute energies and shapes of REC peaks. These studies were prompted by our finding, in another experiment (see Datz, Vane et al., this report), that the REC X-ray peak energy observed for S^{16+} channeled in silicon was slightly lower than expected according to simple energy conservation considerations. Silicon, sulfur, and calcium ions obtained from the Holifield Heavy Ion Research Facility (HHIRF) tandem accelerator were axially channeled through thin silicon crystals aligned in the <110> orientation. X rays emitted at 46.5° with respect to the beam axis were detected with a well-calibrated, high-resolution Si(Li) detector. A typical spectrum is shown in Fig. 4.10 for 180-MeV S^{16+} channeled in a 0.4-μm-thick Si<110> crystal. The measured REC centroid energies were found to be consistently about 100 eV lower than predicted. On the other hand, the peak shapes indicated that REC was proceeding as expected, arising mainly from capture of weakly bound electrons residing in the crystalline channels. A plot of measured and calculated REC peak centroid energies and widths is displayed in Fig. 4.11.

We decided to repeat these measurements in gas targets, to eliminate solid state effects, and at high enough energies to ensure that charge-state contamination of the incident ion beam did not shift the REC peak position. Bare oxygen ions at 100 to 225 MeV obtained from the *HHIRF tandem* were passed through a closed gas cell containing hydrogen or helium at pressures of 5 to 30 Torr. The cell entrance window was a 1.7-mg/cm² Al foil. At the lowest energy, the predicted equilibrium fraction of bare (8+) oxygen was 85%. At energies greater than 160 MeV, the 8+ fraction was more than 95%. X rays were measured at 90° with a Si(Li) detector which was energy-calibrated before, after, and during the run. Results of these measurments are shown in Fig. 4.12. As indicated there, centroid energies very nearly match the calculated values at all energies tested.

ORNL-DWG 88-19128

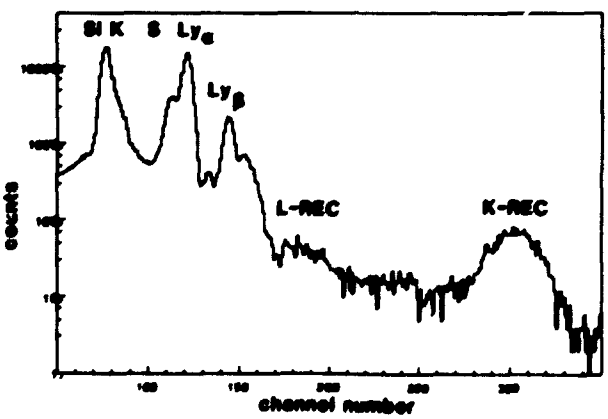

Fig. 4.10. X rays generated by 180 MeV S^{16+} ions channeled through a 0.42-μm-thick silicon crystal along with <110> axis. Observation angle was 46.5° in the lab frame.

ORNL-DWG 88-19124

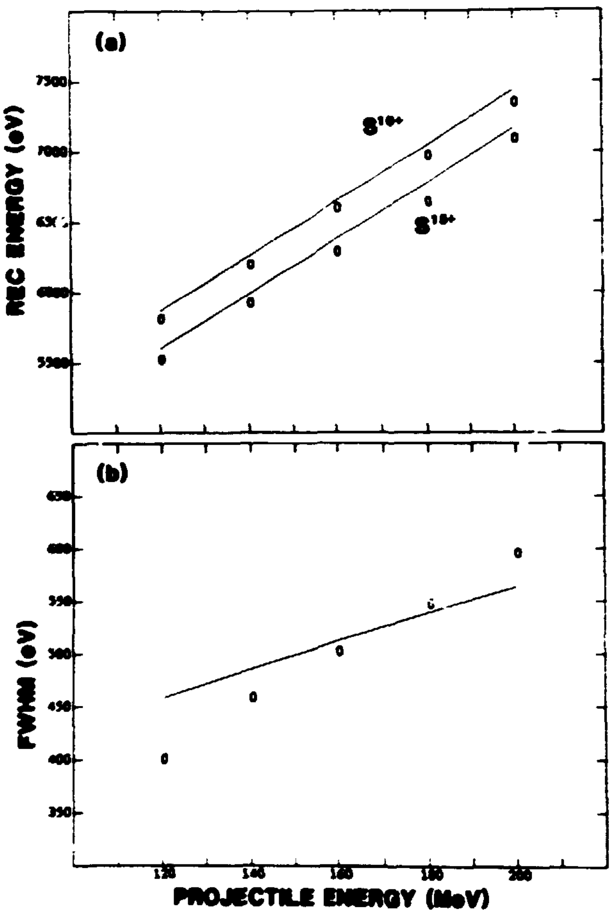

Fig. 4.11. (a) Peak centroid energies for REC by S^{16+} and S^{15+} ions channeled through a 0.41-μm Si <110> crystal. Solid line displays the results of theory corrected for projectile energy loss in the target and Doppler shift effects, including those due to intensity variation of REC radiation over the viewed solid angle aperture. (b) Measured and calculated REC peak widths (FWHM) for S^{16+} channeled through 0.42-μm Si <110>. Calculations assume a Fermi distribution of target electron momenta with Fermi energy of 1[illegible] eV.

It appears then that the REC peak energy shift observed for silicon targets represents a solid-state effect of unknown specific origin. We are currently exploring theoretically the possibility that shielding of the projectile charge by wake electrons traveling with the ion in the silicon and subsequent lowering of the projectile K-shell binding energy might lead to such an effect.

---

1. ORAU Postdoctoral Research Associate.

2. Graduate student on assignment from the University of Heidelberg, Heidelberg, West Germany.
3. Partial support provided by the Joint Institute for Heavy Ion Research.
4. Analytical Chemistry Division, ORNL.
5. ORAU, University of Tennessee at Chattanooga.

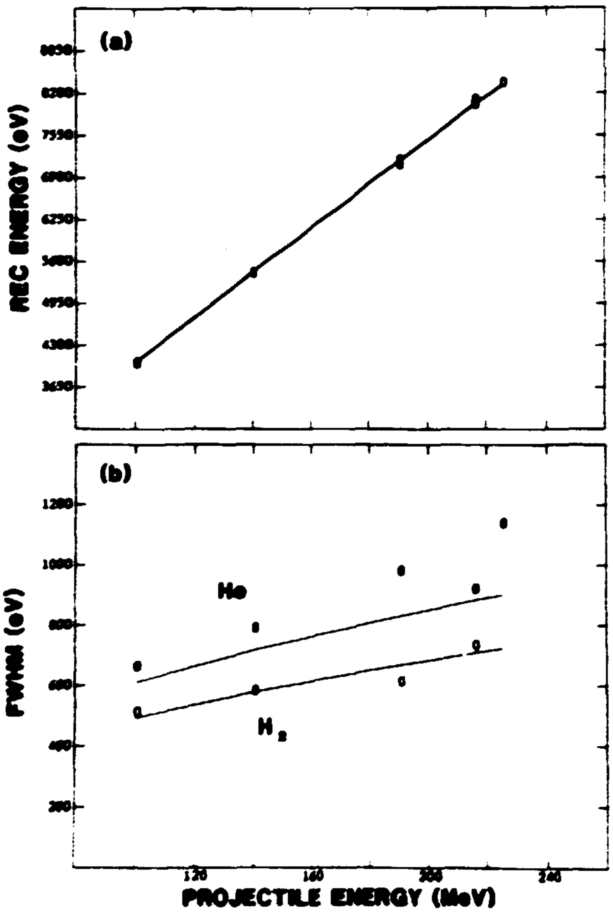

Fig. 4.12. (a) Peak centroid energies for REC by O^{8+} colliding with hydrogen and helium gases at 5 to 30 Torr. Solid line displays the results of theory corrected for projectile ion energy loss in the gas cell entrance window and in the gas and relativistic Doppler shift at the viewing angle of 89.1°. (b) Measured and calculated REC peak widths (FWHM) for O^{8+} colliding with H_2 and He. Calculations assume target hydrogenic 1s wave functions.

ATOMIC PHYSICS FACILITY AT HHIRF

P. F. Dittner

An AIM project to construct two beam lines dedicated to atomic physics in the recently constructed south annex (T109) to the HHIRF has been completed. An overview of the beam lines is shown in Fig. 4.13. The transfer line (beam line 41) is an in-line continuation of the HHIRF rotatable line 17 (BL 17). Beam line 41 (BL 41) consists of the following components (starting at the juncture with BL 17): a pneumatic isolation valve (1), an 800 ℓ/s cryopump (2), a magnetic quadrupole triplet (3), a set of horizontal and vertical adjustable slits (4), a pneumatic isolation valve (5), a magnetic horizontal and vertical steerer (6), a beam profile monitor (7), a Faraday cup (8), a 60-position foil changer (9), a 1500 ℓ/s cryopump (10), a magnetic horizontal and vertical steerer (11), a magnetic quadrupole (12), a set of horizontal and vertical adjustable slits (13), and a pneumatic isolation valve (14). BL 41 terminates at a dipole magnet (15) used to steer the ion beam to any one of four ports of the vacuum chamber (16) in the magnet. A pressure of 6×10^{-9} Torr has been achieved in BL 41. The elements of BL 41 were chosen such that BL 41 has the optics and the required pressure to also serve as the first part of the transfer line from HHIRF to the planned heavy ion storage ring for atomic physics.

Two beam lines exit from the magnet chamber (16), beam line 43 (BL 43), at +15° with respect to BL 41, and beam line 45 (BL 45), at -22.5°. The chamber has two other ports, presently blanked off, for beam lines 42 and 46 at +30° and -45°, respectively. The magnet chamber is pumped by a 400 ℓ/s cryopump (17) and a pressure of 2×10^{-8} Torr has been achieved. BL 43 is a multipurpose beam line with the availability of good collimation for crystal channeling experiments. BL 43 consists of the following elements: a pneumatic isolation valve (18), two widely separated (2 m) sets of horizontal and vertical adjustable slits (19), a multipurpose chamber (20) having 14 flanges from 2.75" to 8" in diameter, a 450 ℓ/s turbomolecular pump (21), a 6" cross (22), and a 1500 ℓ/s cryopump (23). A pressure of 2×10^{-8} Torr has been reached in BL 43.

BL 45 is designed to make measurements of dielectronic recombination and consists of the

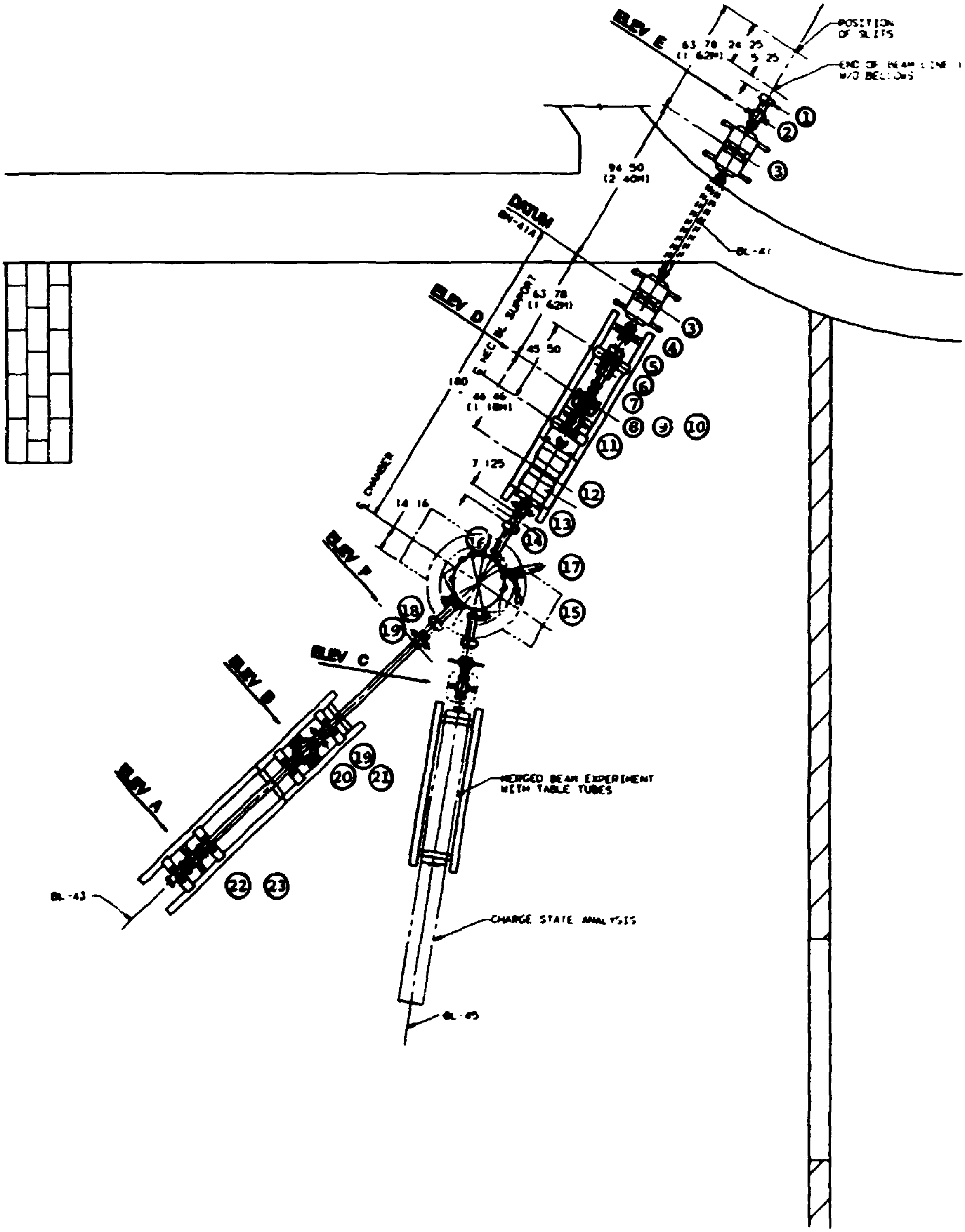

Fig. 4.13. Overview of beam lines 41, 43, and 45 in room T109 of Building 6000.

electron target and charge state analyzer previously located at the EN tandem. BL 45 is bakeable (150° C) and is pumped by three 220 ℓ/s combination ion and Ti sublimation pumps, and two 1500 ℓ/s cryopumps, achieving 1×10^{-9} Torr pressure. The electron beam has been operated at 1 kV and the magnetic charge-state analyzer is operational.

In early September, a beam of Gd ions was succesfully transported as far as the switching magnet as part of the commissioning of the beam lines. Success of this test has allowed us to schedule the first experiments using the merged beam apparatus.

EN TANDEM OPERATIONS

N. L. Jones P. F. Dittner

During the past year, the EN-12 was operated for 2300 hours in support of the accelerator-based atomic physics program. Several changes were made to upgrade the performance and reliability of EN-12. New acceleration tubes of an improved design were installed in November, resulting in reduced radiation and improved performance. Several ion source power supplies were either replaced or updated for improved source stability and performance. A failed charging belt was replaced in May after 8700 hours of use. A new radiation monitoring system was received in February to replace the original equipment that had failed due to age. Replacement of the high-energy vacuum system and installation of a high-speed turbo pump is planned for December 1988. This will be coupled with replacement of ~40 column grading resistors, an upgrade to the terminal stripper gas control value, and finally an increase in tank insulating gas pressure. It is anticipated that completion of these items will provide stable operation at terminal voltages up to 7.2 MV, and that the full benefits expected from the new acceleration tubes will be realized.

OBSERVATION OF LANDAU RESONANCES AT LOW MAGNETIC FIELD STRENGTH IN A HIGH-RESOLUTION LASER PHOTODETACHMENT STUDY OF O^-

H. F. Krause[1]

Studies of the photodetachment process ($A^- + h\nu \rightarrow A + e$) performed in the presence of a strong laboratory magnetic field (1 — 8 tesla) have been reported for atomic negative ions of sulfur and selenium.[2,3] When low-density ions contained in a Penning ion trap were illuminated by a narrow-band CW dye laser, the photodetachment yield was observed to increase periodically close to the reaction threshold (i.e., $h\nu$ = electron affinity) whenever the laser was tuned to quantized states of the free electron (i.e., Landau resonances separated by the classical electron cyclotron frequency, 28.2 GHz/tesla). The observed frequency of each broad resonance (Δf = 6 GHz) could be explained by the use of a simple theoretical model that assumed no interaction between the neutral atom and the departing electron.

More recent theoretical work of Crawford,[4] who assumed a realistic postcollision interaction, indicated that additional resonances associated with this interaction (e.g., Feshbach resonances) might also be observable if the experimental resolution, $f/\Delta f$, could be greatly increased. A much larger photodetachment cross section enhancement (i.e., a much stronger photodetachment yield at a resonance) also should occur under the improved conditions. Development of a greatly improved high-resolution apparatus would therefore allow the study of Landau spectroscopy at unprecedented levels of precision, provide the basis for a new photodetachment scheme that can produce a neutral particle beam at greatly reduced laser power, and perhaps give rise to a new method for producing spin-polarized neutral beams.[5] A novel beam concept for achieving dramatic improvements in spectral resolution was proposed by Krause.[5] The beam arrangement allows the effects of Doppler and Stark broadening to be reduced well below those experienced in a Penning trap (e.g., improvement of 10 – 100x) at the same magnetic field strength. Apparatus construction was completed in this reporting period. Preliminary results indicate that the apparatus resolution is 50x higher than achieved heretofore (e.g., spectral bandwidth below 100 MHz). The results provide the first evidence that (1) strong Landau resonances occur at a very weak magnetic field (0.03 tesla), (2) resonances are observable well above the reaction threshold (e.g., 4 x 10^{+13} Hz above threshold) at large Landau quantum number (L = 40,000), and (3) the study of magnetic field effects in O^- photodetachment is feasible.

In the shakedown experiments, O^- ions from a Colutron ion source were accelerated to 1.6 keV, momentum analyzed, and then collimated before injection into an E x B photoneutralizer (Wien filter). The ion beam (0.5-mm dia., ΔE = 2 eV) was collimated for a Doppler spread below 20 MHz inside the Wien filter. The ion beam intersected with a chopped laser beam at the Doppler-free angle in the center of the Wien filter (i.e., beams nominally perpendicular at this beam energy). The laser beam, which was linearly polarized in the direction of the magnetic field and propagated parallel to the direction of electrostatic field lines inside the Wien filter, was produced by a near-infrared, single-frequency diode laser. The CW laser delivered 20 mW of power within a linewidth of 50 MHz. Neutrals were detected downstream on a high-resolution two-dimensional position-sensitive detector (TDPSD). The ion beam was deflected into a Faraday cup between the Wien filter and the TDPSD. The beam line had to be maintained under ultrahigh vacuum conditions (i.e., 5 x 10^{-10} Torr) to minimize the neutral yield resulting from beam-gas electron detachment processes.

High-resolution spectra were obtained at a fixed laser frequency in Doppler tuning scans by varying the O^- beam direction in very small angular steps (i.e., 25 μrad/step) corresponding to a Doppler frequency shift below 10 MHz/step. Throughout these scans, the ion beam entered the Wien filter at a fixed location. By introducing a small imbalance electric field on the Wien filter about the balance condition, $\varepsilon = v_0B$, the ion beam direction changed before it crossed the laser beam. Since the neutral particles produced at the beam intersection region traveled to the TDPSD in a linear trajectory, the measured angle for each event indicated the direction of the O^- beam with respect to the laser beam at the time of photodetachment. The distribution of neutral intensity vs angle, derived from six-parameter list-mode data while the perturbing E field was rastered, was converted directly to an intensity vs frequency distribution using the known beam velocity and laser frequency.

High-resolution photodetachment spectra for O^-, obtained for a magnetic field strength of 306 G, is shown in Fig. 4.14. The same spectra accumulated while the rotating chopper wheel blade was blocking the laser beam were flat, and at least 20 times lower intensity. The observed

ORNL-DWG 88-14840

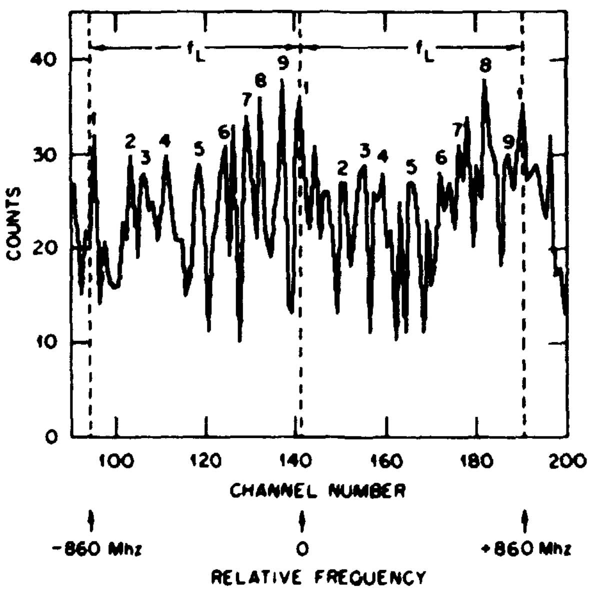

Fig. 4.14. High-resolution photodetachment spectra for $O^-(^2P_{3/2,1/2}) \to O(^3P_{2,1,0})$ in a magnetic field of 306 G. Numbered resonances are duplicated in two Landau cycles. The electric field vector of the laser was parallel to the applied magnetic field (i.e., $\Delta M = 0$ transitions). The wavelength of the laser was 7772.183 [A].

strength of the largest resonances (peak-valley ratio = 4) is large at this small field compared to the Se observations made at 200x higher magnetic field.[2] The total angular range for a complete scan was large enough to allow the periodic spectra (862 MHz Landau frequency) to be observed twice in the same scan. Fig. 4.14 shows that nine different resonances were resolved within each Landau cycle. The centroid position of each structure seen in the left Landau cycle is duplicated in the right Landau cycle within 20 MHz. Each observed peak corresponds to a Landau resonance at the most probable Zeeman lines (e.g., $\Delta M = 0$ transitions) for any of six electronic band systems of $O^-(^2P;\ J = 1/2,\ 3/2) \rightarrow O(^3P;\ j = 2,\ 1,\ 0)$. Landau quantum numbers that are different for each band system lie within the range 9,000 — 39,000. Spectra of the same appearance but with shifted phase were observed when the laser frequency was changed by a noninteger multiple of the Landau frequency. The repeat frequency of all spectra were shown to agree with the classical electron cyclotron frequency for magnetic field intensities in the range, 0.02 — 0.1 tesla. Also, measured spectra were flat when a broadband laser was substituted for the single-frequency laser. These tests appear to eliminate the possibility that the observations resulted from a hidden apparatus defect.

Although the O^- spectra are extremely complicated, identification of the most prominent lines in terms of the O^- electronic structure should be possible using computer simulation techniques. However, data of higher statistical significance at other laser wavelengths will be required. Important issues such as the possible occurrence of additional lines (e.g., Feshbach resonances) cannot be addressed until the ongoing effort to assign resonances has been completed.

---

1. Work supported by the U.S. Army SDC, Huntsville, Alabama.

2. W. A. M. Blumberg, W. M. Itano, and D. J. Larson, Phys. Rev. Lett. 40, 1320 (1978).
3. R. E. Elmquist et al., Phys. Rev. Lett. 58, 333 (1987).
4. O. H. Crawford, Proc. 4th Int. Symp. on Production and Neutralization of Negative Ions and Beams, James G. Allessi, ed., Brookhaven National Laboratory, AIP Conf. Proc. No. 158 (1987) p. 663.
5. H. F. Krause, Ibid., p. 673.

ENERGY- AND ANGLE-RESOLVED PHOTOELECTRON SPECTROSCOPY OF FAST-MOVING NEGATIVE IONS

D. J. Pegg[1] J. Dellwo[2]
J. S. Thompson[2] G. D. Alton
R. N. Compton[3]

We have used the energy- and angle-resolved technique of photoelectron detachment spectroscopy to investigate the interaction of a fast beam of metastable He^- ions with radiation. The spectral dependence of the kinetic energies, yields, and angular distributions of the electrons ejected in photodetachment has been studied. Such measurements allow us to determine the electron affinity, the asymmetry parameters, and the photodetachment cross sections, qualities associated with the structure of the He^- ion and its interaction with photons.

The apparatus used in this work is shown schematically in Fig. 4.15. The apparatus has been described in detail in the paper by Pegg et al.[4] and in the previous Physics Division *Progress Report* (ORNL-6420). A fast beam of He^- ions is crossed, in a perpendicular geometry, by an energy-resolved beam of photons from a pulsed laser. As a result of the interaction, known

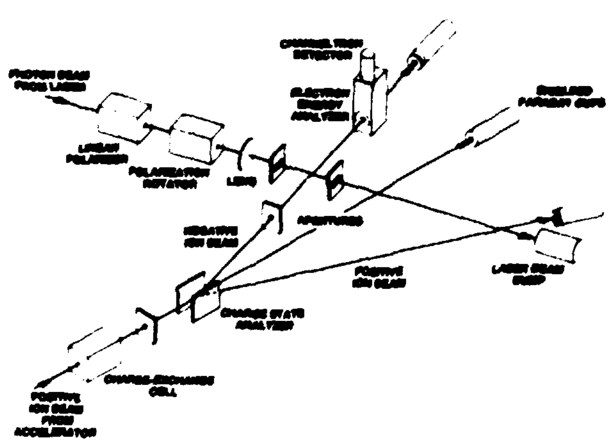

Fig. 4.15. Schematic of the crossed laser-ion beams apparatus used in the fast-beam photodetachment measurements.

amounts of energy and angular momentum are transferred to the ions. The tenuous beam of He^- ions is produced by double-charge transfer collisions when a momentum-selected beam of He^+ ions from an accelerator is passed through a Li-vapor charge-exchange cell.

Since the source of negative ions used in these experiments is a fast, unidirectional beam, the reference frame in which the "physics" occurs moves with respect to the laboratory frame in which measurements are made. Consequently, there will be kinematic modifications of the kinetic energies, yields, and angular distributions of the photoelectrons which are ejected from the moving ions. Effects such as kinematic line shifting and peak doubling are frequently exploited in our measurements.

During the past year, most of our work has been concentrated on an investigation of the photodetachment of the metastable negative ion, He^-, which is formed in the spin-aligned $(1s2s2p)^4P$ state as a result of an electron attaching itself to a He atom in the metastable $(1s2s)^3P$ state. Figure 4.16 shows a spectrum of electrons produced when a 40-keV beam of He^- ions was photodetached using a laser wavelength of 698.5 nm. Peaks 2 and 3 are associated with the photodetachment exit channels that leave the residual He atom in the $(1s2p)^3P$ and $(1s2s)^3S$ states, respectively. As part of a longer term goal of measuring the partial cross sections for these two competing processes, we have made measurements of the angular distributions of the electrons associated with peaks 2 and 3. These angle-resolved measurements determine the asymmetry parameter, β, which characterizes the shape of the electron emission pattern. The measurements are made by determining the yield of each photoelectron peak as a function of the angle, θ, between a fixed collection direction (in our case, the direction of motion of the ion beam) and the variable direction defined by the electric field vector of the linearly polarized laser beam. A typical measurement is shown in Fig. 4.17. For the present case of plane-polarized radiation in the electric dipole approximation and an independent electron model, the shape of the angular distribution should take the form $1 + \beta P_2(\cos\theta)$, where $P_2(\cos\theta)$ is the second-order Legendre polynomial. The apparatus has been tested on reference beams of Li^- and D^- ions, and the expected $\cos^2\theta$ ($\beta = 2$) distributions were obtained in each case.

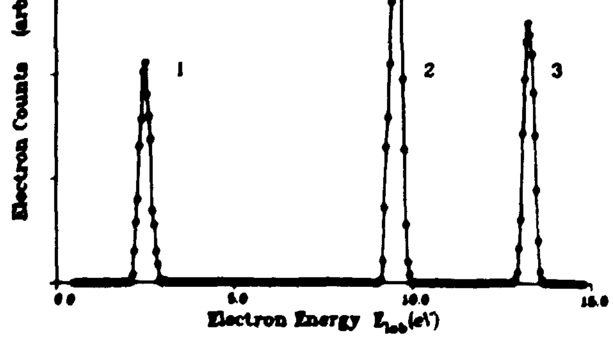

Fig. 4.16. A spectrum of electrons photodetached from a beam of He^- ions. The origins of peaks 2 and 3 are described in the text. Peaks 1 and 2 form a kinematically doubled pair.

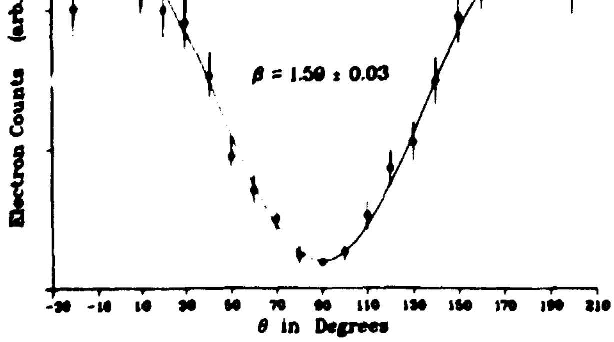

Fig. 4.17. Angular distribution of electrons photodetached from 30 keV beam of He^- ions. The solid curve is a weighted least squares fit of the data to the form $1 + \beta P_2(\cos\theta)$.

The results of the measurements of β, as a function of photon energy, for peak 2 is shown in Fig. 4.18. These electrons are ejected in the process: $h\nu + He^-(1s2s2p\ ^4P) \rightarrow He(1s2p^3P) + e^-$. Since an s-orbital electron is ejected, the outgoing electron should carry away, if correlation is neglected, one unit of orbital angular momentum, i.e., it is a p wave. This situation corresponds to $\beta = 2$ or a $\cos^2\theta$ distribution for all photon energies. A value of $\beta = 2$ was obtained at a photon energy of 2.46 eV, but the value of β for this process is seen to decrease rather sharply and then level off at lower photon energies. Apparatus tests were made using

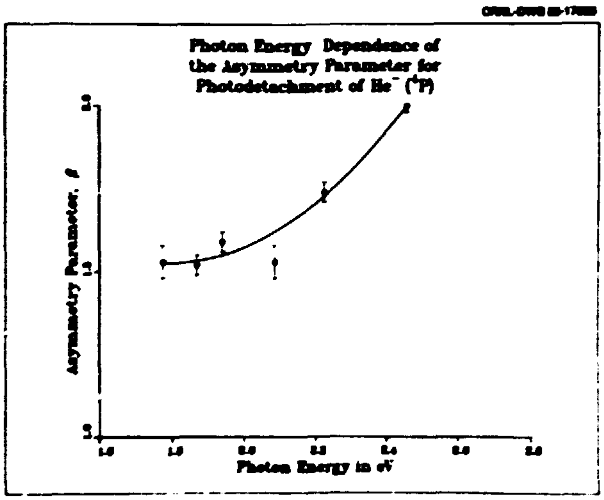

Fig. 4.18. The spectral dependence of the asymmetry parameter, β, for the photodetachment process, $h\nu + He^-(1s2s2p\ ^4P) \rightarrow He(1s2p^3P) + e^-$.

D^- ions at these lower energies and $\beta = 2$ was obtained, as expected. An explanation of this anomolous behavior in β, which must be associated with correlation of some form, is presently being sought.

---

1. Adjunct staff member from the Department of Physics, University of Tennessee, Knoxville, TN 37996.
2. Graduate student from the Department of Physics, University of Tennessee, Knoxville, TN 37996.
3. Health and Safety Research Division, ORNL, and Department of Chemistry, University of Tennessee, Knoxville, TN 37996.
4. D. J. Pegg et al., Phys. Rev. Lett. 59, 2267 (1987).

ARGON RECOIL-ION CHARGE-STATE DISTRIBUTIONS PRODUCED BY BEAMS OF 23 MeV $Cl^{5+,8+,10+}$

J. C. Levin[1] H. Cederquist[2]
C.-S. O[1] C. Biedermann[1]
I. A. Sellin[3]

Multiple-vacancy production in target gases by energetic charged projectiles is of fundamental theoretical interest. As a probe of the strong interactions between projectile and target electrons, such collisions epitomize the many-body collision problem. Measurements of recoil-ion charge distributions in coincidence with the scattered projectile charge state have been made for many systems, but only rarely have recoil-ion spectra for coincident single or multiple projectile-electron capture or loss been obtained for the same collision partners.[4] Further, calculated cross sections for capture of one to four electrons from an argon target by 1.4 MeV/u U^{44+} ions are said by the authors[5] to reproduce well the maxima of the recoil-ion charge-state distributions but to describe poorly their widths.

We have measured argon recoil-ion distributions produced by beams of 23 MeV $Cl^{5+,8+,10+}$ as a function of the degree of projectile capture or ionization. Ion beams produced by the Oak Ridge National Laboratory EN Tandem Facility were used to produce Ar recoil ions in a dilute gas target maintained in the extraction region of a time-of-flight analyzer. Ar^+ recoil, detected in a dual channel-plate detector ~ 1 μsec subsequent to creation, provided the start pulses to a time-to-amplitude converter (TAC). Projectiles were dispersed by an electrostatic charge sorter and the detected particles, suitably delayed, provided the stop pulses to the TAC.

Recoil ion time-of-flight spectra for single or double capture to, or loss from, beams of 23 MeV Cl^{8+} incident on argon are illustrated in Fig. 4.19. Peak widths are observed to increase as a function of final projectile charge state indicating greater recoil energy associated with such processes.[6,7] More striking is the similarity between spectra corresponding to single loss and single capture, and between spectra corresponding to double loss and double capture.

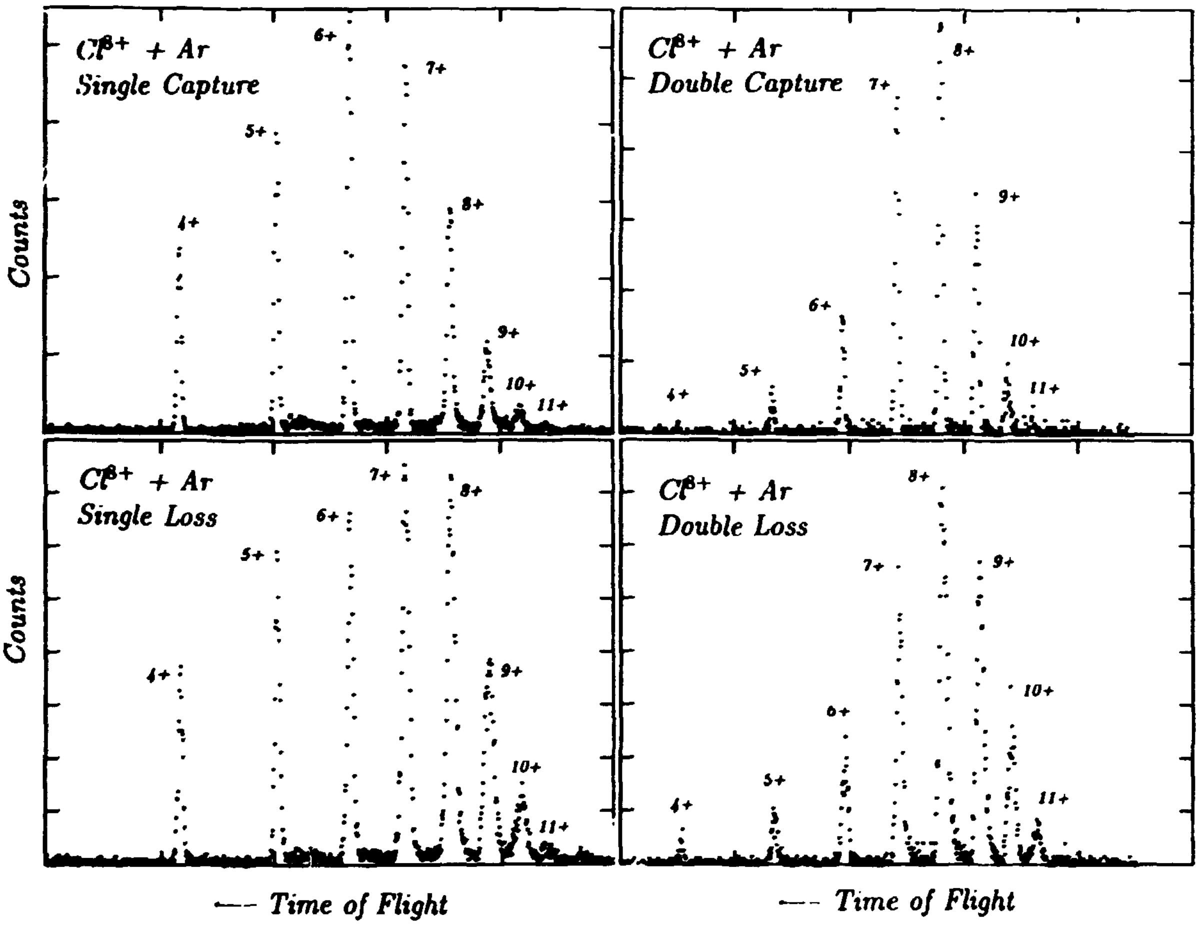

Fig. 4.19. Time-of-flight spectra for argon recoil ions produced by beams of 23 MeV Cl^{8+}.

Determination of impact parameters which characterize these interactions indicates that capture occurs primarily from the argon L shell[7] accompanied by some M-shell ionization. The resultant charge-state distributions for single and double capture can be described well by the assumption of Auger decay of one or two argon L-shell vacancies superimposed upon a binomial distribution of M-shell ionization. The similarity of the loss spectra to the capture spectra suggests that the mechanism by which projectile electrons are lost is through direct interaction with target electrons, producing inner-shell vacancies in the target. This is in contrast to classical trajectory Monte Carlo calculations which indicate that the systems similar to that being studied here, target L-shell ionization, is accompanied by nearly complete ionization of the M shell by the projectile.[5]

---

1. Department of Physics, University of Tennessee, Knoxville, TN 37996.
2. Research Institute of Physics, Stockholm, Sweden.
3. Adjunct staff member from the University of Tennessee, Knoxville, TN 37996.
4. A. Müller et al., Z. Phys. D-Atoms, Molecules and Clusters 7, 210 (1987).
5. A. Müller et al., Phys. Rev. A 33, 3010 (1986).
6. J. C. Levin et al., Phys. Rev. A 36, 1649 (1987).
7. J. C. Levin et al., Phys. Rev. A 38, 2674 (1988).

RECOIL ION, SCATTERED ION, FREE ELECTRON TRIPLE COINCIDENCE MEASUREMENTS

M. Breinig[1] J. E. Freyou[2]

Fast collisions between highly charged heavy ions and neutral gas targets are characterized by many processes, such as projectile and target excitation and ionization and target electron transfer to projectile-centered, bound, and continuum states. Often many of these processes are involved in the same collision. To characterize a collision as completely as possible, the goal of the experimentalist must be to simultaneously determine as many collision parameters as possible, such as projectile and target charge state and state of excitation, projectile and target velocity (speed and direction), and the velocity of any free electrons leaving the collision.

For 1 MeV/u bare and one-electron oxygen and carbon projectiles colliding with neon targets,[3-5] we have coincidentally measured the projectile ion charge state and the target recoil-ion charge state after the collision, and the energy of a free electron emerging from the same collision with a velocity close to the beam velocity. The goal of this experiment is to answer the following questions:

(1) If a free electron moving with a velocity close to the beam velocity is produced, what is the most probable recoil-ion charge state?

(2) If, in addition, the exit charge state of the projectile is determined, what is the most probable recoil-ion charge state?

(3) If a recoil ion of a particular charge state and a projectile ion of a particular charge state are produced in the same collision, how probable is the production of a free electron moving with a velocity close to the beam velocity?

Most cusp electrons accompany a projectile which does not change charge. The most probable recoil-ion charge state for this case lies between two and three. Where the projectile captures a target electron into a bound state in addition to a cusp electron being produced, the recoil-ion charge-state distribution shifts towards higher charge states. Electron loss by the projectile does not produce such a large shift. This points to cusp electrons produced in coincidence with projectile electron loss and produced by projectiles which do not change charge being associated with a more gentle, larger impact, parameter collision. Cusp electron production, in addition to bound state capture, requires at least two target electrons to be involved which probably happens at smaller impact parameters and leads to higher recoil-ion charge states.

Except for the cases in which a cusp electron is produced in coincidence with projectile electron loss, the probability of producing a cusp electron if a recoil ion is produced increases with increasing recoil-ion charge state for all incident projectile ions. If the cusp electron is produced in coincidence with projectile ion electron loss, the probability of detecting a cusp electron if a recoil ion is produced decreases with increasing recoil-ion charge state for C^{5+} and O^{7+} projectile ions. The probability of producing a cusp electron, if a recoil ion is produced, is highest if the cusp electron is associated with a projectile-ion electron loss event and a low charge-state recoil ion.

---

1. Adjunct staff member from the University of Tennessee, Knoxville, TN 37996.
2. Department of Physics, University of Tennessee, Knoxville, TN 37996.

3. C. L. Cocke, Phys. Rev. A 20, 749 (1979).
4. A. S. Schlachter et al., Phys. Rev. A 27, 3372 (1983).
5. W. G. Graham et al., Phys. Rev. A 30, 722 (1984).

PRODUCTION AND TRANSPORT OF CONVOY ELECTRONS IN AMORPHOUS CARBON FOILS

J. P. Gibbons[1] C. E. Gonzalez-Lepera[1]
S. B. Elston[2] O. Heil[3]
R. DeSerio[1] H.-P. Hülskötter[1]
C. Biedermann[1] H. Rothard[3]
M. Breinig[2] I. A. Sellin[2]
C. R. Vane

In recent years, a picture has been emerging of an abundant population of electrons characterized by high angular momenta that accompany an ion during its passage through a thin solid target. Experiments leading to this view have observed both X-ray[4] and convoy electron emission.[5] The convoy secondary electron emission distribution produced by fast ions in foil targets becomes enriched in higher-order multipoles with increasing projectile speed. This can be interpreted as reflecting excitation of states having high n and ℓ (in an approximate hydrogenic basis) during passage through the bulk material, followed by electron loss processes[6] which populate the cusp region of the spectrum.

It is not yet clear how this high-ℓ population is formed, although there is general agreement that it is established in the bulk solid.[4,5,7,8] The expected continuity of transition amplitudes across the ionization threshold of free ions[6] suggests a close connection between these experiments and those that detect large populations of high Rydberg states of projectiles emerging from the target.[8] Thus, one might suppose a population of a complex of dynamic states in the solid analogous to Rydberg states in free atoms which relaxes upon exit from the target into free Rydberg states below threshold and continuum or convoy states of the projectile above threshold, the quantal version of the classical picture underlying the Monte Carlo stochastic perturbation calculations of Burgdörfer and Bottcher.[9]

The experiments we describe, performed at HHIRF, address the questions of production of convoy electrons having high angular momenta, and of the transport of such electrons in thin solid-foil targets. Collisions of 115-MeV O^{q+} ions (projectile velocity v_p = 17 a.u.), with q = 5 – 8 with self-supporting carbon-foil targets, were observed with an electrostatic, spherical-sector electron spectrometer equipped with position-sensitive detection (PSD) to provide angle-resolved emission distribution measurements. Most of the apparatus has been described in detail previously.[10] The output of the PSD system is decoded to recover the emission angles that, in combination with the spectrometer pass energy, determine the emission velocity components of the detected electron. By scanning the spectrometer deflection field, the entire three-dimensional $\vec{v}$- distribution of the cusp can be obtained.

Figure 4.20 displays a selection of results of such velocity distribution measurements. The data shown are contours of equal intensity in the emission-energy and polar-emission-angle plane of v_P = 17.0 a.u. O^{6+} and O^{7+} ions incident on carbon foil targets. The axes are scaled so that equal intervals in either direction represent approximately equal intervals in longitudinal projectile frame emission velocity v_ℓ and transverse projectile frame emission velocity v_t. The strong transverse emission observed is in agreement with our earlier work[6] demonstrating substantial higher-order multipole strengths, but we now find this true even for the thinnest self-supporting targets available, showing that this excitation occurs within the first few layers of the target at these collision velocities. In fact, our data show little (if any) evolution in multipole content with increasing target thickness, implying that the interactions which dominate the development of the ℓ-distribution have cross sections sufficiently large to produce mean excitation distances less than or on the order of the thickness of the thinnest target observed, and that we observe in the present experiment emission from an early established, nearly equilibrium n,ℓ distribution. The observation of high n,ℓ excitation and the rapidity with which an apparent equilibrium of such excitation is established is in at least qualitative agreement with recent theory.[9] The emission distributions show a gradual broadening with increasing foil thickness which we attribute to elastic and inelastic scattering of the convoy electron distribution in the bulk of the solid. This effect is further demonstrated by the plot, in Fig. 4.21, of the emission contour widths of one-electron oxygen projectiles on foils of varying thickness.

---

1. Department of Physics, University of Tennessee, Knoxville, TN 37996.
2. Adjunct staff member from the University of Tennessee, Knoxville, TN 37996.
3. Institut für Kernphysik, J. W. Goethe Universität, D-6000, Frankfurt am Main, FRG.
4. H.-D. Betz, D. Röschenthaler, and J. Rothermel, Phys. Rev. Lett. 50, 34 (1983).
5. S. D. Berry et al., J. Phys. B 19, L149 (1986).
6. J. Burgdörfer, Phys. Rev. Lett. 51, 374 (1983); J. Burgdörfer, Lecture Notes in Physics; Forward Electron Ejection in Ion Collisions, eds. K. O. Groeneveld, W. Mechbach, and I. A. Sellin (Springer-Verlag, Berlin, 1984), p. 32.
7. Y. Yamazaki et al., Phys. Rev. A 34, 4493 (1986).

8. E. P. Kanter et al., Nucl. Instrum. Meth. in Phys. Res. B10/11, 36 (1985).
9. J. Burgdörfer and C. Bottcher, to be published; J. Burgdörfer, Lecture Notes in Physics 294 (Springer-Verlag, Berlin, 1988), p. 344.
10. S. B. Elston, Nucl. Instrum. Meth. in Phys. Res. B24/25, 214 (1987).

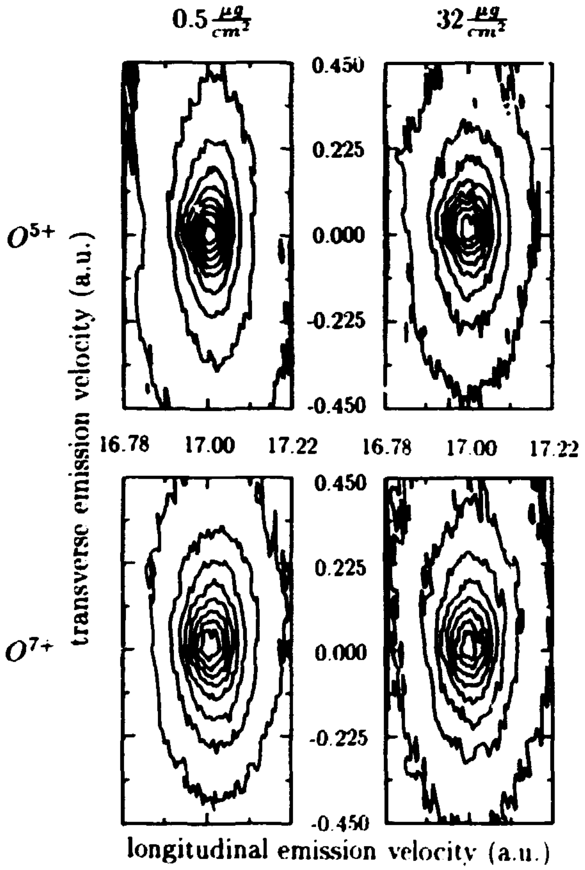

Fig. 4.20. Contour plots of equal convoy emission intensity of O^{5+} and O^{7+} at v_p = 17 a.u in carbon foils of nominal (uncalibrated) thicknesses 0.5 μm/cm² and 32 μg/cm². Contours shown represent multiples of 10% of the peak height. Scaling of the axes is chosen so that isotropic emission would produce essentially circular contours.

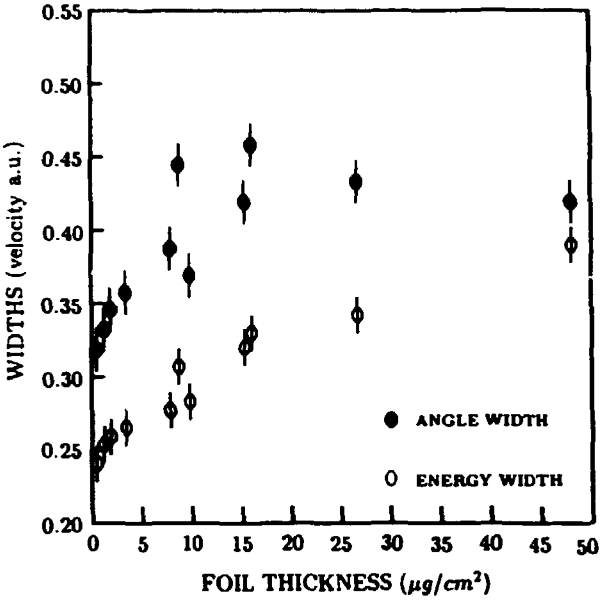

Fig. 4.21. Widths of the O^{7+} convoy distributions as a function of target thickness. The angular width is measured at the 50% contour (FWHM), but expressed as the equivalent projectile frame velocity (= $v_p\Delta\theta$). The energy width is similarly expressed in velocity units, and is measured at the 30% contour to avoid the dominance of the instrumental response near the singularity associated with the cusp.

ATOMIC PHYSICS FOR FUSION PROGRAM

ELECTRON-IMPACT IONIZATION OF MULTIPLY CHARGED CHROMIUM IONS

M. Sataka[1] D. Swenson[3]
S. Ohtani[2] D. C. Gregory

Absolute cross sections have been measured from below threshold to 1500 eV for electron-impact single ionization of chromium ions in initial charge states 6+, 7+, 8+, and 10+. The measurements utilized the ORNL-ECR ion source and electron-ion crossed beams apparatus. Chromium is an important constituent of wall materials in most modern plasma confinement devices, and an accurate knowledge of the characteristics of its ions is vital in order to understand edge-plasma behavior.

The ions in this study all have $3s^2 3p^n$ ground electron configurations, and we might expect the cross section curves to exhibit similar characteristics. Measurements on the lowest three charge states (6+, 7+, and 8+) are represented by the Cr^{7+} data shown in Fig. 4.22. Also shown in that figure are semiempirical Lotz[4] calculations for direct ionization from the ground ($3s^2 3p^5$ — lower curve) and metastable ($3s^2 3p^4 3d$ — upper curve) configurations. Clearly, the measured ionization threshold indicates the presence of metastable ions in the incident beam. The direct ionization calculation for metastable ions is in fairly good

RECOMBINATION RESONANCES IN ELECTRON-IMPACT IONIZATION OF MULTIPLY CHARGED URANIUM IONS

D. C. Gregory M. Sataka[2]
M. S. Huq[1] D. Swenson[3]
F. W. Meyer S. Chantrenne[4]

Single-ionization cross sections for uranium ions with initial charges 10+, 13+ and 16+ have been measured utilizing the ORNL-ECR ion source and electron-ion crossed beams apparatus. The indirect process of excitation of inner-subshell electrons followed by autoionization dominates the cross section, contributing up to a factor of 20 times more than direct ionization to the total. Double ionization of U^{10+} and U^{13+} were also measured in order to evaluate the branchings between single and double ionization for those ions.

The resonant recombination of an incident electron with a target ion (capture of a free electron to an excited level of an ion accompanied by excitation of one of the target-ion electrons) can decay to one of three final states: a stable ion and a free electron (a resonance or excitation event, resulting in no change in the ion charge); a stable ion (a dielectronic recombination event, resulting in an ion of lower charge); or a stable ion and two free electrons (an ionization event, resulting in an ion of higher charge than the target). The final path is the one considered here. The importance of this process to the overall magnitude of selected cross sections has been the subject of speculation[5] since 1981. Recombination resonance ionization proved elusive to experimentalists, with the first clear observations coming only recently.[6,7]

The first successful recombination resonance ionization measurements in this laboratory are presented in Fig. 4.24 for U^{13+}. Individual or closely spaced resonances are clearly resolved in the single ionization channel, with the cross section for the best-resolved feature of 4×10^{-19} cm^2. The 2 eV FWHM resolution of this feature (on the left in Fig. 4.24) is consistent with the predicted energy resolution of the

ORNL-DWG 88-14816

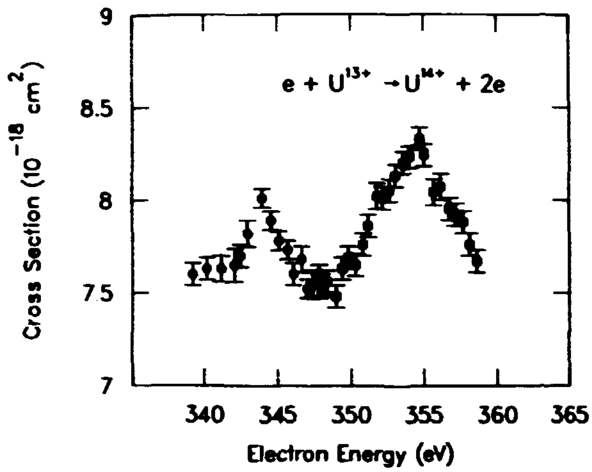

Fig. 4.24. Recombination resonant ionization features in U^{13+}. The circles and boxes represent two data scans. The energy width of the feature at lower energy is consistent with our predicted electron beam energy spread.

electron beam at this energy. The other feature (at higher energy) is broader and is due to several unresolved resonances. We speculate that the resonances in U^{13+} involve excitation of a 4f electron, but the complicated structure of uranium ions makes positive identification of these specific resonances unlikely. A similar pair of resonance structures were measured between 520 and 540 eV in ionization measurements on U^{16+}, but again positive identification of the resonances has not been made. Several improvements in our apparatus are planned which may make resonant recombination ionization measurements feasible in simpler systems where identification of levels will be possible.

---

1. ORAU Postdoctoral Research Associate.
2. Department of Physics, Japan Atomic Energy Research Institute, Japan.
3. Joint Institute for Laboratory Astrophysics, Boulder, Colorado, and ORNL.
4. Lawrence Livermore National Laboratory, Livermore, California.
5. Y. J. LaGattuta and Y. Hahn, Phys. Rev. A 24, 2273 (1981).
6. A. Müller, K. Tinschert, G. Hofmann, E. Salzborn, and G. H. Dunn, Phys. Rev. Lett. 61, 70 (1988).
7. A. Müller, G. Hofmann, K. Tinschert, and E. Salzborn, Phys. Rev. Lett. 61, 1352 (1988).

ELECTRON SPECTROSCOPY OF DOUBLE ELECTRON CAPTURE INTO AUTOIONIZING STATES FORMED IN LOW-ENERGY MULTICHARGED ION-ATOM COLLISIONS

F. W. Meyer M. S. Huq[1]
J. K. Swenson[1] R. A. Phaneuf
D. C. Griffin[2] K. Sommer[3]
C. C. Havener N. Stolterfoht[3]

Our collaborative study of Auger electron emission during low-energy ion-atom collisions has continued this fiscal year. Primary emphasis this year was on the determination of the ℓ-distributions of nonequivalent electron configurations populated in low-energy double-electron capture collisions. From an analysis of high resolution $1s^2 2pn\ell$ (n=6 and 7) Coster-Kronig electron spectra that was based on Hartree-Fock transition energy calculations, we were able to show that very high angular momentum states are produced,[4] as illustrated in Fig. 4.25. As was shown in an earlier publication,[5] production of the nonequivalent $2pn\ell$ (n>6) configuration must involve an electron-electron interaction (or electron correlation) in which energy is exchanged between the two transferred electrons, leaving one of the electrons in a tightly bound 2p orbital, while the other is promoted to a loosely bound Rydberg state. From our analysis of the ℓ-distributions produced in these same collisions, we arrived at the conclusion that these correlated two-electron transitions involve not only an exchange of energy, but also an exchange of angular momentum, which enhances the probability that the Rydberg electron occupies a state of very high angular momentum.

In addition to the analysis of ℓ-distributions, measurements of Auger electron emission were also carried out for the C^{6+} + He system. For this collision system, the $2pn\ell$ doubly excited states formed by double electron capture cannot decay by Coster-Kronig transitions, due to the near-degeneracy of the 2s/2p levels for fully stripped ions. Rather, they decay by KLX transitions, which occur at energies of a few hundred eV, an energy range much less subject to instrumental effects than the very low energies (<16 eV) at which the $1s^2\ 2pn\ell$ Coster-Kronig transitions occur in the O^{6+} + He system (see Fig. 4.25). Hopefully, the measurements on the C^{6+} + He system will provide an independent estimate for the importance of correlation effects in low-energy double-electron capture collisions. Analysis of the measured electron energy spectra for this system is in progress.

1. ORAU Postdoctoral Research Associate.
2. Consultant, Rollins College, Winter Park, Florida.
3. Permanent address: Hahn-Meitner Institut GmbH, Berlin, FRG.
4. F. W. Meyer et al., Phys. Rev. Lett. 60, 1821 (1988).
5. N. Stolterfoht et al., Phys. Rev. Lett. 57, 74 (1986).

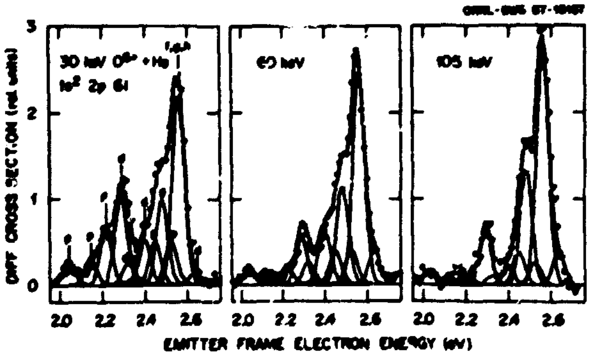

Fig. 4.25. Measured Coster-Kronig electron spectra for O^{6+} + He collisions at 30, 60, and 105 keV; shown also are twelve-Gaussian fits to spectra, based on Hartree-Fock atomic structure calculations. Labels in 30-keV spectrum indicate configurations contributing to each group.

ANGULAR ASYMMETRY IN THE EJECTED ELECTRON SPECTRUM PRODUCED IN He^+ + He COLLISIONS

J. K. Swenson[1] C. C. Havener
F. W. Meyer N. Stolterfoht[2]

In a follow-up experiment intended to provide an absolute normalization of the work described above, we performed measurements of the Auger electrons emitted from the symmetric He^+ + He system in the forward direction. This system had been studied by Bordenave-Montesquieu et al.,[3] who provided absolute cross sections for Auger electron emission into laboratory frame observation angles in the range 20 to 160°. These workers were able to show that, below about 15-keV projectile energy, the production of doubly excited states was equally probable in the target and projectile. On the basis of these earlier measurements, we expected to see in our 0° measurements of 10-keV He^+ + He collisions two sets of Auger lines of equal cross section (after the appropriate frame transformation), corresponding to target transitions and Doppler-shifted projectile transitions. Contrary to this expectation, we observed a strong enhancement of the target Auger transitions relative to the corresponding ones in the projectile, as is shown in Fig. 4.26. Also shown in Fig. 4.26 is a subsequently measured Auger electron spectrum for emission in the backward direction, in which the projectile Auger transitions are strongly enhanced. The results of a detailed experimental study of the dependence of this strong target/projectile asymmetry on the Auger transition rate, observation angle, and projectile energy can be submitted as follows. The enhancement occurs for observation angles that require the emitted fast Auger electron to "pass" the slowly moving singly charged collision partner. Strong enhancement is confined to angles within about 20° of the forward/backward direction. The enhancement is strongest for the shortest-lived Auger transitions, but increases with increasing projectile energy in the range 5 to 15 keV.

To explain these observations, a model based on the idea of Coulomb deflection of the ejected Auger electron as it passes the singly charged collision partner on its way to the electron spectrometer was developed.[6] In this model the target/projectile asymmetry observed at 0° is due to an amplification of the target electron solid angle collected by the electron analyzer. Due to deflection in the Coulomb field of the charged projectile, all target electrons emitted into an annular cone are collected. In the absence of deflection, only those electrons whose directions lie within the acceptance of the analyzer can be collected. Figure 4.27 shows the strongly forward-peaked angular distribution calculated for target $2s^2\ ^1S$ Auger electron emission. In the absence of "Coulomb focusing," the angular distribution of electron emission from this doubly excited state, shown as the dash-dot line in the figure, is, of course, isotropic. The model calculations, which incorporate the time dependence of the electron emission and Coulomb deflection processes, also accurately reproduce the observed dependence of the asymmetry on Auger decay rate.

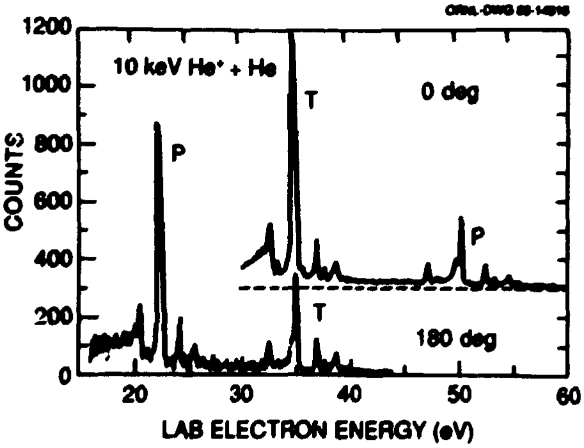

Fig. 4.26. Auger electron spectra for 10-keV He^+ + He collisions, measured at 0 and 180 degrees. Note enhancement of target-based transitions (group labeled T) relative to the corresponding projectile-based transitions (labeled P) at 0°, and the reverse trend at 180°.

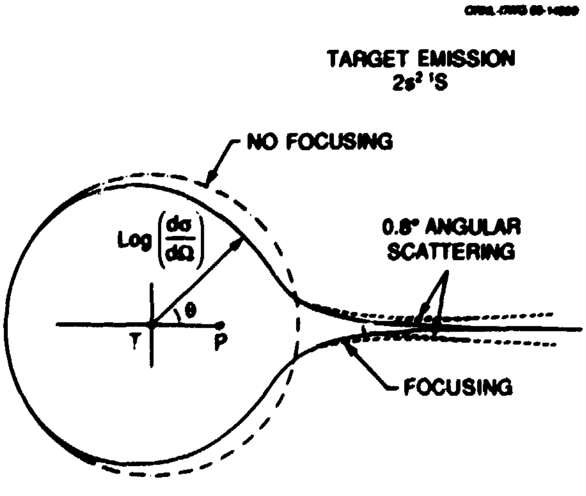

Fig. 4.27. Calculated angular asymmetry for target $2s^2\ ^1S$ emission following 10-keV He^+ + He collisions due to Coulomb focusing; a calculation including the effect of projectile angular scattering is shown as dashed lines.

Qualitatively, the longer the Auger lifetime of the state in question, the larger is the mean initial separation between Auger electron and charged collision partner, and the weaker the net deflection of the emitted electron. This results in a smaller asymmetry, in accord with the observed trend. The observed enhancement of the asymmetry with increasing projectile energy is at least partially explained by considering the energy dependence of the projectile angular scattering that occurs in the double excitation collisions. In general, angular scattering has an inverse dependence on projectile energy. Since the direction about which Coulomb focusing occurs is along the lines joining target and (scattered) projectile, the enhancement is smeared out over progressively larger angles as angular scattering increases, i.e., as collision energy decreases. As a result, a progressively smaller fraction of the enhancement will lie within the angular acceptance of the electron analyzer, giving a smaller net asymmetry at lower energies, in accord with the observed trend.

Further calculations will be performed to investigate the possibility of interference effects during Coulomb focusing, since there are, in general, always at least two different trajectories around the charged collision partner that result in the same electron scattering angle in the laboratory frame. Further experimental work is planned to investigate Coulomb focusing in multicharged collision systems where the effect will be even more pronounced.

---

1. ORAU Postdoctoral Research Associate.
2. Permanent address: Hahn-Meitner Institut GmbH, Berlin, FRG.
3. A. Bordenave-Montesquieu et al., Phys. Rev. A 25, 245 (1982).
4. J. K. Swenson et al., submitted to Physical Review Letters.

ELECTRON CAPTURE IN N^{3+} + H(D) COLLISIONS AT eV-keV ENERGIES USING MERGED BEAMS

M. S. Huq[1] C. C. Havener
R. A. Phaneuf

Using the ion-atom merged-beams apparatus, we have continued to measure total cross sections for electron capture resulting from collisions of various multicharged ions ($N^{3,4,5+}$) with H(D) atoms in the relative energy range extending from tenths of an eV/amu to over one thousand eV/amu.[2] Such measurements are important in astrophysics and in the edge plasma of magnetic fusion devices and provide a benchmark for collision theory. We are able to obtain such low collision energies by merging a relatively fast (~q × 10 keV) multicharged ion beam from the ORNL-ECR ion source with a neutral H beam traveling at nearly the same velocity. The 99%-pure ground-state H is produced by photodetachment as a beam of H^- passes through the inner cavity of a 1.06-μm Nd:Yag laser. The 80-cm-long interaction path of the beams is maintained at an average pressure of 2×10^{-10} Torr. Details of the apparatus and technique can be found elsewhere.[3]

Absolute total cross sections for single electron capture σ_{32} for collisions of N^{3+} with H(D) are shown in Fig. 4.28 as a function of relative collision energy expressed in eV/amu. As can be seen in the figure, the measurements agree with previous experimental measurements at the higher energies and with the theoretical calculations throughout the entire energy range. It should be noted that most of the N^{3+} (>90%) ions produced by the ECR source are in the metastable state, whereas the calculations are

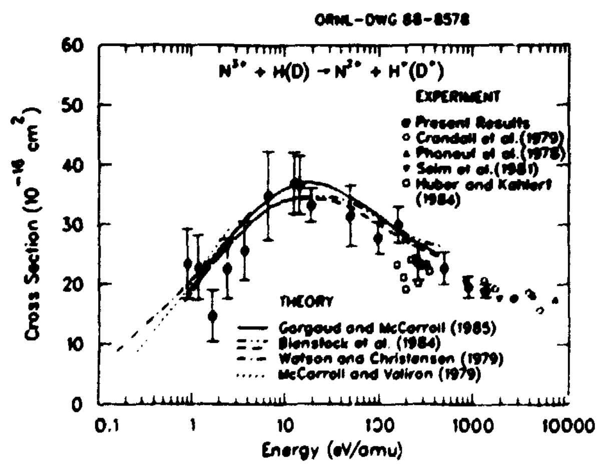

Fig. 4.28. Comparison of merged beams data for electron capture in N^{3+} + H(D) collisions with previous measurements and theory. The error bars denote estimated relative experimental uncertainties estimated at a 90% confidence level.

performed for ground-state incident N^{3+} ions. The good agreement between the calculations and the measurements indicates that the metastable cross section is the same as the ground-state cross section.

Measurements for single electron capture σ_{43} for collisions of N^{4+} + H(D) are shown in Fig. 4.29. Agreement is shown to be good with the previous experimental measurement at the highest energy and the theoretical calculation at the lowest energy. We attempted to extend the measurements below 1 eV/amu, but were prevented by poor signal-to-noise ratios caused by a combination of the low cross section (1×10^{-15} cm^2) and the low target thickness (as the interaction energy approaches zero the beams no longer interact). Since the Li-like N^{4+} ion beam does not have any metastable components in it, the measurements presented here correspond to ground-state reactants and have high enough accuracy such that future theoretical calculations can be compared critically against these data.

Measurements for the collisions of N^{5+} with H(D) are shown in Fig. 4.30. There is considerable scatter in the data due to the instability of the N^{5+} beam produced by the ECR ion source. Theoretical calculations[4] reveal that charge transfer for this system occurs primarily into

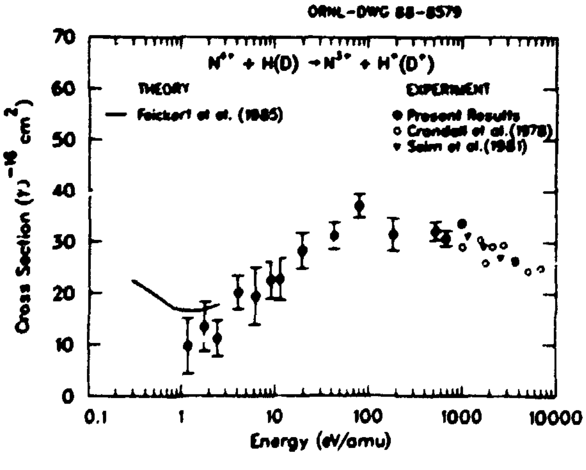

Fig. 4.29. Comparison of merged-beams data for electron capture in N^{4+} + H(D) collisions with previous measurements and theory.

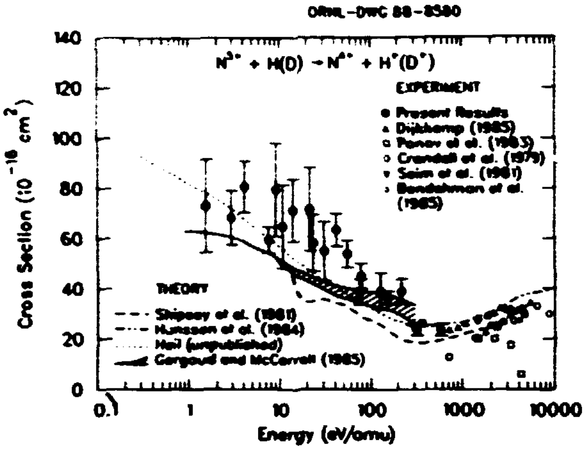

Fig. 4.30. Comparison of merged-beams data for electron capture in N^{5+} + H(D) collisions with previous measurements and theory.

the $(1s^2 4s)^2S$ state of N^{4+}. Capture into the 3s, 3p, and 3d states are found[4] to contribute negligibly at energies less than 1 keV/amu. Despite the large scatter present in the data, the measurements reproduce the general trend of σ_{54} as predicted by theory.

Previous measurements[3] with O^{5+} which showed a discrepancy with theory at the lowest energies has led toward the speculation that capture plus excitation channels may be important for the O^{5+} + H(D) system below 20 eV/amu.[5] In contrast, these present measurements have agreed well with theory and experiment (where they exist) and have increased our confidence in this technically difficult technique.

---

1. ORAU Postdoctoral Research Associate.
2. Summary of paper: M. S. Huq, C. C. Havener, and R. A. Phaneuf, "Low-Energy Electron Capture by N^{3+}, N^{4+}, and N^{5+} from Hydrogen Atoms Using Merged Beams," to be submitted to Physical Review A.
3. C. C. Havener et al., "Merged-Beams Measurements of Electron-Capture Cross Sections for O^{5+} + H at eV Energies," in press, Physical Review A.
4. M. Gargaud and R. McCarroll, J. Phys. B. 18, 463 (1985); E. J. Shipsey, J. C. Browne, and R. E. Olson, J. Phys. B. 14, 869 (1981).
5. C. C. Havener et al., "Electron Capture by Multicharged Ions at eV Energies," in press, Journal de Physique.

ELECTRON SPECTROSCOPY OF MULTICHARGED ION-SURFACE INTERACTIONS

F. W. Meyer   S. H. Overbury[2]
C. C. Havener   K. J. Reed[3]
D. M. Zehner[1]   K. J. Snowdon[4]

In our continuing collaborative investigations of multicharged ion-surface interactions, progress this year has been made on two fronts. Firstly, we have obtained a more detailed picture of the role of inner shell processes in the production of the discrete Auger transition features observed in the emitted electron energy distributions. Secondly, the experimental apparatus used for the surface interaction studies has been substantially improved.

Our understanding of the role of inner-shell vacancy transfer processes in multicharged ion-surface interactions has improved by implementing the variable screening model of Eichler and Wille[5] to calculate adiabatic molecular orbital (MO) energy levels for a number of the collision systems we have experimentally studied. The calculations give information about the range of internuclear separations at which MO pseudocrossings or rotational couplings may occur. They also give a more realistic picture of the possible pathways along which inner-shell excitations occur, and how sensitive these pathways are to the collision partners making up the quasi-molecule. For example, the calculations have provided a qualitative explanation for our experimental observation that projectile K-shell excitation occurs for N, O, and F ions incident on a Cu target, but does not occur for those same ions incident on Au (see Fig. 4.31).

The apparatus used in our studies of multicharged ion-surface interactions was also significantly upgraded this year. The first improvement was the addition of a beam collimation/monitoring section upstream of the target manipulator. This monitor allows more convenient normalization of the measured emitted electron spectra to the incident ion flux. The main improvement in the apparatus, however, was replacement of the fixed-position CMA electron spectrometer by a small hemispherical-sector electron analyzer mounted on a rotation feedthrough to permit measurements of electron spectra over a large range of emission angles. The electron spectrometer also has a deceleration/focusing stage, by which the electron pass energy can be reduced with only a minimum of signal loss. The new electron spectrometer thus provides the capability for angle- as well as energy-resolved measurements. Figure 4.32 shows sample electron energy spectra at three different emission angles acquired with this new spectrometer for 70-keV O^{7+} projectiles incident on Au at 10°. From the well defined Doppler shifts of the KLL Auger features one can deduce that essentially all of the neutralization of the multicharged ion occurs prior to

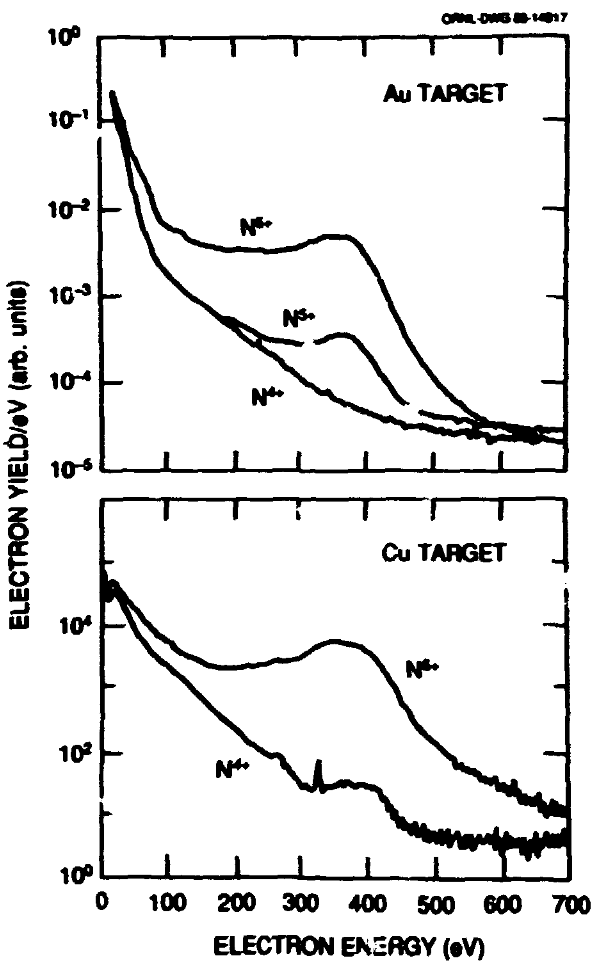

Fig. 4.31. Energy distribution of electrons emitted during collisions of N^{q+} ions incident on Au and Cu targets at 5°, measured using a fixed-position cylindrical mirror (CMA) electron energy analyzer. Note the presence of a projectile KLL Auger feature at 400 eV electron energy for N^{6+} incident on Cu, and the absence of this feature for the same ion incident on Au.

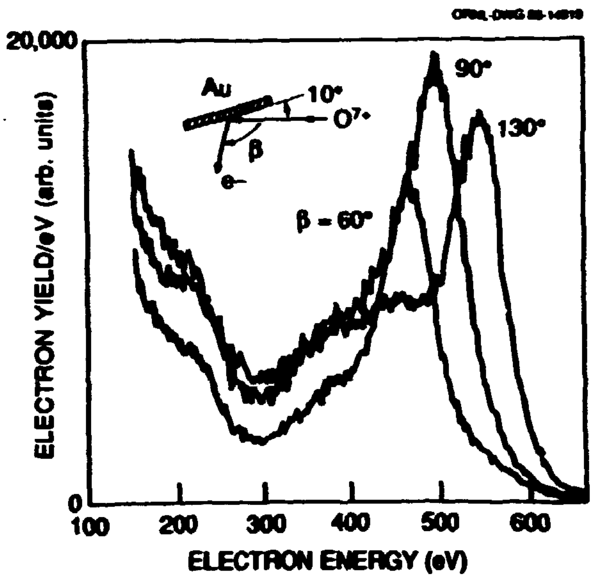

Fig. 4.32. Ejected electron energy distributions for O^{7+} ions incident on a Au surface for three different emission angles (for geometry of measurement, see inset), measured using the new rotatable hemispherical-sector electron analyzer.

penetration of the surface. Extensive measurements are planned for FY 1989 to exploit the utility and flexibility of the new apparatus by measuring angular distributions of electron emission, and investigating at higher resolution the discrete features observed in our earlier electron energy spectra.

---

1. Solid State Division, ORNL.
2. Chemistry Division, ORNL.
3. Lawrence Livermore National Laboratory, Livermore, California.
4. Osnabrück University, Osnabrück, FRG.
5. J. Eichler and U. Wille, Phys. Rev. A 11, 1973 (1975).

5. THEORETICAL PHYSICS

Major areas of research in the theoretical physics program in the Division deal with topics in atomic and nuclear physics. There is a significant overlap of interests of researchers in the two areas, particularly in the field of computational physics. This is particularly true where various aspects of relativity and the Coulomb force are involved. This has led us, in the past year, to initiate the development of an Institute for Computational Physics in cooperation with the University of Tennessee and Vanderbilt University. It is envisaged that this institute will involve the offering of courses in computational physics at the universities, joint seminar series, the development of a dedicated parallel processor computing facility, and most important, a close and stimulating interaction among researchers at the three institutions.

The main areas of our studies in nuclear physics are relativisitic heavy-ion physics, heavy-ion reactions at low and intermediate energies, and nuclear structure physics. These areas complement programs in experimental nuclear physics in the Division carried out at the Holifield Heavy Ion Research Facility, CERN, and GANIL. Similarly, the atomic theory programs to study various charge transfer, capture, and ionization processes reflects much of the experimental atomic physics program on the EN Tandem Accelerator and within the Atomic Cross Sections for Fusion program.

In the past year, the theory program has been significantly enhanced by new appointments to the UT-ORNL Distinguished Scientist Program. In January of 1988 F. E. Close joined that program and has already expanded the division research program in the area of physics at the particle-nuclear interface. In July of 1988, J. H. Macek joined the group in theoretical atomic physics. The atomic theory effort at the Laboratory has almost doubled in the past year with the addition of one postdoc position and the establishment of the Distinguished Scientist program in atomic theory.

Finally, it is with extreme sorrow that we note the death of Georg Leander in the past year. The strengths he brought to the nuclear structure theory effort by his intellectual strengths and vibrant personality are sorely missed.

LEPTON PAIR PRODUCTION IN HEAVY-ION COLLISIONS

W-BOSON PAIR PRODUCTION IN ULTRA-RELATIVISTIC HEAVY-ION COLLISIONS

J. Wu[1] C. Bottcher
M. R. Strayer

Many processes have been discussed as probes of the formation and the decay of the quark-gluon plasma phase of matter in ultrarelativistic heavy-ion collisions.[2,3] Recently, a model[4] has been proposed to calculate the lepton pair production from the decay of vacuum excitations induced by the colliding nuclei. In this model the electromagnetic fields are approximated by the classical fields which are very strong and sharply pulsed near nuclei colliding at relativistic velocities, and the production processes are treated with the perturbative method. For the lowest-order processes the production cross section can be obtained in terms of phase space integrals. As a direct extension of this model, we may calculate the production of pairs of W-bosons.

In the standard electroweak model[5] the electromagnetic and weak interactions are unified in a common SU(2) × U(1) gauge structure. The interactions between the electromagnetic and charged boson fields arise from the self-interactions of the non-abelian SU(2) gauge fields as follows:

$$\begin{aligned} \mathscr{H}_3 = -ie\{(\partial_\mu A_\nu - \partial_\nu A_\mu)W^{-\mu}W^{+\nu} \\ + (\partial_\mu W^+_\nu - \partial_\nu W^+_\mu)A^\mu W^{-\nu} \\ + (\partial_\mu W^-_\nu - \partial_\nu W^-_\mu)W^{+\mu}A^\nu\}, \end{aligned} \quad (1)$$

and

$$\mathscr{H}_4 = -e^2(W^+_\mu W^{-\mu}A_\nu A^\nu - W^+_\mu W^-_\nu A^\mu A^\nu). \quad (2)$$

The lowest-order processes are shown in Fig. 5.1. The W-pair production cross section is

$$\sigma = \int d^2b \sum_{p,q} |< p^{(+)}q^{(-)} | S | 0 >|^2, \quad (3)$$

where the p,q are the indices for momentum and polarization (k,λ), and b is the impact parameter.

A dimensional analysis leads to the following cross section for the W-pair production:

$$\sigma = Z^4\alpha^4/M_W^2 \, f_W(\gamma,M_W), \quad (4)$$

where f_W is a slowly varying function of the energy γ and W-boson mass M_W. A conservative estimate is

$$f_W(\gamma,M_W) \sim \frac{\ln(\gamma,M_W/M_W)}{\ln(\gamma,M_W/m_e)} f_e(\gamma,m_e), \quad (5)$$

which is obtained by scaling the result of the corresponding calculation for the electron pair production. This gives a W-pair cross section for Au + Au at the energy of 100 GeV per nucleon hundreds of times larger than the cross section for the detection of W-bosons in a $p\bar{p}$ collider.

ORNL-DWG 88-14483

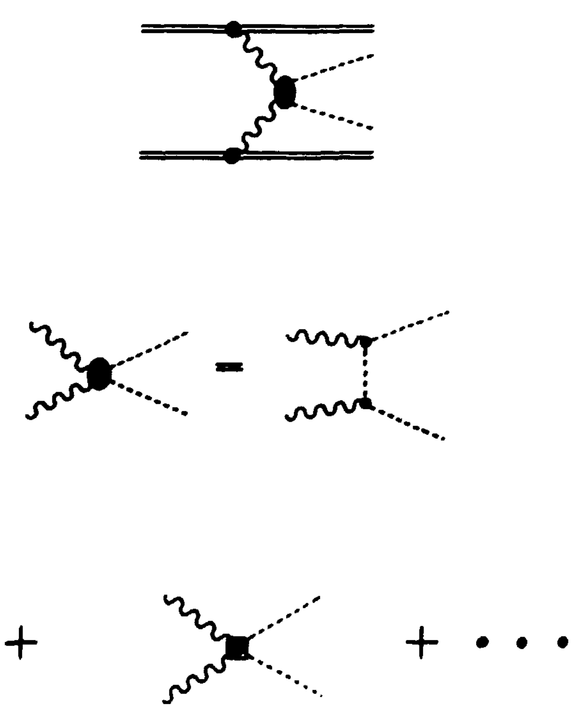

Fig. 5.1. The processes for W-pair production in heavy-ion collisions.

For the lowest-order processes, we can take the effective noninteracting Lagrangian for the charged W-boson fields with a mass term, i.e.,

$$\mathcal{L}_0 = -\frac{1}{2} W^+_{\mu\nu}W^{-\mu\nu} + M_W^2 W^+_\mu W^{-\mu}, \quad (6)$$

where $W_{\mu\nu} = \partial_\mu W_\nu - \partial_\nu W_\mu$. Equation (3) can be reduced to a phase space integral: $\int dk_p dk_q dk_\perp$, where k_p, k_q, and $k_\perp$ are the momenta of W^+, W^-, and the transverse momentum of the electromagnetic fields, respectively. This integration can be carried out by Monte Carlo methods with adequate precision.[5] The results will give us the qualitative behavior and a more detailed quantitative estimation for the background of W-boson production in ultrarelativistic heavy-ion collisions.

---

1. Joint Institute for Heavy Ion Research, ORNL.
2. G. Domokos and J. Goldman, Phys. Rev. D 23, 203 (1981); Phys. Rev. D 28, 123 (1983).
3. K. Kajantie and H. I. Miettenen, Z. Phys. C 9, 341 (1981); Z. Phys. 14, 357 (1982).
4. C. Bottcher and M. R. Strayer, to be published in Physical Review D.
5. See, for example, C. Itzykson and C. Zuber, Quantum Field Theory (McGraw-Hill, New York, 1980).

EFFECTS OF ELECTROMAGNETIC FORM FACTORS ON HEAVY LEPTON PAIR PRODUCTION

C. Bottcher   M. R. Strayer
D. J. Ernst[1]   J. Wu[2]

The point charge results discussed above, which apply directly to electron-positron production, can be generalized to the production of muons and tauons.[3] However, we note important differences in the production and emission of these heavy leptons. In contrast to electron pair production:

(1) Heavy lepton production occurs mainly within the interior of the nucleus, and is sensitive to details of the nuclear charge distribution. Because of the relatively small Compton sizes of the muon and tauon, and the correspondingly large Compton momentum, it is important to include effects from the nucleus and nucleon charge form factor. The Compton wavelength of the muon is about 2 fm, so that there is the

possibility that muon production will take place coherently over the interior region of the nucleus.

(2) Tauons with a rest mass of about 1.8 GeV/c^2 require substantial energy momentum transfer from the electromagnetic fields, with correspondingly large inelastic nuclear excitations. This necessitates a detailed description of the nuclear currents in terms of structure functions.

(3) The cross section yields for muons and tauons must be very different from those predicted by the equivalent photon approximation, which cannot correctly treat the nuclear currents. Here again, the details of the form factors and the structure functions can dramatically alter cross-section yields.

The inclusion of finite nucleus and nucleon elastic form factors into the two photon process follows from the usual procedure of vertex modification. We have employed the dipole form of the proton form factor, while the charge distribution coming from the nucleus was expressed as a Woods-Saxon form, with parameters adjusted to fit elastic electron scattering data.

We have surveyed muon pair production for nuclei and energies of interest to the RHIC design group. Several important features have been noted.

(1) There is some evidence of coherent muon production. The charge number dependence of these cross sections is roughly $Z^{2.4}$. This dependence is significantly less than predicted by calculations with point sources and serves to underscore the importance of the nuclear form factor.

(2) There is a strong dependence on the charge structure of the proton. This is evidenced by the comparison of the point charge and form factor results for the proton collisions.

(3) The largest effects of the proton form factor occurs at high energies. In our calculations the point charge electromagnetic interaction is "weakened" by the nuclear charge distributions. This leads to a domain of energies where perturbation theory is valid.

We are also examining tauon production. An interesting feature here is that proton-proton collisions produce the largest yields of tauons at high energy. Nonetheless, the yield of tauons is greatly supressed by the inclusion of the form factors.

---

1. Consultant from Texas A&M University, College Station, TX 77843.
2. Joint Institute for Heavy Ion Research.
3. C. Bottcher and M. R. Strayer, submitted to Physical Review.

ELECTRON PAIR PRODUCTION FROM PULSED ELECTROMAGNETIC FIELDS IN RELATIVISTIC HEAVY-ION COLLISIONS[1]

C. Bottcher M. R. Strayer

We present calculations of the electron pair production cross sections in relativistic heavy-ion collisions. The electron pairs arise from the decay of vacuum excitations induced by the very strong and sharply pulsed electromagnetic fields near nuclei which collide at relativistic velocities. We present an exact Monte Carlo evaluation of the two-photon terms describing this process, and we discuss at length the inadequacies of the approximation schemes that are inherent to the usual virtual photon approaches. Typical results for collisions corresponding to experiments at the AGS, CERN, and RHIC are discussed.

---

1. Abstract of paper submitted for publication in Physical Review D.

ANOMALOUS ELECTRON PAIR PRODUCTION IN HIGH ENERGY $\pi^- + p$ REACTIONS

D. J. Ernst[1] C. Bottcher
M. R. Strayer

In studies of hadron-hadron collisions, single lepton and dilepton production has been examined extensively. There has emerged from these studies a systematic result that the ratio of electron to pion yields are large and not understandable in terms of known meson decays. Experiments observing anomalous single electrons also have yields of positrons which are consistent with the possibility of a parent e^+e^- source.

Specifically, we are investigating anomalous electron pair yields from 17 GeV/c collisions of $\pi^- + p$.[2] In this experiment, the total cross section for forming anomalous pairs is about 0.25 μb. The pair distribution is measured as a function of the Feynman x-variable. All of the anomalous pairs occur at small values of the invariant mass and transverse momentum of the pair. We have calculated the leptons produced from the long-range electromagnetic fields in the foregoing collision, initially including the lowest-order two-photon diagrams. Two important points have emerged:

(1) The two-photon backgrounds are usually evaluated by using the Weizsäcker-Williams method. For large values of the invariant mass, $0.2 < M < 0.6$ GeV/c^2, the exact Monte Carlo evaluation of the long-range contribution to the two-photon diagrams predicts considerably enhanced yields.

(2) The dilepton production from the long-range electromagnetic fields are sharply peaked at low values of the invariant mass. This contribution to the $\pi^- + p$ experiment only comes from the tail of the distribution. Thus we expect the diagrams with an extra outgoing photon leg to dramatically increase the result, and we are in the process of calculating these diagrams.

---

1. Consultant from Texas A&M University, College Station, TX 77843.
2. M. R. Adams et al., Phys. Rev. D 27, 1977 (1983).

PROBING THE VACUUM WITH HIGHLY CHARGED IONS[1]

C. Bottcher M. R. Strayer

The physics of the fermion vacuum is briefly described and applied to pair production in heavy-ion collisions. We consider, in turn, low energies (< 50 MeV/nucleon), intermediate energies (< 5 GeV/nucleon), and ultrahigh energies such as would be produced in a ring collider. At high energies, interesting questions of Lorentz and gauge invariance arise. Finally, some applications to the structure of high Z atoms are examined.

---

1. Abstract of paper: Nucl. Instrum. & Meth. B31, 122 (1988).

OSCILLATIONS OF THE POLARIZED VACUUM AROUND A LARGE Z "NUCLEUS"[1]

A. Iwazaki[2] S. Kumano[3]

We explain sharp e^+ peaks in heavy-ion collisions by analyzing pure QED with a large atomic number external source. We show that a highly polarized vacuum around the source has at least two neutral oscillation modes, whose energies are predicted to be 1.75 MeV and 1.49 MeV with an appropriate choice of the radius of the source. They decay into a pair of $e^\pm$ only through electromagnetic interactions.

---

1. Abstract of paper to be published in Physics Letters B.
2. Nishogakusha University, Nakahagi, Japan.
3. Guest Assignee from University of Tennessee, Knoxville, TN 37996-1200.

ELECTRON PAIR PRODUCTION AND CAPTURE IN HEAVY-ION COLLISIONS

A. S. Umar[1] M. R. Strayer
V. E. Oberacker[1] C. Bottcher

Pair production with the capture of an electron is a leading mechanism for destroying the intersecting RHIC beams (beamsstralung). Capture of heavier leptons is also measurable, and it could provide an interesting probe of the nuclear interior. Nonperturbative methods must be developed, at the very least, to calibrate perturbative formulations. They will also be central to any attack on QCD.

Our approach to problems in three space dimensions, which we are also following in nonrelativistic and atomic problems, is to discretize on a Cartesian lattice. While time is also discretized, the system variables are usually updated in every successive time step, so that time does not require another index. The use of Cartesian coordinates avoids the pathologies of rotating frames and the complicated metrics of spherical coordinate systems. The resulting algorithms have a pleasing conceptual and logical simplicity, which far outweighs any loss of efficiency because the representation is suboptimal.

In our basis-spline-collocation approach, the Hamiltonian is replaced by a matrix whose structure is sparse and blocked. The solution of the time-dependent Dirac equation is reouced to a series of matrix X vector operations, which can be implemented efficiently on vectorizing or parallel computers.

A complete solution of the pair production problem requires the propagation in time of a complete set, or at least a substantial sample, of vacuum states. We have deferred a direct attack on this problem for the present, though we are pursuing simplified approaches. Rather, we have focussed on the more tractable problem of pair production with capture. This requires only that the final bound state be propagated backwards in time. Such calculations have been completed, with demonstrated convergence, for screened Coulomb potentials. The experience accumulated can be extrapolated to estimate the resources needed for calculations with the correct Coulomb potentials.

The calculations were performed in the frame of one nucleus (the target), while the other nucleus (the projectile) was Lorentz-boosted. The dependence of the capture probability on impact parameter was calculated at two energies. The probabilities were observed to converge to physically well-behaved limits, when the mesh spacing is about one-fifth the Compton wavelength of the lepton, or less. The model was tuned so that this limit was reached with 25-40 mesh points in each direction. We estimate that realistic calculations on e^- or μ^- capture require 70-100 points in each direction, corresponding to 10's of hours of computing at 200-300 Mflops, and consuming 100 Mwords of shared memory.

---

1. Consultant from Vanderbilt University, Nashville, TN 37235.

ULTRARELATIVISTIC HEAVY-ION PHYSICS COLLISIONS

A MULTIPLE COLLISION MODEL FOR HIGH-ENERGY NUCLEUS-NUCLEUS COLLISIONS[1]

Cheuk-Yin Wong Zhong-Dao Lu[2]

We use a Glauber multiple-collision model to examine the dynamics of nucleus-nucleus collisions. The model assumes that the incident and the target baryons make multiple collisions as the collision process proceeds, their probability of collision being given by the baryon-baryon inelastic cross section. In each collision the baryons lose energy and momentum. The model introduces a stopping law which describes how a baryon loses energy in a basic baryon-baryon collision. The baryon energy loss in each basic collision results in the production of particles. The momentum distribution of the produced particles is described by a particle production law. It is found that the zero-degree calorimeter spectra of the WA80 experiments with ^{16}O ions at 60 GeV and 200 GeV per nucleon on various targets are well described by a stopping law which reveals a high degree of stopping in these high-energy nuclear collisions. The transverse energy spectra, however, indicate that there are additional contributions to the transverse energy which may come from other sources.

---

1. Summary of invited talk presented at the International Conference on Medium- and High-Energy Nuclear Physics, Taipei, Taiwan, May 1988, and paper submitted for publication in Physical Review D.
2. Institute of Atomic Energy, Beijing, PRC.

INTERMEDIATE-ENERGY PHYSICS

STUDIES OF THE NUCLEAR SINGLE-PARTICLE RESPONSE FUNCTION IN A SIMPLE MODEL[1]

G. D. White[2] K.T.R. Davies
P. J. Siemens[3]

An expansion for the single-particle response function for a collection of noninteracting fermions in a localized potential well is developed with particular emphasis on applications to nuclei (including Δ-hole excitations), computational techniques, and comparisons to an infinite Fermi gas. Ground states and excited systems can both be treated with this formalism, although the latter involves a significantly more difficult analysis. Also, a useful dispersion relation is obtained for the response function. Then, an accurate method is presented for evaluating bound state and continuum single-particle wave functions in momentum space, the representation in which one most naturally derives the appropriate single-particle normalization factors. However, it is argued that for calculating folding integrals of two single-particle wave functions coordinate space may be superior to momentum space. Our main results show that for any reasonable description of light nuclei excited by pions, the continuum states must be included. Also, in these systems the overall response of the continuum states is dramatically dependent on the real part of the Δ-particle optical potential.

---

1. Abstract of paper to be published in Annals of Physics.
2. Consultant from Northwestern State University, Natchitoches, LA 71457.
3. Consultant from Oregon State University, Corvallis, OR 97331.

GENERALIZATIONS OF THE POINCARÉ-BERTRAND THEOREM AND APPLICATIONS TO NUCLEAR DISPERSION RELATIONS

K.T.R. Davies

When the product of two principal-value terms occurs in a double integral, it is well known that one must be careful about reversing the order of integration.[1] In particular, the Poincaré-Bertrand theorem[1,2] states that

$$\int dx \frac{\mathcal{P}}{(x-u)} \int dy \frac{\mathcal{P}}{(y-x)} f(x,y) = \int dy \int dx \frac{\mathcal{P}}{(x-u)} \frac{\mathcal{P}}{(y-x)} f(x,y) - \pi^2 f(u,u), \tag{1}$$

where $\mathcal{P}$ indicates the principal value. Note the extra term on the righthand side of Eq. (1) which arises from reversing the order of integration. This important theorem can be proven very generally without recourse to complex variable theory,[2] so that its validity does not depend on the analytic behavior of the function f(x,y). (However, it is assumed that f(x,y) is "well behaved" within the x,y domain of integration.)

Equation (1) can be used to prove very easily a well-known result from complex variable theory: If one function, f(x), is the Hilbert transform of another function, g(x), then g(x) is also the Hilbert transform of f(x). This little exercise nicely illustrates the usefulness of Eq. (1).

There are many applications of this theorem in nuclear physics, particularly in studies of the nuclear response functions arising from nucleon-delta-mesonic interactions.[3,4] Consider a causal Green's function, G_α, whose spectral representation obeys the well-known dispersion relation[5]

$$\mathrm{Re}[G_\alpha(\omega)] = \frac{1}{\pi}\int_{-\infty}^{\infty} d\omega' \frac{\mathcal{P}}{(\omega'-\omega)} \mathrm{Im}[G_\alpha(\omega')]n_\alpha(\omega'), \tag{2}$$

where

$$n_\alpha(\omega) = \begin{cases} \tanh[(\omega-\mu_\alpha)/2k_BT] & \text{for bosons} \\ \coth[(\omega-\mu_\alpha/2k_BT] & \text{for fermions,} \end{cases} \tag{3}$$

and k_B is the Boltzmann constant, T is the temperature, and μ_α is the chemical potential. Then, a typical response function[3,5] is proportional to the integral

$$U_{\alpha\beta}(\omega) = i\int_{-\infty}^{\infty} d\omega' \, G_\alpha(\omega+\omega')G_\beta(\omega'), \tag{4}$$

and from Eqs. (1), (2), and (3) one can show that

$$\mathrm{Re}[U_{\alpha\beta}(\omega)] = \frac{1}{\pi}\int_{-\infty}^{\infty} d\omega' \frac{\mathcal{P}}{(\omega'-\omega)} \mathrm{Im}[U_{\alpha\beta}(\omega')]n_{\alpha\beta}(\omega') \tag{5}$$

where

$$n_{\alpha\beta}(\omega) = \begin{cases} \tanh(\omega-\mu_\alpha+\mu_\beta)/2k_BT & \text{if } \alpha \text{ and } \beta \text{ refer to the same kind of particle} \\ \coth(\omega-\mu_\alpha+\mu_\beta)/2k_BT & \text{if } \alpha \text{ and } \beta \text{ refer to different kinds of particles} \end{cases} \tag{6}$$

Comparing Eqs. (3) and (6), we see that, as far as the statistics are concerned, two bosons or two fermions behave like a boson, while a boson and a fermion behave like a fermion, which is a very satisfying result.

Finally, we mention that the basic theorem in Eq. (1) is presently being generalized to include the cases of multiple integrals and of higher-order poles. In particular, the case of multiple integrals appears to have direct application to various products of T=0 Green's functions and response functions. Such products are the basic components occurring in the solution of Dyson's equations, either in nuclear matter or in finite nuclei.[3-5]

---

1. R. Balescu, Statistical Mechanics of Charged Particles (Interscience Publishers, New York, 1963), p. 399.
2. N. I. Muskelishvili, Singular Integral Equations (P. Noordhoff, New York, Groningen, The Netherlands, 1953), pp. 56-61.
3. G. D. White, K.T.R. Davies, and P. J. Siemens, to be published in Annals of Physics.
4. G. D. White, P. J. Siemens, M. Soyeur, and K.T.R. Davies, to be published.
5. A. J. Fetter and J. D. Walecka, Quantum Theory of Many-Particle Systems (McGraw-Hill, New York, 1971), pp. 292-298.

THEORY AND CALCULATIONS OF THE DYSON EQUATIONS INVOLVING NUCLEON-DELTA-MESONIC INTERACTIONS

K.T.R. Davies　P. J. Siemens[2]
G. D. White[1]　M. Soyeur[3]

To give a quantitatively reliable description of nuclear collisions at center-of-mass energies of a few hundred MeV per nucleon, a theoretical model must incorporate many aspects of our extensive experience of nuclear structure and forces. It must give a good account of NN and πN scattering in this energy regime, because the particles in the final state of the collision collide with each other pairwise after the density of the matter has been attenuated but before they are detected. It must accurately describe the motion of nucleons and pions in normal nuclei, including the scattering of nucleons and pions from nuclei, not only because the model must be tested in known cases, but also because of the presence of spectator fragments of nuclear matter in the final state of many relativistic heavy-ion collisions. It must have free parameters to adjust the properties of hot and cold high-density nuclear matter, because the comparison of a range of model predictions to measured data is essential to the process of inductive reasoning from which conclusions on the significance of experiments must be drawn. The theory also should include the main known aspects of nuclear collective motion, since we are hoping to uncover collective effects in the hot dense matter. Of course, it has to be built within the framework of relativistic quantum mechanics.

We are presently pursuing formally such a theory. At the same time, we have initiated a program of practical calculations which will embody the essential ingredients of our formal theory. In particular, we have begun to solve self-consistently the Dyson equations in infinite nuclear matter. So far, we are considering only nucleon-delta and nucleon-pion interactions, but eventually we plan to include the effects of heavier mass mesons.

The most difficult numerical part of such calculations involves the evaluation of certain "loop integrals" (see Fig. 5.2). For example, we have made a number of calculations of the loop integral containing the nucleon and delta propagators:

$$U_{N\Delta}(p) = i \int d^4q \, [f^2(2q+p)G_N(p+q)G_\Delta(q) + f^2(2q-p)G_N(-p+q)G_\Delta(q)], \quad (1)$$

ORNL-DWG 87-19429

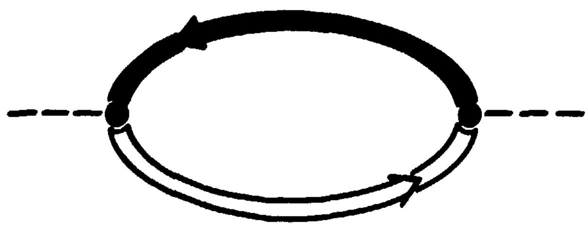

Fig. 5.2. A Feynman diagram for computing the response function. Such a loop integral occurs in the solution of Dyson's equations.

where $p = (E,\vec{p})$ is a four vector and f is a "form factor" which promotes rapid convergence of general nuclear matter loop integrals. Figures 5.3 and 5.4 show typical results for the real and imaginary parts of $U_{N\Delta}$.

From the Poincaré-Bertrand theorem, it can be shown that both the real and imaginary parts of $U_{N\Delta}$ can be obtained from the imaginary parts of G_N and G_Δ. The function G_N is the usual non-

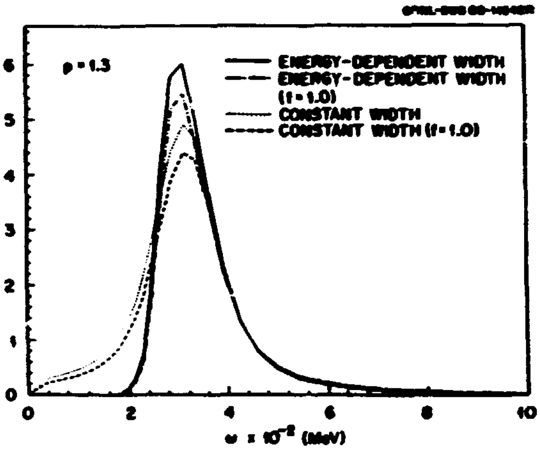

Fig. 5.3. The imaginary part of $U_{N\Delta}$ as a function of the energy E = ω for $p = |\vec{p}| = 1.3$ fm^{-1}. Two different cases are displayed, each shown with and without the form factor.

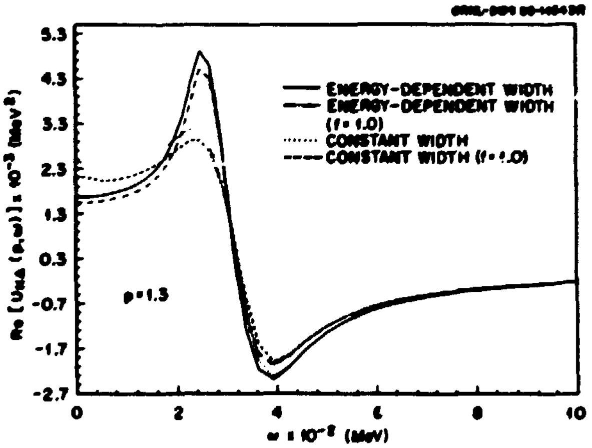

Fig. 5.4. The real part of $U_{N\Delta}$ as a function of E = ω for p = 1.3 fm^{-1}. This function is calculated from the $Im(U_{N\Delta})$ via a dispersion relation.

relativistic, mean-field nuclear matter propagator, while the $Im(G_\Delta)$ is given by

$$Im\ G_\Delta(E,\vec{p}) = -\frac{1}{2}\frac{\Gamma_\Delta(E)\theta(E-\mu_\Delta)}{(E-\epsilon_\Delta(p))^2 + \frac{1}{4}\Gamma_\Delta^2(E)}\ , \quad (2)$$

where $\epsilon_\Delta(\vec{p})$ is the delta single-particle energy, $\Gamma_\Delta(E)$ is the delta width, μ_Δ is the chemical potential, and $\theta(x)$ is a step function. In Figs. 5.3 and 5.4 we considered two different options: (1) using a constant width, $\Gamma_\Delta(E) = \Gamma_\Delta(o) = 115$ MeV, and (2) using an energy-dependent width, which vanishes for $E \lesssim m_N + m_p$ and which rises to a value of $\Gamma_\Delta(E) = \Gamma_\Delta(0)$ at E = 1244 MeV, after which it remains constant. The latter option corrects certain phase-space difficulties and discontinuities associated with the former one. It can also be seen from Figs. 5.3 and 5.4 that the form factor has little effect on the nucleon-delta loop integral. However, this form factor will be essential for convergence of the nucleon-pion loop integral.

Once calculated, $U_{N\Delta}$ will be inserted as a correction into the free-particle pion propagator. Then the nucleon-pion loop integral can be evaluated, and this will be inserted as a correction into the Green's function in Eq. (2), thus giving a new delta propagator. The whole process will be repeated until one obtains self-consistency. How rapidly the process converges remains to be determined.

---

1. Consultant from Northwestern State University, Natchitoches, LA 71457.
2. Consultant from Oregon State University, Corvallis, OR 97331.
3. C.E.N. Saclay, F 91191 Gif-sur-Yvette Cedex, France.

INCLUSIVE γ AND π^0 CROSS SECTIONS IN HEAVY-ION REACTIONS[1]

D. J. Ernst[2]   M. R. Strayer

Perturbation theory in a time-dependent basis is used to derive formal expressions for pion and gamma emission in heavy-ion reactions. The structure of the theory motivates an external mean-field phenomenology as a representation of the actual mean field plus lowest-order collision dynamics. The source function for the emission process is identified as a Wigner function constructed from the time Fourier transform of the nuclear wavefunctions. A simple model of the Wigner function is constructed and used to relate the production cross section for π^0 and γ in the reaction ^{14}N + Ni at a laboratory bombarding energy per nucleon of 35 MeV. A direct relation between π^0 and γ cross sections is predicted to hold in the region of high gamma-ray energy where the gamma emission is dominated by spin currents.

---

1. Abstract of paper: J. Phys. G 14, L37 (1988).
2. Consultant from Texas A&M University, College Station, TX 77843.

PHENOMENOLOGICAL LOCAL POTENTIAL MODEL FOR PION-NUCLEUS SCATTERING

G. R. Satchler

Pion-nucleus elastic and inelastic scattering measurements are usually analyzed in terms of a momentum-dependent "microscopic" optical model potential and the impulse approximation. It is of interest to see whether a good, phenomenological description of these data can be given in terms of simple and local potential models (e.g., Woods-Saxon), and what can be learned from such a description. Preliminary investigations of some elastic scattering have been made with relativistic kinematics but otherwise using the Schrödinger equation (equivalent to a certain approximation to the Klein-Gordon equation.) The results suggest that a simple Woods-Saxon model is sufficient when there is strong absorption, such as at energies near the (3,3) resonance, but that this shape may be inadequate at lower energies.

One interesting question is whether certain features, such as $\sigma(\pi^+)/\sigma(\pi^-)$ ratios for inelastic scattering, depend sensitively on the interaction model used or whether they are largely model-independent. Early results suggest the latter, at least when there is strong absorption; provided the elastic scattering is fitted, the inelastic follows from deforming the optical potential. This parallels our experience with other hadronic scattering, and implies that the apparently anomalous interpretation of the π^+/π^- ratios found[1] for exciting the giant quadrupole resonance is probably not due to inadequacies in the interaction model used. Similarly, the dominance of the imaginary interaction at these energies makes the Coulomb-nuclear interference contribution to the π^+/π^- ratio quite small.

---

1. S. J. Seestrom-Morris et al., Phys. Rev. C 33, 1847 (1986).

N(e,e′γ) AND THE N-Δ TRANSITION QUADRUPOLE MOMENT[1]

S. Kumano[2]

The N(e,e′γ) reaction is investigated to find the N-Δ transition quadrupole moment. The cross section is expressed in terms of N-Δ transition form factors, and it shows a typical dipole radiation pattern if the quadrupole moment vanishes. Given a finite transition quadrupole moment, the dipole radiation pattern rotates. In the laboratory frame, the radiation is peaked in the forward direction due to the Δ motion. Measurement in the out-of-scattering plane is suggested to find the quadrupole moment. The exchange diagram contribution to the cross section is calculated to be at most 3% if we use the isobar model for the Δ propagator.

---

1. Abstract of paper submitted for publication in Nuclear Physics A.
2. Guest Assignee from University of Tennessee, Knoxville, TN 37996-1200.

PIONIC CONTRIBUTION TO THE SCALAR AND LONGITUDINAL N-Δ TRANSITION QUADRUPOLE FORM FACTORS[1]

S. Kumano[2]

The pionic contribution to the scalar and longitudinal proton→Δ^+ transition quadrupole form factors is calculated. It is shown that the πN channel contributes +0.023-i 0.093 fm^2 at photon momentum q = 400 MeV (EMR = +1.4-i 5.7%).

This might be larger than the "core" quadrupole moment, and one should be careful in comparing experimental data and theoretical predictions. This pionic contribution makes the measurement of the phase of the quadrupole moment more interesting.

1. Abstract of paper to be published in Physics Letters B.
2. Guest Assignee from the University of Tennessee, Knoxville, TN 37996-1200.

HEAVY-ION REACTIONS

RELATION BETWEEN M_n, M_p, AND HADRONIC EXCITATION STRENGTHS WHEN THERE IS STRONG ABSORPTION: THE $^{A}Zr(\alpha,\alpha')$ REACTIONS[1]

G. R. Satchler

We study the relationship between the r^{ℓ} radial moments M_n and M_p of neutron and proton transition densities and the corresponding interaction strengths at the large radii sampled by a hadronic probe when there is strong absorption. We use a folding model and a Gaussian alpha-nucleon interaction to generate the transition potentials for $^{A}Zr(\alpha,\alpha')$ reactions at 35.4 MeV. Simple transition density models were considered, as well as a valence-plus-core polarization model, and applied to some 2_1^+ and 3_1^- excitations for A = 90, 92, and 96. We show that the M_n/M_p ratios extracted can be very sensitive to the shapes assumed for the transition densities. The ratios deduced from the $^{A}Zr(\alpha,\alpha')$ data are smaller than those deduced recently using an implicit procedure, but still are considerably larger than N/Z for A > 90. Explicit consideration of a few valence nucleons can produce significant variations.

1. Abstract of paper submitted for publication in Nuclear Physics A.

THE THRESHOLD ANOMALY FOR HEAVY-ION SCATTERING[1]

G. R. Satchler

The real parts of optical potentials deduced from heavy-ion scattering measurements become rapidly more attractive as the bombarding energy is reduced close to the top of the Coulomb barrier. This behavior is explained as a coupled-channels effect, and is related to the corresponding reduction in the absorptive potential through a dispersion relation which expresses the consequences of causality. Another manifestation of this "anomaly" is the striking enhancement observed for the near- and sub-barrier fusion of two heavy ions. The barrier penetration model of fusion is examined critically in this context. It is also stressed that similar anomalies could appear in the energy dependence of nonelastic scattering.

1. Abstract of paper: p. 276 in Proceedings 11th Oaxtepec Symposium on Nuclear Physics, Notas de Fisica, Vol. 11, No. 1 (1988).

FOLDING MODEL ANALYSIS OF $^{12,13}C + {}^{12}C$ AND $^{16}O + {}^{12}C$ SCATTERING AT INTERMEDIATE ENERGIES USING A DENSITY-DEPENDENT INTERACTION[1]

M. E. Brandan[2] G. R. Satchler

Scattering data for $^{12}C + {}^{12}C$, $^{13}C + {}^{12}C$, and $^{16}O + {}^{12}C$ at energies E/A = 9 to 120 MeV per nucleon have been analyzed, using a folded potential based on the density- and energy-dependent DDM3Y interaction. The renormalization required for the real potential is about unity at all energies. A unified description of these data is obtained with a relatively weakly absorbing imaginary potential. Furthermore, only this type of potential provides a successful description of the $^{12}C + {}^{12}C$ data at 140 and 159 MeV which cover almost the whole angular range. Potential ambiguities are discussed.

1. Abstract of paper to be published in Nuclear Physics A.
2. Universidad Nacional Autonoma de Mexico, 01000 Mexico, D.F., Mexico.

SPIN-ORBIT FORCE IN TDHF CALCULATIONS OF HEAVY-ION COLLISIONS[1]

A. S. Umar[2] P.-G. Reinhard[3]
M. R. Strayer K.T.R. Davies
S.-J. Lee[4]

We discuss the time-dependent Hartree-Fock (TDHF) equations which maintain independent nucleon spin degrees of freedom, and which include spin-orbit interactions. The complex numerical task of including the spin-orbit force in reaction studies is described in detail. Calculations are presented which demonstrate that the spin-orbit force produces a significant enhancement in dissipation for both light and heavy systems. The fusion window in $^{16}O + ^{16}O$ collisions disappears, due to the increased dissipation. For the $^{86}Kr + ^{139}La$ system at E_{lab} = 610 MeV, the inclusion of the spin-orbit force results in fusion for central collisions and considerably longer interaction times for deep inelastic collisions. As a consequence of the long sticking times, we observe an orbiting-type phenomenon with a large particle transfer for orbital angular momenta in the vicinity of 110ħ.

---

1. Abstract of paper submitted for publication in Physical Review C.
2. Consultant from Vanderbilt University, Nashville, TN 37235.
3. Consultant from University of Erlangen, Erlangen, West Germany.
4. McGill University, Montreal, Quebec H3A 2T8, Canada.

DISSIPATION AND FORCES IN TIME-DEPENDENT HARTREE-FOCK CALCULATIONS[1]

P.-G. Reinhard[2] K.T.R. Davies
A. S. Umar[3] M. R. Strayer
S.-J. Lee[4]

We have performed time-dependent Hartree-Fock calculations for the $^{16}O + ^{16}O$ system using various parametrizations of the Skyrme force. These calculations also include the spin-orbit part of the Skyrme force. We have refitted, with improved accuracy, the finite-range version of the Skyrme force to the ground state properties of eight nuclei. Particular emphasis is given to comparisons of calculations with and without the spin-orbit force. We see a strong sensitivity of the results to the different parametrizations of the effective interaction. The spin-orbit force introduces a significant enhancement of the dissipation. A schematic model of heavy-ion scattering is used to investigate the origin of the observed sensitivity. We find that the dissipation is essentially determined by the additional residual interaction.

---

1. Abstract of paper: Phys. Rev. C 37, 1026 (1988).
2. Consultant from Universität Erlangen, D-8520 Erlangen, West Germany.
3. Consultant from Vanderbilt University, Nashville, TN 37235.
4. McGill University, Montreal, Quebec H3A 2T8, Canada.

FURTHER OPTICAL MODEL STUDIES OF ^{16}O SCATTERING AT E/A = 94 MeV[1]

A. M. Kobos[2] M. E. Brandan[3]
G. R. Satchler

We present the results of further optical model analyses of data for the scattering of ^{16}O at E/A = 94 MeV. In particular, we explored the use of real potential shapes more general than the Woods-Saxon or folded ones. Evidence was found that fits to the $^{16}O + ^{12}C$ data were sensitive to the real potential even at small radii, and involved potentials with relatively weak absorption (S-wave S-matrix elements with $|S_0| \approx 0.1$). Significant modifications to the DDM3Y folded potential were required for the best fits to these data. The optimum potentials are represented well by a conventional Woods-Saxon potential with a real depth of 80 MeV. The more general shapes did not improve the agreement with the data for heavier targets.

---

1. Abstract of paper to be published in Nuclear Physics A.
2. Myrias Research Corporation, Edmonton, Alberta T5K 2P7, Canada.
3. Universidad Nacional Autonoma de Mexico, 01000 Mexico, D.F., Mexico.

FURTHER STUDIES OF DENSITY-DEPENDENT INTERACTIONS FOR THE EXCITATION OF COLLECTIVE STATES[1]

M. El-Azab Farid[2] G. R. Satchler

The density-dependent DDM3Y effective nucleon-nucleon interaction was used in a double-folding model with macroscopic transition densities to explore further density-dependent effects on the inelastic scattering of α-particles and protons. In particular, we investigate whether transition densities with a node near the nuclear surface, such as occurs for the giant monopole (breathing mode) resonance, are particularly sensitive to density dependence in the interaction. We also study the imposition of a consistency condition on the use of density dependence for inelastic scattering. In both situations, the effects are small (≲20%) for α-particles but large for protons. The consistency condition is discussed further in an appendix.

---

1. Abstract of paper: Nucl. Phys. A481, 542 (1988).
2. Teachers Training College, Salalah, Sultanate of Oman.

NUCLEAR STRUCTURE

REFLECTION-ASYMMETRIC ROTOR MODEL OF ODD-A ~ 219-229 NUCLEI[1]

G. A. Leander[2]   Y. S. Chen[3]

The low-energy spectroscopy of odd-A nuclei in the mass region A ~ 219-229 is modeled by coupling states of a deformed shell model including octupole deformation to a reflection-asymmetric rotor core. Theory and experiment are compared for the nuclei in which data are available: ^{219,221,223,225}Rn, ^{221,223,225,227}Fr, ^{219,221,223,225,227}Ra, ^{219,223,225,227,229}Ac, ^{221,223,225,227,229}Th, and ^{229}Pa. Overall agreement requires an octupole deformation $\beta_3 \sim 0.1$. The results throughout the region are synthesized to evaluate the model.

---

1. Abstract of paper: Phys. Rev. C 37, 2744 (1988).
2. Deceased.
3. Institute of Atomic Energy, Beijing, China.

NUCLEAR STRUCTURE OF LIGHT THALLIUM ISOTOPES AS DEDUCED FROM LASER SPECTROSCOPY ON A FAST ATOM BEAM[1]

J. A. Bounds[2]   G. A. Leander[5]
C. R. Bingham[3]   R. L. Mlekodaj[6]
H. K. Carter[4]   E. H. Spejewski[7]
W. M. Fairbank, Jr.[8]

The neutron-deficient isotopes $^{189-194}$Tl have been studied using collinear fast atom beam laser spectroscopy with mass-separated beams of 7×10^4 to 4×10^5 atoms per second. By laser excitation of the 535-nm atomic transitions of atoms in the beam, the $6s^27s\,^2S_{1/2}$ and $6s^26p\,^2P_{3/2}$ hyperfine structures were measured, as were the isotope shifts of the 535-nm transitions. From these, the magnetic dipole moments, spectroscopic quadrupole moments, and isotopic changes in mean-square charge radii were deduced. A large isomer shift in ^{193}Tl was observed, implying a larger deformation in the $9/2^-$ isomer than in the $1/2^+$ ground state. The ^{189,191,193}Tl^m isotopes have deformations that increase as the mass decreases. A deformed shell model calculation indicates that this increase in deformation can account for the drop in energy of the $9/2^-$ bandhead in these isotopes. An increase in neutron pairing correlations, having opposite and compensating effects on the rotational moment of inertia, maintains the spacing of the levels in the $9/2^-$ strong-coupled band. Results for ^{194}Tl^m differ from previously published values, but are consistent with the ^{190,192}Tl^m data.

---

1. Abstract of paper: Phys. Rev. C 36, 2560 (1987).
2. Los Alamos National Laboratory, Los Alamos, NM 87545.
3. Adjunct staff member from University of Tennessee, Knoxville, TN 37996-1200.
4. UNISOR, Oak Ridge Associated Universities.
5. Deceased.
6. Environmental and Health Protection Division, ORNL.
7. Oak Ridge Associated Universities.
8. Colorado State University, Fort Collins, CO 80523.

SHELL MODEL STRUCTURE OF YRAST STATES IN N = 50-52 ISOTOPES WITH Z = 88-98

J. B. McGrory

A region where the spherical shell model has been applied with considerable success is the mass 89-94 region. (See Ref. 1 for a summary.) Assuming a ^{88}Sr core and an active valence space with protons in the $p_{1/2},g_{9/2}$ orbits, and neutrons in the $d_{5/2},s_{1/2}$ orbits, the low-lying spectra of nuclei near the closed shell have been accurately described in the shell model.

In recent years, refinement of analysis of heavy-ion-induced reactions have greatly expanded the body of data available in nuclei in this mass region. In particular, the nuclei with N = 50 (no valence neutrons in this model) from ^{89}Y - ^{94}Ru are very accurately described by $(p_{1/2},g_{9/2})$ configurations, i.e., they are very spherical. On the other hand, there is evidence of a clear transition to collective rotational behavior in the Zr isotopes (two valence protons) near A ≈ 100. This region then presents a possible region where such a transition might be described quantitatively in a spherical shell model. However, such a description must involve an expanded shell model space, which, at a minimum, must involve the $g_{7/2}$ orbit to take advantage of the strong deformation inducing n-p interaction between the $g_{9/2}$ proton and the $g_{7/2}$ neutron. The interactions involving the $g_{7/2}$ neutron are not known. They should be clearly established if one studied the N = 51,52 isotopes in this mass region. As a first step of a study of this region, an investigation of the known N = 50,51,52 levels in nuclei with Z = 38-48 has been carried out. The two-body matrix elements in the five-orbit space, where the $g_{7/2}$ orbit is added to the model space described above, are treated as parameters. The p-p interaction is fixed by the N = 50 levels. The n-p interaction is fixed by the N = 51 isotopes. Unfortunately, almost all the levels in the nuclei treated are quite well fit without the $g_{7/2}$ orbit. Two levels can be fit only with the inclusion of the $g_{7/2}$ orbit, and these levels are used to fit the $g_{7/2}$ single-particle energy and the center-of-gravity of the $g_{9/2}$-$g_{7/2}$ n-p interaction. The p-p and p-n matrix elements were left fixed by the N = 50,51 results, and we are developing a complete n-n interaction from the N = 52 isotopes from ^{90}Sr to ^{100}Cd. Here again, the yrast levels are generally the only ones with firm spin assignments, and most of these are well fit without the $g_{7/2}$ orbit. There is a consistent problem with the yrast J = 6 levels in the heavier N = 52 isotopes. This is the highest spin available in the $(g_{7/2})$ configuration, and it appears that these levels and a few other "troublesome" levels may provide a first fix on the n-n interaction for the $g_{7/2}$ orbit. Examples of typical N = 51,52 spectra are shown in Fig. 5.5. There the calculated and observed spectra of low-lying states in the N = 51 nucleus ^{90}Nb are shown, as are the spectra of the N = 52 nuclei ^{97}Rh and ^{98}Pd. The effects of the $g_{7/2}$ orbit are treated in ^{90}Nb, while the N = 52 results do not include the $g_{7/2}$ orbit. The qualitative disagreement of the J = 6^+ state in ^{98}Pd is seen to a similar extent in ^{96}Ru, and much more distinctly in ^{100}Cd. In ^{97}Rh the positions of the calculated 19/2, 23/2, 27/2, and 31/2 (not shown) states are distinctly too high. It is possible that these defects will be significantly reduced in the expanded space.

---

1. J. B. McGrory and B. H. Wildenthal, Ann. Rev. Nucl. Part. Sci. 30, 383 (1980).

SYSTEMATICS OF $B(E2;0_1^+ \rightarrow 2_1^+)$ VALUES FOR EVEN-EVEN NUCLEI[1]

S. Raman C. W. Nestor, Jr.[2]
K. H. Bhatt[3]

We have completed a compilation of experimental results for the electric quadrupole transition probability B(E2)↑ between the 0^+ ground state and the first 2^+ state in even-even nuclei. The adopted B(E2)↑ values have been employed to test the various systematic, empirical, and theoretical relationships proposed by several authors (Grodzins, Bohr and Mottelson, Wang et al., Ross and Bhaduri, Patnaik et al., Hamamoto, Casten, Möller and Nix, and Kumar) on a global, local, or regional basis. These systematics offer methods for making reasonable predictions of unmeasured B(E2) values. For nuclei away from closed shells, the SU(3) limit of the intermediate boson approximation implies that the B(E2)↑ values are proportional to $(e_pN_p + e_nN_n)^2$, where $e_p(e_n)$ is the proton(neutron) effective charge and $N_p(N_n)$ refers to the number of valence protons(neutrons). This proportionality is consistent with the observed behavior of B(E2)↑ vs N_pN_n. For deformed nuclei and the actinides, the B(E2)↑ values calculated in a schematic single-particle "SU(3)" simulation or

ORNL-DWG 88-14479

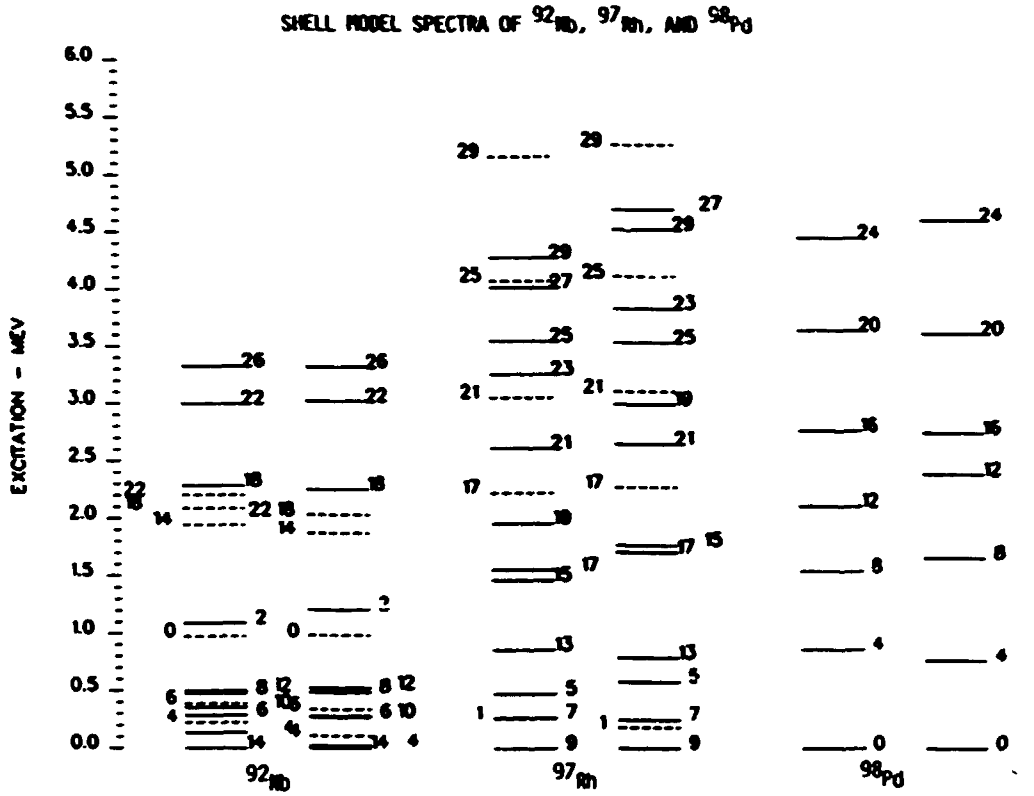

Fig. 5.5. Observed and calculated spectra of Yrast states in N = 51,52 nuclei. For the three nuclei, the observed spectra is to the left, and the calculated spectra to the right. In all spectra, positive parity states are indicated by solid lines, and negative parity states by dotted lines. The spins indicated are 2*J. Spin assignments for negative states are at the left end of the legend, while those for positive parity states are at the right end of the legend.

large single-j simulation of major shells successfully reproduce not only the empirical variation of the B(E2)↑ values but also the observed saturation of these values when plotted against N_pN_n.

---

1. Abstract of paper: Phys. Rev. C 37, 805 (1988).
2. Computing and Telecommunications Division.
3. Western Kentucky University, Bowling Green, KY 42101.

FINITE PARTICLE NUMBER EFFECTS AND THE RELATIONSHIP OF THE FERMION DYNAMICAL SYMMETRY MODEL WITH THE NILSSON MODEL[1]

H. Wu[2] D. H. Feng[2]
C. L. Wu[3] M. W. Guidry[4]

The spherical shell model is the fundamental microscopic model of nuclei. However, because of the lack of obvious truncation schemes to reduce the huge matrices encountered in nuclei where collective behavior is dominant, the shell model approach can, at best, be considered only as the underpinning; little detailed information can be extracted from it for deformed nuclei. However, the recently proposed fermion dynamical symmetry model (FDSM) is based on a symmetry-dictated truncation of the spherical shell model. It allows truncated shell model calculations for strongly deformed nuclei.

We have used the FDSM to study the rotational levels of an odd-mass deformed nucleus with the unpaired particle in an abnormal parity level. By using a strong coupling basis, we have demonstrated an analytical correspondence between the FDSM (which is an approximation to the spherical shell model) and the deformed shell model

(Nilsson model). In particular, we have shown that the FDSM accounts for the ground-state spins of odd-mass, deformed nuclei. By considering the geometrical particle-rotor model as an infinite particle-number approximation to the FDSM, we have suggested a microscopic origin for the Coriolis attenuation problem. This effect originates in the finite number of particles for the physical quantum rotor. According to the FDSM, the Coriolis attenuation should depend in a definite way on the orbital of the unpaired particle as well as the number of particles in the valence shells. In the strong coupling region the same finite particle-number effects may be viewed as providing a renormalization of the moment of inertia and the deformation.

---

1. Summary of paper: Phys. Rev. C 37, 1739 (1988).
2. Drexel University, Philadelphia, PA 19104.
3. Joint Institute for Heavy Ion Research. Permanent address: Jilin University, Changchun, People's Republic of China.
4. Adjunct staff member from University of Tennessee, Knoxville, TN 37996-1200.

THE NUCLEAR OBLATE WINDOW[1]

C. L. Wu[2] D. H. Feng[3]
W. M. Zhang[3] M. W. Guidry[4]
L. L. Riedinger[4]

A long-standing problem in low-energy nuclear structure is an understanding of the narrow window for the occurrence of oblate geometry, especially for the rare earths. Although there are several approaches which can reproduce the general trends in deformation,[5] there is no simple and convincing microscopic explanation as to why nature prefers prolateness over oblateness. In this paper we show that a narrow oblate window occurs naturally in the fermion dynamical symmetry model (FDSM).[6] The suppressed importance of oblate geometry in the FDSM can be deduced immediately without numerical calculations, but in Fig. 5.6 we show a simple numerical FDSM calculation of rare-earth shapes. The numerical

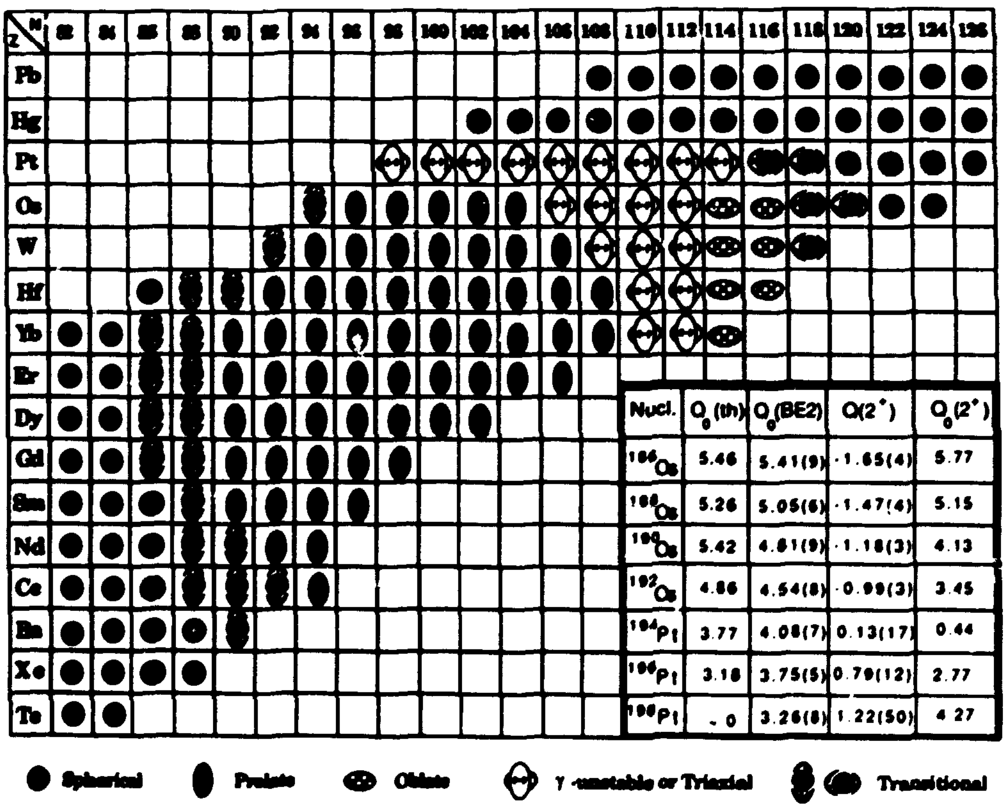

Nucl.	Q_0(th)	Q_0(BE2)	Q(2$^+$)	Q_0(2$^+$)
^{186}Os	5.46	5.41(9)	-1.65(4)	5.77
^{188}Os	5.26	5.05(6)	-1.47(4)	5.15
^{190}Os	5.42	4.81(9)	-1.18(3)	4.13
^{192}Os	4.86	4.54(8)	-0.99(3)	3.45
^{194}Pt	3.77	4.08(7)	0.13(17)	0.44
^{196}Pt	3.18	3.75(5)	0.79(12)	2.77
^{198}Pt	~ 0	3.26(8)	1.22(50)	4 27

Fig. 5.6. The narrow oblate window for rare-earth nuclei.

calculations show clearly that the window for oblate geometry in the rare-earth region is very narrow, as observed experimentally. We find that the narrowness of the FDSM oblate window is fundamental, and originates in the FDSM separation of normal and abnormal parity orbitals, and in the FDSM dynamical Pauli effect.[6] It can be predicted without calculation; the numerical results just provide quantitative details. Thus, the FDSM gives at once a transparent reason for the subsidiary role of oblate rare-earth geometry, and a microscopic formulation in which the geometry can be calculated quantitatively.

---

1. Abstract of paper submitted to Physics Letters B.
2. Joint Institute for Heavy Ion Research. Permanent address: Jilin University, Changchun, People's Republic of China.
3. Drexel University, Philadelphia, PA 19104.
4. Adjunct staff member from University of Tennessee, Knoxville, TN 37996-1200.
5. R. Bengtsson et al., Phys. Lett. 183B, 1 (1987); K. Kumar and M. Baranger, Nucl. Phys. A122, 241 (1968); P. Moller and J. R. Nix, At. Data Nucl. Data Tables 26, 165 (1981).
6. C. L. Wu et al., Phys. Lett. 168B, 313 (1986); Phys. Rev. C 36, 1157 (1987); J. Q. Chen, D. H. Feng, and C. L. Wu, Phys. Rev. C 34, 2269 (1986).

DYNAMICAL PAULI EFFECTS AND THE SATURATION OF NUCLEAR COLLECTIVITY[1]

D. H. Feng[2] M. W. Guidry[4]
C. L. Wu[3] Z. P. Li[5]

Recently, a symmetry-dictated truncation scheme for the spherical shell model called the fermion dynamical symmetry model (FDSM) was proposed by Wu et al.[6,7] The FDSM links the concept of dynamical symmetry to the underlying shell structure by assuming that low-energy collective modes are dominated by coherent S(L=0) and D(L=2) fermion pairs.

An important feature of the FDSM is that there exists a dynamical Pauli effect. A dynamical Pauli effect is defined as a restriction on allowed representations brought about by requirements of the Pauli principle in a particular fermion dynamical symmetry more stringent than those imposed by the particle-hole shell symmetry.

The dynamical Pauli effects predicted by the FDSM are confirmed by experimental B(E2) systematics. It is demonstrated that the saturation of E2 collectivity for deformed nuclei can be well described by a minimal implementation of the FDSM, and that it is a consequence of these Pauli effects. On the other hand, the minimal implementation of the interacting boson model (IBM) fails to produce the E2 saturation behavior. The FDSM B(E2) calculations are also superior to the geometrical model (GM) calculations of Ref. 8. However, the GM results (unlike the IBM) show the correct position of the onset of saturation and can be brought into better agreement by a simple rescaling of radius parameters. The FDSM calculations presented here are comparable to the best large-scale numerical calculations in accuracy and far exceed them in transparency; yet they are an analytical approximation to the spherical shell model, requiring only three adjustable parameters for all heavy nuclei.

---

1. Abstract of paper: Phys. Lett. 205B, 156 (1988).
2. Drexel University, Philadelphia, PA 19104.
3. Joint Institute for Heavy Ion Research. Permanent address: Jilin University, Changchun, People's Republic of China.
4. Adjunct staff member from University of Tennessee, Knoxville, TN 37996-1200.
5. University of Tennessee, Knoxville, TN 37996-1200.
6. C.-L. Wu et al., Phys. Lett. B 168, 313 (1986).
7. C.-L. Wu et al., Phys. Rev. C 36, 1157 (1987).
8. P. Moller and J. R. Nix, At. Data Nucl. Data Tables 26, 165 (1981).

PHYSICS OF (e^+,e^-) SYSTEMS

MICRO-POLYELECTRONS — THE CONDENSATION OF (e^+e^-) DUE TO NONCENTRAL, SHORT-RANGE ELECTROMAGNETIC INTERACTIONS[1]

Cheuk-Yin Wong

The experimental data from heavy-ion reactions with a very large combined charge indicates the possible existence of a neutral object at an energy of 1.6-1.8 MeV.[2,3] Without introducing new forces, we[4] suggested that such an object maintained its stability through the electromagnetic interaction of its constituents of electron(s) and positron(s).

Previously, we studied a model (magnetic moment)-(charge current) interaction between an electron and a positron in a Dirac equation and found, for the $J^{PC} = 0^{++}$ state, an effective potential pocket at the distance about 1 fm, which is deep enough to hold a resonance separated from the ordinary positronium state by a centrifugal barrier.[4] We have recently initiated a more rigorous treatment of the relativistic (e^+e^-) two-body bound-state problem in terms of the relativistic constraint dynamics.[5,6] When we worked out the effective interaction V_{eff}, we found that, for the 0^{++} state in question, the noncentral spin-orbit and tensor force interactions are attractive and strong enough to overwhelm the centrifugal barrrier at short distances to lead to the presence of a barrier separating the long-distance region from the short-distance region. In terms of the radial separation in the center-of-mass system, the noncentral interactions, which vary as $1/r^3$ at large distances, now behave in this relativistic treatment as $1/r^2$ at short distances. For the 0^{++} state, the total effective interaction, including the centrifugal $\ell(\ell+1)/r^2$ term, behaves as $(-1/4 - \alpha^2)/r^2$ at short distances, where α is the fine-structure constant. The (e^+e^-) two-body system at short distances is therefore supercritical in the 0^{++} state.[6]

The supercritical behavior of the (e^+e^-) system implies that in the 0^{++} state there will be the production of (e^+e^-) pairs, which we can take to be coupled to the 0^{++} state, so that there are no net quantum number changes in pair production. The pairs created will act back repulsively on the particles producing the pairs until the attractive interaction is reduced to prevent the collapse of the particles to the center. A condensation of the (e^+e^-) pairs will take place to lead to a micro-polyelectron system.

The supercritical behavior of the (e^+e^-) system in this 0^{++} state can be described in terms of an imaginary mass m and a repulsive self-interaction. There are then two minima of the potential of the scalar (e^+e^-) field. Oscillation about these two minima will give rise to approximately equally spaced energy levels that are doubly degenerate. The double degeneracy is split by the tunneling between the minima. The splittings are expected to be greater for the higher-lying states than for the lower-lying states. Thus, a condensation of e^+e^- will show approximately equally spaced levels which are nearly doubly degenerate. Experimental data of the positions of the positron lines do indeed exhibit approximately such a feature.

---

1. Summary of paper to be published in the proceedings of the Fifth International Conference on Clustering Aspects in Nuclear and Subnuclear Systems, Kyoto, Japan, July 25-29, 1988, and the International Conference on Medium- and High-Energy Nuclear Physics, Taipei, Taiwan, May 23-27, 1988.

2. T. Cowan and J. Greenberg, p. 111 in Physics of Strong Fields (Proceedings, NATO International Advanced Courses on Physics of Strong Fields, Maratea, Italy, June 1986), Plenum Publishing Corp., New York, 1987.
3. P. Kienle, Ann. Rev. Nucl. Part. Sci. 36, 605 (1986).
4. C. Y. Wong and R. L. Becker, Phys. Lett. 182, 251 (1986).
5. H. W. Crater and P. van Alstine, Phys. Rev. Lett. 53, 1577 (1984).
6. H. W. Crater, C. Y. Wong, R. L. Becker, and P. van Alstine, submitted for publication in Physical Review D.

INTERACTION OF A COMPOSITE PARTICLE IN A STRONG COULOMB FIELD[1]

Cheuk-Yin Wong

We study the responses of a composite particle to a strong external Coulomb field. We find a new type of composite effect which arises from the term quadratic in the Coulomb potential. For a charged composite particle, it modifies the effective Coulomb interaction, and for a neutral particle with charged constituents, it leads to an attractive, central interaction with a medium range. If the constituents are fermions, there are additional effects due to the spinor degrees of freedom. These effects may lead to the spontaneous production of composite (e^+e^-) particles in a strong Coulomb field.

---

1. Summary of paper to be published in the proceedings of the International Conference on Medium- and High-Energy Nuclear Physics, Taipei, Taiwan, May 23-27, 1988, and in Progress of Theoretical Physics 81 (1989), in press.

PROGRESS ON A NONPERTURBATIVE, COVARIANT TREATMENT OF NEUTRAL LEPTON-ANTILEPTON SYSTEMS

R. L. Becker H. W. Crater[1]
Cheuk-Yin Wong P. van Alstine[2]

Motivated by the desire to better understand the spectroscopy of quark-antiquark systems[3] and to study the possibility of electrodynamic resonances in lepton-antilepton systems,[4] we are exploring a nonperturbative, relativistic approach to two-fermion systems based on Dirac's "constraint mechanics." The method yields two two-particle Dirac equations which must be compatible. The constraints arising from compatibility require that the mutual interaction, referred to as the quasipotential, depends on the relative coordinate four-vector only through its space-like part, $x_\perp$, which is transverse to the total four momentum. In a center-of-mass frame, $x_\perp$ reduces to the displacement $\vec{r}$ of the two particles. Consequently, the relative time can be eliminated from the equations, thereby removing a difficulty which occurs when employing directly the Bethe-Salpeter (BS) equation. Moreover, the constraint dynamical wave function, Ψ, has been shown[5] to be a transform of the BS one, χ. The quasipotential is an integral, over three four-vectors and a longitudinal coordinate, of the kernel of the BS equation times a factor involving the kernel of the inverse transform, giving χ in terms of Ψ. Because this multiple integral would be extremely difficult to evaluate except with drastic approximations, we have proceeded, instead, by expanding the quasipotential in terms of Dirac operators multiplied by invariant functions, and restricting the invariant functions by comparison with quantum electrodynamical (QED) perturbation theory. The constraint potential can be derived[3] perturbatively from the field theoretic scattering amplitude by way of a form of the Todorov quasipotential equation.

For the case of positronium (Ps), we reported last year[6] that with the invariant function for the one-photon-exchange quasipotential chosen[7] as

$$\mathcal{A}^{(1)}(r) = e_1e_2/r \quad , \quad r = |x_\perp| \, , \tag{1}$$

we succeeded in reducing the 16-component equations to an equation of Schrödinger-Pauli form for the positive energy, four-component piece, Ψ_{++}. All terms in the quasipotential could be treated nonperturbatively in all angular-momentum eigenstates except for the $^3P_0$ states for which the spin-orbit term is strongest. We verified that the ground-state "hyperfine" splitting, $E(^3S_1)-E(^1S_0)$, agreed with perturbative QED to order $mc^2\alpha^4$, for which only relativistic kinematics and one-photon-exchange contribute. We conjectured that virtual annihilation might remove the overcriticality in the $^3P_0$ state.

We have now derived the reduced equation for the unequal mass case, which includes muonium (μ^+e^-) and hydrogen (with a point proton), and have found that the overcriticality persists. Thus, virtual annihilation could not be a universal cure. We then re-examined the choice of the invariant function, $\mathcal{A}(r)$. The spin-independent part of the quasipotential is denoted by $\Phi_{S.I.}$. Agreement with low-order QED requires that

$$\Phi_{S.I.} \equiv 2\epsilon_w\mathcal{A} - \mathcal{A}^2 \sim 2\epsilon_w\mathcal{A}^{(1)} - \mathcal{A}^{(1)2} + \mathcal{O}(\mathcal{A}^{(1)3}) \quad , \quad r \to \infty \tag{2}$$

where

$$\epsilon_w = (w^2 - m_1^2 - m_2^2)/2w,$$

with w the total energy in the CM frame. This rules out a term in $\mathcal{A}$ proportional to r^{-2}. Moreover, the requirement that $\Phi_{S.I.}$ be no more singular at $r = 0$ than r^{-2} rules out any polynomial in r^{-1}. A further restriction arises from consideration of an invariant function $G(\mathcal{A})$ which enters linearly into the Maxwell four-vector potentials A_i^μ, $i = 1,2$, and which is defined in terms of $\mathcal{A}$ by

$$G^2(\mathcal{A}) = [1-2\mathcal{A}(r)/w]^{-1}. \qquad (3)$$

With the original choice for $\mathcal{A}$, G is singular at $r_s = 2\alpha/w$ for the case of two particles with charges of the same sign, e.g., e^-+e^-. For $w = 2m_e$, r_s equals the classical radius of the electron, $r_e \approx 2.8$ fm, which is in the region where the spin-dependent interactions are dominant for e^+e^- in our equations. To avoid a singularity at some $r_s > 0$, we must have $\mathcal{A} < w/2$ for all r, when $e_1 = e_2$. For example, one phenomenological form giving a nonsingular G is

$$\mathcal{A}(r) = \mathcal{A}^{(1)}(r)\left[1 + C(2\mathcal{A}^{(1)}(r)/w)^2\right]^{-1}, \quad C > 1/4, \qquad (4)$$

which also satisfies Eq. (2). For this choice $|\mathcal{A}|_{max} = (2C^{1/2})^{-1}\, w/2$ at $r_x = (2C^{1/2}\, m/w)r_e$. For e^-e^- or e^+e^+ G reaches its maximum value at r_x and approaches 1, rather than 0 at $r \to 0$. An important task, on which we are now working, is to pin down the actual $\mathcal{A}(r)-\mathcal{A}^{(1)}(r)$ by examining higher-order terms in classical and quantum electrodynamics.

For positronium, virtual annihilation into a single photon is known to contribute a shift of the order $m\alpha^4$ to the energy of the ortho ($^3S_1$) state, which has odd charge parity, $\mathcal{C} = (-)^{L+S}$, but not to contribute to the even charge-parity states, e.g., the para ground state ($^1S_0$) and $^3P_0$. We needed to verify that the constraint formalism respects the charge-parity argument. We did so by adapting a proof which we constructed for the Bethe-Salpeter formalism. The Bethe-Salpeter wave function can be expressed as a 4 × 4 matrix, χ. In the CM system with the relative momentum, $\vec{p}$, restricted to a hemisphere and helicities h_1 and h_2, we can expand χ in Dirac plane-wave spinors

$$\chi(\vec{p}) = \sum_{h_1,h_2} [a(\vec{p},h_1,h_2)u(\vec{p},h_1)\bar{v}(-\vec{p},h_2) + a(-\vec{p},h_1,h_2)u(-\vec{p},h_1)\bar{v}(\vec{p},h_2)] \qquad (5)$$

with

$$a(-\vec{p},h_2,h_1) = -\mathcal{C}\, a(\vec{p},h_1,h_2). \qquad (6)$$

The vertex for annihilation into a single photon can be expressed as

$$V_\mu(p) = \mathrm{Trace}[\gamma_\mu\chi(\vec{p})] = \mathrm{Tr}[C\gamma_\mu C^{-1}\, C\chi(\vec{p})C^{-1}] \qquad (7)$$

where C is the charge conjugation matrix. But

$$C\gamma_\mu C^{-1} = -\gamma_\mu^T,$$

and we can show

$$C\chi(\vec{p})C^{-1} = \mathcal{C}\chi^T(\vec{p})$$

where χ^T is the transpose of χ. Therefore $V_\mu = -\mathcal{C}V_\mu$, which vanishes for $\mathcal{C} = +1$.

The quasipotential in the constraint formalism is expressed in a coupling scheme in which one particle is at one vertex and the other particle is at the second vertex, whereas the virtual annihilation diagram has both particles at both vertices. This change of coupling requires a Fierz rearrangement in which the vector particle-antiparticle interaction becomes a sum of virtual particle exchanges for which the vertices have various tensorial characters (scalar, pseudoscalar, vector, and axial vector). Compatibility had been worked out previously for a sum of scalar and vector interactions.[7] After much work, it has now been extended to include the other types.[8] A nonperturbative calculation, including virtual annihilation for the ortho state, is being studied. A number of technical difficulties remain. Further along, we hope to treat the virtual annihilation into two photons for application to the ^1S and ^3P states.

---

1. Consultant from University of Tennessee Space Institute, Tullahoma, TN 37388.
2. Pacific Sierra Research Corporation (Eaton), Los Angeles, CA 90025.
3. H. W. Crater and P. van Alstine, Phys. Rev. D 37, 1982 (1988).
4. C. Y. Wong and R. L. Becker, Phys. Lett. 56, 444 (1986).
5. H. Sazdjian, Phys. Lett. 156B, 381 (1982).
6. R. L. Becker, C. Y. Wong, H. W. Crater, and P. van Alstine, p. 390 in Electronic and Atomic Collisions, Abstracts (Proceedings, XV International Conference on the Physics of Electron and Atomic Collisions, Brighton, England, July 1987.)
7. H. W. Crater and P. van Alstine, Phys. Rev. D 36, 3007 (1987).
8. H. W. Crater et al., in Proceedings of Workshop on Relativistic Nuclear Many-Body Physics, Ohio State University, June 1988, to be published.

A NOVEL (e^+e^-) RESONANCE BEHAVIOR FOR A HIGHLY ENERGY-DEPENDENT, EFFECTIVE INTERACTION

Cheuk-Yin Wong   H. W. Crater[1]
R. L. Becker   P. van Alstine[2]

Previously, we investigated the nonperturbative properties of the (e^+e^-) system under their mutual electromagnetic interaction with a two-body Dirac equation derived from constraint dynamics.[3] The vector interaction in the quasi-potential of the equation was obtained by matching it to the one-photon exchange potential in the perturbative limit. For the 0^{++} ($^3P_0$) state of special interest, the interaction at short distances is supercritical. In the course of our investigation of the effect of the annihilation potential, we found that a one-photon annihilation potential can be represented by a combination of scalar, vector, pseudovector, and pseudoscalar interactions through the Fierz transformation. An interesting phenomenological study of high-order diagrams unrelated to the annihilation diagram is to include some of these interactions in the relativistic constraint dynamics. Because the potential becomes much more complicated when we include the time-like component of the pseudovector interaction, we examine the case of a vector electromagnetic interaction, in conjunction with only the addition of scalar, vector, pseudoscalar, and the space-like part of the pseudovector interaction. For these additional interactions, the requirement of the compatibility of constraint dynamics leads to a pair of Dirac equations of the form

$$S_i\psi = [G\theta_i p + E_i\theta_i P + M_i\theta_{5i} + T_i\theta_i\hat{P} + N_i\theta_{5i} + G(i\theta_i\cdot\partial \ln G\ \theta_{1\perp}\cdot\theta_{2\perp} + i\theta_i\cdot\partial Z\theta_{1\perp}\cdot\theta_{2\perp} + i\theta_{i'}\cdot\partial C + i\theta_2\cdot\partial J\theta_i p\theta_i p - i\theta_{i'}\cdot\partial L\ \theta_{51}\theta_{52})]\psi;\ i = 1, 2 \text{ and } i' \neq i$$

where

$$\theta_i = i\sqrt{\frac{\hbar}{2}}\,\gamma_5\gamma^\mu,\quad \theta_s = i\sqrt{\frac{\hbar}{2}}\,\gamma_5,\quad p = (p_1 - p_2)/2$$

is the relative momentum, $P = p_1 + p_2$ is the total momentum. The term $\theta_{i'}\cdot\partial \ln G\theta_{1\perp}\cdot\theta_{2\perp}$ is due to the vector one-photon exchange interaction which was considered previously;[3] Z is from the space-like pseudovector interaction; C is from the pseudoscalar interaction; J is from the time-like component of the additional vector interaction; and L is from the scalar interaction. The terms E_i, M_i, and T_i are related to the other basic functions.

We include these additional interaction terms by using a Yukawa form of the potential with an $e^{-wr/\sqrt{2}}/r$ energy-dependent range $\sqrt{2}\,\hbar/w$, where w is the total energy of the (e^+e^-) system with their strengths fixed to match the perturbative results for the annihilation potential for the $^3S_1$ state. We found that the effective potential for the 0^{++}($^3P_0$) state is no longer supercritical. There is now a potential pocket at the distance of ~0.2-2 fm. The attractive part of the potential arises mainly from the pseudoscalar interaction. The interaction is very energy-dependent (Fig. 5.7). The integration of the Schrödinger-like equation derived from Eq.

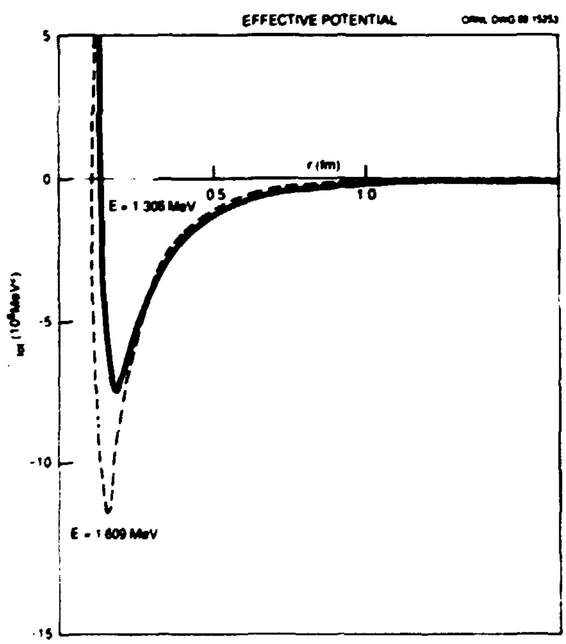

Fig. 5.7. The radial dependence of the effective potential V for the 0^{++} state. The solid curve is the effective potential for the eigenstate at E = 1.306 MeV, and the dashed curve is the effective potential for the eigenstate at E = 1.609 MeV. Note the strong dependence of the potential on the energy.

(1) gives two resonances at E = 1.306 MeV and E = 1.609 MeV. The wave functions for these two resonances have the same interior nodal structure (Fig. 5.8). In order to verify the correctness of the calculations, we have separately

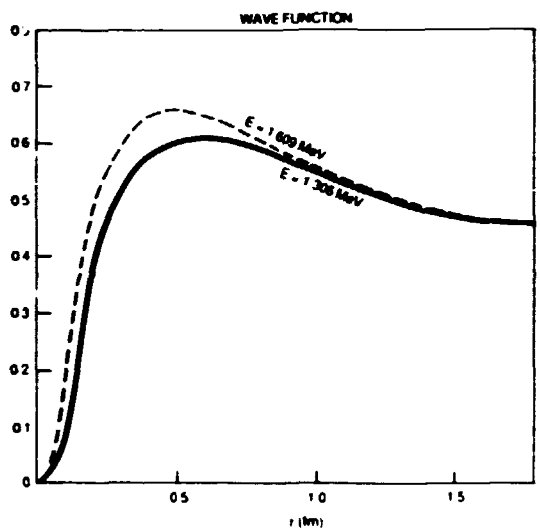

Fig. 5.8. Unnormalized wavefunction in the short-distance region obtained with the potentials of Fig. 5.7. The solid curve is for E = 1.306 MeV, and the dashed curve is for E = 1.609 MeV. The two wave functions have the same nodal structure.

calculated the phase shift as a function of energy using the phase equation.[4] We found that the phase shifts δ(E) make a sudden change at these energies and they cross the value of π/2 at E = 1.304076 MeV and E = 1.609315 MeV (Figs. 5.9 and 5.10), confirming the results of eigenvalue solutions obtained by a very different method. From the energy variation of the phase shifts, we obtain a width of Γ = 0.125 keV for the E = 1.609315 MeV state and a width Γ = 45.3 eV for the E = 1.304076 MeV state.

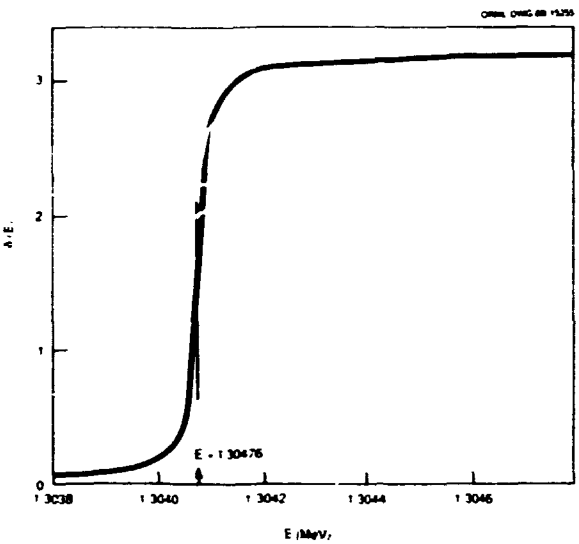

Fig. 5.9. The phase shift function δ(E) as a function of energy in the neighborhood of E = 1.30476 MeV. The phase function δ(E) is equal to π/2 at E = 1.30476 MeV.

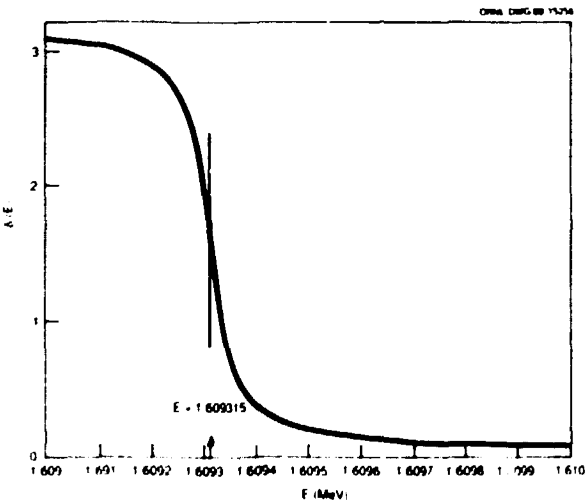

Fig. 5.10. The phase shift function δ(E) as a function of energy in the region of E = 1.609315 MeV. The phase function δ(E) is equal to π/2 at E = 1.609315 MeV.

It is of interest to note a few novel features of the results here. First, strong energy dependence of the effective potential can lead to resonances with similar interior nodal structure, in contrast to energy-independent potentials where the nodal structure of the different eigenstates are different. Second, potential pockets in the (e^+e^-) system may lead to sharp resonances, in spite of the large zero-point oscillation which arises from squeezing the system smaller than the size of the Compton wavelength of the constituents. Thirdly, for the resonance at ~1.3 MeV the phase shift rises with energy, as one expects from a normal potential resonance. However, for the ~1.6 MeV resonance the phase shift decreases as a function of energy. Such a decrease is different from the "echo" of a resonance observed in energy-independent potentials, which has a width much broader than that of the associated resonance. To demonstrate this difference, we have calculated the phase shift function δ(E) for potentials associated with energies below and above 1.609 MeV, and we treat the potential as energy-independent. Then the phase shifts increase with energy to give resonances at energies below and above 1.609 MeV (Fig. 5.11). (Phase shifts increase with energy near the resonances.) Thus, because of the strong dependence on energy, only at 1.609315 MeV does the energy-dependent potential give rise to a resonance at the same energy. Finally, multiple resonances may result from strong energy dependence. It should, however, be noticed that the occurrence of a resonance arises from a cancellation of the kinetic energy and the attractive short-range force. The location of these resonances at around 1.5 MeV may therefore appear accidental.

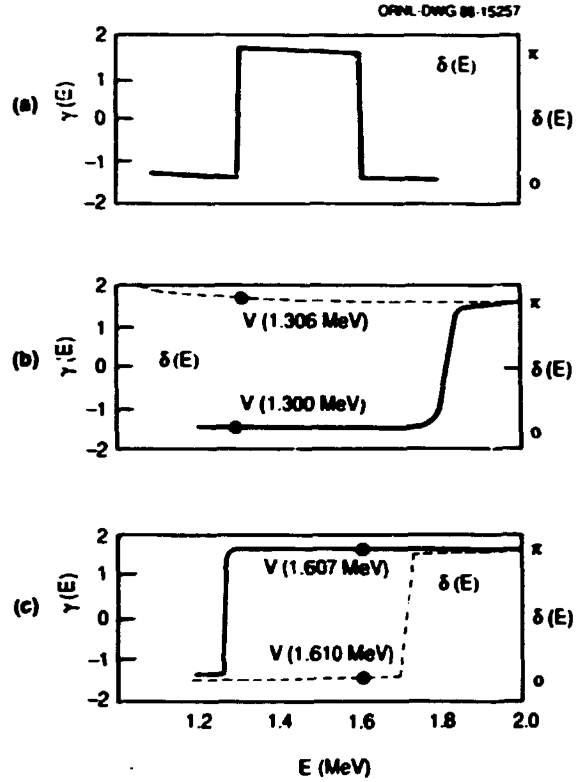

Fig. 5.11. To investigate whether the resonance at E = 1.609315 MeV is an "echo" or a real resonance, we study the phase function δ(E) with energy-dependent and energy-independent potentials. When the energy dependence of the potential V(E) is included, we obtain δ(E) as shown in Figs. 5.11a, 5.9, and 5.10. When we fix the potential V(E) as obtained at E = 1.300 MeV and use the energy-independent potential V(1.300 MeV) to calculate the phase shift δ(E) for other energies, we obtain δ(E) as the solid curve in Fig. 5.11b. When we use an energy-independent potential V(1.306 MeV) where the energy is fixed at 1.306 MeV, we obtain δ(E) as the dashed curve in Fig. 5.11b. Similarly, with energy-independent potentials V(1.609 MeV) and V(1.610 MeV), where the energies are fixed at 1.607 MeV and 1.610 MeV, respectively, we obtain δ(E) as the solid and the dashed curve in Fig. 5.11c. Note the sensitivity of the phase function on the potential.

---

1. Consultant from University of Tennessee Space Institute, Tullahoma, TN 37388.
2. Pacific Sierra Research Corporation (Eaton), Los Angeles, CA 90025.
3. H. W. Crater, C. Y. Wong, R. L. Becker, and P. van Alstine, submitted for publication.
4. F. Calogero, Variable Phase Approach to Potential Scattering (Academic Press, New York, 1967).

COMPUTATIONAL PHYSICS

PERIODIC TIME-DEPENDENT HARTREE-FOCK SOLUTIONS FROM THE BASIS SPLINE METHOD

R. Y. Cusson[1] C. Bottcher
J. Wu[2] M. R. Strayer

The basis spline collocation method in coordinate space[3] is now a well-established method for numerical calculations in physical problems.[4] Recently, this method has been extended to problems in Euclidean times.[5] The time B-spline method, which combines the B-spline method with the traditional variational principles to obtain numerical solutions to partial differential equations, turns out to be unconditionally stable and very efficient, and may find extensive applications. As an example, we propose the calculation of periodic time-dependent Hartree-Fock (TDHF) solutions, from which the collective energy levels could be obtained.[6]

The application of the B-spline method to TDHF lies in the expansion of single-particle wavefunctions in terms of basis spline functions in space-time, i.e.,

$$\psi_i(x,t) = \sum_{\alpha,\beta} \psi_i^{\alpha,\beta}\, u_\alpha(x) u_\beta(t). \qquad (1)$$

For periodic solutions, we simply use periodic basis spline functions, and the above expansion guarantees the periodicity. Rather than writing down the equations at a set of discrete points, we minimize the error functional:[5]

$$S = \int dxdt \,|\, G\Psi \,|^2, \qquad (2)$$

where $G\Psi = 0$ corresponds to the time-dependent Schrödinger equations:[6]

$$\left[i \frac{\partial}{\partial t} - K - U(t)\right] \psi_i^P(x,t) = -\lambda_i \psi_i^P(x,t), \qquad (3)$$

where λ_i are Floquet parameters. The integration of the basis spline functions in the error functional can be carried out. Variational principles would lead to the set of equations determining the expansion coefficients $\psi_i^{\alpha,\beta}$. We believe that an efficient way to minimize the error functional is to combine the B-spline collocation method and time B-spline method.[5] From the quantization rule for periodic TDHF solutions, we could then obtain the collective energy levels.

---

1. Science Applications International Corp., Los Altos, CA 94022.
2. Joint Institute for Heavy Ion Research.
3. C. de Boor, A Practical Guide to Splines (Springer-Verlag, New York, 1978).
4. C. Bottcher and M. R. Strayer, Ann. Phys. (N.Y.) 175, 64 (1987).
5. R. Y. Cusson, P.-G. Reinhard, C. Bottcher, M. R. Strayer, and J. Wu, to be published.
6. I. Zahed and M. Baranger, Phys. Rev. C 29, 1010 (1984).

THE BASIS SPLINE COLLOCATION METHOD APPLIED TO THE DIRAC EQUATION

J. Wu[1] C. Bottcher
M. R. Strayer

Techniques for obtaining highly accurate numerical solutions to problems in quantum field theory have been developed in recent years.[2] One of these is the basis spline collocation method for a relativistic theory of fermions.[3] In this approach, both state vectors and fields are expanded in spline functions, and a lattice in space time is introduced, on which the equations of motion for the state vectors and fields are transformed to coupled matrix equations. For relativistic fermion fields on lattices, problems related to doubling of the spectrum and boundary conditions are crucial in the numerical formulation. We propose general algorithms to treat these problems in the B-spline collocation method, which provide great flexibility in a number of applications.

The difficulties of constructing lattice solutions to the Dirac equation can be addressed by considering the Dirac kinetic energy operator in one space dimension:

$$K_D = \begin{pmatrix} m & -i\partial_x \\ -i\partial_x & -m \end{pmatrix}. \qquad (1)$$

In Ref. 3 a factorization of the collocation matrix of the kinetic energy operator into a lower and upper triangular form is suggested, i.e.,

$$2T = -D_2 = D^- D^+, \qquad (2)$$

where D_2 is the second derivative operator, and the Dirac kinetic energy operator is taken as

$$K_D = \begin{pmatrix} m & -iD^+ \\ iD^- & -m \end{pmatrix}. \qquad (3)$$

Here we suggest that the Dirac kinetic energy operator is in the form:

$$K_D = \begin{pmatrix} m & -iD \\ iD^t & -m \end{pmatrix}, \qquad (4)$$

where D is a matrix appropriate for the first derivative and D^t is its transpose.[4] For problems with periodic boundary conditions, it can be proved that D, D^t are commuting and $-D_2 = DD^t$ is a faithful second-order derivative operator.

Moreover, if D is properly chosen, the second derivative operator thus constructed leads to a better dispersion relation. For the finite difference scheme, the forward and backward derivatives are one example of the D, D^t scheme. However, by a judicious choice of D, we can achieve an optimized dispersion relation for D_2. For other boundary conditions, only the matrix elements at the end points are affected, since splines are local functions.

Boundary conditions in the B-spline collocation method can be simply imposed. They are constructed by taking as many independent spline functions, each of which satisfies the boundary conditions, as the number of collocation points. Generally, in the way[3] the collocation points are chosen, the number of spline functions is larger than (or equal to) the number of collocation points. This allows us to impose side conditions[5] to the system. If we reinterpret these side conditions as boundary conditions, the number of independent splines can be reduced to the number of collocation points such that the transformation between the spline expansion coefficients and collocation points is well conditioned. Thus, all differential operators can be converted to matrix operators in the framework of the B-spline collocation method, where all of the boundary conditions are automatically satisfied.

1. Joint Institute for Heavy Ion Research.
2. S. L. Adler and T. Piran, Rev. Mod. Phys. 56, 1 (1984).
3. C. Bottcher and M. R. Strayer, Ann. Phys. (N.Y. 175, 64 (1987).
4. C. Bottcher, M. R. Strayer, and J. Wu, to be published.
5. C. de Boor, A Practical Guide to Splines (Springer-Verlag, New York, 1978).

ITERATIVE METHOD FOR THE TIME-DEPENDENT RELATIVISTIC MEAN-FIELD THEORY

J. Wu[1] J. J. Bai[2]
P. Y. Cusson[3]

The relativistic mean-field theory provides us with a model[4,5] to replace the nonrelativistic TDHF calculations based on the Schrödinger equation. In this model, nuclei are described as bound states of many Dirac nucleons interacting through meson fields. This theory is correctly time-dilated, Lorentz-contracted, and has retarded interactions and covariant propagations. Therefore, it is preferred in the numerical simulation of heavy-ion collisions at intermediate energies. However, the relativistic calculation in three (space) dimensions involves large amounts of numerical work. We propose an iterative method for the evolution of quantum systems aimed at the reduction of computer time.

The evolution of a quantum system can be described by the Hamiltonian, H, in the time-dependent equation

$$i \frac{\partial}{\partial t} \Psi(x,t) = H\Psi(x,t), \quad (1)$$

where $\Psi(x,t)$ is a state vector. Since we are mainly concerned with many-body systems, Ψ, in general, may have more than one component. The numerical simulation of the time evolution can be realized by the discretization of Eq. (1) on a set of mesh points and discrete time steps. Therefore, Eq. (1) is replaced by the difference scheme

$$\Psi_\beta^{n+1} = \sum_\alpha \left(1 - iH(\beta,\alpha,n)\tau\right)\Psi_\alpha^n, \quad (2)$$

where $\{\alpha\}$ is the set of mesh points and τ is the time step.

The stability of the difference scheme (2) can be greatly improved by the implicit difference scheme:[6]

$$\sum_\alpha \left(1 + iH(\beta,\alpha,n+1/2)\,\frac{\tau}{2}\right)\Psi_\alpha^{n+1} = \sum_\alpha \left(1 - iH(\beta,\alpha,n+1/2)\,\frac{\tau}{2}\right)\Psi_\alpha^n. \quad (3)$$

The solution of Eq. (3) involves an inverse of the matrix $(1 + iH(n + 1/2)\tau/2)$, which slows down the procedure. In order to avoid the calculation of the inverse of a matrix with very large dimensions, we propose an iterative procedure to solve Eq. (3). First, we write the solution formally as:

$$\Psi_\beta^{n+1} = \left[\sum_\alpha \left(1 - iH(\beta,\alpha,n+1/2)\,\frac{\tau}{2}\right)\Psi_\alpha^n - \sum_{\alpha\neq\beta}\left(iH(\beta,\alpha,n+1/2)\,\frac{\tau}{2}\right) \times \Psi_\alpha^{n+1}\right] \Big/ \left(1 + iH(\beta,\alpha,n+1/2)\,\frac{\tau}{2}\right), \quad (4)$$

and then solve Eq. (4) iteratively. The predictor formula for $\Psi_\beta^{n+1,(o)}$ can be obtained simply by letting Ψ_α^{n+1} in Eq. (4) be Ψ_α^n. This corresponds to an explicit way of evolution. The predictor thus obtained will be corrected by the successive replacement of $\Psi^{n+1,(k-1)}$, $(k = 1,2,\ldots)$ on the righthand side of Eq. (4), i.e.,

$$\Psi_\beta^{n+1,(k)} = \Big[\sum_\alpha \Big(1 - iH(\beta,\alpha,n+1/2)\,\frac{\tau}{2}\Big)\,\Psi_\alpha^n - \sum_{\alpha\neq\beta}\Big(iH(\beta,\alpha,n+1/2)\,\frac{\tau}{2}\Big) \times \Psi_\alpha^{n+1,(k-1)}\Big] \Big/ \Big(1+iH(\beta,\beta,n+1/2)\,\frac{\tau}{2}\Big). \qquad (5)$$

Generally, the iterative process is applied until the convergence is reached, as judged by the difference $|\Psi_\beta^{n+1,(k)} - \Psi_\beta^{n+1,(k-1)}|$. Actually, two more iterations are sufficient to give good results, since the predictor $\Psi_\alpha^{n+1,(o)}$ is already a consistent formula. If the Hamiltonian is dependent on Ψ, we must solve it self-consistently.

The iterative method can be generalized to higher dimensions and to the self-consistent mean-field calculation. As long as the diagonal matrix elements remain the major part, the iterative method is effective. For the relativistic mean-field calculation, the interacting meson fields obey equations of motion which involve second-order derivatives in time. We have to cast them into a form which contains only the first derivatives in time. This can be achieved by introducing additional variables for the first time derivatives. The equations of motion can be factorized as[7]

$$(\beta_\mu \partial_\mu + \kappa)\phi = f, \qquad (6)$$

where ϕ and β's are properly defined arrays. Using these linear equations for the meson fields and Dirac equations for nucleons, we can apply the iterative procedure to the self-consistent calculation. Even though the source terms are nonlinear, we can treat them as the off-diagonal part in the procedure. Some numerical calculation has been done and reported in Ref. 8, where the iterative method did result in immense reduction of computer time.

---

1. Joint Institute for Heavy Ion Research.
2. Duke University, Durham, NC 27706.
3. Science Applications International Corp., Los Altos, CA 94022.

4. J. D. Walecka, Ann. Phys. (N.Y.) 83, 491 (1974).
5. B. D. Serot and J. D. Walecka, in Advances in Nuclear Physics, Vol. 16 (Plenum Press, New York, 1985).
6. R. S. Varga, Matrix Iterative Analysis (Prentice-Hall, Englewood Cliffs, NJ, 1962), p. 273.
7. See, for example, E. M. Corson, Introduction to Tensors, Spinors, and Relativistic Wave Equations, Chapter 5 (Chelsea, New York, 1981).
8. J. J. Bai, R. Y. Cusson, J. Wu, P.-G. einhard, H. Stöcker, W. Greiner, and M. R. ayer, Zeit. Phys. A326, 269 (1987).

NUMERICAL METHOD FOR THE CALCULATION OF CONTINUUM EXCITATION AMPLITUDES IN TIME-DEPENDENT EXTERNAL FIELD PROBLEMS[1]

C. Bottcher A. S. Umar[2]
M. R. Strayer V. E. Oberacker[2]

We introduce a new numerical method for calculating continuum excitation probabilities of complex physical systems under the influence of external, time-dependent, and nonperturbative fields. The method utilizes a discretized form of the Hamiltonian on a space lattice and is particularly suited for large-scale computations involving many-body systems. We perform a comparative study for a model problem by solving the same time-dependent Schrödinger equation in spherical and cylindrical coordinates. As a realistic example, we apply the method to the problem of prompt nucleon emission in low-energy heavy-ion reactions.

---

1. Abstract of paper: Phys. Rev. C 37, 2487 (1988).
2. Consultant from Vanderbilt University, Nashville, TN 37235.

APPLICATION OF VECTOR AND PARALLEL COMPUTER ARCHITECTURES

C. Bottcher G. J. Bottrell[1]
M. R. Strayer J. A. Maruhn[2]

We have been devoting some effort to optimizing codes on presently available systems (mostly the Cray-2), while looking ahead to the massively parallel systems which we expect to be available in the near future.

By forcing vectorization of loops, and by some modification of the algorithms, we now have several codes running at around 150 Mflops on the Livermore Cray-2's. These include the codes for Monte Carlo evaluation of Feynman diagrams and for the nonrelativistic TDHF equations.

Two of us (CB and MRS) attended a course at Los Alamos in March 1988 on the FPS T-series hypercubes, as a first step towards moving some of our problems onto a parallel architecture. We have recently begun to work with the mathematical sciences group in the Engineering Physics Division on a "Grand Challenge" project. This is aimed at implementing our pair production calculations on a hypercube architecture, initially an Intel system at ORNL, and then moving up to a state-of-the-art gigaflop machine.

The usefulness of the hypercube architecture has been demonstrated by J. A. Maruhn, who spent a month bringing up a simple hydrodynamics code on the Intel hypercube, and comparing the run times with those on other computers. It was concluded that codes can be made to run efficiently with a moderate amount of effort.

1. Oak Ridge Associated Universities Postdoctoral Research Associate.
2. Consultant from University of Frankfurt, Frankfurt, West Germany.

MATHEMATICAL PHYSICS

PERIODIC TRAJECTORIES FOR THE TWO-DIMENSIONAL NONINTEGRABLE HÉNON-HEILES HAMILTONIAN

T. Huston[1] K.T.R. Davies
M. Baranger[2]

We have begun a new numerical study of the two-dimensional, nonintegrable Hénon-Heiles Hamiltonian[3] which is given by

$$H = \frac{1}{2}(p_x{}^2 + p_y{}^2) + \frac{1}{2}(x^2 + y^2 + 2x^2y - \frac{2}{3}y^3). \quad (1)$$

The equipotential contours of the potential term in (1) are shown in Fig. 5.12. As in previous studies[4,5] we are calculating the periodic trajectores for this Hamiltonian using the Monodromy matrix method.[6] We are mainly interested in determining the principal periodic

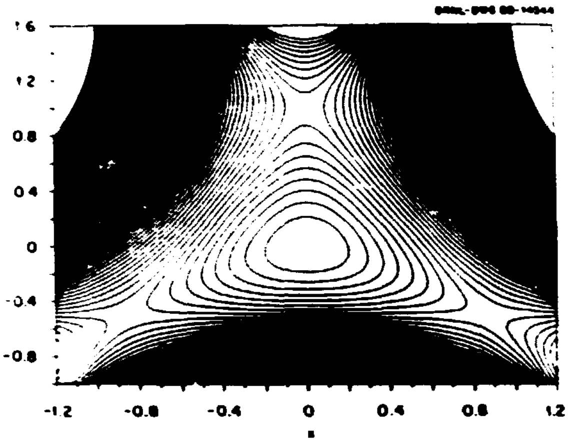

Fig. 5.12. Equipotential contours of the Hénon-Heiles potential.[3]

families and their simplest branchings which originate either at low energies or at small values of the period τ. Also, in order to illuminate the connection with chaotic behavior,[3,4] we are studying representative nonperiodic trajectories which lie "close" in phase space to the periodic families.

One of the main families being studied is the horizontal family, so called because it originates from the horizontal family of small oscillations. This family is shown in Fig. 5.13. You see that for small energies the oscillation is completely in the x-direction; then it rapidly develops a small curve and eventually,

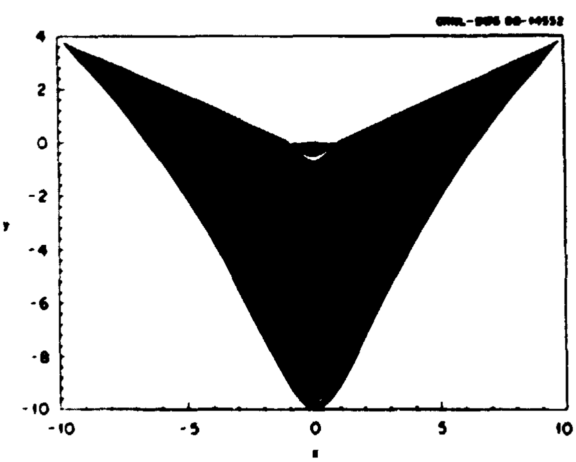

Fig. 5.13. x-y plots of 180 members of the horizontal family. This type of trajectory is a libration.[4]

for large energies, it becomes a very pronounced V shape. This family continues on indefinitely, growing asymptotically to infinite energy. Also, it was determined that this family is always unstable. Even at low energies, the trace of the Monodromy matrix[4-6] is always greater than 4.0. Thus, this family does not allow branching to another family,[4,5] and the nearby nonperiodic trajectories always lie in chaotic regions of phase space.[3,4] Finally, we mention that the potential in Eq. (1) possesses a ternary symmetry, being invariant under rotations of 120°.[3] Thus, for every periodic solution, one can obtain two other valid periodic solutions by rotating the original curve by 120° and by 240°. This is illustrated in Fig. 5.14 for the horizontal family.

---

1. Participant in University of Tennessee Science Alliance Summer Research Program from Hendrix College, Conway, AR 72032.
2. Consultant from M.I.T., Cambridge, MA 02139.
3. M. Hénon, p. 107 in Chaotic Behavior of Deterministic Systems - Les Houches 1981 (North-Holland, Amsterdam, 1983).
4. M. Baranger and K.T.R. Davies, Ann. Phys. (N.Y.) 177, 330 (1987).
5. M.A.M. de Aguiar, C. P. Malta, M. Baranger, and K.T.R. Davies, Ann. Phys. (N.Y.) 180, 167 (1987).
6. M. Baranger, K.T.R. Davies, and J. H. Mahoney, Ann. Phys. (N.Y.) 186, 95 (1988).

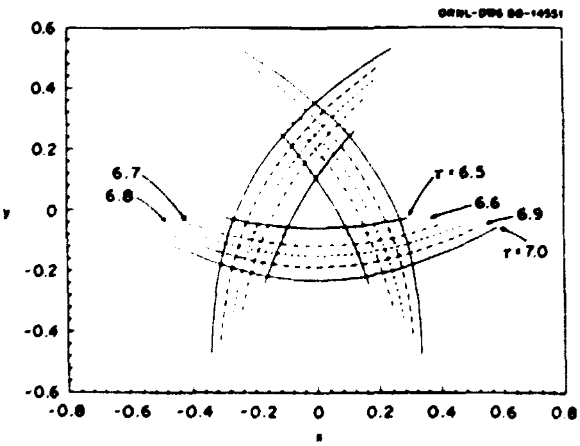

Fig. 5.14. Several low-energy members of the horizontal family and their associated rotated solutions. The horizontal trajectories are the flat, U-shaped curves, and the other two sets of trajectories can be obtained from these by rotations of 120° and 240°.

THE CALCULATION OF PERIODIC TRAJECTORIES[1]

M. Baranger[2]   K.T.R. Davies
J. H. Mahoney[2]

Methods are presented for calculating classical periodic trajectories in a two-dimensional nonintegrable potential problem. The main one is the monodromy method, which consists in refining an approximate solution by using a "once around the trajectory" procedure. This can be done either for a given period or for a given energy. Other methods proceed by searching on the initial conditions until the trajectory closes. We also discuss how to find new periodic families, particularly branchings from already known families, and how to get started when no families are known.

---

1. Abstract of paper: Ann. Phys. (N.Y.) 186, 95 (1988).
2. Massachusetts Institute of Technology, Cambridge 02139.

COMPLEX-PLANE METHODS FOR EVALUATING HIGHLY OSCILLATORY INTEGRALS IN NUCLEAR PHYSICS I[1]

K.T.R. Davies   M. R. Strayer
G. D. White[2]

A general program is being developed for the systematic and careful evaluation of Green's functions in pion-nucleon problems. This paper is the first in a series of projects involving integral methods for the calculation of the pion and nucleon propagators. A method is presented for evaluating efficiently and accurately integrals of the form $\int r^m \, x_{\ell_1}(k_1 r) \, x_{\ell_2}(k_2 r) \ldots x_{\ell_n}(k_n r)dr$, where m and n are arbitrary integers and $x_\ell(x)$ can be either a spherical Bessel function, $j_\ell(x)$, or a spherical Neumann function, $n_\ell(x)$. The range of integration depends upon the particular problem encountered. The prototype integral studied is

$$I_{\ell\ell'L}(kk'p) \equiv \int_0^\infty r^2 \, j_\ell(kr) j_{\ell'}(k'r) \, j_L(pr)dr$$

whose integrand for large r has a slowly decreasing oscillatory behavior. Rapid convergence is insured by rotating, in the complex plane, the upper part of this integral, giving an integrand which decreases exponentially. A scaling formula is used to evaluate $I_{\ell\ell'L}(kk'p)$ for very small or very large values of the momenta. Also, it is shown that, if ℓ, ℓ', and L satisfy triangular inequalities and if $\ell + \ell' + L$ is even, then k, k′, and p must also satisfy triangular inequalities, which is the condition required by the vector delta function $\delta(\vec{k} + \vec{k}' - \vec{p})$. Finally, we present sum rules and integral relations for $I_{\ell\ell'L}(kk'p)$.

---

1. Abstract of paper: J. Phys. G 14, 961 (1988).
2. Consultant from Northwestern State University, Natchitoches, LA 71457.

COMPLEX-PLANE METHODS FOR EVALUATING INTEGRALS WITH HIGHLY OSCILLATORY INTEGRANDS[1]

K.T.R. Davies

An integral whose integrand oscillates rapidly in the asymptotic region may be evaluated by deforming the contour of integration in the complex plane. By proper choice of a contour, the oscillations may be completely eliminated, giving an integrand which decreases exponentially. Such methods may be used to evaluate various types of integrals, the most important of which are of the form $J = \int_R^\infty r^m \chi_{\ell_1}(k_1 r)\chi_{\ell_2}(k_2 r)\ldots\chi_{\ell_n}(k_n r)dr$, where m and n are arbitrary integers and $\chi_{\ell_i}(k_i r)$ is a spherical Bessel or Neumann function. A scaling formula may be used to evaluate J for very large or very small values of the k_i's. Also, it is shown that, for R = 0, m = 2; and when all of the χ_{ℓ_i}'s are Bessel functions, J vanishes if certain vector inequalities involving the k_i's are inconsistent with two sets of relations satisfied by the ℓ_i's.

---

1. Abstract of paper to be published in Journal of Computational Physics.

POTENTIAL GROUP APPROACH TO A CLASS OF SOLVABLE POTENTIALS

J. Wu[1] R. Y. Cusson[2]
Y. Alhassid[3]

Group theoretic techniques have been used in many fields of physics. Most of the applications are for the analysis of bound-state problems. Recently, there have been attempts[4,5] to extend these techniques to scattering problems. In order to understand these extensions, one would like to learn from the examples for which exact connections between simple potential problems and group theory can be established. The solvable class of Natanzon potentials[6] provides us with such examples.

We consider the realization of the SO(2,2) group on the sheet $\sigma = \mathrm{sign}(\rho^2) = +1$ of the (2,2) hyperboloid H^3:[7]

$$\rho^2 = x_1^2 + x_2^2 - x_3^2 - x_4^2 = \text{constant}. \qquad (1)$$

This is a symmetric representation in which the SO(2,2) basis $|\omega,m_1,m_2\rangle$ is characterized by

$$\begin{aligned} C_2|\omega,m_1,m_2\rangle &= \omega(\omega+2)|\omega,m_1,m_2\rangle, \\ J_3|\omega,m_1,m_2\rangle &= m_1|\omega,m_1,m_2\rangle, \\ K_3|\omega,m_1,m_2\rangle &= m_2|\omega,m_1,m_2\rangle. \end{aligned} \qquad (2)$$

If we parametrize the hyperboloid in terms of (χ,ϕ,α) as follows:

$$\begin{aligned} x_1 &= \rho\cosh\chi\cos\phi, \\ x_2 &= \rho\cosh\chi\sin\phi, \\ x_3 &= \rho\sinh\chi\cos\alpha, \\ x_4 &= \rho\sinh\chi\sin\alpha, \end{aligned} \qquad (3)$$

where ϕ and α are rotation angles in 1-2 and 3-4 two-spaces, respectively, the basis can be written explicitly in the form:

$$|\omega,m_1,m_2\rangle = e^{i(m_1\phi+m_2\alpha)}R_{\omega m_1 m_2}(\chi). \qquad (4)$$

After a series of variable transformations from χ, through z to r, where

$$z = \tanh^2\chi,$$

and the transformation $z(r)$ is determined by the differential equation

$$\left(\frac{dz}{dr}\right)^2 = \frac{4z^2(z-1)^2}{R(z)} ,$$

where

$$R(z) = az^2 + b_0 z + c_0 = a(z-1)^2 + b_1(z-1) + c_1,$$

and a similarity transformation

$$F = \left(\frac{dz}{dr}\right)^{-1/2} z^{1/2},$$

we find that $R_{\omega m_1 m_2}(r)$ satisfies the Schrödinger equation with the Natanzon potential

$$H_N R_{\omega m_1 m_2}(r) = \left[-\frac{d^2}{dr^2} + U(r)\right] R_{\omega m_1 m_2}(r) = E R_{\omega m_1 m_2}(r), \quad (5)$$

where

$$U[z(r)] = \frac{fz(z-1) + h_0(1-z) + h_1 z}{R(z)} - \frac{1}{2}\{z,r\}, \quad (6)$$

and the Schwarz derivative of z is defined by

$$\{z,r\} = \frac{z'''}{z'} - \frac{3}{2}\left(\frac{z''}{z'}\right)^2 .$$

In the realization of the Natanzon potential the Hamiltonian of the system is defined as

$$H_N = \left(\frac{z}{R(z)} - \frac{1}{c_1}\right)(\omega+1)^2 - \frac{z}{R(z)}(C_2+1) + \frac{1+h_1}{c_1} , \quad (7)$$

which depends only on the SO(2,2) Casimir operator C_2, where the quantum numbers are determined as

$$(\omega+1)^2 = 1 + h_1 - c_1 E,$$
$$m_1^2 = 1 + f - aE, \quad (8)$$
$$m_2^2 = 1 + h_0 - c_0 E.$$

It is obvious that the states in the same multiplet are at the same energy but belong to different potential strengths, and both bound states and scattering states can be realized in the realization. This approach is known as the potential group approach.[4]

Once the algebraic structure of Natanzon potentials is found, the close forms of their energy spectra and scattering matrices can be understood through purely algebraic construction. The discrete principal series of representations, for which the eigenvalues m_1 of the operator J_3 have a lower bound state, describe the bound states; the continuous principal series of representations describe the scattering states. For the fixed potential strength, we can determine the bound state spectrum by requiring that the state is in a discrete principal series and construct the scattering matrix with the Euclidean connection method.[4,5] These examples reconfirm that the closed forms of bound-state spectra and scattering matrices are closely related to the corresponding group structure.

Since the transformation $z(r)$ contains three parameters, a, b_0, and c_0, and three other parameters, h_0, h_1, and f, are involved in $U(r)$, Natanzon potentials constitute a large class of solvable potentials. The well-known Pöschl-Teller, Eckart, Rosen-Morse, and Manning-Rosen potentials belong to this family. Recently, another important branch of this family was rediscovered by Ginocchio[8] and studied in detail. These analytical solvable potentials are useful in physics, and an understanding of their group structure is very helpful in their applications. For example, they provide us guidelines in formulating realistic algebraic scattering models.

---

1. Joint Institute for Heavy Ion Research.
2. Science Applications International Corp., Los Altos, CA 94022.
3. Yale University, New Haven, CT 06511.
4. Y. Alhassid, F. Gürsey, and F. Iachello, Phys. Rev. Lett. 50, 873 (1983). Ann. Phys. (N.Y.) 148, 346 (1983); Ann. Phys. (N.Y.) 167, 181 (1986).
5. A. Frank and K. B. Wolf, Phys. Rev. Lett. 52, 1737 (1984); Y. Alhassid, J. Engel, and J. Wu, Phys. Rev. Lett. 53, 17 (1984); J. Wu, F. Iachello, and Y. Alhassid, Ann. Phys. (N.Y.) 173, 68 (1987).
6. G. Natanzon, Vestnik Leningrad Univ. 10, 22 (1971); Teoret. Mat. Fiz. 38, 146 (1979) [English transl.].
7. A. Frank and K. B. Wolf, J. Math. Phys. 26, 1973 (1985).
8. J. Ginocchio, Ann. Phys. (N.Y.) 152, 203 (1984); Ann. Phys. (N.Y.) 159, 467 (1985).

POTENTIAL GROUP APPROACH AND DIFFERENTIAL EQUATIONS

J. Wu[1] R. Y. Cusson[2]
Y. Alhassid[3]

Group theoretic techniques find their way into many fields of physics. Most of the applications are involved with symmetry groups and dynamical groups, and designed for bound-state problems. In the attempts to extend these techniques to describe scattering states, another kind of group, the potential group, was suggested.[4] The operators of the potential group connect states at the same energy but belong to different potential strengths. Both bound states and scattering states can be realized with the same group realization.

Consider the differential realization of SO(2,1) algebra

$$J_\pm = e^{\pm i\phi}\left[\pm\frac{\partial}{\partial x} + k_1(x)\left(i\frac{\partial}{\partial\phi} \mp \frac{1}{2}\right) + k_0(x)\right],\qquad J_3 = -i\frac{\partial}{\partial\phi}. \tag{1}$$

The basis for the realization is characterized by

$$C_2\,|\,j,m\rangle = j(j+1)\,|\,j,m\rangle,\qquad J_3\,|\,j,m\rangle = m\,|\,j,m\rangle, \tag{2}$$

and can be written explicitly as

$$|\,j,m\rangle = \Psi_{jm} = \phi_{jm}(x)e^{im\phi}. \tag{3}$$

If the Hamiltonian of a physical system is

$$H = -\left(C_2 + \frac{1}{4}\right), \tag{4}$$

the simultaneous eigenfunction of H and J_3 leads to a one-dimensional Schrödinger equation

$$\left[-\frac{d^2}{dx^2} + (k_1^2(x) - 1)\left(m^2 - \frac{1}{4}\right) + 2m\frac{dk_0(x)}{dx} + k_0^2(x)\right]\phi_{jm}(x) = E\phi_{jm}(x), \tag{5}$$

where the quantum number m appears to be potential strength and $-(j+1/2)^2$ the energy E. Since the Hamiltonian is related only to the Casimir operator, all states in a representation are at the same energy, but correspond to different potential strengths. When the potential strength m is given, the Hamiltonian has a continuous spectrum, which describes the scattering states for the continuous principal series ($j = -1/2 + ik$, $0 < k < \infty$), i.e.,

$$\langle H\rangle = k^2, \qquad 0 < k^2 < \infty$$

and a discrete spectrum, which describes bound states for discrete principal series ($m+j = n$, $n = 0,1,1,\ldots$), i.e.,

$$\langle H\rangle = -(j+1/2)^2 = -(m-n-1/2)^2,$$
$$n = 0,1,2,\ldots(m-1/2).$$

In Fig. 5.15, several Morse potentials are plotted and the SO(2,1) multiplets are shown by the horizontal dashed lines.

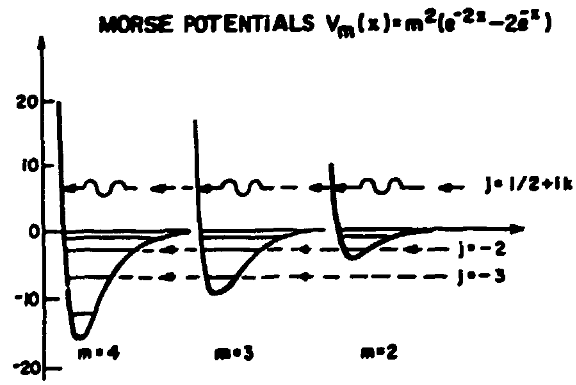

Fig. 5.15. Morse potential $V_m(x) = m^2(e^{-2x} - 2e^{-x})$ for $m = 2,3,4$ are plotted in solid lines. The SO(2,1) multiplets for $j = -2, -3, -1/2+ik$ are shown by the horizontal dashed lines.

Attempts have also been made to apply such realizations to more extensive potentials.[5,6] They can be summarized as:

(1) introduce a similarity transformation $F = e^{S(x)}$ and a variable transformation $x = x(z)$ to the algebra, since the commutation relations are preserved no matter how complicated these transformations could be;

(2) introduce physical systems with more complicated Hamiltonian.

Here we propose the general form of Hamiltonian for the realization of potential group:

$$H = \left(f(z) - a\right)(j+1/2)^2 - f(z)\left(FC_2F^{-1} + 1/4\right), \quad (6)$$

where F is a similarity transformation, z is a related variable transformation, and a > 0. In order to cancel the appearance of the j-dependence in the potential, we have to reinterpret the quantum number m as a function of potential strength, and the energy such that the explicit j-dependence in the Hamiltonian is cancelled by the implicit dependence from the Casimir operator and the potential in the Schrödinger equation is still independent of energy. For example, in the realization of the first class of Ginocchio potentials, the quantum numbers take the following form:[7]

$$\begin{aligned} \langle C_2 + 1/4\rangle &= (j+1/2)^2 = \nu^2 \\ \langle j_3^2\rangle &= m^2 = (\nu+1/2)^2 + \nu^2(1-\lambda^2). \end{aligned} \quad (7)$$

We can apply this approach to realize a class of solvable potentials and, therefore, solve their bound-state spectra and scattering matrices with purely algebraic techniques.[5] We can also realize the confluent hypergeometric equation and hypergeometric equation by using SO(2,1) and SO(m,n) (m,n > 2) groups, respectively. The realizations of these equations imply the general proof that potential problems with analytical solutions in terms of confluent hypergeometric or hypergeometric functions are of the corresponding potential group structure. For further attempts to new solvable classes of potentials, we may have to appeal to other groups and special functions.

---

1. Joint Institute for Heavy Ion Research.
2. Science Applications International Corp., Los Altos, CA 94022.
3. Yale University, New Haven, CT 06511.
4. Y. Alhassid, F. Gürsey, and F. Iachello, Phys. Rev. Lett. 50, 873 (1983); Ann. Phys. (N.Y.) 148, 346 (1983); Ann. Phys. (N.Y.) 167, 181 (1986); A. Frank and K. B. Wolf, J. Math. Phys. 26, 1973 (1985).
5. J. Wu, R. Y. Cusson, Y. Alhassid, and F. Gürsey, to be published.
6. A. O. Barut, A. Inomata, and R. Wilson, J. Phys. A20, 4083 (1987).
7. J. Wu, R. Y. Cusson, and Y. Alhassid, to be published.

QUARKS IN NUCLEI

y-SCALING IN A SIMPLE QUARK MODEL[1]

S. Kumano[2] E. J. Moniz[3]

A simple quark model is used to define a nuclear pair model; that is, two composite hadrons interacting only through quark interchange and bound in an overall potential. An "equivalent" hadron model is developed, displaying an effective hadron-hadron interaction which is strongly repulsive. We compare the effective hadron model results with the exact quark model observables in the kinematic region of large momentum transfer and small energy transfer. The nucleon response function in this y-scaling region is, within the traditional framework, sensitive to the nucleon momentum distribution at large momenta. We find a surprisingly small effect of hadron substructure. Furthermore, we find in our model that a simple parametrization of modified hadron size in the bound state, motivated by the bound quark momentum distribution, is not a useful way to correlate different observables.

---

1. Abstract of paper to be published in Proceedings of the 3rd Conference on the Intersections Between Particle and Nuclear Physics, Rockport, Maine, 1988, and published paper: Phys. Rev. C 37, 2088 (1988).
2. Guest Assignee from University of Tennessee, Knoxville, TN 37996-1200.
3. Massachusetts Institute of Technology, Cambridge, MA 02139.

THE SPIN AND FLAVOR DEPENDENCE OF PARTON DISTRIBUTION FUNCTIONS[1]

F. E. Close[2] A. W. Thomas[3]

Gluon exchange in QCD is shown to lead to systematic flavor and spin-dependent distortion of quark distribution functions. We relate the Δ-nucleon mass difference, the ratio of neutron and proton inelastic structure functions, and the deep inelastic polarization asymmetries. Excellent agreement is found with existing data, and predictions are made for the polarized neutron asymmetry at x > 0.2.

---

1. Abstract of paper to be published in Physics Letters B.

2. UT-ORNL Distinguished Scientist.
3. University of Adelaide, Adelaide SA 5001, Australia.

PARTON DISTRIBUTIONS IN NUCLEI: QUAGMA OR QUAGMIRE?[1]

F. E. Close[2]

Emerging information on the way quark, antiquark, and gluon distributions are modified in nuclei relative to free nucleons is reviewed. Particular emphasis is placed on Drell-Yan and ψ production on nuclei, and caution is urged against premature use of these as signals for quagma in heavy-ion collisions.

1. Abstract of paper to be published in Proceedings of International Conference on Physics and Astrophysics of Quark-Gluon Plasma, Bombay, India, February 8-12, 1988.
2. UT-ORNL Distinguished Scientist.

ATOMIC AND MOLECULAR PHYSICS

TIME-DEPENDENT HARTREE-FOCK STUDIES OF ION-ATOM COLLISIONS

C. Bottcher G. J. Bottrell[1]

We have begun production calculations on ion-atom collisions using the time-dependent Hartree-Fock method. Our implementation uses the basis-spline-collocation technique on a three-dimensional Cartesian lattice.

An interesting check of the method was to compare the static atomic wavefunctions of helium and neon with those tabulated by Herman and Skillman. The differences are hardly visible on a graph.

A study of p + He has been completed, and C^{6+} + Ne is in progress. As indicated in other sections of this report, we have assembled the tools to extract a variety of intricate correlations and differential cross sections for direct comparison with experimental data.

1. Oak Ridge Associated Universities Postdoctoral Research Associate.

CONTINUUM ELECTRON SPECTRA FOR PROTON IMPACT ON HYDROGEN

C. Bottcher G. J. Bottrell[1]
M. R. Strayer

A formalism has been developed for calculating continuum excitation probabilities for time-dependent external field problems.[2] In this formalism the continuum excitation probability is given by

$$P_\alpha(\epsilon) = \langle \psi_\alpha(t) \,|\, F^\dagger(\epsilon)F(\epsilon) \,|\, \psi_\alpha(t)\rangle \quad (1)$$

where

$$F(E) = (\pi\Delta)^{-1/4} \exp[-(H_0-E)^2/(2\Delta^2)] \quad (2)$$

and $\psi_\alpha(t)$ is the final time-evolved wavefunction. We have improved this method by introducing the approximation

$$F(E) = N \left\{1 + \frac{(H_0-E)^2}{2m\Delta^2}\right\}^{-m} \quad (3)$$

with N a normalization constant and m an integer. In the limit $m \to \infty$ this relation is exact. The inversion of the operator necessary to evaluate its action on $\psi_\alpha(t)$ is achieved using a successive over-relaxation (SOR) procedure.

We have used this approach to examine the electrons emitted from both the target and the projectile in collisions of protons with atomic hydrogen. The accuracy of the procedure is comparable to the previous approach which involved using a series expansion to evaluate the Gaussian operator. The great advantage of the present procedure is its speed: an order of magnitude or more improvement over the Gaussian expansion procedure.

In addition, we have performed the deconvolution necessary to evaluate the angular dependence of the emitted electrons. This is accomplished by using the Gaussian form $\exp[-(\hat{n}_i-\hat{r})^2/\delta^2]$ with n_i the i-th direction normal, $\hat{r}$ the integration variable, and δ a factor chosen so that

$$\sum_i \int \exp[-(\hat{n}_i-\hat{r})^2/\delta^2] d^2\hat{r} = 4\pi. \quad (4)$$

We are also working to extend these procedures to the examination of systems involving multi-electron targets.

---

1. Oak Ridge Associated Universities Postdoctoral Research Associate.
2. C. Bottcher, M. R. Strayer, A. S. Umar, and V. E. Oberacker, Phys. Rev. C 37, 2487 (1988).

ON THE CROSS SECTIONS FOR ELECTRON TRANSFER, EJECTION, AND EXCITATION IN COINCIDENCE WITH A HOLE IN A SPECIFIC SHELL[1]

Richard L. Becker

It is a familiar fact that in the independent Fermi particle model the sum of the ion-induced cross sections for inclusive-single direct ionization, electron transfer, and excitation equals that for inclusive single vacancy production. We show, however, that the analogous sum for these processes in coincidence with a hole in a particular shell (i.e., with an Auger electron or X ray) is greater than the inclusive cross section for production of a vacancy in that shell, except in the limit of very weak interactions (exclusively single-electron transitions). These coincidence cross sections are separated into inclusive contributions in which either single or double electron transitions are explicitly specified. Illustrative calculations for He^{2+} and C^{6+} on Ne show the quantitative importance of the double transition terms for direct ionization as well as electron transfer.

---

1. Abstract of paper to be published in the special issue of Acta Physica Hungarica in honor of D. Berényi's 60th birthday.

FORMULATION OF THE OHCE METHOD IN COUPLED CHANNELS THEORY FOR THE CAPTURE OF PROJECTILE ELECTRONS

R. L. Becker

In the theory of energetic ion-atom collisions the case treated most often is that of a structureless projectile ion incident on an atom with one or more active electrons. The ion may be either bare or may contain electrons treated as inert. However, by time reversal invariance, the first-order transition probability from a projectile-centered orbital to a target-centered orbital is equal to that for the reverse transition and should not be ignored.[1] In the independent Fermi particle model (IFPM)[2] the calculation of time-dependent many-electron states is reduced to that of single-electron spin-orbitals. When strong transitions are involved, the coupled-channels approach is called for. If $Z_P \ll Z_T$ a single-center expansion in target-centered states is effective,[3] but when Z_P becomes nearly equal to Z_T, a two-centered expansion appears to be needed. The latter leads to very elaborate and slow calculations. The "one-and-a-half-center-expansion" (OHCE) was developed[4] as a faster, but still fairly accurate, way of treating nearly symmetric collisions. Until now it has been formulated only for the case of an electron initially on the target, described in terms of a basis containing many target orbitals and one projectile orbital, for which case it has been rather successful.[4,5,1] Here we present, for the same basis, the equations for the case of an electron initially on the projectile.

In the impact-parameter method the nuclei move on prescribed trajectories so that the electronic Hamiltonian is time-dependent. It may be decomposed as follows: $H(t) = H^T(t) + V^P(t) = H^P(t) + V^T(t)$, where the V's are residual interactions. The two-center orbital is

$$\psi_\mu(\vec{r},t) = \sum_{n=1}^{N} \chi_n(\vec{r},t)a_{n\mu}(t) + \varphi_\mu(\vec{r},t)b_\mu(t)$$

in which

$$\left(i\hbar\frac{\partial}{\partial t} - H^T\right)\chi_n = 0 = \left(i\hbar\frac{\partial}{\partial t} - H^P\right)\varphi_\mu$$

and

$$\langle\chi_n|\chi_{n'}\rangle = \delta_{nn'},\ \langle\varphi_\mu|\varphi_\mu\rangle = 1.$$

The residual interactions are assumed to drop off more rapidly than r^{-1} so that, if $t = 0$ at the distance of closest approach, the coefficients $a_{n\mu}(t)$ and $b_\mu(t)$ are essentially constant for $t < -t_L$ and $t > t_L$ for some large time t_L. Then the case we consider is defined by the initial conditions

$$a_{n\mu}(-t_L) = 0, \text{ all } n, \text{ and } b_\mu(-t_L) = 1.$$

Moreover,

$$\langle \chi_n(\ ,t) | \varphi_n(\ ,t)\rangle \xrightarrow[t \to \pm t_L]{} 0.$$

The variation of $a_{n\mu}$ leads[3] to

$$\langle \chi_n(\ ,t) | i\hbar \frac{\partial}{\partial t} - H | \psi_\mu\rangle = 0 \qquad (1)$$

or

$$i\hbar\, \dot{a}_{n\mu}(t) - \sum_{n'} V^P_{nn'}(t) a_{n'\mu}(t) = V^T_{n\mu}(t) b_\mu(t)$$

$$- i\hbar \langle \chi_n(\ ,t) | \varphi_\mu(\ ,t)\rangle\, \dot{b}_\mu(t).$$

The time-development matrix U for the target-centered states is defined by

$$i\hbar \frac{\partial}{\partial t} U_{nn'}(t,t') - \sum_{n''} V^P_{nn''}(t) U_{n''n'}(t,t') = 0$$

with

$$U^\dagger(t,t') = U^{-1}(t,t') = U(t',t)$$

so that

$$U_{nn'}(t,t) = \delta_{nn'}.$$

Then

$$a_{n\mu}(t) = -\frac{i}{\hbar} \sum_{n'} \int_{-t_L}^{t} dt'\, U_{nn'}(t,t')$$

$$\times \left[V^T_{n'\mu}(t') b_\mu(t') - i\hbar \langle \chi_{n'}(\ ,t') | \varphi_\mu(\ ,t')\rangle \dot{b}_\mu(t')\right]$$

In the two-center method the variation of $b_\mu(t)$ leads to a differential equation for $b_\mu(t)$. The OHCE method is defined by prescribing in advance the shape of the time-dependence of b_μ and leaving arbitrary only the final value, $b_\mu(t_L)$. The motivation and justification for this approximation, which benefits from our having a large target-centered basis, is discussed in Ref. 4. Let us write

$$b_\mu(t) = 1 + \Delta b\ \beta(t)$$

with

$$\beta(-t_L) = 0,\ \beta(t_L) = 1, \text{ and } \Delta b \equiv b_\mu(t_L) - 1.$$

We then employ a variational principle which leads to

$$\int_{-t_L}^{t_L} dt\ \langle [1+\Delta b\ \beta(t)]\varphi_\mu(\ ,t) | i\hbar \frac{\partial}{\partial t} - H(\ ,t) | \psi_\mu(\ ,t)\rangle = 0. \qquad (2)$$

Together with Eq. (1), this gives

$$\int_{-t_L}^{t_L} dt\ \langle \psi_\mu(\ ,t) | i\hbar \frac{\partial}{\partial t} - H(\ ,t) | \psi_\mu(\ ,t)\rangle = 0$$

so that

$$\langle \psi_\mu(\ ,t_L) | \psi_\mu(\ ,t_\mu)\rangle$$

$$= \langle \psi_\mu(\ ,-t_L) | \psi_\mu(\ ,-t_L)\rangle = 1,$$

which implies the unitarity of the scattering matrix in the basis of atomic orbitals. The optical choice of the mean field in H^T implies that $V^T_{\mu\mu} \equiv 0$. Then, after integration by parts, Eq. (2) with $\beta(t)$ real valued leads to

$$\frac{1}{2}|\Delta b|^2 + \Delta b = -\frac{i}{\hbar} \sum_n \int_{-t_L}^{t_L} dt\ \{[1+\Delta b^* \beta(t)] V^T_{\mu n}(t)$$

$$+ i\hbar\, \Delta b^* \dot{\beta}(t) \langle \varphi_\mu(\ ,t) | \chi_n(\ ,t)\rangle\} \cdot a_{n\mu}(t).$$

The simplest, physically reasonable choice[4] for β is $\beta(t) = \theta(t)$, the step function equal to 0 for $t < 0$ and 1 for $t > 0$. Care at $t = 0$ is needed. We have $\dot{\theta}(t) = \delta(t)$, and in Eq. (2) we encounter

$$\int_{-t_L}^{t_L} dt\ \delta(t)\ \theta(t) = \frac{1}{2}\int_{-t_L}^{t_L} dt \frac{d}{dt}\theta^2(t) = \frac{1}{2},$$

so, effectively, $\theta(0) = 1/2$. For this choice of $\beta(t)$

$$a_{n\mu}(t) = a^{(0)}_{n\mu}(t) + \theta(t) a^{(1)}_{n\mu}(t)\Delta b$$

with

$$a^{(0)}_{n\mu}(t) = -\frac{i}{\hbar}\sum_{n'} \int_{-t_L}^{t} dt'\ U_{nn'}(t,t') V^T_{n'\mu}(t')$$

and

$$a^{(1)}_{n\mu}(t) = -\frac{i}{\hbar}\sum_{n'} \left\{ \int_{0}^{t} dt'\ U_{nn'}(t,t') V^T_{n'\mu}(t') - i\hbar\, U_{nn'}(t,0) \langle \chi_{n'}(\ ,0) | \varphi_\mu(\ ,0)\rangle \right\}.$$

In particular

$$a^{(1)}_{n\mu}(0) = -\langle \chi_n(\ ,0) | \varphi_\mu(\ ,0)\rangle.$$

Then

$$|\Delta b|^2 + 2\Delta b = 2\sum_n \Big\{ -\frac{i}{\hbar}\int_{-t_L}^{t_L} dt\; V^T_{\mu n}(t) a^{(0)}_{n\mu}(t)$$

$$+ \Delta b^* \langle \varphi_\mu(,o) \,|\, \chi_n(,o)\rangle\, a^{(0)}_{n\mu}(o)$$

$$+ \frac{1}{2}|\Delta b|^2 \,|\langle \varphi_\mu(,o) \,|\, \chi_n(,o)\rangle|^2$$

$$- \frac{i}{\hbar}\int_0^{t_L} dt\; V^T_{\mu n}(t)[\Delta b^* a^{(0)}_{n\mu}(t)$$

$$+ (|\Delta b|^2 + \Delta b) a^{(1)}_{n\mu}(t)]\Big\}.$$

Because the only quadratic terms are proportional to $|\Delta b|^2$, one can find a linear combination of the real and imaginary parts of this equation which is linear in ReΔb and ImΔb. Substitution then gives a quadratic equation for ReΔb or ImΔb.

The integrals occurring for this case are similar to those which occurred when the electron was initially on the target,[4] the only difference being that in some of them the limits of integration are different. Thus, numerical calculations of about the same speed and accuracy as previous OHCE calculations appear feasible. A variety of applications would be interesting, including those in which transfer from the target is obtained for projectiles of the same Z_p, but different values of the ionic charge.[1]

---

1. R. L. Becker, Nucl. Instrum. & Meth. B 27, 506 (1987).
2. R. L. Becker, A. L. Ford, and J. F. Reading, Phys. Rev. A 29, 3111 (1984).
3. See R. L. Becker, A. L. Ford, and J. F. Reading, J. Phys. B 13, 4059 (1980).
4. J. F. Reading, A. L. Ford, and R. L. Becker, J. Phys. B 14, 1995 (1981).
5. J. F. Reading, A. L. Ford, and R. L. Becker, J. Phys. B 15, 625 (1982); A. L. Ford, J. F. Reading, and R. L. Becker, J. Phys. B 15, 3257 (1982); R. L. Becker, A. L. Ford, and J. F. Reading, Nucl. Instrum. & Meth. B 10/11, 1 (1985); R. L. Becker, p. 447 in High Energy Ion-Atom Collisions (Springer-Verlag, Berlin, 1988).

IONIZATION IN COLLISIONS BETWEEN ELECTRONS AND COMPLEX IONS[1]

C. Bottcher D. C. Griffin[2]
M. S. Pindzola[3]

Most models of hot plasmas containing complex ions still rely on simple, semi-empirical formulae for electron-impact ionization rates. These formulae often fail when applied to complex ions, through neglect of two factors: (1) indirect ionization mechanisms involving autoionizing states, and (2) long-lived metastable states of the target ion. Extensive calculations and measurements on the iron isonuclear sequence, carried out by groups at Oak Ridge,[4] provide an instructive case study. While the distorted-wave approximation is often adequate, some progress has been made toward more precise calculations. Even approximate calculations on complex systems require extensive computer resources.

---

1. Abstract of talk presented at Gaseous Electronics Conference, Atlanta, Georgia, October 13-16, 1987.
2. Rollins College, Winter Park, FL 32789.
3. Auburn University, Auburn, AL 36849.
4. M. S. Pindzola, D. C. Griffin, and C. Bottcher, Phys. Rev. A 34, 3668 (1986).

ELECTRON-ION COLLISIONS IN THE AVERAGE-CONFIGURATION DISTORTED-WAVE APPROXIMATION[1]

M. S. Pindzola[2] D. C. Griffin[3]
C. Bottcher

Explicit expressions for the electron-impact excitation, ionization, and resonant-recombination cross sections are derived in the average-configuration distorted-wave approximation. Calculations using these expressions are applied to several types of phenomena in electron-ion scattering where comparison with other theoretical methods and experimental measurements can be made.

---

1. Abstract of paper: pp. 75-91 in Atomic Processes in Electron-Ion and Ion-Ion Collisions (Plenum Publishing Corporation, 1986).
2. Auburn University, Auburn, AL 36849.
3. Rollins College, Winter Park, FL 32789.

ELECTRON-IMPACT IONIZATION DATA FOR THE Fe ISONUCLEAR SEQUENCE[1]

M. S. Pindzola[2] C. Bottcher
D. C. Griffin[3] S. M. Younger[4]
H. T. Hunter

Collision processes involving highly ionized iron impurities play an important role in magnetically confined fusion plasmas. Available experimental and theoretical cross-section data for electron-impact ionization of ions in the Fe isonuclear sequence in charge states ranging from 1 to 26 are reviewed, and recommended data for each charge state are presented graphically. Contributions to the ionization cross sections due to inner-shell excitation-autoionization have been considered in detail for each ionization stage and make substantial contributions for the intermediate charge states. The role of metastable levels in ionization is also addressed. Maxwellian collisional rate coefficients are calculated from these recommended cross-section data and presented in tabular, graphical, and parametrized form. Comments are made on current research activities leading to future data for Fe ions.

---

1. Abstract of paper: Nuclear Fusion Special Supplement, 1987.
2. Auburn University, Auburn, AL 36849.
3. Rollins College, Winter Park, FL 32789.
4. Lawrence Livermore National Laboratory, Livermore, CA 94550.

PRODUCTION OF HIGH-ANGULAR MOMENTUM RYDBERG STATES BY STOCHASTIC COLLISIONS[1]

J. Burgdörfer[2] C. Bottcher

Projectile-centered Rydberg states of fast, highly charged ions traversing thin solid targets show an unexpected abundance of high ℓ states. We present a theory for the production of high ℓ states based on classical stochastic dynamics. Diffusion into high ℓ states is shown to be universal for single-particle orbits in three dimensions under the influence of a stochastic perturbation, i.e., largely independent of the details of the interaction potentials. Monte Carlo simulations using a Langevin equation for stochastically perturbed electrons in a dynamically screened Coulomb field yield quantitative agreement with experimental data.

---

1. Abstract of paper submitted to Physical Review Letters.
2. Adjunct staff member from University of Tennessee, Knoxville, TN 37996-1200.

THE v/2 ELECTRON EMISSION IN ION-ATOM COLLISIONS WITH SHORT-RANGE POTENTIALS[1]

J. Burgdörfer[2] J. Wang[3]
A. Bárány[4]

Recent classical trajectory Monte Carlo calculations for $H^+ + H$ collisions by Olson[5] have revealed a qualitatively new feature in the ionization spectrum: a peak near forward direction at $v = v_p/2$ (v_p = projectile velocity) of electrons stranded in between the two potential wells of the target and projectile. Data by Meckbach et al.[6] display a narrowly focused "ridge" in the forward emission spectrum of electrons propagating in the saddle point region of the potential in the exit channel. The "height" of this ridge is not yet unambiguously established.[7] More recently, Olson et al.[8] found a v/2 hump in the differential ionization spectrum at an angle ~20° relative to the forward direction. We have investigated[9] the existence of a "v/2" peak for ion-atom collisions in one dimension where the Coulomb potentials are replaced by Dirac delta potentials. For potentials of zero range (δ potentials) the complete velocity spectrum can be calculated exactly. Despite the absence of a saddle point, we find a hump near $v_p/2$ while the customary ECC and ELC "cusp" electrons near $v_e = v_p$ and $v_e = 0$ are missing (Fig. 5.16). In this case, the excitation process at low and intermediate velocities can be traced to a Fano-Lichten type molecular orbital promotion mechanism at small internuclear distances leading to the excitation of zero-energy (threshold) resonances in the quasimolecular spectrum.[10] This result points to the independence of the primary excitation mechanism from the long-range part of the electron-nucleus interaction. However, the details of the slope of the peak will depend on the long-ranged postcollisional interaction.[6,11] At high velocities the hump near v/2 disappears indicating the breakdown of the quasimolecular excitation mechanism.

---

1. Summary of paper: Phys. Rev. A 38, 4919 (1988).

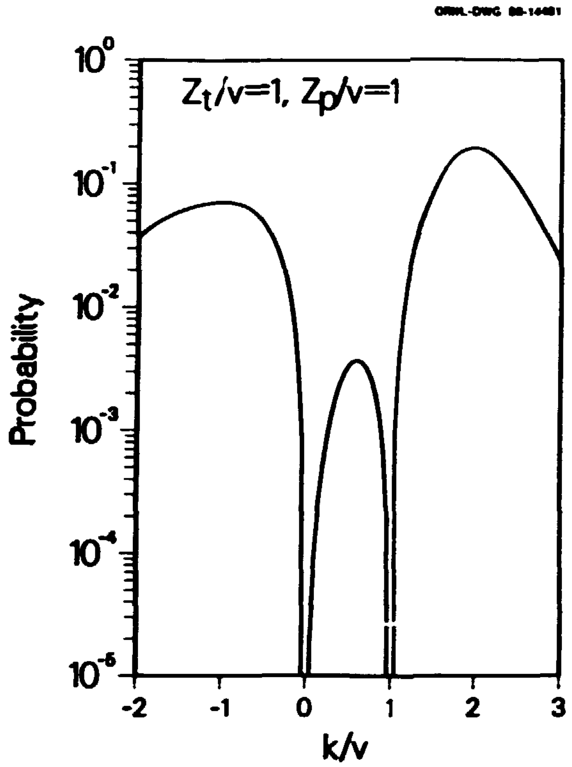

Fig. 5.16. Differential ionization probability vs. electron momentum k (in units of the projectile velocity v_p). $Z_{T,P}$ denotes target (projectile) charge; the v/2 electron hump appears at k/v = 1/2.

2. Adjunct staff member from University of Tennessee, Knoxville, TN 37996-1200.
3. University of Tennessee, Knoxville, TN 37996-1200.
4. Research Institute of Physics, S-10405 Stockholm, Sweden.

5. R. E. Olson, Phys. Rev. A 33, 4397 (1986).
6. W. Meckbach et al., Phys. Rev. Lett. 57, 1587 (1986).
7. C. Garibotti, private communication.
8. R. E. Olson et al., Phys. Rev. Lett. 59, 36 (1987).
9. J. Burgdörfer, J. Wang, and A. Bárány, Phys. Rev. A 38, 4919 (1988).
10. J. Wang and J. Burgdörfer, submitted to Nuclear Instruments and Methods in Physics Research (1988).
11. Conference on the Physics of Electronic and Atomic Collisions, Abstracts of Contributed Papers, Eds. J. Geddes et al. (Brighton, U.K., 1987) p. 605.

TRANSLATION IMBEDDED PERTURBED STATIONARY STATES[1]

G. J. Bottrell[2] T. G. Heil[3]

An extension of the method of perturbed stationary states (PSS) is presented. The translation imbedded perturbed stationary states (TIPSS) method involves an expansion of the total wavefunction in eigenfunctions of the Jacobi nuclear kinetic energies and appropriate electronic states. The resulting equations avoid the usual pitfalls of the PSS approach, i.e., electronic origin ambiguities and long-range dipole couplings. A simple approximation to these equations is examined for the collisions of the bare nuclei He^{2+}, Li^{3+}, and Be^{4+} with atomic hydrogen for velocities v < 1.0 (atomic units). Excellent agreement between theory and experiment is obtained.

---

1. Abstract of paper submitted to Physical Review A.
2. Oak Ridge Associated Universities Postdoctoral Research Associate.
3. University of Georgia, Athens, GA 30602.

NUMERICAL HARTREE-FOCK WAVEFUNCTIONS FOR TRIATOMIC MOLECULES

G. J. Bottrell[1] J. C. Morrison[2]

We have begun a program to solve numerically for the wavefunctions of simple triatomic molecules. This solution is found by expanding the wavefunction in a set of local functions known as basis splines. We then perform a mapping into a collocation space allowing us to work with the actual wavefunction rather than a set of expansion coefficients. The result is a matrix eigenvalue problem for the energies.

This set is solved using the method of imaginary time propagation. In this method an initial trial function ψ_T^0 is chosen. This trial function can be written as an expansion in terms of the exact eigenfunctions ϕ_n as

$$\psi_T^0 = N^0 \left[a_0^0\phi_0 + \sum_n a_n^0\phi_n\right]$$

where ϕ_0 is the ground-state wavefunction, N^0 is a normalization constant, and the sum is over $n \neq 0$. We now operate with the operator $e^{-\tau H}$ where H is the Hamiltonian and τ is a parameter to be chosen. The result after renormalization is the function ψ_T^1, which can be written as

$$\psi_T^1 = N^1 \left[a_0^1\phi_0 + \sum_n a_n^1\phi_n\right]$$

where the a_n^1 are related to the a_n^0 by

$$a_n^1 = e^{-(E_n-E_0)\tau} a_n^0.$$

Since $E_0 < E_n$ for all $n \neq 0$, $a_n^1 < a_n^0$ for all $n \neq 0$, so that ψ_T^1 is richer in ϕ_0 than was ψ_T^0. Repeated iteration allows the resulting function to be arbitrarily close to ϕ_0. The parameter τ is chosen in order to speed up this iteration process with the restriction that it cannot be so large that the expansion of the operator $e^{-\tau H}$ becomes excessively long. Excited state wave-functions are obtained by starting with a trial function that is orthogonal to ϕ_0.

We have applied this method to finding the ground state of the molecular ion H_3^{2+}. Results are in quantitative agreement with other calculations.[3] Plans are under way to improve the accuracy of the results, as well as to allow for exploration of the relevant molecular structure parameters (bond length, bond angle, etc.). Work is also under way to extend this work to multielectron systems, in particular to the helium-like system H_3^+ and the neon-like system H_2O.

---

1. Oak Ridge Associated Universities Post-graduate Research Associate.
2. University of Louisville, Louisville, K. 40292.
3. D. Feller, private communication.

6. LASER AND ELECTRO-OPTICS LAB

The plasma diagnostics development program focuses on the development of advanced diagnostic systems for existing and future magnetic fusion experiments, relying primarily on optical and laser technology. The Laser and Electro-Optics Lab (LEOL) encompasses these activities and makes this technology available to other ORNL programs. The current emphasis is on the application of infrared and far-infrared lasers to the diagnostics of the next generation of ignited fusion reactors. Small-angle Thomson scattering of pulsed CO_2-laser radiation is being developed as a diagnostic of energetic alpha particles produced by the D-T fusion reaction. A multichannel interferometer far-infrared interferometer system is being developed for measurement of electron density profiles in the Advanced Toroidal Facility (ATF) being placed into operation in the ORNL Fusion Energy Division. An infrared laser interferometer/polarimeter system operating at 10.6 and 28 μm has also been proposed for the Compact Ignition Tokamak, whose construction has been proposed at Princeton Plasma Physics Laboratory. Other LEOL activities include measurements of damage to optical materials produced by intense laser irradiation. This work formed part of the ORNL program in support of the Strategic Defense Initiative.

DIAGNOSTIC FOR FUSION-PRODUCED ALPHA PARTICLES BASED ON SMALL-ANGLE THOMSON SCATTERING OF PULSED CO_2 LASER RADIATION

R. K. Richards[1] Y. M. Fockedey[4]
C. A. Bennett[2] H. T. Hunter
L. K. Fletcher[3] D. P. Hutchinson
K. L. Vander Sluis

In a deuterium-tritium fueled fusion reactor the fusion-product alpha-particle behavior is of crucial importance, because the energy transferred to the plasma fuel from the slowing down of these particles is required to maintain ignition. Therefore, the next generation of fusion reactors has as its main physics goal the study of the physics of alpha-particle heating.[5] To study the alpha particle behavior we have examined the feasibility of a Thomson scattering diagnostic based on a high power CO_2 laser.[6] Recent work on this diagnostic is summarized in references 7 and 8. The scattering is expected to produce a spectrum shown in Fig. 6.1. Note that the scattering from the free electrons produces a small background in the measurement of the alpha particles.

Present and future work is directed toward a proof-of-principle test on a nonburning plasma in the Advanced Toroidal Facility (ATF). The goal of this test is to observe the Thomson scattering under similar conditions expected in an experiment having alpha particles. However, with no alpha particles, the test will then be a measurement of only the electrons.

ORNL-DWG 88-14823

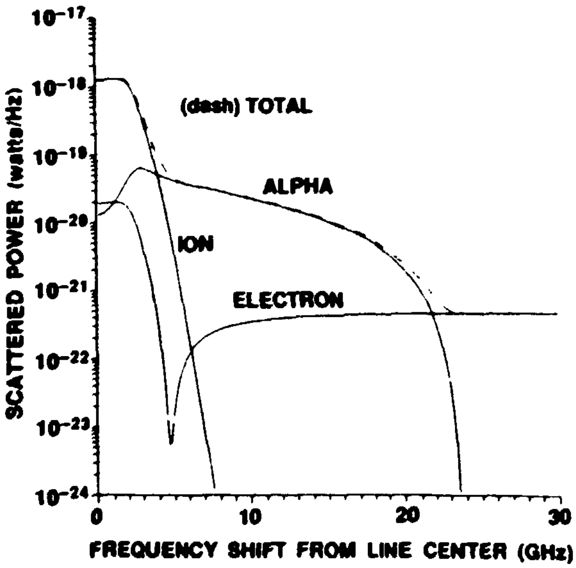

Fig. 6.1. The expected scattered power spectrum from the components in an ignited plasma.

---

1. Fusion Energy Division, ORNL.
2. On sabbatical from University of North Carolina, Asheville.

3. Tennessee Technological University, Cookeville, Tennessee.
4. Catholic University of Louvain, Louvain-la-Neuve, Belgium.
5. D. Post et al., Princeton Plasma Physics Laboratory Report No. 2389 (1986).
6. D. P. Hutchinson et al., Rev. Sci. Instrum. 56, 1075 (1985).
7. R. K. Richards et al., Rev. Sci. Instrum. 59, 1556 (1988).
8. C. A. Bennett, R. K. Richards, D. P. Hutchinson, ORNL/TM-10419, 1988.

DEVELOPMENT OF A SUBMILLIMETER-WAVE MULTICHANNEL LASER INTERFEROMETER FOR THE ADVANCED TOROIDAL FACILITY

C. H. Ma   Y. M. Fockedey[3]
C. A. Bennett[1]   J. Lee[4]
W. H. Casson[2]   K. L. Vander Sluis
D. P. Hutchinson

A 15-channel interferometer operating at a wavelength of 119 μ is being developed for the Advanced Toroidal Facility (ATF) experiment at ORNL. The large number of channels is achieved by the use of reflective beam expansion optics to create a beam 2 cm × 45 cm.[5] After passing through the plasma discharge, the elongated beam produced by the cylindrical mirrors is dissected at the focal plane of the optics system by an array of 15 off-axis paraboloid reflectors, each of which illuminates a single Schottky-diode detector. The use of the beam expanding optics system reduces the average number of optical elements required for the interferometer to approximately 2-3 per channel.

The interferometer was operated on a single channel during the last quarter of FY 1988 using a free-space lens system to transport the laser beam to the ATF device. The atmospheric attenuation of the FIR laser beam due to water vapor was found to be prohibitive and a dry-nitrogen-filled waveguide transmission system was constructed to replace the free-space lens optics. This change resulted in adequate signal levels at the plasma and reference detectors to operate the interferometer. During the first half of FY 1989, the waveguide system will be mated to the beam-expansion-optics set in order to implement the 15-channel interferometer.

---

1. On sabbatical from University of North Carolina, Asheville.
2. ORAU Postdoctoral Research Associate.
3. Catholic University of Louvain, Louvain-la-Neuve, Belgium.
4. University of Tennessee, Knoxville.

5. C.A.J. Hugenholtz and B.J.H. Meddens, Rev. Sci. Instrum. 53, 171 (1982).

PROPOSAL FOR A TWO-COLOR INTERFEROMETER/POLARIMETER FOR THE COMPACT IGNITION TOKAMAK

C. H. Ma   D. P. Hutchinson
K. L. Vander Sluis

During the past year, the feasibility of a two-color infrared interferometer/polarimeter system for simultaneous measurements of electron density and plasma current profiles in the Compact Ignition Tokamak (CIT) has been investigated. A two-color system using CO_2 lasers at a wavelength of 10.6 μm and water-vapor lasers at 28 μm was proposed to correct the measuring errors caused by mechanical vibrations of the optic components. The choice of these wavelengths results mainly from a trade-off, being sufficiently short to limit both the angle of beam refraction by plasma density gradients and the ellipticity of the polarized wave to an acceptable value, yet sufficiently long to obtain adequate sensitivity for the measurements.[1] A schematic diagram of the CO_2 laser system is shown in Fig. 6.2. The detailed theory and description of the system have been reported elsewhere.[2]

In the first of two experiments to determine the performance characteristics of the electro-optic modulation system, a mechanical polarization rotator was inserted in the path of the probing beam, and was set at 45° with respect to the polarization of the incident beam. Under this condition, a Faraday rotation of 90° was simulated. Figure 6.3b shows the output signal of the detector and the modulation signal of the rf modulator. The frequency spectrum of the heterodyne beat signal at 40 MHz and the side-band frequencies of ±70 kHz are illustrated in Fig. 6.3a. It can be seen in the figures that, for a modulation of about 33%, the signal-to-noise ratio of the side-bands is approximately 20 dB. The high signal-to-noise ratio was achieved with only one watt of CO_2 laser power and without any beam focusing. The output

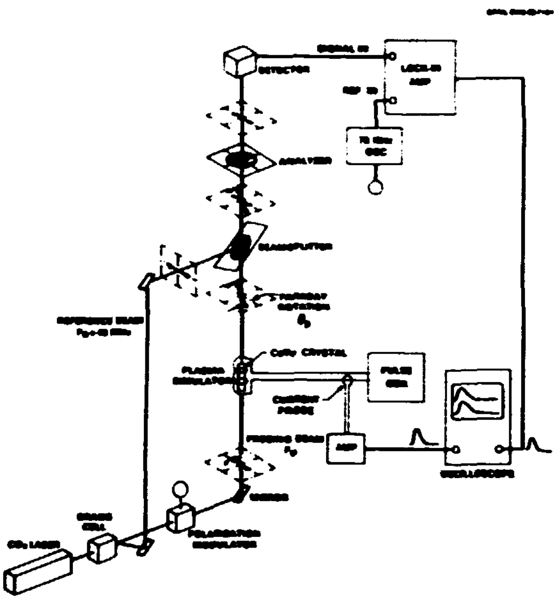

Fig. 6.2. Experimental configuration for the polarization-modulation CO_2 laser polarimeter.

signal can be synchronously detected by two lock-in amplifiers at 40 MHz and 70 kHz. However, due to limited resources, the signal was analyzed by only one lock-in amplifier synchronized to the modulation frequency (October 1987). Since the signal at the modulation frequency is only proportional to the power of the probing beam, this measurement was performed with the reference beam blocked. The output signal of the detector with probing beam only is shown in Fig. 6.4b. The modulation signal is also illustrated in this figure. Figure 6.4a shows the frequency spectrum of the modulated signal. The output voltage of the lock-in amplifier, V, is given by:

$$V = V_0 \sin(2\theta_p) \qquad (1)$$

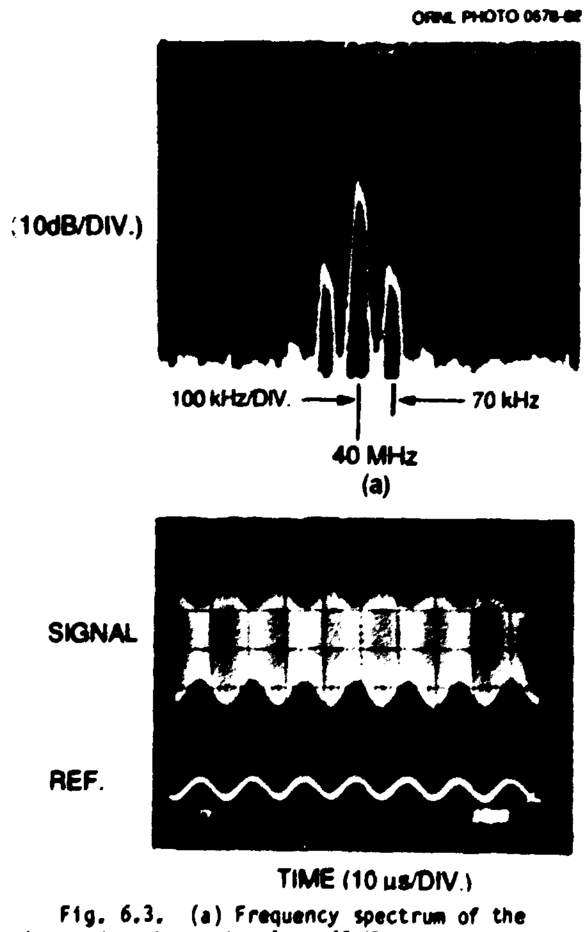

Fig. 6.3. (a) Frequency spectrum of the heterodyne beat signal at 40 MHz and the sideband frequencies of ±70 kHz. (b) Output signal of the detector (upper trace) and the modulation signal at 70 kHz (lower trace) with both probing and reference beams.

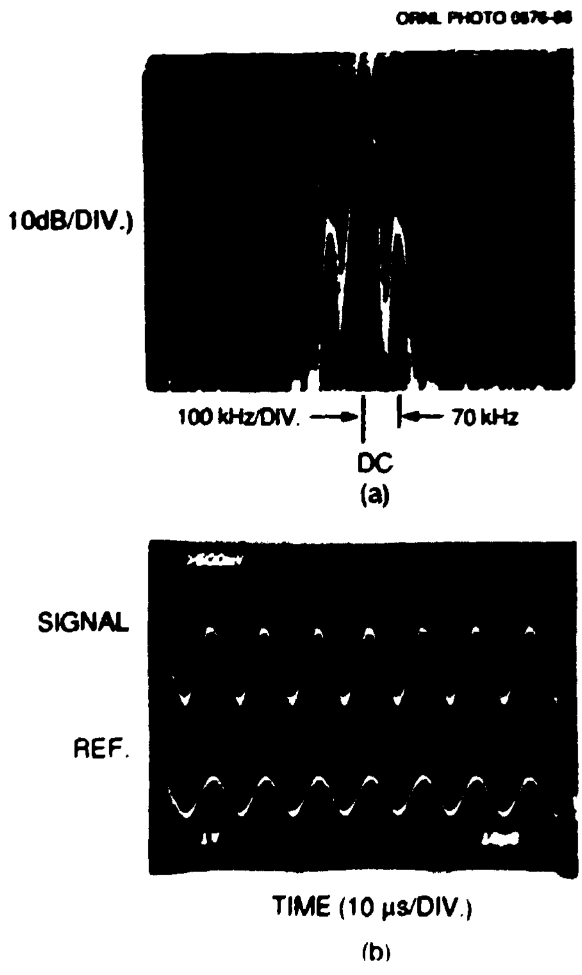

Fig. 6.4. (a) Frequency spectrum of the modulated signal at 70 kHz. (b) Output signal of the detector (upper trace) and the modulation signal (lower trace) with probing beam only.

where θ_p is the Faraday rotation in the plasma, and V_0 is a calibration constant. For CIT plasma parameters, the maximum value of θ_p is approximately 1.5°.[3] Therefore, V can be considered as a direct measure of θ_p and Eq. (1) becomes

$$\theta_p = V/2V_0 \qquad (2)$$

The constant V_0 can be obtained by setting the mechanical polarization rotator at a few degrees (<4°) and measuring the value of V.

Our second experiment studied the transient performance of the polarimeter. The plasma simulator coil was driven by a pulsed current. The rotation caused by this simulator coil was directly proportional to the current, which was monitored by a current probe. The simulated Faraday rotation and the amplifier output were simultaneously displayed on an oscilloscope. Typical oscillograph traces are shown in Fig. 6.5. As shown in the figure, for a simulated rotation of approximately 1.8°, the output voltage of the amplifier is about 330 mV. The base line of the output voltage is in the range of 1 to 2 mV. Therefore, a sensitivity of approximately 0.01° was achieved. The time delay between the simulated and measured rotations was due to the large RC constant (3 ms) of the lock-in amplifier. Evidently, the time resolution of the polarimeter can be improved

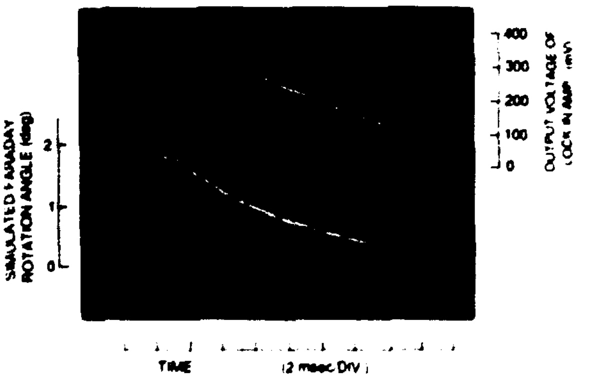

Fig. 6.5. Simulated Faraday rotation angle (lower trace) and the measured lock-in amplifier output (upper trace) vs time for a simulated CIT plasma. Traces indicate that the Faraday rotation measurement has a sensitivity of about 0.01°.

easily by increasing the modulation frequency and using lock-in amplifiers with faster time constants. A magneto-optic polarization modulator was successfully designed, constructed, and tested. The performance characteristics of the polarimeter with this modulator are being investigated.

An interferometer/polarimeter system employing a 28-μm water-vapor laser has been proposed by T. Fukuda et al. and has been tested on a field-reversed theta pinch plasma.[4] To our knowledge, the feasibility of using polarization-modulation techniques in polarimeters has not yet been examined at this wavelength. We are currently designing a 28-μm laser system and intend to investigate the performance of 28-μm polarization modulators.

1. C. H. Ma and D. P. Hutchinson, Bull. Am. Phys. Soc. 32, 1870 (1987).
2. C. H. Ma, D P. Hutchinson, and K. L. Vander Sluis, Rev. Sci. Instrum. 58, 1629 (1988).
3. C. H. Ma et al., Space Power 6, 221 (1986).
4. T. Fukuda et al., Int. J. Infrared MM Waves 5, 1039 (1984).

OPTIC DAMAGE AND IRRADIATION STUDIES

H. T. Hunter R. K. Richards[1]
D. P. Hutchinson

For many years optical materials for high-tech mirrors and windows have been studied to improve their performance in military and commercial applications. ODIS (Optic Damage and Irradiation Studies), as part of the Laser and Electro-Optics Lab, has designed, constructed, and implemented a high power CO_2 pulsed laser system to study the damage thresholds of optical components. A sketch of the basic system components is provided in Fig. 6.6.

The damage thresholds of superpolished mirrors and windows were determined by varying the pulsed laser power density that irradiated the optic surface. To vary the pulsed laser power density, a gas cell was designed to absorb a controlled amount (up to 99.99%) of the pulsed laser 10.6-μm radiation enroute to the sample.

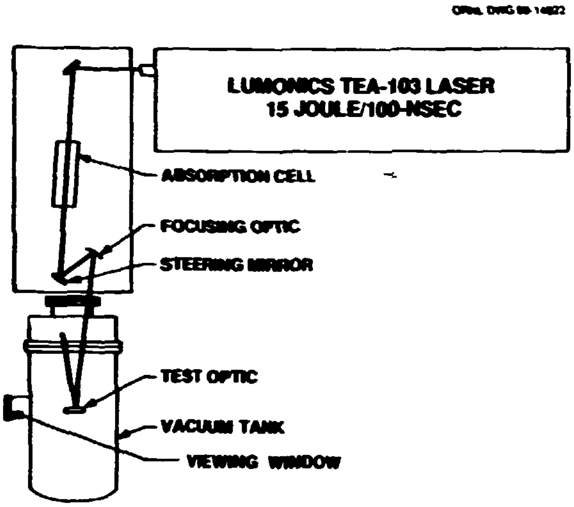

Fig. 6.6. Apparatus (top view).

The extent of optic surface damage was determined by measuring reflectance changes in situ from a 0.633-μm laser scatterometer illuminating the irradiation site. All testing was done while the optic samples were in vacuum. This allowed irradiating the sample with higher CO_2 laser power densities without absorption of the 10.6-μm radiation by air.

Results obtained are considered sensitive material and therefore may not be disclosed for the purpose of this report.

---

1. Fusion Energy Division, ORNL.

7. HIGH ENERGY PHYSICS

H. O. Cohn

The data taking phase of a high energy neutrino interaction experiment at Fermilab has been completed. The experiment was done employing a 1.4 meter freon-filled bubble chamber and a big array of different large area position-sensitive counters. The collaboration that performed the experiment consisted of physicists from Tohoku University, Brown University, Fermilab, Indiana University, Institute for High Energy Physics of Beijing, China, Massachusetts Institute of Technology, University of Tennessee, Tohoku Gakuin University and Oak Ridge National Laboratory. In the following, we describe a new method to investigate the nuclear effect in leptonic interactions (EMC effects).

Since the discovery of the EMC effect,[1] various experiments have been done including muon scattering studies, electron scattering, and deep inelastic neutrino experiments. All of these experiments obtained the ratio of the deep inelastic structure functions, $F_2(x)$, or equivalent of the cross section, $\sigma(x)$, for interactions with a heavy nucleus relative to deuterium. The common features of these data are: a small excess of the ratio in the region ($x < 0.3$), a dip in the middle region ($0.3 < x < 0.7$) and a sharp rise for ($0.8 < x$). Here, x is the Bjorken variable, $x = Q^2/2\ M\nu$, Q^2 being the four momentum transfer squared, M the nucleon mass, and ν the energy transfer between neutrino and muon ($E_\nu - E_\mu$). Although many theoretical interpretations of this effect[2] have been advanced, it would appear that a final resolution of its underlying cause will require either more detailed information or, perhaps, experimental data of a different kind. Our experiment presents a new approach to the study of the nuclear effect.

The basis of our idea is that a nucleus is not uniform for this effect. The more loosely bound surface nucleons may be considered quasi-free while the more tightly bound nucleons experience motion which is strongly correlated with other nucleons, and the EMC effect may be due to interactions involving nucleons of the latter type.

Interactions with the above two categories of nucleons can presumably be differentiated by the nuclear debris associated with neutrino interactions. The dark tracks (stubs) from an interaction vertex in the bubble chamber pictures are thought to be such nuclear debris. It is clear that this procedure will not result in a perfect separation of events due to the two classes of nucleons. Nevertheless, to first order, we shall assume that events with dark tracks are predominantly interactions with deeply bound nucleons while events without dark tracks are primarily interactions with quasi-free surface nucleons. If these assumptions are adequate, we should be able to demonstrate the EMC effect by comparing the two groups of data from a given target nucleus. Furthermore, this should result in a larger effect than is seen in conventional experiments since the latter, perforce, include a large fraction of quasi-free interactions.

The Tohoku 1.4 m High Resolution Freon Bubble Chamber Hybrid System was exposed to the wide band neutrino beam generated by 800 GeV protons from the TEVATRON. The bubble chamber employs a holographic high-resolution camera, in addition to the three normal stereo-optic cameras. In this experiment, the Freon liquid is a mixture of R116, C_2F_6 (27% in weight) and R115, C_2ClF_5 (73%). The ratio of atoms, $^{12}C:^{19}F:^{35}Cl$, is 0.25:0.66:0.09 in the atom numbers and 0.16:0.67:0.17 in the event rate. The average

A is 20.7 in the event rate, so that the average target nucleus approximates ^{19}F.

About half of the neutrino events in this heavy liquid are accompanied by dark tracks at the interaction vertices. They are mostly short stopping tracks referred to as stubs, and their multiplicity distribution, n, tails up to nine and the average multiplicity in the observed dark track events, <n>, is 1.94. The distribution of the dark track length, ℓ, rises sharply as ℓ decreases (the mean length is 35 mm, corresponding to the mean momentum 0.34 GeV/c). The angular distribution of the dark tracks in the laboratory system is quite uniform for P < 0.3 GeV/c. The primary sample of dark tracks contained 2.0% of ($\pi^+ + \mu^+ + e^+$), 0.3% of ($\pi^- + \mu^- + e^-$), and 1.5% of (π^- + neutrals), and we removed these observed pion tracks from our dark track samples for the analysis. Therefore, our dark tracks are believed to be mostly slow protons emerging from the target nucleus and to indicate a strong correlation between the interacting nucleons and surrounding nucleons.

The observation of short dark tracks is affected by the sensitivity of the detector, ℓ_{min}. The data from the holographic sample have a sensitivity ℓ_{min} = 0.5 mm in space and P_{min} = 0.09 GeV/c. Since the analysis of the holograms is time-consuming, in this preliminary report, we include data which is based on the results from normal pictures (84%), where ℓ_{min} = 4 mm in space, corresponding to P_{min} = 0.17 GeV/c. Neutrino charged current events were selected by a kinematical method. A cut was applied to ensure the rejection of neutral curent events and hadron events. The final sample, utilizing a conservative fiducial volume, consisted of 553 events without any dark tracks (n = 0) and 538 events with (n ≥ 1). Our assumption is that the presence of dark tracks is the signature of a strong correlation between the interacting nucleon and its neighbors, and that it is relatively independent of other details of the ν-nucleon deep inelastic interaction. It is estimated that dark track events resulting from rescattering constitute less than 3% of our (n ≥ 1) sample, i.e., the bias due to dark tracks of this origin is negligibly small.

In neutrino interactions, σ(x) is very close to $F_2(x)$ except in the small x region, and the data of all x regions are obtained in a bubble chamber experiment. In order to obtain the ratio of σ(x), the directly measured dN/dx distributions in the two groups are used without any Monte Carlo correction since the corrections are the same for the two groups. Fig. 7.1a shows the ratio of the σ(x) distribution for (n ≥ 1) and (n = 0) groups, R(x) = σ(x)n ≥ 1/σ(x)n = 0. A nuclear effect is clearly seen. The statistics are rather limited in this preliminary result, however, it was checked that the general feature of the ratio was kept for various types of common cuts for both groups.

In Fig. 7.1b-d we compare the data of the present experiment with data from a previous FNAL ν-D experiment,[3] E545. This latter experiment contains 13,106 charged current events,

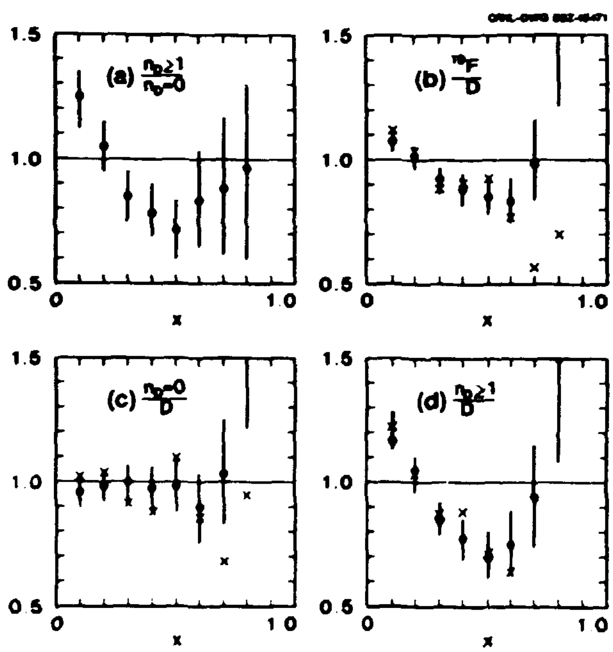

Fig. 7.1. The ratio of σ(x), R(x) = σ(x)I/s(x)II: (a) I = (n ≥ 1) and II = (n = 0), (b) I = (n ≥ 1 + n = 0) and II = (ν-D); the standard EMC plot, σ(x)νF/σ(x)ν-D, (c) I = (n = 0) and II = (ν-D), (d) I = (n ≥ 1) and II = (ν-D), X marks are for E_ν < 100 GeV cut data, error bars about 1.5 times the error bars of total data shown.

which permit improved statistical accuracy of the ratios in these comparisons. Fig. 7.1b shows the standard EMC plot for our full data ν-^{19}F, (n = 0 + n > 1), relative to the deuterium data. The ν-D events were measured and analyzed by substantially the same method as in the pre-set experiment. However, they are independent experiments. Fig. 7.1c represents the ratio $\sigma(x)n = 0/\sigma(x)\nu$-D which shows, as expected, that the effect has essentially disappeared for these events. By contrast, Fig. 7.1d shows $\sigma(x)n > 1/\sigma(x)\nu$-D, where a strong effect is seen. It is clear that the effect seen in Fig. 7.1a is primarily in the (n > 1) group.

The most reasonable conclusion from our results is that the dark track events involve interactions with deeply bound nucleons and show an undiluted nuclear effect while events without dark tracks are dominated by interactions of quasi-free nucleons.

---

1. J. J. Aubert et al., Phys. Lett. 123B, 275 (1983).
2. For example, O. Nachtman, Proceedings of the 11th International Conference on Neutrino Physics (1984), p.405; C. H. Llewellyn Smith, Phys. Lett. 128B, 107 (1983); S. V. Akulinichev et al., Phys. Lett. 158B, 485 (1985).
3. For example, J. Hanlon et al., Phys. Rev. Lett. 45, 1817 (1980); T. Kitagaki et al., Phys. Rev. Lett. 49, 98 (1982); E545 collaboration.

8. COMPILATIONS AND EVALUATIONS

CONTROLLED FUSION ATOMIC DATA CENTER

I. Alvarez[1] · R. K. Janev[5]
C. F. Barnett[2] · M. I. Kirkpatrick
C. Cisneros[1] · E. W. McDaniel[6]
H. B. Gilbody[3] · F. W. Meyer
D. C. Gregory · T. J. Morgan[7]
C. C. Havener · R. A. Phaneuf
H. T. Hunter · M. S. Pindzola[8]
M. S. Huq[b] · J. K. Swenson[b]
E. W. Thomas[6]

The Controlled Fusion Atomic Data Center (CFADC) collects, reviews, evaluates, and recommends numerical atomic collision data which are relevant to controlled thermonuclear fusion research. The CFADC operates with an equivalent of 1.5 full-time staff members and a number of expert consultants under contract. Members of the Experimental Atomic Physics for Fusion group also contribute a small fraction of their time to literature searches and categorization of relevant publications.

The major activities of the data center are:

- the maintenance of an on-line computer data base of fusion-related publications on atomic collision processes, and periodic distribution of updates to other data centers.
- the preparation and publication of compilations of recommended atomic collision data.
- the deduction of scaling laws and parametrization of atomic-collision data for ease of application in fusion research.
- the establishment of a computer data base of recommended atomic-collision data, and a data exchange format to facilitate their application in fusion research.
- the review of the existing atomic-collision data base with respect to current applications in fusion research, and identification of data needs.
- the processing of individual requests for specific data or literature searches on specific processes.

The CFADC participates in the International Atomic and Molecular Data Center Network established by the International Atomic Energy Agency (IAEA) in Vienna and has cooperative agreements with a number of other data centers. These include

- the Atomic and Molecular Processes Information Center at the Joint Institute for Laboratory Astrophysics, Boulder, Colorado.
- the Data Center for Atomic Spectral Lines and Transition Probabilities at the National Institute for Standards and Technology, Gaithersburg, Maryland.
- the IAEA Atomic and Molecular Data Unit in Vienna, Austria.
- the Research Information Center at the Institute of Plasma Physics (IPP), Nagoya University, Japan.
- the Atomic and Nuclear Data Center of the Japan Atomic Energy Research Institute (JAERI), Tokai, Japan.

Updates of our bibliography are sent quarterly on computer diskettes to the IAEA and to both Japanese data centers. This forms the basis for the semiannual IAEA International Bulletin on Atomic and Molecular Data for Fusion. The IAEA publication CIAMDA-87, an indexed bibliography of fusion-relevant atomic and molecular processes covering the 1980-87 period, is based almost entirely on the CFADC bibliography. With supplemental funding from the DOE Office of Fusion Energy, 450 copies of this publication were purchased and distributed by the CFADC to researchers in the United States.

During this reporting period, work has continued on preparation of the five-volume "Redbook" series of recommended data, Atomic Data for Fusion. Three volumes have been published and distributed, and data compilation and evaluation work has recently been completed for a fourth volume, entitled "Collisions of H, H_2, He and Li Atoms and Ions with Atoms and Molecules." Publication and distribution of this volume (ORNL-6086) is planned for the spring of 1989. All tabular and graphical data for this series are computer-generated in publication-ready format. Maxwellian rate coefficients are calculated from the cross-section data, and Chebyshev polynomial fits are given for all the recommended data.

The CFADC also participated in two IAEA-sponsored workshops held in Vienna during the period:

- A Specialists Meeting on Carbon and Oxygen Collision Data for Fusion Plasma Research, where the role of the CFADC was to review the data base for electron collisions and to prepare a summary report, which will be published in a topical issue of Physica Scripta.
- A Consultants Meeting on Atomic Data Base and Plasma Applications Interface.

A major role of the CFADC at the Applications Interface Meeting was to assist with the implementation of a new atomic data interface program, called "ALADDIN," which was developed by R. A. Hulse, a plasma physicist from Princeton Plasma Physics Laboratory. ALADDIN is a FORTRAN code designed to facilitate effective exchange of data and the establishment of a computer data base for "users." It can accept a wide range of data formats, including tabular, parametrized, and fitted data, and it operates on a wide range of computer systems, including personal computers. ALADDIN will facilitate the dissemination of recommended data contained in our "Redbook" series. An entire volume containing data for several hundred reactions can be accommodated along with the ALADDIN program on a single computer diskette.

Work also has continued on the scaling, parametrization, and fitting of recommended atomic collision data using functional forms based on analytical physical models for the process. Often the available data are limited to a narrow energy range, and such "physical" fitting formulae permit extrapolation of the data outside this range with some measure of confidence. Such extrapolation of data is impossible with polynomial fits. This approach has been applied successfully during the period to ionization in collisions of C^{q+} and O^{q+} ions with H, H_2, and He, and work has been initiated on electron-capture collisions for the same reactants.

As a follow-up to a previous IAEA Specialists' Meeting, an assessment of atomic and molecular data requirements for fusion plasma edge studies[9] was prepared during the period in collaboration with the data center at IPP-Nagoya in Japan. Previous data-base assessments for collisions of iron ions were also published[10] during this reporting period.

---

1. Instituto de Fisica, Universidad Nacional Autonoma de Mexico.
2. Consultant, ORNL.
3. Consultant, Queen's University, Belfast, Northern Ireland.
4. ORAU Postdoctoral Research Associate.
5. Consultant, Institute of Physics, Belgrade, Yugoslavia, and International Atomic Energy Agency, Vienna, Austria.
6. Consultant, Georgia Institute of Technology, Atlanta, Georgia.
7. Consultant, Wesleyan University, Middletown, Connecticut.
8. Consultant, Auburn University, Auburn, Alabama.
9. "Atomic and Molecular Data Requirements for Fusion Plasma Edge Studies," H. Tawara and R.A. Phaneuf, Comments on Atomic and Molecular Physics 21, 177-93 (1988).
10. Recommended Data on Atomic Collision Processes Involving Iron and Its Ions, Nuclear Fusion, Special Supplement, 1987:
    R. A. Phaneuf, R. K. Janev, and H. T. Hunter, "Charge Exchange Processes Involving Iron Ions," pp. 7-20.
    M. S. Pindzola et al., "Electron-Impact Ionization Data for the Iron Isonuclear Sequence," pp. 21-41.

NUCLEAR DATA PROJECT

Y. A. Akovali M. J. Martin
M. R. Lay M. R. Schmorak

The Nuclear Data Project (NDP) is one of five data evaluation centers comprising the U.S. Nuclear Data Network (USNDN). The Project is responsible for the evaluation of nuclear structure information in the mass region $A > 199$.

The NDP maintains a complete computer-indexed library of reports and published articles in experimental nuclear structure physics as well as copies of the Evaluated Nuclear Structure Data and Nuclear Structure Reference files (ENSDF, NSR).

The Editor-in-Chief of the Nuclear Data Sheets is a member of the Nuclear Data Project staff. All mass chains from the 14 centers in the International Nuclear Data Network are edited here, and the Editor-in-Chief has the ultimate responsibility for the quality of the mass chains entered into ENSDF and, thus, for what is published in the Nuclear Data Sheets.

Activities

Data Evaluation. During this report period, NDP staff members prepared revised evaluations for the A = 199, 214, 218 and 246-266 (even A) mass chains. These evaluations have been published or are in press in the Nuclear Data Sheets.

Mass Chain Editing and Review. NDP staff members edited and/or reviewed 18 mass chains.

Information Services. NDP staff members responded to requests for specific information by researchers outside the evaluation center. Responses took the form of searches of the ENDSF and NSR files and personal consultation. A list of reports and preprints received by the NDP is prepared and distributed monthly to division staff members.

Research. NDP staff members have participated in research with other groups in the division. Discussion of these activities may be found in the research section of this report.

9. ACCELERATOR DESIGN AND DEVELOPMENT

During this reporting period, work has concentrated on the proposed Heavy Ion Storage Ring for Atomic Physics (HISTRAP) facility which has been described in previous progress reports. HISTRAP is a synchrotron/cooler/storage ring that will allow many new research opportunities in both atomic and nuclear physics. In particular, the ring will be able to accelerate, decelerate, store, and cool ions injected from either the HHIRF tandem accelerator or a dedicated ECR source and RFQ pre-accelerator. In-ring experiments with circulating ions interacting with merged photon, electron, and ion beams will be possible. HISTRAP will have a bending power of 2.67 Tm, which corresponds to a mass-energy product $k = AE/Q^2 = 344$. With tandem injection, this will provide energies for Q/A = 1/2 ions of 82 MeV/nucleon and an energy of 11 MeV/nucleon for uranium. This year, accelerator physics studies of injection stacking and tunable dispersion have been completed. Prototype hardware studies supported by the Laboratory Director's Research and Development Fund have continued. In particular, the vacuum test stand work has been essentially completed, the RF cavity has been assembled, and a prototype dipole and magnet measurement system have been fabricated and tested.

HISTRAP ACCELERATOR PHYSICS DESIGN STUDIES

I. Y. Lee D. K. Olsen
J. B. McGrory G. R. Young

Phase Space Stacking for HISTRAP Injection

A preliminary investigation of beam stacking in horizontal phase space has been made. The design lattice of HISTRAP was used, assuming an ideal beam and no magnetic errors. A single kicker magnet was placed in the lattice in the short straight section between the dipole and the quadrupole triplet. With the kicker so placed, a large distortion of the closed orbit occurs at the middle of the 4-m straight section essentially opposite the kicker magnet. In this study, the kicker magnet which introduced a deflection of 0.05 radians in the closed orbit, produced a 3.38-cm displacement in the center of the 4-m straight. The horizontal acceptance of HISTRAP is limited by the ±5.50-cm of good field in the dipole magnets. The maximum closed orbit displacement produced in any dipole by this same kicker magnet is 3.57 cm and the amplitude of the beta function in the dipole is 12.59 m. Consequently, with the full kicker strength the acceptance of the lattice is 30π mm-mrad.

A zero-width septum was assumed in the center of the 4-m straight at a horizontal distance of 4.7 cm from the equilibrium orbit. A tandem beam with an emittance of 2π mm-mrad, a beta function of 3.0 meters, and an alpha function of zero was injected at 4.95 cm from the equilibrium orbit. Test ions were distributed uniformly on the perimeter of the phase space of this beam and each ion was then tracked through one turn. At the end of each turn, the kicker strength was reduced so that the closed orbit deflection was reduced by the ratio of the distance of the closed orbit at injection to the total number of injected ion bunches. At the end of the injection, the closed orbit was at the normal equilibrium orbit. For each turn, the beta function of the lattice was changed to the value appropriate for the corresponding kicker value, and the beam acceptance was increased to the appropriate value. The beta function and the closed-orbit radius vary almost linearly with the kicker strength, thus a linear approximation was used. After each turn, those ions which were not inside the septum radius were discarded.

Since the lattice has a tune near a one-third integer resonance, the closed orbit should shrink by the diameter of the injected beam after every third turn. In this case, the injected beam diameter was 0.49 cm so that approximately 3 x (3.38cm/0.49cm) = 21 turns should be stackable in HISTRAP with no losses to the septum. And indeed the tracking calculations show that 18 turns can be stacked with no losses. Cases stacking more than 18 turns were studied. Ions were distributed uniformly over the horizontal phase space of the injected beam and tracked. In a typical case, if 500 test ions were distributed in an injected bunch, and all ions tracked for 35 turns, then 98.5% of the injected particles survived. It remains an open question how much ion loss to the septum can be tolerated, and effects of finite septum length and thickness must be considered. It seems very reasonable for preliminary estimates of HISTRAP beam currents to assume that almost all ions will survive for a 35-turn injection. Fig. 9.1 shows the phase-space profiles of the injected bunches for this case.

Tunable Dispersion

The HISTRAP reference design lattice is fourfold symmetric, has four dispersionless straight sections and has two quadrupole and two sextupole families. Other, more flexible, modes of operating this lattice are also possible if the 12 quadrupoles and 16 sextupoles are divided into more families.

One important set of lattice solutions is shown in Fig. 9.2. For these solutions, the lattice was allowed to be twofold symmetric with the design tunes. The quadrupoles were divided as shown into the three families QF1, QD, and QF2. With QF1 = QF2 = 0.93 m^{-1} and QD = 1.05 m^{-1} the lattice operates in the fourfold symmetric design mode with four nondispersed straight sections. If the strength of QF1 is reduced, then dispersion can be introduced into the straight sections as required by the experimentalists. One pair of straight sections S_1 will have positive dispersion, whereas the other pair S_2 will have negative dispersion. The beta functions and dispersions shown in Fig. 9.2 all occur at the design tunes of ν_x =

ORNL-DWG 88-15887

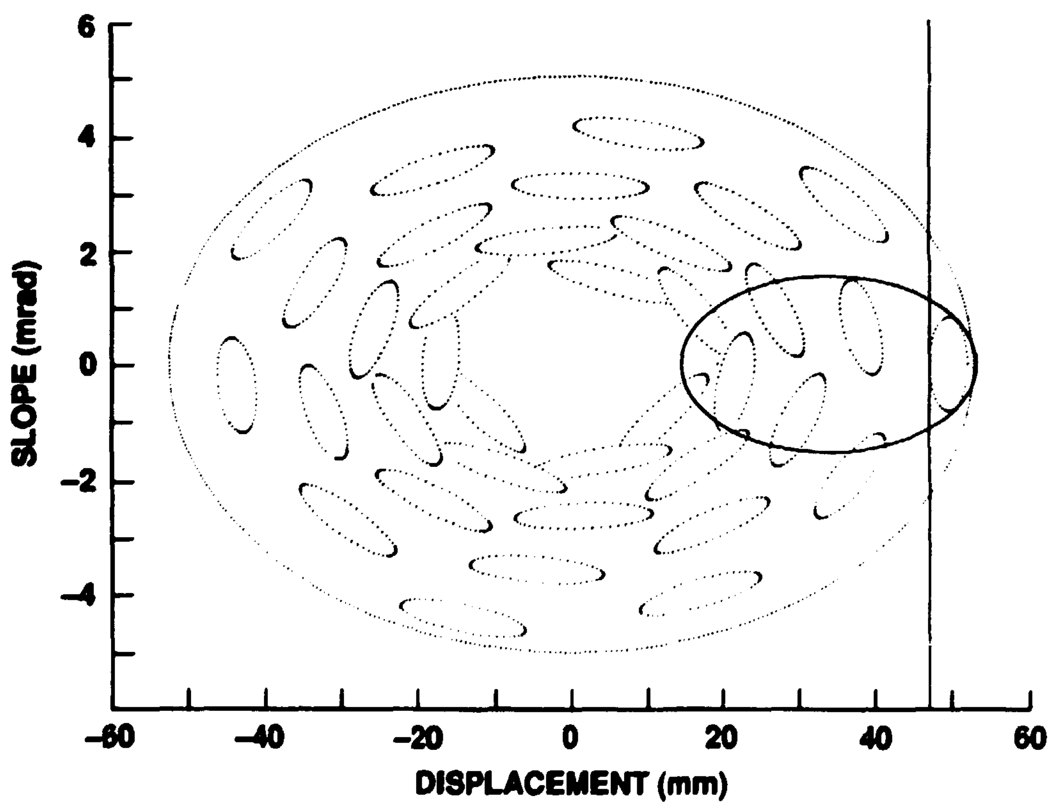

Fig. 9.1. Phase space distribution of 35 turns of ions injected in a perfect HISTRAP lattice. The solid vertical line shows the position of the injected septum. The two large ellipses represent the acceptance of the lattice at injection, kicker on, and after injection, kicker off.

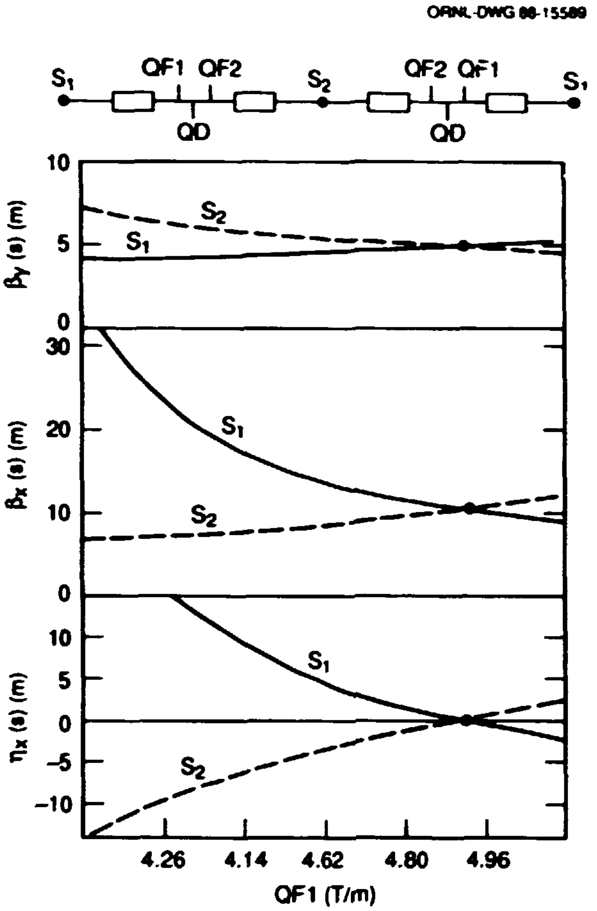

Fig. 9.2. Beta functions and dispersions in the center of straight sections S_1 and S_2 as a function of the quadrupole strength QF1. These lattice solutions all occur with the design tunes so they can be adjusted with beam circulating in HISTRAP.

2.309 and ν_y = 2.274. Consequently, dispersion can be adiabatically introduced as desired into the straight sections while the ion beam is circulating in HISTRAP. These studies show that HISTRAP is very flexible and can provide a variety of beam conditions for in-ring experiments.

HISTRAP PROTOTYPE HARDWARE STUDIES

W. H. Atkins[1] J. W. McConnell
D. T. Dowling W. T. Milner
J. W. Johnson S. W. Mosko
R. S. Lord D. K. Olsen
B. A. Tatum

Ultrahigh Vacuum Test Stand

A vacuum test stand has been designed and constructed to assess the problems associated with obtaining the ultralow pressure of 10^{-12} Torr that is required in the HISTRAP ring. This vacuum test stand, shown in Fig. 9.3, models approximately 1/16 of the ring circumference. The vacuum chamber components and sublimation pump housings were fabricated in house from 316L and 316LN stainless steel and were prebaked at 950°C in a vacuum oven before assembly. Pumping was accomplished by two 1000-ℓ/s titanium sublimation pumps (TSPs) and one 60-ℓ/s magnetic sputter ion pump (SIP). Heating blankets were used for in situ baking at temperatures up to 300°C. Pressures were read with two extraction gauges, one Bayard-Alpert gauge and a residual gas analyzer (RGA).

To eliminate all sources of oil contamination, the roughing system consists of three stages of liquid-nitrogen-cooled sorption pumping, followed by an Air Products 20-cm-diameter closed-cycle gaseous helium cryopump. The cryopump was isolated from the sorption pumps and the UHV system by all-metal valves. The sorption pumps roughed the chamber and the cryopump to 3 x 10^{-3} Torr.

Figure 9.4 shows pressure and temperature profiles as a function of time for a system bakeout cycle. The pressure shown is that measured at the tee containing the roughing valve. After roughing to a pressure of 3 x 10^{-8} Torr, the chamber temperature was increased to 100°C at a rate of 30°C per hour. The temperature was then held fixed at 100°C to check the heating control system. With only the cryopump pumping on the system, the temperature was then raised to 250°C and held for 48 hours. During the 250°C bake, the pressure decreased to 3 x 10^{-8} Torr. Some components which did not have a 250°C upper temperature limit were heated to 300°C.

During cool-down, the temperature was held fixed at 120°C while the TSPs, ion gauges, and RGA were degassed and the SIP was turned on. Cool-down then continued to ambient room temperature and a pressure of 2 x 10^{-11} Torr was obtained. The titanium sublimators were each flashed for four minutes at 47 A and after the pressure recovered to 2 x 10^{-11} Torr, the all-metal valve to the cryopump was closed. The

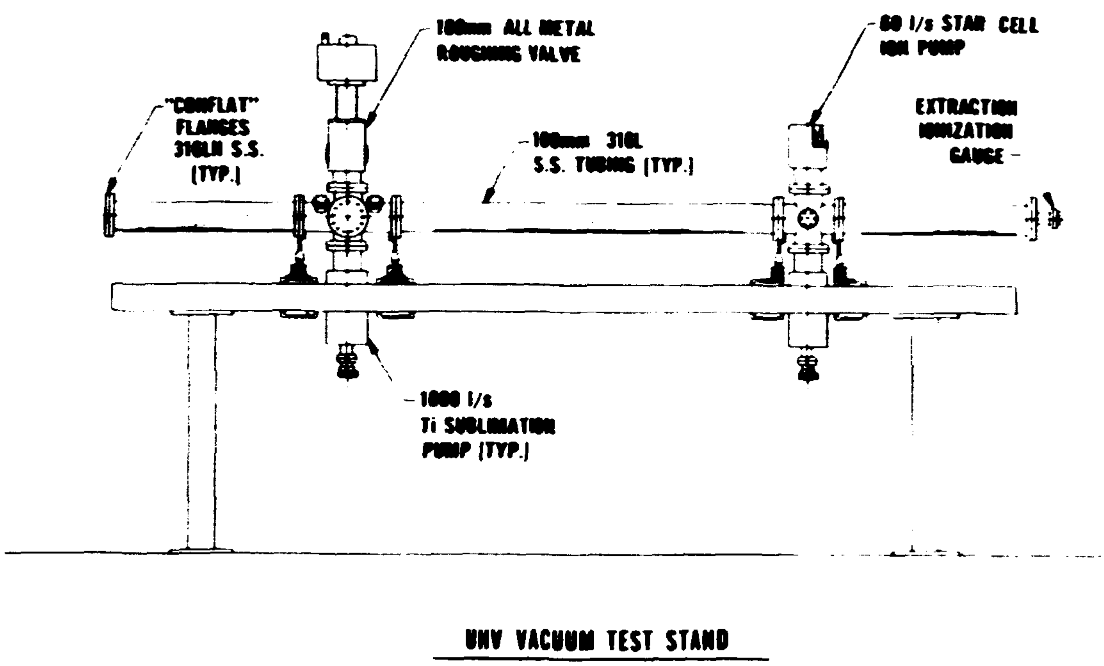

Fig. 9.3. UHV vacuum test stand which models 1/16th of the HISTRAP vacuum system. The stainless steel chambers were initially vacuum baked at 950°C and are covered with heater blankets for in situ bakes at 300°C.

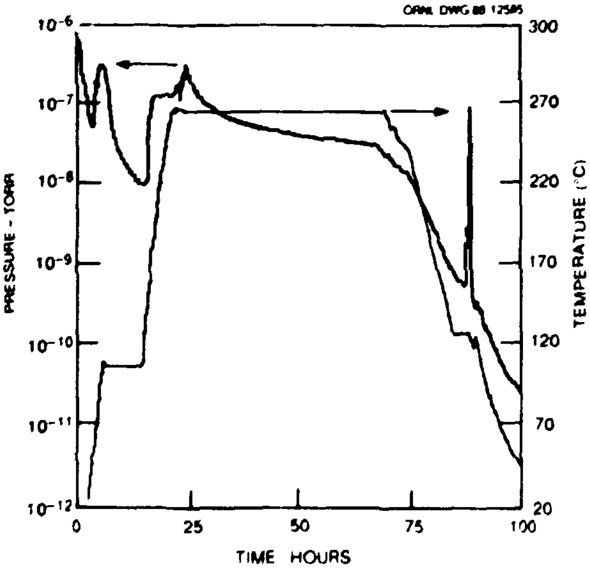

Fig. 9.4. Pressure and temperature profile as a function of time for a bakeout cycle of the vacuum test stand. After a pumpdown cycle of one week, a pressure of 4×10^{-12} Torr was obtained.

pump-down continued with the TSP and SIP and after one week, an ultimate pressure of 4×10^{-12} Torr was achieved. The calculated outgassing rate of the stainless steel for this pressure is 4×10^{-13} Torr L $cm^{-2}s^{-1}$ and an average pressure of 8×10^{-12} Torr is calculated for the equivalent periodic system.

The vacuum firing of the stainless steel at 950°C and the in situ 300°C bakeout produce residual outgassing rates which allow reasonable pump sizes and pump spacing for obtaining pressures on the 10^{-12} scale. The use of a cryopump for roughing during bakeout and cool-down provides a contamination-free method, with high pumping speed, of producing pressures of 2×10^{-11} Torr before the final pumping with the TSP and SIP. This should markedly extend life of the titanium filaments and reduce the time required to reach operating pressure. It appears from this work that the gauges themselves may be the main source of residual gas at these pressures. Figure 9.5 shows a photograph of the assembled vacuum test stand.

Prototype RF Acceleration/Deceleration Cavity

A prototype rf cavity intended to meet the HISTRAP acceleration and deceleration requirements has been designed, constructed, and tested. Estimated characteristics of the cavity are listed in Table 9.1. The cavity is a half-wave, ferrite-loaded configuration with a single accelerating gap. Tuning is accomplished through application of dc bias current to a set of "figure eight" bias windings. A photograph of the cavity is shown in Fig. 9.6.

The center conductors of the cavity are mechanically separate from the high-vacuum beam line which contains a ceramic-insulated accelerating gap. Spring-loaded contact fingers provide electrical contact between the cavity high-voltage electrodes and the beam line. These fingers are retractable so that the beam line can be thermally isolated from the cavity structure during the vacuum bakeout process.

Table 9.1. Characteristics of HISTRAP rf cavity

Accelerating gap voltage	2500 V, p-p
Tuning range	200 kHz-2.5 MHz
Overall length	1.2 m
Beam tube I.D.	0.15 m
Ferrite type	TDK SY7
Ferrite dimensions:	
Number of rings	28
Ring outside diameter	0.5 m
Ring inside diameter	0.3 m
Ring thickness	0.025 m
RF drive power	20 kW
Ferrite power density	200 mW/cc
Ferrite permeability range	8-1400
Typical initial permeability of Ferrite	2500
Peak Ferrite bias current	3000 A-turns
Shunt capacitance required	6000 pF

ORNL PHOTO 4688-88

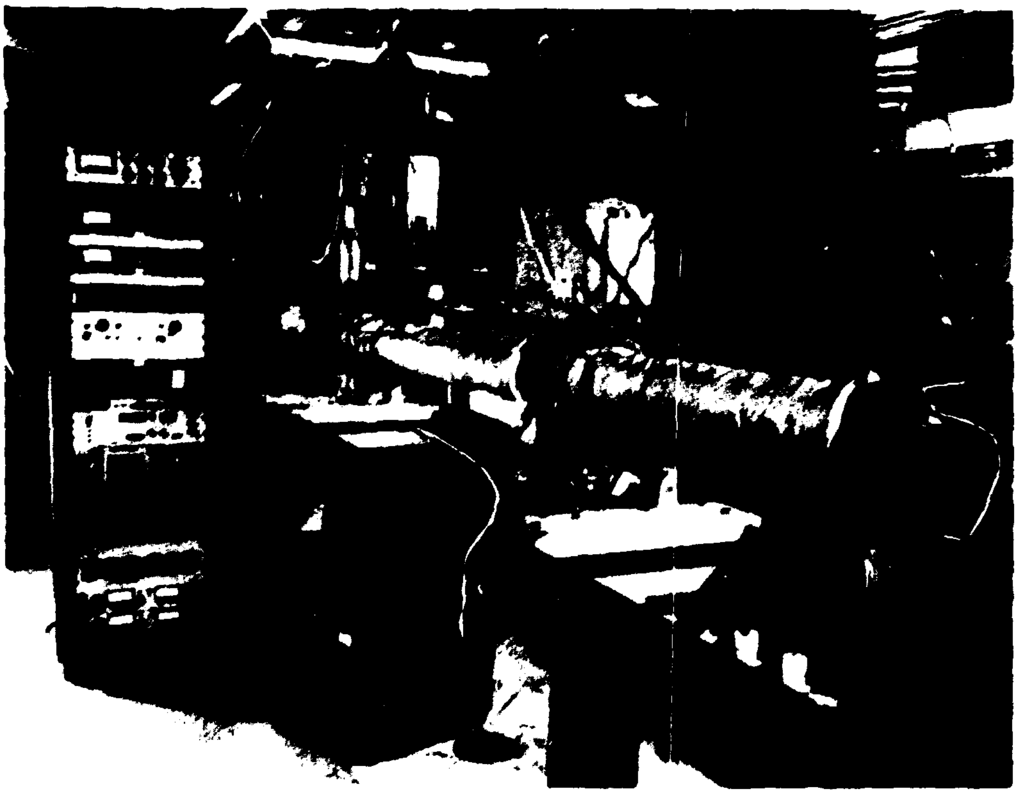

Fig. 9.5. Photograph of the assembled vacuum test stand.

ORNL PHOTO 10257-88

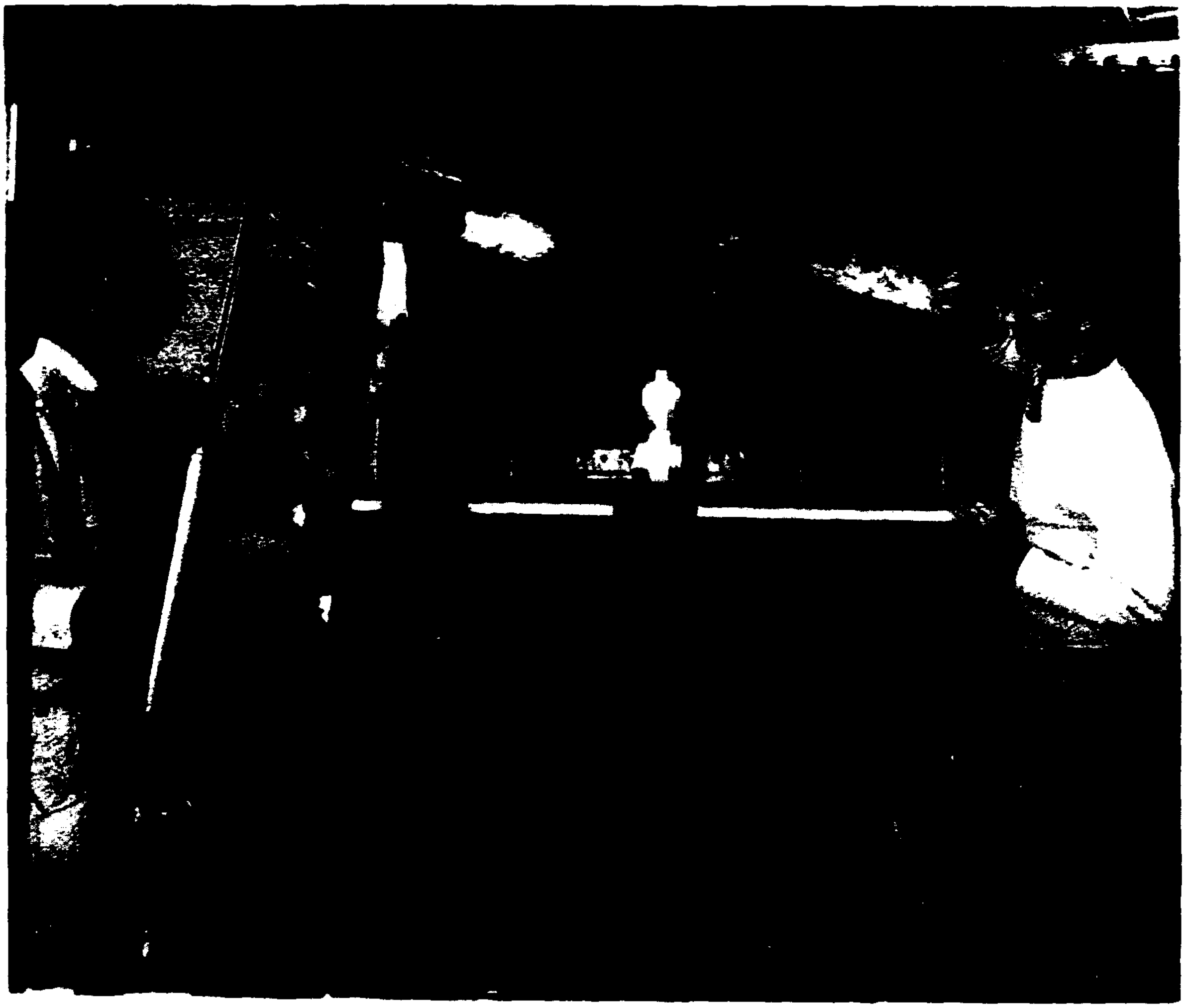

Fig. 9.6. Photograph of the HISTRAP prototype rf cavity with 16 ferrite disks and the upper lid removed.

The complete rf cavity will contain 28 ferrite rings, 14 on each half, which are separated by water-cooled annular copper disks. The ferrite-copper stacks in each half of the cavity are supported by fiberglass end plates which are joined by several steel leadscrews. The prototype cavity has been only partially loaded with 16 ferrite rings. This partial load is sufficient for testing and measuring the tuning and power dissipation characteristics of the configuration. Approximately twice as much gap capacitance and rf drive power are required to operate the cavity with the test 16 rings than the design 28 rings.

Ferrite bias is provided through an array of six independent winding segments, three figure eights on each side of the gap. Each segment is a water-cooled buss with termination outside the cavity. Outside bus connections are used for completing each "figure eight" winding. All three windings may be operated in series, parallel, or other arrangement as may be found suitable for obtaining appropriate bias levels while avoiding rf parasitic modes. The prototype is operating with the three windings in series. A 1000-A dc power supply is sufficient to swing the relative permeability over a 200 to 1 tuning range.

The ferrite rings were individually tested to measure relative permeability as a function of dc bias and rf excitation. Efforts to measure tuning characteristics of the individual rings were unsuccessful due to intrinsic inductance in the test apparatus. Tests with all 16 available rings in the prototype cavity were successful in demonstrating a tuning range from 0.25 to 3.0 MHz using a dc bias excitation from 0 to 1000 A turns, respectively. The actual tuning range of the complete cavity will be within the specified limits when the ferrite load is increased to 28 rings.

Test results are shown in Fig. 9.7 and Fig. 9.8. The low values of "Q" are especially interesting, since it will be possible to drive the cavity to frequencies substantially below resonance on the low end of the tuning range. This provides some possible extension to the tuning range, and will provide needed tuner damping in the low-frequency region where slight increments in ferrite bias cause a huge change in resonant frequency. The shunt resistance at about 80 ohms is nearly constant with respect to frequency. Consequently, the cavity will operate comfortably with a balanced drive connected across the accelerating electrodes.

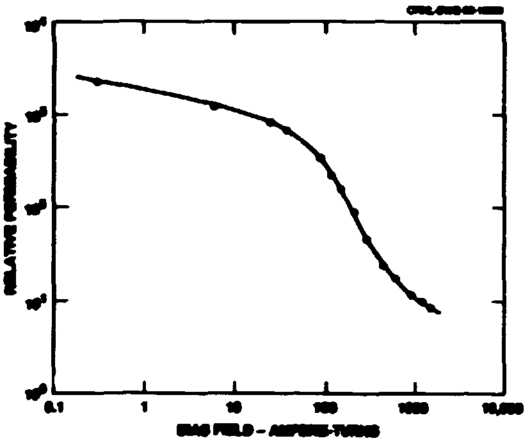

Fig. 9.7. Relative permeability as a function of bias field. The resonant frequency is proportional to the square root of the permeability.

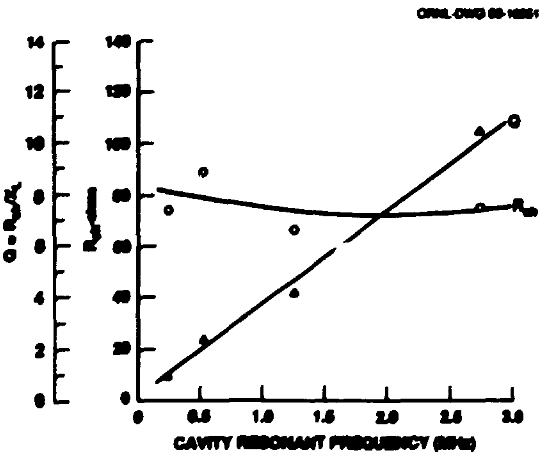

Fig. 9.8. Shunt impedance and resonant Q as a function of cavity frequency.

The several ports in the center area are used for access to the bias winding leads and rf power drive connections. The prototype cavity is driven by a single-ended 400-W rf power amplifier through a ferrite-core transformer which provides a balanced output at an appropriate impedance level. The complete cavity will need a 20-kW amplifier with a balanced output.

Magnetic Field Mapping System

A measurement system was designed and constructed to map the magnetic field of the prototype dipole and other magnetic elements. The field sensing device is a temperature-compensated Hall-effect probe. Positioning of the probe within the field area is accomplished by a personal computer (PC) based, x-y positioning system. The mapping structure, shown in Fig. 9.9, is built on a 4 x 10 ft, non-magnetic, stainless steel, laser table. Two case-hardened and ground-bearing shafts are mounted along the 10-ft dimension at a separation distance of 43.75 in. on center. Twin ball bearing bushings are mounted on each rail and are spanned by an aluminum bridge assembly, to yield one degree of motion. Similarly, two shafts and associated bearings are mounted along the bridge, spanned by an aluminum plate, to yield the second degree of motion. Two slide and vise assemblies are mounted vertically on the top bridge to hold a horizontal boom to position the Hall probe in the dipole gap.

A cantilevered, non-magnetic boom was constructed to hold the Hall probe using lightweight honeycomb paper wrapped with resin-impregnated, graphite tape. Motion in each of

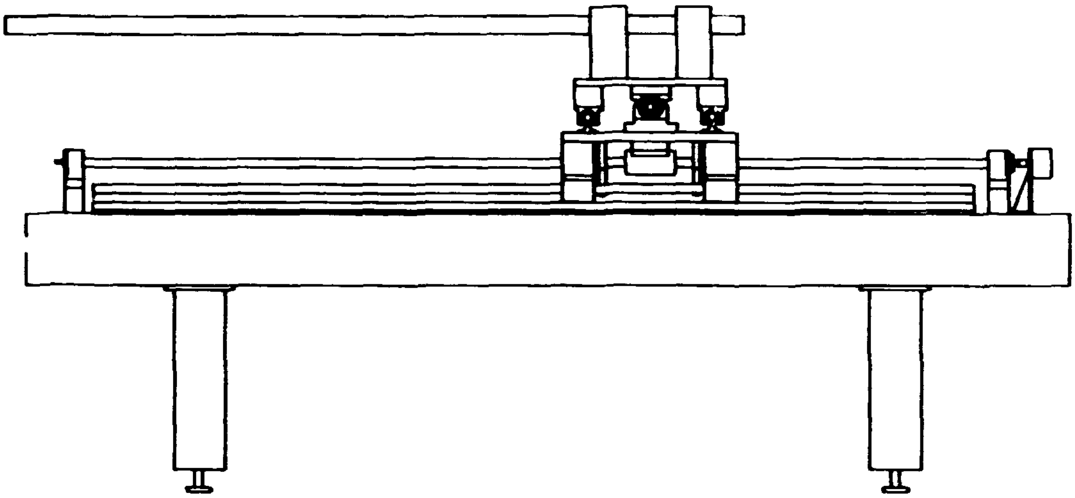

Fig. 9.9. Computer-controlled magnetic field mapping structure. Fields in a horizontal area of about 4 feet by 8 feet can be measured.

the two horizontal degrees of freedom is accomplished by electronic control. Ball screws driven by stepping motors are attached to the bridges by preloaded ball bearing housings. Travel in the horizontal plane is 85 by 35 in. and the maximum manual vertical adjustment is 6 in.

A block diagram of the control and data acquisition system is shown in Fig. 9.10. A stepper motor controller board is mounted in the PC. The board controls the initial and maximum stepping rates, acceleration rate, stepping direction, and number of steps for a maximum of two motors. Step-to-pulse translator/driver/power supply units provide a necessary external interface between the PC board and motors. Each step corresponds to a 1.8° rotation of the motor shaft. Motors are coupled to the ball screws using timing belts to damp out vibrations.

Optical linear scales of 0.01-mm resolution are mounted along each horizontal axis to provide position feedback. Signals from the scales are provided to a digital readout box which converts them to ASCII strings for display and transmission to the PC. The Hall probe contains a thermal sensor and is connected to a controller which compensates for fluctuations in temperature. A removable NMR probe is mounted in the center of the dipole for calibration of the Hall probe. At regular intervals during the mapping process, the Hall probe is positioned over the NMR and comparisons made. Three external thermocouples are used to provide temperature measurements on and near the dipole. Digital panel meters display the temperatures, as well as the power supply current, obtained from a transductor. Each of the above devices provides an RS-232 serial communication interface.

During the mapping process, horizontal motion is controlled by a compiled BASIC program, written in-house, by programming stepping motor controller integrated circuits on the PC board for specified motion patterns. The software also inputs information from the RS-232 devices, displays it, records relative extrema, and writes the information to a floppy disk for later data reduction. Only one PC serial communication port is required due to usage of an RS-232 multiplexer box.

Prototype Dipole Magnet

The dipole magnets, the most important components in HISTRAP, present some special design problems. These dipoles are short with a large sagitta. As a result, they have a complicated three-dimensional geometry and integrated field profiles which depend heavily on end effects.

ORNL-DWG 88-15886

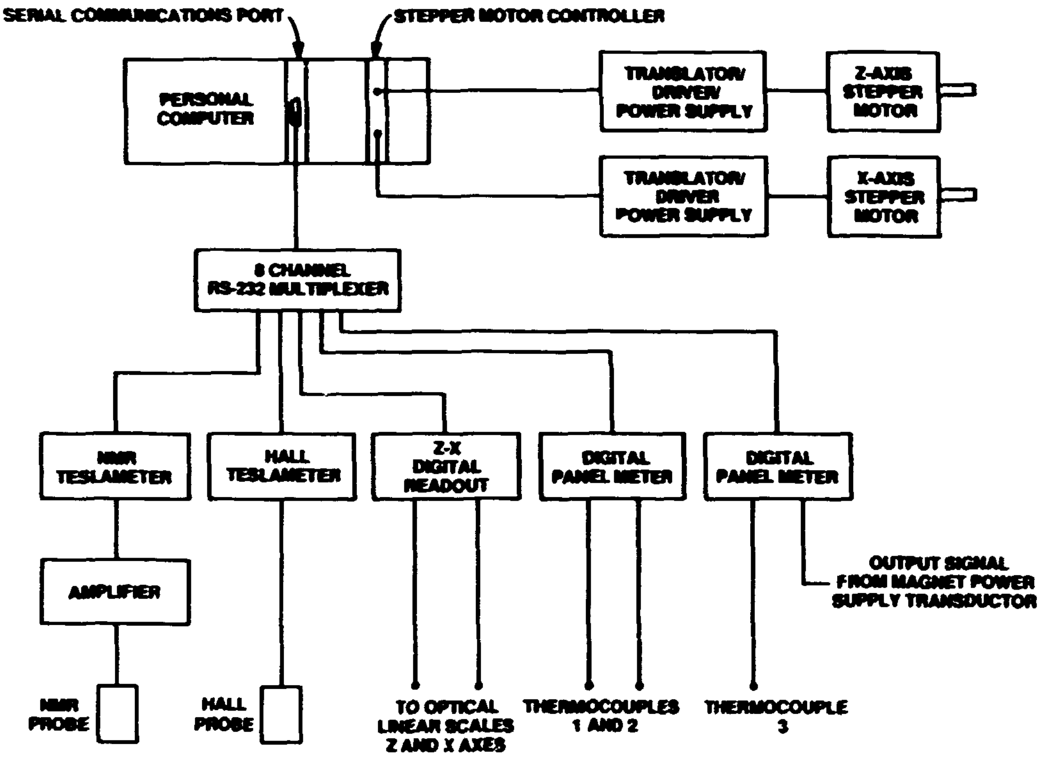

Fig. 9.10. PC-based control and data acquisition system for the magnetic field mapping structure.

In addition, the dipoles have a large gap to provide space for vacuum bakeout insulation; have a "C" design to allow for merged laser beam studies; require a maximum field of 1.6 T; and need good field quality at both high and low excitation. Because of these uncertainties, a prototype dipole has been designed, fabricated, and is being measured.

From the physics design reported in last year's progress report, the prototype dipole magnet was constructed by Fermilab. The yoke design and assembly was similar to that used for the Indiana University Cooler dipoles. In particular, the yoke was fabricated from laminations which were punched from 16-gauge SAE 1004-1006 cold-rolled sheet steel purchased from Inland Steel Corporation. The steel has a phosphate coating to provide electrical insulation between laminations and a measured permeability of 182 at an excitation level of 100 Oersteds. In order to eliminate dimensional problems induced by the stress in the steel, the laminations were punched with a two-stage die. The first punching produced laminations which were about a half-inch larger than desired. These blanks were then allowed to relax overnight before the final dimensions were punched. Sample laminations were dimensionally checked and the pole tips were flat and parallel within 0.001 in.

After being washed to improve adhesion and coated with a thin layer of epoxy, the laminations were stacked in an assembly fixture. This fixture was used to stack both the dipole and end assemblies, which consisted of removable 3.0-in.-thick end packs bolted to 1.0-in.-thick back packs. Four end packs were fabricated; two end packs were machined with the design Rogowski contours, and two are spares should new end cuts be required. The laminations were stacked between these fabricated end assemblies with the gap facing down. The laminations were centered about a vertical spacer projecting into the gap and were stacked on two rails which determined the curvature of the magnet yoke. The yoke was then compressed to the proper length with a 25-ton press and fixed in length with long thru bolts in the stacking fixture. Steel plates, 0.75 in. thick, were welded to the top and bottom of the dipole and four curved plates were welded into the side indentations. Finally, the epoxy between laminations was cured at 300°C for five hours. Laminations were glued together with the exception that the end packs were bolted to the back packs.

The four coil pancakes were wound and cured using only one fixture. The 0.625-in. by 1.750-in. copper conductor was first wrapped with one layer of half-lapped B-stage 7-mil mica tape, and then second wrapped with one layer butted B-stage 7-mil glass tape. Each entire pancake was then wrapped with one layer butted 30-mil scotch ply, and then second wrapped with one layer half-lapped B-stage 7-mil polyester/glass tape. The coils were cured on the winding fixture at a temperature of 300°C for five hours. The electrical leads, water leads, and jumpers connect to the coils at the outside center of the dipole. The coils can be tilted at an angle to the pole face as an adjustment to cancel a measured quadrupole field in the dipole. Figure 9.11 is a photograph of the assembled magnet.

Preliminary mapping of the prototype dipole has been completed at low excitation levels. The field was mapped along 21 orbits. The orbits are separated by 1 cm. Mapping points along an orbit were located such that the path length between points remained constant at 5 mm and a total path length of 209 cm was measured. Positioning accuracy along a single axis is guaranteed to within 0.04 mm.

Measurements have been completed at 50, 100, 180, 300, 400, and 500 A of excitation current spanning a magnetic field range from 430 to 3540 G. The results of these measurements are shown in Fig. 9.12 which plots field profiles in the central region of the dipole and field profiles integrated along the ion path length. These preliminary measurements at 300, 400, and 500 A of excitation, show a small quadrupole component in both the central and integrated profiles. This quadrupole component, which was not predicted by either the TOSCA or POISSON codes, also appears in the Indiana and Heidelberg dipoles. The origin of this difference is not understood. In any event, this quadrupole component can be compensated if needed by adjusting the main quadrupole strengths, fabricating pole face windings, or making small geometrical changes. The measured sextupole and octupole components of the field are small and consistent with the magnet code predictions. With increasing excitation, the quadrupole component decreases and changes sign. This decrease is consistent with a remnant field measurement of 30 G with a ±2 G quadrupole component at ±6 cm. The field quality at about 900 G of excitation, required for storage of decelerated ions, would be excellent. Field maps will be made for the entire range of required excitation levels when the required power supply is delivered.

ORNL PHOTO 10259-88

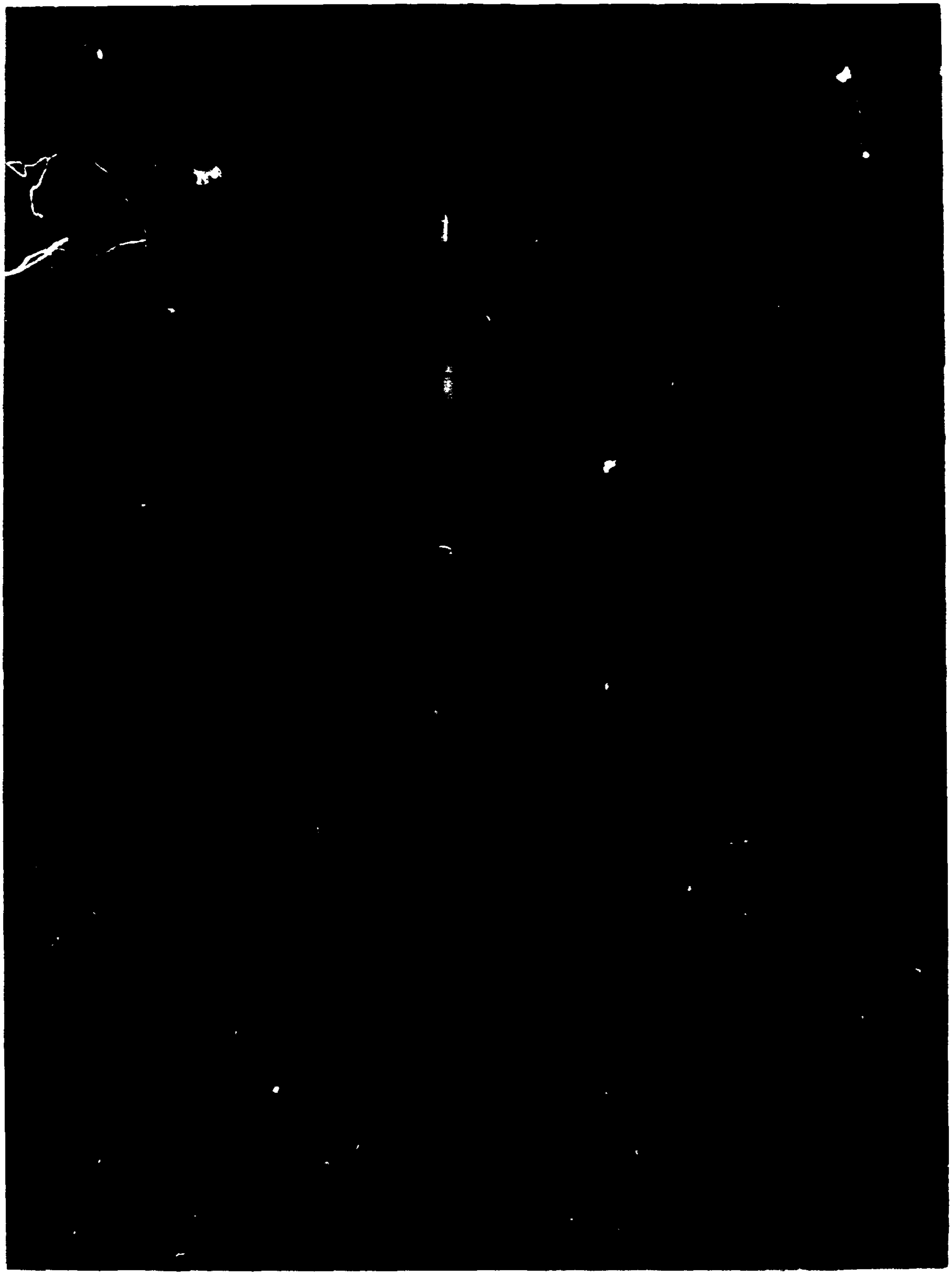

Fig. 9. 11. Photograph of the HISTRAP prototype dipole.

ORNL-DWG 88-16496

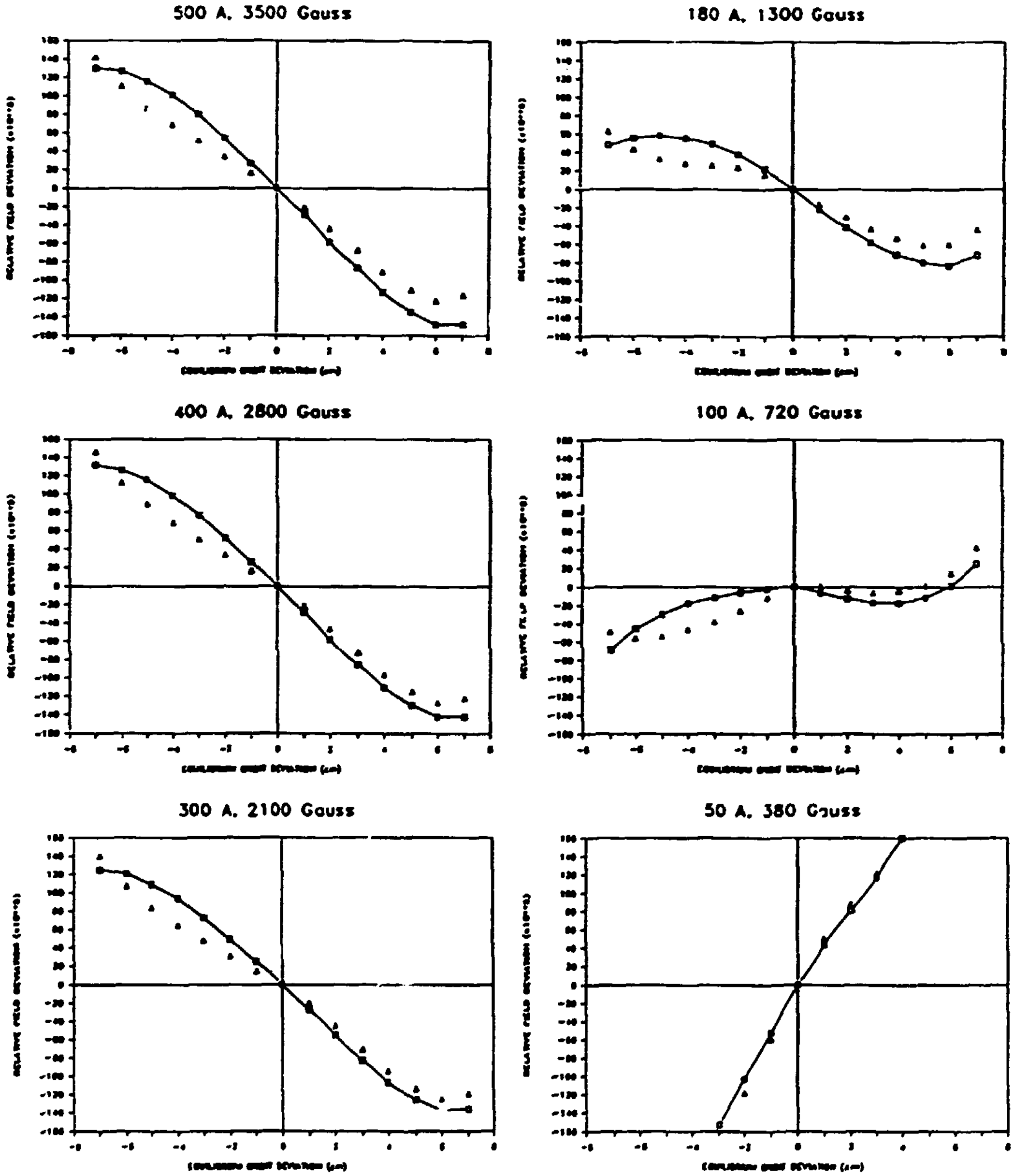

Fig. 9.12. Measured central and integrated magnetic field profiles of the HISTRAP prototype dipole at low excitation levels. The integrated results are the open squares connected by straight lines, whereas the central results are the triangles.

10. PUBLICATIONS

List Prepared by Shirley J. Ball

The following list of publications includes primarily those articles by Physics Division staff members and associates which appeared in print from October 1987 through September 1988. Articles pending publication as of September 30, 1988, are listed immediately following this section.

BOOK, JOURNAL, AND PROCEEDINGS ARTICLES

Ahmad, A., G. Bomar, H. Crowell, J. H. Hamilton, H. Kawakami, C. F. Maguire, W. G. Nettles, R. B. Piercey, A. V. Ramayya, R. Soundranayagam, R. M. Ronningen, O. Scholten, and P. H. Stelson
"Coulomb Excitation of ^{144,146,148,150}Nd," Phys. Rev. C 37, 1836-39 (May 1988)

Albrecht, R., T. C. Awes, C. Baktash, P. Beckmann, F. Berger, R. Bock, G. Claesson, L. Dragon, R. L. Ferguson, A. Franz, S. Garpman, R. Glasow, H. A. Gustafsson, H. H. Gutbrod, J. W. Johnson, K. H. Kampert, B. W. Kolb, P. Kristiansson, I. Y. Lee, H. Loehner, I. Lund, F. E. Obenshain, A. Oskarsson, I. Otterlund, T. Peitzmann, S. Persson, F. Plasil, A. M. Poskanzer, M. Purschke, H. G. Ritter, R. Santo, H. R. Schmidt, T. Siemiarczuk, S. P. Sorensen, E. Stenlund, and G. R. Young (WA80 Collaboration)
"Forward and Transverse Energy Distributions in Oxygen-Induced Reactions at 60 A GeV and 200 A GeV," Phys. Lett. B 199, 297-303 (Dec. 1987)

Albrecht, R., T. C. Awes, C. Baktash, P. Beckmann, F. Berger, R. Bock, G. Claesson, L. Dragon, R. L. Ferguson, A. Franz, S. Garpman, R. Glasow, H. A. Gustafsson, H. H. Gutbrod, K. H. Kampert, B. W. Kolb, P. Kristiansson, I. Y. Lee, H. Loehner, I. Lund, F. E. Obenshain, A. Oskarsson, I. Otterlund, T. Peitzmann, S. Persson, F. Plasil, A. M. Poskanzer, M. Purschke, H. G. Ritter, R. Santo, H. R. Schmidt, T. Siemiarczuk, S. P. Sorensen, E. Stenlund, and G. R. Young
"Photon and Neutral Pion Distributions in 60 and 200 A GeV ^{16}O + Nucleus and Proton + Nucleus Reactions," Phys. Lett. B 201, 390-96 (Feb. 1988)

Albrecht, R., T. C. Awes, C. Baktash, P. Beckmann, F. Berger, R. Bock, G. Claesson, L. Dragon, R. L. Ferguson, A. Franz, S. Garpman, R. Glasow, H. A. Gustafsson, H. H. Gutbrod, J. W. Johnson, K. H. Kampert, B. W. Kolb, P. Kristiansson, I. Y. Lee, H. Loehner, I. Lund, F. E. Obenshain, A. Oskarsson, I. Otterlund, T. Peitzmann, S. Persson, F. Plasil, A. M. Poskanzer, M. Purschke, H. G. Ritter, R. Santo, H. R. Schmidt, T. Siemiarczuk, S. P. Sorensen, E. Stenlund, and G. R. Young
"Charged-Particle Distributions in ^{16}O-Induced Nuclear Reactions at 60 and 200 A GeV," Phys. Lett. B 202, 596-602 (Mar. 1988)

Alton, G. D.
"Characterization of a Cesium Surface Ionization Source with a Porous Tungsten Ionizer. I," Rev. Sci. Instrum. 59, 1039-44 (July 1988)

Alton, G. D.
"Aspects of Negative-Ion Generation and Extraction from a Refocus Geometry Cesium Sputter Negative-Ion Source, II," Rev. Sci. Instrum. 59, 1045-52 (July 1988)

Alton, G. D., and J. W. McConnell (Invited Paper)
"The Emittances and Brightnesses of High-Intensity Negative Ion Sources," Proceedings, Seventh Tandem Conference, Berlin, West Germany, April 6-10, 1987, Nucl. Instrum. Methods Phys. Res. A268, 445-55 (May 1988)

Alton, G. D., Y. Mori, A. Takagi, A. Ueno, and S. Fukumoto
"A Versatile High Intensity Plasma Sputter Heavy Negative Ion Source," Nucl. Instrum. Methods Phys. Res. A270, 194-97 (July 1988)

Andrews, M. C., F. D. McDaniel, J. L. Duggan, P. D. Miller, P. L. Pepmiller, H. F. Krause, T. M. Rosseel, L. A. Rayburn, R. Mehta, and G. Lapicki
"L- and M-Shell X-Ray Production Cross Sections of Nd, Gd, Ho, Yb, Au, and Pb by 25-MeV Carbon and 32-MeV Oxygen Ions," Phys. Rev. A 36, 3699-706 (Oct. 1987)

Aronson, S., T. Awes, P. Braun-Munzinger, P. Gorodetzky, E. Gross, G. Landaud, T. Ludlam, M. Murtagh, A. Shor, J. Stachel, and G. Young (Invited Paper)
"Status of the RHIC Dimuon Detector," pp. 47-105 in Proceedings, Second Workshop on Experiments and Detectors for a Relativistic Heavy Ion Collider (RHIC), Berkeley, California, May 25-27, 1987, CONF-870543, Lawrence Berkeley Laboratory Report LBL-24604, January 1988

Auble, R. L., Editor
"Holifield Heavy Ion Research Facility Newsletter," Issue No. 36 (1988)

Auble, R. L., Editor
""Holifield Heavy Ion Research Facility Newsletter," Issue No. 37 (1988)

Auble, R. L., J. B. Ball, F. E. Bertrand, R. L. Ferguson, I. Y. Lee, R. L. Robinson, and G. R. Young
"Target/Projectile Mass Dependence of Light Ion Yields from Heavy Ion Collisions," Phys. Rev. C 37, 390-92 (Jan. 1988)

Baktash, C. (Invited Paper)
"Energetic M1 Transitions as a Probe of Nuclear Collectivity at High Temperatures," pp. 537-43 in The Variety of Nuclear Shapes (Proceedings, International Conference on Nuclear Shapes, Crete, Greece, June 28-July 4, 1987), World Scientific Publishing, Singapore, 1988

Bannister, M. E., D. W. Mueller, L. J. Wang, M. S. Pindzola, D. C. Griffin, and D. C. Gregory
"Cross Sections for Electron-Impact Single Ionization of Kr^{8+} and Xe^{8+}," Phys. Rev. A 38, 38-43 (July 1988)

Baranger, M., and K.T.R. Davies
"Periodic Trajectories for a Two-Dimensional Nonintegrable Hamiltonian," Ann. Phys. (N.Y.) 177, 330-58 (1987)

Barrette, J., N. Alamanos, F. Auger, B. Fernandez, A. Gillibert, D. J. Horen, J. R. Beene, F. E. Bertrand, R. L. Auble, B. L. Burks, J. Gomez del Campo, M. L. Halbert, R. O. Sayer, W. Mittig, Y. Schutz, B. Haas, and J. P. Vivien
"Coulomb Excitation of Giant Resonances in ^{208}Pb by E = 84 MeV/Nucleon ^{17}O Projectiles," Phys. Lett. B 209, 182-86 (Aug. 1988)

Becker, R. L. (Invited Paper)
"Several Manifestations of Pauli Correlations in Energetic Ion-Atom Collisions," pp. 447-60 in High-Energy Ion-Atom Collisions, Lecture Notes in Physics 294, (Proceedings, Third Workshop on High-Energy Ion-Atom Collision Processes, Debrecen, Hungary, August 3-5, 1987), Springer-Verlag, Berlin, 1988

Beckerman, M.
"Subbarrier Fusion of Two Nuclei," Rep. Prog. Phys. 51, 1047-104 (Aug. 1988)

Beene, J. R., C. E. Bemis, Jr., and M. L. Halbert
"Possibility of Pions Emitted in the Spontaneous Fission of ^{252}Cf," Phys. Rev. C 38, 569-71 (July 1988)

Beene, J. R., R. L. Varner, and F. E. Bertrand (Invited Paper)
"Gamma Decay of Isoscalar and Isovector Giant Resonances Following Heavy-Ion Inelastic Scattering," Proceedings, First Topical Meeting on Giant Resonance Excitation in Heavy-Ion Collisions, Legnaro, Italy, September 21-25, 1987, Nucl. Phys. A482, 407c-20c (May 1988)

Bennett, C. A., R. K. Richards, and D. P. Hutchinson
"Absolute Broadband Calibration Procedures for Infrared Heterodyne Receivers," Appl. Opt. 27, 3324-25 (Aug. 1988)

Berman, B. L., J. O. Kephart, R. H. Pantell, S. Datz, H. Park, R. K. Klein, and B. A. Dahling
"Channeling Radiation Experiments Between 10 and 100 MeV," pp. 239-70 in Relativistic Channeling, Plenum Publishing, New York, 1987

Bertrand, F. E., and J. R. Beene (Invited Paper)
"Excitation and Photon Decay of Giant Resonances Excited by Intermediate Energy Heavy Ions," Nouvelles de GANIL 24, 10 (Feb. 1988)

Bertrand, F. E., and J. R. Beene (Invited Paper)
"Excitation and Photon Decay of Giant Resonances Excited by Intermediate Energy Heavy Ions," pp. 49-71 in Proceedings, Texas A&M Symposium on Hot Nuclei, College Station, Texas, December 7-10, 1987, World Scientific Publishing, Singapore, 1988

Bertrand, F. E., J. R. Beene, and D. J. Horen (Invited Paper)
"Heavy Ion Excitation of Giant Resonances — The Next Generation," Proceedings, First Topical Meeting on Giant Resonance Excitation in Heavy-Ion Collisions, Legnaro, Italy, September 21-25, 1987, Nucl. Phys. A482, 287c-304c (1988)

Bottcher, C., and M. R. Strayer (Invited Paper)
"Lepton Production in Ultra-Relativistic Ion-Ion Collisions," pp. 471-78 in Frontiers of Heavy-Ion Physics, (Proceedings, 6th Adriatic International Conference on Nuclear Physics, Dubrovnik, Yugoslavia, June 15-19, 1987), World Scientific Publishing, Singapore, 1987

Bottcher, C., and M. R. Strayer (Invited Paper)
"Pulsed Electromagnetic Production of Leptons," pp. 279-93 in Proceedings, Second Workshop on Experiments and Detectors for RHIC, Berkeley, California, May 25-29, 1987, CONF-870543, Lawrence Berkeley Laboratory Report LBL-24064, January 1988

Bottcher, C., and M. R. Strayer (Invited Paper)
"Probing the Vacuum with Highly Charged Ions," Proceedings, Symposium on Atomic Spectroscopy and Highly Ionized Atoms, Lisle, Illinois, August 17-21, 1987, Nucl. Instrum. Methods Phys. Res. B31, 122-30 (1988)

Bottcher, C., M. R. Strayer, A. S. Umar, and V. E. Oberacker
"Numerical Method for the Calculation of Continuum Excitation Amplitudes in Time-Dependent External Field Problems," Phys. Rev. C 37, 2487-94 (June 1988)

Bounds, J. A., C. R. Bingham, H. K. Carter, G. A. Leander, R. L. Mlekodaj, E. H. Spejewski, and W. M. Fairbank, Jr.
"Nuclear Structure of Light Thallium Isotopes as Deduced from Laser Spectroscopy on a Fast Atom Beam," Phys. Rev. C 36, 2560-68 (Dec. 1987)

Bracco, A., J. R. Beene, N. Van Gai, P. F. Bortignon, F. Zardi, and R. A. Broglia
"Study of the Breathing Mode of ^{208}Pb Through Neutron Decay," Phys. Rev. Lett. 60, 2603-06 (June 1988)

Chen, X. Y., L. W. Swenson, F. Farzanpay, D. K. McDaniels, Z. Tang, Z. Xu, D. M. Drake, I. Bergqvist, A. Brockstedt, F. E. Bertrand, D. J. Horen, J. Lisantti, K. Hicks, M. Vetterli, and M. J. Iqbal
"Relativistic Medium Effects for ^{208}Pb(p,p') at Intermediate Energies," Phys. Lett. B 205, 436-40 (May 1988)

Claesson, G., R. Albrecht, T. C. Awes, C. Baktash, P. Beckmann, F. Berger, R. Bock, L. Dragon, R. L. Ferguson, A. Franz, S. Garpman, R. Glasow, H. A. Gustafsson, H. H. Gutbrod, J. W. Johnson, K. H. Kampert, B. W. Kolb, P. Kristiansson, I. Y. Lee, H. Loehner, I. Lund, F. E. Obenshain, A. Oskarsson, I. Otterlund, T. Peitzmann, S. Persson, F. Plasil, A. M. Poskanzer, M. Purschke, H. G. Ritter, R. Santo, H. R. Schmidt, T. Siemiarczuk, S. P. Sorensen, E. Stenlund, and G. R. Young
"Charged-Particle Distributions from 60 and 200 A GeV ^{16}O Collisions with Target Nuclei of Carbon, Copper, Silver, and Gold," pp. 129-32 in Proceedings, International Europhysics Conference on High Energy Physics, Vol. I, Uppsala, Sweden, June 25-July 1, 1987, European Physical Society, Petit Lancy, Switzerland, 1987

Close, F. E., and A. W. Thomas
"The Spin and Flavor Dependence of Parton Distribution Functions," Phys. Lett. B212, 227-30 (Sept. 1988)

Datta, S., R. Caplar, N. Cindro, R. L. Auble, J. B. Ball, and R. L. Robinson
"A Refined Coalescence Model for Intermediate-Energy Heavy-Ion Collisions. Application to Deuteron Spectra," J. Phys. G14, 937-48 (July 1988)

Datz, S., Chairman, Committee for the International Survey on Atomic and Molecular Science
"International Survey of Atomic and Molecular Science, 1984-1985," National Academy Press, Washington, D.C., 1987, 55 pages

Datz, S., L. H. Andersen, J.-P. Briand, and D. Liesen (Invited Paper)
"Experimental Atomic Physics in Heavy-Ion Storage Rings," Proceedings, Workshop and Symposium on the Physics of Stored and Trapped Particles, Stockholm, Sweden, June 15-19, 1987, Phys. Scr. T22, 224-27 (1988)

Datz, S., B. L. Berman, R. H. Pantell, and J. O. Kephart (Invited Paper)
"Radiation from Channeled Electrons and Positrons," pp. 185-204 in The Physics of Ionized Gases (Proceedings, XIII International Symposium on Physics in Ionized Gases, Sibenik, Yugoslavia, September 1-5, 1986), World Scientific Publishing, Singapore, 1987

Datz, S., P. F. Dittner, C. M. Fou, P. D. Miller, and P. L. Pepmiller (Invited Paper)
"Dielectronic Recombination of Multiply Charged Ions," pp. 61-76 in The Physics of Ionized Gases (Proceedings, XIII International Symposium on Physics in Ionized Gases, Sibenik, Yugoslavia, September 1-5, 1986), World Scientific Publishing, Singapore, 1987

Davies, K.T.R.
"Complex-Plane Methods for Evaluating Highly Oscillatory Integrals in Nuclear Physics. II," J. Phys. G14, 973-94 (July 1988)

Davies, K.T.R., M. R. Strayer, and G. D. White
"Complex-Plane Methods for Evaluating Highly Oscillatory Integrals in Nuclear Physics. I," J. Phys. G14, 96.-72 (July 1988)

de Aguiar, M.A.M., C. P. Malta, M. Baranger, and K.T.R. Davies
"Bifurcations of Periodic Trajectories in Nonintegrable Hamiltonian Systems with Two Degrees of Freedom: Numerical and Analytical Results," Ann. Phys. (N.Y.) 180, 167-205 (1987)

Defrance, P., S. Rachafi, J. Jureta, F. Meyer, and S. Chantrenne
"Electron Impact Ionization of Ar^{8+}," Proceedings, Conference on the Physics of Multiply Charged Ions, Groningen, The Netherlands, September 16-20, 1986, Nucl. Instrum. Methods. Phys. Res. B23, 265-67 (1987)

DeSerio, R., C. Gonzalez-Lepera, J. P. Gibbons, J. Burgdorfer, and I. A. Sellin
"Measurements of the Hydrogen 2s-2p Coherence Using the Quantum-Beat Technique," Phys. Rev. A 37, 4111-17 (June 1988)

Dittner, P. F. (Invited Paper)
"Dielectronic Recombination Measurements of Multicharged Ions," Proceedings, Workshop and Symposium on the Physics of Low Energy, Stored and Trapped Particles, Stockholm, Sweden, June 14-18, 1987, Phys. Scr. T22, 65-68 (1988)

Dittner, P. F., S. Datz, R. Hippler, H. F. Krause, P. D. Miller, P. L. Pepmiller, C. M. Fou, Y. Hahn, and I. Nasser
"Dielectronic Recombination of the B-Like Ions: N^{2+}, O^{3+}, and F^{4+}," Phys. Rev. A 38, 2762-66 (Sept. 1988)

Dudek, J. (Invited Paper)
"Superdeformed Nuclei. Shells-vs-Liquid Drop, Pairing-vs-Thermal Excitations, Triaxial-vs-Octupole Shapes, Super-Superdeformation," pp. 195-221 in The Variety of Nuclear Shapes (Proceedings, International Conference on Nuclear Shapes, Crete, Greece, June 29-July 3, 1987), World Scientific Publishing, Singapore, 1988

Dudek, J., B. Herskind, W. Nazarewicz, Z. Szymanski, and T. R. Werner
"Pairing, Temperature, and Deformed-Shell Effects on the Properties of Superdeformed ^{152}Dy Nucleus," Phys. Rev. C 38, 940-52 (Aug. 1988)

Dudek, J., T. Werner, and L. L. Riedinger
"Prediction of Hyperdeformed Nuclear States at Very High Spins," Phys. Lett. B211, 252-58 (Sept. 1988)

Ellis-Akovali, Y. A.
"Nuclear Data Sheets for A = 218," Nucl. Data Sheets 52, 789-809 (Dec. 1987)

Ellis-Akovali, Y. A., K. S. Toth, H. K. Carter, C. R. Bingham, I. C. Girit, and M. O. Kortelahti
"α-Decay Reduced Width of ^{194}Pb and Low-Spin Levels in ^{194}Tl Populated in ^{194}Pb β Decay," Phys. Rev. C 36, 1529-39 (Oct. 1987)

Ernst, D. J., and M. R. Strayer
"Inclusive γ and π^0 Cross Sections in Heavy-Ion Reactions," J. Phys. G14, L37-L44 (Feb. 1988)

Farid, M. E., and G. R. Satchler
"Further Studies of Density-Dependent Interactions for the Excitation of Collective States," Nucl. Phys. A481, 542-58 (May 1988)

Feng, D. H., C. L. Wu, M. W. Guidry, and Z. P. Li
"Dynamical Pauli Effects and the Saturation of Nuclear Collectivity," Phys. Lett. B 205, 156-62 (April 1988)

Fewell, M. P., N. R. Johnson, F. K. McGowan, J. S. Hattula, I. Y. Lee, C. Baktash, Y. Schutz, J. C. Wells, L. L. Riedinger, M. W. Guidry, and S. C. Pancholi
"Lifetimes of Yrast and Near-Yrast States of ^{159,160,161}Yb," Phys. Rev. C 37, 101-17 (Jan. 1988)

Garpman, S., R. Albrecht, T. C. Awes, C. Baktash, P. Beckmann, F. Berger, R. Bock, G. Claesson, L. Dragon, R. L. Ferguson, A. Franz, R. Glasow, H. A. Gustafsson, H. H. Gutbrod, J. W. Johnson, K. H. Kampert, B. W. Kolb, P. Kristiansson, I. Y. Lee, H. Loehner, I. Lund, F. E. Obenshain, A. Oskarsson, I. Otterlund, T. Peitzmann, S. Persson, F. Plasil, A. M. Poskanzer, M. Purschke, H. G. Ritter, R. Santo, H. R. Schmidt, T. Siemiarczuk, K. Soderstrom, S. P. Sorensen, E. Stenlund, and G. R. Young
"Preliminary Results from Collisions Between 3.2-TeV ^{16}O and Target Nuclei of C, Cu, and Au," pp. 453-65 in Hadrons, Quarks, and Gluons, Vol. 2 (Proceedings, Hadronic Session of the Twenty-Second Recontre de Moriond, Les Arcs-Savoie, France, March 15-21, 1987), Kim Hup Lee Printing Company, Singapore, 1987

Giese, J. P., and E. Horsdal
"Structure in the Differential Charge-State Fractions of He Following Ionization by Fast Protons," Phys. Rev. Lett. 60, 2018-21 (May 1988)

Girit, I. C., G. D. Alton, C. R. Bingham, H. K. Carter, M. L. Simpson, J. D. Cole, J. H. Hamilton, B. D. Kern, K. S. Krane, and E. F. Zganjar
"UNISOR On-Line Nuclear Orientation Facility," pp. 849-52 in Proceedings, Fifth International Conference on Nuclei Far from Stability, Rousseau Lake, Ontario, Canada, September 14-19, 1987, AIP Conference Proceedings 164, American Institute of Physics, New York, 1988

Goldston, R. J., V. Arunasalam, M. G. Bell, M. Bitter, W. R. Blanchard, N. L. Bretz, R. Budny, C. E. Bush, J. D. Callen, S. Cohen, S. K. Combs, S. L. Davis, D. L. Dimock, H. F. Dylla, P. C. Efthimion, L. C. Emerson, A. C. England, H. P. Eubank, R. J. Fonck, E. Fredrickson, H. P. Furth, G. Gammel, B. Grek, L. R. Grisham, G. Hammett, R. J. Hawryluk, W. W. Heidbrink, D. B. Heifetz, H. W. Hendel, K. W. Hill, E. Hinnov, S. Hiroe, H. Hsuan, R. A. Hulse, K. P. Jaehnig, D. Jassby, F. C. Jobes, D. W. Johnson, L. C. Johnson, R. Kaita, R. Kamperschroer, S. M. Kaye, S. J. Kilpatrick, R. J. Knize, H. Kugel, P. H. LaMarche, B. LeBlanc, R. Little, C. H. Ma, D. M. Manos, D. K. Mansfield, R. T. McCann, M. P. McCarthy, D. C. McCune, K. McGuire, D. H. McNeill, D. M. Meade, S. S. Medley, D. R. Mikkelsen, S. L. Milora, W. Morris, D. Mueller, V. Mukhovatov, E. B. Nieschmidt, J. O'Rourke, D. K. Owens, H. Park, N. Pomphrey, B. Prichard, A. T. Ramsey, M. H. Redi, A. L. Roquemore, P. H. Rutherford, N. R. Sauthoff, G. Schilling, J. Schivell, G. L. Schmidt, S. D. Scott, S. Sesnic, J. C. Sinnis, F. J. Stauffer, B. C. Stratton, G. D. Tait, G. Taylor, J. R. Timberlake, H. H. Towner, M. Ulrickson, V. Vershkov, S. Von Goeller, F. Wagner, R. Weiland, J. B. Wilgen, M. Williams, K. L. Wong, S. Yoshikawa, R. Yoshino, K. M. Young, M. C. Zarnstorff, V. S. Zaveryaev, and S. J. Zweben
"Energy Confinement and Profile Consistency in TFTR," pp. 75-87 in Plasma Physics and Controlled Nuclear Fusion Research 1986, Vol. 1 (Proceedings, Eleventh International Conference on Plasma Physics and Controlled Nuclear Fusion Research, Kyoto, Japan, November 13-20, 1986), International Atomic Energy Agency, Vienna, 1987

Gomez del Campo, J., J. L. Charvet, A. D'Onofrio, R. L. Auble, J. R. Beene, M. L. Halbert, and H. J. Kim
"Studies of Emissions of Complex Fragments and Effective Temperatures for Collisions of $^{58}Ni + ^{58}Ni$ at 11 MeV/Nucleon," Phys. Rev. Lett. 61, 290-93 (July 1988)

Griffin, D. C., R. D. Cowan, and M. S. Pindzola
"Mayer-Fermi Theory and the Long Sequences in the Periodic Table," pp. 25-47 in Proceedings, NATO Advanced Study Institute on Giant Resonances in Atoms, Molecules, and Solids, Les Houches, France, June 16-26, 1986," Plenum Publishing, New York, 1987

Griffin, D. C., M. S. Pindzola, and C. Bottcher
"Distorted-Wave Calculations of the Electron-Impact Ionization of Highly Ionized Na-Like Ions," Phys. Rev. A 36, 3642-53 (Oct. 1987)

Gustafsson, H. A., R. Albrecht, T. C. Awes, C. Baktash, P. Beckmann, F. Berger, R. Bock, G. Claesson, L. Dragon, R. L. Ferguson, A. Franz, S. Garpman, R. Glasow, H. H. Gutbrod, J. W. Johnson, K. H. Kampert, B. W. Kolb, P. Kristiansson, I. Y. Lee, H. Loehner, I. Lund, F. E. Obenshain, A. Oskarsson, I. Otterlund, T. Peitzmann, S. Persson, F. Plasil, A. M. Poskanzer, M. Purschke, H. G. Ritter, R. Santo, H. R. Schmidt, T. Siemiarczuk, S. P. Sorensen, E. Stenlund, and G. R. Young
"Transverse and Zero Degree Energies Observed in ^{16}O-Induced Nuclear Collisions at 60 and 200 A GeV," pp. 125-28 in Proceedings, International Europhysics Conference on High Energy Physics, Vol. I, Uppsala, Sweden, June 25-July 1, 1987, European Physical Society, Petit Lancy, Switzerland, 1987

Hahn, R. L., K. S. Toth, Y. LeBeyec, B. Lagarde, and M. W. Guidry
"Reactions with ^{40}Ar and ^{84}Kr Leading to the Same Compound Nucleus, ^{200}Po," Phys. Rev. C 36, 2132-35 (Nov. 1987)

Halbert, M. L., J. R. Beene, D. C. Hensley, K. Honkanen, T. M. Semkow, V. Abenante, D. G. Sarantites, and Z. Li (Invited Paper)
"Angular Momentum Effects in Subbarrier Fusion," pp. 323-30 in Frontiers of Heavy-Ion Physics (Proceedings, 6th Adriatic International Conference on Nuclear Physics, Dubrovnik, Yugoslavia, June 15-19, 1987), World Scientific Publishing, Singapore, 1987

Harmon, B. A., D. Shapira, P. H. Stelson, B. L. Burks, K. A. Erb, B. Shivakumar, K. Teh, and S. T. Thornton
"Effect of Entrance Channel Asymmetry on Fusion Reactions Leading to Compound Nuclei with A = 40,42," Phys. Rev. C 38, 572-75 (July 1988)

Harris, J. W., B. V. Jacak, K.-H. Kampert, G. Claesson, K.G.R. Doss, R. Ferguson, A. I. Gavron, H.-A. Gustafsson, H. Gutbrod, B. Kolb, F. Lefebvres, A. M. Poskanzer, H.-G. Ritter, H. R. Schmidt, L. Teitelbaum, M. Tincknell, S. Weiss, H. Wieman, and J. Wilhelmy
"Multifragmentation and Flow in Central Collisions of Heavy Systems," Proceedings, Symposium on Central Collisions and Fragmentation Processes, 193rd National Meeting of the American Chemical Society, Denver, Colorado, April 7-10, 1987, Nucl. Phys. A471, 241c-52c (Sept. 1987)

Hicks, K. H., and J. Lisantti
"Analysis of $^{40}Ca(p,p')$ at 500 MeV Using $t\rho$ Optical Potentials in A Collective Framework," Nucl. Phys. A484, 432-44 (July 1988)

Hill, K. W., V. Arunasalam, M. G. Bell, M. Bitter, W. R. Blanchard, N. L. Bretz, R. Budny, C. E. Bush, S. Cohen, S. K. Combs, S. L. Davis, D. L. Dimock, H. F. Dylla, P. C. Efthimion, L. C. Emerson, A. C. England, H. P. Eubank, R. J. Fonck, E. Fredrickson, H. P. Furth, G. Gammel, R. J. Goldston, B. Grek, L. R. Grisham, G. Hammett, R. J. Hawryluk, W. W. Heidbrink, H. W. Hendel, E. Hinnov, S. Hiroe, H. Hsuan, R. A. Hulse, K. P. Jaehnig, D. Jassby, F. C. Jobes, D. W. Johnson, L. C. Johnson, R. Kaita, R. Kamperschroer, S. M. Kaye, S. J. Kilpatrick, R. J. Knize, H. Kugel, P. H. LaMarche, B. LeBlanc, C. H. Ma, D. M. Manos, D. K. Mansfield, R. T. McCann, M. P. McCarthy, D. C. McCune, K. McGuire, D. H. McNeill, D. M. Meade, S. S. Medley, D. R. Mikkelsen, S. L. Milora, W. Morris, D. Mueller, V. Mukhovatov, E. B. Nieschmidt, J. O'Rourke, D. K. Owens, H. Park, N. Pomphrey, B. Prichard, A. T. Ramsey, M. H. Redi, A. L. Roquemore, P. H. Rutherford, N. R. Sauthoff, G. Schilling, J. Schivell, G. L. Schmidt, S. D. Scott, S. Sesnic, M. Shimada, J. C. Sinnis, F. J. Stauffer, J. Strachan, B. C. Stratton, G. D. Tait, G. Taylor, J. R. Timberlake, H. H. Towner, M. Ulrickson, V. Vershkov, S. Von Goeller, F. Wagner, R. Weiland, J. B. Wilgen, M. Williams, K. L. Wong, S. Yoshikawa, R. Yoshino, K. M. Young, M. C. Zarnstorff, V. S. Zaveryaev, and S. J. Zweben
"Impurity and Particle Transport and Control in TFTR," pp. 207-16 in Plasma Physics and Controlled Nuclear Fusion Research 1986, Vol. 1 (Proceedings, Eleventh International Conference on Plasma Physics and Controlled Nuclear Fusion Research, Kyoto, Japan, November 13-20, 1986), International Atomic Energy Agency, Vienna, 1987

Hippler, R., S. Datz, H. F. Krause, P. D. Miller, P. L. Pepmiller, and P. F. Dittner
"Partial Cross Sections for Electron Capture into Specific n States for 0.1- and 0.25-MeV/Nucleon I^{q+} - H_2 Collisions (q = 12-18)," Phys. Rev. A 37, 3201-03 (May 1988)

Hippler, R., S. Datz, P. D. Miller, P. F. Dittner, and P. L. Pepmiller
"Double and Single Electron Capture and Loss in 0.5-2.5 MeV/u O^{q+} - Ne (q = 5, 7, 8) Collisions," Z. Phys. D 8, 163-66 (1988)

Hofmann, H. J., J. Beer, G. Bonani, H. R. von Gunten, S. Raman, M. Suter, R. L. Walker, W. Wolfli, and D. Zimmerman
"Beryllium-10: Half-Life and AMS Standards," Proceedings, Fourth International Symposium on Accelerator Mass Spectrometry, Niagara-on-the-Lake, Ontario, Canada, April 27-30, 1987, Nucl. Instrum. Methods Phys. Res. B29, 32-36 (1987)

Horen, D. J., J. R. Beene, and F. E. Bertrand
"Comment on the Characterization of the Giant Quadrupole Resonance in ^{208}Pb as Reported from π^+/π^- Scattering," Phys. Rev. C 37, 888-90 (Feb. 1988)

Horen, D. J., M.A.G. Fernandes, B. L. Burks, G. R. Satchler, R. L. Auble, F. E. Bertrand, E. E. Gross, D. C. Hensley, R. O. Sayer, and D. Shapira
"Transfer Reactions at High Energy and Ambiguities in Heavy-Ion Potentials," Z. Phys. A 328, 189-93 (Dec. 1987)

Inn, K.G.W., S. Raman, B. M. Coursey, J. D. Fassett, and R. L. Walker
"Development of the $^{10}Be/^{9}Be$ Isotopic NBS Standard Reference Material," Proceedings, Fourth International Symposium on Accelerator Mass Spectrometry, Niagara-on-the-Lake, Ontario, Canada, April 27-30, 1987, Nucl. Instrum. Methods Phys. Res. B29, 27-31 (1987)

Johnson, C. H., D. J. Horen, and C. Mahaux
"Unified Description of the Neutron-^{208}Pb Mean Field Between -20 and +165 MeV from the Dispersion Relation Constraint," Phys. Rev. C 36, 2252-73 (Dec. 1987)

Johnson, C. H., and R. R. Winters
"Evidence for State Dependence of the Imaginary Part of the Empirial Optical Potential," Phys. Rev. C 37, 2340-49 (June 1988)

Johnson, N. (Invited Paper)
"Nuclear Collectivity at High Spins Determined from Lifetime Measurements," pp. 241-52 in Proceedings, International Conference on Nuclear Structure Through Static and Dynamic Moments, Melbourne, Australia, August 25-28, 1987, Conference Proceedings Press, Melbourne, 1987

Jones, C. M., G. D. Alton, J. B. Ball, J. A. Biggerstaff, D. T. Dowling, K. A. Erb, D. L. Haynes, D. E. Hoglund, E. D. Hudson, R. C. Juras, S. N. Lane, C. A. Ludemann, J. A. Martin, M. J. Meigs, S. W. Mosko, D. K. Olsen, and N. F. Ziegler
"The Holifield Heavy Ion Research Facility," Proceedings, Seventh Tandem Conference, Berlin, West Germany, April 6-10, 1987, Nucl. Instrum. Methods Phys. Res. A268, 308-12 (May 1988)

Jones, C. M., K. A. Erb, D. L. Haynes, J. T. Mitchell, N. F. Ziegler, J. E. Raatz, and R. D. Rathmell
"Tests of Compressed Geometry Acceleration Tubes in the Oak Ridge 25URC Tandem Accelerator," Proceedings, Seventh Tandem Conference, Berlin, West Germany, April 6-10, 1987, Nucl. Instrum. Methods Phys. Res. A268, 361-67 (May 1988)

Jones, C. M., K. A. Erb, D. L. Haynes, J. T. Mitchell, N. F. Ziegler, J. E. Raatz, and R. D. Rathmell
"Initial Tests of Compressed Geometry Acceleration Tubes in the ORNL 25URC Tandem Accelerator," pp. 65-76 in Proceedings, XX Symposium of Northeastern Accelerator Personnel, Notre Dame, Indiana, November 3-6, 1986, World Scientific Publishing, Singapore, 1987

Juras, R. C. (Invited Paper)
"Tutorial on Computer Controls," pp. 93-110 in Proceedings, XXI Symposium of Northeastern Accelerator Personnel, Tallahassee, Florida, September 28-October 1, 1987, World Scientific Publishing, Singapore, 1988

Juras, R. C., N. F. Ziegler, M. J. Meigs, R. L. McPherson, D. E. Hoglund, and J. A. Biggerstaff (Invited Talk)
"Evolution and Development of the Oak Ridge 25URC Tandem Accelerator Control System," Proceedings, Seventh Tandem Conference, Berlin, West Germany, April 6-10, 1987, Nucl. Instrum. Methods Phys. Res. A268, 549 (May 1988)

Jury, J. W., P.C.-K. Kuo, K. G. McNeill, C. K. Ross, H. R. Weller, and S. Raman
"Ground-State Photoneutron Reactions in ^{18}O," Phys. Rev. C 36, 1243-48 (Oct. 1987)

Kern, B. D., G. A. Leander, R. L. Mlekodaj, H. K. Carter, M. O. Kortelahti, E. F. Zganjar, R. A. Braga, R. W. Fink, C. P. Perez, P. B. Semmes, and W. Nazarewicz
"Energy Levels and Structure of Light Rare-Earth Nuclei, $^{136,138,140}Sm$ and $^{132,134,136}Nd$, via Beta Decay," pp. 441-44 in Proceedings, Fifth International Conference on Nuclei Far from Stability, Rousseau Lake, Ontario, Canada, September 14-19, 1987, AIP Conference Proceedings 164, American Institute of Physics, New York, 1988

Kern, B. D., R. L. Mlekodaj, M. O. Kortelahti, R. A. Braga, and R. W. Fink
"Energy Levels of ^{136}Pm and ^{136}Nd via Beta Decay of ^{136}Sm and ^{136}Pm," Z. Phys. A 330, 37-43 (1988)

Kern, B. D., R. L. Mlekodaj, G. A. Leander, M. O. Kortelahti, E. F. Zganjar, R. A. Braga, R. W. Fink, C. P. Perez, W. Nazarewicz, and P. B. Semmes
"Transition Through Triaxial Shapes of the Light Samarium Isotopes and the Beta Decay of $^{136,138,140}Eu$," Phys. Rev. C 36, 1514-21 (Oct. 1987)

Krause, H. F. (Invited Paper)
"A Novel High-Resolution Experimental Approach for Studying Laser Photodetachment in a Magnetic Field," pp. 673-81 in Particles and Fields Series 35 (Proceedings, Fourth International Symposium on the Production and Neutralization of Negative Ion Beams, Upton, New York, October 27-31, 1986), AIP Conf. Proc. 158, American Institute of Physics, New York 1987

Leander, G. A.
"Simulation of Nuclear Quasicontinuum Gamma-Ray Spectra," Comput. Phys. Commun. 47, 311-40 (Nov./Dec. 1987)

Leander, G. A.
"Statistical E1 and M1 Gamma Strength Functions from Heavy-Ion,xn$_\gamma$ Data," Phys. Rev. C 38, 728-36 (Aug. 1988)

Leander, G. A., P. Arve, and B. Lauritzen
"Tails of the Rotational Strength Function in the Nuclear Quasicontinuum," Phys. Rev. C 37, 328-35 (Jan. 1988)

Leander, G. A., and Y. S. Chen
"Reflection-Asymmetric Rotor Model of Odd A ~ 219-229 Nuclei," Phys. Rev. C 37, 2744-78 (June 1988)

Lee, I. Y., J. A. Martin, J. B. McGrory, W. T. Milner, D. K. Olsen, and G. R. Young
"Lattice Design of HISTRAP: Heavy Ion Storage Ring for Atomic Physics," pp. 310-12 in Proceedings, 1987 IEEE Particle Accelerator Conference, Washington, D.C., March 16-19, 1987, IEEE Catalog No. 87CH2387-9, Institute of Electrical and Electronics Engineers, New York, 1987

Lee, S. J., J. Fink, A. B. Balantekin, M. R. Strayer, A. S. Umar, P.-G. Reinhard, J. A. Maruhn, and W. Greiner
"Reply to Comment by Furnstahl et al.," Phys. Rev. Lett. 60, 163 (Jan. 1988)

Lee, S.-J., A. S. Umar, K.T.R. Davies, M. R. Strayer, and P.-G. Reinhard
"Enhanced Dissipation in New Mean-Field Studies of Strongly Damped Collisions," Phys. Lett. B 196, 419-23 (Oct. 1987)

Levin, J. C., H. Cederquist, C.-S. O, R. T. Short, I. A. Sellin, L. Liljeby, S. Huldt, S.-E. Johansson, E. Nilsson, and D. A. Church
"Production of Very Cold, Highly Charged Ions by Synchrotron Radiation: Comparisons of the 'Scalpel' and 'Hammer' Methods," Proceedings, Second U.S.-Japan Seminar on the Physics of Highly Charged Ions Produced in Heavy Ion Collisions, Kobe, Japan, March 16-20, 1987, Nucl. Instrum. Methods Phys. Res. A262, 106-09 (Dec. 1987)

Levin, J. C., C.-S. O, H. Cederquist, C. Biedermann, and I. A. Sellin
"Importance of Vacancy Cascades in Argon Recoil-Ion Charge-State Distributions Accompanied by Coincident Projectile-Electron Capture and Loss," Phys. Rev. A 38, 2674-77 (Sept. 1988)

Lisantti, J., F. E. Bertrand, D. J. Horen, B. L. Burks, C. W. Glover, D. K. McDaniels, L. W. Swenson, X. Y. Chen, O. Hausser, and K. Hicks
"Excitation of Giant Resonances in ^{28}Si with 250 MeV Protons," Phys. Rev. C 37, 2408-17 (June 1988)

Loehner, H., R. Albrecht, T. C. Awes, C. Baktash, P. Beckmann, F. Berger, R. Bock, G. Claesson, L. Dragon, R. L. Ferguson, A. Franz, S. Garpman, R. Glasow, H. A. Gustafsson, H. H. Gutbrod, K. H. Kampert, B. W. Kolb, P. Kristiansson, I. Y. Lee, I. Lund, F. E. Obenshain, A. Oskarsson, I. Otterlund, T. Peitzmann, S. Persson, F. Plasil, A. M. Poskanzer, M. Purschke, H. G. Ritter, R. Santo, H. R. Schmidt, T. Siemiarczuk, S. P. Sorensen, E. Stenlund, and G. R. Young
"Multiplicity Dependence of Neutral Transverse Momentum Spectra in 200 A·GeV O + Nucleus Reactions," pp. 133-36 in Proceedings, International Europhysics Conference on High Energy Physics, Vol. I, Uppsala, Sweden, June 25-July 1, 1987, European Physical Society, Petit-Lancy, Switzerland, 1987

Loehner, H., R. Albrecht, T. C. Awes, C. Baktash, P. Beckmann, F. Berger, R. Bock, G. Claesson, L. Dragon, R. L. Ferguson, A. Franz, S. Garpman, R. Glasow, H. A. Gustafsson, H. H. Gutbrod, K. H. Kampert, B. W. Kolb, P. Kristiansson, I. Y. Lee, I. Lund, F. E. Obenshain, A. Oskarsson, I. Otterlund, T. Peitzmann. S. Persson, F. Plasil, A. M. Poskanzer, M. Purschke, H. G. Ritter, R. Santo, H. R. Schmidt, T. Siemiarczuk, S. P. Sorensen, E. Stenlund, and G. R. Young
"Neutral Transverse Momentum Spectra in 60 and 200 A·GeV ^{16}O + Nucleus and Proton + Nucleus Reactions," Proceedings, 6th International Conference on Ultrarelativistic Nucleus-Nucleus Collisions, Schloss Nordkirchen, West Germany, August 24-28, 1987, Z. Phys. C 38, 97-103 (April 1988)

Lund, I., R. Albrecht, T. C. Awes, C. Baktash, P. Beckmann, F. Berger, R. Bock, G. Claesson, L. Dragon, R. L. Ferguson, A. Franz, S. Garpman, R. Glasow, H. A. Gustafsson, H. H. Gutbrod, J. W. Johnson, K. H. Kampert, B. W. Kolb, P. Kristiansson, I. Y. Lee, H. Lohner, F. E. Obenshain, A. Oskarsson, I. Otterlund, T. Peitzmann, S. Persson, F. Plasil, A. M. Poskanzer, M. Purschke, H. G. Ritter, R. Santo, H. R. Schmidt, T. Siemiarczuk, S. P. Sorensen, E. Stenlund, and G. R. Young
"Charged-Particle Spectra in ^{16}O-Induced Nuclear Collisions at the CERN SPS," 6th International Conference on Ultra-Relativistic Nucleus-Nucleus Collisions, Schloss Nordkirchen, West Germany, August 24-28, 1987, Z. Phys. C 38, 51-57 (April 1988)

Ma, C. H., D. P. Hutchinson, and K. L. Vander Sluis
"A Two-Wavelength Infrared Interferometer/Polarimeter System for CIT," Proceedings, 7th Topical Conference on High Temperature Plasma Diagnostics, Napa, California, March 13-17, 1988, Rev. Sci. Instrum. 59, 1629-31 (Aug. 1988)

Mallory, M. L., P. S. Miller, J. Kuchar, and E. D. Hudson (Invited Paper)
"Vacuum Measurements of the K500 Cyclotron Accelerator Chamber," pp. 404-06 in Proceedings, Eleventh International Conference on Cyclotrons and Their Applications, Tokyo, Japan, October 13-17, 1986, Ionics Publishing Company, 1987

Mansfield, D. K., H. K. Park, L. C. Johnson, H. M. Anderson, R. Chouinard, V. S. Foote, C. H. Ma, and B. J. Clifton
"Multichannel Far-Infrared Laser Interferometer for Electron Density Measurements on the Tokamak Fusion Test Reactor," Appl. Opt. 26, 4469-74 (Oct. 1987)

Martin, J. A., D. T. Dowling, D. L. Haynes, E. D. Hudson, C. M. Jones, R. C. Juras, S. N. Lane, C. A. Ludemann, M. J. Meigs, W. T. Milner, S. W. Mosko, D. K. Olsen, and N. F. Ziegler (Invited Paper)
"Operational Experience for Coupled Operation of the Holifield Tandem Electrostatic Accelerator and Isochronous Cyclotron," pp. 38-45 in Proceedings, Eleventh International Conference on Cyclotrons and Their Applications, Tokyo, Japan, October 13-17, 1986, Ionics Publishing Company, 1987

McGuire, K., V. Arunasalam, M. G. Bell, M. Bitter, W. R. Blanchard, N. L. Bretz, R. Budny, C. E. Bush, J. D. Callen, M. Chance, S. Cohen, S. K. Combs, S. L. Davis, D. L. Dimock, H. F. Dylla, P. C. Efthimion, L. C. Emerson, A. C. England, H. P. Eubank, R. J. Fonck, E. Fredrickson, H. P. Furth, G. Gammel, R. J. Goldston, B. Grek, L. R. Grisham, G. Hammett, R. J. Hawryluk, W. W. Heidbrink, H. W. Hendel, K. W. Hill, E. Hinnov, S. Hiroe, H. Hsuan, R. A. Hulse, K. P. Jaehnig, D. Jassby, F. C. Jobes, D. W. Johnson, L. C. Johnson, R. Kaita, R. Kamperschroer, S. M. Kaye, S. J. Kilpatrick, R. J. Knize, H. Kugel, P. H. LaMarche, B. LeBlanc, R. Little, C. H. Ma, J. Manickam, D. M. Manos, D. K. Mansfield, R. T. McCann, M. P. McCarthy, D. C. McCune, D. H. McNeill, D. M. Meade, S. S. Medley, D. R. Mikkelsen, S. L. Milora, D. Monticello, A. W. Morris, D. Mueller, E. B. Nieschmidt, J. O'Rourke, D. K. Owens, H. Park, W. Park, N. Pomphrey, B. Prichard, A. T. Ramsey, M. H. Redi, A. L. Roquemore, P. H. Rutherford, N. R. Sauthoff, G. Schilling, J. Schivell, G. L. Schmidt, S. D.Scott, S. Sesnic, J. C. Sinnis, F. J. Stauffer, B. C. Stratton, G. D. Tait, G. Taylor, J. R. Timberlake, H. H. Towner, M. Ulrickson, S. Von Goeller, F. Wagner, R. Weiland, J. B. Wilgen, M. Williams, K. L. Wong, S. Yoshikawa, K. M. Young, M. C. Zarnstorff, and S. J. Zweben
"Coherent and Turbulent Fluctuations in TFTR," pp. 421-31 in Plasma Physics and Controlled Nuclear Fusion Research 1986, Vol. 1 (Proceedings, Eleventh International Conference on Plasma Physics and Controlled Nuclear Fusion Research, Kyoto, Japan, November 13-20, 1986), International Atomic Energy Agency, Vienna, 1987

Meyer, F. W. (Invited Paper)
"Application of ECR Ion Source Beams in Atomic Physics," pp. 520-46 in Proceedings, International Conference on ECR Ion Sources and Their Applications, East Lansing, Michigan, November 16-18, 1987, MSU National Superconducting Laboratory Report MSUCP-47, Dec. 1987

Meyer, F. W., D. C. Griffin, C. C. Havener, M. S. Huq, R. A. Phaneuf, J. K. Swenson, and N. Stolterfoht (Invited Paper)
"Correlation Effects on Double Electron Capture in Highly-Charged, Low-Energy Ion-Atom Collisions," pp. 673-83 in Proceedings, XVth International Conference on the Physics of Electronic and Atomic Collisions, Brighton, England, July 22-28, 1987, North-Holland, Amsterdam, 1988

Meyer, F. W., D. C. Griffin, C. C. Havener, M. S. Huq, R. A. Phaneuf, J. K. Swenson, and N. Stolterfoht
"Population of High-Angular-Momentum States in Low-Energy Double-Electron-Capture Collisions of O^{6+} with He," Phys. Rev. Lett. 60, 1821-24 (May 1988)

Meyer, F. W., and J. W. Hale
"Operation of the ORNL ECR Source," pp. 319-21 in Proceedings, 1987 Particle Accelerator Conference, Washington, D.C., March 16-19, 1987, IEEE Catalog No. 87CH2387-9, Institute of Electrical and Electronics Engineers, New York, 1987

Nitschke, J. M., P. A. Wilmarth, J. Gilat, P. Moller, and K. S. Toth (Invited Paper)
"Beta-Delayed Proton Decay in the Lanthanide Region," pp. 697-707 in Proceedings, Fifth International Conference on Nuclei Far from Stability, Rousseau Lake, Ontario, Canada, September 14-19, 1987, AIP Conference Proceedings 164, American Institute of Physics, New York, 1988

Nitschke, J. M., P. A. Wilmarth, J. Gilat, K. S. Toth, and F. T. Avignone, III
"Delayed Proton Emission of N = 81 Odd-Odd Precursors: ^{148}Ho, ^{150}Tm, and ^{152}Lu," Phys. Rev. C 37, 2694-703 (June 1988)

Olsen, D. K., G. D. Alton, S. Datz, P. F. Dittner, D. T. Dowling, D. L. Haynes, E. D. Hudson, J. W. Johnson, I. Y. Lee, R. S. Lord, C. A. Ludemann, J. A. Martin, J. B. McGrory, F. W. Meyer, P. D. Miller, W. T. Milner, S. W. Mosko, P. L. Pepmiller, and G. R. Young (Invited Paper)
"The HISTRAP Proposal: Heavy Ion Storage Ring for Atomic Physics," pp. 134-40 in Proceedings, Eleventh Conference on Cyclotrons and Their Applications, Tokyo, Japan, October 13-17, 1986, Ionics Publishing Company, 1987

Olsen, D. K., K. A. Erb, C. M. Jones, W. T. Milner, and N. F. Ziegler
"A Novel Method for Measuring Beam Energies by Time-of-Flight," pp. 114-21 in Proceedings, XX Symposium of Northeastern Accelerator Personnel, Notre Dame, Indiana, November 3-6, 1986, World Scientific Publishing, Singapore, 1987

Pantell, R. H., J. O. Kephart, R. K. Klein, H. Park, B. L. Berman, and S. Datz
"The Study of Material Properties Using Channeling Radiation," pp. 435-53 in Relativistic Channeling (Proceedings, NATO Advanced Research Workshop on Relativistic Channeling, March 31-April 4, 1986, Maratea, Italy), Plenum Publishing, New York, 1987

Pegg, D. J., J. S. Thompson, R. N. Compton, and G. D. Alton
"Evidence for a Stable Negative Ion of Calcium," Phys. Rev. Lett. 59, 2267-70 (Nov. 1987)

Phaneuf, R. A., R. K. Janev, and H. T. Hunter
"Charge Exchange Processes Involving Iron Ions," pp. 7-20 in Recommended Data on Atomic Collision Processes Involving Iron and Its Ions (Reviewed at IAEA Advisory Group Meeting on Atomic Data for Fusion Plasma Modelling, Vienna, Austria, September 18-20, 1985), Special Supplement to Nuclear Fusion, 1987

Pindzola, M. S., and C. Bottcher
"Strong-Field Laser Ionization of Model Atoms," J. Opt. Soc. Am. B4, 752-53 (May 1987)

Pindzola, M. S., D. C. Griffin, and C. Bottcher (Invited Paper)
"Electron-Impact Ionization of Heavy Atomic Ions," pp. 129-45 in Proceedings, XV International Conference on the Physics of Electronic and Atomic Collisions, Brighton, England, July 22-28, 1987, North-Holland, Amsterdam, 1988

Pindzola, M. S., D. C. Griffin, C. Bottcher, S. M. Younger, and H. T. Hunter
"Electron-Impact Ionization Data for the Iron Isonuclear Sequence," pp. 21-41 in Recommended Data on Atomic Collision Processes Involving Iron and Its Ions (Reviewed at IAEA Advisory Group Meeting on Atomic Data for Fusion Plasma Modelling, Vienna, Austria, September 18-20, 1985), Special Supplement to Nuclear Fusion, 1987

Plasil, F., R. Albrecht, T. C. Awes, C. Baktash, P. Beckmann, F. Berger, R. Bock, G. Claesson, L. Dragon, R. L. Ferguson, A. Franz, S. Garpman, R. Glasow, H. A. Gustafsson, H. H. Gutbrod, J. W. Johnson, K. H. Kampert, B. W. Kolb, P. Kristiansson, I. Y. Lee, H. Loehner, I. Lund, F. E. Obenshain, A. Oskarsson, I. Otterlund, T. Peitzmann, S. Persson, A. M. Poskanzer, M. Purschke, H. G. Ritter, R. Santo, H. R. Schmidt, T. Siemiarczuk, S. P. Sorensen, E. Stenlund, and G. R. Young (Invited Paper)
"Nucleus-Nucleus Collisions at Relativistic Energies: The CERN WA80 Experiment," pp. 433-47 in Frontiers of Heavy-Ion Physics (Proceedings, 6th Adriatic International Conference on Nuclear Physics, Dubrovnik, Yugoslavia, June [illegible]-19, 1987), World Scientific Publishing, Singapore, 1987

Platchkov, S., A. Amroun, P. Bricault, J. M. Cavedon, P.K.A. de Witt Huberts, P. Dreux, B. Frois, C. D. Goodman, D. Goutte, J. Martino, V. Meot, G. A. Peterson, X. H. Phan, S. Raman, and I. Sick
"Measurement of the $1f_{7/2}$ Neutron Orbit Radius in ^{41}Ca," Phys. Rev. Lett. 61, 1465-68 (Sept. 1988)

Raman, S., Editor
"Actinide Newsletter," Issue 11 (April 1988)

Raman, S., S. Kahane, and J. E. Lynn (Invited Paper)
"Direct Thermal-Neutron Capture," Proceedings, Sixth International Symposium on Capture Gamma-Ray Spectroscopy, Leuven, Belgium, August 31-September 4, 1987," Inst. Phys. Conf. Ser. No. 88, J. Phys. G14 (Supplement), S223-30 (May 1988)

Raman, S., C. W. Nestor, Jr., and K. H. Bhatt
"Systematics of $B(E2;0_1^+ \rightarrow 2_1^+)$ Values for Even-Even Nuclei," Phys. Rev. C 37, 805-22 (Feb. 1988)

Raman, S., T. A. Walkiewicz, L. G. Multhauf, K. G. Tirsell, G. Bonsignori, and K. Allaart
"Decays of ^{118}In, ^{120}In, and ^{122}In Isomers to Levels in ^{118}Sn, ^{120}Sn, and ^{122}Sn," Phys. Rev. C 37, 1203-28 (Mar. 1988)

Read, P. M., G. D. Alton, and J. T. Maskrey
"High Brightness Sources for MeV Microprove Applications," Proceedings, First International Conference on Nuclear Microprobe Technology and Applications, Oxford, England, September 1-4, 1987, Nucl. Instrum. Methods Phys. Res. B30, 293-99 (1988)

Reinhard, P. G., M. Rufa, J. Fink, J. Maruhn, H. Stocker, W. Greiner, S. Y. Lee, S. Umar, M. R. Strayer, and R. Y. Cusson (Invited Paper)
"Relativistic Mean-Field Theories and Nuclear Properties," pp. 137-63 in Coherent Effects in Highly Excited Nuclei (Proceedings, 18th Mikolajki Summer School on Nuclear Physics, Mikolajki, Poland, September 1-13, 1986," Nuclear Science Research Conference Series, No. 12, Harwood Academic, New York, 1987

Reinhard, P. G., A. S. Umar, K.T.R. Davies, M. R. Strayer, and S. J. Lee
"Dissipation and Forces in Time-Dependent Hartree-Fock Calculations," Phys. Rev. C 37, 1026-35 (March 1988)

Richards, R. K., C. A. Bennett, L. Fletcher, H. T. Hunter, and D. P. Hutchinson
"A CO_2 Laser Thomson Scattering Diagnostic for Fusion Product Alpha Particle Measurement," Proceedings, 7th Topical Conference on High Temperature Plasma Diagnostics, Napa, California, March 13-17, 1988, Rev. Sci. Instrum. 59, 1556-58 (Aug. 1988)

Rufa, M., P.-G. Reinhard, J. A. Maruhn, W. Greiner, and M. R. Strayer
"Optimal Parameterization for the Relativistic Mean-Field Model of the Nucleus," Phys. Rev. C 38, 390-409 (July 1988)

Sarantites, D. G., T. M. Semkow, L. G. Sobotka, V. Abenante, Z. Li, Z. Majka, N. G. Nicolis, D. W. Stracener, D. C. Hensley, J. R. Beene, and H. C. Griffin (Invited Paper)
"A New Look at Reaction Mechanisms with 4π Charged-Particle and Neutron Multiplicity Measurements," pp. 375-91 in Proceedings, Texas A&M Symposium on Hot Nuclei, College Station, Texas, December 7-10, 1987, World Scientific Publishing, Singapore, 1988

Satchler, G. R. (Invited Paper)
"The Threshold Anomaly for Heavy-Ion Scattering," Proceedings, XIth Symposium on Nuclear Physics, Oaxtepec, Mexico, January 4-7, 1988, Notas de Fisica 11, 275-87 (1988)

Schmidt, H. R., R. Albrecht, T. C. Awes, C. Baktash, P. Beckmann, F. Berger, R. Bock, G. Claesson, L. Dragon, R. L. Ferguson, A. Franz, S. Garpman, R. Glasow, H. A. Gustafsson, H. H. Gutbrod, K. H. Kampert, B. W. Kolb, P. Kristiansson, I. Y. Lee, H. Lohner, I. Lund, F. E. Obenshain, A. Oskarsson, I. Otterlund, T. Peitzmann, S. Persson, F. Plasil, A. M. Poskanzer, M. Purschke, H. G. Ritter, R. Santo, T. Siemiarczuk, S. P. Sorensen, E. Stenlund, and G. R. Young (Invited Paper)
"Target Fragmentation in Proton-Nucleus and ^{16}O-Nucleus Reactions at 60 and 200 GeV/Nucleon," 6th International Conference on Ultra-Relativistic Nucleus-Nucleus Collisions, Schloss Nordkirchen, West Germany, August 24-28, 1987, Z. Phys. C 38, 109-15 (April 1988)

Schmorak, M. R.
"Nuclear Data Sheets for A = 199," Nucl. Data Sheets 53, 331-406 (Feb. 1988)

Schuch, R. (Invited Paper)
"Heavy Ion Storage Rings," pp. 163-82 in Proceedings, Workshop on Opportunities for Atomic Physics Using Slow, Highly-Charged Ions, Argonne, Illinois, January 12-13, 1987, Argonne National Laboratory Report ANL-PHY-87-1, 1987

Schuch, R. (Invited Paper)
"Electron Ion Collisions with a Heavy Ion Cooler Ring," Proceedings, Second U.S.-Mexico Symposium on Atomic and Molecular Physics: Two-Electron Phenomena, Mexico City, Mexico, January 8-11, 1986, Notas de Fisica 10, 483-501 (1987)

Schuch, R. (Invited Paper)
"Storage Rings for Investigation of Ion-Atom Collisions," pp. 509-25 in High-Energy Ion-Atom Collisions, Lecture Notes in Physics 294 (Proceedings, Third Workshop on High Energy Ion-Atom Collisions, Debrecen, Hungary, August 3-5, 1987), Springer-Verlag, Berlin, 1988

Schuch, R., S. Datz, P. F. Dittner, R. Hippler, H. F. Krause, and P. D. Miller (Invited Paper)
"Measurement of Inelasticities for Charge Correlated Multiple Ionization of Ne by Fast C^{6+} Ions," Proceedings, Second U.S.-Japan Seminar on the Physics of Highly Charged Ions Produced in Heavy Ion Collisions, Kobe, Japan, March 16-20, 1987, Nucl. Instrum. Methods Phys. Res. A262, 6-9 (Dec. 1987)

Schuch, R., H. Schone, P. D. Miller, H. F. Krause, P. F. Dittner, S. Datz, and R. E. Olson
"Charge- and Angular-Correlated Inelasticities in Collisions of Bare Fast Carbon Ions with Neon," Phys. Rev. Lett. 60, 925-28 (March 1988)

Sellin, I. A. (Invited Paper)
"What Is New in Convoy Electron Physics?," in Dynamical Processes of Highly Charged Ions (Proceedings, International Seminar on Dynamic Processes of Highly Charged Ions, Susono, Japan, August 21-24, 1986), Institute of Plasma Physics Report IPP-AM-48, Nagoya University, Nagoya, Japan, Oct. 1986

Sellin, I. A., J. C. Levin, C.-S. O, H. Cederquist, S. B. Elston, R. T. Short, and H. Schmidt-Bocking (Invited Paper)
"Cold Highly Ionized Ions: Comparison of Energies of Recoil Ions Produced by Heavy Ions and by Synchrotron Radiation X Rays," Proceedings, Workshop and Symposium on the Physics of Low Energy, Stored and Trapped Particles, Stockholm, Sweden, June 14-18, 1987, Phys. Scr. T22, 178-82 (1988)

Semkow, T. M., D. G. Sarantites, K. Honkanen, Z. Li, M. Ross, J. R. Beene, M. L. Halbert, and D. C. Hensley
"Excitation Energy Division in the Quasielastic Region from Reactions of 12 MeV/Nucleon ^{48}Ti with ^{150}Nd," Phys. Rev. C 37, 169-77 (Jan. 1988)

Shapira, D., B. Shivakumar, B. A. Harmon, and S. Ayik (Invited Paper)
"Close Collisions Between Light Nuclei — Orbiting and Fusion," pp. 55-72 in Frontiers of Heavy-Ion Physics (Proceedings, 6th Adriatic International Conference on Nuclear Physics, Dubrovnik, Yugoslavia, June 15-19, 1987), World Scientific Publishing, Singapore, 1987

Silk, J. D., H. D. Holmgren, D. L. Hendrie, T.J.M. Symons, G. D. Westfall, P. H. Stelson, S. Raman, R. L. Auble, J. R. Wu, and K. Van Bibber
"Fragmentation of ^{16}O Projectiles at 100 MeV Per Nucleon," Phys. Rev. C 37, 158-62 (Jan. 1988)

Snowdon, K. J., C. C. Havener, F. W. Meyer, S. Overbury, D. M. Zehner, and W. Heiland
"Technique for Determination of the Metastable Fraction of Multicharged Ion Beams," Rev. Sci. Instrum. 59, 902-05 (June 1988)

Snowdon, K. J., C. C. Havener, F. W. Meyer, S. H. Overbury, D. M. Zehner, and W. Heiland
"Charge Exchange at Molecular-Orbital Pseudocrossings as an Important Mechanism for Nonkinetic-Electron Emission in Slow-Multicharged-Ion ($v < v_0$) Metal-Surface Scattering," Phys. Rev. A 38, 2294-304 (Sept. 1988)

Sobotka, L. G., D. G. Sarantites, Z. Li, E. L. Dines, M. L. Halbert, D. C. Hensley, J. C. Lisle, R. P Schmitt, Z. Majka, G. Nebbia, H. C. Griffin, and A. J. Sierk
"Angular Momentum Dependence of Complex Fragment Emission," Phys. Rev. C 36, 2713-16 (Dec. 1987)

Sobotka, L. G., D. G. Sarantites, Z. Li, E. L. Dines, M. L. Halbert, D. C. Hensley, R. P. Schmitt, Z. Majka, G. Nebbia, H. C. Griffin, and A. J. Sierk (Invited Paper)
"The Angular Momentum Dependence of Complex Fragment Emission," Proceedings, Symposium on Central Collisions and Fragmentation Proceses, 193rd National Meeting of the American Chemical Society, Denver, Colorado, April 7-10, 1987, Nucl. Phys. A471, 131c-48c (Sept. 1987)

Sofield, C. J., P. M. Read, L. B. Bridwell, P. L. Pepmiller, G. D. Alton, D. C. Gregory, and P. D. Miller
"Ionisation of H-, He-, and Li-Like 1 GeV Ni Ions in Solid Carbon Targets," J. Phys. B21, L37-L42 (Feb. 1988)

Sorensen, S. P., R. Albrecht, T. C. Awes, C. Baktash, P. Beckmann, F. Berger, R. Bock, G. Claesson, L. Dragon, R. L. Ferguson, A. Franz, S. Garpman, R. Glasow, H. A. Gustafsson, H. H. Gutbrod, K. H. Kampert, B. W. Kolb, P. Kristiansson, I. Y. Lee, H. Lohner, I. Lund, F. E. Obenshain, A. Oskarsson, I. Otterlund, T. Peitzmann, S. Persson, F. Plasil, A. M. Poskanzer, M. Purschke, H. G. Ritter, R. Santo, H. R. Schmidt, T. Siemiarczuk, E. Stenlund, and G. R. Young (Invited Paper)
"Oxygen-Induced Reactions at 60 A GeV and 200 A GeV Studied by Calorimetry," Proceedings, 6th International Conference on Ultrarelativistic Nucleus-Nucleus Collisions, Schloss Nordkirchen, West Germany, August 24-28, 1987, Z. Phys. C 38, 3-14 (April 1988)

Stelson, P. H.
"Neutron Flow Between Nuclei as the Principal Enhancement Mechanism in Heavy-Ion Subbarrier Fusion," Phys. Lett. 205B, 190-94 (April 1988)

Stolterfoht, N., P. D. Miller, H. F. Krause, Y. Yamazaki, P. F. Dittner, P. L. Pepmiller, I. A. Sellin, and S. Datz
"Production of Autoionizing Rydberg States by Transfer Excitation in High-Energy Ion-Atom Collisions," Proceedings, Second U.S.-Mexico Symposium on Atomic and Molecular Physics: Two-Electron Phenomena, Mexico City, Mexico, January 5-7, 1986, Notas de Fisica 10, 51-61 (1987)

Strayer, M. R. (Invited Paper)
"What Lies Beyond the Mean-Field?," pp. 353-94 in Proceedings, Workshop on Heavy-Ion Reaction Dynamics Studied with Large Counter Arrays, Toronto, Canada, March 26-27, 1987, Report AECL-MISC-283, Atomic Energy of Canada, Ltd., Sept. 1987

Strayer, M. R. (Invited Paper)
"The Time-Dependent Hartree-Fock Method and Chaos in Nuclear Dynamics," p. 157 in Proceedings, Symposia of the American Physical Society Topical Group on Few-Body Systems and Multiparticle Dynamics, Crystal City, Virginia, April 20-23, 1987, AIP Conf. Proc. 162, American Institute of Physics, New York, 1987

Swenson, J. K., N. Stolterfoht, Y. Yamasaki, P. D. Miller, H. Krause, P. F. Dittner, P. L. Pepmiller, and S. Datz
"Observation of Resonant Transfer and Excitation in O^{5+} + He Collisions through High Resolution 0° Auger Electron Spectroscopy," Proceedings, Second U.S.-Mexico Symposium on Atomic and Molecular Physics: Two-Electron Phenomena, Mexico City, Mexico, January 5-7, 1986, Notas de Fisica 10, 85-89 (1987)

Takai, H., C. N. Knott, D. F. Winchell, J. X. Saladin, M. S. Kaplan, L. de Faro, R. Aryaeinejad, R. A. Blue, R. M. Ronningen, D. J. Morrissey, I. Y. Lee, and O. Dietzsch
"Population of High Spin States by Quasi-Elastic and Deep Inelastic Collisions," Phys. Rev. C 38, 1247-61 (Sept. 1988)

Tawara, H., and R. A. Phaneuf
"Atomic and Molecular Data Requirements for Fusion Plasma Edge Studies," Comments At. Mol. Phys. 21, 177-93 (1988)

Teh, K. M., D. Shapira, J. W. McConnell, H. Kim, and R. Novotny
"Data Acquisition for the HILI Detector," Proceedings, 1987 IEEE Nuclear Science Symposium, San Francisco, California, October 19-23, 1987, IEEE Trans. Nucl. Sci. NS-35, 272-76 (1988)

Toth, K. S., Y. A. Ellis-Akovali, H. J. Kim, J. W. McConnell, H. K. Carter, and D. M. Moltz (Invited Paper)
"Nuclear Structure Effects on α Reduced Widths," pp. 665-74 in Proceedings, Fifth International Conference on Nuclei Far from Stability, Rousseau Lake, Ontario, Canada, September 14-19, 1987, AIP Conference Proceedings 164, American Institute of Physics, New York, 1988

Toth, K. S., J. M. Nitschke, P. A. Wilmarth, Y. A. Ellis-Akovali, D. C. Sousa, K. Vierinen, D. M. Moltz, J. Gilat, and M. N. Rao
"Radioactivities with $146 \leq A \leq 152$ Investigated at the OASIS Facility: Evidence for ^{147}Tm β-Decay," pp. 718-21 in Proceedings, Fifth International Conference on Nuclei Far from Stability, Rousseau Lake, Ontario, Canada, September 14-19, 1987, AIP Conference Proceedings 164, American Institute of Physics, New York, 1988

Toth, K. S., D. C. Sousa, J. M. Nitschke, and P. A. Wilmarth
"Beta Decay Properties of ^{148}Er and ^{148}Ho," Phys. Rev. C 37, 1196-202 (Mar. 1988)

Vandenbosch, R., R. C. Connolly, S. Gil, D. D. Leach, T. C. Awes, S. Sorensen, and C. Y. Wu
"Light-Particle Multiplicity Accompanying Projectile Breakup at 20 MeV/Nucleon," Phys. Rev. C 37, 1301-03 (Mar. 1988)

Van Verst, S. P., D. P. Sanderson, K. W. Kemper, D. Shapira, R. L. Varner, and B. Shivakumar
"Sequential Breakup Cross Section of ^{6}Li by ^{40}Ca," Phys. Rev. C 36, 1865-69 (Nov. 1987)

Vierinen, K. S., A. A. Shihab-Eldin, J. M. Nitschke, P. A. Wilmarth, R. M. Chasteler, R. B. Firestone, and K. S. Toth
"Beta Decay of ^{154}Lu and ^{154}Yb," Phys. Rev. C 38, 1509-12 (Sept. 1988)

Vourvopoulos, G., D. L. Humphrey, T. VanCleve, D. C. Hensley, and E. E. Gross (Invited Paper)
"Nuclear Shapes from Heavy Ion Inelastic Scattering," pp. 143-51 in The Variety of Nuclear Shapes (Proceedings, International Conference on Nuclear Shapes, Crete, Greece, June 29-July 3, 1987), World Scientific Publishing, Singapore, 1988

Waggoner, W., C. L. Cocke, L. N. Tunnell, C. C. Havener, F. W. Meyer, and R. A. Phaneuf
"Angular Distributions for Electron Capture from He by Multiply Charged C, N, O, F, and Ne Ions," Phys. Rev. A 37, 2386-92 (Apr. 1988)

Wang, D., J. Rapaport, D. J. Horen, B. A. Brown, C. Gaarde, C. D. Goodman, E. Sugarbaker, and T. N. Taddeucci
"The ^{52,54}Cr(p,n)^{52,54}Mn and ^{57,58}Fe(p,n)^{57,58}Co Reactions at $E_p = 120$ MeV," Nucl. Phys. A480, 285-311 (April 1988)

Wang, L. J., K. Rinn, and D. C. Gregory
"Electron Impact Ionisation of Nickel Ions," J. Phys. B21, 2117-28 (June 1988)

Wang, R. C., and C. Y. Wong
"Finite-Size Effect in Schwinger Particle Production Mechanism," Phys. Rev. D 38, 348-59 (July 1988)

Wilmarth, P. A., J. M. Nitschke, K. Vierinen, K. S. Toth, and M. Kortelahti
"Beta-Delayed Proton Decay of the N = 83 Precursor ^{153}Yb," Z. Phys. A 329, 503-04 (April 1988)

Wong, C. Y. (Invited Paper)
"Theoretical Aspects of High-Energy Heavy-Ion Reactions," pp. 178-230 in Proceedings, 10th INS-Kikuchi Spring School on Quarks and Nuclei, Shimoda, Japan, April 15-18, 1987, INS, University of Tokyo, Japan, Nov. 1987

Wong, C. Y. (Invited Paper)
"On the Possibility of QED (e^+e^-) Resonances at 1.6-1.8 MeV," pp. 296-303 in Windsurfing the Fermi Sea, Vol. II (Proceedings, International Conference and Symposium on Unified Concepts of Many-Body Problems, Stony Brook, New York, September 4-6, 1986), North-Holland, Amsterdam, 1987

Wong, C. Y. (Invited Paper)
"Nuclear Stopping Power in High-Energy Collisions," pp. 241-56 in Proceedings, International Symposium on Medium Energy Physics, Beijing, P.R.C., June 23-28, 1987, World Scientific Publishing, Singapore, 1988

Young, G. R. (Invited Paper)
"A π^0 Spectrometer for Low-Energy Heavy-Ion Reactions," pp. 183-200 in Proceedings, Workshop on Photon and Neutral Meson Physics at Intermediate Energies, Los Alamos, New Mexico, January 7-9, 1987, Report LA-11177-C, Los Alamos National Laboratory, Dec. 1987

Young, G. R. (Invited Paper)
"Luminosity Depletion in RHIC," pp. 155-76 in Proceedings, Workshop on the RHIC Performance, Upton, New York, March 21-26, 1988, Brookhaven National Laboratory Report BNL-41604 (1988)

Young, G. R. (Invited Paper)
"Electromagnetic Dissociation of Nuclei at Relativistic Energies," pp. 253-65 in Proceedings, Workshop on the RHIC Performance, Upton, New York, March 21-26, 1988, Brookhaven National Laboratory Report BNL-41604 (1988)

Zganjar, E. F., M. O. Kortelahti, J. L. Wood, and C. D. Papanicolopulos (Invited Paper)
"Low-Energy E0 Transitions in Odd-Mass Nuclei of the Neutron-Deficient 180 < A < 200 Region," pp. 313-23 in Proceedings, Fifth International Conference on Nuclei Far from Stability, Rousseau Lake, Ontario, Canada, September 14-19, 1987, AIP Conference Proceedings 164, American Institute of Physics, New York, 1988

Ziegler, N. F., G. D. Mills, M. J. Meigs, R. L. McPherson, R. C. Juras, C. M. Jones, D. L. Haynes, and G. D. Alton
"Status of the 25URC Accelerator," pp. 5-10 in Proceedings, XXI Symposium of Northeastern Accelerator Personnel, Tallahassee, Florida, September 28-October 1, 1987, World Scientific Publishing, Singapore, 1988

Ziegler, N. F., W. T. Milner, G. D. Mills, M. J. Meigs, R. L. McPherson, R. C. Juras, C. M. Jones, D. E. Hoglund, D. L. Haynes, J. A. Biggerstaff, and G. D. Alton (Invited Paper)
"Status of the ORNL 25 URC Accelerator," pp. 483-86 in Proceedings, XX Symposium of Northeastern Accelerator Personnel, Notre Dame, Indiana, November 3-6, 1986, World Scientific Publishing, Singapore, 1987

Ziegler, N. F., and R. L. McPherson
"Charging and Corona Modifications to the ORNL 25URC Accelerator," pp. 159-67 in Proceedings, XX Symposium of Northeastern Accelerator Personnel, Notre Dame, Indiana, November 3-6, 1986, World Scientific Publishing, Singapore, 1987

Ziegler, N. F., G. K. Schulze, J. W. Rochelle, W. T. Milner, M. J. Meigs, R. L. McPherson, and R. C. Juras
"Recent Electronic Improvements to the Oak Ridge 25URC Accelerator," Proceedings, Seventh Tandem Conference, Berlin, West Germany, April 6-10, 1987, Nucl. Instrum. Methods Phys. Res. A268, 542-48 (May 1988)

PROGRESS REPORT

Ball, J. B., F. E. Bertrand, S. Datz, C. M. Jones, J. B. McGrory, F. Plasil, and R. L. Robinson
Physics Division Progress Report for Period Ending September 30, 1987, ORNL-6420 (March 1988)

TOPICAL REPORTS

Bennett, C. A., R. K. Richards, and D. P. Hutchinson
Design and Calibration of a Two-Channel Low-Noise Heterodyne Receiver for Use in a CO_2 Laser Thomson Scattering Alpha Particle Diagnostic, ORNL/TM-10419, Mar. 1988

Pindzola, M. S., D. C. Griffin, C. Bottcher, S. M. Younger, and H. T. Hunter
Electron-Impact Ionization Data for the Fe Isonuclear Sequence, ORNL/TM-10297, Nov. 1987

Vane, C. R., M. S. Smith, and S. Raman
A Versatile, Highly Efficient, High-Resolution Von Hamos Bragg Crystal X-Ray Spectrometer, ORNL/TM-10658, Feb. 1988

ARTICLES PENDING PUBLICATION

Akovali, Y. A.
"Nuclear Data Sheets for A = 214," Nuclear Data Sheets

Akovali, Y. A., K. S. Toth, A. L. Goodman, J. M. Nitschke, P. A. Wilmarth, D. M. Moltz, M. N. Rao*, and D. C. Sousa
"Single-Particle States in ^{151}Tm and ^{151}Er; Systematics of Neutron States in N = 83 Nuclei," Physical Review C

Albrecht, R., T. C. Awes, C. Baktash, P. Beckmann, F. Berger, R. Bock, G. Claesson, G. Clewing, L. Dragon, R. L. Ferguson, A. Franz, S. Garpman, R. Glasow, H. A. Gustafsson, H. H. Gutbrod, K. H. Kampert, B. W. Kolb, P. Kristiansson, I. Y. Lee, H. Loehner, I. Lund, F. E. Obenshain, A. Oskarsson, I. Otterlund, T. Peitzmann, S. Persson, F. Plasil, A. M. Poskanzer, M. Purschke, H. G. Ritter, R. Santo, H. R. Schmidt, T. Siemiarczuk, S. P. Sorensen, E. Stenlund, and G. R. Young
"π^0 Momentum Distributions from Central and Peripheral ^{16}O + Au Collisions at 200 A GeV," Zeitschrift fuer Physik

Albrecht, R., T. C. Awes, C. Baktash, P. Beckmann, F. Berger, R. Bock, G. Claesson, L. Dragon, R. L. Ferguson, A. Franz, S. Garpman, R. Glasow, H. A. Gustafsson, H. H. Gutbrod, K. H. Kampert, B. W. Kolb, P. Kristiansson, I. Y. Lee, H. Loehner, I. Lund, F. E. Obenshain, A. Oskarsson, I. Otterlund, T. Peitzmann, S. Persson, F. Plasil, A. M. Poskanzer, M. Purschke, H. G. Ritter, R. Santo, H. R. Schmidt, T. Siemiarczuk, S. P. Sorensen, E. Stenlund, and G. R. Young (Invited Paper)
"Results from CERN Experiment WA80," Proceedings, International Conference on Physics and Astrophysics of the Quark-Gluon Plasma, Bombay, India, February 8-12, 1988

Alton, G. D. (Invited Paper)
"The Sputter Generation of Negative Ion Beams," Proceedings, Seventh International Conference on Ion Implantation Technology, Kyoto, Japan, June 6-10, 1988, Nuclear Instruments and Methods in Physics Research

Alton, G. D. (Invited Paper)
"The Sputter Generation of Negative Ion Beams: Analytical Modeling," Proceedings, Tenth Conference on the Application of Accelerators in Research and Industry, Denton, Texas, November 7-9, 1988, Nuclear Instruments and Methods in Physics Research

Alton, G. D., and G. D. Mills (Invited Talk)
"Production of Atomic Negative Ion Beams of the Group IA Elements," Proceedings, Symposium of Northeastern Accelerator Personnel, New Haven, Connecticut, October 24-27, 1988

Alton, G. D., and G. D. Mills
"A Technique for Generating Atomic Negative Ion Beams of the Group IA Elements," Letter to the Editors, Nuclear Instruments and Methods in Physics Research

Alton, G. D., Y. Mori, A. Takagi, A. Ueno, and S. Fukumoto (Invited Talk)
"A High-Intensity Plasma Sputter Heavy Negative Ion Source," Proceedings, Symposium of Northeastern Accelerator Personnel, New Haven, Connecticut, October 24-27, 1988

Alton, G. D., Y. Mori, A. Takagi, A. Ueno, and S. Fukumoto (Invited Paper)
"A High-Brightness, Plasma-Sputter Heavy Negative Ion Source," Proceedings, Tenth Conference on the Application of Accelerators in Research and Industry, Denton, Texas, November 7-9, 1988, Nuclear Instruments and Methods in Physics Research

Alton, G. D., and P. M. Read
"The Emittances and Brightnesses of $^{69}Ga^+$ Ion Beams Extracted from Needle-Type, Liquid-Metal Ion Sources," Journal of Physics D

Awes, T. C.
"A Neural-Network Approach to the Problem of Photon-Pair Combinatorics," Nuclear Instruments and Methods in Physics Research

Awes, T. C., Albrecht, R., C. Baktash, P. Beckmann, F. Berger, R. Bock, G. Claesson, L. Dragon, R. L. Ferguson, A. Franz, S. Garpman, R. Glasow, H. A. Gustafsson, H. H. Gutbrod, K. H. Kampert, B. W. Kolb, P. Kristiansson, I. Y. Lee, H. Lohner, I. Lund, F. E. Obenshain, A. Oskarsson, I. Otterlund, T. Peitzmann, S. Persson, F. Plasil, A. M. Poskanzer, M. Purschke, H. G. Ritter, R. Santo, H. R. Schmidt, T. Siemiarczuk, S. P. Sorensen, E. Stenlund, and G. R. Young
"Energy Measurements in Oxygen-induced Reactions at 60 A GeV and 200 A GeV," Proceedings, International Workshop XVI on Gross Properties of Nuclei and Nuclear Excitations, Hirschegg, Austria, January 18-22, 1988

Awes, T. C., R. L. Ferguson, F. E. Obenshain, F. Plasil, G. R. Young, S. Pratt, Z. Chen, C. K. Gelbke, W. G. Lynch, J. Pochodzalla, and H. M. Xu
"Extended Emission Sources Observed via Two-Proton Correlations," Physical Review Letters

Awes, T. C., and S. P. Sorensen (Invited Paper)
"Report on the Oak Ridge Workshop on Monte Carlo Codes for Relativistic Heavy-Ion Collisions," Proceedings, Seventh International Conference on Ultrarelativistic Nucleus-Nucleus Colisions, Lenox, Massachusetts, September 26-30, 1988, Nuclear Physics A

Ayik, S., D. Shapira, and B. Shivakumar
"A Transport Description for Capture Processes in Nuclear Collisions," Physical Review C

Baktash, C., Session Chairman Commentary (Invited Paper)
"Understanding the Structure of Nuclei at Finite Temperatures," Proceedings, International Conference on Contemporary Topics in Nuclear Structure, Cocoyoc, Mexico, June 9-14, 1988

Baranger, M., K.T.R. Davies, and J. H. Mahoney
"The Calculation of Periodic Trajectories," Annals of Physics (New York)

Barrachina, R. O., and J. H. Macek
"Theory of Emission-Angle-Dependent Auger Transitions in Ion-Atom Collisions," Journal of Physics B

Becker, R. L.
"On the Cross Sections for Electron Transfer, Ejection, and Excitation in Coincidence with a Hole in a Specific Shell," Acta Physica Hungarica

Bemis, C. E., Jr., F. K. McGowan, J.L.C. Ford, W. T. Milner, R. L. Robinson, P. H. Stelson, G. A. Leander, and C. W. Reich
"Coulomb Excitation of States in ^{229}Th," Physica Scripta

Bertrand, F. E., J. R. Beene, and D. J. Horen (Invited Paper)
"Excitation and Photon Decay of Giant Multipole Resonances — The Role and Future of Medium-Energy Heavy Ions," Proceedings, Third International Conference on Nucleus-Nucleus Collisions, St. Malo, France, June 6-11, 1988, Nuclear Physics A

Bingham, C. R., L. L. Riedinger, L. H. Courtney, Z. M. Liu, A. J. Larabee, M. Craycraft, D.J.G. Love, P. J. Nolan, A. Kirwan, D. Thornley, P. Bishop, A. H. Nelson, M. A. Riley, and J. C. Waddington
"Three Band Crossings in the Yrast Structure of ^{162}Hf," Journal of Physics G

Bottcher, C., and M. R. Strayer
"Electron Pair Production from Pulsed Electromagnetic Fields in Relativistic Heavy-Ion Collisions," Physical Review D

Bottcher, C., and M. R. Strayer
"Electromagnetic Pair Production in Relativistic Heavy-Ion Collisions," Proceedings, Tenth Conference on the Application of Accelerators in Research and Industry, Denton, Texas, November 7-9, 1988, Nuclear Instruments and Methods in Physics Research

Bracco, A., J. R. Beene, F. E. Bertrand, M. L. Halbert, D. C. Hensley, R. L. Auble, D. J. Horen, R. L. Robinson, and R. O. Sayer
"Neutron Decay of Giant Resonances in ^{208}Pb," Physical Review C

Bracco, A., J. R. Beene, N. Van Giai, P. F. Bortignon, F. Zardi, and R. A. Broglia
"Direct Neutron Decay from the Giant Monopole Resonance in ^{208}Pb," Proceedings, Third International Conference on Nucleus-Nucleus Collisions, St. Malo, France, June 6-11, 1988, Nuclear Physics A

Brandan, M. E., and G. R. Satchler
"Folding Model Analysis of ^{12,13}C + ^{12}C and ^{16}O + ^{12}C Scattering at Intermediate Energies Using a Density-Dependent Interaction," Nuclear Physics A

Burgdorfer, J. (Invited Paper)
"Coherence and Correlations in Fast Ion-Atom Collisions," Proceedings, Symposium on Fundamental Processes of Atomic Dynamics, September 21-October 2, 1987, Maraeta, Italy

Burgdorfer, J., and C. Bottcher
"Production of High-Angular Momentum Rydberg and Continuum States by Stochastic Collisions in Solids," Report: 9. Arbeitsbericht, Arbeitsgruppe, Energiereiche Atomare Stosse, Oberstdorf, West Germany

Burgdorfer, J., and C. Bottcher
"Production of High-Angular Momentum Rydberg States by Stochastic Collisions," Physical Review Letters

Burgdorfer, J., and R. Morgenstern
"Coherence and Correlation in Doubly-Excited Helium-Like Atoms," Physical Review A

Burgdorfer, J., J. Wang, and A. Barany
"v/2 Electron Emission in Ion-Atom Collisions with Short-Ranged Potentials," Physical Review A

Burgdorfer, J., J. Wang, J. Muller
"Forward Electron Production in Antimatter-Solid Collisions," Physical Review A

Burks, B. L., Fernandes, M.A.G., G. R. Satchler, D. J. Horen, F. E. Bertrand, J. L. Blankenship, J.L.C. Ford, Jr., E. E. Gross, D. C. Hensley, R. O. Sayer, D. Shapira, and T. P. Sjoreen
"Optical Model and Coupled-Channels Analyses of the Elastic and Inelastic Scattering of ^{18}O from ^{28}Si at 352 MeV," Physical Review C

Carlton, R. F., R. R. Winters, C. H. Johnson, N. W. Hill, and J. A. Harvey
"Total Cross Section and Resonance Spectroscopy for n + ^{86}Kr," Physical Review C

Casson, W. H.
"Far-Infrared Scattering Experiment on a Bumpy Torus," Physics of Fluids

Casson, W. H., C. A. Bennett, L. K. Fletcher, H. T. Hunter, D. P. Hutchinson, J. Lee, C. H. Ma, R. K. Richards, and K. L. Vander Sluis
"Infrared and Far-Infrared Laser Development for Plasma Diagnostics at Oak Ridge National Laboratory," Proceedings, Lasers '87, Tenth International Conference on Lasers and Applications, Lake Tahoe, Nevada, December 7-11, 1987

Claytor, N., B. Feinberg, H. Gould, C. E. Bemis, Jr., J. Gomez del Campo, C. Ludemann, and C. R. Vane
"Electron Impact Ionization of U^{88+} - U^{91+}," Physical Review Letters

Close, F. E. (Invited Paper)
"Parton Distributions in Nuclei: Quagma or Quagmire?," Proceedings, International Conference on Physics and Astrophysics of Quark-Gluon Plasma, Bombay, India, February 8-12, 1988

Close, F. E. (Invited Paper)
"The Nuclear Dependence of Parton Distributions," Proceedings, 3rd Conference on the Intersections Between Particle and Nuclear Physics, Rockport, Maine, May 14-19, 1988

Close, F. E. (Invited Paper)
"The Nuclear Dependence of Parton Distributions," Proceedings, Topical Conference on Nuclear Chromodynamics, Argonne, Illinois, May 19-21, 1988

Close, F. E. (Invited Paper)
"The Parton Distributions in Nuclei and in Polarized Nucleons," Proceedings, 13th International Conference on Neutrino Physics and Astrophysics, Boston, Massachusetts, June 5-11, 1988

Close, F. E. (Invited Talk)
"Where Next in Polarized Leptoproduction?," Proceedings, Symposium on Future Polarization at Fermilab, Batavia, Illinois, June 13-14, 1988

Close, F. E. (Invited Paper)
"Resonance Photo and Electroproduction as a Probe of QCD," Proceedings, CEBAF 1988 Summer Workshop, Newport News, Virginia, June 20-24, 1988

Close, F. E. (Invited Paper)
"Testing QCD with Milli-TeV Electrons," Proceedings, First European Workshop on Hadronic Physics in the 1990's with Multi-GeV Electrons, Seillac, France, June 27-July 1, 1988, Nuclear Physics A

Close, F. E. (Invited Paper)
"Light Quark Spectroscopy," Proceedings, American Physical Society Meeting, Storrs, Connecticut, August 15-18, 1988

Close, F. E. (Invited Talk)
"Exotic Mesons," Proceedings, BNL Workshop on Glueballs, Hybrids, and Exotics, Upton, New York, August 29-September 1, 1988, American Institute of Physics

Close, F. E. (Invited Talk)
"Where is the Proton's Spin?," Proceedings, Spin 88 Conference, Minneapolis, Minnesota, September 12-17, 1988, American Institute of Physics

Crater, H. W., C. Y. Wong, R. L. Becker, and P. Van Alstine
"Nonperturbative Covariant Treatments of the Triplet e^+e^- System Using Two-Body Dirac Equations from Constraint Dynamics," Physical Review D

Datz, S., and P. F. Dittner
"Merged Electron-Ion Beam Studies of Dielectronic Recombination in Multicharged Ions," Zeitschrift fuer Physik D

Davies, K.T.R.
"Complex-Plane Methods for Evaluating Integrals with High Oscillatory Integrands," Journal of Computational Physics

DeSerio, R.
"On Spherical Sector Electrostatic Analyzers for Measurements of Energy and Angular Distributions," Review of Scientific Instruments

Donau, F., J. Zhang, and L. L. Riedinger
"On the Solution to Large-Amplitude Collective Motion in Finite Interacting Fermi Systems," Nuclear Physics A

D'Onofrio, A., J. Gomez del Campo, B. Delaunay, J. Delaunay, H. Dumont, F. Andreozzi, A. Brondi, R. Moro, M. Romano, and F. Terrasi
"Preequilibrium Emision and Target-Projectilelike Correlations for ^{20}Ne + ^{60}Ni at E (^{20}Ne) = 740 MeV," Physical Review C

Dudek, J. (Invited Paper)
"From the Secrets of Nuclear Shapes into Quantum Nuclear Physics," Proceedings, International Conference on Contemporary Topics in Nuclear Structure, Cocoyoc, Mexico, June 9-14, 1988

Dudek, J., and T. Werner (Invited Paper)
"Hyperdeformed Nuclei and the Residual Pseudo-SU(3) Symmetry," Proceedings, Conference on High-Spin Nuclear Structure and Novel Nuclear Shapes, Argonne, Illinois, April 13-15, 1988

Dudek, J., T. Werner, and L. L. Riedinger
"Dependence of the First Saddle-Point Energy on Temperature and Spin in Superdeformed Rare Earth Nuclei," Physics Letters B

Firestone, R. B., J. M. Nitschke, P. A. Wilmarth, K. Vierinen, J. Gilat, K. S. Toth, and Y. A. Akovali
"Decay of ^{149}Er^{9+m} by Positron and Delayed Proton Emission and Electron Capture," Physical Review C

Gaither, C. C., III, M. Breinig, J. Freyou, and T. A. Underwood
"Comparison of Target-Thickness Dependence of the Convoy-Electron Yield and Rydberg-Electron Yield Measured in Coincidence with Exit Charge States in Fast-Ion-Solid Collisions," Proceedings, Tenth Conference on the Application of Accelerators in Research and Industry, Denton, Texas, November 7-9, 1988, Nuclear Instruments and Methods in Physics Research

Gibbons, J. P., S. B. Elston, R. Deserio, C. Biedermann, M. Breinig, C. E. Gonzalez-Lepera, O. Heil, H.-P. Hulskotter, H. Rothard, I. A. Sellin, and C. R. Vane
"Production and Transport of Convoy Electrons in Amorphous Carbon Foils," Proceedings, Tenth Conference on the Application of Accelerators in Research and Industry, Denton, Texas, November 7-9, 1988, Nuclear Instruments and Methods in Physics Research

Giese, J. P., and E. Horsdal
"Differential Charge State Fractions of He Following Ionization by Fast H^- Projectiles," Proceedings, Tenth Conference on the Application of Accelerators in Research and Industry, Denton, Texas, November 7-9, 1988, Nuclear Instruments and Methods in Physics Research

Girit, I. C., G. D. Alton, C. R. Bingham, H. K. Carter, M. L. Simpson, J. D. Cole, J. H. Hamilton, E. F. Jones, P. M. Gore, J. Kormicki, B. D. Kern, K. S. Krane, Y. S. Xu, P. F. Mantica, Jr., B. E. Zimmerman, W. G. Nettles, E. F. Zganjar, M. O. Kortelahti, and W. B. Newbolt
"UNISOR On-Line Nuclear Orientation Facility (UNISOR/NOF)," Proceedings, Workshop on On-Line Nuclear Orientation and Related Topics, Oxford, England, August 31-September 4, 1988

Halbert, M. L.
"Gamma Decay of Giant Resonaces Excited by Heavy Ions," Proceedings, International Symposium on Heavy Ion Physics and Nuclear Astrophysical Problems, Tokyo, Japan, July 21-23, 1988

Halbert, M. L., J. R. Beene, D. C. Hensley, K. Honkanen, T. M. Semkow, V. Abenante, D. G. Sarantites, and Z. Li (Invited Paper)
"Angular Momentum Effects in Subbarrier Fusion," Proceedings, International Symposium on Heavy-Ion Reaction Dynamics in Tandem Energy Region, Hitachi, Japan, August 1-3, 1988

Havener, C. C., M. S. Huq, H. F. Krause, P. A. Schultz, and R. A. Phaneuf
"Merged-Beams Measurements of Electron-Capture Cross Sections for O^{5+} + H at eV Energies," Physical Review A

Havener, C. C., M. S. Huq, F. W. Meyer, and R. A. Phaneuf (Invited Paper)
"Electron Capture by Multicharged Ions at eV Energies," Proceedings, International Conference on the Physics of Multiply Charged Ions, Grenoble, France, September 12-16, 1988, Journal de Physique (Paris)

Horen, D. J., J. Lisantti, R. L. Auble, F. E. Bertrand, B. L. Burks, E. E. Gross, R. O. Sayer, D. K. McDaniels, K. W. Jones, J. B. McClelland, S. J. Seestrom-Morris, and L. W. Swenson
"T = 1, Spin-Dipole Strength in ^{40}Ca," Zeitschrift fuer Physik A

Iwazaki, A., and S. Kumano
"Oscillations of the Polarized Vacuum Around a Large Z 'Nucleus'," Physics Letters B

Janev, R. K., R. A. Phaneuf, and H. T. Hunter
"Recommended Cross Sections for Electron Capture and Ionization in Collisions of C^{q+} and O^{q+} Ions with H, He, and H_2," Atomic Data and Nuclear Data Tables

Jeukenne, J.-P., C. H. Johnson, and C. Mahaux
"Surface Contributions to the Complex Neutron-^{208}Pb Mean Field Between -20 and +20 MeV," Physical Review C

Johnson, C. H., R. F. Carlton, and R. R. Winters
"Extrapolation of the Dispersive Optical Model to the Resonance Region for Neutrons on ^{86}Kr," Physical Review C

Johnson, C. H., and C. Mahaux
"Neutron-^{40}Ca Mean Field Between -80 and +80 MeV from a Dispersive Optical-Model Analysis," Physical Review C

Johnson, J. W., W. H. Atkins, D. T. Dowling, J. W. McConnell, W. T. Milner, and D. K. Olsen
"HISTRAP Vacuum Test Stand for Pressures of 10^{-12} Torr," Proceedings, American Vacuum Society 35th National Symposium and Topical Conference, Atlanta, Georgia, October 3-7, 1988

Jones, C. M.
"25.5 MV Achieved with Oak Ridge Tandem Accelerator," CERN Courier, "Around the Laboratories" Section

Jones, C. M., D. L. Haynes, R. C. Juras, M. J. Meigs, N. F. Ziegler, J. E. Raatz, and R. D. Rathmell
"Improved Voltage Performance of the Oak Ridge 25URC Tandem Accelerator," Nuclear Instruments and Methods in Physics Research

Jones, N. L.
"EN-12 at ORNL," Proceedings, Symposium of Northeastern Accelerator Personnel, New Haven, Connecticut, October 24-27, 1988

Juras, R. C., N. F. Ziegler, G. D. Mills, M. J. Meigs, R. L. McPherson, C. M. Jones, D. L. Haynes, and G. D. Alton
"Oak Ridge 25URC Tandem Accelerator - SNEAP Lab Report," Proceedings, Symposium of Northeastern Accelerator Personnel, New Haven, Connecticut, October 24-27, 1988

Kemmler, J., O. Heil, C. Biedermann, P. Koschar, H. Rothard, K. Kroneberger, K. O. Groeneveld, and I. A. Sellin
"Convoy Electrons in Coincidence with Outgoing Charge States of Ni (920 MeV)," Proceedings, 14th International Conference on X-Ray and Inner-Shell Processes, Paris, France, September 14-18, 1987

Kephart, J. O., R. H. Pantell, B. L. Berman, S. Datz, H. Park, and R. K. Klein
"Measurement of the Occupation Lengths of Channeled 17-MeV Electrons and 54-MeV Electrons and Positrons in Silicon by Means of Channeling Radiation," Physical Review B

Kim, H. J. (Invited Paper)
"Transfer Reactions for the ^{50}Ti + ^{90}Zr System below the Coulomb Barrier," Proceedings, Workshop on Heavy-Ion Interactions Around the Coulomb Barrier, Legnaro, Italy, June 1-4, 1988, Lecture Notes in Physics

Kim, H. J., J. Gomez del Campo, M. Hindi, D. Shapira, and P. H. Stelson
"Transfer Reactions for the ^{50}Ti + ^{90}Zr System Below the Coulomb Barrier," Physical Review C

Kobos, A. M., M. E. Brandan, and G. R. Satchler
"Further Optical Model Studies of ^{16}O Scattering at E/A = 94 MeV," Nuclear Physics A

Kortelahti, M. O., H. K. Carter, R. A. Braga, R. W. Fink, and B. D. Kern
"Non-yrast Level Structure of ^{135}Nd via Beta Decay of ^{135}Tm," Zeitschrift fuer Physik A

Kortelahti, M. O., K. S. Toth, K. Vierinen, J. M. Nitschke, P. A. Wilmarth, R. B. Firestone, R. M. Chasteler, and A. A. Shihal-Eldin
"Decay Properties of ^{152}Yb and ^{153}Tm; Excitation Energies of the $s_{1/2}$ and $h_{1/2}$ Proton States in ^{153}Tm," Physical Review C

Kortelahti, M., E. F. Zganjar, H. K. Carter, C. D. Papanicolopulos, M. A. Grimm, and J. L. Wood
"Nuclear Systematics Far from the Line of Beta Stability: The Low-Lying Excited States of ^{185,187,189}Au," Journal of Physics G

Kumano, S.
"Pionic Contribution to the Scalar and Longitudinal N-Δ Transition Quadrupole Form Factors," Physics Letters B

Kumano, S.
"N(e,e′γ) and the N-Δ Transition Quadrupole Moment," Nuclear Physics A

Lasley, S., M. Breinig, and C. C. Gaither III
"Threshold Behavior of the Cross Section for Collisional Dissociation of Diatomic Molecules," Physical Review A

Lee, I. Y., C. Baktash, J. R. Beene, M. L. Halbert, D. C. Hensley, N. R. Johnson, F. K. McGowan, M. A. Riley, and D. G. Sarantites (Invited Paper)
"High Resolution Correlation Studies of Continuum Gamma Rays of ^{174}Hf," Proceedings, Conference on High-Spin Nuclear Structure and Novel Nuclear Shapes, Argonne, Illinois, April 13-15, 1988

Lee, I. Y., C. Baktash, J. R. Beene, M. L. Halbert, N. R. Johnson, F. K. McGowan, W. T. Milner, H. J. Kim, R. O. Sayer, and D. G. Sarantites
"Spin and Excitation-Energy Dependence of Nuclear Gamma-Ray Energy Correlations," Physical Review Letters

Levin, J. C., C. Biederman, H. Cederquist, C.-S. O, R. T. Short, and I. A. Sellin (Invited Paper)
"Properties of Cold Ions Produced by Synchrotron Radiation and by Charged Particle Impact," Proceedings, Tenth Conference on the Application of Accelerators in Research and Industry, Denton, Texas, November 7-9, 1988, Nuclear Instruments and Methods in Physics Research

Li, B., and C. Y. Wong
"Nuclear Stopping Power and Recoiling Nucleons," Physical Review D

Lisantti, J., D. J. Horen, F. E. Bertrand, R. L. Auble, B. L. Burks, E. E. Gross, R. O. Sayer, D. K. McDaniels, K. W. Jones, J. B. McClelland, S. J. Seestrom-Morris, and L. W. Swenson
"Collective Model DWBA Analysis of 500 MeV Proton Scattering from ^{40}Ca," Physical Review C

Lisantti, J., D. J. Horen, F. E. Bertrand, R. L. Auble, B. L. Burks, E. E. Gross, R. O. Sayer, D. K. McDaniels, K. W. Jones, J. B. McClelland, S. J. Seestrom-Morris, and L. W. Swenson
"Giant Resonance Strength Distribution in ^{40}Ca from Inelastic Scatering of 500 MeV Protons," Physical Review C

Loehner, H., R. Albrecht, T. C. Awes, C. Baktash, P. Beckmann, F. Berger, R. Bock, G. Claesson, L. Dragon, R. L. Ferguson, A. Franz, S. Garpman, R. Glasow, H. A. Gustafsson, H. H. Gutbrod, K. H. Kampert, B. W. Kolb, P. Kristiansson, I. Y. Lee, I. Lund, F. E. Obenshain, A. Oskarsson, I. Otterlund, T. Peitzmann, S. Persson, F. Plasil, A. M. Poskanzer, M. Purschke, H. G. Ritter, R. Santo, H. R. Schmidt, T. Siemiarczuk, S. P. Sorensen, E. Stenlund, and G. R. Young (Invited Paper)
"Momentum Distributions of Neutral Pions in Heavy-Ion Reactions at the CERN-SPS," Proceedings, IX International Seminar on High-Energy Physics Problems – Relativistic Nuclear Physics and Quantum Chromodynamics, Dubna, U.S.S.R., June 14-19, 1988

Loehner, H., R. Albrecht, T. C. Awes, C. Baktash, P. Beckmann, F. Berger, R. Bock, G. Claesson, L. Dragon, R. L. Ferguson, A. Franz, S. Garpman, R. Glasow, H. A. Gustafsson, H. H. Gutbrod, K. H. Kampert, B. W. Kolb, P. Kristiansson, I. Y. Lee, I. Lund, F. E. Obenshain, A. Oskarsson, I. Otterlund, T. Peitzmann, S. Persson, F. Plasil, A. M. Poskanzer, M. Purschke, H. G. Ritter, R. Santo, H. R. Schmidt, T. Siemiarczuk, S. P. Sorensen, E. Stenlund, and G. R. Young

"Neutral Transverse Momentum Spectra in 200 A GeV O + Nucleus Reactions," Proceedings, International Symposium on Collective Phenomena in Nuclear and Subnuclear Long Range Interactions in Nuclei, Bad Honnef, West Germany, May 4-7, 1987

McGowan, F. K., N. R. Johnson, I. Y. Lee, and C. Baktash
"Reply to Comment by S. Raman," Physical Review Letters

Meyer, F. W., C. C. Havener, S. H. Overbury, K. J. Reed, K. J. Snowdon, and D. M. Zehner (Invited Talk)
"Inner-Shell Processes as Probes of Multicharged Ion Neutralization at Surfaces," Proceedings, International Conference on the Physics of Multiply Charged Ions, Grenoble, France, September 12-16, 1988, Journal de Physique (Paris)

Mori, Y., G. D. Alton, A. Takagi, A. Ueno, and S. Fukumoto
"Further Evaluation of the High Intensity Plasma Sputter Heavy Negative Ion Source," Nuclear Instruments and Methods in Physics Research

Morrison, J. D., J. F. Sharpey-Schafer, M. A. Bentley, H. W. Cramer-Gordon, P. Fallon, P. D. Forsyth, D. Howe, A. R. Mokhtar, M. A. Riley, and J. Simpson
"Unpaired Collective Band Crossings in ^{156}Dy Between Spins 35^- and 53^-," Europhysics Letters

Morsch, H. P., W. Spang, J. R. Beene, F. E. Bertrand, R. L. Auble, J. L. Charvet, M. L. Halbert, D. C. Hensley, I. Y. Lee, R. L. Varner D. G. Sarantites, and D. W. Stracener
"Observation of Thermal Narrowing and Shape Effects in the Giant Dipole Resonance Decay of Hot Rare-Earth Nuclei," Physical Review Letters

Mueller, D. W., L. J. Wang, and D. C. Gregory
"Electron-Impact Double Ionization Cross Sections for Xe^{8+}," Physical Review A

Obenshain, F. E., R. Albrecht, T. C. Awes, C. Baktash, P. Beckmann, F. Berger, R. Bock, G. Claesson, L. Dragon, R. L. Ferguson, A. Franz, S. Garpman, R. Glasow, H. A. Gustafsson, H. H. Gutbrod, K. H. Kampert, B. W. Kolb, P. Kristiansson, I. Y. Lee, H. Loehner, I. Lund, A. Oskarsson, I. Otterlund, T. Peitzmann, S. Persson, F. Plasil, A. M. Poskanzer, M. Purschke, H. G. Ritter, R. Santo, H. R. Schmidt, T. Siemiarczuk, S. P. Sorensen, E. Stenlund, and G. R. Young
"Nuclear Stopping in Oxygen-Induced Reactions at 200 A GeV," Proceedings, XIXth International Symposium on Multiparticle Dynamics — New Data and Theoretical Trends, Arles, France, June 13-17, 1988

Papanicolopulos, C. D., M. A. Grimm, J. L. Wood, E. F. Zganjar, M. Kortelahti, J. D. Cole, and H. K. Carter
"Very Converted Transitions and Particle-Core Coupling in Neutron-Deficient Odd-Mass Au Isotopes," Zeitschrift fuer Physik

Pegg, D. J., J. S. Thompson, R. N. Compton, and G. D. Alton (Invited Paper)
"The Structure of the Stable Negative Ion of Calcium," Proceedings, 4th International Conference on Resonance Resonance Ionization Spectroscopy, Gaithersburg, Maryland, April 11-15, 1988

Pegg, D. J., J. S. Thomspon, R. N. Compton, and G. D. Alton (Invited Paper)
"Energy- and Angle-Resolved Photoelectron Spectroscopy of Negative Ions," Proceedings, Tenth Conference on the Application of Accelerators in Research and Industry, Denton, Texas, November 7-9, 1988, Nuclear Instruments and Methods in Physics Research

Peitzmann, T., Albrecht, R., T. C. Awes, C. Baktash, P. Beckmann, F. Berger, R. Bock, G. Claesson, G. Clewing, L. Dragon, A. Eklund, R. L. Ferguson, A. Franz, S. Garpman, R. Glasow, H. A. Gustafsson, H. H. Gutbrod, J. Idh, K. H. Kampert, B. W. Kolb, P. Kristiansson, I. Y. Lee, H. Loehner, I. Lund, F. E. Obenshain, A. Oskarsson, I. Otterlund, S. Persson, F. Plasil, A. M. Poskanzer, M. Purschke, H. G. Ritter, R. Santo, H. R. Schmidt, T. Siemiarczuk, S. P. Sorensen, E. Stenlund, and G. R. Young
"Correlations of Neutral Pions in Ultrarelativistic Heavy Ion Collisions," Proceedings, Seventh International Conference on Ultrarelativistic Nucleus-Nucleus Collisions, Lenox, Massachusetts, September 26-30, 1988, Nuclear Physics A

Phaneuf, R. A., P. Defrance, D. C. Griffin, Y. Hahn, M. S. Pindzola, L. Roszman, and W. Wiese
"IAEA Specialists Meeting on Carbon and Oxygen Collision Data for Fusion Plasma Research," Proceedings, IAEA Specialists' Meeting on Carbon and Oxygen Collision Data for Fusion Plasma Research, Vienna, Austria, May 12-13, 1988, Physica Scripta

Pindzola, M. S., D. C. Griffin, and C. Bottcher
"Theoretical Calculations of Indirect Processes in Electron-Impact Ionization of Atomic Ions," Comments on Atomic and Molecular Physics

Plasil, F., R. Albrecht, T. C. Awes, C. Baktash, P. Beckmann, F. Berger, R. Bock, G. Claesson, L. Dragon, R. L. Ferguson, A. Franz, S. Garpman, R. Glasow, H. A. Gustafsson, H. H. Gutbrod, K. H. Kampert, B. W. Kolb, P. Kristiansson, I. Y. Lee, H. Loehner, I. Lund, F. E. Obenshain, A. Oskarsson, I. Otterlund, T. Peitzmann, S. Persson, A. M. Poskanzer, M. Purschke, H. G. Ritter, R. Santo, H. R. Schmidt, T. Siemiarczuk, S. P. Sorensen, E. Stenlund, and G. R. Young
"Results from CERN Experiment WA80," Proceedings, Winter Workshop on Nuclear Dynamics V, Sun Valley, Idaho, February 22-26, 1988

Poth, H., W. Schwab, B. Seligmann, M. Wortge, A. Wolf, S. Baird, M. Chanel, H. Haseroth, C. E. Hill, R. Ley, D. Manglunki, G. Tranquille, J. L. Valet, and P. F. Dittner
"First Results of Electron Cooling Experiments at LEAR," Zeitschrift fuer Physik

Raman, S. (Invited Paper)
"Selected Topics in Nuclear and Atomic Physics," Proceedings, VIII International School on Nuclear Physics, Neutron Physics, and Nuclear Energy, Varna, Bulgaria, October 19-28, 1987

Raman, S., S. Kahane, and J. E. Lynn (Invited Paper)
"Interplay of Direct and Compound-Nucleus Mechanisms in Neutron Capture by Light Nuclides," Proceedings, International Conference on Nuclear Data for Science and Technology, May 30-June 3, 1988, Mito, Japan

Raman, S., C. W. Nestor, Jr., S. Kahane, and K. H. Bhatt
"Comment on 'Loss of Collectivity at High Spin in ^{172}W'," Physical Review Letters

Raman, S., C. W. Nestor, Jr., S. Kahane, and K. H. Bhatt
"Predictions of B (E2; $0_1^+ \rightarrow 2_1^+$) Values for Even-Even Nuclei," Atomic Data and Nuclear Data Tables

Read, P. M., J. T. Maskrey, and G. D. Alton
"Development of a Lithium Liquid Metal Ion Source for MeV Ion Beam Analysis," Proceedings, European Particle Accelerator Conference, Rome, Italy, June 7-11, 1988, Nuovo Cimento

Riley, M. A., Y. A. Akovali, C. Baktash, M. L. Halbert, D. C. Hensley, N. R. Johnson, I. Y. Lee, F. K. McGowan, A. Virtanen, L. H. Courtney, V. P. Janzen, L. L. Riedinger, L. Chaturvedi, and J. Simpson
"Irregularities at High Spin in the Odd-Odd Nucleus ^{158}Tm," Physical Review C

Riley, M. A., C. Baktash, Y. A. Ellis-Akovali, M. L. Halbert, D. C. Hensley, N. R. Johnson, I. Y. Lee, F. K. McGowan, V. P. Janzen, L. L. Riedinger, and L. Chaturvedi (Invited Paper)
"Alignments, Shape Changes, Band Terminations and Transition Rates in ^{157}Tm," Proceedings, Conference on High-Spin Nuclear Structure and Novel Nuclear Shapes, Argonne, Illinois, April 13-15, 1988

Sataka, M., S. Ohtani, D. Swenson, and D. C. Gregory
"Experimental Cross Sections for Electron-Impact Ionization of Chromium Ions: Cr^{6+}, Cr^{7+}, Cr^{8+}, and Cr^{10+}," Physical Review A

Satchler, G. R.
"Relation Between M_n,M_p and Hadronic Excitation Strengths When There Is Strong Absorption: The ^{A}Zr(α,α') Reactions," Nuclear Physics A

Schmidt, H. R., R. Albrecht, T. C. Awes, C. Baktash, P. Beckmann, F. Berger, R. Bock, G. Claesson, L. Dragon, R. L. Ferguson, A. Franz, S. Garpman, R. Glasow, H. A. Gustafsson, H. H. Gutbrod, J. W. Johnson, K. H. Kampert, B. W. Kolb, P. Kristiansson, I. Y. Lee, H. Lohner, I. Lund, F. E. Obenshain, A. Oskarsson, I. Otterlund, T. Peitzmann, S. Persson, F. Plasil, A. M. Poskanzer, M. Purschke, H. G. Ritter, R. Santo, T. Siemiarczuk, S. P. Sorensen, E. Stenlund, and G. R. Young (Invited Paper)
"Oxygen-Induced Reactions at 200 and 60 GeV/Nucleon," 27th International Summer School for Theoretical Physics, Zakopane, Poland, June 3-15, 1987, Acta Physica Polonica

Schone, H., R. Schuch, S. Datz, P. F. Dittner, J. P. Giese, H. F. Krause, M. Schulz, and Q. C. Kessel
"Charge and Angular Correlated Inelasticities in MeV/Nucleon Ion-Atom Collisions," Proceedings, Tenth Conference on the Application of Accelerators in Research and Industry, Denton, Texas, November 7-9, 1988, Nuclear Instruments and Methods in Physics Research

Schulz, M., S. Datz, P. F. Dittner, J. P. Giese, H. F. Krause, P. D. Miller, H. Schone, J. K. Swenson, C. R. Vane, R. Schuch, E. Justiniano, M. Benhenni, S. M. Shafroth, P. H. Mokler, and S. Reusch
"Transfer and Excitation Processes Studied in H-Like S and Li-Like and H-Like F Colliding with H_2," Proceedings, Tenth Conference on the Application of Accelerators in Research and Industry, Denton, Texas, November 7-9, 1988, Nuclear Instruments and Methods in Physics Research

Schulz, M., J. P. Giese, J. K. Swenson, S. Datz, P. F. Dittner, H. F. Krause, H. Schone, C. R. Vane, M. Benhenni, and S. M. Shafroth
"Electron-Electron Interactions in Transfer and Excitation in $F^{8+} + H_2$ Collisions," Physical Review Letters

Schulz, M., R. Schuch, S. Datz, E.L.B. Justiniano, P. D. Miller, and H. Schone
"Resonant Transfer and Excitation in Li-Like F Colliding with H_2," Physical Review A

Shapira, D. (Invited Paper)
"Nuclear Orbiting," Proceedings, Fifth International Conference on Clustering Phenomena, Kyoto, Japan, July 25-29, 1988

Shapira, D.
"Comment on 'Asymmetric Fission of ^{56}Ni'," Physical Review Letters

Sofield, C. J., L. B. Bridwell, C. D. Moak, P. D. Miller, D. C. Gregory, C. M. Jones, G. D. Alton, P. L. Pepmiller, and J. Hall
"Charge-Exchange Cross Sections for 445 MeV Cl Ions in Solid C Targets," Physical Review A

Stelson, P. H. (Invited Paper)
"Neutron Flow Between Nuclei as the Principal Enhancement Mechanism in Heavy-Ion Subbarrier Fusion," Proceedings, International Symposium on Heavy-Ion Reaction Dynamics in Tandem Energy Region, Hitachi, Japan, August 1-3, 1988

Swenson, L. W., X. Y. Chen, J. Lisantti, D. K. McDaniels, I. Bergqvist, F. E. Bertrand, D. J. Horen, E. E. Gross, C. Glover, R. O. Sayer, B. L. Burks, O. Hausser, K. Hicks, and M. J. Iqbal
"New Continuum Approaches in the Study of Giant Resonances in ^{208}Pb with 400-MeV Protons," Physical Review C

Tinschert, K., A. Muller, G. Hofmann, K. Huber, R. Becker, D. C. Gregory, and E. Salzborn
"Experimental Cross Sections for Electron Impact Ionization of Hydrogenlike Ions Li^{2+}," Journal of Physics B

Toth, K. S., Y. A. Akovali, H. J. Kim, J. M. Nitschke, P. A. Wilmarth, and D. M. Moltz
"Direct and β-Delayed Particle Decays Near Closed Shells," Nuclear Instruments and Methods in Physics Research

Toth, K. S., D. M. Moltz, and J. D. Robertson
"Identification of ^{181}Pb in ^{40}Ca Irradiations of ^{144}Sm," Physical Review C

Toth, K. S., P. A. Wilmarth, J. M. Nitschke, R. B. Firestone, K. Vierinen, M. O. Kortelahti, and F. T. Avignone, III
"Fine Structure in ^{153}Tm α Decay," Physical Review C

Umar, A. S., M. R. Strayer, P.-G. Reinhard, K.T.R. Davies, and S.-J. Lee
"Spin-Orbit Force in TDHF Calculations of Heavy-Ion Collisions," Physical Review C

Wang, J., and J. Burgdorfer
"v/2 ('Ridge') Electron Emission in Ion-Atom Collisions with Short-Ranged Potentials," Report: 9. Arbeitsbericht, Arbeitsgruppe, Energiereiche Atomare Stosse, Oberstdorf, West Germany

White, G. D., K.T.R. Davies, and P. J. Siemens
"Studies of the Nuclear Single-Particle Respone Function in a Simple Model," Annals of Physics (New York)

Wong, C. Y.
"Interaction of a Neutral Composite Particle with a Strong Coulomb Field," Progress of Theoretical Physics

Wong, C. Y. (Invited Paper)
"Origin of Anomalous Positron Peaks in Heavy-Ion Reactions," Proceedings, International Conference on Medium- and High-Energy Nuclear Physics, Taipei, Taiwan, May 23-27, 1988

Wong, C. Y.
"Condensation of (e^+e^-) Due to Short-Range Noncentral Electromagnetic Interaction," Physical Review D

Wong, C. Y. (Invited Paper)
"Condensation of (e^+,e^-) Due to Short-Range Noncentral Electromagnetic Interaction," Proceedings, Fifth International Conference on Clustering Aspects in Nuclear and Subnuclear Systems, Kyoto, Japan, July 25-29, 1988

Wong, C. Y.
"Micropolyelectrons as Possible Sources of the Anomalous Positron Peaks in Heavy-Ion Reactions," Proceedings, Workshop on Microscopic Models in Nuclear Structure Physics, Oak Ridge, Tennessee, October 3-6, 1988, World Scientific Publishing

Wong, C. Y., and Z. D. Lu (Invited Paper)
"The Dynamics of High-Energy Nucleus-Nucleus Collisions," Proceedings, International Conference on Medium- and High-Energy Nuclear Physics, Taipei, Taiwan, May 23-27, 1988

Wong, C. Y., and Z. D. Lu
"A Multiple-Collision Model for High-Energy Nucleus-Nucleus Collisions," Physical Review D

Wu, J., J. J. Bai, and R. Y. Cusson
"Numerical Method for the Time Evolution of Dirac Equation," Physical Review C

Yamazaki, Y., N. Stolterfoht, P. D. Miller, H. F. Krause, P. L. Pepmiller, S. Datz, I. A. Sellin, J. N. Scheurer, S. Andriamonje, D. Bertault, and J. F. Chemin
"Angular Momentum Distributions of Autoionizing States Produced by 1.5-5 MeV C^{q+} Ions in Carbon Foils," Physical Review Letters

Zhang, J.-Y., and J. D. Garrett
"Observation of Diabolical Points in Rapidly-Rotating Nuclei," Physical Review Letters, Comment

11. PAPERS PRESENTED AT SCIENTIFIC AND TECHNICAL MEETINGS

October 1987 Through September 1988

List Prepared by Shirley J. Ball

1987

12th International Conference on Atomic Collisions in Solids, Okayama, Japan, October 12-16, 1987

Read, P. M., C. J. Sofield, G. D. Alton, P. D. Miller, P. L. Pepmiller, D. C. Gregory, and L. B. Bridwell
"Electron Capture Cross Sections to Hydrogenic States of 1-GeV Ni in Solid Carbon"

Snowdon, K. J., C. C. Havener, W. Heiland, F. W. Meyer, S. H. Overbury, and D. M. Zehner
"Direct Evidence for the Dominant Role of Target Core Levels in the Neutralization of Slow Multicharged Ions at Metal Surfaces"

Gaseous Electronics Conference, Atlanta, Georgia, October 13-16, 1987

Bottcher, C., D. C. Griffin, and M. S. Pindzola
"Ionization in Collisions Between Electrons and Complex Ions"

Phaneuf, R. A. (Invited Talk)
"Measurements of Electron-Impact Ionization Cross Sections for Ions"

American Physical Society, Division of Nuclear Physics, New Brunswick, New Jersey, October 15-17, 1987

Awes, T. C., R. L. Ferguson, F. E. Obenshain, F. Plasil, S. Pratt, G. R. Young, Z. Chen, C. K. Gelbke, W. G. Lynch, J. Pochodzalla, and H. M. Xu
"Proton-Proton Correlations in ^{32}S-Induced Reactions on Gold: Reaction Source Geometry," Bull. Am. Phys. Soc. 32, 1550 (Sept. 1987)

Johnson, C. H. (Invited Talk)
"Dispersion Relation Analysis of the Neutron-^{208}Pb Mean Field," Bull. Am. Phys. Soc. 32, 1548 (Sept. 1987)

Lee, I. Y., C. Baktash, J. R. Beene, M. L. Halbert, N. R. Johnson, F. K. McGowan, and D. G. Sarantites
"Gamma-Ray Energy Correlation Studies of ^{170}Hf," Bull. Am. Phys. Soc. 32, 1544 (Sept. 1987)

Lisantti, J., F. E. Bertrand, D. J. Horen, R. L. Auble, B. L. Burks, E. E. Gross, R. O. Sayer, K. W. Jones, J. B. McClelland, S. J. Seestrom-Morris, and L. W. Swenson
"Giant Resonance Strength Distribution in ^{40}Ca as Determined with 500 MeV Protons," Bull. Am. Phys. Soc. 32, 1573 (Sept. 1987)

Penumetcha, V., G. A. Petitt, T. C. Awes, R. L. Ferguson, F. E. Obenshain, F. Plasil, and G. R. Young
"Charge and Mass Distribution of Projectile-like Fragments in the Reaction ^{58}Ni + ^{165}Ho at 15.7 MeV/Nucleon," Bull. Am. Phys. Soc. 32, 1542 (Sept. 1987)

Petitt, G. A., C. Butler, V. Penumetcha, T. C. Awes, J. R. Beene, R. L. Ferguson, F. E. Obenshain, F. Plasil, S. P. Sorensen, and G. R. Young
"Neutron Emission in Damped Reactions of ^{58}Ni + ^{165}Ho at 15.5 MeV/Nucleon," Bull. Am. Phys. Soc. 32, 1550 (Sept. 1987)

Shapira, D., P. H. Stelson, B. L. Burks, B. A. Harmon, B. Shivakumar, and S. T. Thornton
"Effect of Entrance Channel Asymmetry on Fusion Reactions Leading to ^{40}Ca and ^{42}Ca," Bull. Am. Phys. Soc. 32, 1541 (Sept. 1987)

Stelson, P. H.
"Enhancement of Heavy-Ion Sub-barrier Fusion Cross Sections and Neutron Interactions," Bull. Am. Phys. Soc. 32, 1541 (Sept. 1987)

Wong, C. Y.
"Nuclear Stopping Power in High-Energy Collisions," Bull. Am. Phys. Soc. 32, 1551 (Sept. 1987)

Young, G. R. (Invited Talk)
"Experiments with E/A = 200-GeV and 60-GeV Oxygen Beams: Initial Results from CERN Experiment WA80," Bull. Am. Phys. Soc. 32, 1565 (Sept. 1987)

1987 IEEE Nuclear Science Symposium, San Francisco, California, October 19-23, 1987

Teh, K. M., D. Shapira, J. W. McConnell, H. Kim, and R. Novotny
"Data Acquisition for the HILI Detector"

VIII International School on Nuclear Physics, Neutron Physics, and Nuclear Energy, Varna, Bulgaria, October 19-28, 1987

Raman, S. (Invited Talk)
"Selected Topics in Nuclear and Atomic Physics"

Third International Symposium on Laser-Aided Plasma Diagnostics, Los Angeles, California, October 28-30, 1987

Ma, C. H., and D. P. Hutchinson (Invited Talk)
"Feasibility Study of an Infrared Interferometer/Polarimeter System for CIT"

American Physical Society, 29th Annual Meeting of the Division of Plasma Physics, San Diego, California, November 2-6, 1987

Bennett, C. A., D. P. Hutchinson, and R. K. Richards
"Selective Absorption of CO_2 Laser Radiation Using Hot CO_2," Bull. Am. Phys. Soc. 32, 1870 (Oct. 1987)

Hunter, H. T., D. P. Hutchinson, and R. K. Richards
"A High Power Pulsed CO_2 Laser Source for Alpha Particle Measurement by Thomson Scattering," Bull. Am. Phys. Soc. 32, 1870 (Oct. 1987)

Ma, C. H., and D. P. Hutchinson
"An Infrared Interferometer/Polarimeter System for CIT," Bull. Am. Phys. Soc. 32, 1870 (Oct. 1987)

Richards, R. K., H. T. Hunter, and D. P. Hutchinson
"A CO_2 Laser Thomson Scattering Diagnostic for CIT Alpha Particle Measurement," Bull. Am. Phys. Soc. 32, 1922 (Oct. 1987)

Workshop on Advanced Laser Technology for Chemical Measurements, Gaithersburg, Maryland, November 4-6, 1987

Inn, K.G.W., J. D. Fassett, B. M. Coursey, R. L. Walker, and S. Raman
"Development of the NBS Beryllium Isotopic Standard Reference Material"

International Conference on ECR Ion Sources and Their Applications, East Lansing, Michigan, November 16-18, 1987

Meyer, F. W. (Invited Talk)
"Application of ECR Beams in Atomic Physics"

Southeastern Section of the American Physical Society, Nashville, Tennessee, November 23-25, 1987

Awes, T. C. (Invited Talk)
"The Search for the Quark-Gluon Plasma: First Results from CERN Experiment WA80," Bull. Am. Phys. Soc. 32, 2140 (Nov. 1987)

-gdorfer, J. (Invited Talk)
"Stochastic Perturbations of Fast Atoms in Solids," Bull. Am. Phys. Soc. 32, 2132 (Nov. 1987)

Chaturvedi, L., A. V. Ramayya, J. H. Hamilton, C. Girit, J. Kormicki, X. Zhao, S. Zhu, W.-C. Gao, N. R. Johnson, I. Y. Lee, C. Baktash, F. K. McGowan, M. L. Halbert, M. A. Riley, M. O. Kortelahti, and J. D. Cole
"High Spin States and Multiple Band Structures in ^{68}Ge," Bull. Am. Phys. Soc. 32, 2145 (Nov. 1987)

Datz, S. (Invited Talk)
"Channeling Radiation — Atomic and Molecular Physics in One and Two Dimensions," Bull. Am. Phys. Soc. 32, 2128 (1987)

Girit, I. C., J. H. Hamilton, K. S. Krane, H. K. Carter, M. L. Simpson, E. F. Zganjar, J. D. Cole, B. D. Kern, C. R. Bingham
"UNISOR Nuclear Orientation Facility," Bull. Am. Phys. Soc. 32, 2145 (Nov. 1987)

Griffin, J. C., R. W. Fink, C. R. Bingham, H. V. Carmichael, J. L. Wood, M. O. Kortelahti, and H. K. Carter
"Decay of Mass-Separated ^{195}Bi to Levels in ^{195}Pb: Possible Shape-Coexistence in Odd-A Lead Isotopes," Bull. Am. Phys Soc. 32, 2145 (Nov. 1987)

Kormicki, J., J. H. Hamilton, A. V. Ramayya, L. Chaturvedi, Z.-M. Chen, I. C. Girit, W.-C. Ma, S. Wen, X. Zhao, N. R. Johnson, C. Baktash, M. L. Halbert, D. C. Hensley, I. Y. Lee, F. K. McGowan, M. O. Kortelahti, R. B. Piercey, and W. G. Nettles
"High Spin States in ^{182,184}Hg," Bull. Am. Phys. Soc. 32, 2146 (Nov. 1987)

Kortelahti, M. O., B. D. Kern, R. A. Braga, and R. W. Fink
"Energy Levels of Neutron-Deficient Rare-Earth Nuclei via Beta Decay," Bull. Am. Phys. Soc. 32, 2146 (Nov. 1987)

Olive, D. H., and G. D. Alton
"A Quantitative Approach for Determination of Sputter Ratios Based on Scaled Sigmund Theory," Bull. Am. Phys. Soc. 32, 2147 (Nov. 1987)

Raman, S., C. W. Nestor, Jr., and K. H. Bhatt
"Schematic Interpretations of the Systematics of B(E2)↑ Values Throughout the Periodic Table," Bull. Am. Phys. Soc. 32, 2130 (Nov. 1987)

Sellin, I. A. (Invited Talk)
"Convoy Electron Production: Bulk and Surface Effects," Bull. Am. Phys. Soc. 32, 2128 (Nov. 1987)

Simpson, M. L., D. Abraham, and J. M. Rochelle
"High Sensitivity Beam Profile Monitor," Bull. Am. Phys. Soc. 32, 2146 (Nov. 1987)

Young, G. R. (Invited Talk)
"The HISTRAP Proposal: An Accelerator and Storage Ring for Atomic Physics," Bull. Am. Phys. Soc. 32, 2134 (Nov. 1987)

Zganjar, E. F. (Invited Talk)
"Nuclear Shape Coexistence and Electric Monopole Transitions in the 180 < A < 200 Region," Bull. Am. Phys. Soc. 32, 2138 (Nov. 1987)

Zhu, S., L. Chaturvedi, A. V. Ramayya, J. H. Hamilton, C. Girit, J. Kormicki, X. Zhao, W.-B. Gao, N. R. Johnson, I. Y. Lee, C. Baktash, F. K. McGowan, M. L. Halbert, M. A. Riley, M. O. Kortelahti, and J. D. Cole
"High Spin States in ^{65,67}Ga," Bull. Am. Phys. Soc. 32, 2146 (Nov. 1987)

Texas A&M Symposium on Hot Nuclei. College Station, Texas, December 7-10, 1987

Bertrand, F. E., and J. R. Beene (Invited Talk)
"Excitation and Photon Decay of Giant Resonances Excited by Intermediate Energy Heavy Ions"

Sarantites, D. G., T. M. Semkow, L. G. Sobotka, V. Abenante, Z. Li, Z. Majka, N. G. Nicolis, D. W. Stracener, D. C. Hensley, J. R. Beene, and H. C. Griffin (Invited Talk)
"A New Look at Reaction Mechanisms with 4π Charged-Particle and Neutron Multiplicity Measurements"

Lasers '87, Tenth International Conference on Lasers and Applications, Lake Tahoe, Nevada, December 7-11, 1987

Casson, W. H., D. P. Hutchinson, C. H. Ma, R. K. Richards, and K. L. Vander Sluis
"Infrared and Far-Infrared Laser Development for Plasma Diagnostics at Oak Ridge National Laboratory"

12th International Conference on Infrared and Millimeter Waves, Orlando, Florida, December 14-18, 1987

Hutchinson, D. P., W. H. Casson, and C. H. Ma (Invited Talk)
"A Multichannel Far-Infrared Interferometer on ATF"

Ma, C. H., and D. P. Hutchinson
"An Infrared Interferometer/Polarimeter on the Compact Ignition Tokamak"

1988

International Workshop XVI on Gross Properties of Nuclei and Nuclear Excitations, Hirschegg, Austria, January 18-22, 1988

Awes, T. C. (Invited Talk)
"Forward and Transverse Energy Measurements from CERN Experiment WA80"

XIth Symposium on Nuclear Physics, Oaxtepec, Mexico, January 4-7, 1988

Satchler, G. R. (Invited Talk)
"The Threshold Anomaly for Heavy-Ion Scattering"

International Conference on Physics and Astrophysics of the Quark-Gluon Plasma, Bombay, India, February 8-12, 1988

Albrecht, R., T. C. Awes, C. Baktash, P. Beckmann, F. Berger, R. Bock, G. Claesson, L. Dragon, R. L. Ferguson, A. Franz, S. Garpman, R. Glasow, H. A. Gustafsson, H. H. Gutbrod, K. H. Kampert, B. W. Kolb, P. Kristiansson, I. Y. Lee, H. Loehner, I. Lund, F. E. Obenshain, A. Oskarsson, I. Otterlund, T. Peitzmann, S. Persson, F. Plasil, A. M. Poskanzer, M. Purschke, H. G. Ritter, R. Santo, H. R. Schmidt, T. Siemiarczuk, S. P. Sorensen, E. Stenlund, and G. R. Young (Invited Talk)
"Results from CERN Experiment WA80"

Close, F. E. (Invited Talk)
Parton Distributions in Nuclei: Quagma or Quagmire?"

Miniworkshop on Experimental Techniques in Relativistic Heavy-Ion Experiments, Bombay, India, February 13, 1988

Plasil, F. (Invited Talk)
"Calorimetry Applied to Nucleus-Nucleus Collisions at Ultrarelativistic Energies"

Winter Workshop on Nuclear Dynamics V, Sun Valley, Idaho, February 22-26, 1988

Plasil, F., R. Albrecht, T. C. Awes, C. Baktash, P. Beckmann, F. Berger, R. Bock, G. Claesson, L. Dragon, R. L. Ferguson, A. Franz, S. Garpman, R. Glasow, H. A. Gustafsson, H. H. Gutbrod, K. H. Kampert, B. W. Kolb, P. Kristiansson, I. Y. Lee, H. Loehner, I. Lund, F. E. Obenshain, A. Oskarsson, I. Otterlund, T. Peitzmann, S. Persson, A. M. Poskanzer, M. Purschke, H. G. Ritter, R. Santo, H. R. Schmidt, T. Siemiarczuk, S. P. Sorensen, E. Stenlund, and G. R. Young
"Results from CERN Experiment WA80"

7th Topical Conference on High Temperature Plasma Diagnostics, Napa, California, March 13-17, 1988

Ma, C. H., D. P. Hutchinson, and K. L. Vander Sluis
"A Two-Wavelength Infrared Interferometer/Polarimeter System for CIT"

Richards, R. K., C. A. Bennett, L. Fletcher, H. T. Hunter, and D. P. Hutchinson
"A CO_2 Laser Thomson Scattering Diagnostic for Fusion Product Alpha Particle Measurement"

American Physical Society Meeting, New Orleans, Louisiana, March 21-25, 1988

McGuire, S. C., L. P. Clark, J. B. Ball, S. Raman, C. R. Vane, and E. G. Stassinopoulos
"Facility for Heavy-Ion-Induced Single-Event Upset Measurements," Bull. Am. Phys. Soc. 33, 371 (Mar. 1988)

Workshop on the RHIC Performance, Upton, New York, March 21-26, 1988

Young, G. R. (Invited Paper)
Electromagnetic Dissociation of Nuclei at Relativistic Energies"

Young, G. R. (Invited Paper)
"Luminosity Depletion in RHIC"

4th International Conference on Resonance Ionization Spectroscopy, Gaithersburg, Maryland, April 11-15, 1988

Pegg, D. J., J. S. Thompson, R. N. Compton, and G. D. Alton (Invited Talk)
"The Structure of the Stable Negative Ion of Calcium"

Conference on High-Spin Nuclear Structure and Novel Nuclear Shapes, Argonne, Illinois, April 13-15, 1988

Dudek, J., and T. Werner (Invited Talk)
"hyperdeformed Nuclei and the Residual Pseudo-SU(3) Symmetry"

Lee, I. Y., C. Baktash, J. R. Beene, M. L. Halbert, D. C. Hensley, N. R. Johnson, F. K. McGowan, M. A. Riley, and D. G. Sarantites (Invited Talk)
"High Resolution Correlation Studies of Continuum Gamma Rays of ^{170}Hf"

Riley, M. A., C. Baktash, Y. A. Ellis-Akovali, M. L. Halbert, D. C. Hensley, N. R. Johnson, I. Y. Lee, F. K. McGowan, V. P. Janzen, L. L. Riedinger, and L. Chaturvedi (Invited Talk)
"Alignments, Shape Changes, Band Terminations and Transition Rates in ^{157}Tm"

Annual Meeting of the Division of Atomic, Molecular, and Optical Physics, American Physical Society, Baltimore, Maryland, April 18-20, 1988

Bottcher, C., G. J. Bottrell, and M. R. Strayer
"Time-Dependent Hartree-Fock Description of Highly Charged Ion-Atom Collisions: C^{6+} + Ne," Bull. Am. Phys. Soc. 33, 921 (Apr. 1988)

Bottcher, C., G. J. Bottrell, and M. R. Strayer
"Charge Capture in Antiproton-Positronium Collisions: A Numerical Semiclassical Treatment," Bull. Am. Phys. Soc. 33, 1055 (Apr. 1988)

Bottcher, C., and M. R. Strayer
"Fully Three-Dimensional Solution of the Dirac Equation for Heavy-Ion Collisions at Relativistic Velocities," Bull. Am. Phys. Soc. 33, 997 (Apr. 1988)

Breinig, M., S. Datz, R. Hippler, P. D. Miller, H. Schuene, and R. Schuch
"Hot Electrons from Single Ionization and Transfer Ionization in Collisions of I^{q+} with He, H_2, and D_2 Targets," Bull. Am. Phys. Soc. 33, 1054 (Apr. 1988)

Buie, M. J., M. S. Pindzola, S. Chantrenne, and D. C. Gregory
"Electron-Impact Ionization of the Ti^{5+} Ion," Bull. Am. Phys. Soc. 33, 939 (Apr. 1988)

DeSerio, R., and J. P. Gibbons
"Simulation of Measurements of a Dettmann Cusp Using Electrostatic Spherical Sector Spectrometers," Bull. Am. Phys. Soc. 33, 1002 (Apr. 1988)

Freyou, J., M. Breinig, C. C. Gaither, and T. A. Underwood
"Multiple Coincidence in Fast Ion-Atom Collisions," Bull. Am. Phys. Soc. 33, 1054 (Apr. 1988)

Huq, M. S., C. C. Havener, and R. A. Phaneuf
"Total Cross Sections for Electron Capture in Collisions of N^{q+} (q = 3,4,5) with H and D Atoms at keV to eV Energies Using Merged Beams," Bull. Am. Phys. Soc. 33, 1004 (Apr. 1988)

Levin, J. C., C-S. O, H. Cederquist, C. Biedermann, and I. A. Sellin
Recoil-Ion Energy and Impact Parameter Dependence on Coincident Multiple Projectile Electron Capture and Loss," Bull. Am. Phys. Soc. 33, 1054 (Apr. 1988)

Levin, J. C., C-S. O, and I. A. Sellin
"Monte-Carlo Simulations of Time-of-Flight Spectra," Bull. Am. Phys. Soc. 33, 1002 (Apr. 1988)

Meyer, F. W., C. C. Havener, W. Heiland, K. J. Snowdon, and D. M. Zehner
"Electron Emission in Collisions of Highly Charged Ions with Au and Cu Surfaces," Bull. Am. Phys. Soc. 33, 933 (Apr. 1988)

Sataka, M., S. Ohtani, D. Swenson, and D. C. Gregory
"Electron Impact Ionization of Chromium Ions," Bull. Am. Phys. Soc. 33, 939 (Apr. 1988)

Schoene, H., S. Datz, P. F. Dittner, Q. C. Kessel, H. F. Krause, J. K. Swenson, and C. R. Vane
"Zero Degree Electron Spectroscopy in Coincidence with Projectile Charge State in 10-MeV $C(q^+)$-Ne Collisions," Bull. Am. Phys. Soc. 33, 921 (Apr. 1988)

Schulz, M., R. Schuch, S. Datz, E.L.B. Justiniano, P. D. Miller, and H. Schone
"RTE Observed in F^{6+} - H_2 Collisions by X-Ray Coincidences," Bull. Am. Phys. Soc. 33, 1054 (Apr. 1988)

Sellin, I. A., J. Kemmler, O. Heil, C. Biedermann, H. Rothard, K. Kroneberger, and K. O. Groneveld
"Enhanced Transport Length for Convoy Electrons Produced by 15.6 MeV/u Ni Ions in C Targets Observed in Coincidence with Emergent Projectile Charge," Bull. Am. Phys. Soc. 33, 1055 (Apr. 1988)

Swenson, J. K., D. C. Griffin, C. C. Havener, M. S. Huq, F. W. Meyer, R. A. Phaneuf, and N. Stolterfoht
"Spectroscopy of Low Energy Collisions of O^{6+} with He, Ne, and H_2," Bull. Am. Phys. Soc. 33, 1003 (Apr. 1988)

Underwood, T. A., M. Breinig, C. C. Gaither, and J. Freyou
"Measurement of Cross Sections for Cusp Electron Production in Single Ionization and Transfer Ionization Events for .1 MeV/u I^{+13} Incident on He and H_2 Gases," Bull. Am. Phys. Soc. 33, 1054 (Apr. 1988)

Vane, R., S. Raman, S. Kahane, T. Rosseel, S. Stewart, and T. Walkiewicz
"Chemical Sensitivities of Heavy-Ion-Induced X-Rays from Al Compounds and Alloys," Bull. Am. Phys. Soc. 33, 1004 (Apr. 1988)

Wang, J., and J. Burgdorfer
" 'v/2' Electron Emission in Ion-Atom Collisions with Short-Ranged Potentials," Bull. Am. Phys. Soc. 33, 1055 (Apr. 1988)

American Physical Society Meeting, Baltimore, Maryland, April 18-21, 1988

Beene, J. R. (Invited Talk)
"Gamma Decay Studies of Isovector Giant Resonances," Bull. Am. Phys. Soc. 33, 957 (Apr. 1988)

D'Onofrio, A., J. Gomez del Campo, R. L. Auble, J. R. Beene, M. L. Halbert, H. J. Kim, and J. L Charvet
"Population of Excited States of Complex Fragments Emitted in Collisions of 630-MeV ^{56}Ni on ^{58}Ni," Bull. Am. Phys. Soc. 33, 928 (Apr. 1988)

Gomez del Campo, J., R. L. Auble, J. R. Beene, M. L. Halbert, H. J. Kim, J. L. Charvet, and A. D'Onofrio
"Study of Complex Fragments Emitted in Collisions of ^{58}Ni + ^{58}Ni at 11 MeV/Nucleon," Bull. Am. Phys. Soc. 33, 928 (Apr. 1988)

Gross, E. E., D. C. Hensley, J. R. Beene, F. E. Bertrand, M. L. Halbert, G. Vourvopoulos, T. VanCleve, and D. L. Humphrey
"E2 and E4 Matrix Elements for ^{24}Mg from HI Inelastic Scattering," Bull. Am. Phys. Soc. 33, 929 (Apr. 1988)

Johnson, C. H., and C. Mahaux
"Unified Description of the Neutron-^{40}Ca Mean Field for $-80 < E < 80$ MeV," Bull. Am. Phys. Soc. 33, 964 (Apr. 1988)

Kim, H. J., J. Gomez del Campo, M. Hindi, D. Shapira, and P. H. Stelson
"Transfer Reactions for the ^{50}Ti + ^{90}Zr System below the Coulomb Barrier," Bull. Am. Phys. Soc. 33, 1021 (Apr. 1988)

Lisantti, J., F. E. Bertrand, D. J. Horen, B. L. Burks, C. W. Glover, D. K. McDaniels, L. W. Swenson, X. Y. Chen, O. Hausser, and K. Hicks
"Excitation of Giant Resonances in ^{28}Si with 250 MeV Protons," Bull. Am. Phys. Soc. 33, 962 (Apr. 1988)

Lord, R. S., and D. K. Olsen
"Three Dimensional Design of the HISTRAP Prototype Dipole Magnet," Bull. Am. Phys. Soc. 33, 1027 (Apr. 1988)

Penumetcha, V., C. Butler, G. A. Petitt, T. C. Awes, J. R. Beene, R. L. Ferguson, F. E. Obenshain, F. Plasil, S. Sorensen, and G. R. Young
"Mass, Charge, and Excitation Energy Distributions for Heavy Fragments in Strongly Damped Reactions ^{58}Ni + ^{165}Ho at 16 MeV/amu," Bull. Am. Phys. Soc. 33 927 (Apr. 1988)

Saini, S., T. C. Awes, F. E. Obenshain, F. Plasil, D. Shapira, G. R. Young, V. Penumetcha, G. A. Petitt, and G. Nasreen
"Neutron-Neutron and Neutron-Light Ion Correlations in the Reaction ^{32}S + ^{197}Au at 21.9 MeV/Nucleon," Bull. Am. Phys. Soc. 33, 978 (Apr. 1988)

Shivakumar, B., and D. Shapira
"Orbiting Phenomena in Heavy Ion Reactions," Bull. Am. Phys. Soc. 33, 928 (Apr. 1988)

Thompson, J. S., D. J. Pegg, R. N. Compton, and G. D. Alton
"Photoelectron Spectroscopy of Ca$^-$," Bull. Am. Phys. Soc. 33, 1036 (Apr. 1988)

Varner, R. L., J. R. Beene, R. L. Auble, F. E. Bertrand, M. L. Halbert, D. C. Hensley, D. J. Horen, R. L. Robinson, and R. O. Sayer
"Photon Decay Studies in ^{90}Zr and ^{209}Bi," Bull. Am. Phys. Soc. 33, 978 (Apr. 1988)

Wells, J. C., N. R. Johnson, A. Virtanen, M. A. Riley, C. Baktash, I-Y. Lee, and F. K. McGowan
"Gamma-Ray Measurements on High-Spin States of ^{172}Os," Bull. Am. Phys. Soc. 33, 981 (Apr. 1988)

Winters, R. R., and C. H. Johnson
"Evidence for Shell Dependence of the Imaginary Part of the Neutron Optical Potential," Bull. Am. Phys. Soc. 33, 1061 (Apr. 1988)

IAEA Specialists' Meeting on Carbon and Oxygen Collision Data for Fusion Plasma Research, Vienna, Austria, May 12-13, 1988

Phaneuf, R. A., P. Defrance, D. C. Griffin, Y. Hahn, M. S. Pindzola, L. Roszman, and W. Wiese
"IAEA Specialists' Meeting on Carbon and Oxygen Collision Data for Fusion Plasma Research"

3rd Conference on the Intersections Between Particle and Nuclear Physics, Rockport, Maine, May 14-19, 1988

Close, F. E. (Invited Talk)
"The Nuclear Dependence of Parton Distributions"

Topical Conference on Nuclear Chromodynamics, Argonne, Illinois, May 19-21, 1988

Close, F. E. (Invited Talk)
"The Nuclear Dependence of Parton Distributions"

International Conference on Medium- and High-Energy Nuclear Physics, Taipei, Taiwan, May 23-27, 1988

Wong, C. Y. (Invited Talk)
"Origin of Anomalous Positron Peaks in Heavy-Ion Reactions"

Wong, C. Y., and Z. D. Lu (Invited Talk)
"The Dynamics of High-Energy Nucleus-Nucleus Collisions"

International Conference on Nuclear Data for Science and Technology, May 30-June 3, 1988, Mito, Japan

Raman, S. (Invited Talk)
"Validity Between Direct and Compound Nuclear Models of Slow Neutron Capture"

Workshop on Heavy-Ion Interactions Around the Coulomb Barrier, Legnaro, Italy, June 1-4, 1988

Kim, H. J. (Invited Paper)
"Transfer Reactions for the ^{50}Ti + ^{90}Zr System below the Coulomb Barrier"

Seventh International Conference on Ion Implantation Technology, Kyoto, Japan, June 6-10, 1988

Alton, G. D. (Invited Talk)
"The Sputter Generation of Negative Ion Beams"

Alton, G. D., Y. Mori, A. Takagi, A. Ueno, and S. Fukumoto
"A High-Brightness, Plasma-Sputter Negative Ion Source"

13th International Conference on Neutrino Physics and Astrophysics, Boston, Massachusetts, June 5-11, 1988

Close, F. E. (Invited Talk)
"The Parton Distributions in Nuclei and in Polarized Nucleons"

Symposium on On-Line Mass Separators, Radioactive Beams, and Nuclei Far from Stability, American Chemical Society Meeting, Toronto, Canada, June 6-11, 1988

Toth, K. S. (Invited Talk)
"Investigation of Alpha-Particle and Delayed-Proton Decays at and near Closed Shells"

Third International Conference on Nucleus-Nucleus Collisions, St. Malo, France, June 6-11, 1988

Awes, T. C., Z. Chen, R. L. Ferguson, C. K. Gelbke, W. G. Lynch, F. E. Obenshain, F. Plasil, J. Pochodzalla, S. Pratt, H. M. Xu, and G. R. Young
"Extended Emission Sources Observed via Two-Proton Correlations"

Bertrand, F. E., J. R. Beene, and D. J. Horen (Invited Talk)
"Excitation and Photon Decay of Giant Multipole Resonances — The Role and Future of Medium-Energy Heavy Ions"

Bracco, A., J. R. Beene, N. Van Giai, P. F. Bortignon, F. Zardi, and R. A. Broglia
"Direct Neutron Decay from the Giant Monopole Resonance in ^{208}Pb"

Kim, H. J., K. S. Toth, and J. W. McConnell
"Alpha-Particle Decay Studies Near N = 130 with the Use of a Velocity Filter"

Morsch, H. P., W. Spang, J. R. Beene, F. E. Bertrand, R. L. Auble, M. L. Halbert, D. C. Hensley, R. L. Varner, D. G. Sarantites, and D. W. Stracener
"Observation of Temperature Narrowing in the Giant Dipole Resonance Decay of Hot Nuclei and Nuclear Shapes at High T"

Obenshain, F. E.
"Nuclear Stopping in Oxygen-Induced Reactions at 200 A GeV"

European Particle Accelerator Conference, Rome, Italy, June 7-11, 1988

Read, P. M., J. T. Maskrey, and G. D. Alton
"Development of a Lithium Liquid Metal Ion Source for MeV Ion Beam Analysis"

Wolf, A., H. Poth, W. Schwab, B. Seligmann, M. Wortge, P. F. Dittner, H. Haseroth, C. E. Hill, J. L. Vallet, S. Baird, M. Chanel, P. Lefevre, R. Ley, D. Manglunki, D. Mohl, G. Molinari, and G. Tranquille
"Results from Electron Cooling Experiments at LEAR"

International Conference on Contemporary Topics in Nuclear Structure, Cocoyoc, Mexico, June 9-14, 1988

Baktash, C. (Invited Talk), Session Chairman Commentary
"Understanding the Structure of Nuclei at Finite Temperatures"

Dudek, J. (Invited Talk)
"From the Secrets of Nuclear Shapes into Quantum Nuclear Physics"

Symposium on Future Polarization at Fermilab, Batavia, Illinois, June 13-14, 1988

Close, F. E. (Invited Talk)
"Where Next in Polarized Leptoproduction?"

XIXth International Symposium on Multiparticle Dynamics — New Data and Theoretical Trends, Arles, France, June 13-17, 1988

Obenshain, F. E., Albrecht, R., T. C. Awes, C. Baktash, P. Beckmann, F. Berger, R. Bock, G. Claesson, L. Dragon, R. L. Ferguson, A. Franz, S. Garpman, R. Glasow, H. A. Gustafsson, H. H. Gutbrod, K. H. Kampert, B. W. Kolb, P. Kristiansson, I. Y. Lee, H. Loehner, I. Lund, A. Oskarsson, I. Otterlund, T. Peitzmann, S. Persson, F. Plasil, A. M. Poskanzer, M. Purschke, H. G. Ritter, R. Santo, H. R. Schmidt, T. Siemiarczuk, S. P. Sorensen, E. Stenlund, and G. R. Young
"Nuclear Stopping in Oxygen-Induced Reactions at 200 A GeV"

IX International Seminar on High-Energy Physics Problems — Relativistic Nuclear Physics and Quantum Chromodynamics, Dubna, U.S.S.R., June 14-19, 1988

Loehner, H., R. Albrecht, T. C. Awes, C. Baktash, P. Beckmann, F. Berger, R. Bock, G. Claesson, L. Dragon, R. L. Ferguson, A. Franz, S. Garpman, R. Glasow, H. A. Gustafsson, H. H. Gutbrod, K. H. Kampert, B. W. Kolb, P. Kristiansson, I. Y. Lee, I. Lund, F. E. Obenshain, A. Oskarsson, I. Otterlund, T. Peitzmann, S. Persson, F. Plasil, A. M. Poskanzer, M. Purschke, H. G. Ritter, R. Santo, H. R. Schmidt, T. Siemiarczuk, S. P. Sorensen, E. Stenlund, and G. R. Young (Invited Talk)
"Momentum Distributions of Neutral Pions in Heavy-Ion Reactions at the CERN-SPS"

American Physical Society Joint Meeting with the Canadian Association of Physicists, Montreal, Canada, June 20-22, 1988

Dittner, P. F. (Invited Talk)
"Dielectronic Recombination Measurements of Multiply Charged Ions," Bull. Am. Phys. Soc. 33, 1205 (May 1988)

Phaneuf, R. A. (Invited Talk)
"Electron Impact Ionization of Highly Charged Ions," Bull. Am. Phys. Soc. 33, 1205 (May 1988)

CEBAF 1988 Summer Workshop, Newport News, Virginia, June 20-24, 1988

Close, F. E. (Invited Talk)
"Resonance Photo and Electroproduction as a Probe of QCD"

First European Workshop on Hadronic Physics in the 1990's with Multi-GeV Electrons, Seillac, France, June 27-July 1, 1988

Close, F. E. (Invited Talk)
"Testing QCD with Milli-TeV Electrons"

Eleventh International Conference on Atomic Physics (ELICAP), Paris, France, July 4-8, 1988

Burgdorfer, J., and C. Bottcher
"Regular and Stochastic Motion of Rydberg Electrons in Solids"

Levin, J. C., C.-S. O, H. Cederquist, C. Biederman, and I. A. Sellin
"Argon Recoil-Ion Charge-State Distributions Produced by Beams of 23 MeV $Cl^{5+,8+,10+}$"

International Symposium on Heavy Ion Physics and Nuclear Astrophysical Problems, Tokyo, Japan, July 21-23, 1988

Halbert, M. L., R. L. Auble, J. R. Beene, F. E. Bertrand, B. L. Burks, J. Gomez del Campo, D. C. Hensley, D. J. Horen, J. Lisantti, R. L. Robinson, R. O. Sayer, R. L. Varner, W. Mittig, Y. Schutz, B. Haas, J.-P. Vivien, N. Alamanos, F. Auger, J. Barrette, B. Fernandez, A. Gillibert, and A. M. Nathan
"Gamma Decay of Giant Resonaces Excited by Heavy Ions"

Fifth International Conference on Clustering Aspects in Nuclear and Subnuclear Systems, Kyoto, Japan, July 25-29, 1988

Shapira, D. (Invited Talk)
"Nuclear Orbiting"

Wong, C. Y.
"Condensation of (e^+e^-) Due to Short-Range, Non-Central Attractive Forces"

Wong, C. Y.
"Interaction of a Neutral Composite Particle with a Strong Coulomb Field"

International Symposium on Heavy-Ion Reaction Dynamics in Tandem Energy Region, Hitachi, Japan, August 1-3, 1988

Halbert, M. L., J. R. Beene, D. C. Hensley, K. Honkanen, T. M. Semkow, V. Abenante, D. G. Sarantites, and Z. Li (Invited Talk)
"Angular Momentum Effects in Subbarrier Fusion"

Kim, H. J., J. Gomez del Campo, D. Shapira, and P. H. Stelson
"Transfer Reactions for the $^{50}Ti + ^{90}Zr$ System"

American Physical Society Meeting, Storrs, Connecticut, August 15-18, 1988

Close, F. E. (Invited Talk)
"Light Quark Spectroscopy"

BNL Workshop on Glueballs, Hybrids, and Exotics, Upton, New York, August 29-September 1, 1988

Close, F. E. (Invited Talk)
"Exotic Mesons"

Workshop on On-Line Nuclear Orientation and Related Topics, Oxford, England, August 31-September 4, 1988

Girit, I. C., G. D. Alton, C. R. Bingham, H. K. Carter, M. L. Simpson, J. D. Cole, J. H. Hamilton, E. A. Jones, H. Xie, B. D. Kern, K. S. Krane, P. F. Mantica, Jr., W. B. Newbolt, and E. F. Zganjar
"The UNISOR On-Line Nuclear Orientation Facility"

International Conference on the Physics of Multiply Charged Ions, Grenoble, France, September 12-16, 1988

Havener, C. C. (Invited Talk)
"Electron Capture by Multicharged Ions at eV Energies"

Meyer, F. W. (Invited Talk)
"Multicharged Ions as Probes of Surfaces"

Swenson, J. K., C. Bottcher, C. C. Havener, N. Stolterfoht, and F. W. Meyer (Invited Talk)
"Observation of Strong Asymmetry in the Emission of Autoionization Electrons at 0° and 180° Following 10 keV He^+ + He Collisions"

Spin 88 Conference, Minneapolis, Minnesota, September 12-17, 1988

Close, F. E. (Invited Talk)
"Where is the Proton's Spin?"

Seventh International Workshop on Inelastic Ion Surface Collisions, Krakow, Poland, September 19-23, 1988

Havener, C. C. (Invited Talk)
"Interaction of Multicharged Ions with Solid Surfaces"

ACS Symposium on The Interface Between Nuclear Structure and Reactions, Los Angeles, California, September 26-29, 1988

Beene, J. R. (Invited Talk)
"Gamma Decay Studies of Giant Resonances"

Seventh International Conference on Ultrarelativistic Nucleus-Nucleus Collisions, Lenox, Massachusetts, September 26-30, 1988

Awes, T. C., and S. P. Sorensen (Invited Talk)
"Report on the Oak Ridge Workshop on Monte Carlo Codes for Relativistic Heavy-Ion Collisions"

Peitzmann, T., Albrecht, R., T. C. Awes, C. Baktash, P. Beckmann, F. Berger, R. Bock, G. Claesson, G. Clewing, L. Dragon, A. Eklund, R. L. Ferguson, A. Franz, S. Garpman, R. Glasow, H. A. Gustafsson, H. H. Gutbrod, J. Idh, K. H. Kampert, B. W. Kolb, P. Kristiansson, I. Y. Lee, H. Loehner, I. Lund, F. E. Obenshain, A. Oskarsson, I. Otterlund, S. Persson, F. Plasil, A. M. Poskanzer, M. Purschke, H. G. Ritter, R. Santo, H. R. Schmidt, T. Siemiarczuk, S. P. Sorensen, E. Stenlund, and G. R. Young
"Correlations of Neutral Pions in Ultrarelativistic Heavy Ion Collisions"

Wong, C. Y., and Z. D. Lu
"Nuclear Stopping Power in High-Energy Nucleus-Nucleus Collisions"

12. GENERAL INFORMATION

PERSONNEL CHANGES

New Staff Members

A. Scientific Staff

F. E. Close, UT/ORNL Distinguished Scientist, Rutherford Appleton Laboratory, Chilton, England
J. D. Garrett, Niels Bohr Institute, Copenhagen, Denmark
J. H. Macek, UT/ORNL Distinguished Scientist, University of Nebraska, Lincoln, Nebraska
B. A. Tatum, Tennessee Technological University, Cookeville, Tennessee

B. Administrative and Technical Staff

F. P. Ervin, Secretary (transferred from Instrumentation and Controls Division)
B. K. Sizemore, Accelerator Operations
S. D. Taylor, Accelerator Operations

Staff Transfers and Terminations

A. Scientific Staff

C. H. Johnson (retirement)
P. D. Miller, Jr. (retirement)
P. L. Pepmiller (present address: Harvard Medical School, Cambridge, Massachusetts)

B. Administrative and Technical Staff

C. A. Maples, Accelerator Operations (transferred to Metals and Ceramics Division)
R. T. Webber, Secretary (transferred to Central Waste Management Offices)

Temporary Assignments

A. Visiting Scientists

Z. Lu, Institute of Atomic Energy, Beijing, People's Republic of China
M. Sataka, Japan Atomic Energy Research Institute, Tokai-mura, Naka-gun, Ibaraki-ken, Japan
R. Wang, University of Science and Technology of China, Hefei, Anhui, People's Republic of China

B. ORAU Faculty Research Participants

C. A. Bennett, Jr., University of North Carolina, Asheville, North Carolina
W. G. Nettles, Mississippi College, Clinton, Mississippi
T. A. Walkiewicz, Edinboro University of Pennsylvania, Edinboro, Pennsylvania
G. D. White, Northwestern State University, Natchitoches, Louisiana
L. F. Zganjar, Louisiana State University, Baton Rouge, Louisiana

C. Postdoctoral Research Associates

A. D'Onofrio, National Institute of Nuclear Physics, Naples, Italy
Y. M. Fockedey, Catholic University of Louvain, Louvain-la-Neuve, Belgium
J. C. Levin, University of Tennessee, Knoxville, Tennessee
J. E. Lisantti, TRIUMF, University of British Columbia, Vancouver, Canada
A. Ray, University of Tennessee, Knoxville, Tennessee
M. A. Riley, Niels Bohr Institute, Roskilde, Denmark
S. Saini, University of Pennsylvania, Philadelphia, Pennsylvania
M. Schulz, Heidelberg University, Heidelberg, West Germany
K. M. Teh, Vanderbilt University, Nashville, Tennessee
U. Thumm, Freiburg University, Freiburg, West Germany
M. L. Tincknell, Lawrence Berkeley Laboratory, Berkeley, California
A. J. A. Virtanen, University of Jyvaskyla, Jyvaskyla, Finland
J. P. Wieleczko, Commissariat a l'Energie Atomique, Gif-sur-Yvette Cedex, France
J. Wu, University of Tennessee, Knoxville, Tennessee

D. ORAU Postgraduate Research Training Program

G. J. Bottrell, University of Georgia, Athens, Georgia
J. P. Giese, Kansas State University, Manhattan, Kansas
M. S. Huq, College of William and Mary, Williamsburg, Virginia
J. K. Swenson, University of North Carolina, Chapel Hill, North Carolina

E. Graduate Students

H. V. Carmichael, University of Tennessee, Knoxville, Tennessee
M. P. Carpenter, University of Tennessee, Knoxville, Tennessee
R. L. Clark, Vanderbilt University, Nashville, Tennessee
J. Dellwo, University of Tennessee, Knoxville, Tennessee
L. K. Fletcher, Tennessee Technological University, Cookeville, Tennessee
J. E. Freyou, University of Tennessee, Knoxville, Tennessee
C. C. Gaither, University of Tennessee, Knoxville, Tennessee
J. P. Gibbons, University of Tennessee, Knoxville, Tennessee
R. C. Hunt, University of Tennessee, Knoxville, Tennessee
Y-r. Jiang, Vanderbilt University, Nashville, Tennessee
H. Jin, University of Tennessee, Knoxville, Tennessee
E. F. Jones, Vanderbilt University, Nashville, Tennessee
R. W. Kincaid, University of Tennessee, Knoxville, Tennessee
M. Korolija, Ruder Boskovic Institute, Croatia, Yugoslavia
S. E. Lasley, University of Tennessee, Knoxville, Tennessee
X. T. Liu, University of Tennessee, Knoxville, Tennessee
J. Mueller, University of Tennessee, Knoxville, Tennessee
J. D. Richards, University of Tennessee, Knoxville, Tennessee
H. Schone, University of Frankfurt, Frankfurt, West Germany
J. Y. Shea, Vanderbilt University, Nashville, Tennessee
J. S. Thompson, University of Tennessee, Knoxville, Tennessee
T. A. Underwood, University of Tennessee, Knoxville, Tennessee
H. Xie, Vanderbilt University, Nashville, Tennessee
Y-s. Xu, Oregon State University, Corvallis, Oregon
S. Zhu, Vanderbilt University, Nashville, Tennessee

F. ORAU Graduate Research Participants

D. J. Dear, Vanderbilt University, Nashville, Tennessee
M. P. Metlay, University of Pittsburgh, Pittsburgh, Pennsylvania

G. Joint Institute for Heavy Ion Research

K. H. Bhatt, Western Kentucky University, Bowling Green, Kentucky
J. Dudek, Centre de Recherches Nucleaires, Strasbourg, France
W-B. Gao, Vanderbilt University, Nashville, Tennessee
G. J. Garcia-Bermudez, Comision Nacional de Energia Atomica, Buenos Aires, Argentina
J. J. Griffin, University of Maryland, College Park, Maryland
X-L. Han, Jilin University, Changchun, People's Republic of China
S. Kahane, Nuclear Research Center-Negev, Beer Sheva, Israel
L. J. Lantto, University of Oulu, Oulu, Finland
I. Lund, CERN, Geneva, Switzerland
N. B. Neskovic, Boris Kidric Institute of Nuclear Sciences, Belgrade, Yugoslavia
D. Rentsch, University of Giessen, Giessen, West Germany
W-D. Schmidt-Ott, University of Gottingen, Gottingen, West Germany
M. L-A. Soyeur, Commissariat a l'Energie Atomique, Gif-sur-Yvette Cedex, France
J. Wang, Lanzhou University, Lanzhou, People's Republic of China
C-L. Wu, Jilin University, Changchun, People's Republic of China
X. Yang, Institute of Atomic Energy, Beijing, People's Republic of China
J. Y. Zhang, Lanzhou University and Institute of Modern Physics, Lanzhou, People's Republic of China
L. Zhou, Institute of Atomic Energy, Beijing, People's Republic of China

H. ORAU Student Research Participants

G. J. Baker, Southern Methodist University, Dallas, Texas
M. D. Hipshire, University of Tennessee, Knoxville, Tennessee

I. Oak Ridge Science and Engineering Research Semester (ORSERS) Participants

K. A. Childress, Whitworth College, Spokane, Washington
S. M. Sipe, Anderson College, Anderson, Indiana
C. M. Steele, Georgia Southern College, Statesboro, Georgia
R. T. VanHook, Hendrix College, Conway, Arkansas

J. Great Lakes College Association Science Program

A. M. Calabrese, Depauw University, Greencastle, Indiana
S. T. Churchwell, Earlham College, Richmond, Indiana
R. L. Kehoe, Earlham College, Richmond, Indiana
S. S. McWilliams, Earlham College, Richmond, Indiana
M. P. Nesnidal, Lawrence University, Appleton, Wisconsin
B. J. Vartanian, Albion College, Albion, Michigan

K. Great Lakes College Association Faculty Participant

R. R. Winters, Denison University, Granville, Ohio

Summer Assignments

A. ORAU STRIVE Participants

A. J. Domkowski, Webb School of Knoxville, Knoxville, Tennessee
E. M. Wike, Hillsboro High School, Nashville, Tennessee

B. ORAU Professional Internship

D. H. Olive, Jr., Vanderbilt University, Nashville, Tennessee

C. University of Tennessee/ORNL Science Alliance Undergraduate Program

P. K. Card, Hendrix College, Conway, Arkansas
J. M. Gaines, Rhodes College, Memphis, Tennessee
G. M. Howard, Middle Tennessee State University, Murfreesboro, Tennessee
R. C. Hunt, Western Carolina University, Cullowhee, North Carolina
T. E. Huston, Hendrix College, Conway, Arkansas
L. E. Kidder, Drake University, Des Moines, Iowa
E. M. Lowndes, University of Illinois at Urbana-Champaign, Urbana, Illinois
J. S. McCarley, Georgia Institute of Technology, Atlanta, Georgia
S. Naguleswaran, Hanover College, Hanover, Indiana
L. Norman, The Evergreen State College, Olympia, Washington
J. W. Sedler, University of Maryland, College Park, Maryland
S. M. Sipe, Anderson College, Anderson, Indiana

PHYSICS DIVISION SEMINARS: OCTOBER 1987-SEPTEMBER 1988

Seminars arranged by the Physics Division and announced in the ORNL Technical Calendar are listed below. During the period of this report, Terry C. Awes (October 1987) and Edward E. Gross (November 1987-September 1988) served as Seminar Chairmen.

Date	Speaker	Title
1987		
Oct. 6	Shunzo Kumano University of Illinois Urbana, Illinois	"Meson Decay in the Flux Tube Model"
Oct. 8	Carl M. Shakin Brooklyn College of the CUNY Brooklyn, New York	"Condensed Matter Dynamics in Nuclear and Particle Physics"
	Ulrich Brosa Philipps-Universitat Marburg Marburg Federal Republic of Germany	"Fission of the Actinides"
	E. Salzborn Justus-Liebig Universität Giessen Federal Republic of Germany	"Ion-Ion Collisions: Recent Experimental Results for $He^+ + He^+$, $Bi^+ + Bi^+$, $H^+ + H^-$, and $Cs^+ + H^-$"
Oct. 22	Michel Baranger Massachusetts Institute of Technology Cambridge, Massachusetts	"The New Classical Mechanics: Is There a Quantum Equivalent?"
Oct. 29	Tom Humanic GSI, Darmstadt Federal Republic of Germany	"Ultrarelativistic Heavy-Ion Collisions at 200 GeV/A at the CERN SPS"
Oct. 30	Mitsuru Tohyama National Superconducting Cyclotron Laboratory Michigan State University East Lansing, Michigan	"Applications of Quantum Theory of Two-Body Collisions"
Nov. 5	Friedrich Donau ZFK Rossendorf, East Germany	"Spin Orientation in Deformation"
Nov. 12	Y. Sharon Princeton University Princeton, New Jersey	"Analysis of High-Angular-Momentum Yrast States in Even-Even Actinides"
Nov. 17	Daniel R. Bes Comisión Nacional de Energia Atómica Buenos Aires, Argentina	"Gauge Methods in Nuclear Physics"
Nov. 20	M. Sekiguchi Institute for Nuclear Study University of Tokyo, Japan	"Status of the TARN II Project"
Nov. 23	Craig L. Woody Brookhaven National Laboratory Upton, New York	"High-Rate E.M. Calorimetry with BaF_2 Detectors"
Dec. 10	Michael J. Saltmarsh Fusion Energy Division, ORNL	"ORNL's Role in the Fusion Energy Program"

Date	Speaker	Title
1987		
Dec. 17	Da H. Feng Drexel University Philadelphia, Pennsylvania	"Symmetry-Dictated Pauli Effects and the Solution of E2-Collectivity"
1988		
Jan. 14	Dave K. Christen Solid State Division, ORNL	"High-Temperature Oxide Superconductors"
Jan. 18	Dieter Schneider Lawrence Livermore National Laboratory, Livermore, California	"Electron Spectra Measured in the Forward Direction in Ion-Atom Collisions"
Jan. 28	Walter Greiner Frankfurt University, Federal Republic of Germany	"Nuclear Equation of State from Relativistic Heavy Ion Collisions"
Feb. 11	John G. Cramer, Jr. University of Washington Seattle, Washington	"Transactional Interpretation of Quantum Mechanics"
Feb. 25	Gary T. Alley Instrumentation and Controls Division, ORNL	"Recent Developments in Very Large Scale Integrated Circuits"
Mar. 3	Keh-Fei Liu University of Kentucky Lexington, Kentucky	"Role of Binding Energy in the EMC Effect"
Mar. 4	Ivo Slaus Institute Ruder Boskovic Zagreb, Yugoslavia	"Violation of Charge Symmetry"
Mar. 10	Roscoe E. Marrs Lawrence Livermore National Laboratory, Livermore, California	"Studies of Highly Charged Ions in the Electron-Beam Ion Trap at Lawrence Livermore Laboratory"
Mar. 24	G. Claesson Lund University, Lund, Sweden	"Results from WA80 at CERN: Charged-Particle Distributions"
Apr. 7	Edward R. Flynn Los Alamos National Laboratory Los Alamos, New Mexico	Measurement of Magnetic Fields in the Human Brain"
Apr. 11	Manuel Menendez University of Georgia Athens, Georgia	"Electron Dynamics Near the Line Joining Two Coulombic Centers"
Apr. 14	Avi Gover Science Applications International Corporation, McLean, Virginia	"High-Power Electrostatic Accelerator Free-Electron Lasers—Fusion and Other Applications"
Apr. 28	S. Raman Division Staff Member	"Quantulumcunque—Concerning B(E2) Values"
Apr. 29	Michael Thoennessen State University of New York Stony Brook, New York	"Giant Dipole Gamma-Fission Angular Correlation in Excited Heavy Nuclei"
May 6	Reinhold Mann Engineering Physics and Mathematics Division, ORNL	"Intelligent Sensor Systems for Mobile Robots"
May 12	Ralph M. Moon, Jr. Solid State Division, ORNL	"Scientific Opportunities with the Advanced Neutron Facility"

Date	Speaker	Title
1988		
May 19	Rudi Malfliet KVI, Groningen, The Netherlands	"Dirac-Brueckner Approach to Nuclear Matter in Equilibrium and Nonequilibrium"
May 19	Samuel H. Aronson Brookhaven National Laboratory Upton, New York	"Experimental Status of the 5th Force"
May 26	Timothy J. P. Ellison Indiana University Cyclotron Facility, Bloomington, Indiana	"Status Report on the IUCF Cooler Ring"
June 1	Fred E. Bertrand Division Staff Member	"Heavy-Ion Excitation and Photon Decay of Giant Resonances"
June 2	Michael Nitschke Lawrence Berkeley Laboratory Berkeley, California	"Beta-Delayed Proton Decay in the Lanthanide Region"
June 9	Richard C. Durfee Computing and Telecommunications Division, Martin Marietta Energy Systems, Inc.	"Geographic Information Systems Technology and Spatial Modeling"
July 14	Dietrich Pelte University of Heidelberg Federal Republic of Germany	"Investigations of Multifragmentation Processes in Heavy-Ion Collisions"
July 21	Volker Metag University of Giessen Federal Republic of Germany	"High-Energy Photons and Neutral Mesons: Sensitive Probes of Reaction Dynamics in Heavy-Ion Collisions"
Aug. 5	Thomas Weber Institute for Nuclear Physics Giessen, Federal Republic of Germany	"Recent Results of the $^{235,238}U(e,e'f)$ Coincidence Experiments"
Aug. 9	R. F. Bishop University of Manchester, England	"Extended Coupled Cluster Theory: Quantum Many-Body Theory Made Classical"
Aug. 11	J. P. Coffin Centre de Recherche Nucleaire Strasbourg, France	"Prompt and Delayed Charged-Particle Emission from Heavy-Ion Collisions Near the Fermi Energy (~27 MeV per nucleon)"
Aug. 18	Kumar Bhatt Western Kentucky University Bowling Green, Kentucky	"How and Where Are Single Words Processed in the Brain"
Aug. 25	Wolf D. Schmitt-Ott University of Gottingen Federal Republic of Germany	"Neutron-Rich Isotopes Produced in Fragmentation Reactions at GANIL"
Sept. 7	Alan Harmon Lawrence Berkeley Laboratory Berkeley, California	"Observation of Constant Average Angular Momentum in Subbarrier Fusion"
Sept. 15	David J. Pegg Division Staff Member and University of Tennessee	"Photo Detachment of Negative Ions"
Sept. 29	Jerry Garrett Division Staff Member	"Why a Rotating Nucleus Shrinks"

SCIENTIFIC MEETINGS HELD DURING THIS PERIOD

Workshop on the Proposal for a National Gamma-Ray Detector Facility
Oak Ridge, Tennessee, November 19-21, 1987

N. R. Johnson, organizer

Computational Atomic and Nuclear Physics at One Gigaflop
Oak Ridge, Tennessee, April 14-16, 1988

J. B. McGrory, M. R. Strayer, and C. Bottcher, organizers

Workshop on High-Energy Nuclear Collision Monte Carlo Codes

Oak Ridge, Tennessee, September 12-23, 1988

S. P. Sorensen and T. C. Awes, organizers

PHYSICS DIVISION

OCTOBER

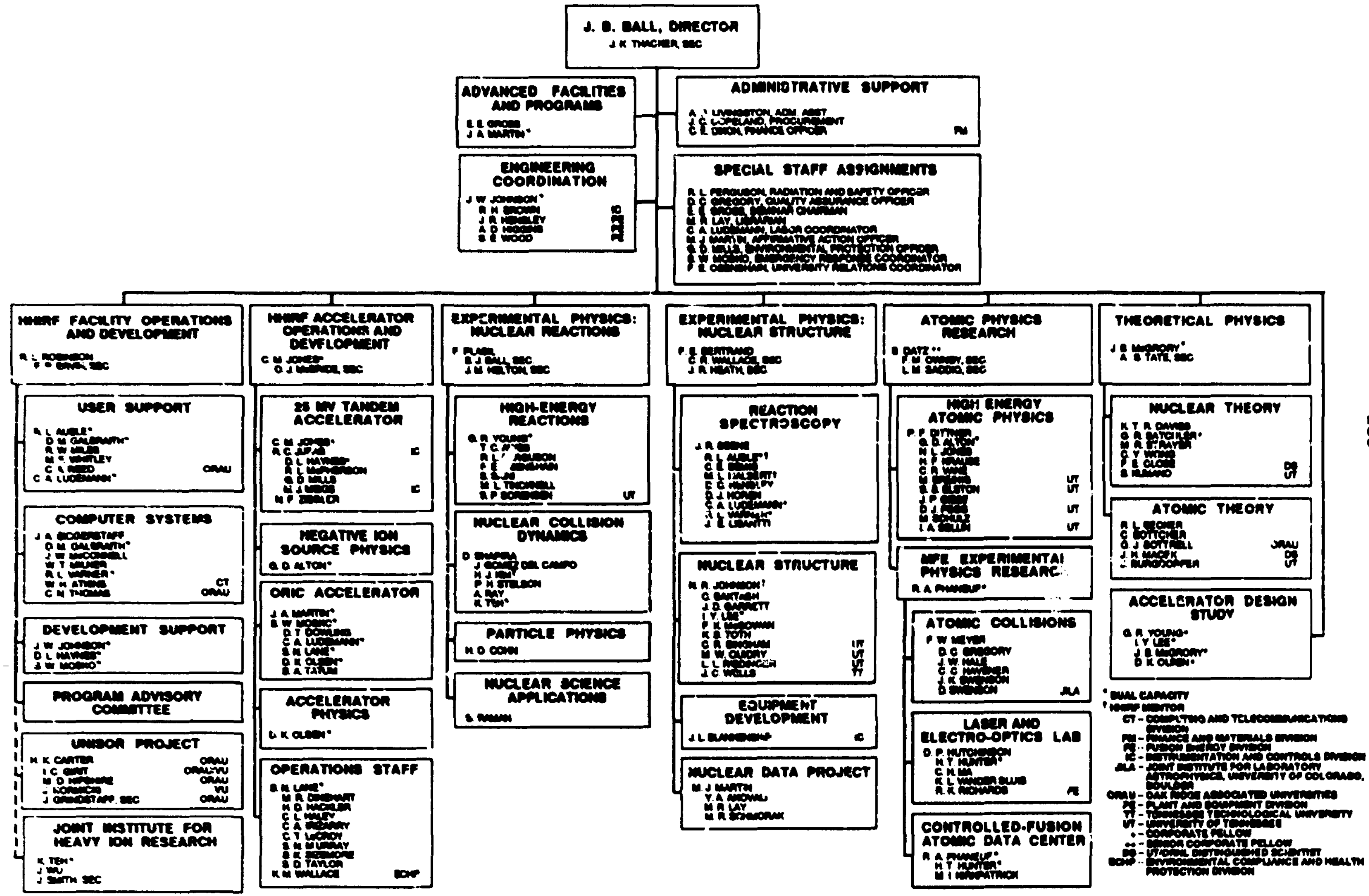

ORNL-6508
Distribution Category
UC-410

INTERNAL DISTRIBUTION

1. E. D. Aebischer
2. Y. A. Akovali
3. G. D. Alton
4. T. D. Anderson
5. B. R. Appleton
6. R. L. Auble
7. T. C. Awes
8. C. Baktash
9-170. J. B. Ball
171. S. J. Ball
172. C. F. Barnett
173. R. L. Becker
174. M. Beckerman
175. J. R. Beene
176. C. E. Bemis, Jr.
177. F. E. Bertrand
178. J. A. Biggerstaff
179. C. R. Bingham
180. Biology Library
181. C. Bottcher
182. H. R. Brashear
183. M. Breinig
184. J. Burgdorfer
185. H. K. Carter
186-187. Central Research Library
188. F. E. Close
189. H. O. Cohn
190. S. Datz
191. K. T. R. Davies
192. P. F. Dittner
193. D. T. Dowling
194. B. G. Eads
195. S. B. Elston
196. F. P. Ervin
197. R. L. Ferguson
198. J. D. Garrett
199. I. C. Girit
200. J. Gomez del Campo
201. J. H. Greene
202. D. C. Gregory
203. E. E. Gross
204. M. W. Guidry
205. E. C. Halbert
206. M. L. Halbert
207. J. A. Harvey
208. C. C. Havener
209. D. L. Haynes
210. J. R. Heath
211. J. M. Helton
212. D. C. Hensley
213. J. R. Hightower
214. D. J. Horen
215. H. T. Hunter
216. D. P. Hutchinson
217. C. H. Johnson
218. J. W. Johnson
219. N. R. Johnson
220. C. M. Jones
221. N. L. Jones
222. R. C. Juras
223. S. V. Kaye
224. H. J. Kim
225. M. I. Kirkpatrick
226. C. H. Krause
227. H. F. Krause
228. E. H. Krieg, Jr.
229-230. Laboratory Records Department
231. Laboratory Records, ORNL R.C.
232. S. N. Lane
233. M. R. Lay
234. I. Y. Lee
235. A. B. Livingston
236 A. L. Lotts
237. C. A. Ludemann
238. C. H. Ma
239. J. H. Macek
240. F. Maienschein
241. J. A. Martin
242. M. J. Martin
243. O. J. McBride
244. J. W. McConnell
245. F. K. McGowan
246. J. B. McGrory
247. G. S. McNeilly
248. P. E. Melroy
249. J. R. Merriman
250. F. W. Meyer
251. R. W. Miles
252. P. D. Miller
253. W. T. Milner
254. O. B. Morgan, Jr.
255. S. W. Mosko
256. F. R. Mynatt
257. F. E. Obenshain
258. D. K. Olsen
259. ORNL - Y-12 Technical Library Document Reference Section
260. F. M. Ownby
261. R. W. Peelle
262. D. J. Pegg
263. F. G. Perey
264. R. A. Phaneuf
265. H. B. Piper
266. Physics Division Library
267. F. Plasil
268. H. Postma
269. M. L. Poutsma
270. S. Raman
271. D. E. Reichle
272. C. R. Richmond
273. L. L. Riedinger
274. R. L. Robinson
275. M. W. Rosenthal
276. T. M. Rosseel
277. T. H. Row
278. L. J. Saddiq
279. G. R. Satchler
280. M. R. Schmorak
281. I. A. Sellin
282. P. B. Semmes
283. U. Shapira
284. J. Sheffield
285. W. D. Shults
286. W. D. Siemens
287. T. P. Sjoreen
288. S. P. Sorensen
289. P. H. Stelson
290. J. O. Stiegler
291. M. R. Strayer
292. A. S. Tate
293. B. A. Tatum
294. J. K. Thacker
295. K. S. Toth
296. A. W. Trivelpiece

297. K. L. Vander Sluis
298. C. R. Vane
299. R. L. Varner
300. C. R. Wallace
301. K. M. Wallace
302. P. J. Walsh
303. D. A. Waters
304. J. C. Wells, Jr.
305. M. Whitley
306. C-Y. Wong
307. F. W. Young
308. G. R. Young
309. N. F. Ziegler
310. A. Zucker

EXTERNAL DISTRIBUTION

311. J. M. Alexander, Department of Physics, SUNY at Stony Brook, Stony Brook NY 11794
312. B. J. Allen, Physics Division, Australian Atomic Energy Commission, Sutherland, N.S.W., Australia
313. J. U. Andersen, Institute of Physics, Aarhus University, DK-8000, Aarhus C, Denmark
314. Sakir Ayik, Tennessee Technological University, Physics Department, Cookeville, TN 38505
315. A. B. Balantekin, Department of Physics, University of Wisconsin, 1150 University Avenue, Madison, WI 53706.
316. Charles A. Barnes, Division of Physics and Astronomy, California Institute of Technology, Pasadena, CA 91125
317. G. A. Bastin, Centre de Spectrometrie Nucleaire et de Spectrometrie de Masse, B. P. 104, 91406 Orsay, France
318. Bates Linear Accelerator, P. O. Box 95, Middleton, MA 01949
319. H. Behrens, Zentralstelle fur Atomkernenergie-Dokumentation, Kernforschungszentrum Karlsruhe 7514, Eggenstein-Leopoldshafen-2, Federal Republic of Germany
320. Ingmar Bergstrom, Nobel Institute of Physics, Stockholm 50, Sweden
321. B. L. Berman, Department of Physics, The George Washington University, Washington, DC 20052
322. Bibliotheque - Madame Belle, Universite de Grenoble, Institut des Sciences Nucleaires, 53, rue des Martyrs, B. P. 21, 38 Grenoble, France
323. J. P. Blaser, Paul Scherrer Institute (PSI), CH-5234 Villigen, Switzerland
324. P. Blasi, Universita di Fierenza, Largo E. Fermi 2, 50125 Fierenza, Italy
325. S. D. Bloom, University of California, Lawrence Livermore National Laboratory, P. O. Box 808, Livermore, CA 94550
326. H. G. Blosser, Cyclotron Laboratory, Michigan State University, East Lansing, MI 48824
327. R. Bock, Gesellschaft für Schwerionenforschung, Postfach 11 05 41, 6100 Darmstadt, West Germany
328. H. Bohn, Physik-Department E12, Technische Universitat, 8046 Garching bei Munchen, Federal Republic of Germany
329. A. Bohr, Copenhagen University, Niels Bohr Institute, Blegdamsvej 17, Copenhagen, Denmark
330. Peter Braun-Munzinger, Department of Physics, SUNY at Stony Brook, Stony Brook, NY 11794
331. L. B. Bridwell, Office of the President, S.W. Missouri State University, 901 South National, Springfield, MO 65804
332. J. S. Briggs, Theoretical Physics Division, Atomic Energy Research Establishment, Harwell, Didcot, Oxfordshire OX 11 ORA, England
333. J. A. Brink, Library Division, The Merensky Institute of Physics, University of Stellenbosch, Stellenbosch, Republic of South Africa
334. H. C. Britt, Lawrence Livermore Laboratory, P. O. Box 808, Livermore, CA 94550
335. Ricardo Americo Broglia, Niels Bohr Institute, Blegdamsvej 17, 2100 Copenhagen 0, Denmark
336. D. A. Bromley, Nuclear Structure Laboratory, Yale University, New Haven, CT 06520
337. Peter Anthony Butler, University of Liverpool, P. O. Box 147, Liverpool L69 3X, United Kingdom
338. T. A. Cahill, Director, Crocker Nuclear Laboratory, University of California, Davis, CA 95616
339. R. Caplar, Ruder Boskovic Institute, Bijenicka 54, 41001 Zagreb, Croatia, Yugoslavia
340. Jose L. S. Carvalho, Instituto de Radioprotecao e Dosimetria, C.N.E.N., Av. das Americas km 11,5 Barra de Tijuca - R. J., 22700 - Rio de Janeiro, R. J. Brazil
341. Yong Shou Chen, Institute of Atomic Energy, Academia Sinica, P. O. Box 275, Beijing, China
342. F. E. Chukreev, Kurchatov Institute of Atomic Energy, Kurchatov Square, 123 182 Moscow, USSR
343. N. Cindro, Ruder Boskovic Institute, Bijenicka 54, 41001 Zagreb, Yugoslavia
344. David Clark, Lawrence Berkeley Laboratory, University of California, Berkeley, CA 94720
345. Douglas Cline, Nuclear Structure Research Laboratory, University of Rochester, Rochester, NY 14627
346. J. D. Cole, EG&G Idaho, Inc., TRA 652, Idaho Falls, ID 83415
347. University of Colorado, Department of Physics, Boulder, CO 80309
348. D. H. Crandall, Branch Chief for Experimental Research, Applied Plasma Physics Division, Office of Fusion Energy, ER 542, G-226, GTN, U.S. Department of Energy, Washington, DC 20545
349. F. L. Culler, Office of the President, Electric Power Research Institute, P. O. Box 10412, 3412 Hillview Avenue, Palo Alto, CA 94303
350. R. E. Culp, Martin Marietta Denver Aerospace, P.O. Box 179, M/S # P0540, Denver, CO 80201

351. T. J. Curtin, Director, Office of Research and Grants Administration, Texas Women's University, Box 22939, TWU Station, Denton, TX 76204
352. R. Y. Cusson, Physics Department, Duke University, Durham, NC 27706
353. Cyclotron Library, Indiana University Cyclotron Facility, 2401 Milo B. Sampson Lane, Bloomington, IN 47405
354. B. A. Dahling, Lawrence Livermore National Laboratory, University of California, Livermore, CA 94550
355. Solange de Barros, Head, Department of Nuclear Physics, Universidade Federal do Rio de Janeiro, Instituto de Fisica - Department Fisica Nuclear, Centro de Technologia - Bloco A, Ilha do Fundao - Rio de Janeiro, Brasil
356. Adriano de Lima, Physics Laboratory, University of Coimbra, Coimbra, Portugal
357. Claude Détraz, Director, GANIL, B.P. 5027, 14021 Caen Cedex, France
358. R. M. Diamond, Chemistry Division, Lawrence Berkeley Laboratory, Berkeley, CA 94720
359. Olacio Dietzsch, Depto. de Fisica Experimental, Instituto de Fisica, Universidade de Sao Paulo, Cx. Postal 20516, Sao Paulo, S.P., Brazil
360. J. L. Duggan, Department of Physics, North Texas State University, Denton, TX 76203
361. K. A. Erb, National Science Foundation, Rm. 341, 1800 G Street NW, Washington, DC 20550
362. John R. Erskine, U.S. Department of Energy, Division of Nuclear Physics, ER-23, GTN, Washington, DC 20545
363. U. Facchini, Physics Department, University of Milan, Via Salidini 50, Milan, Italy
364. Amand Faessler, Institut fur Theoretische Physik, Universitat Tubingen, Auf der Morgenstelle 14, D-7400 Tubingen, West Germany
365. D. H. Feng, Department of Physics, Drexel University, Philadelphia, PA 19104
366. M. P. Fewell, Australian National University, Canberra, 2600 Australia
367. R. W. Fink, School of Chemistry, Georgia Institute of Technology, Atlanta, GA 30332
368. G. N. Flerov, Laboratory for Nuclear Reactions, Dubna Joint Institute for Nuclear Research, Dubna, Moscow Oblast, U.S.S.R.
369. J. S. Forster, Nuclear Physics Branch, Atomic Energy of Canada Limited, Chalk River Nuclear Laboratories, Chalk River, Ontario, Canada KOJ 1J0
370. J. D. Fox, Department of Physics, Florida State University, Tallahassee, FL 32306
371. I. M. Frank, Laboratory for Nuclear Reactions, Dubna Joint Institute for Nuclear Research, Dubna, Moscow Oblast, U.S.S.R.
372. Claus-Konrad Gelbke, National Superconducting Cyclotron Laboratory, Michigan State University, East Lansing, MI 48824
373-382. GLCA-ORS, Attention: R. R. Winters, Denison University, Granville, OH 43023
383. Alan Goodman, Department of Physics, Tulane University, New Orleans, LA 70118
384. Harvey A. Gould, Lawrence Berkeley Laboratory, 1 Cyclotron Blvd., Berkeley, CA 94720
385. H. E. Gove, Nuclear Structure Laboratory, University of Rochester, Bldg. 510A, Rochester, NY 14627
386. Walter Greiner, Institut fur Theoretische Physik der Universitat Frankfurt Main, Robert Mayer-Strasse 8-10, West Germany
387. H. Grunder, Continuous Electron Beam Accelerator Facility (CEBAF), 12070 Jefferson Avenue, Newport News, VA 23606
388. M. Grypeos, University of Thessaloniki, Department of Theoretical Physics, Thessaloniki, Greece
389. H. H. Gutbrod, Gesellschaft für Schwerionenforschung, Postfach 11 05 41, 6100 Darmstadt 1, West Germany
390. J. H. Hamilton, Department of Physics, Vanderbilt University, Nashville, TN 37203
391. Ole Hansen, Brookhaven National Laboratory, Bldg. 901A, Upton, NY 19973
392. J. S. Hattula, Department of Physics, University of Jyvaskyla, Seminaarinkatu 15, SF-40100 Jyvaskyla 10, Finland
393. R. L. Heath, Idaho National Engineering Laboratory, EG&G Idaho, Inc., P. O. Box 1625, Idaho Falls, ID 83401
394. David L. Hendrie, Director, Division of Nuclear Physics, ER 23, Mail Station J-309, U.S. Department of Energy, Washington, DC 20545
395. Ronald Henry, Department of Physics and Astronomy, Louisiana State University, 202 Nicholson Hall, Baton Rouge, LA 70803-4001
396. Bent Herskind, Niels Bohr Institute, Riso, DK-4000 Roskilde, Denmark
397. Rainer Hippler, Universitat Bielefeld, Fakultat fur Physik, University of Bielefeld, Postfach 8640, 4800 Bielefeld 1, West Germany
398. Harry D. Holmgren, Department of Physics, University of Maryland, College Park, MD 20742.
399. J. R. Huizenga, Department of Physics and Astronomy, University of Rochester, Rochester, NY 14627
400. P. Hvelplund, Institute of Physics, Aarhus University, DK-8000, Aarhus C, Denmark
401. H. R. McK. Hyder, Nuclear Physics Laboratory, Oxford University, Keble Road, Oxford OX1 3RH, England
402. M. V. Hynes, Department of Physics, Los Alamos National Laboratory, University of California, Los Alamos, NM 97545
403. Francesco Iachello, Yale University, Department of Physics, New Haven, CT 06520

404. University of Illinois at Urbana-Champaign, Department of Physics, Urbana, IL 61801
405. Institute for Energy Analysis, P. O. Box 117, Oak Ridge, TN 37830
406. Institute of Physics, High Energy and Nuclear Physics Library, C. Postal 20.516,0100 - Sao Paulo, S.P., Brasil
407. I. Iori, Istituto di Science Fisiche, Aldo Pontromoli, Via Celoria 16, 20133 Milano, Italy
408. Iowa State University, Department of Physics, Ames, IA 50011
409. J. M. Irvine, Department of Physics, University of Manchester, Oxford Rd., GB-Manchester M13 9 PL, United Kingdom
410. Beth Jinkerson, ORAU/UPD, Oak Ridge, TN 37831-0117
411. R. C. Johnson, University of Surrey, Guildford, Surrey GU2 5XH, United Kingdom
412. R. Kamermans, Fysisch Laboratorium, Rijksuniversiteit Utrecht, P. O. Box 80.000, 3508 TA UTRECHT, The Netherlands
413. H. Kamitsubo, Head, Cyclotron Laboratory, Institute of Physical and Chemical Research, Wako-shi, Saitama, 351 Japan
414. D. G. Kamke, Ruhr-Universitat Bochum, Dynamitron Tandem Laboratory, Universitatsstr., 150 Gibaunde NT, Postfach 1021 48, 4360 Bochum 1, Federal Republic of Germany
415. University of Kansas, Department of Physics, Lawrence, KS 66045
416. Norihisa Kato, Department of Physics, Kyushu University, 33 Fukuoka, 812, Japan
417. H. Kawakami, Institute for Nuclear Study, University of Tokyo, Midori-cho, Tokyo, Japan
418. J. O. Kephart, Department of Electrical Engineering, Stanford University, Stanford, CA 94305
419. B. D. Kern, Department of Physics & Astronomy, University of Kentucky, Lexington, KY 40506
420. Uwe Keyser, Institut F. Metallphysik und Nukleare, Festkoerperphysik Techn.-Universitaet, D3300 Braunschweig, Mendelssohnstr. 3, Federal Republic of Germany
421. R. K. Klein, Department of Electrical Engineering, Stanford University, Stanford, CA 94305
422. P. K. Kloeppel, Continuous Electron Beam Accelerator Facility, 12070 Jefferson Avenue, Newport News, VA 23606
423. H. Knudsen, Institute of Physics, Aarhus University, DK-8000, Aarhus C, Denmark
424. Steven E. Koonin, Kellogg Radiation Laboratory, California Institute of Technology, Pasadena, CA 91125
425. M. O. Kortelahti, Physics Department, University of Jyvaskyla, Seminaarink 15, 40100 Jyvaskeyla, Finland
426. K. S. Krane, Department of Physics, Oregon State University, Corvallis, OR 97331-6507
427. B. Krishnarajulu, Department of Physics, Gulbarga University, Gulbarga 585106, India
428. Thomas J. Kvale, Department of Physics & Astronomy, University of Toledo, Toledo, OH 43606
429. Michel LeTournel, Centre de Recherches Nucleaires, Service des Accelerateurs, B. P. 20 CRO, 67037 Strasbourg Cedex, France
430. Librarian, Atomic Energy Centre, P. O. Box No. 164, Ramna, Dacca, Bangladesh
431. Librarian, Chen Kin-hai, Institute of Modern Physics, Academia Sinica, P. O. Box 31, Lanzhou, People's Republic of China
432. Librarian, Cyclotron Laboratory, Michigan State University, East Lansing, MI 48824
433. Librarian, Cyclotron Laboratory, RIKEN (The Institute of Physical and Chemical Research), Wako-shi, Saitama 351, Japan
434. Librarian, Department of Physics, Georgia State University, Atlanta, GA 30303
435. Librarian, Fermi National Accelerator Lab., P.O. Box 500, Batavia, IL 60510
436. Librarian, GANIL, B. P. No. 5027, 14004 Caen Cedex, France
437. Librarian, GSI, Postfach 11 05 41, 6100 Darmstadt, Federal Republic of Germany
438. Librarian, Institut des Sciences Nucleaires, B. P. No. 257 - Centre de Tri, 38044 Grenoble Cedex, France
439. Librarian, Institute of Nuclear Research of the Hungarian Academy of Sciences, P.O. Box 51, Debrecen, H-4001 Hungary
440. Librarian, MERT Division Library, Oak Ridge Associated Universities, P. O. Box 117, Oak Ridge, TN 37831-0117
441. Librarian, Nuclear Physics Group, Department of Physics, Schuster Laboratory, The University, Manchester, M13 9PL, United Kingdom
442. Librarian, Nuclear Physics Group, Institute of Physics, Academia Sinica, Taipei, Taiwan 11529, Republic of China
443. Librarian, Nuclear Physics Lab, University of Oxford, 1 Keble Rd., Oxford OX1 3PH, United Kingdom
444. Librarian, Physics Department, 374 Bausch and Lomb Building, University of Rochester, Rochester, NY 14627
445. Librarian, Universidade de Sao Paulo, Instituto de Fisica - Biblioteca Depto Fisica Nuclear, Caixa Postal, 20516 - 01498 - Sao Paulo, Brasil
446. Library of the Institute of Atomic Energy, Beijing, People's Republic of China
447. Rainer M. Lieder, Institut für Kernphysik, Postfach 1913, 5170 Julich, West Germany
448. J. S. Lilley, Daresbury Laboratory, GB-Warrington WA4 4AD Chesnire, England
449. J. C. Lisle, Dept. of Physics, Schuster Laboratory, Manchester University, Manchester M13 9 M13 9 PL, United Kingdom
450. H. Lizurej, Jagellonian University, Institute of Physics, Reymonta 4, 30-059 Krakow 16, Poland
451. Tom Lonnroth, Department of Physics, Abo Akademi, Porthansgatan 3, SF-20500 Turku, Finland

452. Malcolm Macfarlane, Department of Physics, Indiana University, Bloomington, IN 47405
453. A. D. MacKellar, Department of Physics and Astronomy, University of Kentucky, Lexington, KY 40506-0055
454. G. Madurga, Departameto de Fisica Atomica y Nuclear, Facultad de Ciencias, Universidad de Sevilla, Sevilla, Spain
455. Claude Charles Mahaux, Institut de Physique B5 Universite de Liege, Sait Tilman, B-4000 Liege 1, Belgium
456. Robert S. Marianelli, Division of Chemical Sciences, Office of Basic Energy Sciences, U.S. Department of Energy, Mail Station G-334, GTN, Washington, DC 20545
457. Mario Mariscotti, Comision Nacional de Energia Atomica, Departmento de Fisica, Avenida del Libertador 8250, 1429 Buenos Aires, Argentina
458. Niels Marquardt, Universität Dortmund Lehrstuhl für Beschleunigerphysik, P.O. Box 500 500, D-4600 Dortmund 50, West Germany
459. J. V. Martinez, Division of Chemical Sciences, Mail Stop J309 GTN, U.S. Department of Energy, Washington, DC 20545
460. Floyd D. McDaniel, Department of Physics, North Texas State University, Denton, TX 76203
461. W. R. McMurray, Deputy Chief Scientist, Kerninstituut Van Die Suidelike Universiteite, Southern Universities Nuclear Institute, Republic of South Africa
462. G. K. Mehta, Professor of Physics, Van de Graaff Laboratory, Indian Institute of Technology Kanpur, Kanpur 208 016, India
463. Eugen Merzbacher, University of North Carolina, Department of Physics and Astronomy, Chapel Hill, NC 27514
464. R. J. Meyer, Nuclear Physics Department, Fysisch Laboratorium Rijksuniversiteit, P. O. Box 80 000, 3508 TA Utrecht, The Netherlands
465. R. Middleton, Department of Physics, University of Pennsylvania, Philadelphia, PA 19104
466. E. Migneco, INFN Laboratorio Nazionale del Sud, Corso Italia 57, 95127 Catania, Italy
467. Alice C. Mignerey, Department of Chemistry, University of Maryland, College Park, MD 20742
468. J. C. D. Milton, Physics Division, Atomic Energy of Canada Ltd., Chalk River, Canada K0J 1J0
469. University of Minnesota, Physics Department, 116 Church Street SW, Minneapolis, MN 55455
470. C. D. Moak, 332 Louisiana Avenue, Oak Ridge, TN 37830
471. G. C. Morrison, Department of Physics, University of Birmingham, Birmingham B15 2TT, England
472. U. Mosel, Institut fur Theoretische Pysik, Universitat Giessen, 6300 Giessen, West Germany
473. Brian W. Moudry, c/o Ms. Helene Perry, Department of Physics, Loyola College, Baltimore, MD 21210
474. S. C. Mukherjee, Librarian, Saha Institute of Nuclear Physics, 92, Acharya Prafulla Chandra Road, Calcutta - 9, India
475. Shoji Nagamiya, Department of Physics, Columbia University, New York, NY 10027
476. M. A. Nagarajan, Daresbury Laboratory, GB-Warrington WA4 4AD Cheshire, England
477. Y. Nakamura, JPL, Systems Analysis Section, California Institute of Technology, 4800 Oak Grove Drive, Pasadena, CA 91103
478. Witek Nazarewicz, Institute of Physics, Politechnika Warszawska ul. Koszykowa 75, PL-00662 Warszawa, Poland
479. John H. Neiler, 853 West Outer Drive, Oak Ridge, TN 37830
480. Nebojsa Neskovic, Boris Kidric Institute of Nuclear Science - Vinca, Institute for Research in Physics, P.O. Box 522, 11001 Beograd - Yugoslavia
481. John Newton, Dept. of Nuclear Physics, The Australian National University, P. O. Box 4, Canberra ACT 2600, Australia
482. Ray Nix, Nuclear Theory, T-9, MS B279, Los Alamos National Laboratory, Los Alamos, NM 87545
483. Ranier W. Novotny, II. Physikalisches Institut, Justus-Liebig Universitat, Heinrich-Buff-Ring 16, 6300 Giessen, West Germany
484-568. Oak Ridge Associated Universities, Office of Information Services, P. O. Box 117, Oak Ridge, TN 37831-0117
569. Office of Assistant Manager for Energy Research and Development, Department of Energy, Oak Ridge Operations Office, Oak Ridge, TN 37830
570. Yuko Okamoto, Particle Theory Group, Department of Physics, Nara Women's University, Nara-shi 630, Japan
571. Masumi Oshima, Japan Atomic Energy Research Institute, Tokai Establishment, Tokai-mura, Naka-gun, Ibaraki-ken 319-11, Japan
572. Ingvar Otterlund, Division of Cosmic and Subatomic Physics, University of Lund, Sölvegatan 14, S-233 62 Lund, Sweden
573. R. H. Pantell, Department of Electrical Engineering, Stanford University, Standford, CA 94305
574. H. Park, Department of Electrical Engineering, Stanford University, Stanford, CA 94305
575. Peter Paul, Department of Physics, S.U.N.Y. at Stony Brook, Stony Brook, NY 11794
576. Max Peisach, Southern Universities Nuclear Institute, P. O. Box 17, Faure, 7131, Republic of South Africa
577. A. A. Pilt, Tandem Accelerator Laboratory, McMaster University, Hamilton, Ontario, Canada L8S 4K1
578. University of Pittsburgh, Department of Physics, Pittsburgh, PA 15260

579. J. G. Pochodzalla, Gesselischaft fur Schwerionenforschung, Postfach 11 0- 41, Darmstadt 1, West Germany
580. R. E. Pollock, Department of Physics, Indiana University, Bloomington, IN 47405
581. A. M. Poskanzer, Nuclear Science Division, Lawrence Berkeley Laboratory, Berkeley, CA 94720
582. Helmut Poth, C.E.R.N., European Laboratory for Particle Physics, CH-1211, Geneva 23, Switzerland
583. F. Pougheon, Institut de Physique Nucleaire, B.P. No. 1, 91406 Orsay, France
584. B. Povh, Max Planck Institut fur Kernphysik, 69 Heidelberg, Saupfercheckweg, Postfach 1248, Federal Republic of Germany
585. James Purcell, Department of Physics, Georgia State University, Atlanta, GA 30303
586. A. V. Ramayya, Department of Physics, Vanderbilt University, Nashville, TN 37203
587. Jacobo Rapaport, Department of Physics, Ohio University, Athens, OH 45701-0640
588. John Rasmussen, Lawrence Berkeley Laboratory, Building 70A, Berkeley, CA 94720
589. Patrick Richard, Physics Department, Kansas State University Manhattan, KS 66506
590. Shela Robinson, Department of Physics & Astronomy, Western Kentucky University, Bowling Green, KY 42101
591. L. Rosen, Los Alamos National Laboratory, P. O. Box 1663, Los Alamos, NM 87544
592. Ranier Santo, Sektion Physik der Universitat Munchen, 8046 Garching, Beschleuigerlaboratorium (Forschungsgelande), Federal Republic of Germany
593. D. G. Sarantites, Department of Chemistry, Washington University, St. Louis, MO 63130
594. V. Sarantseva, Head, Publishing Department, Joint Institute for Nuclear Research, Head Post Office, P. O. Box 79, Moscow, U.S.S.R.
595. J. P. Schiffer, Physics Division, Argonne National Laboratory, 9700 South Cass Avenue, Argonne, IL 60439
596. K. D. Schilling, Zentralinstitut fur Kernforschung, Rossendorf, Bereich 2, DDR-8051 Dresden, Democratic Republic of Germany
597. Hermann Schweickert, Cyclotron Laboratory, Kernforschungszentrum Karlsruhe, Institut fur Applied Physik, P. O. Box 3640, D-7500 Karlsruhe 1, Federal Republic of Germany
598. David K. Scott, National Superconducting Cyclotron Laboratory, Michigan State University, East Lansing, MI 48824
599. S. Seki, Tandem Accelerator Center, University of Tsukuba, Ibaraki 305, Japan
600. J.P.F. Sellschop, Department of Physics, University of Witwatersrand, Johannesburg, South Africa
601. M. H. Sergolle, Director, Institut de Physique Nucleaire - Orsay , B.P. N° 1, 91406 Orsay Cedex, France
602. J. C. C. Sharp, Information Officer, Daresbury Laboratory, Science Research Council, Daresbury, Warrington WA4 4AD, England
603. J. F. Sharpey-Schafer, Oliver Lodge Laboratory, The University, P. O. Box 147, Liverpool, L69 3BX, United Kingdom
604. N. Shikazono, Division of Physics, Japan Atomic Energy Research Institute, Tokai Research Institute, Postal Area Number 319-11, Tokai-mura, Naka-gun, Ibaraki-ken, Japan
605. R. H. Siemssen, Kernfysisch Versneller Instituit der Rijksuniversiteit Zernikelaan 25, 9747 AA Groningen, The Netherlands
606. C. Signorini, INFN Laboratorio Nazionale di Legnaro, Via Romea 4, 35020 Legnaro-Padova, Italy
607. Raghuvir Singh, North Eastern Hill University, Department of Physics, Laitumkhrah, Shillong-793003, India
608. S. J. Skorka, Tandem Accelerator Laboratory, University of Munich, Munich, Federal Republic of Germany
609. Carl Sofield, Nuclear Physics Division, Bldg. 477, AERE Harwell, Oxfordshire OX 11 ORA, England
610. Hsu Loke Soo, Department of Physics, Nanyang University, Singapore 22, Republic of Singapore
611. C. Speth, Institut fur Kernphysik, KFA, Julich, Postfach 1913, D-5170 Julich, Federal Republic of Germany
612. T. Springer, Institut fur Festkorperforschung der KFA Julich GmbH, Postfach 1913, D-5170 Julich 1, Federal Republic of Germany
613. Stanford University, Department of Physics, Stanford, CA 94305
614. Stephen G. Steadman, Massachusetts Institute of Technology, Room 26-411, Cambridge, MA 02139
615. Alberto Stefanini, Instituto Nazionale di Fisica Nucleare, Laboratori Nazionali di Legnaro, 35020 Legnaro (Padova), Italy
616. Donald K. Stevens, Office of Basic Energy Sciences, U.S. Department of Energy, Mail Station J-304, GTN, Washington, DC 20545
617. R. G. Stokstad, Lawrence Berkeley Laboratory, Bldg. 88, Berkeley, CA 94720
618. N. Stolterfoht, Hahn-Meitner-Institut fur Kernforschung Berlin GmbH, Bereich Kern - und Strahlenphysik, D-1000 Berlin 39, West Germany
619. Kazusuke Sugiyama, Department of Nuclear Engineering, Faculty of Engineering, Tohoku University, Sendai, Japan
620. J. K. Swenson, Department of Physics, University of North Carolina, Chapel Hill, NC 27514
621. T. J. Symons, Nuclear Science Division, Lawrence Berkeley Laboratory, 1 Cyclotron Road, Berkeley, CA 94720

622. Shigyea Tanaka, Japan Atomic Energy Research Institute, Tokai-mura, Ibaraki-ken, Japan
623. Hiroyuki Tawara, Institute of Plasma Physics, Nagoya University, Chikusa-ku Nagoya 464, Japan
624. Lee C. Teng, Fermi National Accelerator Laboratory, Accelerator Division, P. O. Box 500, Batavia, IL 60510
625. The High Energy Group, Institute of Physics, Academia Sinica, Nankang, Taipei, Taiwan, ROC
626. Mauro Donizette Tonasse, Faculdades Integradad de Uberaba, Avenida Afranio de Azevedo no. 115, UBERABA - MG - Brazil
627. P. J. Twin, Daresbury Nuclear Physics Laboratory, Daresbury, Nr. Warrington, Lancashire, England
628. J. P. Unik, Argonne National Laboratory, Building 200, Argonne, IL 60439
629. Robert Vandenbosch, Department of Chemistry, University of Washington, Seattle, WA 98195
630. A. van der Woude, Kernfysisch Versneller Institut der Rijksuniversiteit, Universiteitscomplex Paddepoel, Groningen, The Netherlands
631. H. Verheul, Natuurkundig Laboratorium der Vrije Universiteit de Boelelaan 1081, Amsterdam, The Netherlands
632. VICKSI, Sekretariat, Hahn-Meitner Institut fur Kernforschung Berlin GmbH, Postfach 39 01 28, D-1000 Berlin 39, Federal Republic of Germany
633. Virginia Polytechnic Institute and State University, Department of Physics, Blacksburg, VA 24061
634. A. J. A. Virtanen, Department of Physics, University of Jyvaskyla, Seminaarinkatu 15, SF-40100 Jyvaskyla, Finland
635. W. von Oertzen, Hahn-Meitner Institut fur Kernforschung, Berlin GmbH, Federal Republic of Germany
636. George Vourvopoulos, Department of Physics, Western Kentucky University, Bowling Green, KY 42101
637. Thomas A. Walkiewicz, Edinboro University, Department of Chemistry & Physics, P.O. Box 589, Wetsell Ridge Road, Edinboro, PA 16412
638. A. H. Wapstra, Institute Voor Kernphysisch Onderzoek, Ooster Ringdijk 18, Amsterdam, The Netherlands
639. David Ward, Nuclear Physics Branch, Chalk River Nuclear Laboratories, Ontario, Canada KOJ 1J0
640. Harlan L. Watson, Deputy Staff Director, Subcommittee on Energy Development and Applications, Committee on Science and Technology, U.S. House of Representatives, B374 Rayburn House Office Building, Washington, DC 20515
641. H. E. Wegner, Department of Physics, 901A, Brookhaven National Laboratory, Upton, NY 11973
642. D. C. Weisser, Department of Nuclear Physics, Institute of Advanced Studies, The Australian National University, P. O. Box 4, Canberra ACT 2600, Australia
643. W. G. Weitkamp, Nuclear Physics Laboratory, G-10, University of Washington, Seattle, WA 98195
644. Robert A. Weller, Jr., Department of Physics, Yale University, New Haven, CT 06511
645. Joseph Weneser, Department of Physics, Bldg. 510, Brookhaven National Laboratory, Upton, NY 11973
646. E. P. Wigner, Department of Physics, Princeton University, Princeton, NJ 08540
647. B. H. Wildenthal, Department of Physics & Astronomy, University of New Mexico, 800 Yale NE, Albuquerque, NM 87131
648. University of Wisconsin, Department of Physics, Madison, WI 53706
649. J. L. Wood, School of Chemistry, Georgia Institute of Technology, Atlanta, GA 30332
650. Alexander Xenoulis, Van de Graaff Laboratory, Nuclear Research Center, Demokridos, Aghia Paraskevi Attikis, Athens, Greece
651. Takashi Yamazaki, Research Center for Nuclear Physics, Osaka University (Suita Campus), Ibaraki, Osaka, 567 Japan
652. Yasunori Yamazaki, Research Laboratory for Nuclear Reactors, Tokyo Institute of Technology, Tokyo, Japan
653. Fujia Yang, Director, Institute of Modern Physics, Fudan University, Shanghai, People's Republic of China
654. D. Youngblood, Cyclotron Institute, Texas A&M University, College Station, TX 77940
655. E. F. Zganjar, Department of Physics and Astronomy, Louisiana State University, Baton Rouge, LA 70803
656. K. Ziegler, Hahn-Meitner Institut fur Kernforschung Berlin GmbH, Postfach 39 01 28, D-1000 Berlin 39, Federal Republic of Germany
657-717. Given distribution as shown in DOE/TIC-4500 under UC-410 - General Physics.